STIC-ILL

10/9/10

From: Marx, Irene
Sent: Tuesday, September 10, 2002 9:19 AM
To: STIC-ILL
Subject: 09/777664

411609

Importance: High

Please send to Irene Marx, Art Unit 1651; CM1, Room 10E05, phone 308-2922, Mail box in 11B01

Observations on the ionic composition of blue-green algae growing in saline lagoons
AU Pillai, V. K.
SO Proc. Natl. Inst. Sci. India, (19550000) vol. 21, no. 2, pp. 90-102.
DT Journal

Dalrymple, D.W., 1965, "Calcium carbonate deposition associated with blue green algal mats, Baffin Bay.:, Texas: Institute of Marine Science Publication 10, p. 187-200

Black, M., 1933, "The algal sedimentation... ", Royal Society of London Philosphical transactions, Ser. B, V. 222, p. 165-192

Lowenstam HA (1981), Science, 211:1126-1131

Ferris et al., Earth Sci., 47:233-250 (1993)

Ferris et al., Appl. and Environm. Microbiol.,1989, 55:1249-1257

Kazmierczak et al., (1990), Science, 250:1244-1248

Kempe et al., Facies, 28:1-32, 1993.

Kempe et al., 1994, Bull, Inst. Oceanogr., Monaco no. spec., 13:61-117.

Merz, M.U.E, 1992, Facies, 26:81-102

Pentecost et al., 1986, Calcification in cyanobacteria, In "Biomineralization of Lower plants and animals (Leadbeater et a., ed. 73-90, Clarendon Press, Oxford.

Riding, R., 1982, Nature, 299:814-815

Thompson eta., 1990, Geology, 18:995-998

Irene Marx
Art Unit 1651
CMI 10-E-05,
Mail Box 11-B-01
703-308-2922

CIS TI 9/11

LC 9/11 SMP NOS

STIC-ILL

411606

From: Marx, Irene
Sent: Tuesday, September 10, 2002 9:19 AM
To: STIC-ILL
Subject: 09/777664

Imp rtance: High

Please send to Irene Marx, Art Unit 1651; CM1, Room 10E05, phone 308-2922, Mail box in 11B01

Observations on the ionic composition of blue-green algae growing in saline lagoons
AU Pillai, V. K.
SO Proc. Natl. Inst. Sci. India, (19550000) vol. 21, no. 2, pp. 90-102.
DT Journal

Dalrymple, D.W., 1965, "Calcium carbonate deposition associated with blue green algal mats, Baffin Bay.:, Texas; Institute of Marine Science Publication 10, p. 187-200

Black, M., 1933, "The algal sedimentation... ", Royal Society of London Philosphical transactions, Ser. B, V. 222, p. 165-192

Lowenstam HA (1981), Science, 211:1126-1131

Ferris et al., Earth Sci., 47:233-250 (1993)

Ferris et al., Appl. and Environm. Microbiol.,1989, 55:1249-1257

Kazmierczak et al., (1990), Science, 250:1244-1248

Kempe et al., Facies, 28:1-32, 1993.

Kempe et al., 1994, Bull, Inst. Oceanogr., Monaco no. spec., 13:61-117.

Merz, M.U.E, 1992, Facies, 26:81-102

Pentecost et al., 1986, Calcification in cyanobacteria, In "Biomineralization of Lower plants and animals (Leadbeater et a., ed. 73-90, Clarendon Press, Oxford.

Riding, R., 1982, Nature, 299:814-815

Thompson eta., 1990, Geology, 18:995-998

Irene Marx
Art Unit 1651
CMI 10-E-05,
Mail Box 11-B-01
703-308-2922

2 HC
9/10

No

SEP-11-2002 11:33 Linda Hall Library 816 926 8785 P.03

NOTICE: This material may be protected by copyright law (Title 17, U.S. Code)

Calcium Carbonate Deposition Associated With Blue-Green Algal Mats, Baffin Bay, Texas

DON W. DALRYMPLE[1]

[1] Present address: Phillips Petroleum Company, Bartlesville, Oklahoma.

Rice University, Houston, Texas

Abstract

A distinctive grain type, termed "algal micrite," is forming in association with blue-green algal mats in the Baffin Bay area. This grain type consists essentially of microcrystalline aragonite intermeshed with mucilaginous organic material, and is believed to form by direct precipitation from super-saturated sea water within the lower zones of the mat. The precipitation may be induced by bacterial decomposition of the algal mat.

Introduction

The Baffin Bay complex is situated along the Texas Gulf Coast, some 30 miles south of Corpus Christi, Texas (Fig. 1). High evaporation rates and restricted water circulation result in general hypersalinity within the complex, and this hypersalinity is reflected in the suite of sedimentary grain types being deposited in the area (Rusnak, 1960a). This suite is comprised in part of various non-skeletal, calcium carbonate grain types, including a distinctive grain type which appears to occur almost exclusively in association with the blue-green algal mats of the area. The purpose of this paper is to describe the nature, occurrence, and possible mode of origin of this mat-associated grain type. This work is part of a more complete study of the sediments of Baffin Bay, completed in partial fulfillment of the requirements for an advanced degree at Rice University, Houston, Texas (Dalrymple, 1964). The complete work is intended for publication at a later date.

Petrography

In the interests of brevity and convenience, the grain type described herein will be termed, "algal micrite grains," although the unproven genetic implications of this term are recognized. Rusnak (1960a) described similar aggregates from Baffin Bay, but apparently failed to observe the association of aggregates with algal mats. Rusnak (1960a, p. 172) stated that ". . . nearly all the lumps are associated with oolites and carbonate-coated shell fragments . . ."

In reflected light, algal micrite grains are chalky white to cream colored, and display a rough, uneven, exterior surface (Fig. 2A). A wide range of grain sizes has been observed, from one-sixteenth millimeter to more than 200 millimeters in length. The smaller grains are irregularly equant in shape, while the larger grains are invariably flattened and flake-like in appearance. It is apparent that the large, flattened grains are merely cemented aggregates of the smaller, more equant grains, and this interpretation is readily confirmed by thin section examination (Figs. 2B, C).

In thin section, algal micrite grains are seen to consist primarily of randomly dis-

SEP-11-2002 11:33 Linda Hall Library 816 926 8785 P.04

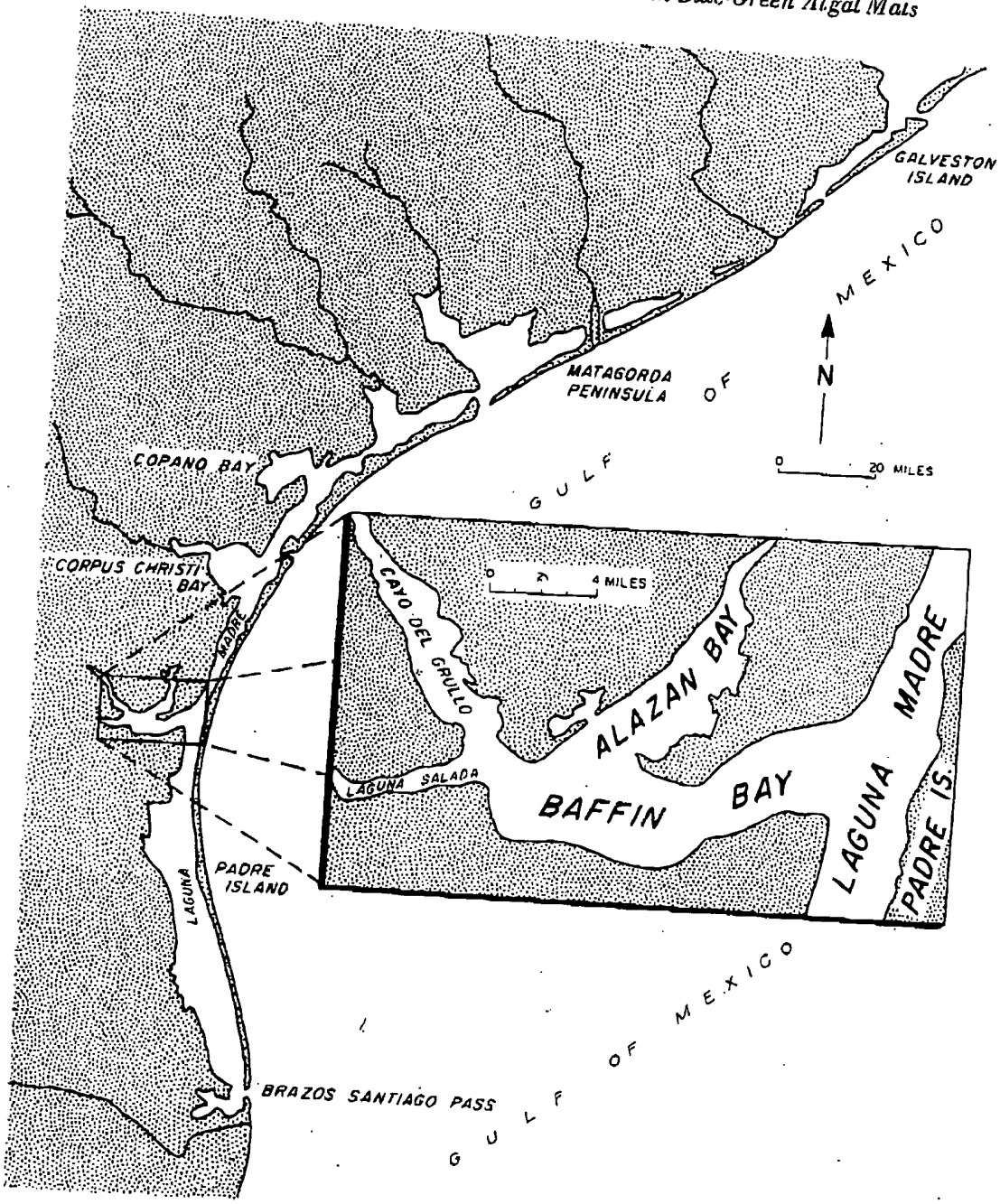

FIG. 1. Index map of Texas Gulf Coast and the Baffin Bay area. After Fisk, 1959.

FIG. 2A. Reflected light photograph of the surface between two layers of an algal-laminated recent stromatolite, Baffin Bay, Texas. The light-colored grains seen on the surface are algal micrite grains. Note the various shapes and states of aggregation of these grains. The dark surface on which the grains are resting is the organic material of the mat itself. Magnification, ×16. B. Thin-section photomicrograph of a small algal micrite grain. This may be a single, "unit" grain, as it is not obviously an aggregate of pre-existing grains (compare with Fig. 2-C). Crossed nicols, ×200. C. Thin-section photomicrograph of a large algal micrite grain, composed of an aggregation of several smaller grains. Note the pore spaces in the interior of the grain (black). Crossed nicols, ×125.

SEP-11-2002 11:34 Linda Hall Library 816 926 8785 P.05

SEP-11-2002 11:34 Linda Hall Library 816 926 8785 P.06

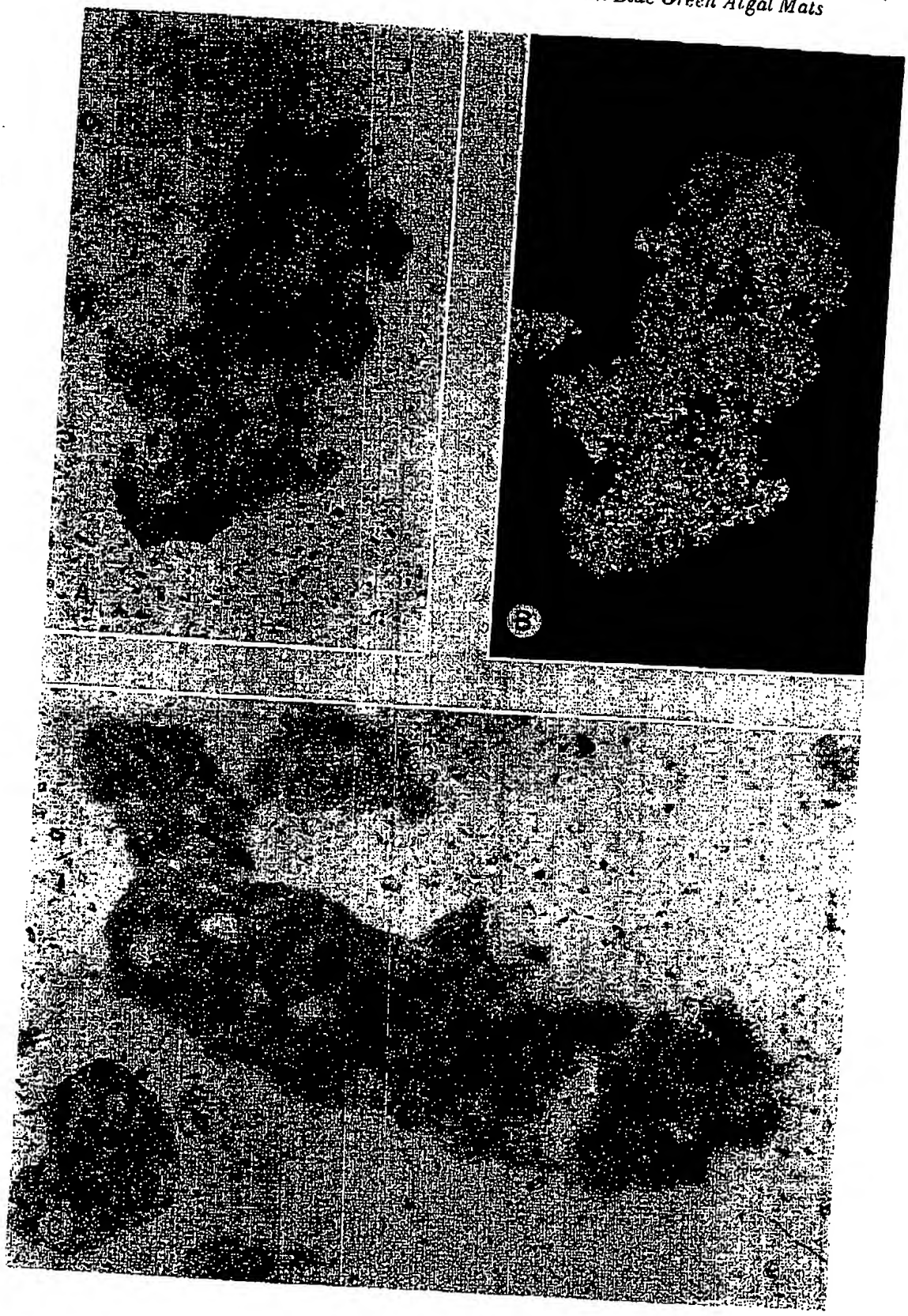

SEP-11-2002 11:35 Linda Hall Library 816 926 8785 P.07

posed, silt- and clay-size crystals of calcium carbonate, or "micrite" (Folk, 1959). The material that joins small, individual algal micrite grains together to form the larger, flattened grains appears to be identical to the grains themselves (Fig. 3A). Indeed, the process by which the larger grains are produced appears to be one of "coalescence" rather than "cementation."

Decalcification of one of the larger grains with dilute acetic acid resulted in a 52% weight loss and left a flexible replica duplicating the size and shape of the original grain. This replica appeared to consist of mucilaginous organic material with some occluded terrigenous clay. The organic matter and clay are probably the chief contributors to the characteristic cloudy, semi-opaque appearance of thin-sectioned algal micrite grains when viewed in transmitted light.

The color of the grains is brownish-gray in plane polarized light, and dark, yellowish-brown between crossed nicols. X-ray analysis indicates that the calcium carbonate of algal micrite grains is aragonite.

Numerous opaque blebs are present in most algal micrite grains (Fig. 3C). Many of these blebs are circular in outline, have an average diameter of perhaps ten microns, and appear white in reflected light. Their appearance is identical to the remains of boring algae commonly seen in pelecypods, and they probably originate in the same way. Their relative abundance in algal micrite grains may be due to the high organic content of these grains.

Larger, irregularly-shaped, opaque or semi-opaque blebs also are observed in some algal micrite grains. The maximum diameter of these blebs is about forty microns. In reflected light their color ranges from light brown to white. An abundance of identical blebs was observed in the organic portions of plastic-impregnated algal mats, suggesting that the blebs may be organic fragments derived from the mat community. In addition, a few blebs of similar size and shape but having a black, metallic appearance in reflected light were observed. Purdy (1963a) interprets black blebs in Bahamian faecal pellets as iron sulphide resulting from the interaction of hydrogen sulphide with iron. The metallic-appearing blebs in Baffin Bay algal micrite grains may have a similar origin; certainly hydrogen sulphide is present in abundance in the lower zones of the algal mats.

It should be noted that algal micrite grains do not always consist exclusively of cryptocrystalline calcium carbonate. Representatives of all of the grain types of the area are seen to be incorporated in algal micrite grains (Fig. 4A). Most of the smaller algal micrite grains and many of the larger aggregates, however, are devoid of these other, "accessory" grain types (Fig. 4B). Thus, algal micrite grains are basically composed of cryptocrystalline carbonate; and the shell fragments, quartz grains, ooids and coated grains which are often incorporated in them are not essential to the integrity of the grain. In this respect, algal micrite grains differ from Bahamian grapestone, which is defined by Purdy (1963a, p. 344) as ". . . cemented aggregates of skeletal and non-

FIG. 3A. Thins-section photomicrograph of an algal micrite grain which is obviously an aggregate of several pre-existing algal micrite grains. In this extremely thin section, it is apparent that the material which cements the original grains together is petrographically identical to the material of the grain themselves. Plane polarized light, ×200. B. Same as Fig. 3-A, but between crossed nicols. Note the pore spaces (black) and the irregular surface of the grain. ×200. C. Thin-section photomicrograph of a large algal micrite grain. Note the elongate, flattened shape and porous interior of this aggregate grain. Note also the numerous opaque blebs, interpreted mainly as organic matter derived from the algal mat community. Plane polarized light, ×160.

SEP-11-2002 11:35 Linda Hall Library 816 926 8785 P.08

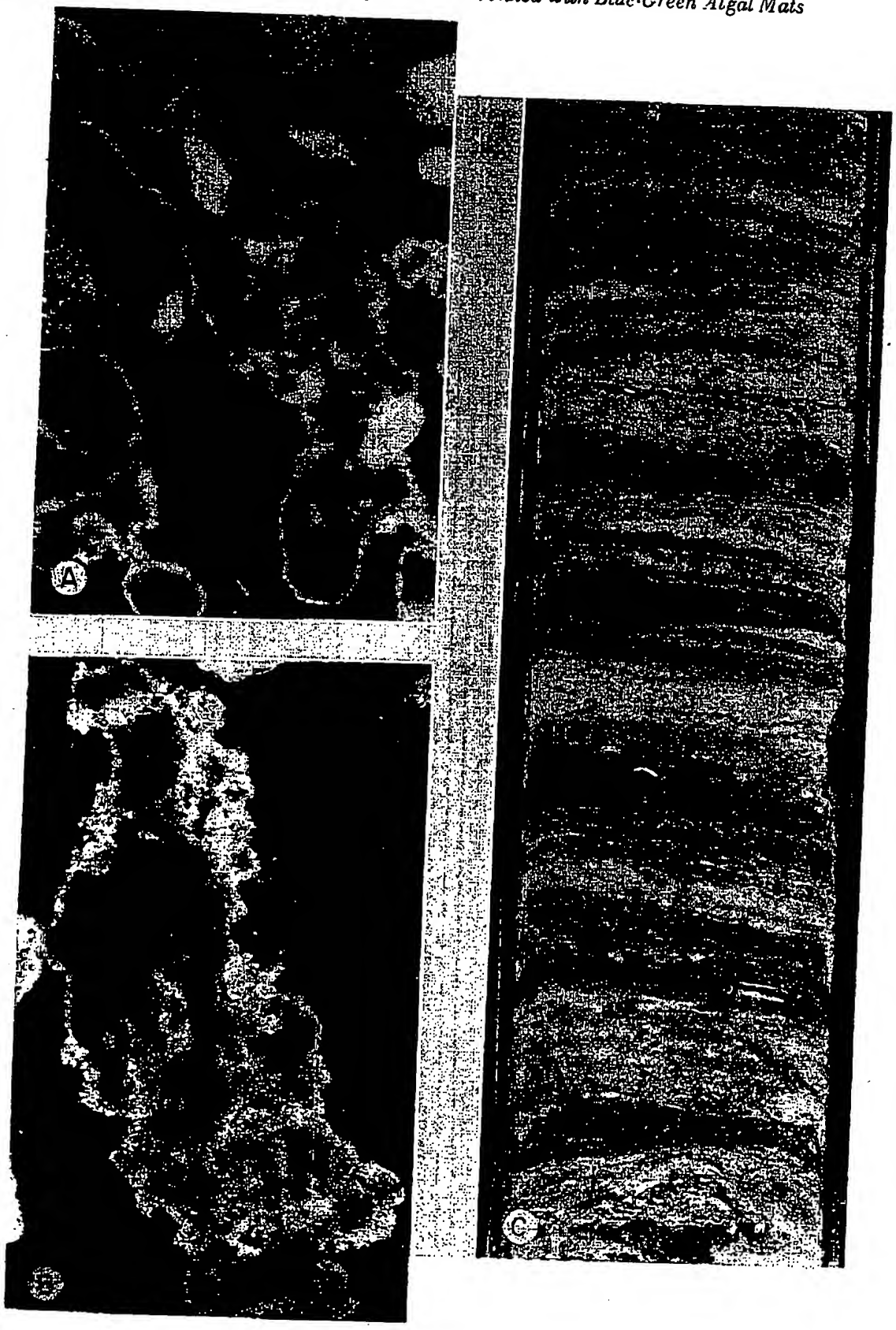

SEP-11-2002 11:35 Linda Hall Library 816 926 8785 P.09

skeletal grains in which the carbonate cement is restricted largely to the aggregates's periphery."

Distribution of Algal Micrite Grains

The distribution of the various grain types comprising the coarse fraction (larger than one-eighth millimeter) of the Baffin Bay sediments was determined by point-count analysis of 200 thin-sections prepared from plastic-impregnated sediment samples. The most outstanding characteristic of the distribution of algal micrite grains was found to be the coincidence of high volume percentages of these grains with observed algal mat development. In view of this apparent association, it is instructive to consider the influence which the Baffin Bay mats exert on sedimentation.

Sediments of Algal Mats

The fur-like surface of living algal mat is composed of minute algal filaments which extend a short distance up into the overlying water. These filaments carry mucilaginous sheaths (Ginsberg, 1960) which, combined with the intertwining nature of the filaments, enables the mat to trap or fix sediment particles that come in contact with it. As the filaments have motility and positive phototropism in moderate light (Sorensen and Conover, 1962), they are able to move up through a continuous layer of sediment recently deposited on them and re-establish a new surface mat (Ginsburg, 1960). Thus, alternation of sedimentation with algal growth and entrapment results in a laminated sediment (Fig. 4C). The first well-documented report relating laminated sediments such as these to the "stromatolites" commonly found in ancient rocks was Black's (1933) investigation of the algal-laminated sediments of the Bahama Islands. Black and later Ginsburg (1960) and Logan (1961) have related the growth forms of modern stromatolites to their various ancient counterparts. In addition, Logan et al. (1962) have recently completed an exhaustive classification of stromatolites, together with an interpretation of their environmental significance.

Several stromatolite samples from the Baffin Bay area were allowed to dry and then were impregnated under a partial vacuum with a polyester resin. Thin section photomicrographs of these impregnations are illustrated in Figs. 5 through 7. These photographs show that nearly every grain size and grain type found in the Baffin Bay area is incorporated into the stromatolite. In general, algal-rich laminae alternate with sediment-rich laminae, indicating either periodicity of algal growth, periodicity of sedimentation, or most likely, a combination of both. Certainly the sediment supply must fluctuate with changing water level, agitation, and turbidity; and the algal growth, or at least the rate of growth, may be varied by seasonal or other ecological factors, as well as by the rate of sedimentation itself.

The stromatolites of the Baffin Bay complex are completely non-indurated. Logan

---

Fig. 4A. Thin-section photomicrograph of an algal micrite grain, showing several detrital quartz grains (white) included in the large, aggregate algal micrite grain. Crossed nicols, ×100. B. Thin-section photomicrograph of a large, complex algal micrite grain composed exclusively of algal micrite. Note the pore spaces (black) and the flattened shape of this rather typical grain. Crossed nicols. ×125. C. Reflected light photograph of a short core of stromatolitic sediment. The lighter-colored layers are composed largely of quartz sand, while the darker layers contain more terrigenous clay and the compressed remains of algal mats. ×1.2.

SEP-11-2002 11:36 Linda Hall Library 816 926 8785 P.10

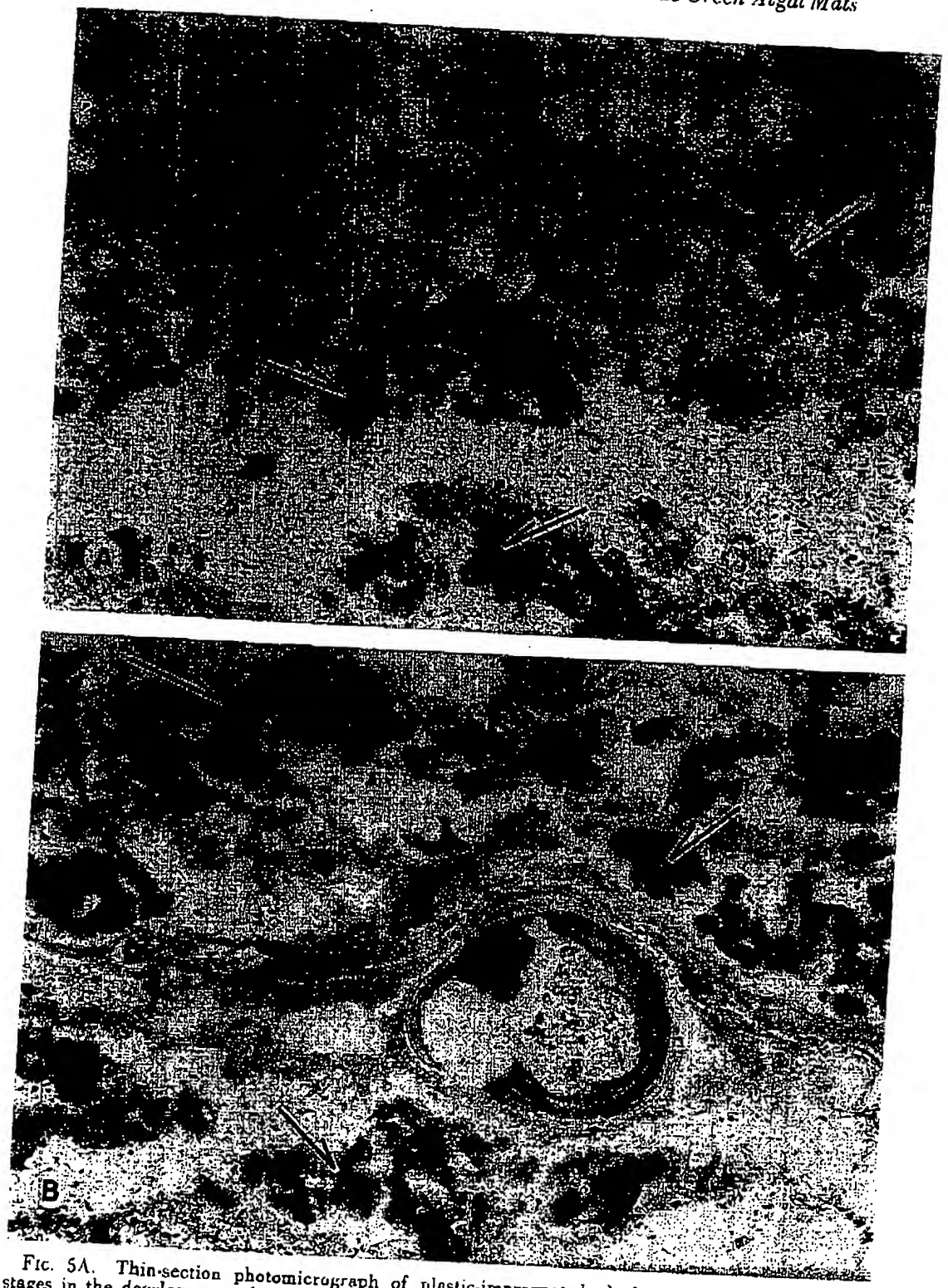

FIG. 5A. Thin-section photomicrograph of plastic-impregnated algal mat, illustrating the first stages in the development of algal micrite grains. At this stage, the algal micrite is difficult to distinguish from the organic material of the mat itself. Arrows point to more obvious areas of algal micrite development. Note the abundant opaque organic fragments within the mat. The large white areas are gaps caused by shrinkage during drying and impregnation. Plane polarized light, ×120. B. Thin-section of mat showing a more advanced stage of algal micrite formation. Distinct micrite grains (arrows) occur among mat laminae. Note the enclosed ooid. Plane polarized light, ×120.

SEP-11-2002 11:36 Linda Hall Library 816 926 8785 P.11

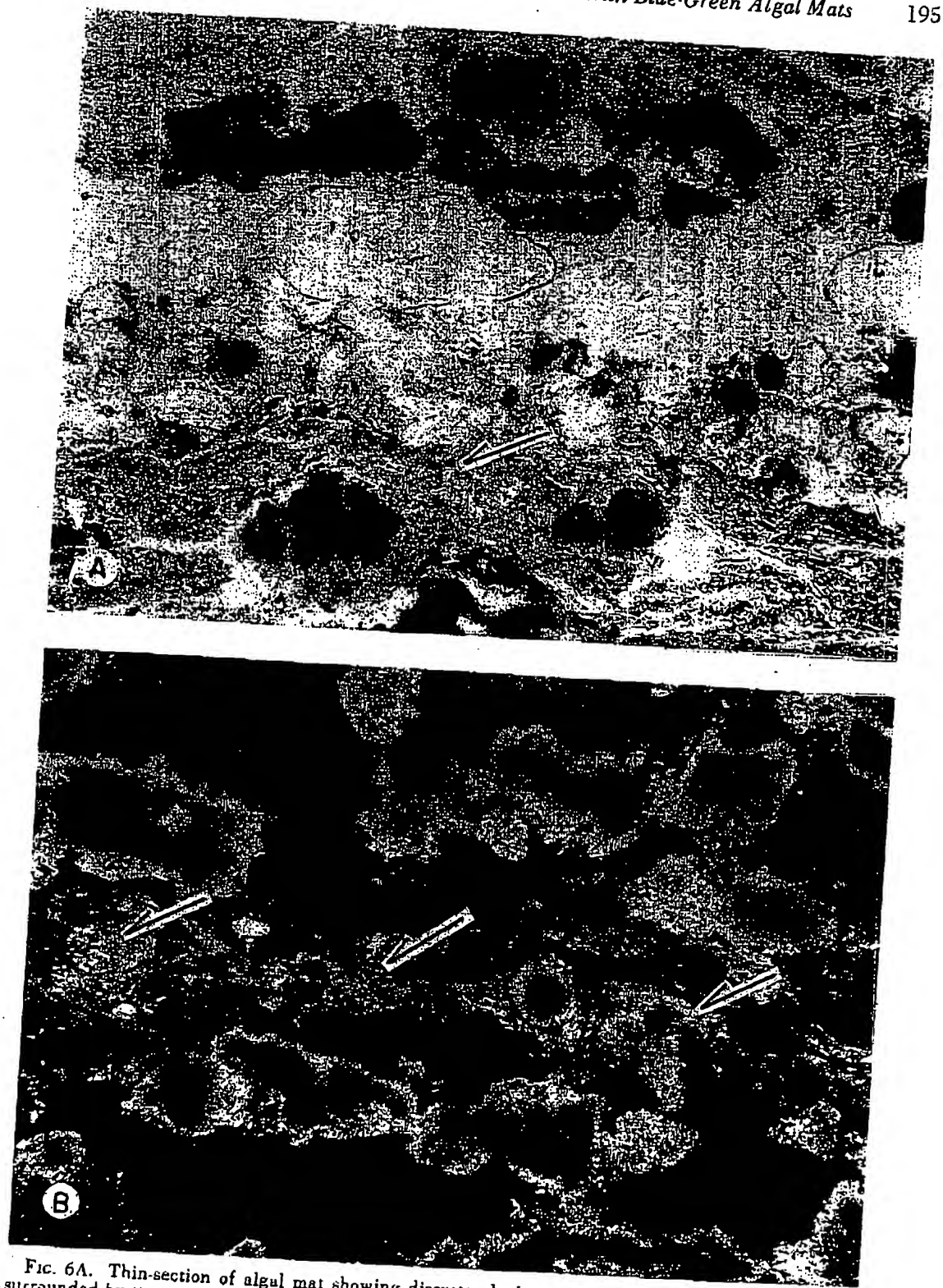

FIG. 6A. Thin-section of algal mat showing discrete algal micrite grains (dark) at two horizons, surrounded by the organic material of the mat (arrow). Plane polarized light, ×140. B. Thin-section of algal mat showing well-developed algal micrite grains within the mat. Note the birefringence of the organic material of the mat (arrows) between crossed nicols. This bright-yellow birefringence is very characteristic, as is the tendency for a given mat lamina to go to extinction as a unit. The black area is pore space resulting from shrinkage of the mat during drying. Crossed nicols, ×120.

SEP-11-2002 11:36 Linda Hall Library 816 926 8785 P.12

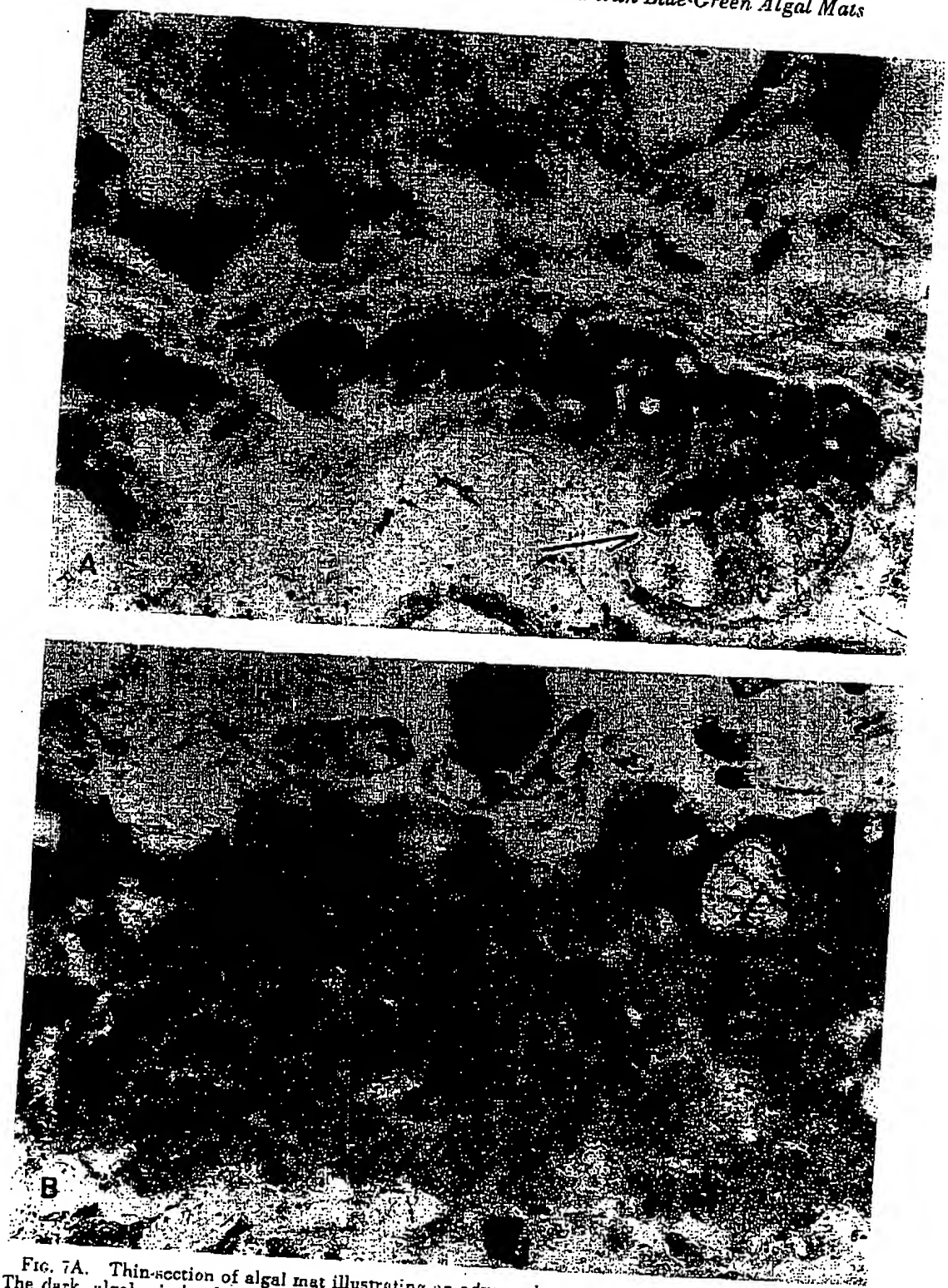

FIG. 7A. Thin-section of algal mat illustrating an advanced stage in the formation of algal micrite. The dark, algal micrite forms a nearly continuous layer across the area of the photograph. Note the partially enclosed foraminifera (arrow). Plane polarizzed light, × 120. B. Thin-section of algal mat showing that the formation of algal micrite has produced a thick, continuous layer of microcrystalline aragonite. Plane polarized light, ×120.

SEP-11-2002 11:37 Linda Hall Library 816 926 8785 P.13

(1961) reported that the discrete, club-shaped or domed algal heads of Shark Bay, Australia, were lithified to varying degrees by a process which he believed to be the usual intertidal precipitation of aragonite. Presumably the process is similar to the formation of beachrock, in which induration is effected by the growth of acicular aragonite crystals into the pore spaces of the rock (Ginsburg, 1953). The acicular crystals have not been observed in the Baffin Bay stromatolites, although they have been reported by Rusnak (1960a) from beachrock in the Baffin Bay area.

Instead, calcium carbonate precipitation of another type is associated with the mats. The grain type resulting from this precipitation has been referred to previously as algal micrite. The origin of algal micrite is of some interest, as this grain type apparently has not been previously described in the literature. Several possible modes of origin will be discussed.

Discussion of the Origin of Algal Micrite

Algal micrite grains certainly do not originate as simple agglomerates of mud, because the mud fraction of Baffin Bay sediments generally contains less than ten percent calcium carbonate (see also Rusnak, 1960a and b), and algal micrite grains contain approximately fifty percent calcium carbonate. Furthermore, algal micrite grains contain little if any terrigenous mud. The non-carbonate portion of algal micrite grains is made up largely of incorporated quartz sand and mucilaginous organic material.

This lack of terrigenous clay in algal micrite grains also rules out the theory that the grains originated as the fecal material of mud-ingesting organisms, or as the fecal material of filter-feeding Lamellibranchs (Jørgensen, 1955). Organisms feeding directly on the organic matter of the mat itself, however, conceivably could produce fecal material essentially devoid of terrigenous clay. Aside from the small clams, *Mulinia lateralis* and *Anomalocardia cuniemeris*, the only macro-invertebrate found in the vicinity of the Baffin Bay mats was a small, red, unidentified worm. This worm was observed only rarely; consequently it seems highly unlikely that its feces could account for the large amounts of algal micrite present in many of the mats. Perhaps the most cogent argument against the theory that algal micrite grains are cemented equivalents of invertebrate fecal material is the observation that the highest abundances of algal micrite grains are found in those stromatolites which are the most regularly laminated, and hence non-burrowed. This indicates that a feces-producing vagile infauna was essentially absent from the algal mat areas when the formation of algal micrite was especially prevalent.

The possibility remains that algal micrite grain formation may be dependent in some way on intertidal exposure. Logan (1961) found that the stromatolites of Shark Bay, Australia, were lithified in the intertidal zone by interstitial precipitation of acicular aragonite in a process similar to the formation of beachrock. The algal micrite of Baffin Bay, however, is decidedly not acicular; therefore it is judged not to be the equivalent of the cement of Shark Bay stromatolites. Inasmuch as the living algal mats of the Baffin Bay complex are restricted to areas where intermittent intertidal exposure is likely to occur, and assuming that algal micrite forms only in association with the mat, the possibility that intertidal exposure is necessary for the formation of algal micrite cannot be entirely negated. Indeed, it seems reasonable that periods of exposure would

SEP-11-2002 11:37 Linda Hall Library 816 926 8785 P.14

allow evaporation to increase the salinity of the water within the mat complex, thus increasing the solubility product and encouraging precipitation.

In considering the possible mode of origin of algal micrite grains, one obvious possibility remains to be considered; namely, that the carbonate is the result of direct precipitation from sea water. Illing (1954) described the cement of Bahamian grapestone as consisting of ". . . finely divided aragonite of varying texture . . . composed of aggregated particles of mud dimensions. From its occurrence, it is clear that it is being precipitated from sea water, yet the particles show no recognizable crystalline shape, and are similar to the material that forms the matrix of the grains themselves" (Illing, 1954, p. 30). In essence, then, Illing finds evidence for the direct precipitation of microcrystalline aragonite from sea water.

The close association of algal micrite grains with well-developed algal mats strongly suggests that the mat or the mat environment in some way influences the formation of the grains. This influence could take a number of forms. For example, the photosynthetic activity of the algae in the upper zones of the mats might initiate calcium carbonate precipitation by extracting carbon dioxide from the water in the immediate vicinity. Eardley (1938) cites this process as one of the causes of precipitation of calcium and magnesium carbonates in the unicellular algal bioherms of Great Salt Lake, Utah. If a similar process is active in the Baffin Bay mats, however, one might expect the precipitated carbonate to occur as crusts around the algal filaments, or to fall as a "rain" of fine crystals on the surface of the mat. Neither of these modes of occurrence was observed in the Baffin Bay mats. Because of the many possible catalytic effects within the mat, however, intuitive expectations as to the form of calcium carbonate precipitation induced by photosynthetic activity are not sufficient to entirely disregard this hypothesis.

Alternatively, decomposition of the abundant organic material in the mats by ammonifying bacteria could result in the production of ammonia and the precipitation of calcium carbonate in the manner described by Purdy (1963b, p. 486).

$$NH_3 + H_2O = NH_4OH \tag{1}$$

$$2NH_4(OH) + Ca(HCO_3)_2 = (NH_4)_2CO_3 + 2H_2O + CaCO_3 \tag{2}$$

Purdy cites this or similar reactions as responsible for the aragonite cement of grapestone, fecal pellets and mud aggregates in Bahamian sediments. Of course, this anaerobic bacterial action would take place only in a reducing environment, but the black, oderiferous character of the lower layers of the algal mats indicates that reducing conditions prevail therein (see also Rusnak, 1960a and b). The presence of a reducing environment in the mat is substantiated by the work of Sorensen and Conover (1962, p. 69) who describe a zone of hydrogen sulphide with ". . . an autotrophic purple bacterium . . . and bacteria including *Beggiota* sp." in their zone E, four to ten millimeters below the surface of the algal mats of the Laguna Madre area.

Algal micrite precipitation induced by organic decay might also account for the intimate interrelationship of algal micrite grains to the organic portion of the mat. As seen in thin sections of plastic-impregnated stromatolites, the algal micrite appears to be in a sense "replacing" the original algal material. For example, all gradations can be seen from pure organic mat, through finely-divided mixtures of mat and micrite, to typical algal micrite grains (Figs. 5 through 7). If micrite precipitation is induced by bacterial destruction of the mat, then such a relationship would be expected.

In addition, the discrete nature of individual, globular grains of algal micrite seen

SEP-11-2002 11:37 Linda Hall Library 816 926 8785 P.15

between many algal laminae could be accounted for by precipitation indirectly induced by organic decay. Because a given layer of organic matter in the lower, reducing zones of an algal mat is probably not a homogeneous body, but rather a complex mixture of various types of organic debris, one might expect such a layer to be attacked by bacteria, not evenly and regularly throughout the layer, but preferentially at loci most suitable for bacterial activity. The discreteness of these loci might even be emphasized by rapid reproduction of the bacteria in these initially more favorable micro-environments. As the organic matter in these favorable areas is consumed and "replaced" by algal micrite, the sites of most active bacterial activity would move through the organic layer, enlarging and combining the initially formed grains and resulting in the aggregate texture commonly seen in the large grains. Confinement of this activity to a given layer or layers within the mat would produce the flattened shape so often observed in the larger aggregates. The ultimate result would be an essentially continuous micrite replica of the original layer.

The factors which determine the location of the postulated centers of micrite deposition are unknown, although it may be that certain types of organic material are more favorable than others for bacterial colonization.

Summary

In summary, several hypotheses for the genesis of algal micrite grains have been considered in light of observations made on the nature and occurrence of these grains in the Baffin Bay area and on similar grains in other areas. Although present information does not permit an unequivocal statement as to the exact genesis of these grains, the following interpretation best accounts for the observed facts. The micrite is precipitated as microcrystalline aragonite directly from super-saturated sea water in association with algal mats. The specific chemical reaction is unknown, but inducement of precipitation by anaerobic bacteria involved in the decomposition of the mat's organic matter may be involved. Thus the precipitation may take place in the lower, reducing zones of the mat. Discrete loci of initial micrite precipitation may be related to more favorable areas for bacterial colonization.

Literature Cited

Black, M., 1933. The algal sediments of Andros Island, Bahamas. Phil. Trans. R. Soc., Series B, V. 122, p. 165–192.

Dalrymple, D. W., 1964. Recent sedimentary facies of Baffin Bay, Texas. Unpublished Ph.D. dissertation, Rice University, Houston, Texas, 192 p.

Eardley, A. J. 1938. Sediments of Great Salt Lake, Utah. Bull. Am. Ass. Petrol. Geol., V. 22, no. 10, p. 1305–1411.

Fisk, H. N., 1959. Padre Island and the Laguna Madre Flats, coastal south Texas, 2d Coastal Geography Conf., Coastal Studies Institute, Louisiana State Univ., Baton Rouge, La. p. 103–152.

Folk, R. L. 1959. Practical petrographic classification of limestones. Bull. Am. Ass. Petrol. Geol., V, 43, no. 1, p. 1–38.

Ginsburg, R. N. 1953. Beachrock in south Florida. J. Sedim. Petrol., v. 23, no. 2, p. 85–92.

———. 1960. Ancient analogues of Recent stromatolites: Int. geol. Congr., XXI Session, Norden, 1960, part XXII. Int. Paleont. Union, Copenhagen, 1960.

Illing, L. V. 1954. Bahamian calcareous sands. Bull. Am. Ass. Petrol. Geol., V. 38. p. 1–95.

Jørgensen, C. B. 1955. Quantitative aspects of filter feeding in invertebrates. Biol. Rev., V. 30, p. 39–54.

SEP-11-2002 11:38 Linda Hall Library 816 926 8785 P.16

Logan, B. W. 1961. Cryptozoon and associate stromatolites from the Recent, Shark Bay, Western Australia. J. Geol., V. 69, no. 5, p. 517–533.

———, R. Rezak, and R. N. Ginsburg, 1962. Classification and environmental significance of stromatolites. Publ. Dep. Oceanogr. Agric. Mech. Univ. Tex., May, 1962.

Purdy, E. G. 1963a. Recent calcium carbonate facies of the Great Bahama Bank 1. Petrography and reaction groups. J. Geol., V. 71, no. 3, p. 334–355.

———. 1963b. Recent calcium carbonate facies of the Great Bahama Bank 2. Sedimentary facies. J. Geol., V. 71, no. 4, p. 472–497.

Rusnak, G. A. 1960a. Sediments of Laguna Madre, Texas, *in* Recent Sediments, Northwest Gulf of Mexico. Am. Ass. Petrol. Geol., Tulsa, Okla., p. 153–196.

———. 1960b. Some observations of Recent oolites. J. Sedim. Petrol., V. 30, no. 3, p. 471–480.

Sorensen, L. O., and J. T. Conover. 1962. Algal mat communities of *Lyngba confervoides* (C. Agardh) Gomont. Publs. Inst. mar. Sci. Univ. Tex., V. 8, p. 61–74.

TOTAL P.16

STIC-ILL

9/10

41619

Fr m: Marx, Irene
Sent: Tuesday, September 10, 2002 9:19 AM
To: STIC-ILL
Subject: 09/777664

Importance: High

Please send to Irene Marx, Art Unit 1651; CM1, Room 10E05, phone 308-2922, Mail box in 11B01

Observations on the ionic composition of blue-green algae growing in saline lagoons
AU Pillai, V. K.
SO Proc. Natl. Inst. Sci. India, (19550000) vol. 21, no. 2, pp. 90-102.
DT Journal

Dalrymple, D.W., 1965, "Calcium carbonate deposition associated with blue green algal mats, Baffin Bay.:, Texas: Institute of Marine Science Publication 10, p. 187-200

Black, M., 1933, "The algal sedimentation... ", Royal Society of London Philosphical transactions, Ser. B, V. 222, p. 165-192

Lowenstam HA (1981), Science, 211:1126-1131

Ferris et al., Earth Sci., 47:233-250 (1993)

Ferris et al., Appl. and Environm. Microbiol.,1989, 55:1249-1257

Kazmierczak et al., (1990), Science, 250:1244-1248

Kempe et al., Facies, 28:1-32, 1993.

Kempe et al., 1994, Bull, Inst. Oceanogr., Monaco no. spec., 13:61-117.

Merz, M.U.E, 1992, Facies, 26:81-102

Pentecost et al., 1986, Calcification in cyanobacteria, In "Biomineralization of Lower plants and animals (Leadbeater et a., ed. 73-90, Clarendon Press, Oxford.

Riding, R., 1982, Nature, 299:814-815

Thompson eta., 1990, Geology, 18:995-998

Irene Marx
Art Unit 1651
CMI 10-E-05,
Mail Box 11-B-01
703-308-2922

COMPLETED

LHC
9/10

ALOG(R)File 28:Oceanic Abst.
(c) 2002 Cambridge Scientific Abstracts. All rts. reserv.

1551677 95-01677
The role of alkalinity in the evolution of ocean chemistry, organization of living systems, and biocalcification processes
Kempe, S.; Kazmierczak, J.; Doumenge, F.; Allemand, D.; Toulemont A. (eds.)
Geol.-Paleontol. Inst., T.H. Darmstadt, Schnittspahnstr. 9, D-64287 Darmstadt, FRG
Past and Present Biomineralization Processes. Considerations about the Carbonate Cycle. IUCN-COE Workshop Monaco (Monaco) 15-16 Nov 1993
PAST AND PRESENT BIOMINERALIZATION PROCESSES. CONSIDERATIONS ABOUT THE CARBONATE CYCLE. IUCN-COE WORKSHOP, MONACO (MONACO), 15-16 NOVEMBER 1993 pp. 61-117, 1994
BULL. INST. OCEANOGR. MONACO
MUSEE OCEANOGRAPHIQUE, MONACO (MONACO)
SUMMARY LANGUAGE - ENGLISH, SPANISH, FRENCH
Languages: ENGLISH

-more-

?
Display 2/9/1 (Item 1 from file: 28)
DIALOG(R)File 28:Oceanic Abst.
(c) 2002 Cambridge Scientific Abstracts. All rts. reserv.
Journal Announcement: V32N2
We have investigated present-day alkaline environments and studied carbonates formed under these conditions. The crater lake of Satonda Island/Indonesia contains seawater which has become slightly more alkaline than average seawater due to the operation of the alkalintiy pump in its deeper parts (the lake is reducing below 22 m) (Kempe and Kazmierczak, 1990b, 1993). The increased alkalinity and pH and the increased calcite and aragonite supersaturations enabled the formation of reefs composed in part of in vivo permineralizing with high Mg-calcite cyanobacterial mats (Kazmierczak and Kempe, 1990, 1992). These are the first in vivo calcifying recent microbialites reported from a modern marine setting (the other modern marine microbialites grow mainly by trapping sediment particles on the mat surface). In a sense, Satonda provides us with a recreation of ancient ocean conditions, when abundant in situ calcifying microbialites (stromatolites and thrombolites) occurred. In Lake Van, Anatolia, Turkey, the largest soda lake on Earth, we found columns of microbial tufa up to 40 m high (Kempe et al., 1991). These form at places where ground water with

-more-

?
Display 2/9/1 (Item 1 from file: 28)
DIALOG(R)File 28:Oceanic Abst.
(c) 2002 Cambridge Scientific Abstracts. All rts. reserv.
high Ca concentrations mixes with the very alkaline lake water (150 meq/l, pH 9.7). The inorganically precipitated mineral phase is calcite which provides a hard ground for coccoid cyanobacterial mats which in turn permineralize with aragonite. The mats stabilize the columns and form a thick outer crust. Theses examples illustrate that Precambrian and Phanerozoic marine calcareous microbialites can best be explained as having formed in an alkaline environment, highly supersaturated with respect to carbonate minerals.
Descriptors: alkalinity; seawater evolution; lakes; chemical limnology; calcification; chemical oceanography; paleoceanography; Precambrian; Phanerozoic; mineralization; microorganisms; fossil sea water; relict lakes ; algal mats; Cyanophyta; Indonesia, Satonda I.; Turkey, Anatolia, Van L.

- end of display -

SEP-11-2002 11:10 LINDA HALL LIBRARYL 816 926 8785 P.03

NOTICE: This material may be protected
by copyright law (Title 17, U.S. Code)

The Role of Alkalinity in the Evolution of Ocean Chemistry, Organization of Living Systems, and Biocalcification Processes

by

Stephan KEMPE [1] and Józef KAŹMIERCZAK [2]

[1] *Geological-Paleontological Institut, T.H. Darmstadt, Schnittspahnstrasse 9, D-64287 Darmstadt, Fed. Rep. Germany;*
[2] *Institute of Paleobiology, Polish Academy of Sciences, Al. Zwirki i Wigury 93, PL-02089 Warszawa, Poland.*

ABSTRACT

The present ocean has an alkalinity ranging from 2.1 to 2.5 meq/l. We suggest that changes in seawater alkalinity (associated with changes in TCO_2, pH and Ca concentration) were a major driving force for the biological evolution, the onset of biocalcification and changes in the pattern of carbonate sedimentation observed throughout Earth's history.

Thermodynamic, mass-balance and kinetic arguments suggest that the Precambrian ocean had a very high alkalinity, similar to the chemistry of modern Soda Lakes (Soda Ocean Hypothesis) (KEMPE and DEGENS, 1985; KEMPE *et al.*, 1989). This high alkalinity must have arisen shortly after the establishment of the first oceans due to the weathering of the early komatiitic crust in the presence of water and carbonic acid (Urey reaction). In the Proterozoic ocean this alkalinity and the associated sodium were slowly extracted by pore water subduction, the consequential formation of albite in the granodioritic crust, the formation of long-lived carbonate deposits and the increase of the sedimentary organic carbon reservoir. Due to decreasing alkalinity, the concentration of the free Ca ion could rise from below 10^{-5} M to 10^{-3} M causing a strong Ca stress for the biota. During that time, the ocean has been highly supersaturated with respect to most carbonate minerals, allowing inorganic and microbially mediated precipitation of Ca and Mg carbonates in places where Ca and Mg were introduced to the ocean (submarine springs, riverine and ground water inputs).

With the increase of oxygen and the oxidation of the reduced sulfur pool to form sulfate in the ocean, a second mechanism modulating seawater alkalinity appeared: sulfate reduction in stagnant oceanic basins (KEMPE, 1990). As exemplified in the

SEP-11-2002 11:10 LINDA HALL LIBRARYL 816 926 8785 P.04

Black Sea today, these basins could function as alkalinity pumps: during the oxidation of sinking organic carbon sulfate is reduced and its negative charge is substituted by bicarbonate ions, increasing the alkalinity in proportion to the lost sulfate. Slow upwelling, eddy diffusion or overturn furnish excess alkalinity to the ocean causing local, regional, or global supersaturation events promoting increased $CaCO_3$ formation. Negative excursions in the $\delta^{13}C$ record noticed in carbonate sequences are interpreted to mark such events of excess alkalinity in Earth history.

In order to substantiate these hypotheses, we have investigated present-day alkaline environments and studied carbonates formed under these conditions. The crater lake of Satonda Island/Indonesia contains seawater which has become slightly more alkaline than average seawater due to the operation of the alkalinity pump in its deeper parts (the lake is reducing below 22 m) (KEMPE and KAZMIERCZAK, 1990b, 1993). The increased alkalinity and pH and the increased calcite and aragonite supersaturations enabled the formation of reefs composed in part of in vivo permineralizing with high Mg-calcite cyanobacterial mats (KAZMIERCZAK and KEMPE, 1990, 1992). These are the first in vivo calcifying recent microbialites reported from a modern marine setting (the other modern marine microbialites grow mainly by trapping sediment particles on the mat surface). In a sense, Satonda provides us with a recreation of ancient ocean conditions, when abundant in situ calcifying microbialites (stromatolites and thrombolites) occurred.

In Lake Van/Anatolia, the largest soda lake on Earth, we found columns of microbial tufa up to 40 m high (KEMPE *et al.*, 1991). These form at places where ground water with high Ca concentrations mixes with the very alkaline lake water (150 meq/l, pH 9.7). The inorganically precipitated mineral phase is calcite which provides a hard ground for coccoid cyanobacterial mats which in turn permineralize with aragonite. The mats stabilize the columns and form a thick outer crust.

Theses examples illustrate that Precambrian and Phanerozoic marine calcareous microbialites can best be explained as having formed in an alkaline environment, highly supersaturated with respect to carbonate minerals.

Le rôle de l'alcalinité dans l'évolution chimique de l'océan, l'organisation des systèmes vivants, et les mécanismes de la biocalcification

RÉSUMÉ

L'alcalinité actuelle des océans varie de 2.1 à 2.5 meq/l. Nous suggérons que les changements d'alcalinité des océans, associés aux variations de TCO_2, de pH et de concentration en ions Ca, ont été une force d'induction pour l'évolution biologique dans l'histoire du globe, et qu'ils ont dû déterminer le début de la biocalcification et les modifications de dépôt des sédiments carbonatés au cours des temps géologiques.

Des arguments thermodynamiques et cinétiques et les bilans de masse semblent montrer que l'océan Précambrien présentait une alcalinité très élevée, similaire à celle des "lacs alcalins" actuels (soda ocean hypothesis). Cette alcalinité élevée est vraisemblablement apparue juste après la formation des premiers océans et a résulté de l'altération de la première croûte "komatiitic" par des eaux riches en acide carbonique (réaction d'Urey). Dans l'océan Protérozoique, l'alcalinité diminue, le sodium est lentement extrait par la subduction de l'eau interstitielle, avec pour conséquence la formation d'albite dans la croûte granodioritique, la formation des dépôts anciens de carbonates, et l'augmentation du réservoir de carbone organique sédimentaire. La diminution de l'alcalinité permettait une augmentation de la concentration en ions libres Ca de 10^{-5} M à 10^{-3} M, provoquant un stress calcique aux organismes vivants. Cet océan était fortement sursaturé en la plupart des minéraux carbonatés, favorisant ainsi la précipitation inorganique ou d'origine microbienne de carbonates de Ca et de Mg dans des sites où le Ca et le Mg arrivaient à l'océan (sources sous-marines, arrivées d'eaux souterraines ou de rivières).

Avec l
allait form
l'alcalinité
stagnants (
peuvent fo
organique
négative e
proportion
d'autres dé
précipitatic
carbonatée
dans l'histo

Dans l
alcalins ac
Satonda e
conséquen
de l'alcalin
de récifs c
(KAZMIER
calcifiants
surtout en
constitue a
trouvaien
thrombolit
nous avons
al., 1991),
alcalines d
fournit un
s'enrichisse
croûte épai
d'origine m
du Précamb
ayant les m
carbonatés.

Avec l'augmentation de l'oxygène, l'oxydation du réservoir de soufre réduit allait former les sulfates des océans, créant ainsi un second mécanisme modulant l'alcalinité de l'eau de mer : la réduction des sulfates dans des bassins océaniques stagnants (KEMPE, 1990). L'exemple actuel de la mer Noire montre que ces bassins peuvent fonctionner comme des pompes alcalines : pendant l'oxydation du carbone organique lors de sa chute vers le fond, les sulfates sont réduits et leur charge négative est remplacée par les ions bicarbonates, ce qui augmente l'alcalinité proportionnellement au sulfate éliminé. A l'occasion de lentes remontées d'eaux ou d'autres déplacements, des sursaturations se produisent dans l'océan, entraînant des précipitations de calcaire. Les écarts négatifs des mesures de $\delta^{13}C$ dans les séquences carbonatées sont interprétés comme des témoins de ces épisodes d'excès d'alcalinité dans l'histoire du globe.

Dans le but de confirmer ces hypothèses nous avons étudié, dans les milieux alcalins actuels, les carbonates formés dans ces conditions. Le lac de cratère de Satonda en Indonésie est légèrement plus alcalin que l'eau de mer normale, conséquence du phénomène de pompe alcaline près du fond. L'augmentation du pH, de l'alcalinité et de la sursaturation en calcite et en aragonite a permis la formation de récifs composés en partie de tapis cyanobactériens riches en calcite magnésienne (KAZMIERCZAK and KEMPE, 1990, 1992). Ce sont les premiers microbialites calcifiants récents signalés en situation marine actuelle; les autres se développent surtout en piégeant les particules de sédiment à la surface des tapis. Satonda constitue ainsi un modèle recréant les conditions de l'océan primitif, dans lequel se trouvaient en abondance des microbialites calcifiants (stromatolithes et thrombolithes). Dans le lac de Van en Anatolie, le plus grand lac alcalin de la terre, nous avons trouvé des colonnes de tuf microbien de plus de 40 m de haut (KEMPE *et al.*, 1991), qui se forment là où les eaux souterraines se mélangent aux eaux très alcalines du lac (150 meq/l, pH 9.7). La phase minérale précipitée, de la calcite, fournit un substrat dur pour les tapis de coccoïdes cyanobactériens qui, à leur tour, s'enrichissent en aragonite. Les tapis consolident les colonnes qu'ils revêtent d'une croûte épaisse. Ces deux exemples de genèse actuelle de revêtements calcaires d'origine microbienne permettent de supposer que les microbialites marins calcaires du Précambrien et du Phanérozoïque se sont développés dans des bassins océaniques ayant les mêmes caractéristiques chimiques : milieu alcalin sursaturé en minéraux carbonatés.

CONTENTS

SEP-11-2002 11:11 LINDA HALL LIBRARYL 816 926 8785 P.06

PROLOGUE 1 (the scientist)

"If the Earth was populated with life so soon after it had been meteoritically sterilized, why did three billion years then go by before fossils of creatures with differently specialized cells began appearing in the fossil record, whereupon there was a huge explosion of diversity? That objection can be met in two ways. First, there was a lot going on. Single-celled organisms can be as complicated as jellyfish, slime moulds and fungi. as someone put it... "they had to learn all that chemistry". But who in any case, says that the acquisition of the biochemical machinery of differentiation and sexual reproduction, the origin of biodiversity, would have been child's play?" (John Maddox, 1994. — Origin of life by careful reading. — *Nature*, 367, p. 409).

PROLOGUE 2 (the novelist)

"Wouldn't intelligence arise again and again?" Barnes said. "Well it barely arose on the Earth" Beth said. "The Earth is 4.5 billion years old, and single-celled life appeared 3.9 billion years ago – almost immediately, geologically speaking. But life remained single-celled for the next three billion years. Then in the Cambrian period ... there was an explosion of sophisticated life forms. Within a hundred million years, the ocean was full of fish. Then the land became populated. Then the air. But nobody knows why the explosion occurred in the first place. And since it didn't occur for three billion years, there's the possibility that on some other planet, it might never occur at all." (Michael Crichton, 1987. — Sphere. — Ballentine Books).

1. INTRODUCTION

Physicists search for the grand unification theory, a sort of world formula describing the physical principals of macro- and microcosms. Geochemists strive to uncover the driving forces behind biogenesis and evolution. Panspermia is only an option if shown beyond doubt that biogenesis was not possible on Earth. Until then, the most plausible assumption is that life originated in the early ocean of Earth, shortly after accretion. The $\delta^{13}C$ signature of the organic carbon preserved in the Isua formation, Greenland, already carries the clear signal of photosynthetic fractionation, 3.8 Ga (giga anni = 10^9 years) before present (SCHIDLOWSKI *et al.*, 1979). The biochemical reactions which we call "life" must have evolved during the first 0.7 Ga of Earth history. This is the Hadean era of which we do not have any preserved record save for a couple of reworked zircon crystals dated to ca. 4.2 Ga (COMPSTON and PIDGEON, 1986). Any hypothesis regarding this part of Earth history must therefore always remain speculative. Nevertheless it should be possible to construct a plausible scenario of early Earth applying geochemical principals. Such a scenario can then be tested if it is compatible with the post-Isua rock record and with biochemical requirements for basic functions of life.

In this paper we present such a scenario which we think is both plausible and which offers geochemical causes for some of the major evolutionary events such as the onset of biocalcification which marks the beginning of the Phanerozoic 0.57 Ga ago.

We attempt to link recent achievements in geochemistry, paleoceanography and paleontology with results of biochemical, biomolecular and physiological experiments, particularly those concerned with the universal function of calcium in living systems. Central to our arguments is the

SEP-11-2002 11:12 LINDA HALL LIBRARYL 816 926 8785 P.07

hypothesis of an early alkaline (sodic) ocean (KEMPE and DEGENS, 1985), which calls for an initially very low Ca content in the seawater. Its subsequent, order-of-magnitude increase during the Precambrian, led to a hypothesis (KAŹMIERCZAK *et al.*, 1985), which explains the sudden onset of biocalcification and biophosphatization processes near the Precambrian/Cambrian boundary as a common Ca detoxification response of the marine biota. This concept expands an early idea of SIMKISS (1977) to a biohistoric time scale. It regards biocalcification as a means to remove the enormously cytotoxic Ca^{2+} ion from cells. Cytophysiologically and ecotoxicologically, Ca^{2+} can be compared with other biologically active metals. These can be essential or beneficial for cells at strictly defined (optimal) levels but are subtoxic or lethal at higher concentrations. Larger than required extracellular Ca concentrations may increase its influx into the cytoplasm and cause "calcium stress". This phenomenon may not only have initiated biocalcification but also controls the formation of (bio)carbonates throughout Earth history, governing the global carbon cycle. In addition, the calcium-evoked excessive extracellular secretion by planktonic algae regulates macrofloc formation and therefore the rate of vertical particle flux in the ocean (DEGENS *et al.*, 1985; DEGENS and ITTEKKOT, 1986).

Here we present arguments that these processes and their temporal and spatial fluctuations can be attributed to changes in seawater alkalinity – the most critical factor in natural waters controlling the acid-base equilibria and the dynamics of ionic exchange in living systems.

2. THE CARBONATE SYSTEM: A SYNOPSIS

Life processes involve the formation or destruction of high molecular weight organic matter, from or to inorganic carbon of very low molecular weight. Withdrawal or addition of inorganic carbon to water or air in contact with water alters the parameters of the carbonate system (a term used to signify all of the reactions involving anions of carbonic acid). Table I lists the most prominent natural processes which cause changes in the carbonate system. These changes are best described as changes in carbonate alkalinity and as changes of the total CO_2 concentration (TCO_2 or sum CO_2). Alkalinity is defined as the sum of the charges of all anions of weak acids and total alkalinity therefore includes not only the carbon-bearing species, HCO_3^- and CO_3^{2-}, but also borates and other ions of weak acids (mostly given in units of meq/kg or μeq/kg). TCO_2 in contrast is the molar sum of all the carbon bearing species (mostly given as mmol/kg or μmol/kg). Neglecting ion pairs the definitions read:

$$\text{Carbonate Alkalinity} = [HCO_3^-] + 2x[CO_3^{2-}]$$

$$TCO_2 = [HCO_3^-] + [CO_3^{2-}] + [CO_2] + [H_2CO_3]$$

Because the contribution of free CO_2 plus carbonic acid to TCO_2 is small in seawater, alkalinity is numerically the larger value of the two. In today's ocean, carbonate alkalinity averages 2.20 and 2.26 meq/kg and TCO_2 2.01 and 2.23 mmol/kg in surface and bottom waters, respectively (BROECKER and PENG, 1982). The differences between the bottom and surface waters arise from photosynthesis and calcite precipitation which occurs in the surface layer of the ocean, forming sinking organic and calcareous particles. While sinking, respiration and redissolution replenish the carbon and the associated nutrients to the lower water column.

TABLE I

Summary of processes changing alkalinity and TCO_2

Process	changes in alkalinity	changes in TCO_2
pCO_2 in air increases	no change	increase
pCO_2 in air decreases	no change	decrease
photosynthesis	slight increase	decrease
respiration	slight decrease	increase
$CaCO_3$ precipitation	decrease	decrease
$CaCO_3$ dissolution	increase	increase
sulfate reduction	increase	increase
sulfide oxidation	decrease	decrease
silicate weathering	increase	increase
silicate deposition	no change	no change

The fact that redissolution can occur in marine bottom waters shows that the saturation with respect to $CaCO_3$ minerals is transgressed somewhere in mid water. The ocean is supersaturated at the surface and undersaturated at the bottom with regard to both aragonite and calcite. To describe the state of saturation the product of the actual ion activities of Ca^{2+} and CO_3^{2-} is compared with the solubility product (K) of the mineral in question:

$$\text{Saturation index (SI)}_{\text{calcite}} = \log([Ca^{2+}] \times [CO_3^{2-}] / K_{\text{calcite}})$$

In this notation positive SI's signify supersaturation, zero is saturation, and negative values indicate undersaturation. Due to the increase of the CO_2 pressure (pCO_2) – caused by remineralization – with depth, the CO_3^{2-} concentration changes from 0.20 to 0.06 mmol/kg. At the same time the solubility product changes due to the increase of hydrostatic pressure. Both effects together – plus the effect of temperature decrease – diminish the $SI_{calcite}$ from between 0.4 to 0.6 in oceanic surface waters to zero at 4,500 m in the N-Atlantic to less than 1,000 m depth in the N-Pacific (e.g. BROECKER and PENG, 1982). In bottom waters the saturation index drops well below zero, i.e. into the undersaturated range.

It is interesting to note that no spontaneous inorganic $CaCO_3$ precipitation occurs in the present surface ocean even though it is substantially supersaturated with both aragonite and calcite. Spontaneous calcite precipitation apparently needs a supersaturation of at least SI = 0.8. SVENSSON (1992) found in laboratory experiments that at this apparent saturation noticeable calcite precipitation terminates. KEMPE and KAŹMIERCZAK (1990a) showed that the $SI_{calcite}$ was equal to or larger than 0.8 in a number of lakes sustaining growth of in situ calcifying cyanobacterial mats (cyanobacterial microbialites).

All marine carbonates precipitated today are formed predominantly by enzymatically controlled processes. This tends to keep the ocean from accumulating Ca^{2+} and CO_3^{2-} ions and keeps it below the threshold of $SI_{calcite} \leq 0.8$ where spontaneous precipitation would finally occur. It is on the other hand also readily understood that small changes in the carbonate ion concentration – and hence in alkalinity – can have a very large effect on the saturation state. In contrast, the same changes in the Ca concentration (as they occur during $CaCO_3$ dissolution) have only a small effect on the saturation index because the present ocean has a large Ca concentration (10 mmol/kg) compared to alkalinity.

The ther
between the
surface wate
this convect
sluggish the
time scales, l
by slow proc
sulfate reduc

Clearly, t
ocean, simpl
present to a
precursors of
– and is – tl
mobilizatior
conditions fo.

Under th
molecular o
differentiated
and a large ra
played the ma
on the miner
silicates with
(UREY, 1951).

kaoli

The react
released to w
minerals bein
thus leaving
concentration
to form today
proportion of
condition, [N
if sufficient t
and MACKEN
associated wi
produce sodiu

3. RIS

3.1 The "

These basi
and DEGENS,
low in alkalir
This scenario
an early Earth
HENDERSON-S
1987; CALDE
ocean than at
having Cl as t
MACKENZIE, I

nges in TCO_2
increase
decrease
decrease
increase
decrease
increase
increase
decrease
increase
no change

vaters shows that
ed somewhere in
undersaturated at
cribe the state of
CO_3^{2-} is compared

$\zeta_{calcite}$)

is saturation, and
ease of the CO_2
lepth, the CO_3^{2-}
e same time the
c pressure. Both
minish the $SI_{calcite}$
1,500 m in the N-
ECKER and PENG,
ow zero, i.e. into

CO_2 precipitation
ly supersaturated
tation apparently
1992) found in
oticeable calcite
showed that the
aining growth of
ites).
edominantly by
cean from accu-
d of $SI_{calcite} \leq 0.8$
n the other hand
on concentration
n the saturation
1 (as they occur
saturation index
. (10 mmol/kg)

1° spécial 13 (1994)

The thermohaline mixing of the present ocean keeps the difference between the surface and the bottom waters low by returning cold N-Atlantic surface water of low carbon concentration to the deep sea. The more vigorous this convection is, the smaller the difference should become. The more sluggish the ocean mixes, the larger the difference should get. On geological time scales, however, oceanic alkalinity and TCO_2 concentrations are governed by slow processes, such as changes in nutrient supply, changes in the extend of sulfate reduction and changes in silicate weathering (and reverse weathering).

Clearly, the carbonate system must have played a key role in the early ocean, simply because enough dissolved inorganic carbon must have been present to allow for the abiogenic formation of organic molecules, the precursors of self-replicating animated systems. Also carbonic acid has been – and is – the most important acid available for weathering and cation mobilization. It is therefore necessary to explore the options of initial conditions for ocean chemistry in view of the carbonate system.

Under the conditions of an abiotic Earth, absence or very low levels of molecular oxygen and hence the absence of sulfate, the absence of a differentiated crust, a high geothermal flux and hence a high volcanic activity, and a large rate of impacting asteroids and comets, silicate weathering must have played the major role in regulating alkalinity and TCO_2 in the ocean. Depending on the mineral weathered, many equations can be written for the reaction of silicates with carbonic acid, collectively they are referred to as Urey reactions (UREY, 1951). Average feldspar is, for example, weathered according to:

$$Na_{0.62}Ca_{0.38}Al_{1.38}Si_{2.62}O_8 + H_2CO_3 \text{ yields}$$

$$\text{kaolinite} + SiO_2 + 0.6\ Na^+ + 0.4\ Ca^{2+} + 0.6\ HCO_3^- + 0.4\ CO_3^{2-}$$

The reaction illustrates that both alkaline and alkaline earth cations are released to water. Upon accumulation in the ocean, the alkaline earth carbonate minerals being less soluble would reach saturation first and would precipitate, thus leaving sodium, potassium and carbonate ions to build up their concentrations further. These are exactly the conditions which allow soda lakes to form today. Soda lakes are terminal lakes which are fed by streams with a proportion of $[HCO_3 + CO_2] > [Ca + Mg]$ (or, which is essentially the same condition, $[Na+K] > [Cl+SO_4]$), and which develop highly alkaline conditions if sufficient time exists to accumulate enough dissolved minerals (GARRELS and MACKENZIE, 1967). Modern soda lakes occur in volcanic regions associated with plate boundaries (Figure 1). There fresh silicate rocks exist to produce sodium and carbonate dominated weathering solutions.

3. RISE AND FALL OF THE EARLY ALKALINE OCEAN

3.1 The "soda ocean hypothesis"

These basic considerations and observations led us to hypothesize (KEMPE and DEGENS, 1985) that the early ocean should have been highly alkaline and low in alkaline earth cations, in short, it should have been a "soda ocean". This scenario for the early ocean contrasts sharply with conventional views of an early Earth with a high pCO_2 atmosphere (HART, 1978; OWEN *et al.*, 1979; HENDERSON-SELLERS *et al.*, 1980; KUHN and KASTING, 1983; KASTING, 1985, 1987; CALDEIRA and KASTING, 1992) and hence a similar or more acidic ocean than at present containing appreciable concentrations of Ca and Mg and having Cl as the main anion (CONWAY, 1943; WEDEPOHL, 1963; GARRELS and MACKENZIE, 1971; MAISONNEUVE, 1982; WALKER, 1983; HOLLAND, 1984).

SEP-11-2002 11:13 LINDA HALL LIBRARYL 816 926 8785 P.10

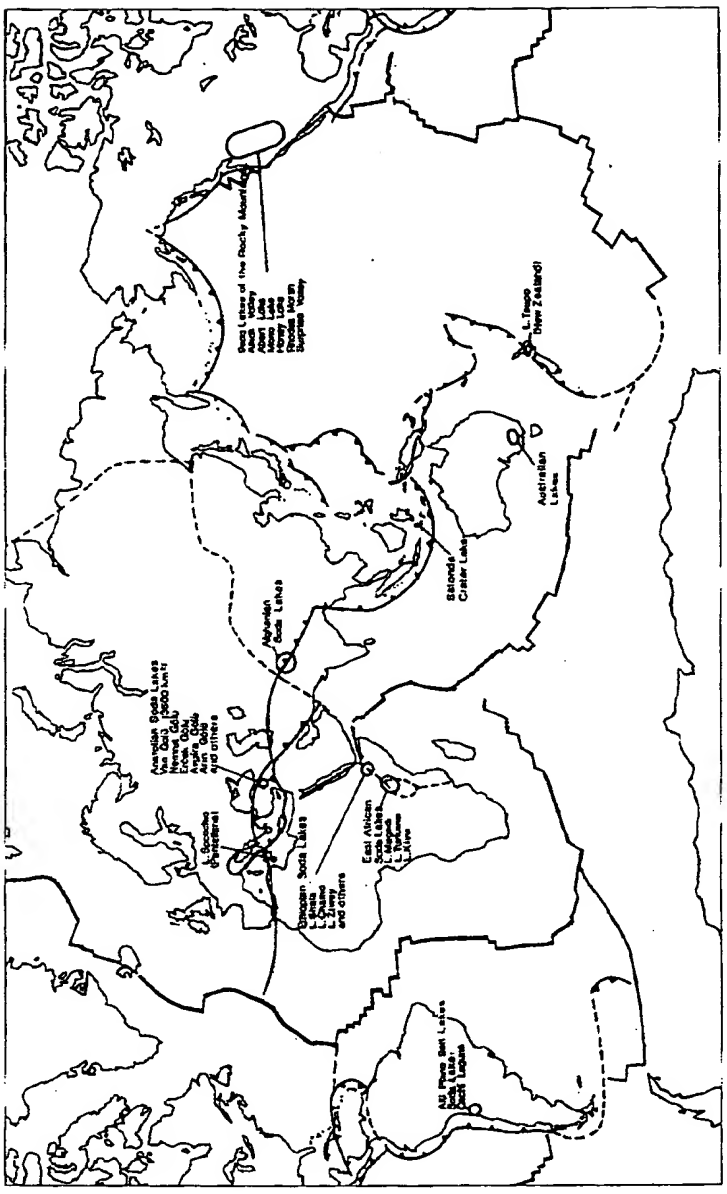

FIGURE 1 – Distribution of modern soda lakes (KEMPE *et al.*, 1989).

Later (K
that the so
bioevolution
concentratio
initial silicat
Supersaturat
higher than t
inorganic an

We will
and will late

3.2 The

Modern
in large natu
feasible. Fo
Lake Van/E
the composi
the presence
In Lake Van
of ion pairs
is much low
biologically
carbonate an

Composition o

Param
N
K
M
C
Cl
S
H
C
P
Si
N
N
N
B
To
pH
pC
Sl
SL
SL

FIGURE 1 – Distribution of modern soda lakes (KEMPE *et al.*, 1989).

Later (KAŽMIERCZAK and DEGENS, 1986; KEMPE *et al.*, 1989) it became clear that the soda ocean hypothesis (SOH) offers also answers for many bioevolutionary and physiological enigmas. Central to these questions is the Ca concentration in seawater. Because of the high primary alkalinity (caused by the initial silicate weathering), the ocean could hold only minute Ca concentrations. Supersaturation with regard to carbonate minerals nevertheless must have been higher than today because – in the absence of enzymatic biocalcification – only inorganic and biologically induced $CaCO_3$ precipitation could proceed.

We will explore rise and fall of the Precambrian sodic ocean in the following and will later review the biological and paleontological evidence in favour of it.

3.2 The rise of the early alkaline ocean

Modern soda lakes illustrate that highly alkaline conditions can be attained in large natural aquifers. Thus, a highly alkaline ocean is thermo-dynamically feasible. For comparison, the composition of the largest recent soda lake, Lake Van/Eastern Anatolia, is given in Table II. In one important aspect does the composition of modern soda lakes differ from a hypothetical early ocean: the presence of diatoms in modern environments keeps the silica content low. In Lake Van the Ca concentration amounts to 10^{-4} mol/kg. Due to the presence of ion pairs between Ca and HCO_3, CO_3, and SO_4, the free Ca^{2+} concentration is much lower, i.e. 22 µmol/kg only (Reimers, pers. comm.). Because of the biologically regulated silica content, Ca concentration is limited only by carbonate and not by silicate mineral equilibria.

TABLE II

Composition of Lake Van waters, sample V25, 200 m depth (REIMER et al., 1993, unpublished).

Parameter	mg/l	mmol/l
Na	7960	346.2
K	432	11.04
Mg	110	4.53
Ca	3.66	0.0913
Cl	5860	165.2
SO_4	2430	25.33
HCO_3	3051	50.02
CO_3	3169	52.82
PO_4	0.49	5.19
SiO_2	5.26	87.5
NH_4	<0.002	
NO_3	<?0.03	
NO_2	0.0005	
B	ca. 93	
Total	23022	
pH	9.87	
pCO_2 ppmv	262	free CO_2 17.8 µmol/kg
$SI_{calcite}$	1.078	
$SI_{aragonite}$	0.917	
$SI_{dolomite}$	3.801	

Since it is not known which Ca silicates would form in highly alkaline solutions and at what supersaturation spontaneous precipitation would occur, it is difficult to model highly alkaline solutions including silicate. Modelling is, however, possible for the carbonate system. In Figure 2 modern seawater is numerically titrated with increments of $NaHCO_3$ using the WATMIX electrolyte model (WIGLEY and PLUMMER, 1976). With increasing alkalinity, the supersaturation of $CaCO_3$ rises sharply. $CaCO_3$ is then subtracted until a $SI_{aragonite}$ of 0.8 is attained. In the model the pCO_2 is prescribed to 300 ppmv. As can be seen, the total Ca concentration drops to only 10^{-4} M at moderate alkalinities, levels out and increases in high alkalinities. This increase is possible because of the increase in the importance of ion pairs at higher carbonate concentrations. The free Ca^{2+} concentration, however, decreases with increasing alkalinity down to almost 10^{-6} M. The pH increases sharply at relatively low alkalinity, and rises to values of above 10.0 when alkalinity increases above 200 meq/l. It should be noted, that at low alkalinities the Ca concentration drops much faster than the alkalinity rises. Close to the present-day seawater composition, an increase in alkalinity from 2.38 to 10.3 meq/l leads to a more than 10-fold decrease in the Ca concentration (i.e. from 44 to 3 mg/l or 10^{-4} to 10^{-5} M).

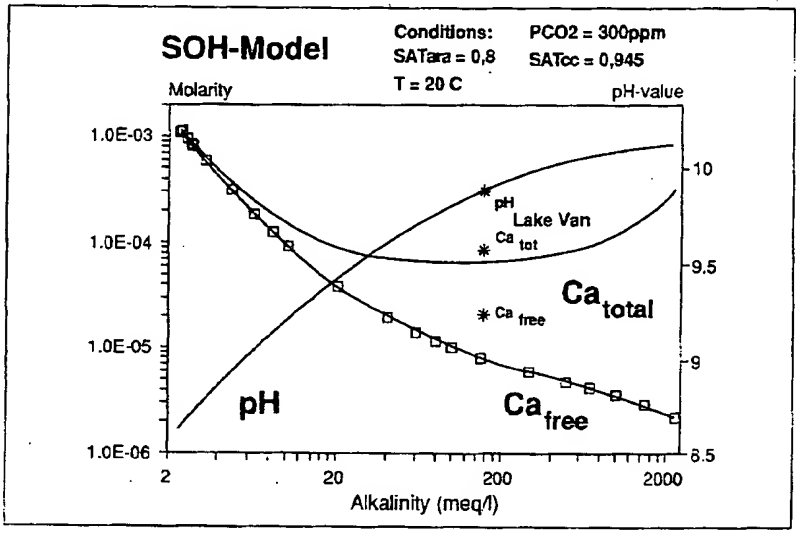

FIGURE 2 – Numeric titration of modern seawater with increments of $NaHCO_3$ (Program WATMIX, WIGLEY and PLUMMER, 1976).

Apart from thermodynamic considerations, kinetic and mass-balance arguments must be considered for the early ocean (KEMPE and DEGENS, 1985). A sodic ocean can only arise if silicate weathering is in fact rapid enough to keep pace with mantle degassing. Present-day volcanic emanation is 0.002 GtC/a (LEAVITT, 1982), while current continental weathering, measured as river transport, is amounting to 0.1 GtC/a (KEMPE, 1979). At present, silicate weathering is therefore far larger than volcanic recharge and consumes one volume of present-day atmospheric CO_2 mass (712 GtC) within 7000 years only. However, present-day silicate weathering proceeds under high soil pCO_2

and its rate is therefore biologically controlled. But even if weathering were a factor of 100-500 lower (the difference between pCO_2 in air and soil air), alkalinity would accumulate fast in an abiotic ocean.

An estimate of abiogenic silicate weathering can be deduced from Lake Taupo, New Zealand (616 km²). It releases Na- and K-balanced alkalinity at a rate of 30.2 t C/a/km² (data: SCHOUTEN, 1984; TIMPERLEY and VIGOR-BROWN, 1985). If this rate were representative for the entire oceanic area (15 GtC/a), then the ocean would acquire enough alkalinity (1 g C/kg H_2O ca. or 80 meq/l) within 100 000 years to surpass a concentration above which alkaline conditions would be established.

These example show that it is unlikely that primordial Earth could have sustained a high pCO_2 atmosphere for any appreciable time. Astrophysicists argue that the early atmosphere must, because of the faint early sun, have had a high pCO_2 (up to a 1000 times the present level) to keep the Earth from freezing (e.g. OWEN *et al.*, 1979; CALDEIRA and KASTING, 1992). This is clearly an ex cathedra conclusion and not substantiated by geochemical considerations. It is instead conceivable that the production of methane in a mostly anaerobic ocean is significant enough to sustain a greenhouse effect strong enough to keep the Earth from freezing (e.g. KONDRATYEV and MOSKALENKO, 1984). Each CH_4 molecule has a 20 times larger greenhouse effect than a CO_2 molecule (e.g. LASHOF and AHUJA, 1990). Furthermore, JENKINS (1993) recently showed that on a faster rotating Earth less clouds would form, allowing a higher fraction of solar radiation to reach the sea surface and partly compensating for the effect of an early faint sun. Also, with a lower fraction of land and a higher percentage of volcanic rocks on land, the general albedo could have been much lower than present-day, further decreasing the necessity for a high greenhouse gas concentration in the early atmosphere.

The build-up of highly alkaline conditions in the ocean must have been a geologically fast process. CO_2 input to the weathering system was a function of mantel degassing and/or the rate of impacts of comets carrying water and CO_2 to the young Earth. Cometary impacts and volcanic eruptions of the primordial magma ocean will have provided blankets of fresh, glassy and fine-grained silicate readily reacted with any available acid. Total masses available on Earth for the three most important acids are: H_2CO_3 = 65.5 x 10^{21} g C = 5.5 x 10^{21} mol; HCl = 52 x 10^{21} g Cl = 1.6 x 10^{21} mol (KEMPE and DEGENS, 1985); H_2SO_4 = 5.2 x 10^{21} g S = 0.16 x 10^{21} mol (e.g. WALKER 1977); i.e., through Earth history, there was 3.7 and 34 times more carbonic than hydrochloric and sulfuric acid available, respectively. On the other hand, the primordial, possibly komatiitic crust had a ratio of [Ca+Mg]/[Na+K] of 1.6 (ROGERS, 1978). Consequently, there was not enough HCl and H_2SO_4 available to balance Na and K which therefore must have been balanced by carbonate and bicarbonate ions in appreciable amounts. Such solutions will lead to highly alkaline conditions if concentrated over long time periods, just as observed in modern soda lakes.

One of the evidences in favor of an early alkaline ocean are recent microbialites and the environment in which they grow. Microbialites are laminated (stromatolitic) or unstructured (thrombolitic) predominantly calcareous deposits caused by the trapping of particles or the extracellular and non-enzymatic permineralization of microbial, mostly cyanobacterial mats (WALTER, 1976). We could show (KEMPE and KAŹMIERCZAK, 1990a) that for those modern sites, in which in situ permineralizing microbialites grow and

for which enough hydrochemical data are available (i.e. Andros Ponds/Bahamas, Lake Tanganyika, and Lake Walker) calcium carbonate supersaturation is much larger (> 0.8 $SI_{calcite}$) than in the present marine environment. Furthermore we discovered the largest currently known microbialitic structures in Lake Van (KEMPE *et al.*, 1991). This discovery proves that microbialites are compatible with highly alkaline conditions and high $CaCO_3$ supersaturation (compare Table II). Similarly, the widespread stromatolites from the Middle Eocene Green River Formation in SW-Wyoming have formed in a soda lake. This is clearly indicated by the trona deposits of the former Lake Gosiute (for review see SURDAM and WRAY, 1976). Even more, our discovery of large microbialitic structures in a marine-derived environment in Satonda Crater Lake (KEMPE and KAZMIERCZAK, 1990b, 1993; KAŻMIERCZAK and KEMPE, 1990, 1992) show that present-day seawater can sustain in situ calcification of cyanobacterial mats if "titrated" to slightly increased alkalinities. These findings are strong indications that the widespread occurrence of stromatolites in the Precambrian rock record (e.g. WALTER, 1983) are witnesses of a highly $CaCO_3$ supersaturated and alkaline early ocean.

3.3 The decline of the early alkaline ocean

With the rapid recycling of the early hot oceanic crust, precipitating Ca and Mg carbonates would also be recycled fast. The only major reservoir for carbon would therefore have been the dissolved carbon pool in the ocean. In fact, nearly all of the carbon of the present-day lithosphere, biosphere, hydrosphere, and atmosphere could be stored as sodium carbonate in an ocean of present-day volume without reaching the saturation limit of sodium carbonate minerals. Only after the continents began to form, carbon could be stored for longer periods in solid form. For the SOH it is not important, if continents accreted gradually (e.g. VEIZER and JANSEN, 1969; HURLEY and RAND, 1969) or rapidly (e.g. WARREN, 1989; ARMSTRONG, 1991). Important is, however, that the granodioritic crust is relatively enriched in alkali metals. With the establishment of deep subduction, ocean water could be trapped as porewaters, be subducted and the dissolved sodium could be incorporated into continental rocks (KEMPE and DEGENS, 1985). This removal would be a slow process, essentially depending on the activity of subduction which in turn is a function of the declining radioactively generated internal heat of the planet. The carbon in turn would be stored in calcareous and carbonaceous rocks accreted to continents. Because of their low density, they would preferentially be protected from re-incorporation into the mantle. In a sense, the cations of the early komatiitic crust would be redistributed, after residing for a long time in the ocean, into granodioritic crust and Ca and Mg carbonate rocks. This process of extracting the original high soda content of the ocean is very slow. Today, water is subducted with roughly 1 km^3/a resulting in half lives of any dissolved substance (if removed in that manner) in the ocean of ca. 1 Ga (KEMPE and DEGENS, 1985). It must therefore have taken several billion years for the soda ocean to decline.

In Figure 3 the rise and fall of the alkaline ocean is condensed into a scenario of ocean development according to the thermodynamic model of Figure 2. In our reasoning, the end of the alkaline ocean is marked by the occurrence of the first widespread marine deposits of gypsum. They could have formed only after the Ca concentration rose to appreciable amounts indicating a substantial decrease of the primary alkalinity. Earliest gypsum

layers, alt
Amadeus I
marine eva
(Hormuz S
System, In
DEGENS, 1
dismissed a
could just a

FIGURE 3 – S
ocean" occup
dominated by
graph) and si
numeric mod
major overtur

4.1 Ope

Toward
atmosphere
(present co
modulate T
stagnant b
reduction p
the removed
as an avera
pycnocline
system. Suc
only large s

(i.e. Andros
ium carbonate
resent marine
rently known
This discovery
conditions and
he widespread
ation in SW-
d by the trona
AM and WRAY,
es in a marine-
KAZMIERCZAK,
at present-day
; if "titrated" to
cations that the
n rock record
rsaturated and

recipitating Ca
or reservoir for
n the ocean. In
re, biosphere,
ate in an ocean
nit of sodium
arbon could be
t important, if
); HURLEY and
). Important is,
alkali metals.
l be trapped as
corporated into
ould be a slow
ich in turn is a
of the planet.
naceous rocks
l preferentially
the cations of
for a long time
ite rocks. This
n is very slow.
lf lives of any
n of ca. 1 Ga
l billion years

densed into a
mic model of
narked by the
n. They could
iable amounts
rliest gypsum

spécial 13 (1994)

layers, albeit of a sabkha environment, date from 0.9 Ga (Proterozoic Amadeus Basin, Australia). The oldest large gypsum deposits as parts of thick marine evaporative series date to the lower Proterozoic ca. 0.7-0.6 Ga ago (Hormuz Series, Persia; the upper Valdai Series, Russian Platform; Vindhyan System, India; Shaler Group, Victoria Island, Canada; see KEMPE and DEGENS, 1985 for more details). Older pseudomorphs of anhydrite can be dismissed as evidence of a higher Ca concentration in the ocean because they could just as well have formed in sediments of lakes and sabkhas.

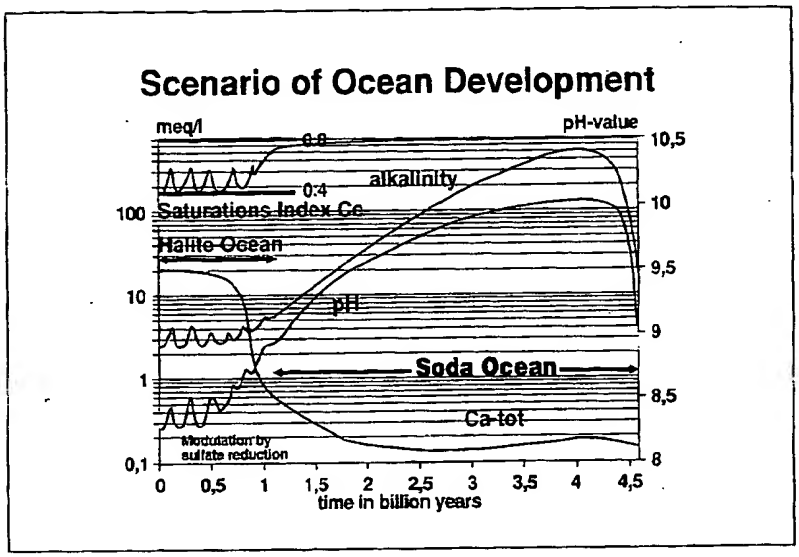

FIGURE 3 – Scenario of ocean development through Earth history. Rise and fall of the "soda ocean" occupied roughly 3.5 billion, whereas late Precambrian and Phanerozoic ocean was dominated by halite. Concentrations of total Ca (lower curve), pH and alkalinity (center of graph) and supersaturation index for aragonite (top of graph) are drawn according to the numeric model of Fig. 1. Fluctuations in the halite ocean period are schematic only, indicating major overturn events.

4. THE PHANEROZOIC "ALKALINITY PUMP"

4.1 Operating the "alkalinity pump"

Towards the end of the Proterozoic the oxygen concentration in the atmosphere increased enough to hold large quantities of sulfate in the ocean (present concentration 28 mmol/kg). Therefore a new powerful mechanism to modulate TCO_2 and alkalinity was available (Table I): sulfate reduction. In stagnant basins and under conditions of sluggish ocean mixing sulfate reduction produces alkalinity needed as a replacement of the charge carried by the removed sulfate ion. The reaction is fueled by organic carbon (formulated as an average Redfield-ratio compound in Figure 4) sinking through the pycnocline at rates larger than the downwelling of molecular oxygen in the system. Such a system was termed an "*alkalinity pump*" (KEMPE, 1990). The only large scale current example of an alkalinity pump is the Black Sea basin.

SEP-11-2002 11:15 LINDA HALL LIBRARYL 816 926 8785 P.16

There alkalinity has, within ca. 7000 years, increased to 4.5 meq/l in the deep water (Figure 4, inset; GOYET *et al.*, 1991). Part of this alkalinity has reached the surface waters by upwelling. Actually the re-oxidation of H_2S t sulfate during upwelling should lead to a backreaction of the bicarbonate to CO_2 and its consequent degassing. However, the extraction of part of the H_2S by iron as insoluble mackinawite and pyrite can lead to excess alkalinity. Also the dissolution of $CaCO_3$ in deeper unsaturated waters leads to an increase of alkalinity and TCO_2. In case of the Black Sea, the latter apparently is the major process for the upwelling of excess alkalinity to the surface layer in the Black Sea (3.3 meq/kg). The concentration is far larger than anywhere else in the ocean. If the surface layer of the Black Sea would not have a low salinity (18.2 permil) and low Ca concentration (6.2 mmol/kg, GOYET *et al.*, 1991), then the surface layer would be highly supersaturated with respect to carbonate minerals. Its actual supersaturation is 0.4 $SI_{calcite}$ and 0.25 $SI_{aragonite}$ only. One of the consequences of alkalinity production by sulfate reduction is that the TCO_2 has a $\delta^{13}C$ much lower than average seawater (-6.6 in deep and +0.8 in surface waters of the Black Sea; FRY *et al.*, 1991) owing to its origin from low $\delta^{13}C$ organic matter (Figure 4, inset).

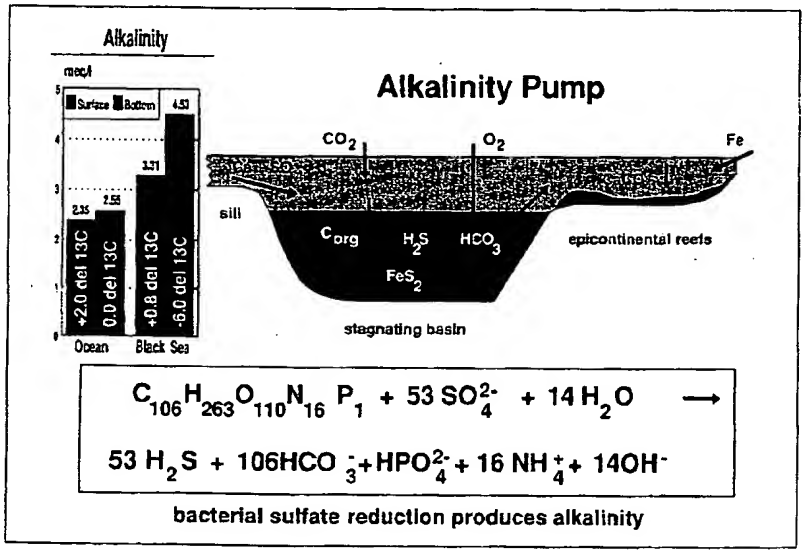

FIGURE 4 – Alkalinity pump and chemical equation of sulfate reduction (fueled by a Redfield ratio-type organic compound) (modified after KEMPE, 1990). Inset compares alkalinity and $\delta^{13}C$ of the present-day ocean and the Black Sea.

An even more striking example of an alkalinity pump is the crater lake of Satonda Island (Figure 5). It is filled with seawater and stratified because of dilution of the epilimnion by rain and concentration of deep layers by continued evaporation during the dry season (KEMPE and KAZMIERCZAK, 1993). Ongoing sulfate reduction in the anoxic waters below 22 m has resulted in very high total alkalinities (6.4 in the middle and up to 50 meq/kg in the lower layer). Some of the alkalinity has reached the upper layer by upwelling or diffusion, increasing its alkalinity to 3.6 meq/kg and its pH to

8.45. In conse
layer and in s
lake (KEMPE
1992). Further
compared to th

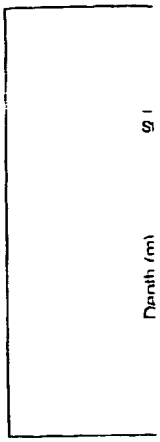

FIGURE 5 – Longi
and the salinity a
(well mixed aer
bottom anaerobic

4.2 Anaer

These exa
modulating al
ocean stratific
regionally o
schematically
below the ch
supersaturatio
adjacent to an
in nature or co
neighbourhood
carbonate seq
exceptions (e.g
largely ignore
concerned wit
climatic factor
TUCKER and W

In Figure
compared with
to the missing
fermentation
reduced iron
sulfides. It is t

8.45. In consequence, the supersaturation has reached 0.8 $SI_{calcite}$ in the surface layer and in situ calcified cyanobacterial reefs grow along the shores of the lake (KEMPE and KAZMIERCZAK, 1990b; KAZMIERCZAK and KEMPE, 1990, 1992). Furthermore, the $\delta^{13}C$ dropped throughout the lake to very low values compared to the $\delta^{13}C$ in the ocean.

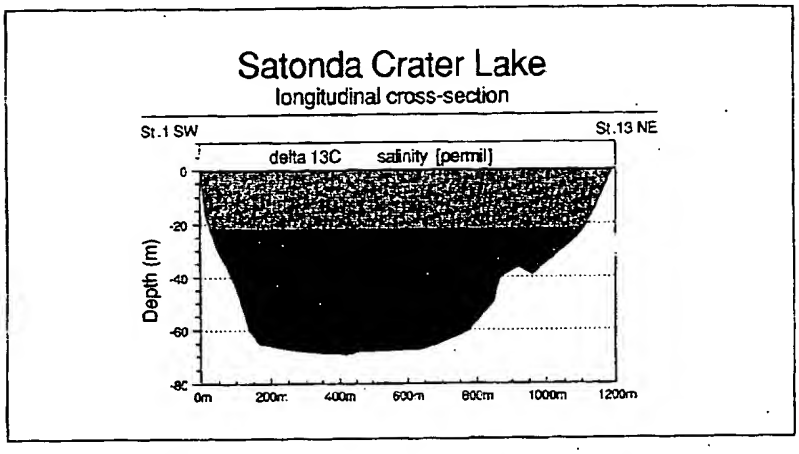

FIGURE 5 – Longitudinal section through the crater lake of Satonda Island/Sumbawa, Indonesia and the salinity and $\delta^{13}C$ values of its three main layers as an example of an alkalinity pump (well mixed aerobic surface layer, 0-22 m; middle well mixed anaerobic layer 22-55 m; bottom anaerobic layer, deeper than 55 m) (after KEMPE and KAZMIERCZAK, 1993).

4.2 Anaerobic basins and carbonate facies

These examples show that sulfate reduction could be the main factor modulating alkalinity in the Phanerozoic ocean. Depending on the extent of ocean stratification, Phanerozoic seawater must have experienced locally, regionally or globally alkalinity and supersaturation excursions as schematically shown in Figure 3. Such alkalinity plumes originating from below the chemocline should lead to increased carbonate mineral supersaturation and enhanced deposition of carbonates in epicontinental areas adjacent to anoxic basins (KEMPE, 1990). These basins could either be oceanic in nature or could occupy deeper sections of the shelf itself, creating in their neighbourhood a facies mosaic as it is characteristic for many epicontinental carbonate sequences (comp. Figure 7b). It should be noted that with a few exceptions (e.g. HAY *et al.*, 1981; CALDEIRA *et al.*, 1990) alkalinity has been largely ignored so far as an important factor in paleoceanographic studies concerned with carbonate sedimentation. Much more attention was given to climatic factors, tectonism and sea level changes (for review: WILSON, 1975; TUCKER and WRIGHT, 1990; PRATT, 1992; WRIGHT, 1992).

In Figure 6 the stagnation of a Phanerozoic marine water body is compared with the situation in a stagnating Precambrian alkaline ocean. Due to the missing sulfate in the early alkaline ocean it would be governed by fermentation and methane production and not by sulfate reduction. Also reduced iron would stay in solution and could not have been removed as sulfides. It is therefore available for upwelling and periodic oxidation in the

surface layer. Together with silica, also available in high concentrations in highly alkaline solutions, it could have formed epicontinental banded iron formations (BIFs). EUGSTER (1969) suggested already that BIFs can be explained best as being formed under highly alkaline conditions. Silica is thought to precipitate during wet seasons, when freshwater input diluted seawater, reduced alkalinity and decreased pH, therefore making SiO_2 less soluble. Import of fresh seawater and upwelling during the dry season could then complete the annual cycle by precipitating iron oxides originated from a large reduced iron pool available in the anaerobic oceanic basins. In the basin itself, black shales with highly insoluble heavy metal sulfides and iron phosphates could have formed, sediments characteristic of Archean rocks.

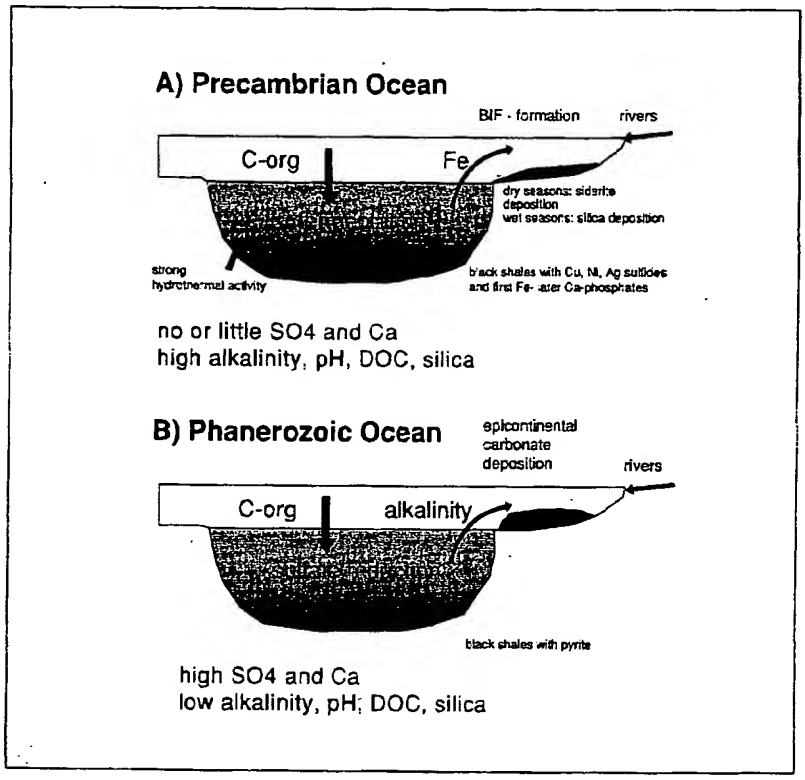

FIGURE 6 – Development of anaerobic basins in the Precambrian (A) and Phanerozoic (B) ocean.

In the final, halite period of the ocean, the anaerobic basins are dominated by free hydrogen sulfide. Iron cannot collect in dissolved form but is incorporated in black shales as pyrite. Exported alkalinity triggers the precipitation of epicontinental carbonates.

According to these models three realms of carbonate formation can be discerned (Figure 7): The soda ocean, the Phanerozoic stagnant and the Phanerozoic well mixed ocean.

FIGURE 7 – C
and well-mix

In the
(Fig. 7A):
carbonate
noticed in
seawater
deposited
could forr
increased
microbiali
open ocear
In the
both in the
carbonate
sinking op
alkalinity
are expose
the supers
corals, ru
supersatur

centrations in
l banded iron
BIFs can be
ions. Silica is
input diluted
ing SiO_2 less
season could
ginated from a
s. In the basin
des and iron
rchean rocks.

ozoic (B) ocean.

e dominated
form but is
triggers the

ation can be
tant and the

scial 13 (1994)

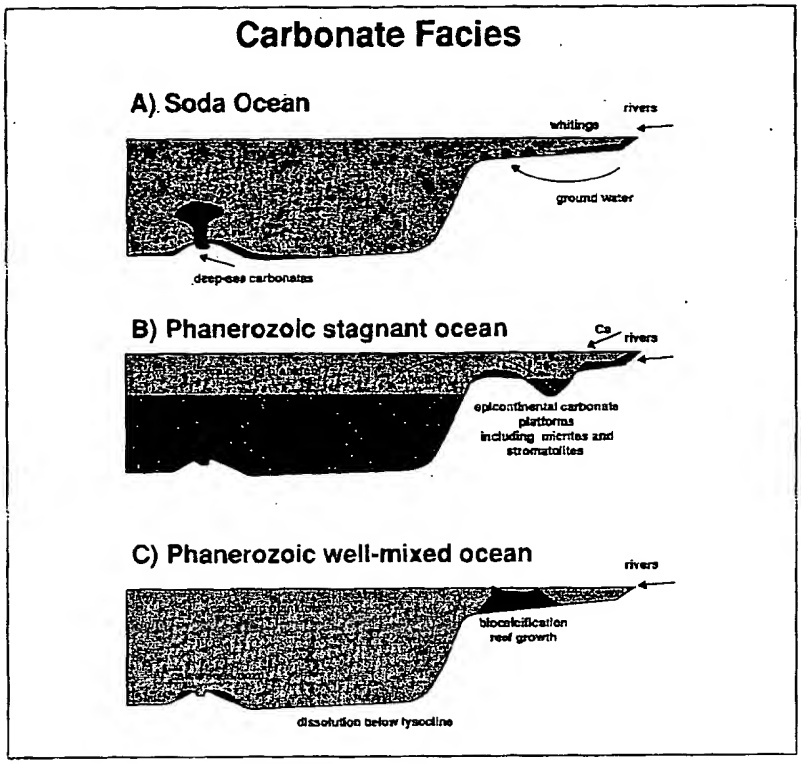

FIGURE 7 – Comparison of general carbonate facies in the soda ocean (A) and in the stagnant (B) and well-mixed (C) Phanerozoic halite ocean.

In the early alkaline ocean carbonates formed where Ca was available (Fig. 7A): At deep sea hydrothermal vents, $CaCO_3$ would precipitate forming carbonate rocks in close association with mafic rocks, an association often noticed in metamorphic basement series. In estuaries, fresh water mixed with seawater and whitings formed fine-grained suspended carbonates which deposited along-shore. At groundwater seepages, shallow-water carbonates could form in situ on the shelf. With decreasing alkalinity and slightly increased Ca concentrations thick sequences of shallow water calcareous microbialites could form. Because no biocalcifying organisms existed, no open ocean biological carbonates were produced.

In the Phanerozoic ocean biocalcifying organisms can produce carbonates both in the open sea and on shelves. In case of a stagnant ocean (Fig. 7B) Ca carbonate deposition would be focused to the shelves because most of the sinking open ocean carbonates would dissolve in deeper waters. TCO_2 and alkalinity would be exported to the shelves. There biomineralizing organisms are exposed to fluctuating levels of alkalinity and supersaturation. As long as the supersaturation can be kept low by the enzymatic calcification, reefs of corals, rudists and other biocalcifyers can form. If, however, the supersaturation is increased too fast and reaches values above roughly 0.8 SI,

then calcareous microbialites can grow (KEMPE and KAŻMIERCZAK, 1990a). Thus carbonate platforms often display a composite of true biomineralizers and of species-poor microbialite dominated sequences.

In case of the Phanerozoic well-mixed ocean (Fig. 7C), alkalinity, TCO_2 and supersaturation will not fluctuate much. These are the conditions for restricted but constant build-up of reefs by enzymatic biocalcifyers. In the open ocean widespread deposits of calcareous ooze can accumulate and dissolution can occur only below a relatively deep lysocline.

This discussion summarizes the possible carbonate facies in view of the high primary alkalinity of the early sodic ocean and in view of the secondary alkalinity produced by temporarily stagnant ocean basins.

4.3 Carbonate platforms, sedimentary discontinuities, and $\delta\ ^{13}C$ excursions

The previous discussion is rather theoretical and we need to explore the evidence for the predicted effects of the alkalinity pump mechanism.

Therefore, it would be instructive to give examples of the coexistence of anaerobic basins and large carbonate deposits in the marine record of the Phanerozoic. Both in the Paleozoic and Mesozoic we find in fact well documented anoxic basins contemporary with extensive carbonate platforms (ramps) and pelagic carbonate deposits (e.g. BYERS, 1977; BERRY and WILDE, 1978; ARTHUR and SCHLANGER, 1979; JENKYNS, 1980, 1988; GRACIANSKY *et al.*, 1984; WILDE, 1987; KOERSCHNER and READ, 1989; TUCKER *et al.*, 1990; WIGNALL and HALLAM, 1992). Curves of the burial rate of $C_{carbonate}$ and $C_{organic}$ have been compiled by HOLSER (1984) for the Phanerozoic (Figure 8).The curves correlate significantly, indicating that in fact there is a temporal connection between high organic carbon burial (indicative of widespread anoxic basins) and epicontinental carbonate deposition. The $C_{carbonate}$ peaks mark periods with the largest extent and thickness of biogenic (microbial and skeletal) reefs (compare NEWELL, 1971; COPPER, 1988; TALENT, 1988).

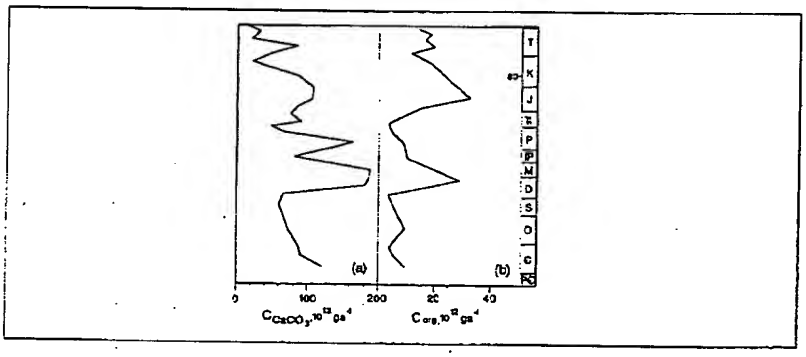

FIGURE 8 – Curves of deposition rates of $C_{carbonate}$ (a) and $C_{organic}$ (b) through the Phanerozoic (from HOLSER, 1984, modified). Note the coincidence of periods of high rates of carbonate deposition with those of high rates of organic deposition. This is particularly evident for the lower Cambrian, Devonian to lower Carboniferous (Mississippian), Jurassic to upper Cretaceous, and for the two Tertiary epoches, Eocene and Miocene. The coincidence can be interpreted as global effects of alkalinity pumps (KEMPE, 1990): anaerobic (stratified) basins conserve organic matter and produce, at the same time, excess alkalinities which are exported to shallow areas causing unusually high calcium carbonate supersaturation levels and intensive carbonate sedimentation.

FIGURE 9 – Compilation of detailed carbon isotope profiles of the transitions Precambrian/Cambrian, Permian/Triassic, and Cretaceous/Tertiary in carbonate profiles. The $\delta^{13}C$ excursions occurring near these major stratigraphic boundaries are here interpreted to indicate destabilization of anaerobic basins. The upwelling of water from below the chemocline exports higher alkalinities with light $\delta^{13}C$ signals to shallow-water areas. (a): Ulakhan-Sulugat, southeastern Siberia; the two wavy horizontal lines on the profile mark probable short sedimentary discontinuities (KOZANOV, 1984) (after MAGARITZ, 1989); (b): Kuh-e-Ali, northwest Iran (after HOLSER and MAGARITZ, 1987); (c): Deep Sea Drilling Project Site 527, South Atlantic (after SHACKLETON and HALL, 1984).

ERCZAK, 1990a).
biomineralizers

alkalinity, TCO_2
conditions for
alcifyers. In the
accumulate and

in view of the
of the secondary

ies, and $\delta^{13}C$

l to explore the
nism.
coexistence of
e record of the
ld in fact well
onate platforms
RY and WILDE;
GRACIANSKY *et*
ER *et al.*, 1990;
arbonate and $C_{organic}$
(Figure 8).The
is a temporal
of widespread
$C_{carbonate}$ peaks
(microbial and
, 1988).

Phanerozoic (from
bonate deposition
nt for the lower
r Cretaceous, and
erpreted as global
ve organic matter
ow areas causing
ite sedimentation.

spécial 13 (1994)

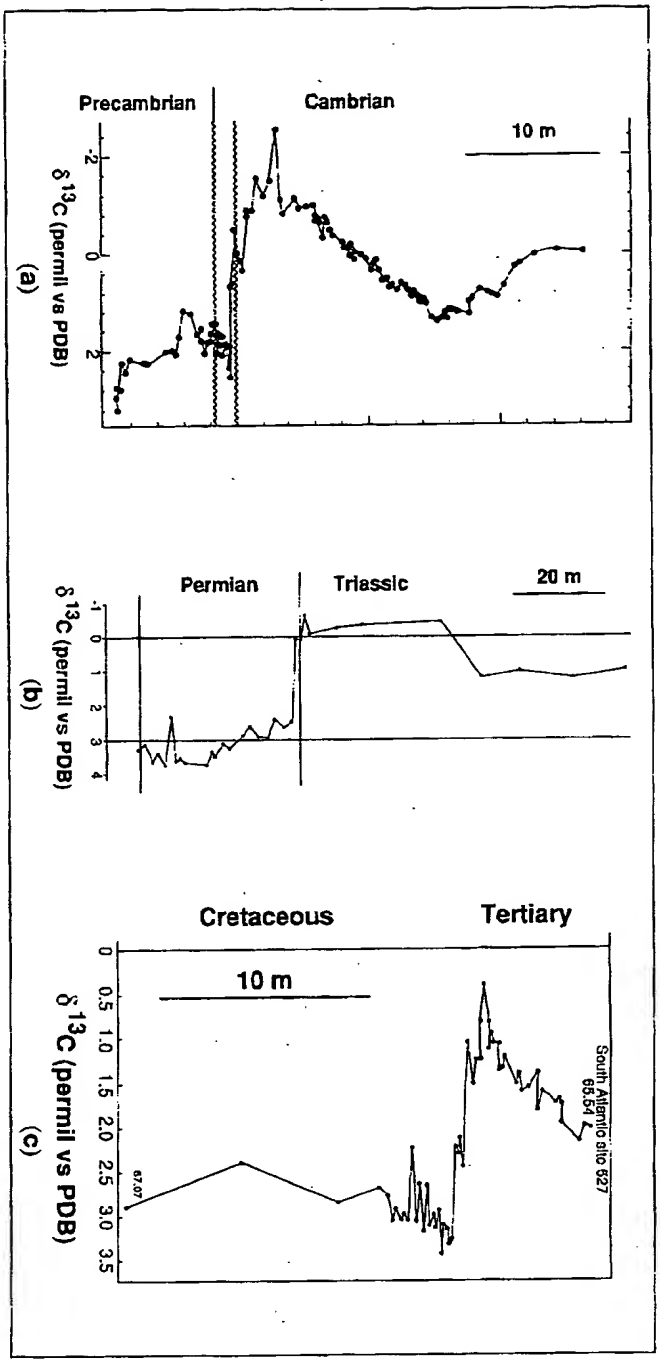

FIGURE 9 – Compilation of detailed carbon isotope profiles of the transitions Precambrian/Cambrian, Permian/Triassic, and Cretaceous/Tertiary in carbonate profiles. The $\delta^{13}C$ excursions occurring near these major stratigraphic boundaries are here interpreted to indicate destabilization of anaerobic basins. The upwelling of water from below the chemocline exports higher alkalinities with light $\delta^{13}C$ signals to shallow-water areas. (a): Ulakhan-Sulugat, southeastern Siberia; the two wavy horizontal lines on the profile mark probable short sedimentary discontinuities (ROZANOV, 1984) (after MAGARITZ, 1989); (b): Kuh-e-Ali, northwest Iran (after HOLSER and MAGARITZ, 1987); (c): Deep Sea Drilling Project Site 527, South Atlantic (after SHACKLETON and HALL, 1984).

SEP-11-2002 11:17 LINDA HALL LIBRARYL 816 926 8785 P.22

One of the most convincing evidences that alkalinity pumps have important influence on carbonate platform sedimentations is derived from the $\delta^{13}C$ record. As we have seen in Satonda Crater Lake and in the Black Sea, waters charged with excess alkalinity upwelling from anaerobic basins, have a lower $\delta^{13}C$ than the average marine $\delta^{13}C$. Records of $\delta^{13}C$ at major geological time boundaries, like the Precambrian/Cambrian, Permian/Triassic, and Cretaceous/Tertiary show distinctive negative excursions (Figure 9). Such excursions have already been interpreted as signs of oceanic overturn (e.g. HOLSER, 1984; MARGARITZ, 1989; HOFFMAN *et al.*, 1991; WIGNALL and HALLAM, 1992; ERWIN, 1994, for review of the P/T boundary). Figure 10 explores the details of the $\delta^{13}C$ response to an overturn in view of the alkalinity pump and stratified basins. Overturn does not need to be complete and the basin, needed to produce specific light $\delta^{13}C$ excursions, can be of varying size according to the regional or global extent of the signal. There are many processes which can cause overturn or partial uplift of anaerobic and higher alkaline bottom waters: (i) enhanced downwelling of cold polar water, uplifting basins water; (ii) enhanced downwelling of highly saline and dense waters from evaporative regions of the ocean, also causing higher rates of upwelling; (iii) geothermal heating of the stagnant water body from below, thereby inducing thermal instability; (iv) Lake Nyos-type gas eruptions which could cause catastrophic self-accelerated uplift of deep water under conditions of a very high pCO_2 accumulated from submarine volcanic sources over long periods (EVANS *et al.*, 1993); (v) sudden large-scale mass wastes at large volcanic islands or along the continental shelves, displacing bottom waters and causing seiches; (vi) cometary impacts displacing water from basins and causing shock waves (rate of impacts reviewed by: CHAPMAN and MORRISON, 1994).

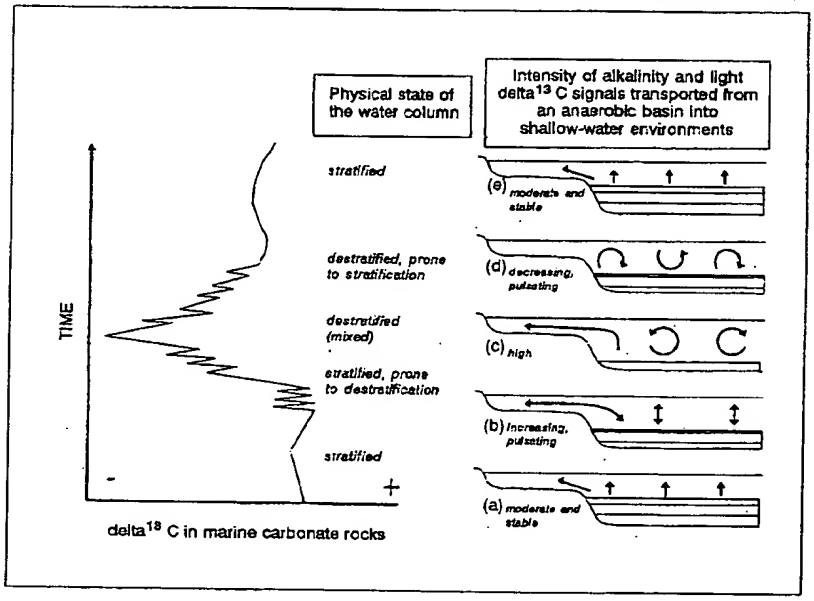

FIGURE 10 – Inferred relationship between excessive alkalinities (arrows) and associated light $\delta^{13}C$ signals transported from anaerobic marine basins to shallow-water environments and the resulting $\delta^{13}C$ values recorded in a sequence of carbonate sediments.

It is interesting to discuss possible causes of omission surfaces and hardgrounds and other sedimentary discontinuities often observed in large carbonate series (e.g. JAANUSON, 1961; KAŹMIERCZAK and PSZCZÓKOWSKI, 1968; FÜRSICH, 1979; HOLMER, 1983; GRUSZCZYŃSKI, 1986; WENDT, 1988). In view of the alkalinity pump two factors may cause these phenomena: Overturns involving deep basin waters with a very high pCO_2 could temporarily increase atmospheric pCO_2 and decrease supersaturation in oceanic surface waters. Lighter $\delta^{13}C$ signals associated with some of the discontinuity surfaces (GRUSZCZYŃSKI *et al.*, in press) could be interpreted as supportive evidence for such a scenario. It could also be possible that pulses of higher alkalinity waters and enhanced $CaCO_3$ deposition deplete the Ca concentration in surface waters enough to later stop or decrease the rate of deposition temporarily when upwelling of deeper water ceases.

Two distinct discontinuities corresponding with strong negative $\delta^{13}C$ excursions are reported from the boundary Precambrian/Cambrian (Pϵ/ϵ) in the stratotypical section at Ulakhan Sulugur, southeastern Siberia (compare Figure 9a). Generally, the Pϵ/ϵ boundary is associated with the strongest negative $\delta^{13}C$ excursions. They are recorded in the Himalaya (AHARON *et al.*, 1987), China, and Iran (BRASIER *et al.*, 1990), Morocco and Siberia (MAGARITZ *et al.*, 1991), and South Australia (TUCKER, 1989). In fact, several such $\delta^{13}C$ excursions predate the Pϵ/ϵ transition (e.g. KNOLL *et al.*, 1986; KNOLL, 1991) probably recording several overturns of deep stagnating ocean basins which originated after the continental break-up at the end of the Proterozoic (MCKERROW *et al.*, 1992). Overturn of any of these basins or even of Panthalassa itself would exert high and sudden Ca, PO_4, alkalinity and supersaturation stresses upon the shallow water biota. The onset of biocalcification was in all probability a response to these severe environmental challenges.

5. BIOLOGICAL AND EVOLUTIONARY IMPLICATIONS OF THE EARLY ALKALINE OCEAN HYPOTHESIS

Progress was achieved recently as to "how", "when", and "at what site" organisms deposit minerals (for extensive review: LOWENSTAM and WEINER, 1989; MANN *et al.*, 1989; SIMKISS and WILBUR, 1989). Also some questions concerning composition, structure, mode of nucleation and growth of many biominerals have been clarified (ADDADI *et al.*, 1987; BERMAN *et al.*, 1993; MANN *et al.*, 1993). The question "why" mineral skeletal structures appeared almost simultaneously in the evolution of many different groups of organisms close to the boundary Precambrian/Cambrian remains principally unanswered, however. Also what was the reason causing the later Phanerozoic skeletonization events which, among others, involved groups of organisms whose representatives must have existed long before in a non-skeletonized form (e.g. coccolithophorids, radiolarians and planktonic foraminifers). Another matter of considerable controversy and speculation concerns the primary function(s) of skeletal structures. Two hypotheses explaining the onset of biocalcification processes (understood as "true", i.e. biologically controlled or enzymatic deposition of calcareous and Ca phosphatic skeletal structures) at the transition Precambrian/Cambrian have been advanced.

The "predation hypothesis" claims that mineral skeletons originated as a response of organisms to an increased rate of predation (HUTCHINSON, 1961; ROMER, 1963; STANLEY, 1973; VERMEIJ, 1989).

SEP-11-2002 11:18 LINDA HALL LIBRARYL 816 926 8785 P.24

It is based on observations of recent externally skeletonized animals (so called durofaunas) which apparently defend themselves through heavy skeletons (even though not always effectively) against predators, and on a few findings of early Cambrian invertebrate skeletons bearing holes or scratches. These are interpreted as evidence for a dramatically increased predation pressure counterbalanced by the invention of mineral skeletons by prey organisms.

The "depot hypothesis" considers skeletons as primary deposits of metabolic waste- or by-products, many of which have subsequently been adjusted to perform other important life functions (JONES, 1969; HALSTEAD, 1969; LEHNINGER, 1983; DEGENS, 1979). As a modification KAŹMIERCZAK *et al.* (1985) proposed that the onset of biocalcification was a common detoxification response of marine biota which – after a long existence in a relatively calcium-poor environment – was near the transition Precambrian/Cambrian rapidly exposed to subtoxic Ca^{2+} concentration.

This "Ca^{2+} detoxification" hypothesis is based on the universal function of calcium in cell physiology and on the sophisticated Ca regulation systems functioning in eukaryotic organisms for keeping the optimal cytoplasmic Ca^{2+} concentration at very low levels (below 10^{-7} M) against extracellular Ca^{2+} concentrations about 10,000 to 30,000 times higher (10^{-3}-10^{-2} M). The ability of living cells to respond to changes in their ionic environment may be regarded as one of their most fundamental properties. In response to changes in external Ca concentration, cells will adjust various intracellular processes in order to maintain overall homeostasis. As will be shown below, the advantage of the hypothesis of the calcium-poor early alkaline ocean, compared to other hypotheses proposed thus far to explain the key events in the evolution of life as, for instance, the widely accepted role of the increasing atmospheric oxygen concentration as a determinant for the evolution of complex life (e.g. CLOUD, 1976; KNOLL, 1991; DERRY *et al.*, 1992), rest not only on geological and paleontological evidence but also on data from biochemistry, molecular biology, physiology, and developmental biology.

5.1 Calcium and pH in the Precambrian ocean

As indicated above, one of the consequences of a high alkalinity in the early ocean and a low atmospheric pCO_2 could have been a high pH and a very low concentration of free, ionic calcium [Ca^{2+}] in seawater. For obvious reasons, there is no possibility to determine [Ca^{2+}] or pH levels in the early Archean ocean precisely. Plausible values can, however, be proposed in analogy with modern highly alkaline lakes. Total Ca concentrations of < 5 mg/l (< 10^{-4} M) and pH values of > 9.5 are typical for modern soda lakes (e.g. KEMPE, 1977; MELACK, 1983; BISCHOFF, 1991) with free calcium [Ca^{2+}] levels even lower (ca. 10^{-5} M). In the early ocean inorganic Ca complexing biopolymers and ion pairs formed with phosphate and silica were additional factors depressing the Ca^{2+} concentration further, possibly to < 10^{-6} M.

During the gradual decrease of alkalinity towards the late Precambrian, Ca^{2+} concentration could have risen sharply from values lower than 10^{-5} M to about 10^{-2} M, and pH could have decreased to < 8.5. Before discussing possible consequences of such dramatic chemical changes for the evolution of life we want to illuminate the role of calcium for cellular processes, focusing on those cytophysiological processes and biomolecular patterns, which support a highly alkaline paleoceanographic scenario.

"Complex life appears to be a consequence of calcium functionality"

could be – without much exaggeration – the quintessence of the multitude of biochemical, physiological and biomolecular papers dealing with various aspects of calcium in living systems.

5.2 Calcium in the cell: function and regulation as testimony for the Ca-poor cell ambience in the geological past

The versatility of calcium in biological systems is related to the highly adaptable coordination geometry of Ca^{2+}, and the ease it can coordinate or cross-link in complex biochemical molecules. Calcium links extracellular changes of voltage, chemical concentrations or mechanical activity to cell processes, because this ion is characterized by a divalent charge, modest binding energies, fast reaction kinetics and does not participate in redox reactions (WILLIAMS, 1974, 1989). These unique properties most likely determined during the early stages in the evolution of life that calcium became the messenger for and the integrator of basic cell functions (KRETSINGER, 1977a, b). To perform precisely these functions and to prevent Ca^{2-} stress, calcium has to be present in the cells in correct concentration, at the right site, and at the proper time.

Generally, Ca^{2-} concentrations in cytoplasms ($[Ca^{2+}]_i$) is $< 10^{-7}$ M in all non-activated cells, i.e., about four orders of magnitude lower than the average extracellular calcium concentration $[Ca^{2+}]_o$ (ca. 10^{-3} M in blood and body fluids, and ca. 10^{-2} M in seawater). This extremely asymmetrical distribution of Ca^{2+} across the plasma membrane allows cells to generate both electrical and chemical intracellular signals.

The concentration of cytosolic free calcium ($[Ca^{2+}]_i$) is critically important for many cell functions and its accurate control represents a fundamental property of all living cells (e.g. BORLE, 1981; CAMPBELL, 1983; MARMÉ, 1985; CARAFOLI, 1987). The maintenance of this level appears to be an ancient and

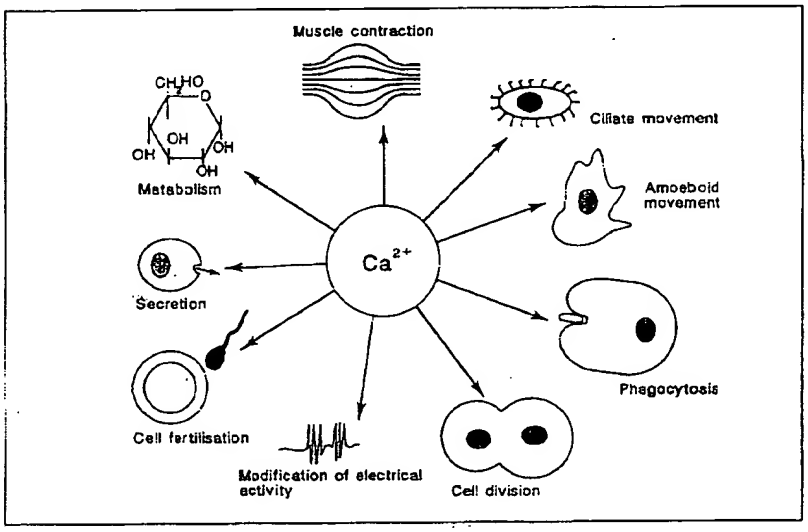

FIGURE 11 – Examples of phenomena activated by an increase in intracellular free Ca^{2+}. Metabolic and secretory pathways involved in Ca extrusion processes are instrumental in matrix-dominated (enzymatic) biocalcification (after CAMPBELL, 1983, slightly modified).

universal condition of life (KRETSINGER, 1983). An increase of $[Ca^{2+}]_i$ to 10^{-6} – 10^{-5} M normally activates the cell and is responsible for a wide spectrum of effects, for example, membrane transport and permeability (excitability), cell locomotion, gene expression, and stimulation of integrated processes such as mitosis, contraction, secretion of hormones, neurotransmitters, and exocrine products (compare Figure 11).

Excessive influx of Ca^{2+} to cytosol calcium can be toxic and is considered to be the common cause of cell injury and ultimately cell death (e.g. SCHANNE *et al.*, 1979; FARBER, 1981; TRUMP and BEREZESKY, 1985, 1992), probably because of the untrammeled action of Ca^{2+}-stimulated phospholipases and proteases (CARAFOLI, 1987). The cytotoxic effects of calcium result also from the very low solubility product of $[Ca^{2+}]$ and $[PO_4^{3-}]$ leading to precipitation of calcium phosphate deleterious to cell functioning. The universal phosphate-based cell energetics is of very ancient origin and is not compatible with higher concentrations of Ca^{2+} at neutral or basic pH typical for the cytosol (KRETSINGER, 1977a, 1983).

The general mechanisms by which most cells regulate intracellular Ca^{2+} is shown in Figure 12 (for extensive review see e.g. EXTON, 1988; TSIEN and TSIEN, 1990). Ca^{2+} entering the cell via systems of regulated membrane ion channels is extruded from the cell by the activity of (Ca^{2+}-Mg^{2+}) ATPase Ca^{2+} pumps located in the plasma membrane. There are also Na^+/Ca^{2+} exchange systems that can operate either to extrude or take up Ca^{2+}. They occur both in prokaryotic and eukaryotic cells. Mechanisms by which eukaryotic cells return to a low resting value of cytosolic calcium include – beside Ca^{2+} extrusion across the surface membrane – Ca^{2+} sequestration to internal Ca^{2+} stores such as the endoplasmic (sarcoplasmic) reticulum, mitochondria, and plasma membrane. All cells also possess various Ca^{2+}-binding proteins and other compounds that contribute to the intracellular buffering of free Ca^{2+} (CARAFOLI, 1987; PUTNEY, 1990). The endoplasmic reticulum has the highest capacity for storing calcium under physiological conditions, while mitochondria contribute only at abnormal (damaging) cytosolic Ca concentrations, exceeding 10^{-6} M, often leading to their pathological calcification, and are

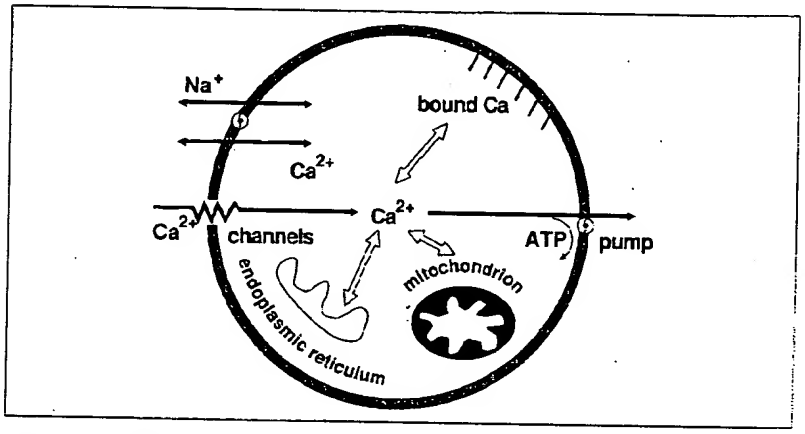

FIGURE 12 – Main pathways and stores controlling cytosolic Ca^{2+} in an eukaryotic (here mammalian) cell (after EXTON, 1988, modified).

rather insensitive to lower Ca^{2+} concentrations. Interestingly, the endoplasmic reticulum has a Ca^{2+} ATPase pump with a high affinity for Ca^{2+}, whereas mitochondria have a separate mechanism for releasing Ca^{2+} based mainly on a Na^{+}/Ca^{2+} exchanger. A possible explanation for this phenomenon within the bioevolutionary scenario implied by the SOH will be discussed below.

One of the most intriguing aspects of calcium regulation systems in eukaryotic cells is the great variety of proteinaceous Ca channels located at the plasma membrane. Although they all serve transmembrane Ca^{2+} transport into the cell, they do this in separate and often very complex ways. At least four different kinds of calcium channels have been recognized: leak channels, stretch-sensitive or mechanically-operated channels (MOCs), voltage-operated channels (VOCs), and receptor-operated channels (ROCs) (for review: MELDOLESI and POZZAN, 1987; TSIEN and TSIEN, 1990). The Ca influx through the stretch-sensitive and leak channels (the latter noticed mainly in vascular smooth muscles) is a consequence of the large electrochemical gradient across the cell membrane tending to drive Ca ions into the cell, and the fact that no membrane is perfectly impermeable, particularly when mechanically perturbed. This non-gated pathway of Ca influx cannot strictly be termed "channel". As VOCs are defined channels which are gated by membrane potential, whereas as ROCs those, which are activated as a consequence of neurotransmitter or hormone binding to specific membrane receptors.

Best known is the diverse group of VOCs which includes depolarization-dependent activation, selectivity by high-affinity binding of Ca^{2+}, and selective modulation by some external signals, e.g. extracellular Ca^{2+} concentration. VOCs can be divided into several subgroups, known, according to their functional classification, as L, T, N, and P channels, respectively. They differ significantly in their kinetics of activation, single channel conductance, and the duration of their openings and closings (e.g. NOWYCKY *et al.*, 1985; JAN and JAN, 1989; BEAN, 1989; TSIEN and TSIEN, 1990). Given this diversity, it is worthwhile asking what feature VOCs have in common apart from their steep voltage dependance. It is their >1000-fold higher selectivity for Ca^{2+} over Na^{+} or K^{+}, a selectivity much larger than other Ca^{2+} entry pathways. This extreme Ca^{2+} selectivity appears paradoxical in view of the very steep Ca^{2+} gradient occurring normally across the cell membrane. It may, however, make sense if considered an evolutionary remainder from times when the normal extracellular Ca concentration was much lower than today.

Under conditions of a steep transmembrane Ca gradient, Ca influx is apparently much better modulated by the ROCs, which activate Ca influx in the absence of changes in membrane potential. Two groups can be discerned: "true" ROCs where channel and receptor functions reside in the same molecule, and ROCs activated by second messengers generated following receptor activation (second messenger-operated channels, SMOCs). The latter are of particular interest because of their close connection with a great array of processes triggered by second messenger-activated redistribution of Ca^{2+} signals and the resulting interactions with other processes regulated by different second messengers. Compared to VOCs and ROCs, the action of SMOCs is primarily the prolongation of $[Ca^{2+}]_i$ signals and the generation of a cascade of slow-developing cellular processes. One of the best studied second messengers is inositol (1,4,5,)-trisphosphate ($InsP_3$). By generating internal calcium signals, it controls diverse processes such as fertilization, cell growth,

transformation, secretion, smooth müscle contraction, sensory perception and neuronal signalling (see BERRIDGE, 1993 for extensive review).

Generally more than one type of Ca^{2+} channels occurs in cells. This has been demonstrated in invertebrates (e.g. HAGIWARA *et al.*, 1975) and particularly in vertebrates (e.g. NOWYCKY *et al.*, 1985; KOSTYUK, 1989), for both excitable and non-excitable cells. The largest variability of Ca channels in a single cell has been observed in vertebrates. It is obvious that the diverse types of Ca channels, designed basically to transport Ca across the surface membrane, could not have appeared simultaneously in evolution. In view of this diversity we can join BERRIDGE (1993, p. 315) who, after asking the dramatic question: "Why did this diversity arise?" answers: "We can only surmise that a few basic signalling systems emerged in evolution and were then modified in subtle ways to meet the unique signalling requirements of different cells". We agree with that suggestion and can offer a plausible environmental foundation for such an evolutionary development through the hypothesis of a Ca-poor early alkaline ocean.

It is clear from this short review that the purpose of all Ca regulation and Ca extrusion systems is to keep the cytosolic Ca^{2+} concentration below the 10^{-6} M threshold so dangerous for cell functioning. The necessity of fast removal mechanisms in order to diminish the cytotoxicity of Ca was in all probability the reason for the development of the complex Ca-associated signalling and regulation systems observed in cells. MACCALLUM (1926) already suggested that life may have originated in an environment with a Ca concentration near cytosolic level, grew adjusted to it, and, as KRETSINGER (1983) added, developed elaborate mechanisms to maintain it. Our hypothesis meets all these presumptions well.

5.3 Biological and paleontological evidences for the early alkaline ocean

Interesting conclusions supporting the SOH can also be drawn from experimental and theoretical studies concerned with the origin of life. Environmental conditions favorable to biogenesis are still a matter of debate (PACE, 1991 for review).

Although acidic or neutral anaerobic hydrothermal systems have been considered by some authors (HOLM, 1992 for extensive review) to be the most probable settings for the origin of life, it is worth mentioning that an alkaline environment with pH values ranging between 8 and 9 has been postulated by ABELSON (1966). Under such conditions HCN and formaldehyde could inorganically be synthesized and ultraviolet irradiation could cause formation of various amino acids and other important biological substances. Abelson's experiments showed that the HCN polymerization reactions producing amino acids are very sensitive to pH, a 1 M solution of HCN will not polymerize at a pH of 4.6 and polymerization does also not occur at very high pH. The process proceeds, however, well at pH 8-9 and Abelson suggested such a pH range for the primitive ocean. Also experiments designed to simulate the origin of reproducing protocells have shown (SNYDER and FOX, 1975) that the assembly and stability of microspheres formed from any kind of proteinoids (preprotein) is limited by pH. The most stable mixture of acidic and basic microspheres displaying cell-like properties (enzyme-like activities) has been obtained in alkaline solutions with a pH up to 9.

The SOH allows not only low initial Ca concentrations but at the same time permits high phosphate levels. In this context the observations of FOX

(1968) and GABEL (1990) that inorganic phosphates and polyphosphates affect significantly composition and yield of proteinoids becomes important. DOSE and RAUCHFUSS (1972) reported the production of acidic and basic proteinoids in a single preparation by heating an alkaline mixture of amino acids with sodium polyphosphate.

Mitochondria have a specific and – for all eukaryotic cells – uniform relation to calcium which offers indirect clues as to the Ca^{2+} concentration in the early ocean. As mentioned above, mitochondria have low Ca storage capacities at cytosolic Ca^{2+} concentrations below 10^{-5} M. They increase their Ca intake capacity at higher cytosolic Ca^{2+} concentrations enormously, displaying, however, often symptoms typical of calcium intoxication. According to the widely accepted endosymbiotic theory of eukaryotic cell origin (e.g. MARGULIS, 1981; CAVALIER-SMITH, 1981), mitochondria represent prokaryotic organisms engulfed during eukaryogenesis by microbial host cells. After incorporation into the cytosol of a foreign cell, the mitochondrial organism could survive only at Ca^{2+} concentrations approaching those of their original environment, which in our reasoning should not be higher than 10^{-6} M. Furthermore, the Ca extrusion system in mitochondria is adjusted to low Ca levels only, because it is based on the rather simple Na^+-Ca^{2+} exchange mechanism which would not allow survival in a present-day extracellular Ca^{2+} concentration but was effective at the pre-mitochondrial stage of evolution.

Cyanobacteria seem to be particularly good indicators of ancient highly alkaline environments. Microfossils closely resembling filamentous and coccoid cyanobacteria are known already from early Archean sediments and the oldest are reported from 3.5 to 3.7 Ga old strata (AWRAMIK *et al.*, 1983; SCHOPF and PACKER, 1987; WALSH, 1992; SCHOPF, 1993). All modern cyanobacteria are without exception alkalophilic or at least alkalotolerant organisms (BROCK, 1973; KROLL, 1990) having extremely low requirements for Ca (GERLOFF and FISHBECK, 1969). Even slightly increased external Ca and/or Mg levels stimulate in cyanobacteria excretion of thick mucopolysaccharide sheaths (FOERSTER, 1964), which bind the surplus of extracellular Ca or Mg, keeping them out of the cell. These sticky compounds were in all probability the main factor responsible for the early establishment of benthic cyanobacterial communities which produced various microbialitic structures at sites of higher Ca influx into the Ca-poor Archean ocean (e.g. restricted evaporitic basins, vicinities of Ca-rich hydrothermal vents, areas influenced by terrestrial runoff or supratidal environments – see WALTER, 1983, for review).

Sodium appears to be essential for cyanobacterial growth (KRATZ and MYERS, 1955, ALLEN and ARNON, 1955), a further support for the SOH. Experiments have shown (e.g. ABE *et al.*, 1987) that under high Na concentration both CO_2 and HCO_3^- were actively transported into cells whereas under Na^+-deficient condition transport of both of these species was suppressed. Na^+ ions can substitute H^+ as the energy coupling ions in cyanobacteria as well as in many other bacteria (e.g. LANYI, 1979). According to SKULACHEV (1989, 1992), the reason for this substitution in marine bacteria is the adaptation to alkaline conditions, in which the concentration of protons is larger in the cytoplasm than outside and in which the electrochemical potential of the cells can be maintained by discharging Na^+ instead of protons. The large number of bacteria (including cyanobacteria) possessing primary Na^+ pumps (DIMROTH, 1990) and adapted to high pH indicates, according to

SEP-11-2002 11:20 LINDA HALL LIBRARYL 816 926 8785 P.30

SKULACHEV (1989), that this "sodium world" arose early in evolution and still occupies a large fraction of the biosphere. It is interesting to note that Na^+ is directly involved in energy transduction also in mitochondria and chloroplasts, as recently shown by SKULACHEV (1989). Should these organelles once have been free living, they must have been part of the highly alkaline "sodium world".

5.4 Calcium build-up in the ancient sea: a promoter of major steps in the evolution of life

Compared to other hypotheses of early ocean chemistry (for review see: RONOV, 1968; GARRELS and MACKENZIE, 1971; HOLLAND, 1972; MAISONNEUVE, 1982; WALKER, 1983) the hypothesis of an alkaline ocean has a substantial advantage: it provides a plausible geochemical scenario for major innovations in the evolution of early life. Changes in extracellular Ca^{2+} level are known to induce and control many critical metabolic and morphogenetic processes, in fact some of these can only be initiated at strictly defined extracellular Ca^{2+} levels. Taking this into account, KAŹMIERCZAK and DEGENS (1986) and KEMPE *et al.* (1989) have interpreted some of the key events in the evolution of Precambrian life, such as eukaryogenesis, increase in morphological diversity of unicellular eukaryotes, origin of multicellularity, and the onset of biocalcification, as the result of gradually increasing Ca^{2+} pressure upon the evolving biota. The interpretation has been supported by data derived from cell physiology, developmental biology and ecotoxicology and confronted with the known Precambrian paleontological record. As the paper presenting most of the data was published in a periodical of rather limited circulation, particularly among biologists, we feel that it may be beneficial for the current presentation to recapitulate its main points.

One of the most critical innovations in evolution was undoubtedly eukaryogenesis (eukaryosis), which arose, according to the most widely accepted theory, by serial endosymbiosis (MARGULIS, 1981; SITTE, 1993, for review). The eukaryotic (or better proto-eukaryotic) ancient "host" cell acquired chloroplasts and mitochondria symbionts by means of endocytosis (e.g. CAVALIER-SMITH, 1981; MUSCATINE, 1982). In experimental transfer of isolated mitochondria into yeast protoplast (KOVAC *et al.*, 1989; SULO *et al.*, 1989) it was found that an optimal frequency of transfer and satisfactory protoplast-to-protoplast fusions were obtained when the isolated mitochondria and protoplasts have been pretreated with Ca^{2+} ions (introduced to the medium as 10 mM $CaCl_2$). Apparently the Ca^{2+} ions are instrumental in firmly binding the mitochondria to the surface of protoplasts. Furthermore, experiments with various amoebas show that the two fundamental types of endocytosis, i.e., pinocytosis and phagocytosis, are Ca-dependant, with maximum uptake at 10^{-4} M external Ca^{2+} level (PRUSCH and MINCK, 1985; YOUNG, 1985). Decline in extracellular Ca^{2+} below 10^{-5} M diminishes profoundly the endocytotic capacity of amoeba. Transferring these Ca^{2+} thresholds to the scenario of the Ca-poor Precambrian ocean, it can be concluded that the sustenance of the first endosymbiotic cellular systems leading to the origin of true eukaryotic cells was most probably not possible until the extracellular Ca^{2+} level was well $>10^{-5}$ M (Fig. 3). This level could have been attained quite early, judging from recent paleontological findings of eukaryotic fossils in sediments 2.1 Ga old (HAN and RUNNEGAR, 1992). An origin of eukaryotic cells much earlier than 2 Ga is also suggested by extrapolating the rate of protein evolution (e.g. WOESE, 1987). This may implicate that some of the eukaryogenic events

could have occurred at sites of higher Ca inputs (e.g. at hydrothermal or river influxes) into the otherwise Ca-poor ocean.

Ca has probably been also involved in nucleus formation in protoeukaryotes. The Ca level plays a crucial role in maintaining chromosome configuration (BAJAJ *et al.*, 1971) and modulates the distribution of condensed and diffused chromatin (AARONSON and WOO, 1981; MATSUMOTO and TAKYU, 1986). Ca^{2+} is reported to regulate various nuclear activities in animals, for instance the initiation of DNA synthesis (BOYNTON *et al.*, 1980), assembly and disassembly of microtubules in chromosome movement during mitosis (HEPLER, 1992), and regulation of cell proliferation (SASAKI and HIDAKA, 1982). Nuclear Ca^{2+} appears to be regulated independently of cytoplasmic Ca^{2+} by gating mechanisms in the nuclear envelope (WILLIAMS *et al.*, 1985). This strongly implies that the shift of the genetic material to the cell interior in protoeukaryotes and its membranization could have been an adaptive response to protect the genetic material against the deteriorating influx of excessive Ca^{2+}, due to its build-up in the environment. Cell nucleus formation had not to be necessarily associated with a significant increase in cell size as usually proposed by students of Precambrian microfossils (e.g. SCHOPF, 1978; KNOLL, 1983; VIDAL, 1984).

According to CAVALIER-SMITH (1987), the key step in the evolution of eukaryotes was the development of the cytoskeleton which enables the cell to keep the structural integrity – a basic prerequisite to have a fluid outer membrane. There are indications that both synthesis and disassembly of basic cytoskeletal proteins (tubulin and actin) comprising cytosolic microtubules and microfilaments are highly Ca^{2+} and Mg^{2+}-dependent (e.g. GAL *et al.*, 1988; STOSSEL, 1989). The changes in microtubule organization caused by changing external concentrations of these cations are in certain organisms very fast and often associated with impressive morphogenetic effects (GOODWIN, 1989).

Besides in cyanobacteria, extremely low Ca requirements have been observed in some fungi and unicellular algae. Particularly interesting in that regard are some unicellular and coenobial algae, (e.g. some species of *Chlorella* and *Scenedesmus*; see O'KELLEY, 1968; GERLOFF and FISHBECK, 1969) which bear some resemblance to Precambrian larger unicells called acritarchs. Small (10-15 µm in diameter), spherical acritarch-like microfossils appear first in deposits ca. 2.4-2.3 Ga old (e.g. HOFMANN, 1976). In sediments ca. 2.0 Ga old larger and morphologically diversified unicells appear which are known as acanthomorph acritarchs (e.g. PFLUG and REITZ, 1985; HOFMANN and GROTZINGER, 1985). In our opinion, they may represent a response of acritarch organisms to increasing marine Ca^{2+} concentration. Environmental Ca^{2+} level has a profound impact both on size and shape of algal cells. For example, cells of *Chlorella* growing in Ca^{2+}-depleted water are much smaller than cells from Ca^{2+}-rich media (STEGMANN, 1940). Media with Ca^{2+} concentrations < 10^{-4} M caused not only a decrease in cell size in the green alga *Scenedesmus* but evoked also change in the shape of the cells from typically spindle-like to ellipsoidal or spherical (KYLIN and DAS, 1967; TRAINOR, 1969). Prominent phenotypic expressions have been exerted in the siphonalean green algae *Acetabularia* by changing extracellular Ca levels (HARRISON and HILLIER, 1985; GOODWIN, 1989; GOODWIN and TRAINOR, 1985).

During the Proterozoic, acritarchs increased considerably in diversity and near the turn Precambrian/Cambrian some of them achieved impressive sizes, for unicellular organisms, while others developed great varieties of shapes

(e.g. VIDAL and KNOLL, 1982; VIDAL, 1984; WANG, 1985). It may be presumed that the evolutionary tendency of acritarchs to increase size and shape diversity was a survival strategy invented by these unicells to cope with the dramatic increase of Ca^{2+} concentration in the ambience. The great influx (uptake) of this dangerous cation (similarly as in case of other metal ions) pushed the cells to increase the rate of its excretion. An optimal excretionary surface to volume ratio in initially small cells could be achieved either by increasing the cell diameter or by development of various secondary structures, like appendages or spines, increasing the cell surface without radical change in cell diameter. In the fossil record, the first strategy is represented by the giant, spherical *Chuaria* (e.g. HOFMANN, 1985), the second by an array of variously sculptured late Proterozoic acritarchs (e.g. VIDAL and KNOLL, 1982; WANG, 1985; MOCZYDOWSKA *et al.*, 1993) attaining often also remarkably large sizes (e.g. VIDAL, 1990).

Large phosphogenic events noticed near the end of the Precambrian (SHELDON, 1981; COOK and SHERGOLD, 1984) intensified probably the Ca stress experienced by the planktonic algae. It is known that Ca migration into cells is enhanced in the presence of higher extracellular concentrations of inorganic phosphate (COTMORE *et al.*, 1971; BORLE, 1981) and synergistic action of Ca^{2+} and PO_4^{3-} may even produce sublethal or lethal effects (DZIAK and BRAND, 1974; HELLMAN and ANDERSON, 1978). Planktonic algae respond to simultaneous excess of Ca^{2+} and PO_4^{3-} by copious excretion of mucopolysaccharides and glycoproteins (CHROST, 1978) and often also with an increase in cell size (FRIEBELE *et al.*, 1978; SMITH and KALF, 1982).

The function of Ca in cell contact physiology in metazoans and aggregates of protists and fungi permits to draw far-reaching conclusions concerning the significance of increasing Ca^{2+} concentration in the early ocean for promoting the origin of multicellular life forms. Of particular interest are here the definite extracellular Ca^{2+} concentration thresholds indispensable for cell-to-cell adhesion, cell aggregation and many other cell contact phenomena reported from various groups of organisms.

Colony formation in the green alga *Coelastrum* is directly controlled by extracellular Ca^{2+} levels (CHAN, 1976). A medium with a Ca^{2+} concentration of ca. 2×10^{-4} M supported only growth of unicells. Formation of colonies was induced by raising the Ca^{2+} level to 2×10^{-3} but further increase to 10^{-2} M and higher had inhibitory effect on *Coelastrum* growth.

Extracellular Ca^{2+} levels of about 10^{-5} M is needed for initiating cell aggregation in yeast (e.g. ROSE, 1984) and slime mold (BONNER, 1971). Ca^{2+} is linking anionic groups of cell wall components of adjacent cells and may act as co-factor in activating the binding capacity of certain glycoprotein component to carbohydrate (BURGER and MISEVIC, 1985).

The presence of the oldest coenobial algae (? protovolvocaeans) in the ca. 1.9 Ga old Gunflint Iron Formation (KAZMIERCZAK, 1976) can be taken as an indication that the critical environmental Ca^{2+} level of about 10^{-4} M needed for inducing cell aggregation in algal protists was probably established by that time. A significant increase in abundance and variety of coenobial and colonial algae occurred during the late Proterozoic (e.g. TIMOFEEV, 1969; LINDGREN, 1982; TYNNI and UCTELA, 1984). The intensive aggregation of algal cells during that time was probably enhanced by the aforementioned simultaneous excess of Ca^{2+} and PO_4^{3-} in seawater.

It seems that calcium was directly involved in the origin of metazoan life

forms. Early observations of HERBST (1900) and HOLTFRETER (1943) showed that in extremely Ca-deficient solutions cells of gastrulating embryos and tissues fail to adhere and that cell aggregates disintegrate. It follows that a certain critical concentration of free Ca^{2+} is absolutely necessary to keep metazoan cells together. Sponges provide a classical example of Ca^{2+}-dependent cell aggregation. *Microciona* and *Haliclona* cells disintegrate if the Ca level falls below 10^{-5} M and they reaggregate after the Ca concentration has been increased above this level (KRETSINGER, 1977a). Similar experiments carried out on embryos and tissues of various animals demonstrate that in most of them cells failed to adhere when the extracellular Ca^{2+} level is $< 10^{-4}$ M. This is because withdrawal of Ca leads to a disruption of intercellular junctional complexes (e.g. GILULA and EPSTEIN, 1976; FRANCHI and CAMATINI, 1982; VOLBERG *et al.*, 1986). For instance, LANE (1968) reported that for this reason hydroids cease growth when external Ca^{2+} is $< 10^{-4}$ M, and ARTHUR and SANDBON (1969) observed the same for nematodes.

It has also been demonstrated that extracellular Ca^{2+} and other divalent cations can trigger cell membrane lysis and cause cell fusion (PAPAHADJOPOULOS *et al.*, 1990 for review). Biomembrane fusion is a basic event which is essential for a large number of biological processes like the formation of bi- and multinucleate syncytia and giant cells, polykaryons and heterokaryons (e.g. MCCONACHIE and O'DAY, 1986; SALHANI *et al.*, 1985; LEE and BROWN, 1987). The cell fusion process can be accelerated by, for instance, preincubating the cells in a medium with high pH (> 10), a temperature of about 37°C and subsequent addition of Ca (TOISTER and LOYTER, 1971). Similar cell fusion phenomena could have been promoted in the alkaline Precambrian ocean at sites where Ca was injected (hydrothermal vents or groundwater seepage), which – in the case of heterotrophic unicells – may have led to the origin of polykaryon (multinuclear) organization (e.g. some ciliates) and – in the case of algal cells – to a coenocytic Bauplan (e.g. siphonalean algae). Some nonseptate or sparingly septate, branched filamentous fossils appearing in sediments ca. 2 Ga old and younger (compare CLOUD, 1976; AWRAMIK and BARGHORN, 1977) may already represent first coenocytic algae. Many megascopic carbonaceous fossils (vendotaenids, beltinids, moranids etc.) ranging from the early Proterozoic into the Phanerozoic (e.g. HOFMANN, 1985; STEINER *et al.*, 1992) represent probably coenocytic organization as well. They also showed a tendency towards an increase in cell size with time similar to the already discussed unicellular and colonial algae (HOFMANN, 1985, for review).

These observations allow the general conclusion that extracellular Ca^{2+} levels of between 10^{-5} to 10^{-4} M could be a chemical prerequisite for the origin of metazoan, coenobial, colonial, syncytial, and polykaryon organizational stages in evolution. Such Ca^{2+} levels could have been reached in the ocean quite early, presumably in the early Proterozoic, due to the intensified riverine input of Ca as a result of the rapid cratonization beginning at the end of the Archean (VEIZER and COMPSTON, 1976; KRÖNER, 1984; VEIZER, 1985).

5.5 Biocalcification: an evolutionary product of Ca extrusion systems in Ca-stressed cells

Explaining the onset of the biocalcification at the Pϵ/ϵ boundary as the common response of many groups of marine biota to a dramatically increased Ca level (KAŹMIERCZAK *et al.*, 1985) is a logic extension of the soda ocean hypothesis (KEMPE and DEGENS, 1985). The concept of "Ca stress" (DEGENS

et al., 1985) implies that temporally high Ca concentrations exert a physiological pressure upon the evolving biota. Ca stress has been supposed to be the geochemical factor triggering the onset of biocalcification and subsequent events of heavy calcification as well as the later carbonate and phosphate skeletonization in additional marine groups (chordates, benthic and planktonic foraminifers, coccolithophorids, calpionellids, scleractinian corals, bryozoans, etc.). However, even though the external Ca concentration is very important to the organisms, the influx of Ca into the cells is usually mediated (enhanced or impeded) by a number of other factors such as light, pH, alkalinity, and the concentrations of oxygen, Mg, and PO_4^{3-}. Light, hypoxia, increased pH, alkalinity, and PO_4^{3-} are known, for instance, to enhance Ca migration into cells (e.g. BORLE, 1981; ROOS and BORON, 1981; CAMPBELL, 1983; TRUMP and BEREZESKY, 1985, 1992). These synergisms must also have been instrumental for the onset of biologically controlled (enzymatic) biocalcification at the Pє/є boundary.

Cells of biomineralizing systems can create conditions in which ions reach sufficiently high concentrations to cause mineral deposition in association with various biopolymers within fluid microenvironments. Some 60 different mineral types have been identified from 55 organismal phyla (LOWENSTAM and WEINER, 1989; SIMKISS and WILBUR, 1989). In most of the phyla nucleation and mineral growth occurs within a preformed matrix that almost always includes acidic macromolecules rich in carboxylate, sulfate, and/or phosphate moieties (WEINER *et al.*, 1983; ADDADI *et al.*, 1989; WEINER and ADDADI, 1991).

SIMKISS (1976) and WILBUR (1980) formulated three basic rules for the functioning of eukaryotic mineralizing systems (summarized in WILBUR, 1984), enclosing those consisting of an epithelium, of single cells, and of mineralizing intracellular vacuoles: (I) the ion activity product must exceed the solubility product of the precipitating mineral; (II) biomineralization is associated with secretion of organic matter by mineralizing cells; and (III) crystal formation occurs usually in fluid microenvironments.

Rule III is straightforward, but the others need comment. In matrix/crystal interaction (rule II) it is generally assumed that the organic matrix plays a critical role in regulating growth and morphology of the mineral phase (e.g. CRENSHAW, 1982; WEINER *et al.*, 1983; WHEELER and SIKES, 1984). Dissolving the biomineral with EDTA or other weak acids yields a soluble matrix fraction (SM) which is capable of binding Ca. The presence of SM is often cited as evidence that the matrix initiates and controls crystal growth (ADDADI and WEINER, 1989; MANN *et al.*, 1989, for review). WHEELER *et al.* (1987) and WHEELER and SIKES (1989), however, expressed the opinion that the hypotheses which rely on SM Ca-binding need to be re-evaluated because crystal-binding, rather than Ca-binding by the SM is responsible for the initiation of biomineral formation.

We already discussed how Ca^{2+} enters cells and which modes of Ca^{2+} capacitation exist within cells. In order to meet rule I it would, however, be interesting to explore the way (or ways) on which Ca^{2+} is transported to the site of precipitation and where the HCO^{3-} and PO_4^{3-} are derived from to produce biominerals.

Biomineralization is apparently linked to the proficiency of living systems to cope with reactive metal ions in the environment. To utilize some of them as key constituents in growth and metabolism was an essential achievement of evolution. Biocalcification could, therefore, be interpreted to be an

evolutionary derivative of the function the reactive Ca^{2+} plays in cells (KAŹMIERCZAK and DEGENS, 1986; SIMKISS, 1989).

The messenger function of Ca is, according to our scenario, of very ancient origin and the gradually (or sometimes spasmodically) increasing environmental Ca concentration must have caused life to evolve suitable Ca regulation and extrusion mechanisms. These include extracellular Ca-binding polymers and Na^{+}-Ca^{2+} exchanger in prokaryotes and a variety of Ca^{2+} channels and sophisticated Ca^{2+} regulation systems in eukaryotes. An excessive influx of Ca^{2+} into eukaryotic cells, leading to a physiological Ca^{2+} stress, must have been compensated by an increased efflux of this cation. This may have resulted in the evolution of a large array of Ca^{2+}-affine secretory macromolecules carrying Ca in a complexed (bound) form via the endoplasmic reticulum, Golgi stack and Ca-ATPase pump to intra- and/or extracellular sites. Acidic glycoproteins, sulfated proteoglycans, glycosaminoglycans, acidic polysaccharides, phosphoproteins, or phospholipids are associated with cytoplasmic vacuoles, lysosomes, secretory granules, matrix vesicles, and membrane bound vesicles in eukaryotes ranging from protoctists to vertebrates (e.g. NILSSON and COLEMAN, 1977; ANDERSON, 1985; MANN *et al.*, 1986; BEAUDOIN and GRONDIN, 1991; NICAISE *et al.*, 1992). All of these macromolecules have a high Ca storage capacity and are involved in post-translational processing of carbohydrate moieties of membrane and secretory proteins (including functional calciproteins such as calmodulin, troponin-C and parvalbumin), part of which are sequestered on that way before exocytosis. Secretion therefore serves a dual purpose: metabolic waste discharge and Ca^{2+} detoxification. Because the same as above groups of high affinity Ca-binding acidic macromolecules are typical components of the so-called calcifying matrices identified in almost all carbonate and phosphatic biominerals (e.g. VEIS *et al.*, 1977; WHEELER and SIKES, 1984; KEMP, 1984; WEINER *et al.*, 1983; WEINER and ADDADI, 1991), biocalcification can also be considered as a means of Ca detoxification or at least as part of the cellular Ca extrusion system.

It still needs to be explained why the same Ca-loaded polymers are in one site associated with biominerals but not in others. Apparently biomineralization depends on the ability of cellular systems to provide for a space where a supersaturated solution can be sustained to facilitate a continuous biomineral growth (rule I). This implies (i) that Ca^{2+} is liberated from its carrier at the calcification site; that (ii) Ca^{2+} is provided at similar rates as carbonate and phosphate ions; and that (iii) the reaction space must be fluid in nature.

The catabolic degradation of the Ca^{2+}-binding polymers is poorly understood. It may occur after leaving trans Golgi (DEGENS, 1976 for review). Solubilization by uronic acids or similarly acting sugars and subsequent action of proteases could liberate Ca^{2+} from its carrier. Discovery of Ca-dependent non-lysosomal proteases (calpains) active at cellular membranes (MURACHI *et al.*, 1981; PONTREMOLI and MELLONI, 1986) indicates that such enzymatically controlled Ca^{2+} source is feasible. Ca-dependent proteases can act as a kind of homeostat, autoactivating when cytosolic Ca^{2+} concentration is significantly elevated (MELLGREN, 1987), suggesting that cleavage of Ca carriers could be triggered by Ca^{2+} influx into cells.

The carbonate and phosphate ions for biomineralization are supplied by carbonic anhydrase (CA) and alkaline phosphatase (AP), enzymes which are known to be associated with biocalcification.

CA catalyses the reversible hydration of CO_2 to HCO_3^- and may therefore liberate the carbonate ions needed to form $CaCO_3$ (WILBUR and SALEUDDIN, 1983; KINGSLEY and WATABE, 1987) or it may function in the reverse direction removing H^+, thereby increasing pH and enhancing calcification (WHEELER, 1975). CA may also facilitate CO_2 transfer from the external medium to the calcification site (CHEN and LAWRENCE, 1987). Evidence in general suggest that dissolved inorganic carbon, i.e. the substratum for the CA activity at calcification sites, is primarily derived metabolically even though external supply may also occur (SIKES and WHEELER, 1983; SIMKISS and WILBUR, 1989).

AP is associated with mineralization in vertebrates but also in several groups of invertebrates (for review: WUTHIER and REGISTER, 1985; DONACHY *et al.*, 1990). It increases the concentration of inorganic phosphate locally, acts as a phosphate carrier, and mediates the hydrolysis of organic phosphate compounds thereby increasing the concentration of PO_4^{3-} at sites of biomineral formation (e.g. KAKUTA *et al.*, 1985; HUNTER *et al.*, 1993).

There is little doubt that these enzymatic systems existed long before the onset of biocalcification as an integral part of the cell's metabolic system responsible for sequestration, degradation and extrusion of metabolic waste products, including metal detoxification. Two different strategies of metal detoxification have evolved : (i) transition and trace metals are bound to PO_4^{3-} and neutralized in ortho- and polyphosphate metal-enriched granules (SIMKISS and MASON, 1983; SIMKISS and TAYLOR, 1989); and (ii) calcium is bound to macromolecules of high Ca^{2+} affinity and transported together with metabolic phosphate to final neutralization sites. Either they are diffused in ionic form to the external environment or kept inside as tiny intra- and extracellular Ca phosphate "packages". In light of the early alkaline ocean hypothesis one can assume that the first detox-systems derived from times when metal cations were abundant but Ca concentration was low. The later Ca^{2+} increase caused acute problems for the cells because higher Ca^{2+} influx required higher Ca^{2+}-binding capacities in Ca-transporting macromolecules and raised problems at Ca^{2+} diffusion sites. The dramatic Ca^{2+} buildup in the seawater near the Proterozoic limited the effectiveness of diffusion and lead to increased supersaturation at epithelial extrusion sites causing mineral nucleation. The high environmental PO_4^{3-} concentrations derived from anaerobic basins and the accompanying Ca^{2+} shifted the ion activity product of the first exoskeletons in favour of Ca phosphate minerals. With the rapid depletion of phosphate from the ocean, biomineral formation shifted, with the exception of chordate endoskeletons and a few invertebrate groups, to calcium carbonate.

Two principally different biomineralization processes are distinguished (e.g. LOWENSTAM and WEINER, 1989): biologically induced or non-enzymatic mineralization, resulting from the interaction of the organisms with its environment, and biologically controlled or enzymatic (called also, after LOWENSTAM, 1981, organic matrix-mediated) mineralization, which is conducted under strict cellular control through the influence of organic polymers.

The **biologically induced** calcification characterizes bacteria and lower plants (algae). It is usually the result of CO_2 fixation by photoassimilation whereby minerals precipitate at the cell surface because of the increasing CO_3^{2-} ion activity and therefore $CaCO_3$ supersaturation in the cell ambience. Good examples for this mineralization are the modern and fossil in situ calcified cyanobacterial mats known as stromatolites and thrombolites (GOLUBIĆ, 1973; KRUMBEIN, 1979; PENTECOST and RIDING, 1986, for review).

As already mentioned (Chapter 3.2) cyanobacterial mat calcification is initiated only at high carbonate mineral supersaturations ($SI_{aragonite} > 0.8$; KEMPE and KAŹMIERCZAK, 1990a). As an example, the modern in vivo calcified cyanobacterial mat from Satonda Crater Lake is shown in Figure 13 (KEMPE and KAŹMIERCZAK, 1990b, 1993). It demonstrates that the stromatolitic structure is actually the product of two different biologically induced calcification processes: (i) the in vivo precipitation of high Mg-calcite at the surface of the cyanobacterial mat (dark laminae), due to the high calcite supersaturation of the lake water during the dry season, and (ii) the early postmortem permineralization with aragonite (light laminae) of remnants of non-calcified cyanobacteria (possibly grown during the wet season at lower supersaturation in the lake water) triggered by an alkalinity increase within the decaying mat due to the action of sulfate reducing bacteria (KAŹMIERCZAK and KEMPE, 1990, 1992). Such microbialites can be seen as analogues of Precambrian stromatolites which were, up to the appearance of skeleton-bearing organisms at the P€/€ boundary, the only macroscopic products of marine biocalcification. In the highly alkaline and Ca poor Archean seawater they could have formed only at places of notable Ca and Mg influx where not only high supersaturations of carbonate minerals could arise but where also enough divalent ions were available. With the beginning of the Proterozoic, a decreasing alkalinity caused an increase in Ca^{2+} and enough Ca was available in seawater to trigger widespread growth of stromatolites in open marine shallow waters. In the Riphean (late Proterozoic) the peak of this development was reached and widespread, thick series of microbialitic limestones formed (GROTZINGER, 1989, for review). Thus, high carbonate mineral supersaturation in seawater can be taken as the major factor responsible for the intensive formation of carbonate microbialites during the Precambrian (GROTZINGER, 1990; KEMPE and KAŹMIERCZAK, 1990a).

The first wave of **biologically controlled** biocalcification close to the P€/€ boundary led predominantly to the evolution of phosphatic skeletons (LOWENSTAM and MARGULIS, 1980; BENGTSON and CONWAY MORRIS, 1992). At that time seawater must have had a high PO_4^{3-} concentration as witnessed by large contemporary phosphorite deposits (SHELDON, 1981). It has even been suggested that this "phosphogenic event" was the triggering mechanism for skeletonization by increasing the metabolic rates of many organisms (COOK and SHERGOLD, 1984). Knowing, however, that increased PO_4^{3-} levels increase the migration of Ca^{2+} into cells (as described above), it can easily be conceived that such synergism caused phosphate precipitation in cells due to enhanced supersaturation of calcium phosphates close to the cell membranes.

The high phosphate concentration at the P€/€ boundary is most probably connected with oceanic overturns (for review: BRASIER, 1992; TUCKER, 1992). In our scenario the increase of PO_4^{3-} in anaerobic basins is easily explained with our "alkalinity pump" concept: the increased sulfate concentration of the late Proterozoic ocean made sulfide available in excess of iron which prior to the availability of sulfate regulated phosphate concentrations (compare also Fig. 6). Furthermore, these anaerobic basins produced spikes of alkalinity further stressing the evolving organisms. Experiments by BACHRA (1963) showed that in solutions containing Ca^{2+} and PO_4^{3-} shifts in HCO_3^- concentration can alter the proportion of the precipitated Ca carbonates versus the Ca phosphates (Figure 14).

The previous suggestions that increased oxygen levels promoted the origin of metazoans and the onset of biomineralization (TOWE, 1971, 1981; KNOLL, 1991)

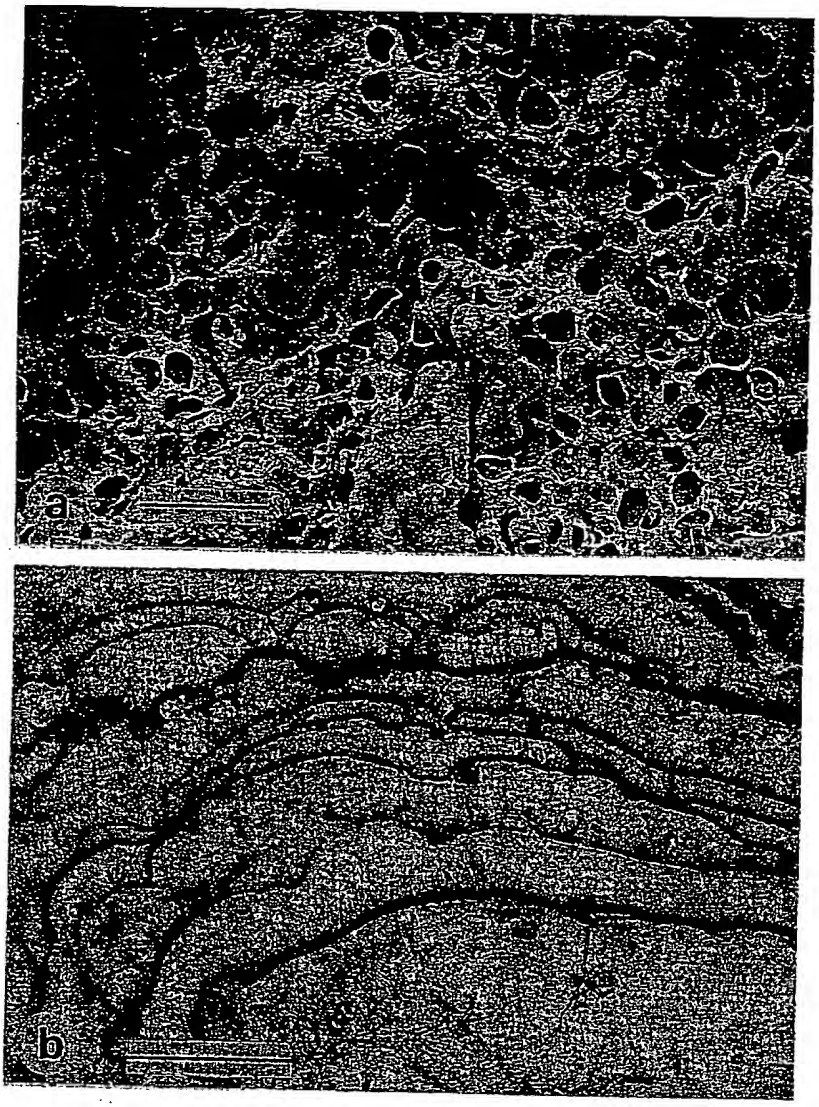

FIGURE 13 – Modern analogue of ancient calcareous stromatolites produced by in situ calcification of benthic cyanobacterial mat evoked by high but fluctuating level of calcium carbonate saturation in the environment. a: SEM view of living surface of a coccoid cyanobacterial mat in part heavily permineralized with microgranular high-Mg calcite; b: microscopic vertical cross section of a stromatolitic structure built by coccoid cyanobacteria shown in (a); the fine lamination is the result of alternation of in vivo with permineralized cyanobacterial layers (dark laminae) and early post-mortem with aragonite permineralized cyanobacterial layers (light laminae). The critical factor controlling the mineralogy and mode of permineralization in these microbialitic structures are seasonal fluctuations in calcium carbonate saturation in the water column (KAŹMIERCZAK and KEMPE, 1990). Satonda Crater Lake, Indonesia; bar scales equal: in (a) – 50 µm, in (b) – 300 µm.

Figure 14 – Exp
phosphate and ap
calcium, carbonat
and 22 mM HCC
diagrams sugge
biocalcification
simultaneous Ca
Under slightly inc
phosphate deposit

are weakened
(algal) life for
RIDING, 1992)
already in the e

It should b
near the Pϵ/ϵ
appeared. In th
to detoxify no
abundant in t
microscopic bi

Special me
metabolically
insoluble gra
skeletonized an
1989; BROWN,

ced by in situ
vel of calcium
: of a coccoid
h-Mg calcite;
lt by coccoid
f in vivo with
with aragonite
ontrolling the
s are seasonal
K and KEMPE,
(b) – 300 µm.

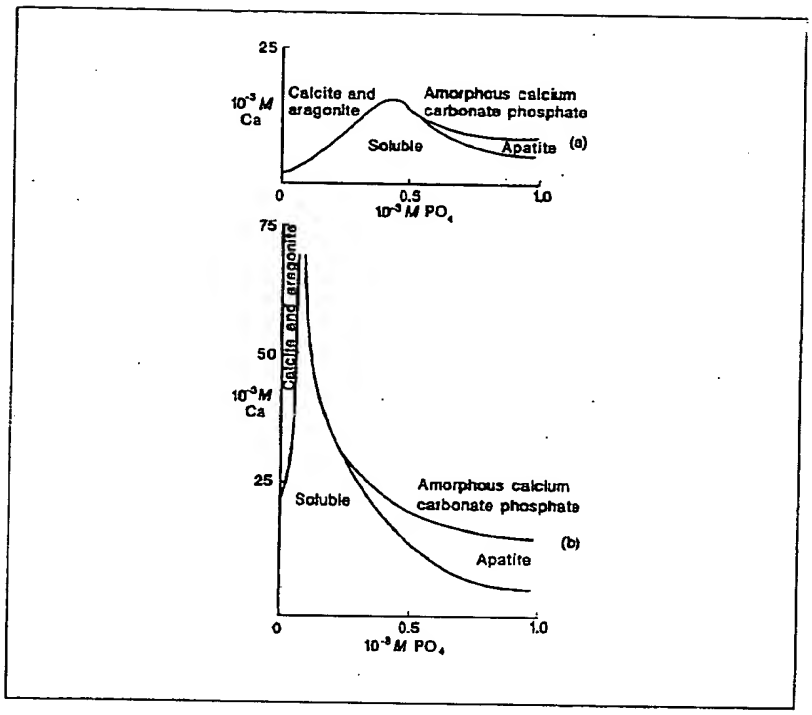

Figure 14 – Experimental carbonate (calcite and aragonite) and phosphate (amorphous Ca phosphate and apatite) mineral deposition from solutions containing various concentrations of calcium, carbonate and phosphate ions. Two series of solutions were employed: 110 mM (a) and 22 mM HCO_3^- (b) (from BACHRA, 1963, modified by WILBUR and SIMKISS, 1968). The diagrams suggest that the predominance of phosphatic skeletons during the onset of biocalcification at the transition Precambrian/Cambrian could be a synergistic effect of simultaneous Ca^{2+}, PO_4^{3-}, and HCO_3^- excess in shallow waters caused by oceanic overturn(s). Under slightly increased PO_4^{3-} concentrations even at lower HCO_3^- and Ca^{2+} concentrations Ca phosphate deposits clearly predominate over carbonate minerals.

are weakened by recent findings documenting the existence of eukaryotic (algal) life forms 2.1 Ga old (HAN and RUNNEGAR, 1992, and a comment by RIDING, 1992), which require an at least mildly oxygenated atmosphere already in the early Proterozoic (RUNNEGAR, 1991).

It should be stressed that during the impressive skeletonization events near the Pϵ/ϵ boundary mostly calcareous and phosphatic macroskeletons appeared. In the much longer pre-macroskeletal period during which cells had to detoxify not only Ca but predominantly transition and heavy metals abundant in the Precambrian sea, the formation of less spectacular, microscopic biomineral structures could be expected.

Special mechanisms of cell detoxification by binding excessive metals to metabolically produced phosphates and precipitating them in the form of insoluble granules which are widely distributed in extant both non-skeletonized and skeletonized animals (SIMKISS, 1981; SIMKISS and TAYLOR, 1989; BROWN, 1982), may be reminders of this ancient detoxification

SEP-11-2002 11:25 LINDA HALL LIBRARYL 816 926 8785 P.40

mechanism. Interestingly, these spherical granules, 1-100 µm in diameter, are formed in close association with the Golgi complex, endoplasmic reticulum, lysosomes and membrane-bound vesicles. Also the metal-affine organic matrix is similar for sites producing granules and for sites forming macroskeletons. However, even if these microscopic mineral deposits predate the Pϵ/ϵ skeletonization events by far, they would be difficult to find and to extract from the rock record. Similarly, various spicular elements, abundant in many extant lower metazoans (particularly members of marine meiofauna – compare e.g. RIEGER and STERRER, 1975), could have been existing prior to the onset of macroscopic skeletons. We therefore agree with SIMKISS (1989) that the cellular mechanisms, involved in the macroskeleton formation, must have existed prior to the Pϵ/ϵ transition for several hundred millions of years.

Among the Phanerozoic skeletonization events, the emergence of the calcareous nannoplankton (coccolithophorids) in the early Jurassic and of the planktonic foraminifers in the late Triassic (HERMAN, 1979) are the most important. Both groups certainly existed long before they started calcification, which was, in our opinion, a response to a Ca stress which arose after the great Permian/Triassic oceanic overturn and after the Permian extraction of Ca as sulfate and carbonate deposits which lead to a low overall Ca balance for the ocean. Also the reestablishment of anoxic basins and the production of excess alkalinity played a role. It is known that higher Ca^{2+} concentration and pH enhances coccolith formation in coccolithophorids, whereas lower pH and Ca^{2+} concentrations suppresses coccolith formation even though viable cells have been observed both in nature and in culture (e.g. SWIFT and TAYLOR, 1966; SIKES and WILBUR, 1980). Other Phanerozoic skeletonization events, like for example, the appearance of calcareous benthic foraminifera in the Devonian or of scleractinian corals in the Triassic, could also have been caused by environmental Ca stress to which the non-calcifying predecessors of these groups have been exposed.

6. OUTLOOK

The coupled changes of alkalinity, calcium and $CaCO_3$ supersaturation through Earth history provide a powerful mechanism which could have promoted evolution of living systems (Figure 15). The Precambrian alkaline ocean and the "alkalinity pump" operating on and off in the Phanerozoic ocean are geochemically plausible scenarios. In the discussion we tried to show the evidence in favour of these scenarios. From the many arguments which we present, two seem to be the most convincing for us:

- The close comparability of present day environments generating in situ calcified microbialites with the alkaline Precambrian seas sustaining calcareous stromatolites; the recurrence of such microbialites in Phanerozoic epicontinental seas due to alkalinity plumes from anaerobic basins.
- The role of calcium for the biochemistry and physiology of the cell, which could have evolved only in an environment of very low ionic calcium concentration, such as is provided in highly alkaline waters.

Integrating a large body of knowledge from a wide spectrum of geological, chemical and biological sciences is a difficult task. If all of the observations, which we cite in favour of our hypotheses, will stand closer inspection will be seen in the future. We think that the early alkaline ocean offers new explanations for many aspects in the evolution of life and in the geologic history, which so far were not explained satisfactorily.

FIGURE 15 – Curves representing changes in oceanic Ca^{2+} concentration through geologic time as inferred from the hypothesis of the early alkaline (sodic) ocean. Some major biogeochemical and bioevolutionary events associated with changes in Ca^{2+} levels are indicated as well as sources of alkalinity controlling the saturation levels with respect to carbonate minerals and the intensity of biocalcification in the marine environment. The distinct distortion of the curve near the transition Archean/Proterozoic corresponds with the onset of cratonization which resulted in an increased riverine transport of Ca^{2+}. The zigzag shape of the Ca^{2+} curve in Phanerozoic times reflects large scale changes in Ca^{2+} concentration associated with major oceanic overturns.

n in diameter, are
lasmic reticulum,
al-affine organic
ır sites forming
l deposits predate
ult to find and to
ients, abundant in
rine meiofauna –
existing prior to
h SIMKISS (1989)
formation, must
nillions of years.
mergence of the
rassic and of the
'9) are the most
ted calcification,
ı arose after the
ian extraction of
erall Ca balance
he production of
oncentration and
as lower pH and
ugh viable cells
IFT and TAYLOR,
nization events,
aminifera in the
also have been
ng predecessors

supersaturation
ich could have
mbrian alkaline
he Phanerozoic
ion we tried to
iany arguments

; in situ calcified
ing calcareous
n Phanerozoic
ins.
the cell, which
ionic calcium

spectrum of
k. If all of the
ill stand closer
alkaline ocean
life and in the

spécial 13 (1994)

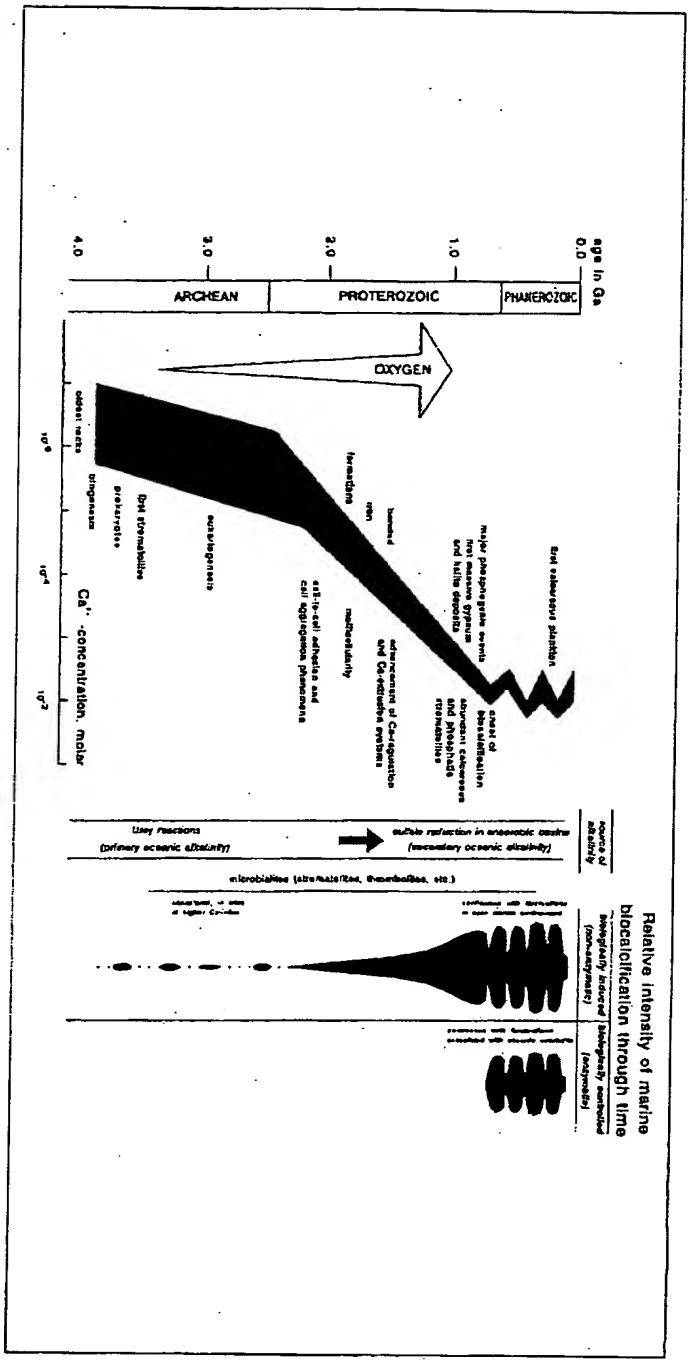

FIGURE 15 – Curves representing changes in oceanic Ca^{2+} concentration through geologic time as inferred from the hypothesis of the early alkaline (sodic) ocean. Some major biogeochemical and biocvolutionary events associated with changes in Ca^{2+} levels are indicated as well as sources of alkalinity controlling the saturation levels with respect to carbonate minerals and the intensity of biocalcification in the marine environment. The distinct distortion of the curve near the transition Archean/Proterozoic corresponds with the onset of cratonization which resulted in an increased riverine transport of Ca^{2+}. The zigzag shape of the Ca^{2+} curve in Phanerozoic times reflects large scale changes in Ca^{2+} concentration associated with major oceanic overturns.

7. ACKNOWLEDGEMENTS

This paper was made possible by grants from the German Research Council (Wo 395/4/1-4; Ke 287/9/1-3) to S.K., by an European Community fellowship, a grant from the Committee of Scientific Research (Komitet Badań Naukowych - No 0022/P2/92/03) and by the continued financial assistance from the Polish Academy of Sciences to J.K. The cooperation by G. Landmann, A. Lipp, A. Reimer, U. Svensson, Dr. M. Duman, Y. Dogan, and Prof. T. Konuk during the Lake Van and Satonda expeditions is gratefully acknowledged. Without the strong encouragement and support in the early phase of the development of the SOH by Prof. E.T. Degens, this paper could not have been written. We also owe thanks to many colleagues who, in the last years, discussed implications of our hypotheses with us and provided valuable information and insight. This paper is a contribution to the German Research Council Programme "Globale und regionale Steuerungsfaktoren biogener Sedimentation".

8. REFERENCES

AARONSON R.P., WOO E., 1981. — Organization in the cell nucleus: divalent cations modulate the distribution of condensed and diffuse chromatin. — *Journal of Cell Biology*, **90**: 181-186.

ABE T., TSUZUKI M., MIYACHI S., 1987. — Transport and fixation of inorganic carbon during photosynthesis of *Anabaena* grown under ordinary air. II. Effect of sodium concentration during growth on the induction of active transport system for IC. — *Plant Cell Physiology*, **28**: 671-677.

ABELSON P.H., 1966. — Chemical events on the primitive Earth. — *Proceedings of the National Academy of Sciences USA*, **55**: 1365- 1372.

ADDADI L., BERMAN A., MORADIAN OLDAK J., WEINER S., 1989. — Structural and stereochemical relations between acidic macromolecules of organic matrices and crystals. — *Connective Tissue Research*, **21**: 127-135.

ADDADI L., WEINER S., 1989. — Stereochemical and structural relations between macromolecules and crystals in biomineralization. — *In*: Biomineralization – Chemical and Biochemical Perspectives. Mann S., Webb J., and Williams R.J.P. (eds.), VCH Verlagsgesellschaft, Weinheim, p. 133-156.

AHARON P., SCHIDLOWSKI M., SINGH I.B., 1987. — Chronostratigraphic markers in the end-Precambrian carbon isotope record of the lesser Himalaya. — *Nature*, **327**: 699-702.

ALLEN M.B., ARNON D.I., 1955. — Studies on nitrogen-fixing blue-green algae. II. The sodium requirement of *Anabaena cylindrica*. — *Physiologia Plantarum*, **8**: 653-660.

ANDERSON H.C., 1985. — Normal biological mineralization - role of cells, membranes, matrix vesicles, and phosphatase. — *In*: Calcium in Biological Systems. Rubin R.P., Weiss G.B., Putney J.W.Jr. (eds.), Plenum Publishing Corporation, New York, p. 599-606.

ARMSTRONG R.L., 1991. — The persistent myth of crustal growth. — *Australian Journal of Earth Sciences*, **38**: 613-630.

ARTHUR E.J., SANBON R.C., 1969. — Osmotic and ionic regulation in nematodes. — *In*: Chemical Zoology, vol. 3. Florkin M. and Scheer B.T. (eds.), Academic Press, New York, p. 429-464.

ARTHUR M.
as cas
Ameri
AWRAMIK S
Preca
AWRAMIK S
bacteri
20: 35
BACHRA B.
from
Scienc
BAJAJ Y.P.S.
analys
749-7
BEAN B.P.,
Annua
BEAUDOIN A
the ce
Biochi
BENGTSON S
phyla.
Signor
BERMAN A.,
1993.
adaptir
BERRIDGE M
Nature
BERRY W.B.
explan
Americ
BISCHOFF J.
at Mo
1743-1
BONNER J.T.
molds.
BORLE A.B.,
Revie
BOYNTON A
stimul
Biophy
BRASIER M.
record.
BRASIER M.
LIN, J
carbon
bounda
Magaz
BROCK T.D.,
evoluti

Bulletin de l'In

ARTHUR M.A., SCHLANGER S.O., 1979. — Cretaceous "oceanic anoxic events" as casual factor in development of reef-reservoired giant oil fields. — *American Association of Petroleum Geologists Bulletin*, **63**: 870-885.

AWRAMIK S.M., BARGHORN E.S., 1977. — The Gunflint microbiota. — *Precambrian Research*, **5**: 121-142.

AWRAMIK S.M., SCHOPF J.W., WALTER M.R., 1983. — Filamentous fossil bacteria from Archean of Western Australia. — *Precambrian Research*, **20**: 357-374.

BACHRA B.N., 1963. — Precipitation of calcium carbonate and phosphates from metastable solutions. — *Annals of the New York Academy of Sciences*, **109**: 251-255.

BAJAJ Y.P.S., RASMUSSEN H.P., ADAMS M.W., 1971. — Electron-microprobe analysis of isolated plant cells. — *Journal of Experimental Botany*, **22**: 749-752.

BEAN B.P., 1989. — Classes of calcium channels in vertebrate cells. — *Annual Review of Physiology*, **51**: 367-384.

BEAUDOIN A.R., GRONDIN G., 1991. — Shedding of vesicular material from the cell surface of eukaryotic cells: different cellular phenomena. — *Biochimica et Biophysica Acta*, **1071**: 203-219.

BENGTSON S., CONWAY MORRIS S., 1992. — Early radiation of biomineralizing phyla. — *In*: Origin and Evolution of the Metazoa. Lipps J.H. and Signor P.W. (eds.) Plenum Press Corporation, New York, P. 447-481.

BERMAN A., HANSON J., LEISEROWITZ L., KOETZLE T., WEINER S., ADDADI L., 1993. — Biological control of crystal texture: a widespread strategy for adapting crystal properties to function. — *Science*, **259**: 776-779.

BERRIDGE M.J., 1993. — Inositol trisphosphate and calcium signalling. — *Nature*, **361**: 315-325.

BERRY W.B.N., WILDE P., 1978. — Progressive ventilation of the oceans – an explanation for the distribution of the Lower Paleozoic black shales. — *American Journal of Science*, **278**: 257- 275.

BISCHOFF J.L., HERBST D.B., ROSENBAUER R.J., 1991. — Gaylussite formation at Mono Lake, California. — *Geochimica et Cosmochimica Acta*, **55**: 1743-1747.

BONNER J.T., 1971. — Aggregation and differentiation in the cellular slime molds. — *Annual Review of Microbiology*, **25**: 78-92.

BORLE A.B., 1981. — Control, modulation and regulation on cell calcium. — *Review of Physiology, Biochemistry and Pharmacology*, **90**: 14-153.

BOYNTON A.L., WHITFIELD J.F., MACMANUS J.P., 1980. — Calmodulin stimulates DNA synthesis by rat liver cells. — *Biochemical and Biophysical Research Communications*, **95**: 746-759.

BRASIER M.D., 1992. — Nutrient-enriched waters and the early skeletal fossil record. — *Journal of the Geological Society, London*, **149**: 621-629.

BRASIER M.D., MAGARITZ M., CORFIELD R., LUO HUILIN, WU XICHE, OUYANG LIN, JIANG ZHIWEN, HAMDI B., HE TINGGUI, FRASER A.G., 1990. — The carbon- and oxygen-isotope record of the Precambrian-Cambrian boundary interval in China and Iran and their correlation. — *Geological Magazine*, **127**: 319-332.

BROCK T.D., 1973. — Lower pH limit for the existence of blue-green algae: evolutionary and ecological implications. — *Science*, **179**: 480-483.

BROECKER W.S., PENG T.-H., 1982. — Tracers in the Sea. — El Digio Press, Lamont-Doherty Geological Observatory, Palisades, N.Y., 690 p.

BROWN B.E., 1982. — The form and function of metal-containing "granules" in invertebrate tissues. — *Biological Reviews*, **57**: 621-667.

BURGER M.M., MISEVIC G., 1985. — Cell encounter: molecular and biological aspects of initial contacts. — *In*: Cellular and Molecular Control of Direct Cell Interactions. Marthy H.J. (ed.), Plenum Publishing Corp., New York, p. 3-26.

BYERS C.W., 1977. — Biofacies patterns in euxinic basins: a general model. — *In*: Deep-water Carbonate Environments. Cook H.E. and Enos P. (eds.), *The Society of Economic Paleontologists and Mineralogists, Special Publication*, **25**: 5-17.

CALDEIRA K., KASTING J.F., 1992. — Susceptibility of the early Earth to irreversible glaciation caused by carbon dioxide clouds. — *Nature*, **359**: 226- 228.

CALDEIRA K., RAMPINO M.R., VOLK T., ZACHOS J.C., 1990. — Biogeochemical modeling at mass extinction boundaries: atmospheric carbon dioxide and ocean alkalinity at the K/T boundary. — *In*: Extinction Events in Earth History. Kaufman E.G. and Walliser O.H. (eds.), Springer-Verlag, Berlin, p. 333-345.

CAMPBELL A.K., 1983. — Intracellular Calcium - Its Universal Role as a Regulator. — John Wiley and Sons Ltd., Chichester, 556 p.

CARAFOLI E., 1987. — Intracellular calcium homeostasis. — *Annual Review of Biochemistry*, **56**: 395-433.

CAVALIER-SMITH T., 1981. — The origin and early evolution of the eukaryotic cell. — *Symposia of the Society of General Microbiology*, **32**: 33-84.

CHAN K.Y., 1976. — Control of colony formation in *Coelastrum microporum* (Chlorococcales, Chlorophyta). — *Phycologia*, **15**: 149- 154.

CHAPMAN C.R., MORRISON D., 1994. — Impacts on the Earth by asteroids and comets: assessing the hazard. — *Nature*, **367**: 33-40.

CHEN C.P., LAWRENCE J.M., 1987. — The role of carbonic anhydrase in facilitating the transport CO_2 in the tooth of *Lytechinus variogatus* (Echinodermata: Echinoidea). — *Comparative Biochemistry and Physiology*, **87A**: 327-331.

CHROST R.J., 1978. — Extracellular release in *Chlorella vulgaris* culture and role of bacteria accompanying algae in this process. — *Acta Microbiologica Polonica*, **27**: 55-62.

CLOUD P., 1976. — Beginnings of biospheric evolution and their biogeochemical consequences. — *Paleobiology*, **2**: 351-387.

COMPSTON W., PIDGEON R.T., 1986. — Jack Hills, evidence of more very old zircons in Western Australia. — *Nature*, **321**: 766-769.

CONWAY E.J., 1943. — The chemical evolution of the ocean. — *Proceedings of the Royal Irish Academy*, Sect. B, **XLVIII**: 161-212.

COOK P., SHERGOLD J.H., 1984. — Phosphorus, phosphorites and skeletal evolution at the Precambrian/Cambrian boundary. — *Nature*, **308**: 231-236.

COPPER P., 1988. — Ecological succession in Phanerozoic reef ecosystems: is it real? — *Palaios*, **3**: 136-152.

COTMORE J.M., NICHOLS J.JR., WUTHIER R.E., 1971. — Phospholipid calcium phosphate complex: enhanced calcium migration in the presence of

phosphate. — *Nature*, **172**: 1339-1341.

CRENSHAW M.M., 1982. — Mechanisms of normal biological mineralization of calcium carbonates. — *In*: Biological Mineralization and Demineralization. Nancollas G.H. (ed.), Springer Verlag, Berlin, p. 243-257.

DEGENS E.T., 1976. — Molecular mechanisms of carbonate, phosphate, and silica deposition in the living cell. — *Topics in Current Chemistry*, **64**: 1-112.

DEGENS E.T., 1979. — Why do organisms calcify? — *Chemical Geology*, **25**: 257-269

DEGENS E.T., ITTEKKOT V., 1986. — Ca^{2+}-stress, biological response and particle aggregation in the aquatic habitat. — *Netherlands Journal of Sea Research*, **20**: 109-116.

DEGENS E.T., KAZMIERCZAK J., ITTEKKOT V., 1985. — Cellular response to Ca^{2+}-stress and its geological implications. — *Acta Palaeontologica Polonica*, **30**: 115-135.

DERRY L.A., KAUFMAN A.J., JACOBSEN S.B., 1992. — Sedimentary cycling and environmental change in the Late Proterozoic: Evidence from stable and radiogenic isotopes. — *Geochimica et Cosmochimica Acta*, **56**: 1317-1329.

DIMROTH P., 1990. — Mechanisms of sodium transport in bacteria. — *Philosophical Transactions of the Royal Society of London*, B, **326**: 465-477.

DONACHY J.E., WATABE N., SHOWMAN R.M., 1990. — Alkaline phosphatase and carbonic anhydrase activity associated with arm regeneration in the seastar *Asterias forbesi*. — *Marine Biology*, **105**: 471-476.

DOSE K., RAUCHFUSS H., 1972. — On the electrophoretic behavior of thermal polymers of amino acids. — *In*: Molecular Evolution: Prebiological and Biological. Rohlfing D.L. and Oparin A.I. (eds.), Plenum Press, New York, p. 199.

DZIAK R., BRAND J.S., 1974. — Calcium transport in isolated bone cells. — *Journal of Cell Physiology*, **84**: 74-75.

ERWIN D.H., 1994. — The Permo-Triassic extinction. — *Nature*, **367**: 231-236.

EUGSTER H.P., 1969. — Inorganic bedded cherts from the Magadi area, Kenya. — *Contributions to Mineralogy and Petrology*, **22**: 1-31.

EVANS W.G., KLING G.W., TUTTLE M.L., TANYILEKE G., WHITE L.D., 1993. — Gas buildup in Lake Nyos, Cameroon: the recharge process and its consequences. — *Applied Geochemistry*, **8**: 207-221.

EXTON J.H.,1988. — Mechanism of action of calcium-mobilizing agonists: some variations on a young theme. — *FASEB Journal*, **2**: 2670-2676.

FARBER J.L., 1981. — The role of calcium in cell death. — *Life Sciences*, **29**: 1289-1295.

FOERSTER J.W., 1964. — The use of calcium and magnesium ions to stimulate sheaths formation in *Oscillatoria limosa* (Roth) C.A. Agardh. — *Transactions of the American Microscopical Society*, **83**: 420-427.

FOX W.W., 1968. — Natural polymers: abiotic polymerization and self-organization. — *In*: Encyclopedia of Polymer Science and Technology, vol. 9. Mark H.F., Gaylord N.G., and Bikales W.M. (eds.), Interscience, New York, p. 284-291.

FRANCHI E., CAMATINI M., 1985. — Evidence that a Ca^{2+} chelator and a calmodulin blocker interfere with the structure of inter-Sertoli junctions. — *Tissue and Cell*, **17**: 13-25.

FRIEBELE E.S., CORREL D.L., FAUST M.A., 1978. — Relationship between plankton size and the rate of orthophosphate uptake: in situ observations of an estuarine population. — *Marine Biology*, **45**: 39-52.

FRY B., JANNASCH H.W., MOLYNEAUX S.J., WIRSEN C.O., MURAMOTO J.A., KING S., 1991. — Stable isotope studies of the carbon, nitrogen and sulfur cycles in the Black Sea and the Cariaco Trench. — *Deep-Sea Research*, **38**: 1003-1019.

FÜRSICH F.T., 1979. — Genesis, environments, and ecology of Jurassic hardgrounds. — *Neues Jahrbuch für Geologie und Paläontologie, Abhandlungen*, **158**: 1-63.

GABEL N.W., 1990. — A realistic chemical basis for the origin of life. — *Evolutionary Theory*, **9**: 181-209.

GAL V., MARTIN S., BAYLEY P., 1988. — Fast disassembly of microtubule induced by Mg^{2+} and Ca^{2+}. — *Biochemical and Biophysical Research Communications*, **155**: 1464-1470.

GARRELS R.M., MACKENZIE F.T., 1967. — Origin of the chemical composition of some springs and lakes. — *In*: Equilibrium Concepts in Natural Water Systems. *American Chemical Society Advances in Chemistry*, **67**: 222-242.

GARRELS R.M., MACKENZIE F.T., 1971. — Evolution of Sedimentary Rocks. — W.W. Norton and Comp. Inc., New York, 397 p.

GERLOFF G.C., FISHBECK K.A., 1969. — Quantitative cation requirements of several green and blue-green algae. — *Journal of Phycology*, **5**: 109-114.

GILULA N., EPSTEIN M.L., 1976. — Cell-to-cell communication, gap junction and calcium. — *Symposia of the Society of Experimental Biology*, **30**: 257-272.

GOLUBIĆ S., 1973. — The relationship between blue-green algae and carbonate deposits. — *In*: The Biology of Blue-Green Algae. Carr N.G. and Whitton B.A. (eds.), Blackwell, Oxford, p. 434-472.

GOODWIN B.C., 1989.— Unicellular morphogenesis. — *In*: Cell Shape. Stein W.D. and Bronner F. (eds.), Academic Press, San Diego, p. 365-391.

GOODWIN B.C., TRAINOR L.E.H., 1985. — Tip and whorl morphogenesis in *Acetabularia* by calcium-regulated strain fields. — *Journal of Theoretical Biology*, **117**: 79-106.

GOYET C., BRADSHAW A.L., BREWER P.G., 1991. — The carbonate system in the Black Sea. — *Deep-Sea Research*, **38**: 1049-1068.

GRACIANSKY P.C. DE, DEROO G., HERBIN J.P., MONTADERT L., MÜLLER C., SCHAAF A., SIGAL J., 1984. — Ocean-wide stagnation episode in the Late Cretaceous. — *Nature*, **308**: 346-349.

GROTZINGER J.P., 1989. — Facies and evolution of Precambrian carbonate depositional systems: emergence of the modern platform archetype. — *The Society of Economic Paleontologists and Mineralogists Special Publications*, **44**: 79-106.

GROTZINGER J.P., 1990. — Geochemical model for Proterozoic stromatolite decline. — *In*: Proterozoic Evolution and Environments. Knoll A.H. and Ostrom J.H. (eds.), *American Journal of Science* (Special volume dedicated to the memory of P.E. Cloud), **290-A**: 80-104.

GRUSZCZYŃSKI M., 1986. — Hardgrounds and ecological succession in the light of early diagenesis (Jurassic, Holy Cross Mts., Poland). — *Acta Palaeontologica Polonica*, **31**: 163-212.

GRUSZCZYŃSKI M., COLEMAN M., KAŹMIERCZAK J., GOLDRING R., ISAACS M.C., 1994. — Origin of hardgrounds: a step of understanding. —

Sedimentology (in press).

HAGIWARA S., OZAWA S., SAND O., 1975. — Voltage clamp analysis of two inward current mechanisms in the egg cell membrane of a starfish. — *Journal of General Physiology*, **65**: 617-644.

HALSTEAD L.B., 1969. — Are mitochondria directly involved in biological mineralization? — *Calcified Tissue Research*, **3**: 103-104.

HAN T.-M., RUNNEGAR B., 1992. — Megascopic eukaryotic algae from 2.1-billion-year-old Negaunee Iron-Formation, Michigan. — *Science*, **257**: 232-235.

HARRISON L.G., HILLIER N.A., 1985. — Quantitative control of *Acetabularia* morphogenesis by extracellular calcium: A test of kinetic theory. — *Journal of Theoretical Biology*, **114**: 177-192.

HART M. H., 1978. — The evolution of the atmosphere of the Earth. — *Icarus*, **33**: 23-39.

HAY W.W., BARRON E.J., SLOAN II J.L., SOUTHAM J.R., 1981. — Continental drift and the global pattern of sedimentation. — *Geologische Rundschau*, **70**: 302-315

HELLMAN B., ANDERSON T., 1978. — Calcium and pancreatic ß-cell function. IV. Evidence that glucose and phosphate stimulate ^{45}Ca incorporation into different intracellular pools. — *Biochimica et Biophysica Acta*, **541**: 483-491.

HENDERSON-SELLERS A., BENLOW A., MEADOWS A.J., 1980. — The early atmospheres of the terrestrial planets. — *Quarterly Journal of the Royal Astronomical Society*, **21**: 74-81.

HEPLER P.K., 1992. — Calcium and mitosis. — *International Review of Cytology*, **138**: 239-268.

HERBST C., 1900. — Über das Auseinandergehen von Furchungs- und Gewebezellen in kalkfreiem Medium. — *Archiv für Entwicklungs mechanik*, **9**: 424-463.

HERMAN Y., 1979. — Plankton distribution in the past. — *In*: Zoogeography and Diversity of Plankton. Van der Spoel S. and Pierrot-Bults A.C. (eds.), Bunge Scientific Publishing, Utrecht, p. 29-49.

HOFFMAN A., GRUSZCZYŃSKI M., MAKOWSKI K., 1991. — On the interrelationship between temporal trends in $\delta^{13}C$, $\delta^{18}O$, and $\delta^{34}S$ in the world ocean. — *Journal of Geology*, **99**: 355-370.

HOFMANN H.J., 1976. — Precambrian microflora, Belcher Island, Canada: significance and systematics. — *Journal of Paleontology*, **50**: 1040-1073.

HOFMANN H.J., 1985. — Precambrian carbonaceous megafossils. — *In*: Paleoalgology: Contemporary Research and Applications. Toomey D.F. and Nitecki M.H. (eds.), Springer-Verlag, Berlin, p. 20-33.

HOFMANN H.J., GROTZINGER J.P., 1985. — Shelf-facies microbiota from the Odjick and Rocknest Formations (Epworth Group; 1.89 Ga), northwestern Canada. — *Canadian Journal of Earth Sciences*, **22**: 1781-1792.

HOLLAND H.D., 1972. —The geologic history of seawater – An attempt to solve the problem. — *Geochimica et Cosmochimica Acta*, **36**: 637-651.

HOLLAND H.D., 1984. — The Chemical Evolution of the Atmosphere and Oceans. — Princeton University Press, Princeton, 582 p.

HOLM N.G. (ed.), 1992. — Marine Hydrothermal Systems and the Origin of Life. — *Origins of Life* (Special Issue), **22**: 1-242

HOLMER L.E., 1983. — Lower Viruan discontinuity surfaces in central Sweden. — *Geologiska Föreningens i Stockholm Förhandlingar*, **105**: 29-42.

HOLSER W.T., 1984. — Gradual and abrupt shifts in ocean chemistry during Phanerozoic time. — *In*: Patterns of Change in Earth Evolution. Holland H.D. and Trendall A.F. (eds.), Dahlem Konferenzen, Springer-Verlag, Berlin, p. 123-143.

HOLSER W.T., MAGARITZ M., 1987. — Events near the Permian-Triassic boundary. — *Modern Geology*, **11**: 155-180.

HOLTFRETER J., 1943. — Properties and functions of the surface coat in amphibian embryos. — *Journal of Experimental Zoology*, **93**: 251-323.

HUNTER G.K., HOLMYARD D.P., PRITZKER K.P.H., 1993. — Calcification of chick vertebral chondrocytes grown in agarose gels: a biochemical and ultrastructural study. — *Journal of Cell Science*, **104**: 1031-1038.

HURLEY P.M., RAND J.R., 1969. — Pre-drift continental nuclei. — *Science*, **164**: 1220-1242.

HUTCHINSON G.E., 1961. — The biologist poses some problems. — *In*: Oceanography. Sears M. (ed.), *American Association for the Advancement of Science, Publication*, **67**: 85-93.

JAANUSON V., 1961. — Discontinuity surfaces in limestones. — *Bulletin of the Geological Institute University of Uppsala*, **40**: 221-241.

JAN L.Y., Jan Y.N., 1989. — Voltage-sensitive ion channels. — *Cell*, **56**: 13-25.

JENKINS G.S., 1993. — A general circulation model study of the effects of faster rotation rate, enhanced CO_2 concentration, and reduced solar forcing: implications for the faint young sun paradox. — *Journal of Geophysical Research*, **98**: 20803-20811.

JENKYNS H.C., 1980. — Cretaceous anoxic events: from continents to oceans. — *Journal of the Geological Society of London*, **137**: 171-188.

JENKYNS H.C., 1988. — The early Toarcian (Jurassic) anoxic event: stratigraphic, sedimentary and geochemical evidence. — *American Journal of Science*, **288**: 101-151.

JONES A.R., 1969. — Mitochondria, calcification, and waste disposal. — *Calcified Tissue Research*, **3**: 363-365.

KAKUTA S., GOLUB E.E., SHAPIRO I.M., 1985. — Morphochemical analysis of phosphorous pools in calcifying cartilage. — *Calcified Tissue International*, **37**: 293-299.

KASTING J.F., 1985. — Photochemical consequences of enhanced CO_2 levels in Earth's early atmosphere. — *In*: The Carbon Cycle and Atmospheric CO_2: Natural Variations Archean to Present. Sundquist E.T. and Broecker W.S. (eds.), *Geophysical Monographs*, **32**: 612-622.

KASTING J.F., 1987. — Theoretical constraints on oxygen and carbon dioxide concentrations in the Precambrian atmosphere. — *Precambrian Research*, **34**: 205-229.

KAŹMIERCZAK J., 1976. — Devonian and modern relatives of the Precambrian *Eosphaera*: possible significance for the early eukaryotes. — *Lethaia*, **9**: 39-50.

KAŹMIERCZAK J., DEGENS E.T., 1986. — Calcium and the early eukaryotes. — Mitteilungen aus dem Geologisch-Paläontologischen Institut der Universität Hamburg, **61**: 1-20.

KAŹMIERCZAK J., KEMPE S., 1990. — Modern cyanobacterial analogs of

Paleo
KAŹMIERCZ
Paleo
294-3
KAŹMIERCZ
the L
Polon.
KAŹMIERCZ
time:
Palä.
KEMP N.E.,
scales
KEMPE S.,
Geoch
dem
47: 12
KEMPE S.,
Cycle.
Repor
KEMPE S.,
shallo
KEMPE S.,
Geolo.
KEMPE S., K
the fo
Biogeo
(eds.).
Spring
KEMPE S., K
linke
Precar
KEMPE S.,
Hydro
KEMPE S., K
its be
Mode
(ed.),
Arling
KEMPE S., I
1991.
— *Na*
KINGSLEY
calcifi
Exper
KNOLL A.H.
In: Bi
Teves
New
KNOLL A.H
265: 6

Paleozoic stromatoporoids. — *Science*, **250**: 1244-1248.

KAŻMIERCZAK J., KEMPE S., 1992. — Recent cyanobacterial counterparts of Paleozoic *Wetheredella* and related problematic fossils. — *Palaios*, **7**: 294-304.

KAŻMIERCZAK J., PSZCZÓKOWSKI A., 1968. — Sedimentary discontinuities in the Lower Kimmeridgian of the Holy Cross Mts. — *Acta Geologica Polonica*, **18**: 587-612.

KAŻMIERCZAK J., ITTEKKOT V., DEGENS E.T. 1985. — Biocalcification through time: environmental challenge and cellular response. — *Paläontologische Zeitschrift*, **59**: 15-33.

KEMP N.E., 1984. — Organic matrices and mineral crystallites in vertebrate scales, teeth and skeletons. — *American Zoologist*, **24**: 956-976.

KEMPE S., 1977. — Hydrographie, Warven-Chronologie und organische Geochemie des Van Sees, Ost Türkei. — Ph.D. Thesis, *Mitteilungen aus dem Geologisch-Paläontologischen Institut der Universität Hamburg*, **47**: 123-208.

KEMPE S., 1979. — Carbon in the rock cycle. — *In*: The Global Carbon Cycle. Bolin B., Degens E.T., Kempe S., and Ketner P. (eds.), SCOPE Report 13, Wiley & Sons, Chichester, p. 343-377.

KEMPE S., 1990. — Alkalinity: The link between anaerobic basins and shallow water carbonates? — *Naturwissenschaften*, **77**: 426-427.

KEMPE S., DEGENS E.T., 1985. — An early soda ocean? — *Chemical Geology*, **53**: 95-108.

KEMPE S., KAŻMIERCZAK J., 1990a. — Calcium carbonate supersaturation and the formation of in situ calcified stromatolites. — *In*: Facets of Modern Biogeochemistry. Ittekkot V.A., Kempe S., Michaelis W., and Spitzy A. (eds.), Festschrift for E.T. Degens on occasion of his 60th birthday, Springer-Verlag, Berlin, Heidelberg, New York, p. 255-278.

KEMPE S., KAŻMIERCZAK J., 1990b. — Chemistry and stromatolites of the sea-linked Satonda Crater Lake, Indonesia: A recent model for the Precambrian sea? — *Chemical Geology*, **81**: 299-310.

KEMPE S., KAŻMIERCZAK J., 1993. — Satonda Crater Lake, Indonesia: Hydrogeochemistry and biocarbonates. — *Facies*, **28**: 1-32.

KEMPE S., KAŻMIERCZAK J., DEGENS E.T., 1989. — The soda ocean concept and its bearing on biotic and crustal evolution. — *In*: Origin, Evolution and Modern Aspects of Biomineralization in Plants and Animals. Crick, R.E. (ed.), Proceedings 5th International Symposium on Bio-mineralization, Arlington, Texas, May, 1986, Plenum Press, New York: 29-43.

KEMPE S., KAŻMIERCZAK J., LANDMANN G., KONUK T., REIMER A., LIPP A., 1991. — Largest known microbialites discovered in Lake Van, Turkey. — *Nature*, **349**: 605-608.

KINGSLEY R.J., WATABE N., 1987. — Role of carbonic anhydrase in calcification in the gorgonian *Leptogorgia virgulata*. — *The Journal of Experimental Zoology*, **241**: 171-180.

KNOLL A.H., 1983. — Biological interactions and Precambrian eukaryotes. — *In*: Biotic Interactions in Recent and Fossil Benthic Communities. Tevesz M.J.S. and McCall P.L. (eds.), Plenum Publishing Corporation, New York, p. 251-283.

KNOLL A.H., 1991. — End of the Proterozoic eon. — *Scientific American*, **265**: 65-73.

SEP-11-2002 11:28 LINDA HALL LIBRARYL 816 926 8785 P.50

KNOLL A.H., HAYES J.M., KAUFMAN A.J., SWETT K., LAMBERT I.B., 1986. — Secular variation in carbon isotope ratios from the Upper Proterozoic successions of Svalbard and East Greenland. — *Nature*, **321**: 832-838.

KOERSCHNER III W.F., READ J.F., 1989. — Field and modelling studies of Cambrian carbonate cycles. — *Journal of Sedimentary Petrology*, **59**: 654-687.

KONDRATYEV K.YA., MOSKALENKO N.I., 1984. — The role of carbon dioxide and other minor gaseous components and aerosols in the radiation budget. — *In*: The Global Climate. Houghton J.T. (ed.), Cambridge University Press, London: 225-233.

KOSTYUK P.K., 1989. — Diversity of calcium in channels in cellular membranes. — *Neuroscience*, **28**: 253-261.

KOVAC L., GRIAC P., KLOBUCNIKOVA V., SULO P., 1989. — Transfer of isolated organelles into cells: an experimental approach to the evolutionary origin of cell organelles. — *Origins of Life*, **19**: 436-437.

KRATZ W., MEYRS J., 1955. — Nutrition and growth of several blue-green algae. — *American Journal of Botany*, **42**: 282- 287.

KRETSINGER R.H., 1977a. — Why does calcium play an informational role unique in biological systems? — *In*: Metal-Ligand Interactions in Organic Chemistry and Biochemistry (9th Jerusalem Symposium), part 2. Pullman B. and Goldbleum N. (eds.), E. Lidel Publishing Company, Dordrecht, p. 257-263.

KRETSINGER R.H., 1977b. — Evolution of the informational role of calcium in eukaryotes. — *In*: Calcium Binding Proteins and Calcium Function. Wasserman R.H., Corradino R.A., Kretsinger R.H., MacLennnan D.H., and Siegel F.L. (eds.), North Holland Publishers, New York, p. 63-72.

KRETSINGER R.H., 1983. — A comparison of the roles of calcium in biomineralization and in cytosoling signalling. — *In*: Biomineralization and Biological Metal Accumulation. Westbroek P. and De Jong E.W. (eds), D. Reidel Publishing Co., Dordrecht, p. 123-131.

KROLL R.G., 1990. — Alkalophiles. — *In*: Microbiology of Extreme Environments. Edwards C. (ed.), Open University Press, Milton Keynes, p. 55-92.

KRÖNER A., 1984. — Evolution, growth and stabilization of the Precambrian lithosphere. — *Physics and Chemistry of the Earth*, **15**: 69-106.

KRUMBEIN W.E., 1979. — Calcification by bacteria and algae. — *In*: Biogeochemical Cycling of Mineral-Forming Elements. Trudinger P.A. and Swain D.J. (eds.), Elsevier, Amsterdam, p. 47-68.

KUHN W.R., KASTING J.F., 1983. — The effects of increasd CO_2 concentrations on surface temperature of the early Earth. — *Nature*, **301**: 53-55.

KYLIN A., DAS G., 1967. — Calcium and strontium as micronutrients and morphogenetic factors for *Scenedesmus*. — *Phycologia*, **6**: 201- 210.

LANE C.E., 1968. — Coelenterata: chemical aspects of ecology, pharmacology and toxicology. — *In*: Chemical Zoology, vol. 7. Florkin M. and Scheer B.T. (eds.), Academic Press, New York, p. 263-284.

LANYI J.K., 1979. — The role of Na^+ in transport processes of bacterial membranes. — *Biochimica et Biophysica Acta*, **559**: 377-397.

LASHOF D.A., AHUJA D.R., 1990. — Relative contribution of greenhouse gas emissions to global warming. — *Nature*, **344**: 529-531.

LEAVITT S
fro
LEE S.Y.,
sipl
Ple
LEHNINC
pho
Bio
D. I
LINDGRE
Rip
Co
LOWENST
Pha
LOWENST
112
LOWENST
Uni
MACCAL
tiss
MAGARI
fau
MAGARI
A.
isot
and
MAISONN
—
MANN B.
as
MANN S.
Ch
We
MANN S.
ME
org
261
MARGUL
Fra
MARMÉ
Ber
MATSUM
tem
MCCONA
ext
Bio
MCKERR
cor
Lor

LEAVITT S.W., 1982. — Annual volcanic carbon dioxide emission: an estimate from eruption chronologies. — *Environmental Geology*, **4**: 15-21.

LEE S.Y., BROWN R.M.Jr., 1987. — Experimental cell fusion with selected siphonocladalean algal cells. — *In*: Cell Fusion. Sowers A.E. (ed.), Plenum Publishing Corp., New York, p. 167-178.

LEHNINGER A.L., 1983. — The possible role of mitochondria and phosphocitrate in biological calcification. — *In*: Biomineralization and Biological Metal Accumulation. Westbroek P. and De Jong E.W. (eds.), D. Reidel Publishing Co., Dordrecht, p. 107-121.

LINDGREN S., 1982. — Algal coenobia and leiospheres from the Upper Riphean of the Turukhansk region, eastern Siberia. — *Stockholm Contributions to Geology*, **38**: 1-20.

LOWENSTAM H., MARGULIS L., 1980. — Evolutionary prerequisites for early Phanerozoic calcareous skeletons. — *BioSystems*, **12**: 27-41.

LOWENSTAM H.A., 1981. — Minerals formed by organisms. — *Science*, **211**: 1126-1131.

LOWENSTAM H.A., WEINER S., 1989. — On Biomineralization. — Oxford University Press, Oxford, 324 p.

MACCALLUM A.B., 1926. — The paleochemistry of the body fluids and tissues. — *Physiological Review*, **6**: 316-357.

MAGARITZ M., 1989. — $\delta^{13}C$ minima follow extinction events: A clue to faunal radiation. — *Geology*, **17**: 337-340.

MAGARITZ M., KIRSCHVINK J., LATHAM A.J., ZHURAVLEV A.YU., ROZANOV A.YU., 1991. — Precambrian/Cambrian boundary problem: Carbon isotope correlations for Vendian and Tommotian time between Siberia and Morocco. — *Geology*, **19**: 847-850.

MAISONNUEVE J., 1982. — The composition of the Precambrian ocean waters. — *Sedimentary Geology*, **31**: 1-11.

MANN B., HANNINGTON J.P., WILLIAMS R.J.P., 1986. — Phospholipid vesicles as a model system for biomineralization. — *Nature*, **324**: 565-567.

MANN S., WEBB J., WILLIAMS R.J.P. (eds.), 1989. — Biomineralization - Chemical and Biomineral Perspectives. — VCH Verlagsgesellschaft, Weinheim, 541 p.

MANN S., ARCHIBALD D.D., DIDYMUS J.M., DOUGLAS T., HEYWOOD B.R., MELDRUM F.C., REEVES N.J., 1993. — Crystallization at inorganic-organic interfaces: biominerals and biomimetic synthesis. — *Science*, **261**: 1286-1292.

MARGULIS L., 1981. — Symbiosis and Cell Evolution. — Freeman, San Francisco, 419 p.

MARMÉ D., 1985. — Calcium and Cell Physiology. — Springer-Verlag, Berlin, 390 p.

MATSUMOTO H., TAKYU T., 1986. — Effect of calcium on the structure and template activity of pea chromatin. — *Plant Cell Physiology*, **27**: 293-302.

MCCONACHIE D.R., O'DAY D.H., 1986. — The immediate induction of extensive cell fusion by Ca^{2+} addition in *Dictyostelium discoideum*. — *Biochemistry and Cell Biology*, **64**: 1281-1287.

MCKERROW W.S., SCOTESE C.R., BRASIER M.D., 1992. — Early Cambrian continental reconstruction. — *Journal of the Geological Society, London*, **149**: 599-606.

MELACK J.M., 1983. — Large, deep salt lakes: a comparative limnological analysis. — *In*: Saline Lakes. Hammer U.T. (ed.), Junk, The Hague: 223-230.

MELDOLESI J., POZZAN T., 1987. — Pathways of Ca^{2+} influx at the plasma membrane: voltage, receptor-, and the second messenger-operated channels. — *Experimental Cell Research*, **171**: 271-283.

MELLGREN R.L., 1987. — Calcium-dependent proteases: an enzyme system active at cellular membranes? — *Federation of American Societies for experimental Biology Journal*, 1: 110-115.

MOCZYDOWSKA M., VIDAL G., RUDAVSKAYA V.A., 1993. — Neoproterozoic (Vendian) phytoplankton from the Siberian Platform, Yakutia. — Palaeontology, 36: 495-522.

MURACHI T., TANAKA K., HATANAKA M., MURAKAMI T., 1981. — Intracellular Ca^{2+}-dependent protease (calpain) and its high-molecular weight endogenous inhibitor (calpastatin). — *Advances in Enzyme Regulation*, **19**: 407-424.

MUSCATINE L., 1982. — Establishment of photosynthetic eukaryotes as endosymbionts in animal cells. — *In*: On the Origins of Chloroplasts. Schiff J.A. (ed.), Elsevier/North Holland, New York, p. 77-92.

NEWELL N.D., 1971. — An outline history of tropical organic reefs. — *American Museum Novitates*, **2465**, 37p.

NICAISE B., MAGGIO K., THIRION S., HOROYAN M., KEICHER E., 1992. — The calcium loading of secretory granules. A possible key event in stimulus-secretion coupling. — *Biology of the Cell*, 75: 89-99.

NILSSON J.R., COLEMAN J.R., 1977. — Calcium-rich refractile granules in *Tetrahymena pyriformis* and their possible role in the intracellular ion-regulation. — *Journal of Cell Science*, **24**: 311-325.

NOWYCKY M.C., FOX A.P., TSIEN R.W., 1985. — Three types of neuronal calcium channel with different calcium agonist sensitivity. — *Nature*, **316**: 440-443.

O'KELLEY J., 1968. — Mineral nutrition of algae. — *Annual Review of Plant Physiology*, **19**: 89-112.

OWEN T., CESS R.D., RAMANATHAN V., 1979. — Enhanced CO_2 greenhouse to compensate for reduced solar luminosity on early Earth. — *Nature*, 277: 640-642.

PACE N.R., 1991. — Origin of life – facing up to the physical setting. — *Cell*, **65**: 531-533.

PAPAHADJOPOULOS D., NIR S., DÜZGÜNES N., 1990. — Molecular mechanisms of calcium-induced membrane fusion. — *Journal of Bioenergetics and Biomembranes*, **22**: 157-179.

PENTECOST A., RIDING R., 1986. — Calcification in cyanobacteria. — *In*: Biomineralization in Lower Plants and Animals (The Systematic Association Special Vol. No. 30). Leadbeater B.S.C. and Riding R. (eds.), Oxford University Press, Oxford, p.73-90.

PFLUG H.D., REITZ E., 1985. — Earliest phytoplankton of eukaryotic affinity. — *Naturwissenschaften*, 72: 656-657.

PONTREMOLI S., MELLONI E., 1986. — Extralysosomal protein degradation. — *Annual Review in Biochemistry*, **55**: 455-481.

PRATT B.R., 1992. — Peritidal carbonates. — *In*: Facies Models: Response to

Sea Le
Associa
PRUSCH R.D.,
Amoeb
Tissue
PUTNEY J.W.
Calciun
REIMER A., L
seiner Z
395/2-1
RIDING R., 19
RIEGER R.M.,
the occ
zoologi
ROGERS J.J.V
variati
Geoche
p. 25-3
ROMER A.S.,
York Ac
RONOV A.B.,
the cou
ROSE A.H.,
Saccha
Adhesic
Springe
ROSS A., Bor
296-43
ROZANOV A.
— *Epis*
RUNNEGAR I
biochen
Palaeo
SALHANI N.,
R.H., E
synthe
interkin
SASAKI Y., I
Biocher
SCHANNE F.A
depend
206: 70
SCHIDLOWSKI
isotope
Greenla
Geochi
SCHOPF J.W.
Americ
SCHOPF J.W.,

SEP-11-2002 11:30 LINDA HALL LIBRARYL 816 926 8785 P.53

Sea Level Change. Walker R.G. and James N.P. (eds.), Geological Association of Canada, Ottawa, p. 303-322.

PRUSCH R.D., MINCK D.R., 1985. — Chemical stimulation of phagocytosis in *Amoeba proteus* and the influence of external calcium. — *Cell and Tissue Research*, **242**: 557-564.

PUTNEY J.W.JR., 1990. — Capacitative calcium entry revisited. — *Cell Calcium*, **11**: 611-624.

REIMER A., LANDMANN G., KEMPE S., 1993. — Wasserchemie des Van Sees, seiner Zuflüsse und der Porenwässer. — Final Report DFG Project Wo 395/2-1 to 2-4, Hamburg, 42 p. (unpublished).

RIDING R., 1992. — The algal breath of life. — *Nature*, **359**: 13-14.

RIEGER R.M., STERRER W., 1975. — New spicular skeletons in Turbelaria, and the occurrence of spicules in marine meiofauna. — *Zeitschrift für zoologische Systematik und Evolutionsforschungs*, **13**: 207-278.

ROGERS J.J.W., 1978. — Inferred composition of early Archean crust and variation in crustal composition through time. — *In*: Archean Geochemistry. Windley B.F., Naqvi S.M. (eds.), Elsevier, Amsterdam, p. 25-39.

ROMER A.S., 1963. — The "ancient history" of bone. — *Annals of the New York Academy of Sciences*, **109**: 168-176.

RONOV A.B., 1968. — Probable changes in the chemistry of seawater during the course of geologic time. — *Sedimentology*, **10**: 25-43.

ROSE A.H., 1984. — Physiology of cell aggregation: flocculation by *Saccharomyces cerevisiae* as a model system. — *In*: Microbial Adhesion and Aggregation (Dahlem Conferences). Marshall K.C. (ed.), Springer-Verlag, Berlin, p. 323-335.

ROSS A., Boron W.F., 1981. — Intracellular pH. — *Physiological Review*, **61**: 296-434.

ROZANOV A.Yu., 1984. — The Precambrian-Cambrian boundary in Siberia. — *Episodes*, **7**: 20-24.

RUNNEGAR D., 1991. — Precambrian oxygen levels estimated from the biochemistry and physiology of early eukaryotes. — *Palaeogeography, Palaeoclimatology, Palaeoecology (Global Change)*, **97**: 97-111.

SALHANI N., VIENKEN J., ZIMMERMANN U., WARD M., DAVEY M.R., CLOTHIER R.H., BALLS M., COCKING E.C., LUCY J.A., 1985. — Haemoglobin synthesis and cell wall regeneration by electric field-induced interkingdom heterokaryons. — *Protoplasma*, **126**: 30-36.

SASAKI Y., HIDAKA H., 1982. — Calmodulin and cell proliferation. — *Biochemical and Biophysical Research Communications*, **104**: 451-456.

SCHANNE F.A.X., KANE A.B., YOUNG E.E., FARBER J.L., 1979. — Calcium dependence of toxic cell death: a final common pathway. — *Science*, **206**: 700-702.

SCHIDLOWSKI M., APPEL P.W., EICHMANN R., JUNGE C.E., 1979. — Carbon isotope geochemistry of the 3.7×10^9 yr old Isua sediments, West Greenland: Implications for the Archaean carbon and oxygen cycles. — *Geochimica et Cosmochimica Acta*, **43**: 189-199.

SCHOPF J.W., 1978. — The evolution of the earliest cells. — *Scientific American*, **239**: 85-102.

SCHOPF J.W., 1993. — Microfossils of the early Archean Apex Chert: new

evidence of the antiquity of life. — *Science*, **260**: 640-646.

SCHOPF J.W., PACKER B.M., 1987. — Early Archean (3.3-billion to 3.5-billion-year-old) microfossils from Warrawoona Group, Australia. — *Science*, **237**: 70-73.

SCHOUTEN C.J., 1984. — Budget of water and its constituents for Lake Taupo (New Zeland). — *In*: Dissolved Loads of Rivers and Surface Water Quantity/Quality Relationships. Proceeding I.A.H.S. Symposium, Hamburg, Aug. 1983, *International Association of Hydrological Sciences*, Publication **141**: 277-297.

SHACKLETON N.J., HALL M.A., 1984. — Carbon isotope data from leg 74 sediments. — *In*: Initial reports of the Deep Sea Drilling Project. Moore T.C.Jr. and Rabinowitz P.D. (eds.), U.S. Government Printing Office, Washington, D.C., p. 613-619.

SHELDON R.O., 1981. — Ancient marine phosphorites. — *Annual Review of Earth and Planetary Sciences*, **9**: 251-284.

SIKES C.S., WHEELER A.P., 1983. — A systematic approach to some fundamental questions of carbonate calcification. — *In*: Biomineralization and Biological Metal Accumulation. Westbroek P. and de Jong E.W. (eds.), D. Riedel, Dordrecht, p. 285-289.

SIKES C.S., WILBUR K.M., 1980. — Calcification by coccolithophorids: effects of pH and Sr. — *Journal of Phycology*, **16**: 433-436.

SIMKISS K., 1976. — Cellular aspects of calcification. — *In*: The Mechanisms of Mineralization in the Invertebrates and Plants. Watabe N. and Wilbur K.M. (eds.), University of South Carolina Press, Columbia, p. 205-224.

SIMKISS K., 1977. — Biomineralization and detoxification. — *Calcified Tissue Research*, **24**: 199-200.

SIMKISS K., 1981. — Calcium, pyrophosphate and cellular pollution. — *Trends in Biochemical Sciences*, **IV**(Apr.): iii-v.

SIMKISS K., 1989. — Biomineralization in the context of geological time. — *Transactions of the Royal Society of Edinburgh: Earth Sciences*, **80**: 193-199.

SIMKISS K., MASON A.Z., 1983. — Metal ions: metabolic and toxic effects. — *In*: The Mollusca. Vol. 2. Hochachka P. (ed.), Academic Press, New York, p. 101-164.

SIMKISS K., TAYLOR M.G., 1989. — Convergence of cellular systems of metal detoxification. — *Marine Environmental Research*, **28**: 211- 214.

SIMKISS K., WILBUR K.M., 1989. — Biomineralization. Cell Biology and Mineral Deposition. — Academic Press, San Diego, 337 p.

SITTE P., 1993. — Symbiogenetic evolution of complex cells and complex plastids. — *European Journal of Protistology*, **29**: 131-143.

SKULACHEV V.P., 1989. — Bacterial Na^+ energetics. — *Federation of European Biochemical Societies Letters*, **250**: 106-114.

SKULACHEV V.P., 1992. — The laws of cell energetics. — *European Journal of Biochemistry*, **208**: 203-209.

SMITH R.E.H., KALF J., 1982. — Size-dependent phosphorus uptake kinetics and cell quota in phytoplankton. — *Journal of Phycology*, **14**: 275-284.

SNYDER W.D., FOX S.W., 1975. — A model for the origin of stable protocells in a primitive alkaline ocean. — *BioSystems*, **7**: 222- 229.

STANLEY S.M., 1973. — Fossil data and the Precambrian-Cambrian

evolut
STEGMANN (
Zeitsc.
STEINER M.,
of nev
"mega
Berlin
STOSSEL T.
cytopl
264: 1
SULO P., GR
efficie
Curre
SURDAM R.(
Forma
Amste
SVENSSON U
Calcin
Ph.D.
Selbst
SWIFT E., T.
coccol
121-1
TALENT J.A
symbi
TIMOFEEV B
146 p.
TIMPERLEY
sedim
Taupo
Chemi
TOISTER Z.,
— *Bio*
TOWE K.M.,
record
781-78
TOWE K.M.,
In: Lif
Ma., p
TRAINOR F.I
spine f
TRUMP B.F.,
hypoth
TRUMP B.F.
injury,
227-23
TSIEN R.W.,
— *Ann*
TUCKER M.

evolutionary transition. — *American Journal of Science*, **276**: 56-76.

STEGMANN G., 1940. — Die Bedeutung der Spurenelemente für *Chlorella*. — *Zeitschrift für Botanik*, **35**: 385-422.

STEINER M., ERDTMANN B.-D., JUNYUAN C., 1992. — Preliminary assessment of new Late Sinian (Late Proterozoic) large siphonous and filamentous "megaalgae" from eastern Wulingshan, north-central Hunan, China. — *Berliner geowissenschaftliche Abhandlungen* (E), **3**: 305-319.

STOSSEL T.P., 1989. — From signal to pseudopod. How cells control cytoplasmic actin assembly. — *The Journal of Biological Chemistry*, **264**: 1961-1964.

SULO P., GRIAC P., KLOBUCNIKOVA V., KOVAC L., 1989. — A method for the efficient transfer of isolated mitochondria into yeast protoplasts. — *Current Genetics*, **15**: 1-6.

SURDAM R.C., WRAY J.L., 1976. — Lacustrine stromatolites, Eocene River Formation, Wyoming. — *In*: Stromatolites. Walter M.R. (ed.), Elsevier, Amsterdam, p. 535-541.

SVENSSON U., 1992. — Die Lösungs- und Abscheidungskinetik natürlicher Calcitminerale in wässrigen CO_2-Lösungen nahe dem Gleichgewicht. — Ph.D. Thesis, Univ. Bremen, Fachbereich Geowissenschaften, Selbstverlag, Bremen, 113 p.

SWIFT E., TAYLOR W.R., 1966. — The effect of pH on the division rate of the coccolithophorid *Cricosphaera elongata*. — *Journal of Phycology*, **2**: 121-125.

TALENT J.A., 1988. — Organic reef-building: episodes of extinction and symbiosis. — *Senckenbergiana lethaea*, **69**: 315-368.

TIMOFEEV B.V., 1969. — Proterozoic Sphaeromorphida. — Nauka, Leningrad, 146 p. (Russian)

TIMPERLEY M., VIGOR-BROWN R.J., 1985. — Weathering of pumice in the sediments as a possible source of major ions for the waters of Lake Taupo, New Zealand. — *In*: Water-Rock Interaction. Kitano Y. (ed.), Chemical Geology, Special Issue, 49: 43-52.

TOISTER Z., LOYTER A., 1971. — Ca^{2+}-induced fusion of avian erythrocytes. — *Biochimica et Biophysica Acta*, **242**: 719-724.

TOWE K.M., 1971. — Oxygen-collagen priority and the early metazoan fossil record. — *Proceedings of the National Academy of Sciences USA*, **65**: 781-788.

TOWE K.M., 1981. — Biochemical keys to the emergence of complex life. — *In*: Life in the Universe. Billingham J. (ed.), MIT Press, Cambridge, Ma., p. 297-306.

TRAINOR F.R., 1969. — *Scenedesmus* morphogenesis. Trace elements and spine formation. — *Journal of Phycology*, **5**: 185-190.

TRUMP B.F., BEREZESKY I.K., 1985. — Cellular ion regulation and disease: A hypothesis. — *Current Topics in Membranes and Transport*, **25**: 279-319.

TRUMP B.F., BEREZESKY I.K., 1992. — The role of cytosolic Ca^{2+} in cell injury, necrosis and apoptosis. — *Current Opinion in Cell Biology*, **4**: 227-232.

TSIEN R.W., TSIEN R.Y., 1990. — Calcium channels, stores, and oscillations. — *Annual Review of Cell Biology*, **6**: 715-760.

TUCKER M.E., 1989. — Carbon isotopes and Precambrian-Cambrian

boundary geology, South Australia: ocean basin formation, seawater chemistry and organic evolution. — *Terra Nova*, **1**: 573-582.

TUCKER M.E., 1992. — The Precambrian-Cambrian boundary: seawater chemistry, ocean circulation and nutrient supply in metazoan evolution, extinction and biomineralization. — *Journal of the Geological Society London*, **149**: 655-668.

TUCKER M.E., WRIGHT V.P., 1990. — Carbonate Sedimentology. — Blackwell Scientific, Oxford, 482 p.

TUCKER M.E., WILSON J.L., CREVELLO P.D., SARG J.R., READ J.F. (eds.), 1990. — Carbonate Platforms - Facies, Sequences and Evolution. — *International Association of Sedimentologists*, Special Publication **9**, Blackwell Scientific, Oxford, 328 p.

TYNNI R., UUTELA A., 1984. — Microfossils from the Precambrian Muhos Formation in Western Finland. — *Geological Survey of Finland Bulletin*, **350**: 5-38.

UREY H.C., 1951. — The origin and development of the Earth and other terrestrial planets. — *Geochimica et Cosmochimica Acta*, **1**: 209-277.

VEIS A., SHARKEY M., DICKSON I., 1977. — Non-collagenous proteins of bone and dentin extracellular matrix and their role in organized mineral deposition. — *In*: Calcium Binding Proteins and Calcium Function. Corradino R.A., Carafoli E., Kretsinger R.H., MacLeannan D.H., and Siegel F.L. (eds.), North Holland, New York, p. 409-418.

VEIZER J., 1985. — Carbonates and ancient oceans: isotopic and chemical record on times scales of 10^7-10^9 years. — *In*: The Carbon Cycle and Atmospheric CO_2: Natural Variations Archean to Present. Geophysical Monographs 32. Sundquist E.T. and Broecker W.S. (eds.), American Geophysical Union, Washington, p. 595-601.

VEIZER J., COMPSTON W., 1976. — $^{87}Sr/^{86}Sr$ in Precambrian carbonates as an index of crustal evolution. — *Geochimica et Cosmochimica Acta*, **40**: 905-915.

VEIZER J., JANSEN S.L., 1969. — Basement and sedimentary recycling and continental evolution. — *Journal of Geology*, **87**: 342-370.

VERMEIJ G.J., 1989. — The origin of skeletons. — *Palaios*, **4**: 585- 589.

VIDAL G., 1984. — The oldest eukaryotic cells. — *Scientific American*, **250**: 48-57.

VIDAL G., 1990. — Giant acanthomorph acritarchs from the Upper Proterozoic in southern Norway. — *Palaeontology*, **33**: 287-298.

VIDAL G., KNOLL A.H., 1982. — Radiations and extinctions of plankton in the late Proterozoic and early Cambrian. — *Nature*, **302**: 518-520.

VOLBERG T., GEIGER B., KARTENBECK J., FRANKE W.W., 1986. — Changes in membrane-microfilament interaction in intercellular adherens junctions upon removal of extracellular Ca^{2+} ions. — *The Journal of Cell Biology*, **102**: 1832-1842.

WALKER J.C.G., 1977. — Evolution of the Atmosphere. — Macmillan, New York.

WALKER J.C.G., 1983. — Possible limits on the composition of the Archean ocean. — *Nature*, **302**: 518-520.

WALSH M.M., 1992. — Microfossils and possible microfossils from the Early Archean Onverwacht Group, Barberton Mountain Land, South Africa. — *Precambrian Research*, **54**: 271-293.

WALTER M.R., 1976 (ed.). — Stromatolites. — Elsevier, Amsterdam, 790p.

WALTER M.R., 1983. — Archean stromatolites: evidence of the Earth's earliest benthos. — *In*: Earth's Earliest Biosphere. Schopf J.W. (ed.), Princeton University Press, Princeton, p. 187-213.

WANG F., 1985. — Middle-Upper Proterozoic and lowest Phanerozoic microfossil assemblages from SW China and contiguous areas. — *Precambrian Research*, **29**: 33-43.

WARREN P.H., 1989. — Growth of the continental crust: a planetary-mantle perspective. — *Tectonophysics*, **161**: 165-199.

WEDEPOHL K.H., 1963. — Einige Überlegungen zur Geschichte des Meerwassers. — *Fortschritte in der Geologie von Rheinland und Westfalen*, **10**: 129-150.

WEINER S., ADDADI L., 1991. — Acidic macromolecules of mineralized tissues: the controllers of crystal formation. — *Trends in Biochemical Sciences*, **16**: 252-256.

WEINER S., TRAUB W., LOWENSTAM H.A., 1983. — Organic matrix in calcified exoskeletons. — *In*: Biomineralization and Biological Metal Accumulation. Westbroek P. and de Jong E.W. (eds.), D. Reidel, Dordrecht, p. 205-224.

WENDT J., 1988. — Condensed carbonate sedimentation in the late Devonian of the eastern Anti-Atlas (Morocco). — *Eclogae geologiae Helvetiae*, **81**: 155-173.

WHEELER A.P., 1975. — Oyster mantle carbonic anhydrase: evidence for plasma membrane-bound activity and for a role in biocarbonate transport. — Ph.D. Thesis, Duke University, Durham N.C.

WHEELER A.P., SIKES C.S., 1984. — Regulation of carbonate calcification by organic matrix. — *American Zoologist*, **24**: 933-944.

WHEELER A.P., SIKES C.S., 1989. — Matrix-crystal interactions in $CaCO_3$ biomineralization. — *In*: Biomineralization - Chemical and Biochemical Perspectives. Mann S., Webb J., and Williams R.J.P. (eds.), VCH Verlagsgesellschaft, Weinheim, p. 95-131.

WHEELER A.P., RUSENKO K.W., GEORGE J.W., SIKES C.S., 1987. — Evaluation of calcium binding by molluscan shell organic matrix and its relevance to biomineralization. — *Comparative Biochemistry and Physiology*, **87B**: 954-960.

WIGLEY T.M.L., PLUMMER L.N., 1976. — Mixing of carbonate waters. — *Geochimica et Cosmochimica Acta*, **40**: 989-995.

WIGNALL P.B., HALLAM A., 1992. — Anoxia as a cause of the Permian/Triassic mass extinction: facies evidence from northern Italy and the western United States. — *Palaeogeography, Palaeoclimatology, Palaeoecology*, **93**: 21-46.

WILBUR K.M., 1980. — Cells, crystals, and skeletons. — *In*: The Mechanisms of Biomineralization in Animals and Plants. Omori M. and Watabe N. (eds.), Tokai University Press, Tokyo, p. 3-121.

WILBUR K.M., 1984. — Many minerals, several phyla, and a few considerations. — *American Zoologists*, **24**: 839-845.

WILBUR K.M., SALEUDDIN A.S.M., 1983. — Shell formation. — *In*: The Mollusca. Vol. 4. Saleuddin A.S.M. and Wilbur K.M. (eds.), Academic Press, New York, p. 236-287.

SEP-11-2002 11:32 LINDA HALL LIBRARYL 816 926 8785 P.58

WILBUR K.M., SIMKISS K., 1968. — Calcified shells. — *In*: Comprehensive Biochemistry, vol 26, part A. Florkin M. and Stotz E.H. (eds.), Elsevier Publishing Co., Amsterdam, p. 229-295.

WILDE P., 1987. — Model of progressive ventilation of the late Precambrian-early Paleozoic ocean. — *Geology*, **19**: 1093-1095.

WILLIAMS D.A., FOGARTY K.E., TSIEN R.Y., FAY F.S., 1985. — Calcium gradients in single smooth muscle cells revealed by the digital imaging microscope using Fura-2. — *Nature*, **318**: 558-561.

WILLIAMS R.J.P., 1974. — Calcium ions: their ligands and their function. — *Biochemical Society Symposia*, **39**: 133-138.

WILLIAMS R.J.P., 1989. — Calcium and cell steady states. — *In*: Calcium Binding Proteins in Normal and Transformed Cells. Pochet R., Lawson D.E.M., and Heizmann C.W. (eds.), Plenum Publishing Corporation, New York, N.Y., p. 7-16.

WILSON J.L., 1975. — Carbonate Facies in Geologic History. — Springer-Verlag, New York, 470 p.

WOESE C.R., 1987. — Bacterial evolution. — *Microbiological Review*, **51**: 221-271.

WRIGHT V.P., 1992. — Speculations on the controls on cyclic peritidal carbonates: ice-house versus greenhouse eustatic controls. — *Sedimentary Geology*, **76**: 1-5.

WUTHIER R.E., REGISTER T.C., 1985. — Role of alkaline phosphatase, a polyfunctional enzyme in mineralizing tissues. — *In*: The Chemistry and Biology of Mineralized Tissues. Butler W.T. (ed.), Ebsco Media, Inc., Birmingham, p. 113-124.

YOUNG J.D.E., 1985. — Role of ionic events in the triggering of phagocytosis. — *Journal of Theoretical Biology*, **116**: 475-478.

La función de la alcalinidad en la evolución química del océano, la organización de los ecosistemas, y los mecanismos de la biocalcificación

RESUMEN

La alcalinidad actual de los océanos varía entre 2.1 y 2.5 meq/l. Se sugere que las variaciones de la alcalinidad de los océanos, asociadas a las variaciones de TCO_2, del pH y de la concentración de iones Ca, han sido una fuerza de inducción para la evolución biológica en la historia del globo, y que deben haber determinado el comienzo de la biocalcificación, y las modificaciones del modelo de los sedimentos carbonatados a lo largo de la historia de la tierra.

Diferentes argumentos de tipo termodinámico, relacionados con el equilibrio de masas de agua, asi como aspectos cinéticos parecen mostrar que el océano Precámbrico presentaba una alcalinidad muy alta, similar a la de los "lagos alcalinos" actuales (Soda Ocean hypothesis)(KEMPE and DEGENS,1985 ; KEMPE *et al.*, 1989). Esta alta alcalinidad apareció probablemente justo después de la formación de los primeros océanos y como resultado de la colada de la primera costra "komatiitic" por aguas ricas en ácido carbónico (Reacción de Urey). En el Océano Proterozoico, la alcalinad disminuye, el sodio es extraido lentamente por el agua intersticial de subducción, dando

como consec
depósitos mu
orgánico sedi
de la concen
estrés cálcico
sobresaturac
favoreciendc
carbonatos d
océano (fuent

Con el a
reducido forr
mecanismo m
sulfatos en las
del Mar Neg
alcalinas : du
fondo, los sul
biocarbonatac
de sulfato. E
difusión, se p
ocasiona sob
resultado un i
de las medid
muestras de l
confirmar est
carbonatos fo

El lago e
levemente má
bomba alcalin
22 m) (KEMPE
y aragonito y
de arrecifes, e
de cianobacte
Son los prime
(los demás ag
una reconstit
"microbialitos

En el lago
columnas de t
columnas se f
se mezcla cor
inorgánica sii
produce arag
espesa.

Estos dos
del Precámbr
medio alcalinc

como consecuencia, la formación de albita en la costra granodiorítica, los depósitos muy antiguos de carbonatos y el aumento del depósito de carbono orgánico sedimentario. La disminución de la alcalinidad permite un aumento de la concentración en calcio libre de 10^{-5} M a 10^{-3} M, lo que provoca un estrés cálcico para los organismos vivientes. Aquel océano estaba fuertemente sobresaturado con relación a la mayoría de los carbonatos minerales, favoreciendo asi la precipitación inorgánica o de orígen microbiano de carbonatos de calcio y de magnesio en lugares donde el calcio llegaba al océano (fuentes submarinas, entradas de aguas freáticas o ríos).

Con el aumento del oxígeno y la oxidación del depósito de azufre reducido formó los sulfatos del océano dando lugar a la aparición de otro mecanismo modulador de la alcalinidad del agua de mar : la reducción de los sulfatos en las cuencas océanicas estancadas (KEMPE, 1990). El ejemplo actual del Mar Negro muestra que estas cuencas pueden funcionar como bombas alcalinas : durante la oxidación del carbono orgánico que desciende sobre el fondo, los sulfatos son reducidos y su carga negativa es sustituida por iones biocarbonatados, aumentando la alcalinidad en concordancia con la pérdida de sulfato. En los afloramientos de poca intensidad, en los remolinos de difusión, se producen excesos del nivel de alcalinidad en el océano lo que ocasiona sobresaturaciones, locales, regionales o globales, que dan como resultado un incremento en la formación de $CaCO_3$. Las diferencias negativas de las medidas de $\delta^{13}C$ en las secuencias carbonatadas se interpretan como muestras de los excesos de alcalinidad en la historia del globo. Con el fin de confirmar estas hipótesis, se han estudiado, en medios alcalinos actuales, los carbonatos formados bajo estas condiciones.

El lago existente en el crater de la isla de Satonda en Indonesia es levemente más alcalino que el agua de mar normal, debido a la acción de una bomba alcalina en su zona más profunda (el lago es reductor por debajo de los 22 m) (KEMPE and KAZMIERCZAK, 1990b, 1993). La sobresaturación de calcita y aragonito y el aumento de alcalinidad y del pH pudo ocasionar la formación de arrecifes, en parte por una premineralización en vivo mediante el soporte de cianobacterias con Mg y calcita (KAZMIERCZAK and KEMPE, 1990, 1992). Son los primeros "microbialitos" recientes señalados en el mar que calcifican (los demás aglomeran sobretodo los granos de sedimento). Satonda representa una reconstitución de las condiciones en el océano antiguo, cuando los "microbialitos" abundaban (stromatolitos, trombolitos).

En el lago Van / Anatolia, el mayor "soda lake" del mundo, se pueden ver columnas de tapices bacterianos, de 40 m de altura (KEMPE *et al.*, 1991). Estas columnas se forman en lugares donde el agua del fondo es muy rica en Ca y se mezcla con el agua muy alcalina del lago (150 meq/l, pH 9.7). La calcita inorgánica sirve de substrato duro a una capa cianobacteriana que luego produce aragonito. Esta capa estabiliza las columnas y forma una costra espesa.

Estos dos ejemplos muestran que los "Microbialitos" calcáreos y marinos del Precámbrico y Fanerozoico, se han desarollado probablemente en un medio alcalino muy sobresaturado con minerales carbonatados.

STIC-ILL

09/10

From: Marx, Irene
Sent: Tuesday, September 10, 2002 9:19 AM
T : STIC-ILL
Subject: 09/777664

411610

Imp rtance: High

Please send to Irene Marx, Art Unit 1651; CM1, Room 10E05, phone 308-2922, Mail box in 11B01

Observations on the ionic composition of blue-green algae growing in saline lagoons
AU Pillai, V. K.
SO Proc. Natl. Inst. Sci. India, (19550000) vol. 21, no. 2, pp. 90-102.
DT Journal

Dalrymple, D.W., 1965, "Calcium carbonate deposition associated with blue green algal mats, Baffin Bay.:, Texas: Institute of Marine Science Publication 10, p. 187-200

Black, M., 1933, "The algal sedimentation... ", Royal Society of London Philosphical transactions, Ser. B, V. 222, p. 165-192

Lowenstam HA (1981), Science, 211:1126-1131

Ferris et al., Earth Sci., 47:233-250 (1993)

Ferris et al., Appl. and Environm. Microbiol.,1989, 55:1249-1257

Kazmierczak et al., (1990), Science, 250:1244-1248

Kempe et al., Facies, 28:1-32, 1993.

Kempe et al., 1994, Bull, Inst. Oceanogr., Monaco no. spec., 13:61-117.

Merz, M.U.E, 1992, Facies, 26:81-102

Pentecost et al., 1986, Calcification in cyanobacteria, In "Biomineralization of Lower plants and animals (Leadbeater et a., ed. 73-90, Clarendon Press, Oxford.

Riding, R., 1982, Nature, 299:814-815

Thompson eta., 1990, Geology, 18:995-998

LC
9/11
SMP
Completed
0
20
4.00

Irene Marx
Art Unit 1651
CM1 10-E-05,
Mail Box 11-B-01
703-308-2922

salt water p 86 (ament)

The Systematics Association
Special Volume No. 30

Biomineralization in Lower Plants and Animals

Edited by

Barry S. C. Leadbeater
Department of Plant Biology,
University of Birmingham

Robert Riding
Department of Geology,
University College,
Cardiff

Published for the SYSTEMATICS ASSOCIATION by the
CLARENDON PRESS · OXFORD
1986

QR88
.B57
1986

Oxford University Press, Walton Street, Oxford OX2 6DP
Oxford New York Toronto
Delhi Bombay Calcutta Madras Karachi
Kuala Lumpur Singapore Hong Kong Tokyo
Nairobi Dar es Salaam Cape Town
Melbourne Auckland
and associated companies in
Beirut Berlin Ibadan Nicosia

Oxford is a trade mark of Oxford University Press

Published in the United States
by Oxford University Press, New York

© *The Systematics Association, 1986; Chapter 6*
© *Macaulay Institute for Soil Research, 1986*

All rights reserved. No part of this publication may be reproduced, stored in a retrieval system, or transmitted, in any form or by any means, electronic, mechanical, photocopying, recording, or otherwise, without the prior permission of Oxford University Press

British Library Cataloguing in Publication Data
Biomineralization in lower plants and animals. —
(The Systematics Association special volume; no. 30)
1. Biomineralization
I. Leadbeater, Barry S. C. II. Riding, Robert
III. Systematics Association IV. Series
574.19'214 QH512
ISBN 0-19-857702-8

LIBRARY OF CONGRESS
5
JAN 0 9 1987
COPY
CIP

Library of Congress Cataloging in Publication Data
Main entry under title:
Biomineralization in lower plants and animals.
(The Systematics Association special volume:
no. 30)
Includes index.
1. Microbial metabolism — Congresses. 2. Biomineralization — Congresses. 3. Algae — Physiology — Congresses. 4. Protozoa — Physiology — Congresses. 5. Lichens — Physiology — Congresses. I. Leadbeater, Barry S. C. II. Riding, Robert. III. Systematics Association. IV. Title.
QR88.B57 1986 576'.119214 85-31951
ISBN 0-19-857702-8

Typeset by Dobbie Typesetting Service, Plymouth, Devon
Printed in Great Britain by
Richard Clay (The Chaucer Press) Ltd,
Bungay, Suffolk

Biomineral
akin to the
Earth. It p
alive, and v
from river
products of
Consequer
geologists
Earth and

At the ri
the concen
for their p
materials a
simple stat
have value
in biomine
to the proc
existence
significanc
diverse suit
of this boc

We take
algae, lich
for two rea
of study an
of the subj
the field. S
have led u
important
in diatoms
similar, wi
and most i
also exist i
and scales.
exhibit con

5. Calcification in cyanobacteria

ALLAN PENTECOST and ROBERT RIDING

Abstract

Cyanobacterial calcification is primarily due to the extracellular nucleation of crystals of calcium carbonate within and upon the sheath. Trapping and binding of particulate sediment is a separate process which alone, or together with calcification, is responsible for stromatolite formation. Several taxa, particularly filamentous forms, show specificity for calcification, but none appears to be an obligate calcifier. Calcification is dependent upon favourable environmental conditions, as well as upon sheath characters. The mineralogy and composition of cyanobacterial calcium carbonate is consistent with that expected to form by inorganic precipitation from the surrounding water. In freshwater this is normally low-magnesian calcite.

In the Recent, calcification is virtually restricted to freshwater where species belonging to *Homeothrix*, *Phormidium*, *Plectonema*, *Rivularia*, *Schizothrix*, and *Scytonema* are commonly affected. These produce oncoids and contribute significantly to tufa deposits in lacustrine and fluviatile environments. Recent marine stromatolites principally form by trapping and binding processes associated with cementation, and are not normally calcified by precipitation on or within cyanobacterial sheaths. Calcification was common in marine cyanobacteria from the Cambrian (590 million years) to the Cretaceous (65 million years), possibly indicating a difference in sea-water chemistry in comparison both to the Precambrian and the Cenozoic.

Introduction

Cyanobacteria are widely distributed micro-organisms with a long geological record. Calcification makes them much more conspicuous than they would otherwise be and can lead to the formation of thick crusts of sediment in marine, hypersaline, fresh-water, and hot-spring environments. The best known of these deposits are tufa, stromatolites, and the nodular stromatolites termed oncolites or oncoids.

Despite long recognition of their participation and importance in calcium carbonate deposition, uncertainties remain concerning both the

processes and products of cyanobacterial calcification. The fact that no cyanobacterium is known to be an obligate calcifier raises doubts concerning the degree of control over, and specificity for, the process of calcification. So far as products are concerned, it is difficult to distinguish between fine-grained carbonate sediment trapped by the cyanobacterium and that which is precipitated upon or within it. These problems are further compounded by the general difficulty of sometimes recognizing whether cyanobacteria merely colonize sediment or are active in its deposition.

These problems are central to any discussion of cyanobacterial calcification. In order to focus them we propose to begin this review with the following statements which attempt to summarize both our present state of knowledge and the problems which still require resolution. These statements must therefore be regarded as working hypotheses covering the most important areas for consideration of cyanobacterial calcification.

1. Calcification is defined here as the nucleation of calcium carbonate upon and/or within the cyanobacterial sheath. It is distinct from the trapping and binding of particulate sediment which is the main process in the formation of Recent marine stromatolites.
2. Calcification is primarily associated with the polysaccharide sheath of cyanobacteria; this appears to provide sites favourable to the nucleation of calcium carbonate crystals.
3. The mineralogy and composition of cyanobacterial calcium carbonate is consistent with that to be expected from essentially inorganic precipitation.
4. Several cyanobacteria exhibit specificity for calcification, but none is known to be an obligate calcifier.
5. Cyanobacterial calcification is only partly within the influence of the organism. It requires suitable environmental conditions favouring precipitation of calcium carbonate, together with the presence of a sheath to provide a site for crystal nucleation.
6. Stromatolites may be formed by either, or both, (a) calcification (as defined in statement 1), and (b) trapping of particulate sediment by cyanobacteria.
7. Since the Cretaceous (65 million years) calcification in cyanobacteria has only been common in fresh water. Prior to that, and since the early Cambrian (590 million years) cyanobacterial calcification was common in the sea. In the Precambrian, when marine stromatolites were abundant, there is little direct evidence that cyanobacterial calcification occurred.

Deposition of calcium carbonate in association with cyanobacteria

The sheath provides the normal site for calcification. Nucleation of calcium carbonate crystals may occur within the sheath (impregnation)

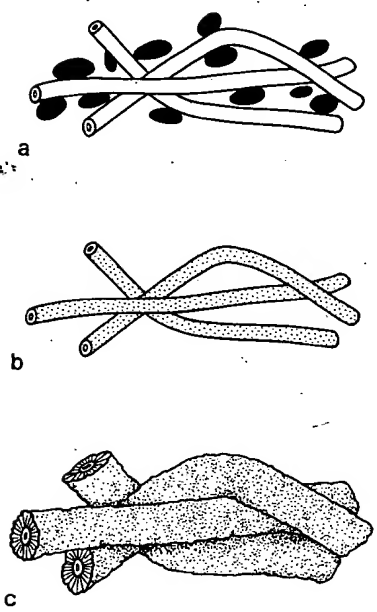

Fig. 5.1. Deposition of calcium carbonate associated with filamentous cyanobacteria. (a) Trapping and binding of particulate sediment; (b) calcification of the sheath interior (impregnation); (c) calcification of the sheath exterior (encrustation).

and upon it (encrustation) (Riding 1977*a*, p. 40, Fig. 5). In addition, the sheath can trap sediment particles which are then bound into the cyanobacterial mat as growth continues (Fig. 5.1). Trapping and binding is not here regarded as calcification, although it may be associated with it.

In filamentous forms, calcification (impregnation) of the sheath interior results in the formation of a calcareous macaroni-like tube providing fossils which may preserve the size and shape of the sheath for hundreds of millions of years. *Girvanella* Nicholson & Etheridge exemplifies this type of preservation (Riding 1977*a*).

Calcification of the sheath exterior (encrustation) may develop as an external crust on the sheath surface, in which case it is indistinguishable from cementation. These crystals are commonly larger than those impregnating the sheath interior (Riding 1977*a*, Fig. 5). They commonly form in tufa deposition. External calcification may also develop through outward extension of crystals within the sheath, as shown in *Scytonema* by Lowenstam (Chapter 1, this volume).

Calcification of coccoid forms appears to be a post-mortem effect associated with cementation, as in the *Entophysalis* mats of the Shark Bay stromatolites (Golubic 1983).

Thus, sheath calcification and trapping and binding of particulate sediment are not mutually exclusive processes. Stromatolites formed with and without calcification have been termed skeletal and non-skeletal stromatolites respectively (Riding 1977*b*), but skeletal stromatolites always include some component of trapped sediment.

Site and mechanism

The site of calcification is the surface, outer layers, and interior of the mucilaginous sheath (Wallner 1934; Gleason 1972; Golubic 1973; Pentecost 1978; Casanova and Tiercelin 1982; Wood 1984). SEM images show that calcification occurs at the sheath surfaces of *Phormidium*

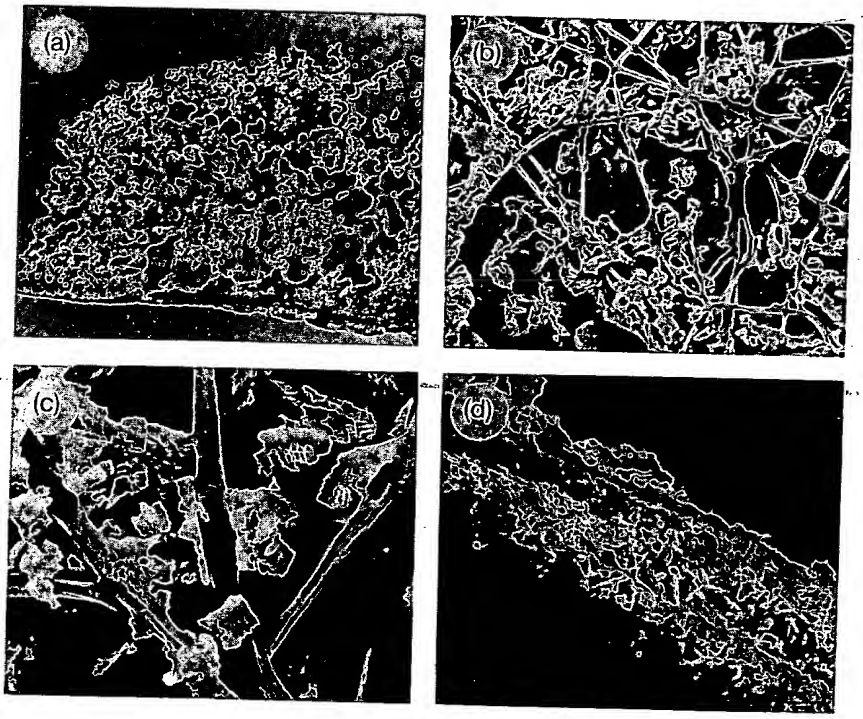

Fig. 5.2. (a) Carbonate-encrusted nodules of *Phormidium incrustatum* from Ingleton Glen, Yorkshire, × 7. (b) SEM picture of *S. calcicola* trichomes showing calcite crystals attached to the sheaths at the deposit surface. Ingleton Glen, Yorkshire. × 425, Au–Pd coated. (c) SEM picture of *S. calcicola* showing calcite encircling but not penetrating the sheaths. Note collapse of the sheath caused by desiccation. Ingleton Glen, Yorkshire. × 1600, Au–Pd coated. (d) SEM picture of *Phormidium incrustatum* sheath surface. Anhedral and acicular crystals are visible, probably of calcite. Ingleton Glen, Yorkshire. × 3400, Au–Pd coated.

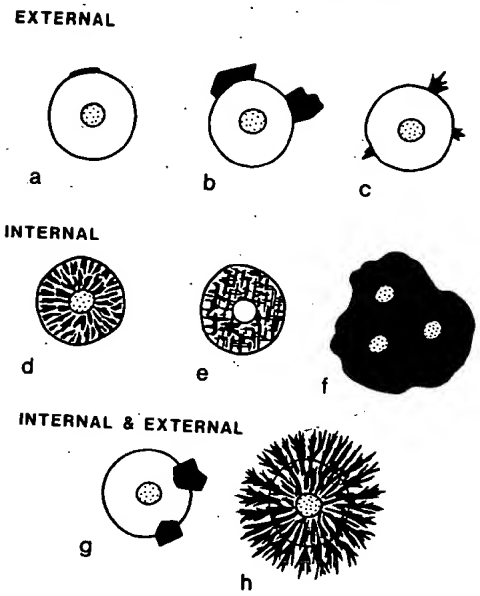

Fig. 5.3. Styles of calcification in filamentous cyanobacteria illustrated by transverse sections. (a–c) External, partial; (d–f) internal, relatively complete; (g, h) internal and external. (a) Thin crust (e.g. *Microcoleus*); (b) rhombs (e.g. *Scytonema*); (c) blades and needles (e.g. *Schizothrix*); (d) blades and needles within the sheath (e.g. *Plectonema*); (e) dendrites within the sheath (e.g. *Geitleria*); (f) solid $CaCO_3$ mass surrounding several trichomes (e.g. *Rivularia*); (g) rhombs (e.g. *Scytonema*); (h) blades, needles, and polycrystalline dendrites (e.g. *Scytonema*). Cells stippled; sheath clear; $CaCO_3$ black.

incrustatum, *Schizothrix calcicola* (Fig. 5.2), and *Rivularia haematites* (unpublished observations). Unfortunately, the highly hydrated sheaths of these organisms collapse during preparation (Fig. 5.2(c)) and the outer layers of the sheaths of *Rivularia* are diffluent and poorly defined, so that penetration of calcite into these layers may well occur but be difficult to demonstrate. Sheath calcification certainly occurs in *Scytonema* (Gleason 1972), *Plectonema gloeophilum* (Riding 1977*a*), and in the cave species, *Geitleria calcarea* and *G. floridana* (Friedmann 1979; Couté 1982).

Although the crystals are closely associated with the filaments, there is not always clear crystallographic orientation with respect to the sheath. Pentecost (1978, 1985*a*) found no evidence for orientation in *Phormidium*, *Rivularia*, and *Schizothrix*. However, the three-dimensional network of calcite found in *Geitleria* appears to be directed parallel to the lines of rhombohedral cleavage (Couté 1982) and indicates a strong directional influence of the sheath (Fig. 5.3(e)), and the calcite crystals in the sheath of *Plectonema* form tufted clusters crudely orientated normal to the surface of the filament (Riding 1977*a*, p. 36) (Fig. 5.3(d)).

Where carbonate-depositing waters associated with cyanobacteria were analysed in detail, calcite precipitation was found to have been thermodynamically favoured (Pentecost 1981). In the absence of inhibitors, nucleation is likely to occur and there are at least three ways by which the calcite could contact and grow on the sheath. Sheath polysaccharides of cyanobacteria, including those associated with carbonate deposition, contain acidic groups, mainly ionizable uronic acids (Drews and Weckesser 1982; Pentecost 1985*a*). These would attract oppositely charged calcium ions, perhaps giving rise to epitaxial growth and heterogeneous nucleation. Alternatively, nucleation might occur on attached bacteria or clay and silt particles. Third, nucleation could occur on bacteria or inorganic particles in suspension which could then become attached to the sheath. For particles 0.1 μm or less in diameter, the forces of molecular bombardment could overcome the repulsive potential energy barrier between two surfaces allowing bonds to form. For larger particles, the energy barrier is higher and adhesion could only occur if isolated chains of polymer protruded from the sheath (Rogers 1979).

These processes may operate singly or together and trapping of calcite particles in suspension can also provide additional sediment on the sheaths. Silt trapping certainly occurs in calcified colonies and the silt content may exceed 10 per cent by weight, even in fresh-water deposits. Calcite precipitation often occurs in productive alkaline lakes due to phytoplankton photosynthesis and this could provide a source of calcite in lacustrine sites (Golubic 1973; Jones and Wilkinson 1978). A careful study of the initial stages of deposition is obviously required although, in any case, crystal growth certainly continues at the sheath surface. This is particularly clear in *Rivularia* where crystal size increases further into the colony (Wallner 1934, 1935) and the crystals themselves sometimes appear zoned as a result of continued growth (Casanova 1981). Golubic (1973) noted in the green alga *Gongrosira* that some calcification within the colonies was probably the result of respiratory dissolution and photosynthetic precipitation leading to recrystallization. This could also occur in cyanobacteria.

The sheaths of cyanobacteria differ widely in their physical and chemical properties (Drews and Weckesser 1982) but sheath development may be environmentally induced in some genera (Rippka *et al.* 1979; Pentecost 1985*b*). Sheaths vary both in their thickness and consistency with a tendency for calcified species to have sheaths which are thick (2–10 μm) and gelatinous, with the notable exception of *Scytonema* and some forms of *Plectonema* which have thick, non-gelatinous sheaths. In these genera sheath thickness appears to influence the degree of false-branching (Pentecost 1985*b*).

Two basic types of trichome organization are found in the calcified species. In the '*semiglobosa*' form of *Schizothrix calcicola*, *Homeothrix janthina*,

and especially *Rivularia* a radiating pattern is apparent. The trichomes become aligned, often within a common sheath, and grow outwards to form nodular, often densely calcified colonies 1 mm to several cm in diameter. This has little influence on crystal growth, although in *Rivularia* the crystals commonly grow parallel to the trichome surfaces, presumably following the line of least resistance (Fig. 5.3(f)). Radial growth also occurs in the nodules formed by *Phormidium incrustatum* (Fig. 5.2(a)) but sections reveal a less pronounced radial structure in most cases. The reasons for these differences are unclear but phototaxy, motility, and false-branching could all play a part. It should also be noted that doubt remains concerning the separate identity of *Homeothrix janthina* and *S. calcicola* f. *semiglobosa*. The trichomes of the former can be distinguished by their gradual attentuation to hair-like points, whilst in the latter attenuation is slight. Intermediate forms seem to occur and this warrants further study.

The second group consists of 'unstructured' mats. These are most frequently composed of *S. calcicola* (Fig. 5.2(b)) where no preferred orientation of the trichomes is apparent. Unstructured mats are also formed by *Scytonema/Plectonema*, mainly in semiterrestrial sites.

Cyanobacterial calcium carbonate

Mineralogy and composition

Freshwater calcified cyanobacteria normally contain, or are encrusted by, crystals of low-magnesian calcite (Gleason 1972). Marine influence produces high-magnesian calcite (Monty 1967, p. B74) and aragonite (Golubic and Campbell 1981). These changes in composition with environment reflect the normal response for physiochemical precipitates relative to water-chemistry (Folk 1974).

Little is known concerning the original calcium carbonate of fossil cyanobacteria. Diagenetic changes cause both aragonite and high-magnesian calcite to be replaced by low-magnesian calcite. However, James and Klappa (1983) reported that the style of preservation of the possible cyanobacterial fossil *Renalcis* in Cambrian limestones suggests that it was probably originally composed of high-magnesian calcite.

Morphology

Ancient calcified cyanobacteria have skeletons with micritic structure ($CaCO_3$ grains smaller than 4 μm in size) which appear to have been recrystallized. Recent specimens also commonly consist of micritic carbonate, but the individual crystals have their original form and arrangement in contradistinction to the more equidimensional and

apparently unorganized grains of fossil examples. Some recent calcified cyanobacteria, however, show extensive development of calcium carbonate which forms a solid mass, pierced by trichomes. The following styles of calcification are known.

1. Rhomb-like crystals within or upon the sheath, e.g. *Scytonema hofmanni* (Monty 1965, quoted in Gleason 1972, p. 76), *Microcoleus lyngbyaceous* (Gleason 1972, p. 76);

2. Acicular crystals within, and sometimes extending beyond the sheath, e.g. *Schizothrix calcicola* (Gleason 1972, p. 66), *Plectonema gloeophilum* (Riding 1977*a*);

3. Thin platy crystals on the sheath surface, e.g. *Microcoleus lyngbyaceous* (Gleason 1972, p. 77). Gleason calls these low-relief crystals 'plaque';

4. Dendritic networks of fine crystallites within and extending beyond the sheath, e.g. probably in *Schizothrix calcicola* (Gleason 1972, p. 66), in *Geitleria* (Friedmann 1979; Couté 1982), and in *Scytonema* (Lowenstam, Chapter 1, this volume);

5. Crystal masses surround several, or many, trichomes, e.g. *Rivularia*, although the inner part of the sheath is not normally calcified.

These are illustrated in Fig. 5.3. Crystals within the sheath probably have arrangements which relate to sheath structure (see 'Site of calcification').

Taxonomy and specificity

It is only recently that the cyanobacteria were classified using bacteriological methods. They were originally placed with the algae and classified accordingly, primarily on morphological grounds. The current position is such that whilst the techniques for a full bacteriological classification are available, we are not in a position to apply them since so many cyanobacteria are difficult to obtain as pure cultures. Rippka *et al.* (1979) provided a provisional classification consisting of five sections. Most calcifying forms belong to section III, subdivision *Oscillatoria*, but this subdivision is unsatisfactory and requires revision. The scheme is useful, however, because it allows organisms to be classified to some extent according to their morphology, although many morphological features, e.g. sheath thickness and extent of lamination, have been found to be unreliable. Instead, other methods have been applied such as DNA base composition (Herdman *et al.* 1979). Considerable time will elapse before these methods are widely applied and in the meantime the 'traditional' system of Geitler (1932) is probably the most useful. Field observations suggest that a small number of cosmopolitan phenotypes or 'pleomorphs' are inhabiting niches whose main characteristics are determined by the depositing environment rather than the overall climate.

This presumes either genetic stability or the tendency for several genotypes to undergo a convergence of form under similar conditions. Considering the similarity of cyanobacterial deposits worldwide, the former hypothesis seems reasonable although there is *in vivo* evidence for genetic translation and probably transduction (Herdman 1982).

Pia (1934) listed 76 species belonging to 23 genera associated with deposition. However, only five reasonably well-defined filamentous species are recognized as being of common occurrence here, namely *Schizothrix calcicola*, *Phormidium incrustatum*, *Homeothrix janthina*, *Rivularia haematites*, and *Scytonema hoffmanii*. The species belonging to group III can be distinguished by their trichome diameters and morphology. *Plectonema* can be regarded as a non-heterocystous form of *Scytonema* and the taxonomy of two *Phormidium* species was clarified by Kann (1973). It was suggested that the coccoid form *Pleurocapsa* also shows specificity for calcification (Krumbein and Giele 1979).

Golubic (1973), in reviewing the specificity problem, concluded that carbonate deposition could not be upheld as a species character. However, if we accept that sheath surface chemistry is one of the determinants of deposition this view may have to be modified.

Photosynthetic activity plays an important role in the calcification of eukaryotic algae but it appears to play little part in cyanobacterial calcification. There are no specialized anatomical features to promote calcification and the growth rates of the species involved are often low, particularly at high latitudes. However, the situation varies considerably depending upon the biomass per unit area and the rate of flow of water. Under extreme conditions, with a low flow and high biomass, photosynthesis may become an important factor although this should be regarded as exceptional.

Products

Microfabrics created by individual colonies

Tangled tubes (e.g. *Plectonema* and fossil *Girvanella*), fan-like arrays of tubes (e.g. *Rivularia* and fossil equivalents), and dense micritic (fine-grained) calcareous bush-like masses (e.g. *Schizothrix* and fossil *Angulocellularia*) constitute the principal morphological styles of calcified cyanobacterial filaments and colonies (Fig. 5.4). These are present among the earliest calcified cyanobacteria in the Lower Cambrian (Riding and Voronova 1985). Most Palaeozoic and Mesozoic fossils of this type are known from marine environments whereas their Recent analogues only appear to be present in fresh water (Riding 1977*a*; Riding and Voronova 1982).

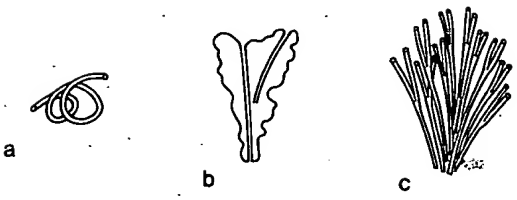

Fig. 5.4. Morphology of individual calcified filaments and colonies which provide the basic microfabrics from which larger stromatolitic, reef, and tufa deposits are constructed. (a) Tangled tubes, e.g. fossil *Girvanella*; (b) micritic bushes, e.g. fossil *Angulocellularia*; (c) fan-like arrays of branched tubes, e.g. fossil *Botomaella*.

Calcified coccoid cyanobacteria such as *Pleurocapsa* (Krumbein and Giele 1979) appear to be responsible for the clotted microfabrics in thrombolites and also occur in the sub-Recent tufas of the Dead Sea area (Buchbinder 1981). Thrombolites are a variety of stromatolite which lack the laminated fabric normally diagnostic of stromatolites. The term was introduced by Aitken (1967) (also see Monty 1976, p. 22).

Reefs

Clusters, layers, and veneers, all representing in-place accumulations of individual calcified cyanobacteria, are present in many if not all marine reefs of Palaeozoic and Mesozoic age (Wray 1969). Normally they are intimately associated with metazoan reef builders, as well as with carbonate sand and mud, so that the resulting rock fabric is complex. In the Lower Palaeozoic, clusters of microscopic bush-like masses of *Angulocellularia* are intimately associated with sponge-like organisms in Cambrian and Lower Ordovician mounds (see references in Riding and Voronova 1982*a*). In the early-Mesozoic calcified cyanobacteria occur with scleractinian coral- and sponge-dominated reefs of Triassic age (Schäfter and Senowbari-Daryan 1983). Bioherms constructed mainly by *Rivularia* occur in the Pleistocene of Greece (Richter *et al.* 1979).

Tufa

Freshwater calcareous deposits with which cyanobacteria are associated can be classified into two types—those which develop and remain *in situ*, consisting of thin incrustations or developing into massive layers of many varieties (tufa and travertine) and spherical or flattened bodies terms oncolites or oncoids, detached from the substrate and subject to rolling by gentle currents (< 1 m s^{-1}) or growing more or less in place on the beds of lakes and rivers. Oncoids may be regarded as loose

tufa-like cyanobacteria-dominated nodules, but are more commonly classed as spherical stromatolites (see below).

Tufa forms under many conditions, but usually in streams with steep gradients subject to turbulent flow. It is commonly developed at springs and waterfalls in limestone areas. Loss of CO_2 from the water due to turbulence and evaporation results in $CaCO_3$ precipitation on any available surface, particularly the plants which thrive in these moist, well-lit environments. Consequently, not only cyanobacteria but algae, especially chlorophytes, together with bryophytes, grass, and other plants are involved in and incorporated into tufa and the resulting deposit is often highly porous. Cyanobacteria commonly dominate the wettest zones and create fabrics similar to those seen in skeletal stromatolites (see below).

The surface layers of tufa consist mainly of deposits formed by *Phormidium incrustatum* and *Schizothrix calcicola* overgrowing bryophytes, with *P. incrustatum* usually more abundant under less turbulent conditions. *Rivularia* usually occurs in areas of moderate flow (0.2–1.5 m s^{-1}), often close to the water surface, but is not normally a major tufa former.

Lacustrine tufa deposits which appear to be mainly cyanobacterial were described from Great Salt Lake, Utah (Eardley 1938; Halley 1976) and tufa/stromatolite deposits from Green Lake, New York (Eggleston and Dean 1976). Sub-Recent examples occur in the Dead Sea area (Buchbinder 1981).

Stromatolites

Persistent difficulty in satisfactorily defining the term stromatolite is due to the absence, in most ancient stromatolites, of direct evidence of the organisms responsible for them. Consequently a genetic definition, stipulating the involvement of cyanobacteria, can be applied to Recent examples but is inappropriate for most ancient ones which are merely laminated calcareous deposits *thought*, by analogy with modern forms, to be cyanobacterial in origin. It has also been pointed out that numerous micro-organisms, including bacteria and algae, can also be involved in stromatolite formation (Hofmann 1973). Consequently, both genetic and non-genetic definitions have been developed. Walter (1976, p. 1) recommended a 1974 definition by S. M. Awramik and L. Margulis: Stromatolites are organosedimentary structures produced by sediment trapping, binding and/or precipitation as a result of the growth and metabolic activity of micro-organisms, principally cyanophytes. An alternative, descriptive definition is given in Semikhatov *et al.* (1979, p. 993): an attached, laminated, lithified, sedimentary growth structure, accretionary away from a point or limited surface of initiation.

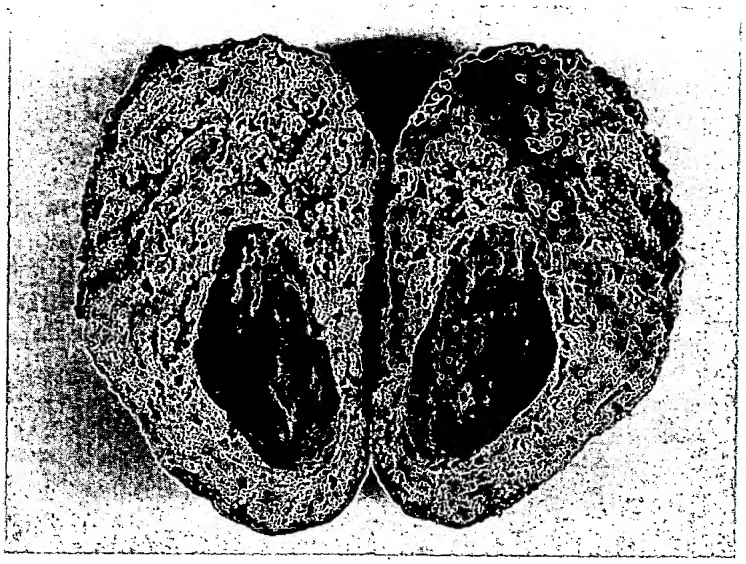

Fig. 5.5. Recent oncoids, formed mainly by *Schizothrix calcicola* and *Phormidium incrustatum*, cut to show the pebble nucleus and laminated structure. The oncoid is 8 cm long and 5 cm wide. River Alz, Bavaria.

Stromatolites formed primarily by calcification of cyanobacteria have been termed 'skeletal stromatolites' in contradistinction to 'non-skeletal stromatolites' formed by trapping and binding of sediment and in which little or no trace of calcified sheath material is preserved (Riding 1977*b*). Skeletal oncoids (nodular stromatolites) 'constructed by calcified cyanophytes' have been termed cyanoids (Fig. 5.5) (Riding 1983).

In general, in marine deposits, skeletal stromatolites and cyanoids are less common than non-skeletal stromatolites and oncoids. Modern subtidal stromatolites, such as those described from Bermuda by Gebelein (1969, p. 59), are not calcified whereas those in fresh-water environments adjacent to the sea are (Monty 1973, p. 614). The Shark Bay stromatolites of Western Australia are lithified by a process described by Golubic (1983) as post-mortem calcification of the sheaths of the coccoid species *Entophysalis major*. This appears to be due to the intertidal location of the stromatolites studied, desiccation of the *Entophysalis* mat killing the cyanobacterium and promoting $CaCO_3$ deposition. Subtidal stromatolites at Shark Bay appear to be lithified by cementation. In none-marine environments, calcified cyanobacteria are relatively common. However, *in situ* calcified cyanobacteria in fresh-water usually contribute to tufa formation, rather than to stromatolites. This is due to the additional presence of other plants in these environments which lead to the production of porous tufa fabrics rather than to the formation of

more densely laminated stromatolites. Nevertheless, cyanoids are widespread in fresh-water because they develop under water where many tufa-forming bryophytes and angiosperms are excluded. Cyanoids generally range in size from 0.5 to 30 cm and are formed by accretion on a foreign nucleus. Major Recent components are *Homeothrix janthina*, *Schizothrix calcicola*, *Phormidium incrustatum*, and occasionally *Rivularia*, and the ultimate size attained is probably related to current speed (Golubic 1973).

Environment

Two major environmental gradients significantly affect calcification in cyanobacteria. The first is variation in water movement in freshwater, the second is change in salinity. In limestone areas where freshwater is supersaturated in dissolved $CaCO_3$, loss of dissolved CO_2 results in spontaneous carbonate precipitation. Evasion of CO_2 initially takes place where groundwater surfaces in springs and subsequently is stimulated by turbulent flow and evaporation until equilibrium with the atmosphere is re-established (Golubic 1973, pp. 435–6). Consequently, springs, waterfalls, and fast-flowing streams show high rates of $CaCO_3$ precipitation which affect all surfaces and result in tufa deposition and oncoid formation (Fig. 5.6). In slow-flowing streams downstream from these sites, and in lakes, inorganic precipitation is reduced and calcification becomes species-specific (Golubic 1973, p. 440).

Many of these deposits show a regular lamination (Monty 1976, pp. 205–8). In *Rivularia*, this has been used to distinguish some species (Geitler 1932; Golubic 1973) although the variation is such that this cannot reasonably be upheld. The zones are caused by seasonal differences in growth, perhaps augmented by seasonal changes in water chemistry which are known to occur in many calcareous streams. Densely calcified zones are produced in the winter when growth is slow, followed by wider, lightly calcified zones in the summer. Superimposed on this cycle may be discontinuities caused by emersion during periods of low water. Zonation also occurs in other genera but the zones are often less clear although the cause appears to be the same (Pentecost 1978). In some cases, oncoids appear to be colonized by alternating layers of *Phormidium/Rivularia* and *S. calcicola*.

In the second major environmental gradient, between freshwater and marine environments, species-specific calcification ceases as marine influence increases (Geitler 1932; Monty 1973, p. 614). This is due to the lower rates of inorganic precipitation caused by the strong buffering of seawater (see Golubic 1973, pp. 446–7). The initial stages of this gradient, where calcification continues, are associated with a change from

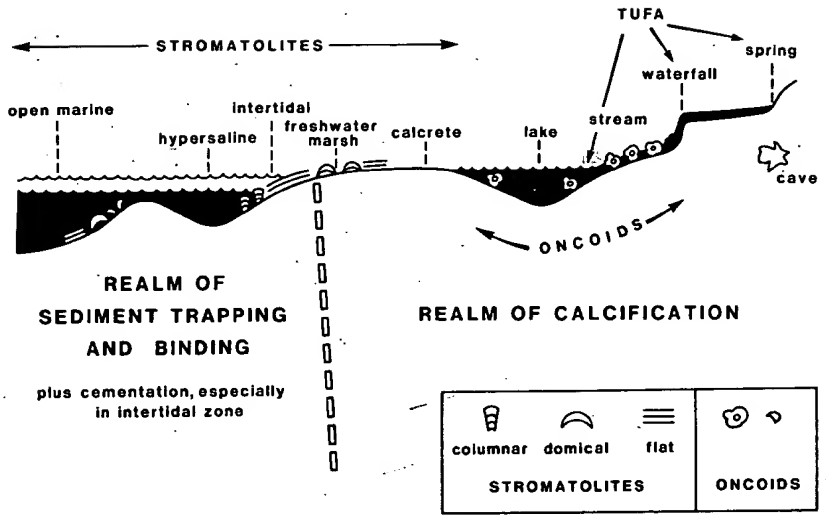

Fig. 5.6. Environmental distribution of Recent carbonate deposits associated with cyanobacteria. Sediment trapping and binding is the dominant process operating in modern marine environments. It also occurs in fresh water although in tufa and oncoid deposits it is subordinate to calcification.

low- to high-magnesian calcite precipitation on cyanobacteria as sea-water influence increases, reflecting the greater Mg^{2+} concentration in sea water (see 'Cyanobacterial calcium carbonate', above).

Oncoids have been described from the margins of soda lakes in Africa (Casanova and Tiercelin 1982) where accretion may be the result of evaporation. Evaporation is also an important agent in fresh water in warm climates (Pentecost, 1985*a*). A few cyanobacteria are known to exist as halophilic strains (Whitton and Potts 1982) whilst others show considerable halotolerance but there are no studies so far on calcified species.

Little is known of the effects of light and temperature on deposition. Tufaceous material formed by cyanobacteria was reported from Arctic and tropical latitudes, both containing Oscillatoriaceae, probably *S. calcicola*. Golubic (1973) demonstrated light-orientated growth of cave travertine caused by the phototactic responses of cyanobacteria. The abundance of *S. calcicola* in low-light regimes was noted (Pentecost 1978; 1982); light obstruction caused by the deposits themselves appears to provide favourable habitats just below the tufa surface.

The geological record of marine calcified cyanobacteria indicates major long-term influences which may include sea-water chemistry. The first appearance of heavily calcified cyanobacteria is an abrupt event near the base of the Cambrian (~590 million years) (Riding and Voronova

1984) which introduced forms such as *Angulocellularia* and *Girvanella*, comparable with extant taxa such as *Schizothrix calcicola* and *Plectonema gloeophilum* (Riding and Voronova 1982*a*; Riding 1977*a*). This sudden appearance in the geological record of abundant calcified cyanobacteria suggests a change in calcification potential related either to environmental factors or to some change in cyanobacterial morphology and/or metabolism.

From the Cambrian until the Cretaceous calcified cyanobacteria are common and locally very abundant components of shallow marine carbonate deposits, in addition to occurring in fresh water. From the mid-Cretaceous (~100 million years) they become less common in the sea and by the early Cenozoic (~60 million years) calcified cyanobacteria appear to be absent in normal marine environments. Reversals of the Mg^{2+}/Ca^{2+} ratio, related to pCO_2 in the late Precambrian and to Ca^{2+} deposition by plankton in the Cretaceous, could account for development of marine calcification near 590 million years and its loss near 100 million years (Riding 1982). This suggests that cyanobacterial calcification can be seen as an index of changes in sea-water chemistry and $CaCO_3$ precipitation rates which has considerable importance for studies of marine geochemistry and carbonate sedimentation.

References

Aitken, J. D. (1967). Classification and environmental significance of cryptalgal limestones and dolomites, with illustrations from the Cambrian and Ordovician of southwestern Alberta. *J. Sediment. Petrol.* **37**, 1163–78.

Buchbinder, B. (1981). Morphology, microfabric and origin of stromatolites of the Pleistocene precursor of the Dead Sea, Israel. In *Phanerozoic stromatolites* (ed. C. Monty), pp. 181–96. Springer, Berlin.

Casanova, J. (1981). Etude d'un milieu stromatolitique continental: les travertins plio-pléistocenes du Var (France). Thèse docteur, Université Aix-Marseille II.

—— and Tiercelin, J-J. (1982). Constructions stromatolitiques en milieu carbonaté sodique: les oncolites des plains inondables du lac Magadi. *C. R. hebd. Seanc. Acad. Sci., Paris* sér. II, **295**, 1139–44.

Couté, A. (1982). Ultrastructure d'une cyanophycée aérienne calcifée cavericole: *Geitleria calcarea* Friedmann. *Hydrobiologia* **97**, 255–74.

Drews, G. and Weckesser, J. (1982). Function, structure and composition of cell walls and external layers. In *The biology of cyanobacteria* (ed. N. G. Carr and B. A. Whitton), pp. 333–58. Blackwell, London.

Eardley, A. J. (1938). Sediments of the Great Salt Lake, Utah. *Bull Am. Ass. Petrol. Geol.* **22**, 1305–1411.

Eggleston, J. R. and Dean, W. E. (1976). Freshwater stromatolitic bioherms in Green Lake, New York. In *Stromatolites* (ed. M. R. Walter), pp. 479–88. Developments in Sedimentology, Vol. 20, Elsevier, Amsterdam.

Folk, R. L. (1974). The natural history of crystalline calcium carbonate: effect of magnesium content and salinity. *J. Sediment. Petrol.* **44**, 40–53.

Friedmann, E. I. (1979). The genus *Geitleria*: distribution of *G. calcarea* and *G. floridana* n sp. *Plant Syst. Evol.* **131**, 169–78.

Gebelein, C. D. (1969). Distribution, morphology, and accretion rate of Recent subtidal algal stromatolites, Bermuda. *J. Sediment. Petrol.* **39**, 49–69.

Geitler, L. (1932). *Cyanophyceae*. In *Kryptogamen-Flora von Deutschland, Österreich und der Schweiz 14* (ed. L. Rabenhorst). Akademische Verlagsgesellschaft, Leipzig.

Gleason, P. J. (1972). The origin, sedimentation and stratigraphy of a calcitic mud located in the southern fresh-water Everglades. Thesis, Department of Geosciences, Pennsylvania State University, University Park, Pennsylvania.

Golubic, S. (1973). The relationship between blue-green algae and carbonate deposits. In *The biology of blue-green algae* (ed. N. G. Carr and B. A. Whitton), pp. 434–72. Blackwell, London.

—— (1983). Stromatolites, fossil and Recent: a case history. In *Biomineralization and biological metal accumulation* (ed. P. Westbroek and E. W. de Jong), pp. 313–26. D. Reidel, Dordrecht.

—— and Campbell, S. E. (1981). Biogenically formed aragonite concretions in marine *Rivularia*. In *Phanerozoic stromatolites* (ed. C. Monty), pp. 209–29. Springer, Berlin.

Halley, R. B. (1976). Textural variation within Great Salt Lake algal mounts. In *Stromatolites* (ed. M. R. Walter), pp. 435–45. Developments in Sedimentology, Vol. 20, Elsevier, Amsterdam.

Herdman, M. (1982). Evolution and genetic properties of the genome. In *The biology of cyanobacteria* (ed. N. G. Carr and B. A. Whitton), pp. 263–306. Blackwell, London.

—— Janvier, M., Waterbury, J. B., Rippka, R., Stanier, R. Y., and Mandel, M. (1979). Deoxyribonucleic acid base composition of cyanobacteria. *J. gen. Microbiol.* **111**, 63–71.

Hofmann, H. J. (1973). Stromatolites: characteristics and utility. *Earth Sci. Rev.* **9**, 339–73.

James, N. P. and Klappa, C. F. (1983). Petrogenesis of early Cambrian reef limestones, Labrador, Canada. *J. Sediment. Petrol.* **53**, 1051–96.

Jones, F. G. and Wilkinson, B. H. (1978). Structure and growth of lacustrine pisoliths from recent Michigan marl lakes. *J. Sediment. Petrol.* **48**, 1103–11.

Kann, E. (1973). Bemerkungen zur Systematik und Ökologie einiger mit Kalk inkrustierter *Phormidium* arten. *Schweiz. Z. Hydrol.* **35**, 141–51.

—— and Giele, C. (1979). Calcification in a coccoid cyanobacterium associated with the formation of desert stromatolites. *Sedimentology* **26**, 593–604.

Monty, C. L. V. (1967). Distribution and structure of Recent stromatolitic algal mats, eastern Andros Island, Bahamas. *Ann. Soc. Géol. Belg.* **90**, 55–100.

—— (1973). Precambrian background and Phanerozoic history of stromatolitic communities, an overview. *Ann. Soc. Géol. Belg.* **96**, 585–624.

—— (1976). The origin and development of cryptalgal fabrics. In *Stromatolites* (ed. M. R. Walter), pp. 193–249. Developments in Sedimentology, Vol. 20. Elsevier, Amsterdam.

Pentecost, A. (1978). Blue-green algae and freshwater carbonate deposits. *Proc. R. Soc., London* **B200**, 43–61.

—— (1981). The tufa deposits of the Malham district, north Yorkshire. *Fld. Stud.* **5**, 365–87.

—— (1982). A quantitative study of calcareous stream and Tintenstriche algae from the Malham district, northern England. *Brit. phycol. J.* **17**, 443–56.

—— (1985*a*). Association of cyanobacteria with tufa deposits: identity, enumeration and nature of the sheath material revealed by histochemistry. *Geomicrobiol. J.* **4**, 285–98.

—— (1985*b*). Investigation of variation in heterocyst numbers, sheath development and false-branching in natural populations of Scytonemataceae (Cyanobacteria). *Arch. Hydrobiol.* **102**, 343–53.

Pia, J. (1934). Die Kalkbildung durch Pflanzen. *Beih. bot. Zbl.* **52**, 1–72.

Richter, D. K., Herforth, A., and Ott, E. (1979). Pleistozäne, brackische Blangrünalgenriffe mit *Rivularia haematites* auf der Perachorahalbinsel bei Korinth (Griechenland). *N. Jb. Geol. Paläont. Abh.* **159**, 14–40.

Riding, R. (1977*a*). Calcified *Plectonema* (blue-green algae), a Recent example of *Girvanella* from Aldabra Atoll. *Palaeontology* **20**, 33–46.

—— (1977*b*). Skeletal stromatolites. In *Fossil algae, recent results and developments* (ed. E. Flügel), pp. 57–60. Springer, Berlin.

—— (1982). Cyanophyte calcification and changes in ocean chemistry. *Nature* **299**, 814–15.

—— (1983). Cyanoliths (cyanoids): oncoids formed by calcified cyanophytes. In *Coated grains* (ed. T. M. Peryt), pp. 276–83. Springer, Berlin.

—— and Voronova, L. (1982*a*). Recent freshwater oscillatoriacean analogue of the Lower Palaeozoic calcareous alga *Angulocellularia*. *Lethaia* **15**, 105–14.

—— —— (1984). Assemblages of calcareous algae near the Precambrian/Cambrian boundary in Siberia and Mongolia. *Geol. Mag.* **121**, 205–10.

—— —— (1985). Morphological groups and series in Cambrian calcareous algae. In *Paleoalgology* (ed. D. F. Toomey and M. H. Nitecki), pp. 56–78. Springer, Berlin.

Rippka, R., Deruelles, J., Waterbury, J. B., Herdman, M., and Stanier, R. Y. (1979). Generic assignments, strain histories and properties of pure cultures of cyanobacteria. *J. gen. Microbiol.* **111**, 1–61.

Rogers, H. J. (1979). Adhesion of microorganisms to surfaces: some general considerations of the role of the envelope. In *Adhesion of micro-organisms to surfaces* (ed. D. C. Elwood and P. Rutler), pp. 6–29. Academic Press, London.

Schäfer, P. and Senowbari-Daryan, B. (1983). Die Kalkalgen aus der Obertrias von Hydra, Griechenland. *Palaeontographica* **B185**, 83–142.

Semikhatov, M. A., Gebelein, C. D., Cloud, P., Awramik, S. M., and Benmore, W. C. (1979). Stromatolite morphogenesis—progress and problems. *Can. J. earth Sci.* **16**, 992–1015.

Wallner, J. (1934). Über die Beteiligung Kalkablagender Pflanze bei der Bildung südbayerischer Tuffe. *Biblthca Bot.* **111**, 1–30.

—— (1935). Zur Kenntis der Kalkbildung in der Gattung *Rivularia*. *Beih. bot. Zbl.* **A54**, 151–5.

Walter, M. R. (1976). Introduction. In *Stromatolites* (ed. M. R. Walter), pp. 1–3. Developments in Sedimentology, Vol. 20, Elsevier, Amsterdam.

Whitton, B. A. and Potts, M. (1982). Marine littoral. In *The biology of cyanobacteria* (ed. N. G. Carr and B. A. Whitton), pp. 515–42. Blackwell, London.

Wood, P. (1984). Structural and physiological studies of the effects of mineral deficiencies on the Rivulariaceae (Cyanobacteria). PhD Thesis, University of Durham and Sunderland Polytechnic, UK.

Wray, J. L. (1969). Algae in reefs through time. *Proc. N. Am. Paleont. Convention* Sept. 1969, Part J, pp. 1358–73.

6.

The int
in the
extrace
minera
the fun
thus lea
The typ
The m
and we
of mag
copper
zinc, a
coloniz
of iron
minera
more i
metal-
on silic
format
in or c

Lowe
biomi
can b
occur
a stro
by o
biom

STIC-ILL

Marx
QI, 534

Fr m: Marx, Irene
Sent: Tuesday, September 10, 2002 9:19 AM
T : STIC-ILL
Subject: 09/777664

Imp rtance: High

Please send to Irene Marx, Art Unit 1651; CM1, Room 10E05, phone 308-2922, Mail box in 11B01

Observations on the ionic composition of blue-green algae growing in saline lagoons
AU Pillai, V. K.
SO Proc. Natl. Inst. Sci. India, (19550000) vol. 21, no. 2, pp. 90-102.
DT Journal

Dalrymple, D.W., 1965, "Calcium carbonate deposition associated with blue green algal mats, Baffin Bay.:, Texas: Institute of Marine Science Publication 10, p. 187-200

Black, M., 1933, "The algal sedimentation... ", Royal Society of London Philosphical transactions, Ser. B, V. 222, p. 165-192

Lowenstam HA (1981), Science, 211:1126-1131

Ferris et al., Earth Sci., 47:233-250 (1993)

Ferris et al., Appl. and Environm. Microbiol.,1989, 55:1249-1257

Kazmierczak et al., (1990), Science, 250:1244-1248

Kempe et al., Facies, 28:1-32, 1993.

Kempe et al., 1994, Bull, Inst. Oceanogr., Monaco no. spec., 13:61-117.

Merz, M.U.E, 1992, Facies, 26:81-102

Pentecost et al., 1986, Calcification in cyanobacteria, In "Biomineralization of Lower plants and animals (Leadbeater et a., ed. 73-90, Clarendon Press, Oxford.

Riding, R., 1982, Nature, 299:814-815

Thompson eta., 1990, Geology, 18:995-998

Irene Marx
Art Unit 1651
CMI 10-E-05,
Mail Box 11-B-01
703-308-2922

of 10 km, this gives a slip of 2.9 m for 1.2 m of slip at Loma Prieta ($x \approx 3$ km). A more precise three-dimensional dislocation calculation yields a slip of 2.5 ± 0.4 m from the surface to 10 km.

9. M. Lisowski, W. H. Prescott, J. C. Savage, M. J. Johnston, *Geophys. Res. Lett.* 17, 1437 (1990).
10. T. A. Clark *et al.*, *ibid.*, p. 1215.
11. The EDM measurements were made to station Eagle; the GPS occupations were at Eagle Un, ~40 m away. In the calculation the two markers were treated as one. On Loma Prieta the GPS occupations and the south-directed EDM lines were from LP1, whereas the EDM lines to the north were from Loma USE. We have corrected all measurements to LP1. For this solution there are 59 observations, 46 unknowns (2 for each of 23 stations), and no null space.
12. For strike slip on a vertical dislocation extending from the earth's surface to depths of 5 to 15 km, the mean-square lack of fit [the residual sum of squares corrected for misclosure; see (*4*)] is 1.4. For strike slip on a plane dipping 70° to the southwest the mean-square lack of fit is 1.5. Both models provide acceptable fits to the data. W. Thatcher and G. Marshall [*Eos* 17, 554 (1990)] presented similar results. In contrast, if the slip vector is constrained so that the strike-slip component is 1.4 times the dip-slip component, the mean-square lack of fit is 2.8, a significantly poorer fit. With 18 linearly independent observations and three parameters, models with mean-square lack of fit greater than 1.7 are rejectable at the 95% confidence level. The variance in the triangulation measurements estimated from the network misclosure is completely consistent with the a priori estimate of the data variance.
13. Near Loma Prieta a total of 33 to 38 mm/yr of slip is partitioned between the San Andreas and Calaveras faults. Estimates of slip on the San Andreas fault range from 13 mm/yr [W. H. Prescott, M. Lisowski, J. C. Savage, *J. Geophys. Res.* 86, 10,853 (1981)] to 26 mm/yr [M. Matsa'ura, D. D. Jackson, A. Cheng, *ibid.* 91, 12,661 (1986)].
14. W. C. Bradley and G. B. Griggs [*Geol. Soc. Am. Bull.* 87, 433 (1976)] estimated uplift rates of as much as 0.26 mm/yr. T. C. Hanks, R. C. Bucknam, K. R. Lajoie, and R. E. Wallace [*J. Geophys. Res.* 89, 5771 (1984)] estimated an uplift rate of 0.35 mm/yr. All rates apply to the Santa Cruz coastline, the uplift rate at the fault trace is not well known.
15. R. S. Anderson, *Science* 249, 397 (1990); Valensise and Ward, in preparation.
16. The average rate of slip on the San Andreas fault in the Carrizo Plains has been 33.9 ± 2.9 mm/yr during the last 3,700 years and 35.8 + 5.4/−4.1 mm/yr during the last 13,250 yr [K. E. Sieh and R. H. Jahns, *Geol. Soc. Am. Bull.* 95, 883 (1984)]; the geodetically determined slip-rate somewhat northwest on the creeping segment of the fault has been 33 ± 1 mm/yr over the last 100 years [W. Thatcher, *J. Geophys. Res.* 84, 2283 (1979)].
17. J. Olson, *Geophys. Res. Lett.* 17, 1492 (1990).
18. As pointed out by T. Heaton (personal communication). Erect a coordinate system with x'_1 horizontal and normal to fault strike, x'_2 horizontal and parallel to fault strike, and x'_3 vertical. The condition that the vertical fault be pure strike-slip is $\sigma'_{13} = 0$. If we assume that one principal stress is near vertical, then σ'_{23} must also vanish. The horizontal and vertical shear stresses acting on the dipping fault are given by $\tau_h = \sigma'_{12}\sin(\delta)$ and $\tau_v = (\sigma'_{11} - \sigma'_{33})\sin(\delta)\cos(\delta)$, where δ is the fault dip. Consider the intermediate principal stress (σ_2) to be vertical and the minimum compression (σ_3) to be at an angle θ clockwise from x'_1. The observed rake of the slip vector in the Loma Prieta earthquake requires that $\tau_h = \beta\tau_v$; $\beta \sim 1.4$ or $\phi = \sin^2(\theta) - \sin(\theta)\cos(\theta)/\beta\cos(\delta)$ where the parameter $\phi \equiv (\sigma_2 - \sigma_3)/(\sigma_1 - \sigma_3)$ describes the shape of the stress ellipsoid. Note that $\phi \geq 0$, as required by definition, for $\theta \geq \tan^{-1}[1/\beta\cos(\delta)] \approx 64°$. The direction of maximum compression, consistent with the slip vector in the two earthquakes, ranges from $64° \leq \theta < 90°$. The minimum value of θ (N16°E) occurs when $\sigma_2 = \sigma_3$, the maximum (N42°E) when $\sigma_2 = \sigma_1$.
19. A. G. Lindh, *U.S. Geol. Surv. Open-File Rep. 83-63* (1983); L. R. Sykes and S. P. Nishenko, *J. Geophys. Res.* 89, 5905 (1984); C. H. Scholz, *Geophys. Res. Lett.* 12, 17 (1985).
20. H. Kanamori (personal communication) pointed out that the two 1985 Nahani earthquakes, M_s 6.6 (October 1985) and M_s 6.9 (December 1985) had epicenters only 2 to 3 km apart, coincident aftershock zones, and similar focal mechanisms; these common features suggest that they either ruptured the same plane or closely spaced parallel planes; R. J. Wetmiller *et al.*, *Bull. Seismol. Soc. Am.* 78, 590 (1988); G. L. Choy and J. Boatwright, *ibid.*, p. 1627.

21. We thank R. Kovach, T. Heaton, and H. Kanamori for valuable discussions; D. Richards, C. Williams, and Y. Du for assistance in the numerical calculations; J. Savage, W. Thatcher, D. Oppenheimer, G. Beroza, B. Ellsworth, and K. Lajoie for comments. This work was supported by the U.S. Geological Survey and by National Science Foundation grant EAR 90-03575 to Stanford University.

23 July 1990; accepted 19 October 1990

Modern Cyanobacterial Analogs of Paleozoic Stromatoporoids

JÓZEF KAŹMIERCZAK AND STEPHAN KEMPE

Recent and subfossil calcareous structures resembling cystose and subclathrate Paleozoic stromatoporoids have been discovered in a sea-linked, stratified, alkaline crater lake on Satonda Island, Indonesia. The structures are produced by mats of coccoid cyanobacteria growing along the lakeshore from the water surface down to the O_2-H_2S interface located at a depth of 22.8 meters. Calcification of the mats is controlled by seasonal changes in calcium carbonate supersaturation in the epilimnion. The internally complex structures are a product of two different calcification processes: (i) periodic in vivo calcification of the surficial cyanobacterial layers by low-Mg calcite, and (ii) early postmortem calcification of the cyanobacterial aggregates below the mat surface by microbially precipitated aragonite. The finding supports the idea that Paleozoic stromatoporoids represent fossilized cyanobacteria (stromatolites). It also implies that the stromatoporoid-generating epicontinental seas during the early Paleozoic may have been more alkaline and had a higher carbonate mineral supersaturation than modern seawater.

STROMATOPOROIDS ARE CALCAREOUS marine fossils common in many lower Paleozoic shallow-water carbonate deposits. The characteristic specimens came from Devonian limestones in Germany (*1*). These true stromatoporoids occur in mid-Ordovician to lowermost Carboniferous (Strunian) rocks. Most of the upper Paleozoic and Mesozoic fossils ascribed to stromatoporoids are sponges, predominantly calcified demosponges known as sclerosponges or coralline sponges (*2, 3*). They differ significantly from the Paleozoic stromatoporoids in their skeletal architecture, microstructure, and in the presence of spicules. Such pseudo-stromatoporoid fossils have been usually treated as separate groups and have been variously named Disjectoporida, Sphaeractinoidea, and Spongiomorphida (*4*). The practice of calling them stromatoporoids (*3, 5, 6*) should be abandoned because it is misleading.

Paleozoic stromatoporoids have been ascribed to various groups of organisms, in recent years to coelenterates (mostly hydrozoans) (*7*) and sponges (particularly sclerosponges) (*8*). No conclusive evidence for such affinities has been presented, however. Stromatoporoids have also been hypothesized (*9*) to form from in vivo calcification of coccoid cyanobacterial mats comparable to certain fossil and recent calcareous stromatolites. This suggestion has been supported by findings of remnants of coccoid cyanobacteria within skeletal elements of various stromatoporoids (*10*). Because living stromatoporoid-like stromatolites have not been found, the main question of this hypothesis is how the calicifying mats could produce the diversified and in many cases quite regular patterns that characterize many stromatoporoids. Some workers have suggested that these patterns are too advanced to be products of prokaryotic organisms (*11*).

In this report we describe modern calcified cyanobacterial mats that closely resemble certain Paleozoic stromatoporoids. These mats were discovered in the crater lake on Satonda Island (Indonesia) during the Indonesian-Dutch SNELLIUS II Expedition in November 1984, and we studied them in detail during the Indonesian-German SONNE 45B cruise in the fall of 1986 (*12*).

Satonda Island, ~2 km in diameter, is

J. Kaźmierczak, Institute of Paleobiology, Polish Academy of Sciences, Al. Zwirki i Wigury 93, PL-02089 Warszawa, Poland.
S. Kempe, Institute of Biogeochemistry and Marine Chemistry, University of Hamburg, Bundesstrasse 55, D-2000 Hamburg 13, Germany.

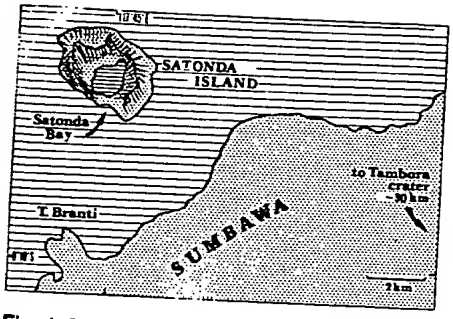

Fig. 1. Index map to Satonda Island, Indonesia.

located about 2.5 km offshore Sumbawa, northwest of the famous Tambora volcano (Fig. 1). Its central part is occupied by a seawater-filled crater lake 1.2 by 0.9 km wide. The steep slopes of the crater rim rise up to 300 m above lake level. The lake is 44 m deep on average and has a central plain 60 to 69 m deep. Satonda volcano has not been active for several thousand years. It was, however, covered by 50 to 80 cm of ash and pumice from the April 1815 cataclysm of Tambora.

The lake is midwater stratified (*12*) by a pronounced pycnocline at a depth of 22.8 m that separates an oxic epilimnion, 12.5% less salty than seawater, from an anoxic hypolimnion, 4.5% more saline than seawater. The oxic layer has a partial pressure of CO_2 (p_{CO_2}) in equilibrium with that of the atmosphere (~350 ppmv); whereas, in the anoxic layer, p_{CO_2} increases to up to 240,000 ppmv at depth. The dissolved inorganic carbon gave $\delta^{13}C$ values of −8.4, −11.4, and −21.4 per mil PDB (*13*) from depths of 10, 40, and 60 m, respectively. These negative values strongly suggest that the main source of the high p_{CO_2} is organic matter washed in from the crater rim. Reduction of sulfate to H_2S and the production of HCO_3^- or dissolution of fresh volcanic silicates under high p_{CO_2} has increased the total alkalinity in the crater lake. In the epilimnion it reaches 3.5 to 3.6 meq/kg (the alkalinity of seawater is 2.1 meq/kg), and it increases to 48 meq/kg at the lake bottom. The *p*H at the lake surface reaches 8.42, significantly higher than in normal surface seawater. The constant withdrawal of $CaCO_3$ by the calcifying cyanobacterial mats has lowered the Ca concentration to about half and the Mg concentration to about 85% of the values in seawater and increased the Mg/Ca molar ratio to 8 to 9 (the ratio of seawater is 5). Because of the high alkalinity and in spite of the low Ca concentration, the epilimnion is highly supersaturated with respect to carbonate minerals: the saturation indices (*14*) reach 0.70 for aragonite, 0.84 for calcite, and 2.81 for dolomite [Table 1, sample from 10 m depth, calculated with WATEQ (*15*)]. These conditions favor the chemical precipitation of aragonite and low-Mg calcite (*16*). The stromatolitic carbonate is precipitated nonenzymatically, that is, it shows the typical shifts of about +5 per mil toward higher $\delta^{13}C$ values (13 samples, mean ± SD = −3.5 ± 1.0 per mil) compared to dissolved carbonates [−8.4 per mil (*12*)].

The history of the crater lake and of its stromatolites is complex. Beneath the calcareous mounds we found organic mud; the presence of this mud indicates that the crater was originally filled with fresh water. Wood from that layer yielded a ^{14}C age of 3920 ± 30 years ago. We believe that at that time, part of the crater wall collapsed and seawater infiltrated through the remnant of the crater wall, which was less than 20 m wide. The lake was colonized by marine gastropods (*Ocenebra*, *Nerita*, and *Cerithium*) and pelecypods (*Pinctada* and perhaps *Lioconcha*). Eventually the bottom layer turned anoxic and produced excess alkalinity, which probably through eddy diffusion significantly alkalized the epilimnion. As the lake became alkaline, the marine mollusks would have been forced into extinction quickly. The alkaline environment apparently favored the growth of calcifying cyanobacterial mats. On rocky grounds along the lakeshore, 13 large stromatolitic reefs have been formed. They are more than 1 m thick and occur as low mounds and irregular crusts forming steep and partly overhanging walls down to the present O_2-H_2S interface at depths >23 m.

The next event in the lake's history was uplift of the island by >1 m after 310 ± 50 years ago (^{14}C dates of uplifted beach deposits). This uplift forced the beach line to recede ~100 m and ended the hydraulic connection between lake and sea. Input of rainwater would have diluted the surface layer and established a new pycnocline at midwater depths (which probably sank gradually to its present depth at 22.8 m).

Today the lake level stands 1.8 m above the highest sea level in the wet season and 0.8 m above it at the end of the dry season. Dilution of surface waters by rainfall has enhanced colonization of red algae (*Peyssonnelia* and *Lithoporella*), nubecullinid foraminifera, and serpulids, which, together with the coccoid cyanobacteria, form the present living reef surface. This association is overgrown down to 8 m depth by a thick carpet of filamentous green algae (siphonocladaleans), which themselves do not calcify. A large population of small cerithiid gastropods (*Rhinoclavis sinensis*) grazes on the cyanobacteria and green algae. Down to the O_2-H_2S interface the reef surface is densely overgrown by monaxonid demosponges (*Suberites* sp.).

The living surface of the calcified cyanobacterial mat has a pustular to cauliflower-like appearance to a depth of ~8 m, whereas deeper, it is almost smooth with occasional small protuberances. Analysis with the scanning electron microscope (SEM) shows that the mat surface is dotted with numerous fine tubercles that are typically located on more or less regularly distributed larger knobs (Fig. 2, A and B). The living zone of the mat is composed of a thin layer of subglobular aggregates of coccoid cyanobacteria (Fig. 2, B and C), which, according to current classification (*17*), can be assigned to the *Pleurocapsa* group. The gelatinous capsules (sheaths) surrounding groups of living pleurocapsalean cells are locally covered with anhedral granules of low-Mg calcite.

The weakly permineralized living cyanobacterial layers grade below the surface continously into a massive, finely laminated limestone composed of alternating micritic and sparitic sheets. These are visible in transmitted light as dark and light laminae, respectively. In the uppermost 3 to 5 cm of the crusts, the laminated structures occur as little nodules and thin interlayers between the foliaceous thalli of calcareous red algae.

Table 1. Chemical data of Satonda Crater Lake water; p_{CO_2} and mineral saturation indices (SI) for aragonite (Ara), calcite (Cc), and dolomite (Dol) have been calculated with the program WATEQ (*15*); 1, sample from 10 m depth; 2, sample diluted by 5%; 3, dilution and decrease in temperature by 5°; 4 and 5, dilution, cooling, and p_{CO_2} increase; 6, sample from 30 m; 7, sample from 30 m degassed to atmospheric p_{CO_2}: 8, for comparison, seawater sample from Satonda Bay; *T*, temperature; Sal., salinity, Alk, alkalinity.

Parameter	1	2	3	4	5	6	7	8
T (°C)	29.9	29.9	25	25	25	29.8	29.8	29.5
Sal. (per mil)	30.87	29.32	29.32	29.32	29.32	36.82	36.82	34.37
*p*H	8.42	8.41	8.41	8.35	8.30	7.27	8.60	8.27
p_{CO_2} (ppmv)	359	359	354	420	482	12040	340	289
Ca (mmol/kg)	5.42	5.15	5.15	5.15	5.15	6.47	6.47	10.6
Mg (mmol/kg)	42.17	40.06	40.06	40.06	40.06	50.11	50.11	50.11
C-Alk (meq/kg)	3.47	3.30	3.30	3.30	3.30	6.28	6.28	1.99
SI_{Ara}	0.70	0.66	0.62	0.57	0.54	−0.01	1.09	0.59
SI_{Cc}	0.84	0.80	0.76	0.72	0.68	0.13	1.23	0.73
SI_{Dol}	2.81	2.74	2.61	2.52	2.44	1.40	3.61	2.39

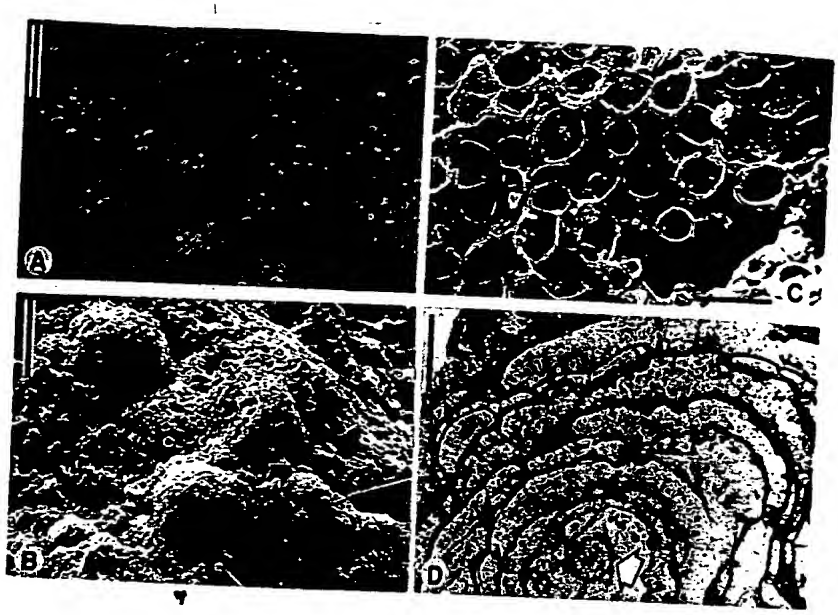

Fig. 2. (**A**) An SEM view of the slightly calcified living surface of the coccoid cyanobacterial mat from Satonda Crater Lake with fine tubercles and larger knobs; depth 9 m; scale bar is 500 μm. (**B**) Magnification of (A) showing globular capsules (sheaths) of the pleurocapsalean cell aggregates forming the mat and a few spicules of the monaxonid sponge (*Suberites* sp.) patchily overgrowing the cyanobacterial mat; scale bar is 100 μm. (**C**) Enlarged fragment of the above showing details of the living surface of the pleurocapsalean mat; scale bar is 30 μm. (**D**) Vertical section (transmitted light) of a subfossil part of a calcareous coccoid cyanobacterial buildup (microstromatolite) from Satonda Crater Lake. The lighter aragonitic layers alternate with darker calcitic layers arranged in a cystose to subclathrate pattern typical of some Paleozoic stromatoporoids. Arrow indicates cross section of a filament of siphonocladalean algae encrusted by cyanobacterial carbonate; sample was at water level; scale bar is 250 μm.

Farther down, the limestone is composed entirely of variously sized, elongated, and irregularly twisted laminated bodies mingled into a hard, massive rock. The center of each laminated body is occupied by typically one or rarely two or three empty, cylindrical tubes, 90 to 220 μm in diameter (Fig. 2D). The size and shape of these tubes indicate that they are molds of siphonocladalean thalli and are essentially similar to the filaments of *Cladophoropsis* associated with the living surface. The central position of the tubes in the laminated structures indicates that the siphonocladalean filaments originally formed the growth base of the laminated encrustations.

The dark laminae are much thinner (15 to 50 μm) than the light ones (20 to 300 μm) and are arranged in a subhorizontal to subcystose or cystose manner (Fig. 2D). At junctions between neighboring cysts, subvertical to vertical column- and pillar-like structures occur; the latter typically has a characteristic spool-like shape (Fig. 3A). Analysis by SEM and energy-dispersive x-ray mapping of EDTA-etched sections revealed that the dark and light laminae differ fundamentally both in microstructure and mineralogy. The dark laminae display an irregularly porous microstructure and are composed of low-Mg calcite, whereas the light ones are compact and made of fibrous aragonite (Fig. 3C).

The SEM analyses demonstrate that the subfossil laminated bodies are calcareous stromatolites (microbialites) produced by coccoid cyanobacteria identical to those forming the mat surface today. Remnants of these cyanobacteria are still identifiable in the dark as well as in the light laminae. In the dark laminae, clusters of coccoid microfossils representing capsules or molds of capsules of pleurocapsalean cyanobacteria are seen embedded in a granular, calcitic matrix (Fig. 3C). Similar if not identical capsules are known from other modern and fossil stromatolites (*10, 18*). In the light laminae, residues of the outer common sheaths (glycocalyx) that surround the coccoid cell aggregates in vivo can be identified in only a few samples. With careful etching of the aragonite laminae with EDTA, however, the traces of a continuous mass of coccoid aggregates became visible. These traces form rounded depressions that correspond in size and distribution to the better preserved pleurocapsalean aggregates from the dark laminae. This observation provides evidence of a uniform microbial origin of the entire stromatolitic structure.

We suggest that the following events lead to the observed laminated microstructure (Fig. 4). First, the cyanobacteria grow to dome-like aggregate a few hundred micrometers thick. Then the outer layer is mineralized in vivo by low-Mg calcite. Decay of the now encased inner aggregates by sulfate reduction increases the alkalinity beneath the calcitic cyst and triggers crystallization of aragonite. Thus the aragonite preserves largely decayed cell aggregates in contrast to the in vivo permineralized aggregates in the calcite layer. The interpretation of the aragonite as postmortem precipitate is substantiated by the occurrence of threadlike struc-

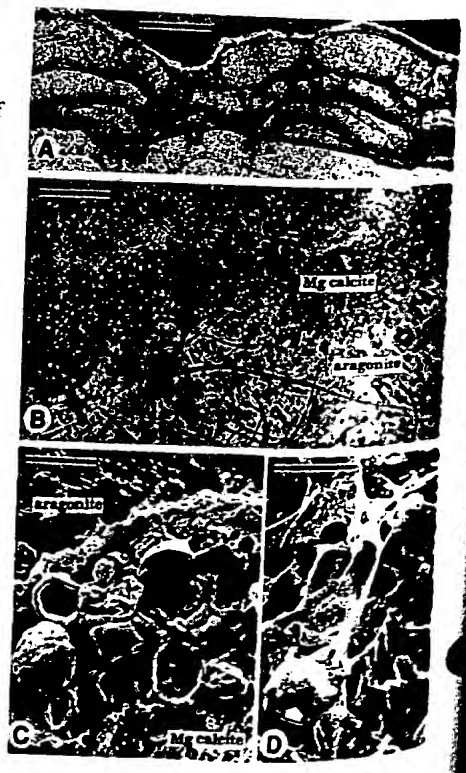

Fig. 3. (**A**) Vertical section (transmitted light) of the subfossil part of a calcareous microstromatolite from Satonda Crater Lake. It shows stromatoporoid-like arrangement of the darker calcitic components among which skeletal elements like cysts, laminae, spool-like pillars, and thicker columns typical of many Paleozoic stromatoporoids can be distinguished; sample was at water level; scale bar is 100 μm. (**B**) Enlarged micrograph of the above illustrating the mineralogical and textural differences between the in vivo (low-Mg calcite) and early postmortem (aragonite) permineralized coccoid cyanobacterial mat. Numerous filaments of saprotrophic fungi are visible in the aragonitic layer; scale bar is 50 μm. (**C**) SEM photomicrograph (vertical section, EDTA etching) of the contact between the calcitic and aragonitic laminae as shown in (B). Note the well-preserved capsules of pleurocapsalean cyanobacteria in the granular calcitic lamina and the fibrous character of the aragonitic lamina. Scale bar is 5 μm. (**D**) SEM picture (vertical section, EDTA etching) of an aragonitic lamina from the specimen shown in (B). Arrow indicates remnant of an almost totally decomposed coccoid cyanobacterial aggregate in the dense network of filaments of decomposing fungi and bacteria; scale bar is 25 μm.

tures in this layer (Fig. 3, B and D) that closely resemble hyphae of saprotrophic fungi or sheaths of sulfur bacteria indicative of anaerobic decay. Calcification as a consequence of anaerobic decomposition by sulfate reduction is a well-known process below the zone of photosynthesis in modern cyanobacterial mats (*19*).

This model does not, however, answer why the coccoid aggregates can grow nonmineralized for some time and what triggers calcite precipitation on the mat surface. High $CaCO_3$ supersaturation is believed to be the crucial factor inducing in vivo calcification of cyanobacteria (*20*), although the deposition of $CaCo_3$ can be initiated in different ways (*21*). Fluctuations in supersaturation can be caused by changes in three factors: temperature, pCO_2, and the concentrations of the Ca^{2+} and CO_3^{2-}. Satonda has two seasons: a cool rainy season and a hot dry season. During the rainy season the lake level rises by ~1 m, and the epilimnion could be diluted by about 5%. The lake probably also cools by a few degrees Celsius. At the same time, organic debris washed into the lake produces a temporary increase in pCO_2.

We have calculated the effects of variations in the three factors on supersaturation (Table 1). These calculations show that supersaturations of aragonite and calcite can indeed be lowered to values comparable to their respective seawater supersaturations (column 8), that is, to values that apparently do not sustain in vivo calcification of the cyanobacterial mat. Under a reduced supersaturation, cyanobacteria might grow rapidly without triggering significant calcite precipitation (Fig. 4A). With warming and evaporation during the dry season, the critical calcite supersaturation (at about $SI = 0.8$) is surpassed and calcite is precipitated at the mat surface (Fig. 4B).

The calculations are valid only for the present conditions. The massive laminated bodies apparently formed, however, before the present epilimnion was established. Exact chemical conditions at that time are difficult to reconstruct. If one assumes that the water below the present pycnocline represents the former epilimnic water, one can calculate its supersaturation at atmospheric pCO_2 (Table 1, columns 7 and 8). The resulting supersaturations are large and would sustain spontaneous carbonate precipitation. These supersaturations are the consequence of a few hundred years of alkalinity increase caused by sulfate reduction and by dissolution of carbonate particles sinking into the anoxic bottom layer. Model calculations for the present epilimnic conditions illustrate that seasonal variations in supersaturations may be strong enough to cause the observed lamination in the cyanobacterial buildups.

The textural patterns observed closely resemble those described in many Paleozoic stromatoporoids. The similarity is particularly striking for the cystose, subcystose, and subclathrate stromatoporoids characterizing the initial, Ordovician, and the final, Fammenian-Strunian, periods in the history of the group. The Ordovician examples include stromatoporoids classified to *Cystostroma* (*22, 23*), *Pseudostylodictyon* (*22, 24, 25*), or *Clathrodictyon* (*23, 25, 26*); the Fammenian-Strunian examples include forms described as *Pseudolabechia* (*27*) or *Stylostroma* (*28*). Cystose and subcystose patterns remarkably similar to those occurring in Satonda stromatolites have also been described from early Proterozoic marine stromatolites (*29*) and Quaternary lacustrine microbial tuffas (*30*).

The dark laminae of the Satonda microbialites are similar to the skeletal elements of Paleozoic stromatoporoids, whereas the light laminae may correspond to interskeletal spaces. In fossil stromatoporoids, the spaces are filled with sparry low-Mg calcite that most likely originated from diagenetic transformation of primary aragonite or represents neospar filling the fenestral spaces remaining in the cyanobacterial mats after the decay of the noncalcified coccoid aggregates. The presence of primary aragonite in stromatoporoids has been suggested from studies on authigenic quartz inclusions in Devonian *Actinostroma* and *Stromatopora* (*31*). Also megaquartz crystals have been observed in Devonian stromatoporoids (*32*); the quartz is associated with closed spaces filled with organic material that acts as nucleating agent. All these observations are in agreement with the interpretation of stromatoporoid morphogenesis given above. Irregular stellate patterns (the so-called "astrorhizae") occurring in some stromatoporoids (*24*) are not present in the Satonda mats. The abundance of molds of filaments of siphonocladalean green algae in the stromatolites studied indicate, however, that such patterns could be easily produced by rhizoids or branched thalli of similar algae overgrown by the calcifying cyanobacterial mat.

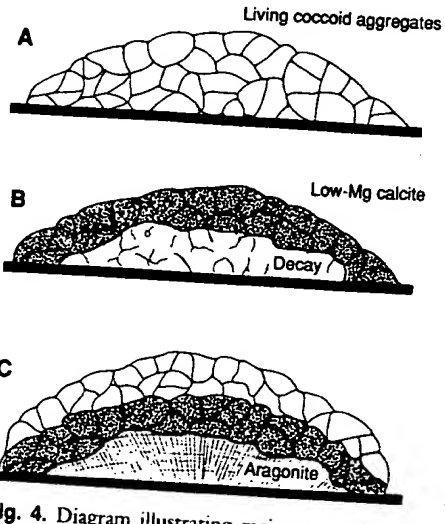

Fig. 4. Diagram illustrating major stages in the formation of an arcuate cyst plate in a cystose stromatoporoid-like calcareous stromatolite. (**A**) Dome-shaped aggregate of living coccoid cyanobacteria. (**B**) Periodic in vivo permineralization of the surficial cells with low-Mg calcite. The noncalcified coccoids remaining below the calcitic cyst have been obliterated by heterotrophic microorganisms post-mortem. (**C**) The metabolic activity of the decomposing microbiota mediates an early diagenetic formation of aragonite in the cryptic microenvironment.

The species-poor biota of the mildly alkaline Satonda Crater Lake parallels the low or even extremely low diversity biota associated with the extensive stromatoporoid banks and mounds that characterize the Silurian and Devonian carbonate platforms worldwide (*33*). Considering the devastating impact of alkaline seawater on the marine mollusks that once lived in Satonda lake, we conclude that a similar increase in alkalinity accompanied by changes in the main ionic composition may also have caused temporal impoverishment of normal marine organisms and enhanced development of in vivo calcifying stromatoporoid-like cyanobacterial mats in the early Paleozoic epicontinental seas. All cyanobacteria are alkaliphilic microorganisms (*34*), and their abundance can be taken per se to indicate that an environment is alkaline. At Satonda Crater Lake, the generation of stromatoporoid-like stromatolites requires, in addition to increased alkalinities, fluctuations in $CaCO_3$ supersaturation levels. The widely accepted models of stratified or sluggish early Paleozoic seas (*35*) imply that similar conditions may have produced stromatoporoids there. Deeper, anoxic basins of those epicontinental seas could have easily produced excess alkalinity, and these waters, through temporal destratification of the water column or upwelling systems, could have periodically invaded the shallow areas and generated high $CaCO_3$ supersaturation levels that promote the formation of stromatoporoid stromatolites. The periodic changes in $CaCO_3$ supersaturation combined with other changing environmental factors important for cyanobacterial growth such as O_2 and PO_4^{3-} levels, temperature, and light intensities could alter the organization of cyanobacterial colonies and produce a plethora of mat configurations.

A large number of textural patterns have been produced by the temporally in vivo calcifying mats. On the basis of these textures, taxonomists have designated over

2000 species of Paleozoic stromatoporoids (*36*). Compared to their Satonda counterparts, the Paleozoic stromatoporoids are characterized by generally thicker growth increments and more regular textures that sometimes show almost perfect superposition of pillars and columns. This texture could have been caused by a larger temporal and spatial persistence of regular fluctuations in the Paleozoic seas compared to the hydrochemically less stable and geologically short-lived Satonda Crater Lake.

Stromatoporoids apparently survived the Frasnian-Fammenian crisis and became extinct during the lowermost Carboniferous (Strunian). Their disappearance has been mostly attributed to ocean cooling or meteorite impact (*37*). From our studies on Satonda stromatolites we suggest that a worldwide decrease in alkalinity and in carbonate mineral supersaturation following the Fammenian oceanic turnover (*38*) may better account for the fading of stromatoporoid stromatolites from the late Paleozoic geological record.

REFERENCES AND NOTES

1. A. Goldfuss, *Petrefacta Germaniae*, vol. I (Arnz, Düsseldorf, 1826).
2. J. Kaźmierczak, *Palaeontology* **17**, 341 (1974).
3. R. A. Wood, *Spec. Pap. Palaeontol.* **37**, 1 (1987); ———, J. Reitner, R. R. West, *Lethaia* **22**, 85 (1989).
4. O. Kühn, in *Handbuch der Paläozoologie*, O. H. Schindewolf, Ed. (Borntraeger, Berlin, 1939), vol. 2A, pp. 3–68; E. Flügel, *Palaeontol. Z.* **49**, 369 (1975).
5. Y. Dehorne, *Mém. Serv. Explication Carte Géol. Detaill. France* (1920); H. Yabe and T. Sugiyama, *Sci. Rep. Tohoku Imp. Univ. Sendai Ser. 2* **14**, 135 (1935); R. G. S. Hudson, *Palaeontology* **2**, 180 (1960).
6. R. A. Wood and J. Reitner, *Palaeontology* **29**, 469 (1986); J. Wendt, *Neues Jahrb. Geol. Palaeontol. Abh.* **150**, 111 (1975).
7. H. Nestor, *Lethaia* **14**, 21 (1981); K. Mori, *Stockholm Contrib. Geol.* **37**, 167 (1982); O. V. Bogoyavlenskaya, *Stromatoporaty Paleozoya* (Nauka, Moscow, 1984).
8. W. D. Hartman and T. E. Goreau, *Symp. Zool. Soc. London* **25**, 205 (1970); C. W. Stearn, *Lethaia* **5**, 369 (1972).
9. J. Kaźmierczak, *Nature* **264**, 49 (1976).
10. ———, *Acta Palaeontol. Pol.* **25**, 243 (1980); ——— and W. E. Krumbein, *Lethaia* **16**, 207 (1983).
11. R. Riding and S. Kershaw, *Nature* **268**, 178 (1977); C. T. Scrutton, in *The Origin of Major Invertebrate Groups*, M. R. House, Ed. (Academic Press, London, 1979), pp. 167–207; C. Monty, in *Phanerozoic Stromatolites*, C. Monty, Ed. (Springer, Berlin, 1981), pp. v–viii.
12. S. Kempe and J. Kaźmierczak, *Chem. Geol.* **81**, 299 (1990).
13. $\delta^{13}C = [(^{13}C_{sample}/^{12}C_{sample})/(^{13}C_{PDB}/^{12}C_{PDB})]1000$, where PDB is the Pee Dee Belemnite standard.
14. The saturation index (SI) is defined as $\log [(IAP)/K_{mineral}]$, that is for calcite (Cc): $\log([Ca^{2+}][CO_3^{2-}]/K_{Cc})$; *IAP* = ion activity product.
15. L. N. Plummer, B. F. Jones, A. H. Truesdell, *U.S. Geol. Surv. Water Res. Invest. Pap. 76-13* (1976; revised 1978, 1984).
16. G. Müller, G. Irion, U. Förstner, *Naturwissenschaften* **59**, 158 (1972); R. L. Folk, *J. Sediment. Petrol.* **44**, 40 (1974).
17. R. Rippka, J. W. Waterbury, R. Y. Stanier, in *The Prokaryotes*, M. P. Starr *et al.*, Eds. (Springer, Berlin, 1981), vol. 1, pp. 247–256.
18. R. J. Horodyski and S. Vonder Haar, *J. Sediment. Petrol.* **45**, 894 (1975); W. E. Krumbein and C. Giele, *Sedimentology* **26**, 593 (1979); C. J. R. Braithwaite, J. Casanova, T. Frevert, B. A. Whitton, *Palaeogeogr. Palaeoclimatol. Paleoecol.* **69**, 145 (1988).
19. W. E. Krumbein and Y. Cohen, in *Fossil Algae*, E. Flügel, Ed. (Springer, Berlin, 1977), pp. 37–56; W. E. Lyons *et al.*, *Geology* **12**, 623 (1984).
20. K. Simkiss, in *Biomineralization in Lower Plants and Animals*, B. S. C. Leadbeater and R. Riding, Eds. (Clarendon, Oxford, 1986), pp. 19–37; S. Kempe and J. Kaźmierczak, in *Facets of Modern Biogeochemistry*, V. Ittekkot, S. Kempe, W. Michaelis, A. Spitzy, Eds. (Springer, Berlin, 1990), pp. 252–275.
21. W. E. Krumbein, in *Biogeochemical Cycling of Mineral-Forming Elements*, P. A. Trudinger and D. J. Swaine, Eds. (Elsevier, Amsterdam, 1979), pp. 47–68; A. Pentecost, *Geomicrobiol. J.* **4**, 285 (1985); A. Pentecost and J. Bauld, *ibid.* **6**, 129 (1988).
22. J. J. Galloway and J. St. Jean, Jr., *Bull. Am. Paleontol.* **43**, 5 (1961).
23. T. E. Bolton, *Geol. Surv. Can. Bull.* **379**, 17 (1988).
24. J. J. Galloway, *Bull. Am. Paleontol.* **37**, 345 (1957).
25. H. E. Nestor, *Ordovician and Llandoverian Stromatoporoidea of Estonia* (Valgus, Tallinn, 1964).
26. B. D. Webby, *Palaeontology* **12**, 637 (1969).
27. C. W. Stearn, *J. Paleontol.* **62**, 411 (1988).
28. D. Y. Dong, *Acta Palaeontol. Sin.* **12**, 280 (1964).
29. M. R. Walter, in *Earth's Earliest Biosphere*, J. W. Schopf, Ed. (Princeton Univ. Press, Princeton, 1983), pp. 187–213.
30. J. Casanova, *Sci. Géol. Bull.* **40**, 135 (1987); C. Hilaire-Marcel and J. Casanova, *Palaeogeogr. Palaeoclimatol. Palaeoecol.* **58**, 155 (1987).
31. D. K. Richter, *Sedimentology* **19**, 211 (1972).
32. R. A. Henderson, *J. Sediment. Petrol.* **54**, 1138 (1984).
33. L. F. Laporte, Ed., *Soc. Econ. Paleontol. Mineral Spec. Publ.* **18** (1974); D. F. Toomey, Ed., *ibid.* **30** (1981).
34. T. D. Brock, *Science* **179**, 480 (1973).
35. W. B. N. Berry and P. Wilde, *Am. J. Sci.* **278**, 257 (1978); P. Wilde and W. B. N. Berry, *Palaeogeogr. Palaeoclimatol. Palaeoecol.* **48**, 143 (1984); W. T. Holser, M. Magaritz, J. Wright, in *Global Bio-Events*, O. Walliser, Ed. (Springer, Berlin, 1986), pp. 63–74; J. Wright, H. Schrader, W. T. Holser, *Geochim. Cosmochim. Acta* **51**, 631 (1987).
36. E. Flügel and E. Flügel-Kahler, in *Fossilium Catalogus*, I. F. Westphal, Ed. (Jung, Gravenhage, 1968), pp. 1–681.
37. P. Copper, *Geology* **14**, 835 (1986); C. W. Stearn, *ibid.* **15**, 677 (1987); D. J. McLaren, *ibid.* **13**, 170 (1985).
38. H. H. J. Geldsetzer, W. D. Goodfellow, D. J. McLaren, M. J. Orchard, *Geology* **15**, 393 (1987); U. Brand, *Palaeogeogr. Palaeoclimatol. Palaeoecol.* **76**, 311 (1989).

39. We thank G. Landmann, A. Lipp, Y. Surachman, and D. Susanto for field assistance. The paper has been reviewed by H. K. Wong, W. E. Krumbein, and A. Nissenbaum. Supported by the German Federal Ministry of Research and Technology, Polish Academy of Sciences, and a fellowship from the A. V. Humboldt Foundation (to J.K.). The paper is a contribution to the IGCP Project No. 261, "Stromatolites."

15 May 1990; accepted 22 August 1990

Simulation of Tsunamis from Great Earthquakes on the Cascadia Subduction Zone

MAX K.-F. NG, PAUL H. LEBLOND,* TAD. S. MURTY

Large earthquakes occur episodically in the Cascadia subduction zone. A numerical model has been used to simulate and assess the hazards of a tsunami generated by a hypothetical earthquake of magnitude 8.5 associated with rupture of the northern sections of the subduction zone. Wave amplitudes on the outer coast are closely related to the magnitude of sea-bottom displacement (5.0 meters). Some amplification, up to a factor of 3, may occur in some coastal embayments. Wave amplitudes in the protected waters of Puget Sound and the Strait of Georgia are predicted to be only about one fifth of those estimated on the outer coast.

THE CASCADIA SUBDUCTION ZONE IS the area where the Juan de Fuca plate and smaller adjacent plates slip below the North American continent (Fig. 1). The possibility of a massive earthquake in this area has recently been recognized (*1*). A seismic sea wave, or tsunami, would be a major risk associated with such an event. In this report, we present calculations that quantify this risk and allow identification of the factors that would determine flooding levels along the adjacent coast.

A critical element in tsunami modeling is the nature of the initial sea-level displacement that starts the wave. Because the rupture takes place on a time scale that is short compared to the response time of the ocean waters, the sea-surface displacement, which causes the tsunami, is practically identical to that of the sea bottom. Geophysical arguments (*2*) suggest that a vertical uplift of 5 m of the ocean bottom along the deformation front, decreasing linearly to zero at the coast line, is possible during a large earthquake. We have modeled only the rupture of the northern sections of the Cascadia subduction zone (north of 48°N). A maximum earthquake magnitude of 8.2 is estimated for rupture of each of the Winona and Explorer segments and of about 8.5 for simultaneous rupture of all segments north of 48°N (Fig. 1).

Tsunami propagation from an impulsive

M. K.-F. Ng and P. H. LeBlond, Department of Oceanography, University of British Columbia, Vancouver, BC Canada V6T 1W5.
T. S. Murty, Institute of Ocean Sciences, Post Office Box 6000, Sidney, BC Canada V8L 4B2.

STIC-ILL

From: Marx, Irene
Sent: Tuesday, September 10, 2002 9:19 AM
T : STIC-ILL
Subject: 09/777664

Importance: High

411607

Please send to Irene Marx, Art Unit 1651; CM1, Room 10E05, phone 308-2922, Mail box in 11B01

Observations on the ionic composition of blue-green algae growing in saline lagoons
AU Pillai, V. K.
SO Proc. Natl. Inst. Sci. India, (19550000) vol. 21, no. 2, pp. 90-102.
DT Journal

Dalrymple, D.W., 1965, "Calcium carbonate deposition associated with blue green algal mats, Baffin Bay.:, Texas: Institute of Marine Science Publication 10, p. 187-200

Black, M., 1933, "The algal sedimentation... ", Royal Society of London Philosphical transactions, Ser. B, V. 222, p. 165-192

Lowenstam HA (1981), Science, 211:1126-1131

Ferris et al., Earth Sci., 47:233-250 (1993)

Ferris et al., Appl. and Environm. Microbiol.,1989, 55:1249-1257

Kazmierczak et al., (1990), Science, 250:1244-1248

Kempe et al., Facies, 28:1-32, 1993.

Kempe et al., 1994, Bull, Inst. Oceanogr., Monaco no. spec., 13:61-117.

Merz, M.U.E, 1992, Facies, 26:81-102

Pentecost et al., 1986, Calcification in cyanobacteria, In "Biomineralization of Lower plants and animals (Leadbeater et a., ed. 73-90, Clarendon Press, Oxford.

Riding, R., 1982, Nature, 299:814-815

Thompson eta., 1990, Geology, 18:995-998

Irene Marx
Art Unit 1651
CMI 10-E-05,
Mail Box 11-B-01
703-308-2922

EARTH SCIENCE (CHIKYU KAGAKU)
Vol.47, No.3, pp.233—250.
MAY 1993

Microbial biomineralization in natural environments

F. G. Ferris*

Abstract Microorganisms contribute to the precipitation of a tremendous range of minerals in natural environments. This phenomenon is known as microbial biomineralization. The importance of microbial biomineralization stems not only from the great diversity of environments that are populated by microorganisms, but also arises from their distinctive physiology and unique cellular structure. For example, microbial sulfate-reduction is the major source of sulfide in anaerobic sediments where low temperature (ca. <100℃) precipitation of metal sulfides occurs. At the same time, microorganisms exhibit a profound ability to bind metallic ions, and this allows cells to serve directly as nucleation templates for the precipitation of authigenic mineral phases. There are many examples of microbial biomineralization in modern environments, and there is abundant evidence that similar processes contributed to thegenesis of some mineral deposits in the past. Frequent documentation of microbial biomineralization in environments disrupted by mining or other industrial activity indicates further that mineral precipitation by microorganisms may be a sensitive indicator for environmental change.

I Introduction

The precipitation of minerals by living organisms is a widespread phenomenon that is generally referred to as biomineralization (Lowenstam and Weiner, 1989). Familiar products of biomineralization in eukaryotic plants and animals include various types of shells, bones, and teeth ; however, biological mineral precipitation is not carried out by higher organisms alone. Many prokaryotic microorganisms (*i.e.*, bacteria) are potent catalysts of biomineralization, and contribute to the formation of a tremendous range of minerals (Beveridge, 1989). In this regard, microbial biomineralization is not a trivial affair .

The significance of microbial biomineralization is emphasized by the fact that microorganisms are the most abundant life form on earth and live in an unparalled variety of environments (Ferris and Beveridge, 1985). Microorganisms exist where there is liquid water up to temperatures of about 110 ℃, and thrive in the harshest environments from the high Arctic to the depths of the oceans and porous terrestrial strata (Stetter, 1982 ; Yayanos, 1986 ; Johnston and Kipphut, 1988 ; Ghiorse and Wilson, 1988). Moreover, microbial life is as old as the geologic record, stretching back at least 3.8 billion years (Schidlowski, 1988). The implications of these observations are clear. Microbial biomineralizaiton is important on a global scale and has helped shape the planet throughout geological time.

II The Early Earth and Microorganisms

The earth is estimated to have taken form about 4.2 to 4.4 billion years ago, and the first components of a biosphere probably developed shortly thereafter. Althougth there are no rocks from this early epoch, fossilized stromatolites are common in Archean sediments (Walter, 1983). These organo-sedimentary structures nor-

Received October 16, 1992 ; accepted February 4, 1993.
*Department of Geology, University of Toronto, 22 Russell Street, Toronto, Ontario. M5S 3B1, Canada

mally appear as laminated organic-rich cherts and siliceous carbonates. The fine layering and upraised conical or dome shapes are in many ways comparable to modern microbial mats that grow in a variety of modern aquatic environments (Stolz and Margulis, 1984). Among the Archean stromatolites, the oldest are from the Onverwacht group in South Africa and Warawoona group in Western Australia (Awramik *et al.*, 1983 ; Awramik, 1986). These benchmark formations are of unequaled importance in that they document the presence of relativelycomplex microbial communities well into the past.

The occurence of fossilized stromatolites increases dramaticially in progressing from Archean to Proterozoic sediments. These more recent stromatolitic assemblages are distinguished by abundant cellularly preserved microfossils that are generally absent from their Archean counterparts (Awramik, 1971; Awramik and Barghoorn, 1977). This apparent increase in microbial biomass about 2.5 billion years ago is commonly taken to be a result of the development of facultative oxygenic photoautotrophs (*i.e.*, primative cyanobacteria). These ancient photosynthetic microorganisms, using water as a source of reducing power, must have been highly competetive and probably quickly dominated the biosphere (Fay, 1992). At the same time, the activity of these microorganisms initiated a tremendous period of environmental change on Earth.

The small initial amounts of atmosphereic oxygen were most likely involved in oxidation reactions with exposed crustal minerals (Schlesinger, 1991). The oxidation of reduced minerals, such as pyrite (FeS_2), is thought to have contributed to the deposition of oxidized iron in sedimentary formations known as Red Beds. The earliest occurence of Red Beds around 2.0 billion years ago is approximately coincident with the latest deposition of Banded Iron Formations. This provides compelling evidence which suggests that the development of a stable oxic atmosphere was delayed until the oceans were cleared of reduced metals because of microbial production of oxygen. The oxidative precipitation of iron in the Precambrian has been cited as a form of microbial biomineralization (Laberge, 1973) ; however, there is considerable debate on this point. Even then, when the rate oxygen of evolution finally exceeded its rate of consumption by the oxidation of reduced substances, O_2 started to accumulate in the atmosphere towards its present day level of 20% (Schlesinger, 1991). Also, with the build-up of an oxygen-rich atmosphere, obligate aerobic microorganisms developed by the end of the Proterozoic (Fay, 1992).

Ⅲ Microorganisms and Mineral Formation

Minerals that develop in association with microorganisms can be treated as being authigenic in origin. This essentially involves the precipitation of ions from an oversaturated solution (Leeder, 1982). Basically, the overall process can conveniently be divided into two stages, nucleation and crystal growth. Distinctions between the two stages can in turn be made based on the energy changes associated with crystallization, and causative physicochemical conditions that contribute to authigenic processes (Berner, 1980).

In general terms, nucleation represents an activation energy barrier that inhibits or blocks the spontaneous formation of a solid phase from a supersaturated solution (Berner, 1980). If the concentration of ions in a solution gradually increases and exceeds the solubility product of a solid mineral phase, insoluble precipitates will not form until a certain degree of supersaturation has been reached. Stable nuclei can only develop after the activation energy required to form a new interface is overcome by the energy released as a consequence of bond formation in the solid phase. The process during which the maximum free energy is attained is known as nucleation, and involves the growth of critical

mally appear as laminated organic-rich cherts and siliceous carbonates. The fine layering and upraised conical or dome shapes are in many ways comparable to modern microbial mats that grow in a variety of modern aquatic environments (Stolz and Margulis, 1984). Among the Archean stromatolites, the oldest are from the Onverwacht group in South Africa and Warawoona group in Western Australia (Awramik *et al.*, 1983 ; Awramik, 1986). These benchmark formations are of unequaled importance in that they document the presence of relativelycomplex microbial communities well into the past.

The occurence of fossilized stromatolites increases dramaticially in progressing from Archean to Proterozoic sediments. These more recent stromatolitic assemblages are distinguished by abundant cellularly preserved microfossils that are generally absent from their Archean counterparts (Awramik, 1971; Awramik and Barghoorn, 1977). This apparent increase in microbial biomass about 2.5 billion years ago is commonly taken to be a result of the development of facultative oxygenic photoautotrophs (*i.e.*, primative cyanobacteria). These ancient photosynthetic microorganisms, using water as a source of reducing power, must have been highly competetive and probably quickly dominated the biosphere (Fay, 1992). At the same time, the activity of these microorganisms initiated a tremendous period of environmental change on Earth.

The small initial amounts of atmosphereic oxygen were most likely involved in oxidation reactions with exposed crustal minerals (Schlesinger, 1991). The oxidation of reduced minerals, such as pyrite (FeS_2), is thought to have contributed to the deposition of oxidized iron in sedimentary formations known as Red Beds. The earliest occurence of Red Beds around 2.0 billion years ago is approximately coincident with the latest deposition of Banded Iron Formations. This provides compelling evidence which suggests that the development of a stable oxic atmosphere was delayed until the oceans were cleared of reduced metals because of microbial production of oxygen. The oxidative precipitation of iron in the Precambrian has been cited as a form of microbial biomineralization (Laberge, 1973) ; however, there is considerable debate on this point. Even then, when the rate oxygen of evolution finally exceeded its rate of consumption by the oxidation of reduced substances, O_2 started to accumulate in the atmosphere towards its present day level of 20% (Schlesinger, 1991). Also, with the build-up of an oxygen-rich atmosphere, obligate aerobic microorganisms developed by the end of the Proterozoic (Fay, 1992).

Ⅲ Microorganisms and Mineral Formation

Minerals that develop in association with microorganisms can be treated as being authigenic in origin. This essentially involves the precipitation of ions from an oversaturated solution (Leeder, 1982). Basically, the overall process can conveniently be divided into two stages, nucleation and crystal growth. Distinctions between the two stages can in turn be made based on the energy changes associated with crystallization, and causative physicochemical conditions that contribute to authigenic processes (Berner, 1980).

In general terms, nucleation represents an activation energy barrier that inhibits or blocks the spontaneous formation of a solid phase from a supersaturated solution (Berner, 1980). If the concentration of ions in a solution gradually increases and exceeds the solubility product of a solid mineral phase, insoluble precipitates will not form until a certain degree of supersaturation has been reached. Stable nuclei can only develop after the activation energy required to form a new interface is overcome by the energy released as a consequence of bond formation in the solid phase. The process during which the maximum free energy is attained is known as nucleation, and involves the growth of critical

nuclei which are unstable relative to resolution. When the critical nucleus is formed, continued increases in the number of ions or atoms is accompanied by a decrease in free energy. This process goes on spontaneously, and is known as crystal growth.

Nucleation may occur either homogenously or heterogeneously (Berner, 1980). In homogeneous reactions, critical nuclei are formed simply by random collisions of ions or atoms in solution. Conversely, heterogenous nucleation involves development of critical nuclei on surfaces of foreign solids which catalyze nucleation by reducing the activation energy barrier. The surface of the heteronucleus may be viewed as a template of similar atomic spacing that promotes mineral precipitation. Favorable heterogenous nucleation templates typically possess sites where strong surface chemical interactions occur (*i.e.*, adsorption or bonding).

The activation energy barrier to nucleation can be reduced by lowering the interfacial energy of the solid phase, and/or increasing the degree of solution supersaturation. Supersaturation levels may be regulated, to a certain extent, by the metabolic activity of microorganisms. For example, growth of ammonia generating, denitrifying, or sulfate-reducing bacteria may promote an increase in solution pH which is more supportive towards the precipitation of carbonate minerals (Berner, 1971). Conversely, interfacial energies can be lowered by the presence of organic surfaces that promote chemical bonding at the nucleation site (Mann, 1988).

Much of organic matter in natural environment exists as small colloidal aggregates of highly cross-linked heteropolymeric material (Beveridge *et al.*, 1983). At least some of the more durable polymeric networks are derived from the cell walls and external sheaths of bacteria (Philip and Calvin, 1976). These cellular structures are not only very resistant to degradation, but also possess reactive anionic sites that can adsorb dissolved metallic ions and, under favorable geochemical conditions, promote mineral precipitation as expected for a surface induced lowering of the interfacial energy of the solid phase.

Crystal growth involves transport of ions, atoms, or molecules to the surface of a crystal and various surface reations, such as adsorption, dehydration, ion exchange, etc., that result in incorpoation of the ions into a crystal lattice (Berner 1980). The rate of crystal growth may be limited by either transport, surface chemical reactions, or by a combination of both processes. The implications of transport and surface chemical reactions for crystal growth in microbial biomineralization are not particularly well understood ; however, bacteria are so small that a low Reynolds number of about 10^{-5} applies to them (Beveridge, 1989). This means that microorganisms cannot outswim their local aqueous environment. Instead, they drag it around with themselves, no matter how fast they move. Consequently, microorganisms rely entirely on diffusion for their subsistence and live in a microenvironment that may be chemically quite different than the bulk aqueous phase. Thus, mineral phases may be precipitated by microorganisms in an environment where otherwise unfavorable geochemical conditions seem to prevail.

Microbial biomineralization is obviously a very complex phenomenon that can proceed in a number of different ways. For example, metal cations can be precipitated directly from solution as a result of microbial metabolic activity. This happens on the inside, outside, or even at some distance way from cells (Beveridge, 1989). Indirect bacterial mineral precipitation as a consequence of regional geochemical conditions is also possible and involves passive epicelluar crystal nucleation and growth on the outside of bacterial cells. This later process can be attributed to the inherent metal-binding capacity of anionic structual polymers in the cell walls and external sheaths of bacteial cells (Beveridge, 1989). In natural environments, passive and active microbial biomineralization often oc-

cur simultaneously and are not easy to distinguish as separate processes ; however, as shown in this paper there are many examples of microbial supported mineralization in modern environments, and there is abundant evidence that similar kinds of processes contributed to the formation of some mineral deposits in the past.

Ⅳ Phosphogenesis

Accumulations of phosphate minerals commonly occur in both ancient and modern sediments deposited in shallow near shore marine environments under high biological productivity (Dahanayake and Krumbein, 1985 ; Glenn and Arthur, 1988). The formation of phosphate minerals in these environments arises from a series of complex biogeochemical reactions in which phosphate is initially supplied to sediments and then to interstitial pore waters via microbial degradation of phosphate-rich organic matter. Subsequent inorganic phosphate precipitation generally leads to the development of irregular rims and coatings of fine grained micritic mineralization on preexisting hard substrates, including organic matter derived from microbial cells (Southgate, 1986) (Fig. 1). In this way, organic matter serves in phosphogenesis not only as a vehicle by which inorganic phosphate is supplied to sediments, but also as a substrate upon which phosphate preferentially nucleates.

Phosphate beds that occur in sequences of laminated carbonates and chert of the Upper Cretaceous-Lower Eocene Mishash Formation of Isreal provide compelling evidence for the dual role of microorgnisms in phosphogenesis(Soudry and Champtier, 1983). Paleoenvironemtal analyses of the Negev phosphorites suggest that they were deposited on the shelf of a receding epicontinental sea in association with partly degraded decomposing cyanobacterial mats. In many areas, dense apatite overgrowths occur on the fossilized remains of cyanobacterial sheaths along with fragmented phosphatitic colonies of coccoid bacterial cells infilled with apatite. The same pattern of mineralization has been observed in the Djebel-Onk microbial mat generated phosphorites near the Algeria-Tunisia frontier, and within phosphatidic carbonates of the Georgina Basin, Australia (Dahanayake and Krumbein, 1985 ; Southgate, 1986). These close associations between fossilized microbial structures and phosphate mineralization clearly indicate that bacterial cells, and their organic remains, act nucleation sites for phosphate precipitation.

Ⅴ Carbonate Precipitation

The majority of recent carbonate sediments are formed in marine environments. They are found throughout the oceans where they are closely associated with regions of upwelling along mid-ocean ridges and continental shelves (Leeder, 1982). The predominent carbonate minerals in these sediments are the $CaCO_3$ polymorphs calcite and aragonite. Recent shallow-water tropical and subtropical deposits consist mostly of aragonite and high-magnesium calcite, whereas temperate shallow-water deposits contain predominantly calcite. This difference in the oceanic distribution of carbonate minerals has been attributed to high levels of magnesium in warmer tropical waters, for this metal severely retards the precipitation of calcite.

Bacteria have been implicated as causative agents for carbonate precipitation in a number of laboratory investigations (Krumbein, 1974 ; Krumbein, 1979). In these experiments, the bacterial cells actually functioned as nucleation elements for the formation of aragonite and high magnesium calcite. These minerals first deveveloped on the surfaces of the bacteria and not in the cells, as expected for a direct chemcial precipitation of cell-bound calcium or magnesium. Similar patterns of carbonate mineralization are commonly observed in association with microbial mats from various intertidal zones. Fossilized remnants of these stratified microbial communities are also widely distributed in silicified carbonates from the Pre-

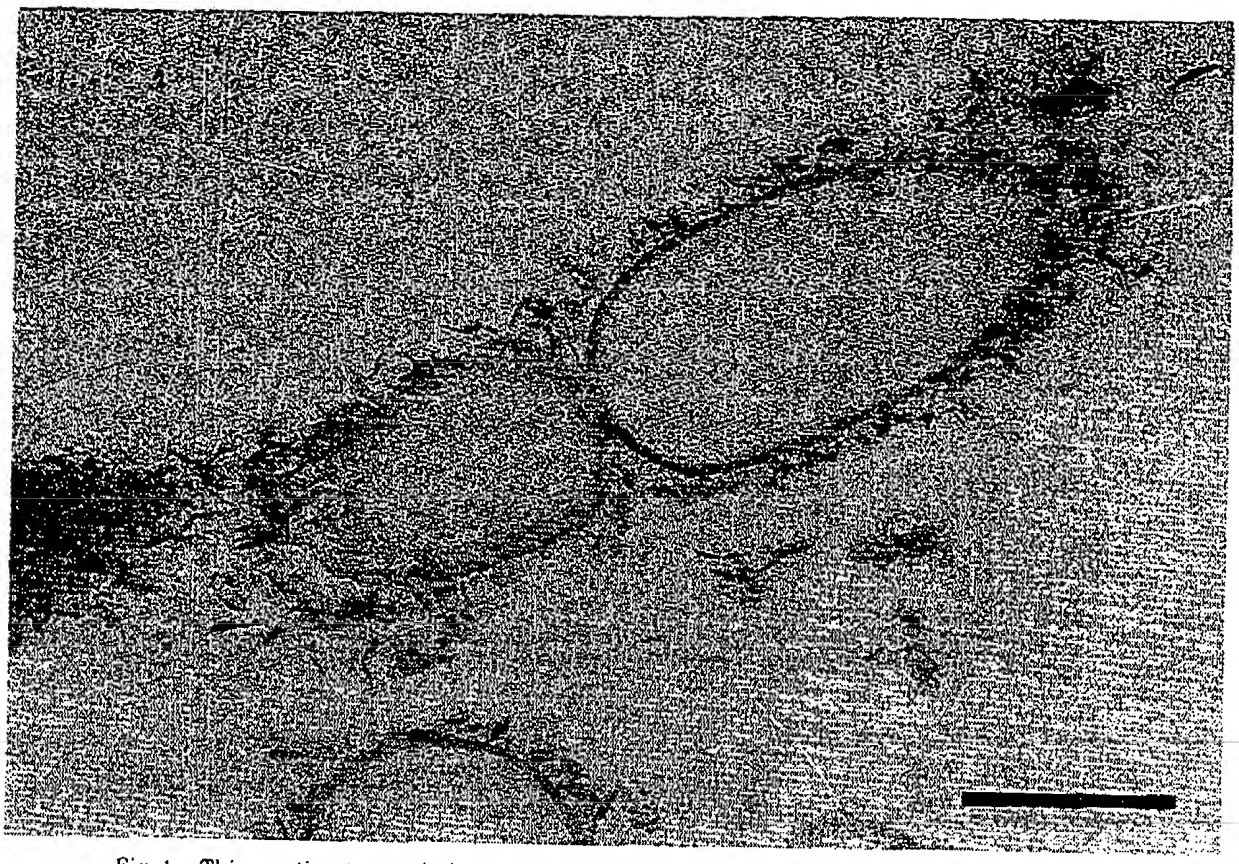

Fig. 1. Thin-section transmission electron micrograph of a bacterium partially encrusted by uranium phosphate microcrystals. The specimen was prepared by first exposing the bacteria to an aqueous uranyl acetate solution. The cell-bound uranyl ions were subsequently precipitated by suspending the cells in a solution containing potassium phosphate (bar=500nm).

cambrian era (Knoll, 1985).

High-magnesium calcite peloids are commonly found in cemented marine carbonate accumulations from quiet water lagoons and microcavities in reefs (Chafetz, 1986). These peloids are elliptical to spheroidal bodies 20 to 60 mm in diameter with crystalline dentate rims. The nuclei are generally fine grained and often contain fossilized clumps of bacteria encased within anhedral micron-sized crystals of high-magnesium calcite. In contrast, the euhedral crystalls rimming the peloids are larger and devoid of organic matter. This difference in the degree of crystallinity between the peloid nucleus and rims presumably reflects different rates of precipitation. A rapid precipitation of calcite initiated by bacteria probably accounts for the smaller anhedral crystals of the nuclei, whereas the rim developed more slowly after a complete mineralization of the bacteial cells. Fossilized clumps of bacteria have also been found in silt-sized particles from freshwater travertine deposits (Chafetz and Folk, 1984).

Partly consolidated deposits of carbonate sediment occur in many tropical and subtropical marine intertidal zones. These deposits are commonly known as beach rock and develop as uniform layers or partially eroded masses at the sediment-water interface (Leeder, 1982). Spherical carbonate particles called ooliths are often found in these formations, particularly where strong tidal currents come about (Loreau and Purser, 1973). The ooliths normally range in diameter from 0.1 to 1.5 mm with alternating

laminations of aragonite and organic matter. The nature and precise origin of these laminations are not welly understood ; however, microorganisms have been implicated in the formation of some oolitic structures (Dahanayake and Krumbein, 1985). Moreover, carbonate precipitating bacteria can be isolated from beach rock formations (Krumbein, 1979).

The role of photosynthetic cyanobacteria in the formation of calcareous microbialite (thrombolite) deposits in an alkaline freshwater lake has recently been evaluated (Thompson *et al.*, 1990 ; Thompson and Ferris, 1990). In this study, a pure culture of Synechococcus sp. was isolated from homogenized actively growing material from the thrombolite and inoculated into cold filter-sterilized lake water. Sequentially progressive epicellular biomineralization of gypsum, calcite (Fig. 2), and magnesite was observed by transmission electron microscopy. Measured changes in the chemistry of the inoculated lake water were consistent with the observed pattern of biomineralization (Thompson and Ferris, 1990). Gypsum was initially precipitated on the surface of Synechococcus because of the binding of calcium cations and the presence of high sulfate concentrations in the lake water. Then cellular precipitates of calcite and magnesite developed as the pH of the lake water increased owing to the photosynthetic metabolism of the cyanobacterium. A similar pattern of biomineralization involving mats of coccoid cyanobacteria from the Pleurocapsa group may account for the growth of enormous tower-like (ca. 40m high) microbialites from alkaline (pH > 9.7) Lake Van in eastern Anatolia, Turkey (Kempe *et al.*, 1991).

VI Metal Sulfides and Associated Paragenetic Minerals

The precipitation of sulfide minerals during low temperature diagenesis involves a number of interdependent biological and geochemical events. Dissimilatory bacterial sulfate reduction is the major mechanism by which sulfide is produced in modern anoxic sedimentary environments (Berner, 1980). This process is carried out by a widely distributed group of anaerobic bacteria that energate energy for growth by coupling the oxidation of simple organic molecules to the reduction of sulfate (Pfenning, 1989). Sulfide minerals are generally precipitated as a direct result of bacterial sulfate reduction. Patterns of sulfur isotope fractionation in many sedimentary sulfide deposits are consistent with this form of biomineralization, and support the bacteriogenic origin of reduced sulfur (Trudinger *et al.*, 1985).

In fine-grained anoxic sediments, sulfide minerals are frequently found to be in close association with high molecular weight organic materials. A number of studies suggest that the formation of organometallic complexes directly in natural environments plays a vital role in the transfer of metallic ions into sulfide phases (Forstner, 1982). This perception is strengthened by results from direct microscopic examinations of marine and to a lesser extent fresh water sediments. In these environments, metal sulfides are commonly precipitated on the surfaces of bacterial cells (Degens and Ittekkot, 1982 ; Ferris *et al.*, 1987 b) (Fig. 3). The formation of sulfide minerals on the outside surfaces of bacteria can be attributed to an uptake and retention of metallic ions. In actuality, the bacteria serve as nucleation templates because they efficiently concentrate the metals before they react with bacterigenic sulfide. There is further experimental evidence which implies that metallic ions bound by bacterial cells tend to be more chemically reactive toward sulfide than when they are in solution (Mohagheghi et al., 1985).

The most important environmental parameter controlling sulfide production in natural sediments is the availability of low molecular weight organic molecules that can be easily metabolized by sulfate-reducing bacteria (Pfenning, 1989 ; Jorgensen, 1982). For this reason, it is not suprising to find that mineralized zones

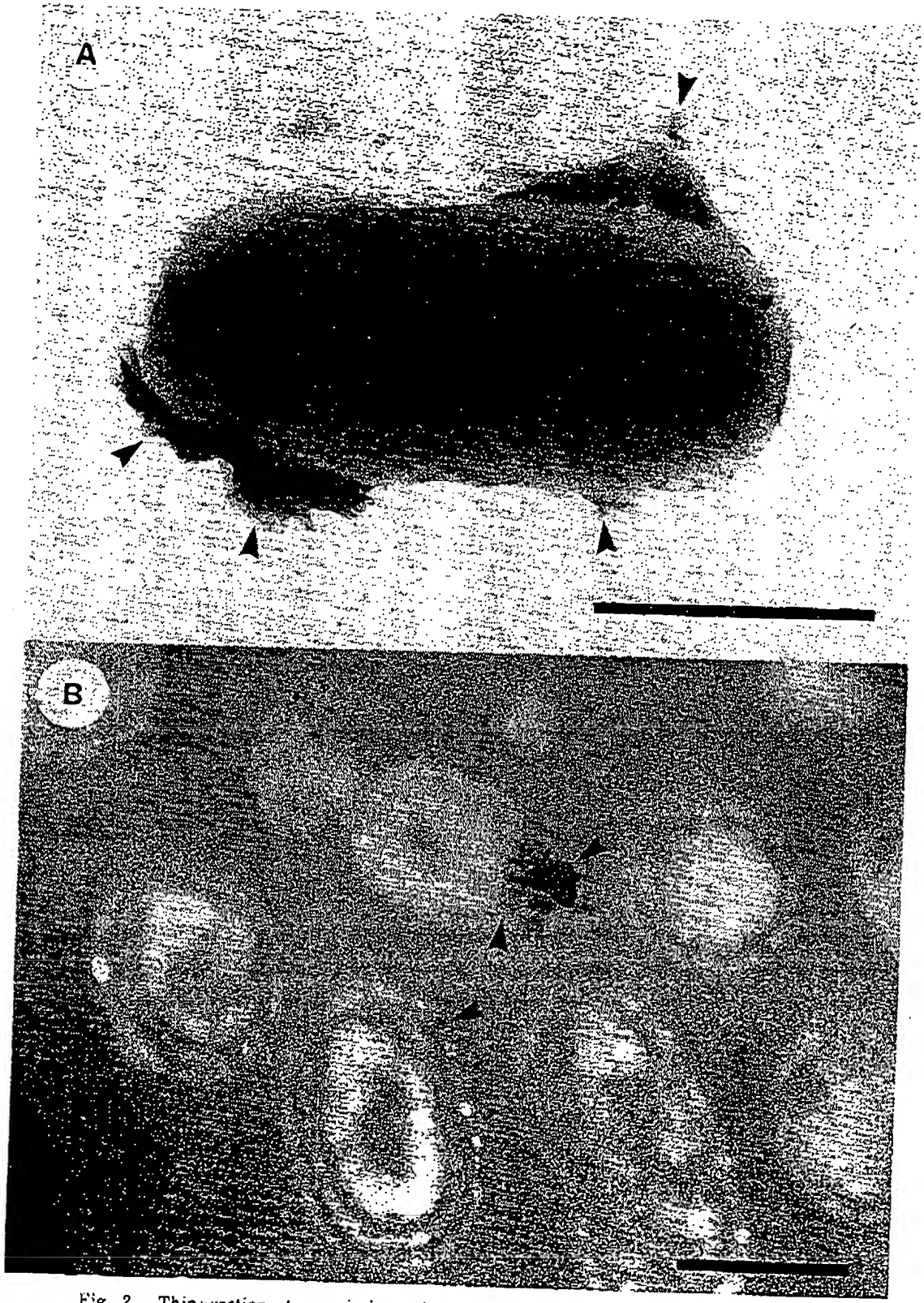

Fig. 2. Thin-section transmission electron micrographs of *Synnechococcus* sp (acyanobacterium) with cell surface deposits, indicated by arrows, of (A) gypsum and (B) calcite (bars = 500nm).

of copper, lead, zinc, and iron frequently occur in association with stromatolitic formations. For example, the Woodcutter's deposit in the Northern Territory of Australia developed in a shallow water restricted basin where bacterial degradation of dense microbial mats and activity of sulfate-reducing bacteria caused a coprecipitation of lead and zinc sulfides along with precursors of the host dolomite rock (Roberts, 1973). Similar accumulations of metal sulfides are found in fine-grained organic-rich maine shales that were deposited under conditions of high biological productivity in shallow oxygen-free, sulfide-rich basins (Raiswell and Berner, 1986).

During sulfate reduction in sediments organic matter is consumed as sulfide, phosphate, and metabolic carbon dioxide are released to the pore water system (Berner, 1971). Because sulfide is a comparatively strong base, it readily reacts with metabolic carbon dioxide to form the much weaker base HCO_3^-. This increase in the concentration of carbonate alkalinity may cause the equilibrium ion product for calcium carbonate to be exceeded. If this happens, precipitation of calcium carbonate can occur. Similarly, if the concentration of phosphate in the sediment pore water system becomes sufficiently high, phosphate minerals can precipitate. Thus, it is not surprising that pyrite formation in marine sediments is nearly coincident with the precipitation of carbonate and phosphate minerals (Glenn and Arthur, 1988). Typically, paragenetic carbonate phases tend to become more predominant with depth, as might be expected from increasing alkalinity and depletion of sulfate caused by bacterial sulfate reduction at deeper levels in the sediment.

The formation of many sedimentary uranium

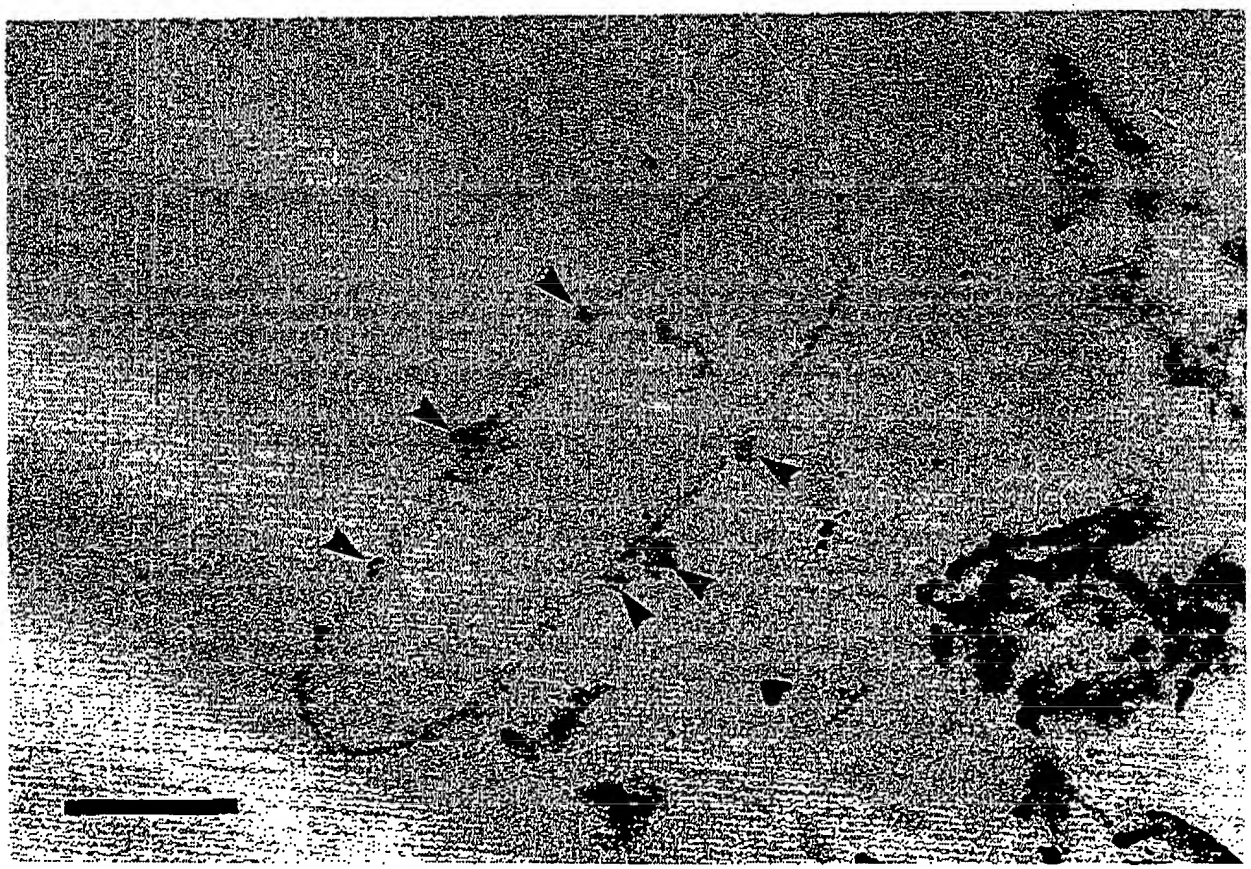

Fig. 3. A thin-section profile showing small electron dense metal sulfide deposits (arrows) on the membranous remains of a bacterial cell in a metal contaminated lake sediment from Sudbury, Ontario, Canada (bar = 500nm).

ores has been attributed to the reduction of relatively soluble uranyl ions – U (VI) –to insoluble uranium (IV) oxides and silicates by aqueous sulfide species (Mohagheghi et al., 1985). This implies at least an indirect role for sulfate-reducing bacteria in the genesis of some sediment hosted uranium deposits. ; however, detailed laboratory growth studies with Desulfovibrio desulfuricans show that sulfate reducing bacteria have an influence on uranyl ion precipitation beyond the simple production of sulfide reductant. A number of microorganisms, including D. desulfuricans and some Fe (III) –reducing bacteria, are now known to be directly capable of enzymatically reducing U (VI) to U (IV) (Lovley *et al.*, 1991 ; Lovley and Phillips, 1992). Enzymatic reduction of U (VI) proceeds much faster than nonenzymatic reduction of U (VI) by sulfide, and rapidly brings about extracellular and epicellular precipitation of uraninite. These observations are consistent with recent descriptions of uranium- and sulfide-mineralized microorganisms in peat bog and flood plain silts of mudflats along Solway Firth in southwest Scotland (Milodowski *et al.*, 1990).

Ⅶ Iron and Manganese Oxides

Bacteria that oxidize iron or manganese are widely distributed in nature and have been studied extensively (Ghiorse, 1984). The growth of these microorganisms is typically accompanied by the development of cell surface deposits of Fe (III) or Mn (IV) oxides. This extracellular deposition of iron or manganese depends strongly on the production of anionic metal binding surface polymers by the bacteria (Fig. 4). At times, fresh isolates of ferromanganese depositing bacteria lose their ability to oxidize Mn (II), suggesting that the process is actively catalyzed by enzymes which the microorganism produces. In contrast, the ability to accumulate Fe oxides is usually not lost because Fe (II) oxidizes spontaneously at neutral pH in the presence of oxygen. Thus, iron depositing bacteria only have to bind the reduced metallic ion or hydrous cationic colloidal forms to precipitate iron oxides.

Fossil structures that resemble modern ferromanganese depositing bacteria have been found in laminated black cherts from the Gunflint Iron Formation (Laberge, 1973) ; however, there is some doubt that the formation of massive Precambrtian iron formations can be attributed entirely to microbial metal precipitation. Nevertheless, electron microprobe and analytical electron microscopic studies have demonstrated that significant amounts of iron are associated with fossil bacteria (Laberge, 1973 ; Tazaki *et al.*, 1992). In addition, more recent naturally occuring iron oxides commonly contain organic matter, and accumulate in environments favorable for the growth of bacteria (Yapp and Poths, 1986 ; Ferris *et al.*, 1989 b).

In an electron microscopic study of sediments receiving acid drainage from mine tailing and coal refuse impoundments, individual bacterial cells were prominent as nucleation sites for the development of iron oxide mineralization. The bacteria were not only serving as templates for the deposition of iron, but their organic remains were being trapped and incorporated into the mineral precipitates during crystal growth (Ferris *et al.*, 1989a ; Ferris *et al.*, 1989b) (Fig. 5). There are numerous acidophilic bacterial genera and species present in acid mine drainage environments, including some that acquire energy for growth from the oxidation of Fe (II), such as Thiobacillus ferrooxidans. On the other hand, many are conventional heterotrophs which utilize organic compounds to grow (Harrison, 1984). This later group of bacteria are not usually viewed as being capable of directing the precipitation of iron ; however, the iron mineralization in the acid mine drainage sediments was not associated with any specifc morphological group of bacteria, and commonly developed on the organic remains of dead cells (Ferris *et al.*, 1989a ; Ferris *et al.*, 1989b). The implication is that bacteria, regardless of trophic classification or physiological state, are indeed capable

of serving as passive nucleation elements for iron oxides in sediments.

Microbiological precipitation of magnetite is now known to proceed in two different ways. Dissimilatory Fe (III) reducing bacteria living in anaerobic sediments can convert amorphous ferric oxide to magnetite by coupling the reduction of iron to the oxidation of organic compounds. In this case, the magnetite precipitates are deposited extracellularly and the crystals have the typical octahedral shape for magnetite (Lovley *et al.*, 1987). Conversely, magnetotactic bacteria produce a morphologically distinct varieties (*i.e.*, hexagonal prisms, cuboidal, or tear drop crystals) of magnetite intracellularly in a membrane-bounded structure that is called a magnetosome (Blakemore, 1982 ; Towe and Moench, 1981 ; Mann *et al.*, 1984) (Fig. 6). The magnetite crystals inside magnetotactitic bacteria also have a unique size distribution, ranging in length from 0.05 to 0.3 mm (Towe and Moench, 1981). This has facilitated the recognition of magnetite crystals from magnetotactic bacteria in soils, sediments, and ancient stromatolites (Chang *et al.*, 1989 ; Fassbinder *et al.*, 1990 ; Stolz *et al.*, 1986). Microbial biomineralization of ferrimagnetic iron sulfide minerals (e.g., greigite, Fe_3S_4) in magnetotactic bacteria inhabiting brackish, sulfide-rich sediments has also been documented (Farina *et al.*, 1990 ; Mann *et al.*, 1990).

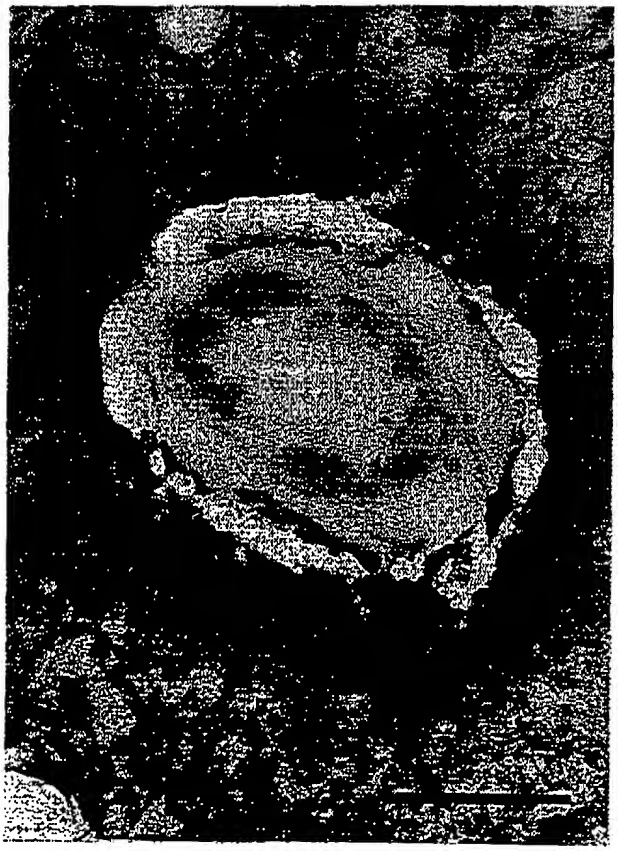

Fig. 4. A manganese oxide encrusted bacterial cell in a thin-section of a hot spring microbial mat from Yellowstone National Park, Wyoming, USA (bar=500nm).

The formation of marine manganese nodules, freshwater and hotspring manganese precipitates and desert varnish has been attributed to manganese oxidizing bacteria (Ehrlich and Zapkin, 1985 ; Mustoe, 1981 ; Ferris et al., 1987a ; Ehrlich, 1974). Also, the development of at least some of the manganese oxide deposits that arise near deep ocean hydrothermal vents can be attributed to the activity of manganese oxidizing bacteria (Ehrlich, 1983) In addition, recent studies show that bacteria cells scavenge manganese in hydrothermal plumes at a distances at least 7 km away from the vent source (Cowen *et al.*, 1986). This later observation suggests that bacteria play an important role in precipitating manganese over large areas in the oceans.

Ⅷ Siliceous Minerals

The influence of bacteria on silica precipitation and authigenic clay formation has always been an interesting, but difficult problem in microbial biomineralization. In any event, high molecular weight humic substances are sometimes incorporated into clays (Wang and Huang, 1986). Moreover, fossil remnants of bacterial cells are commonly found in cherty sequences of siliceous carbonates as well as sandstones, siltstones, and shales (Knoll, 1985). These observations suggest that sites of diagenetic silicification and clay formation are apt to

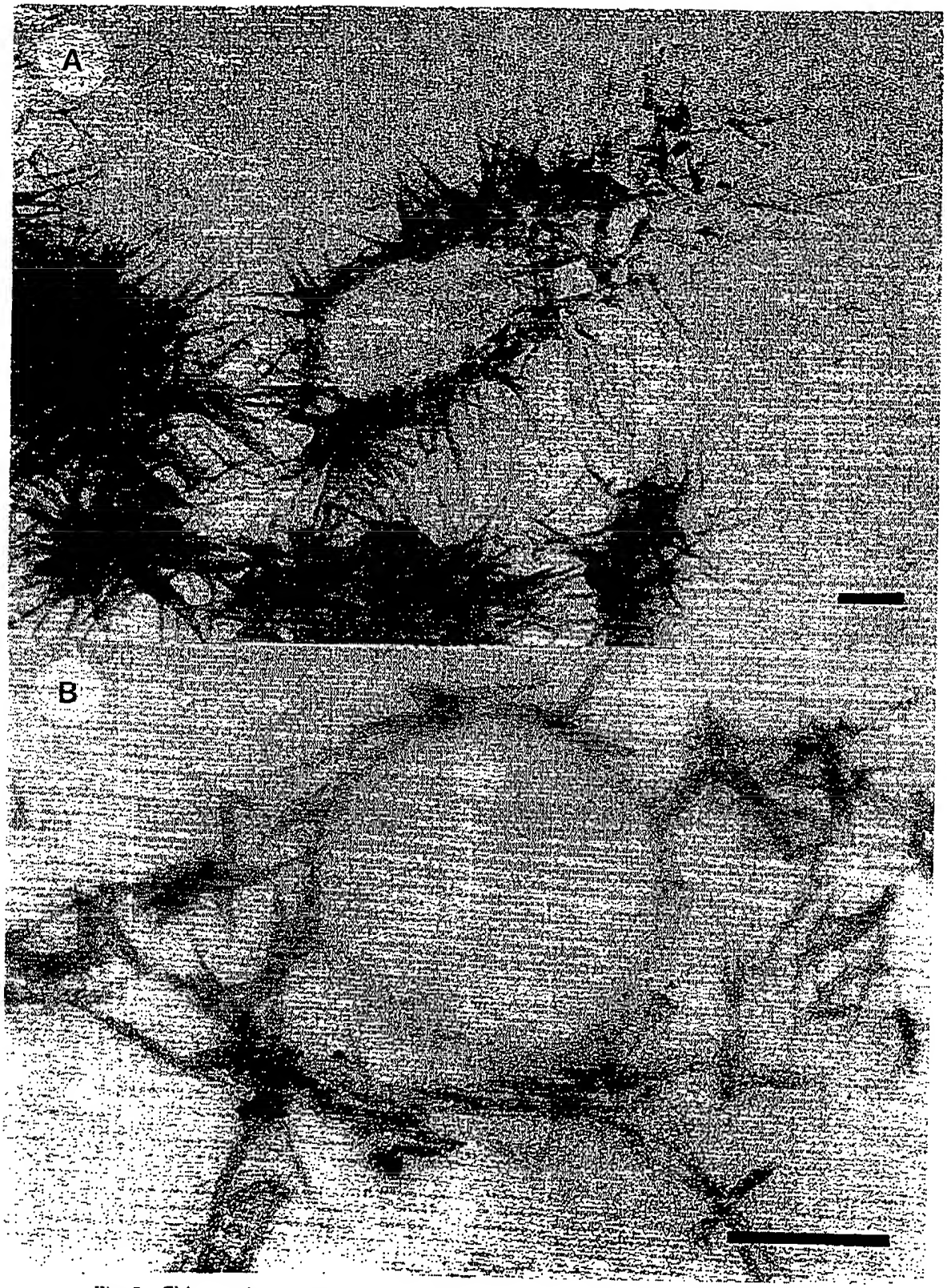

Fig. 5. Thin-section electron micrographs of bacterial cells with surface deposits of (A) amorphous ferrihydrite and (B) microcrystalline hematite in acid mine drainage sediments (bars = 250nm).

be found in sedimentary environments where relatively high concentrations of organic matter accumulate.

Direct examination of terrestrial acidic hot spring sediments by analytical transmission electron microscopy has revealed bacterial cells in successive stages of mineralization by amorphous iron-silica crystallites (Ferris *et al.*, 1986). The iron was probably bound by the anionic surface polymers of the bacteria, whereas the silica crystallites presumably developed from mono-or polysilicic acid that was hydrogen bonded to available hydroxyl groups. Similar epicellular deposits of silica on bacterial cells have been reported in laboratory experiments (Birnbaum and Wireman, 1985 ; Ferris *et al.*, 1988) (Fig. 7). These data not only confirm that bacteria are capable of precipitating silica, but also provide an explanation for the close association between early diagenetic silica and organic matter derived from microorganisms in Precambrian sedimentary formations.

Cell surface deposits of a complex iron-aluminum-silicate have been found on bacterial cells growing in a metal contaminated lake sediment (Ferris *et al.*, 1987). These precipitates ranged from a poorly structured granular material to a more well developed crystalline phase (Fig. 8). Selected area electron diffraction patterns and energy dispersive X-ray spectroscopy suggested that this polymorphic iron-aluminum-silicate was chamosite [$(Fe_5\,Al)(Si_3\,Al)O_{10}(OH)_8$]. The exact role of bacteria as nucleating elements for an iron-rich limonitic clay can be understood in terms of their ability to immobilize metallic ions. Hydrous iron-alu-

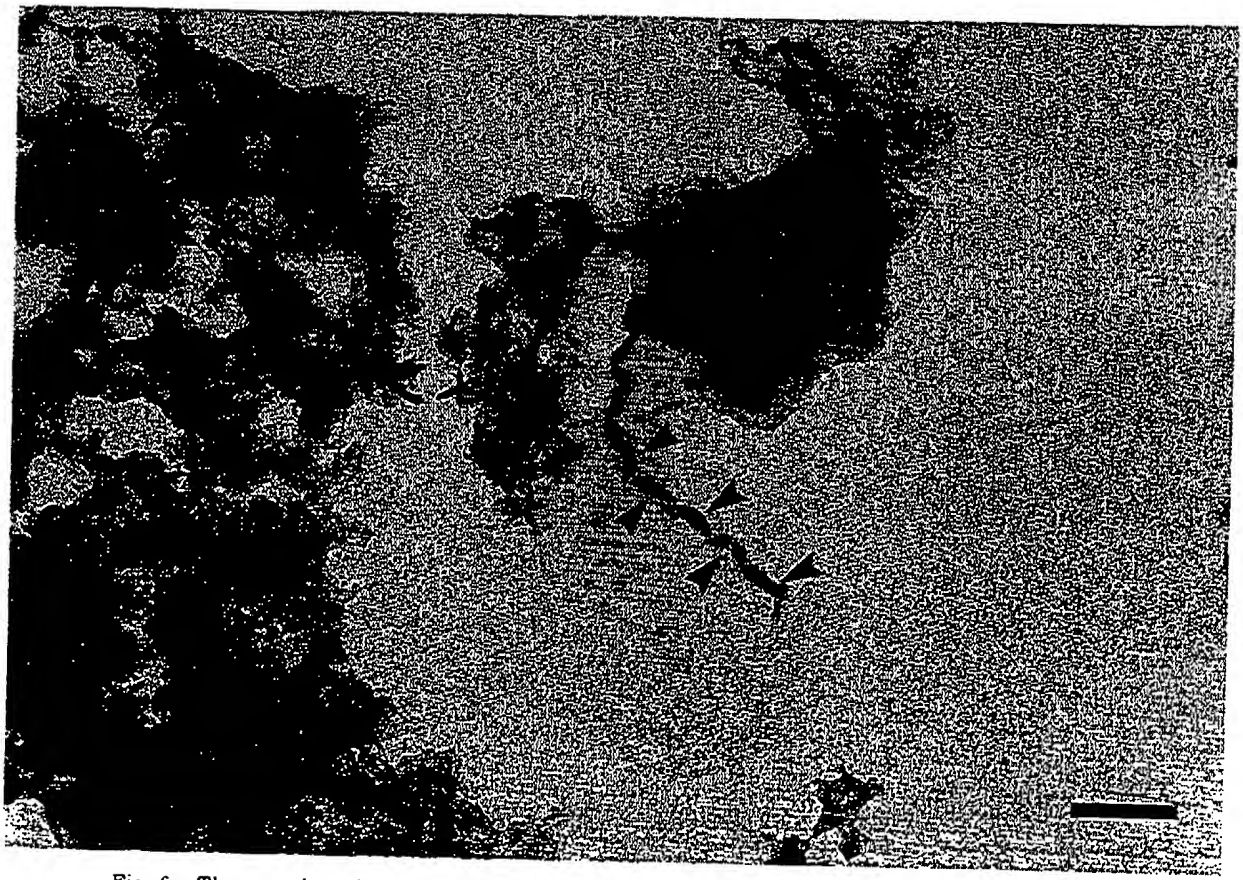

Fig. 6. The remains of a magnetotactic bacterium with internal tear-drop shaped magnetite particles (arrows) in a whole mount of sediment from a metal contaminated lake sediment near Sudbury, Ontario, Canada (bar=250nm).

Fig. 7. Thin-section electron micrographs of iron silica crystallites deposited on the surface of bacteria in(A)a hot spring sediment from Yellowstone National Park, Wyoming, USA (bar = 1.0 mm) and(B)an experimental laboratory simulation (bar-500nm).

minum-silicate species could be precipitated directly by dissolved silicic acid from metals complexed by the cells, or alternatively, cationic colloidal species formed initially in the sediment pore water systems could be bound. These processes, either separately or together, would account for the formation of a gel-like phase from which the crystalline forms typically evolve during structural rearrangement and layer growth in the solid state (Amouric and Parron, 1985).

Glauconite is a common potassium-containing iron-aluminum-silicate that frequently occurs in organic rich marine sediments where phosphogeneis takes place (Glenn and Arthur, 1988). In these systems, glauconites are generally precipitated early with phosphate, pyrite, and carbonate precipitation taking place at progressively deeper levels in the sediment in association with microbial sulfate reduction. This paragenetic sequence signifies a change from oxidizing conditions to a more strongly reducing environment that favors the reduction of iron and its precipitation as pyrite during bacterial sulfate reduction. In this context, the development of glauconite, is thought to be related to partial microbial reduction of Fe (III) under mildlly reducing conditions. Also, it is conceivable that the bacteria act in a dual role as nucleation elements for glauconite precipitation.

IX Concluding Remarks

Microbial biomineralization has contributed to the formation of a tremendous range of sedimentary mineral deposits. The development of such bacteriogenic mineral deposits is usually

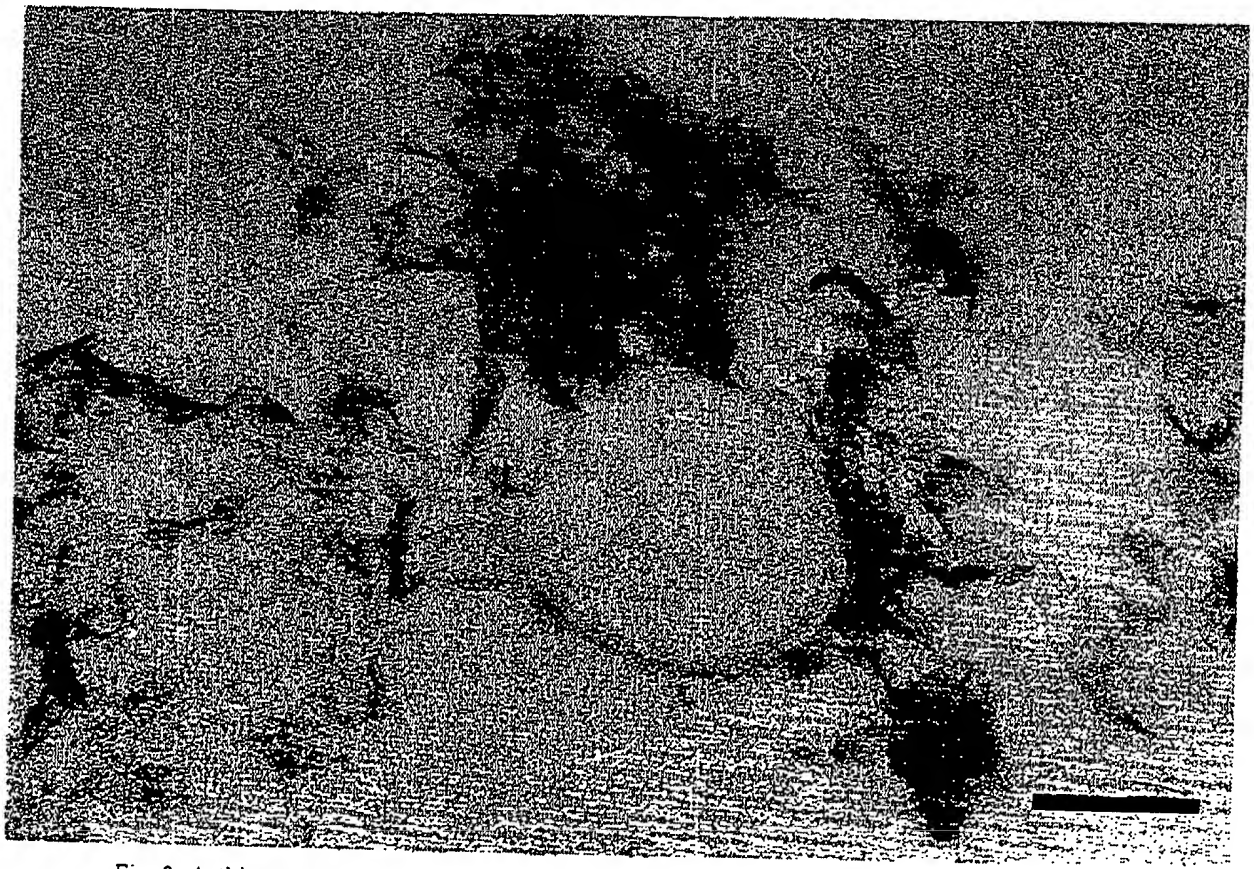

Fig. 8. A thin-section electron micrograph of a bacterial cell with surface deposits of a complex iron-aluminum-silicate. The specimen was obtained from a lake near Sudbury, Ontario, Canada (bar = 250nm)

explained in terms of geologic time : however, laboratory investigations indicate that bacteria are capable of supporting high rates of mineral precipitation. For example, cultures of bacteria isolated from marine beachrock have been shown to precipitate up to 4.7 mg. L^{-1}. hr^{-1} of calcite (Krumbein, 1979). Simple calculations suggest that approximately 1.8×10^8 tonnes of calcite would be precipitated at this rate of mineral precipitation over 1000 years in a shallow (*i.e.*, 5.0m depth) 1 km 2 body of water. While this unreasonably assumes a uniform distribution of calcite precipitating bacteria, constant rate of mineralization, and no dissolution of calcite, the implications are clear. Microbial biomineralization is not a trivial affair, particularly if one considers that bacteria live in virtually every kind of environment on Earth where liquid water is freely available. It is also interesting to note that many examples of microbial biomineralization come from environments that have been disrupted by mining or other industrial activity. At the same time, some of the best examples of microbial biomineralization in the geological record come from the Precambrian era, a period in Earth's history that is reknown for environmental change. The picture that emerges from these considerations is intriguing. Microbial biomineralization may be a sensitive indicator of trends in global environmental change. This interesting possiblity gives grounds to believe that microbial biomineralization must be studied in greater detail, particularly in view of current concerns about the deteriorating condition of our planet.

Acknowledgement

The author's work is supported by the Natural Science and Engineering Research Council (NSERC) of Canada.

References

Amouric, M. and Parron, C. (1985) Structure and growth mechanisms of glauconite as seen by high resolution transmission electron microscopy. *Clays and Clay Minerals*, 33, 474–482.

Awramik, S. M. (1971) Precambrian columnar stromatolite diversity : Reflection of metazoan appearance. *Science*, 174, 825–827.

——— (1986) New fossil finds in old rocks. *Nature*, 319, 446–447.

———, and Barghoorn, E.S. (1977) The Gunflint microbiota. *Precambrian Res.*, 5, 121–142.

———, Schopf, J. W., and Walter, M. R. (1983) Filamentous fossil bacteria from the Archean of Western Australia. *Precambrian Res.*, 20, 357–374.

Berner, R. A. (1971) Bacterial processes effecting the precipitation of calcium carbonate in sediments. *The Johns Hopkins University Studies in Geology*, 19, 247–251.

——— (1980) *Early diagenesis, A theoretical approach*. Princeton University Press, Princeton.

Beveridge, T. J. (1989) Role of cellular design in bacterial metal accumulation and mineralization. *Ann. Rev. Microbiol.*, 43, 147–171.

———, Meloche, J. D., Fyfe, W. S., and Murray, R. G. E. (1983) Diagenesis of metals chemically complexed to bacteria : Laboratory formation of metal phosphates, sulfides and organic condensates. *Appl. Environ. Microbiol.*, 45, 1094–1108.

Birnbaum, S. J. and Wireman, J. W. (1985) Sulfate-reducing bacteria and silica solubility : A possible mechanism for evaporite diagenesis and silica precipitation in banded iron formations. *Can. J. Earth Sci.*, 22, 1904–1909.

Blakemore, R. P. (1982) Magnetotactic bacteria. *Ann. Rev. Microbiol.*, 36, 217–238.

Chafetz, H. S. (1986) Marine peloids : A product of bacterially induced precipitation of calcite. *J. Sediment. Petrol.*, 54, 812–817.

———, and Folk, R. L. (1984) Travertines : Depositional morphology and the bacterially constructed constituents. *J. Sediment. Petrol.*, 54, 289–316.

Chang, S. R., Stolz, J. F., Kirschvink, J. L., and Awramik, S. M. (1989) Biogenic magnetite in

stromatolites II : Occurenc in ancient sedimentary environments. *Precambrian Res.*, 43, 305－315.

Cowen, J. P., Massoth, G. J., and Baker, E. T. (1986) Bacterial scavenging of Mn and Fe in a mid-to far-field hydrothermal particle plume. *Nature*, 322, 169－171.

Dahanayake, K. and Krumbein, W. E. (1985) Ultrastructure of a microbial mat generated phosphorite. *Mineral. Deposita*, 20, 260－265.

Degens, E. T. and Ittekkot, V. I. (1982) In situ metal staining of biological membranes in sediments. *Nature*, 298, 262－264.

Ehrlich, H. L. (1974) The formation of ores in the sedimentary environment of the deep sea with microbial participation:The case for ferromanganese concretions. *Soil Sci.*, 119, 36－41.

——— (1983) Manganese oxidizing bacteria from a hydrothermally activeregion on the galapagos rift. *Ecol. Bull.*, 35, 357－366.

——— and Zapkin, M. A. (1985) Manganese-rich layers in calcareous deposits along the western shore of the Dead Sea may have a bacterial origin. *Geomicrobiol. J.*, 4, 207－221.

Farina, M., Motta, Esquivel, D. M. S., and Lin de Barros, H. G. P. (1990) Magneticiron-sulfur crystals from a magnetotactic microorganism. *Nature*, 343, 256－258.

Fassbinder, J. W. E., Stanjek, H., and Vali, H. (1990) Occurence of magnetic bacteria in soil. *Nature*, 343, 161－163.

Fay, P. (1992) Oxygen relations of nitrogen fixation in cyanobacteria. *Microbiol. Rev.*, 56, 340－373.

Ferris, F. G. and Beveridge, T. J. (1985) Functions of bacterial cell surface structures. *BioScience*, 35, 172－177.

———, ——— and Fyfe, W. S. (1987a). Manganese oxide deposition in a hot spring microbial mat. *Geomicrobiol. J.*, 5, 33－42.

Ferris, F. G., Fyfe, W. S., and Beveridge, T. J. (1986) Iron-silica crystallite nucleation by bacteria in a geothermal sediment. *Nature*, 320, 609－611.

———, ——— and ——— (1987b) Bacteria as nucleation sites for authigenic minerals in a metal contaminated lake sediment. *Chem. Geol.*, 63, 225－232.

———, ——— and ——— (1988) Metallic ion binding by Bacillus subtilis:Implications for the fossilization of microorganisms. *Geology*, 16, 149－152.

———, Schultze, S., Witten, T. C., Fyfe, W. S., and Beveridge, T. J. (1989a) Metal interactions with microbial biofilms in acidic and neutral pH environments. *Appl. Environ. Microbiol.*, 55, 1249－1257.

———, Tazaki, K., and Fyfe, W. S. (1989b) Iron oxides in acid mine drainage environments and their association with bacteria. Chem. Geol. 74, 321－330

Forstner, U. (1982) Accumulative phases for heavy metals in limnic sediments. *Hydrobiologia*, 91, 269－284.

Ghiorse, W. C. (1984) Biology of iron-and manganese-depositing bacteria. *Ann. Rev. Microbiol.*, 38, 515－550.

——— and Wilson, J. T. (1988) Microbial ecology of the terrestrial subsurface. Adv. *Appl. Microbiol.*, 33, 107－132.

Glenn, C. R. and Arthur, M. A. (1988) Petrology and major element geochemistry of Peru margin phosphorites and associated diagenetic minerals:Authigenesis in modern organic-rich sediments. *Marine Geol.*, 80, 231－267.

Harrison, A. P. (1984) The acidophilic Thiobacilli and other acidophilic bacteria that share their habitat. *Ann. Rev. Microbiol.*, 38, 265－292.

Johnston, C. G. and Kipphut, G. W. (1988) Microbially mediated Mn (II) oxidation in an oligotrophic artic lake. *Appl. Environ. Microbiol.*, 54, 1440－1445.

Jorgensen, B. B. (1982) Ecology of the bacteria of the sulfur cycle with special reference to anoxic-oxic interface environments. *Phil. Trans. R. Soc. London, B298*, 543－561.

Kempe, S., Kazmierczak, J., Landmann, G., Konuk, T., Reimer, A., and Lipp, A. (1991)

Largest known microbialites discovered in Lake Van, Turkey. *Nature*, 349, 605–608.

Knoll, A. H. (1985) Exceptional preservation of photosynthetic organisms in silicified carbonates and silicified peats. *Phil. Trans. R. Soc. London.*, B311, 111–122.

Krumbein, W. E. (1974) On the precipitation of aragonite on the surface of marine bacteria. *Naturwissenschaften*, 61, 167–168.

——— (1979) Photolithotrophic and chemoorganotrophic activity of bacteria and algae as related to beachrock formation and degradation (Gulf of Aqaba, Sinai). *Geomicrobiol. J.*, 1, 139–203.

Laberge, G. L. (1973) Possible biological origin of Precambrian iron formations. *Econ. Geol.*, 68, 1098–1109.

Leeder, M. R. (1982) *Sedimentology:Process and product.* George Allen and Unwin, London.

Loreau, J. P. and Purser, B. H. (1973) Distribution and ultrastructure of holoceneooids in the Persian Gulf. In *The Persian Gulf-Holocene Carbonate Sedimentation and Diagenesis in a Shallow Epicontinental Sea.* (Purser, B. H., ed.), Springer, Heidelberg, pp. 279–328.

Lovley, D. R., Stolz, J. F., Nord, G. L., and Phillips, E. J. P. (1987) Anaerobic production of magnetite by a dissimilatory iron reducing microorganism. *Nature*, 330, 252–254.

———, Phillips, E. J. P., Gorby, Y. A., and Landa, E. R. (1991) Microbial reduction of uranium. *Nature*, 350, 413–416.

——— and E. J. P. Phillips. (1992) Reduction of uranium by Desulfovibriodesulfuricans. *Appl. Environ. Microbiol.*, 58, 850–856.

Lowenstam, H. A. and Weiner, S. W. (1989) *On Biomineralization.* Oxford University Press, New York.

Mann, S. (1988) Molecular recognition in biomineralization. *Nature*, 332, 119–124

———, Frankel, R. B., and Blakemore, R. P. (1984) Structure, morphology, and crystal growth of bacterial magnetite. *Nature*, 310, 405–407.

Mann, S., Sparks, N. H. C., Frankel, R. B., Bazylinski, D. A., and Jannasch, H. (1990) Biomineralization of ferrimagnetic greigite and iron pyrite in a magnetotactic bacterium. *Nature*, 343, 258–261.

Milodowski, A. E., West, J. M., Pearce, J. M., Hyslop, E. K., Basham, I. R., and Hooker, P. J. (1990) Uranium-mineralized microorganisms associated with uraniferous hydrocarbons in southwest Scotland. *Nature*, 347, 465–467.

Mohagheghi, A., Updegraff, D. M., and Goldhaber, M. B. (1985) The role of sulfate-reducing bacteria in the deposition of sedimentary uranium ores. *Geomicrobiol. J.*, 4, 153–173.

Mustoe, G. E. (1981). Bacterial oxidation of manganese and iron in a modern cold spring. *Bull. Geol. Soc. Am.*, 92, 147–153.

Pfenning, N. (1989) Metabolic diversity among the dissimilatory sulfate-reducing bacteria. *Antonie van Leeuwenhoek*, 56, 127–138.

Philip, R. P. and Calvin, M. (1976) Possible origin for insoluble organic (kerogen) debris in sediments from insoluble cell wall materials of algae and bacteria. *Nature*, 262, 134–136.

Raiswell, R. and Berner, R. A. (1986) Pyrite and organic matter in Phanerozoic normal marine shales. *Geochim. Cosmochim. Acta*, 50, 1967–1976.

Roberts, W. M. B. (1973) Dolomitization and the genesis of the Woodcutters lead-zinc prospect, Northern Territory, Australia. *Mineral. Deposita*, 8, 35–56.

Schidlowski, M. (1988) A 3,800 million year isotopic record of life from carbon in sedimentary rocks. *Nature*, 333, 313–318.

Schlesinger, W. H. (1991) *Biogeochemistry : An analysis of global change.* Academic Press, San Diego.

Soudry, D. and Champtier, Y. (1983) Microbial processes in Negev phosphorites (Southern Isreal). *Sedimentology*, 30, 411–423.

Southgate, P. N. (1986) Cambrian phoscreteprofiles, coated grains, and microbial processes in phosphogenesis:Georgina basin, Australia.

J. Sediment. Petrol., 56, 429－441.

Stetter, K. O. (1982) Ultrathin mycelia forming organisms from submarine volcanic areas having optimum growth temperature of 105℃. *Nature*, 300, 258－260.

Stolz, J. F. and Margulis, L. (1984) The stratified microbial community at LagunaFigueroa, Baja California, Mexico : A possible model for prephanerozoic laminated microbial communities preserved in cherts. *Origins of Life*, 14, 671－679.

————, Chang, S. R., and Kirschvink, J. L. (1986) Magnetotactic bacteria and single domain magnetite in hemipelagic sediments. *Nature*, 321, 849－851.

Tazaki, K., Ferris, F. G., Wiese, R. G., and Fyfe, W. S. (1992) Iron and graphite associated with fossil bacteria in chert. *Chem. Geol.*, 95, 313－325.

Thompson, J. G. and Ferris, F. G. (1990) Cyanobacterial precipitation of gypsum, calcite, and magnesite from natural alkaline lake water. *Geology*, 18, 995－998.

Thompson, J. B., Ferris, F. G., and Smith, D. A. (1990) Geomicrobiology and Sedimentology of the mixolimnion and chemocline in Fayetteville Green Lake, New York. *Palaios*, 5, 52－75.

Towe, K. M., and Moench, T. T. (1981) Electron optical characterization of bacterial magnetite. *Earth Plant. Sci. Lett.*, 52, 213－220.

Trudinger, P. A., Chambers, L. A., and Smith, J. W. (1985) Low temperature sulfate reduction : Biological versus abiological. *Can. J. Earth Sci.*, 22, 1910－1918.

Walter, M. R. (1983) Archean Stromatolites : Evidence of the Earth's earliest benthos. In *Earth's Earliest Biosphere* (Schopf, J. W., ed.) Princeton University Press, Princeton, pp. 187－213.

Wang, M. C. and Huang, P. M. (1986) Humic macromolecule intelayering in nontrominte through interactions with phenol monomers. *Nature*, 323, 529－531.

Yapp, C. J. and Poths, H. (1986) Carbon in natural goethites. *Geochim. Cosmochim. Acta.*, 50, 1213－1220.

Yayanos, A. A. (1986) Evolutional and ecological implications of the properties of deep-sea barophilic bacteria. *Proc. Natl. Acad. Sci. USA*, 83, 9542－9546.

自然環境における微生物の生体鉱物化作用

F. G. Ferris

要　旨

微生物は，自然環境下で，極めて多種多様な鉱物を沈積させるのに役立っている．この現象は，微生物による生体鉱物化作用として知られている．微生物による生体鉱物化作用の重要性は，単に，微生物の生息する環境がきわめて多様というばかりでなく，微生物が独特な生理と独特な細胞構造をもつことにある．例えば，100℃以下の温度，嫌気的な堆積物の中で，微生物が硫酸塩を還元させ，硫化物の沈殿を行っている．同時に，微生物は，金属イオンを結合する能力をそなえており，その能力によって，細胞を核形成の場として，自生鉱物を沈殿させている．現在の環境下でも多くの微生物が，広く生体鉱物化作用を行っているが，過去においても，鉱床の形成にバクテリアが寄与したと思われる証拠が多く見出されている．さらに，鉱山や工業活動により破壊された環境下において，微生物による生体鉱物化作用の数多い記録は，微生物による鉱物の沈殿が環境変化の敏感な指示計となり得ることを示している．

STIC-ILL

Fr m: Marx, Irene
S nt: Tuesday, September 10, 2002 9:19 AM
To: STIC-ILL
Subject: 09/777664

Imp rtance: High

Please send to Irene Marx, Art Unit 1651; CM1, Room 10E05, phone 308-2922, Mail box in 11B01

Observations on the ionic composition of blue-green algae growing in saline lagoons
AU Pillai, V. K.
SO Proc. Natl. Inst. Sci. India, (19550000) vol. 21, no. 2, pp. 90-102.
DT Journal

Dalrymple, D.W., 1965, "Calcium carbonate deposition associated with blue green algal mats, Baffin Bay.:, Texas: Institute of Marine Science Publication 10, p. 187-200

Black, M., 1933, "The algal sedimentation... ", Royal Society of London Philosphical transactions, Ser. B, V. 222, p. 165-192

Lowenstam HA (1981), Science, 211:1126-1131

Ferris et al., Earth Sci., 47:233-250 (1993)

Ferris et al., Appl. and Environm. Microbiol.,1989, 55:1249-1257

Kazmierczak et al., (1990), Science, 250:1244-1248

Kempe et al., Facies, 28:1-32, 1993.

Kempe et al., 1994, Bull, Inst. Oceanogr., Monaco no. spec., 13:61-117.

Merz, M.U.E, 1992, Facies, 26:81-102

Pentecost et al., 1986, Calcification in cyanobacteria, In "Biomineralization of Lower plants and animals (Leadbeater et a., ed. 73-90, Clarendon Press, Oxford.

Riding, R., 1982, Nature, 299:814-815

Thompson eta., 1990, Geology, 18:995-998

Irene Marx
Art Unit 1651
CMI 10-E-05,
Mail Box 11-B-01
703-308-2922

APPLIED AND F[illegible]ONMENTAL MICROBIOLOGY, May 1989, p. 1249–1257
0099-2240/89/051249-09$02.00/0
Copyright © 1989, American Society for Microbiology
Vol. 55, No. 5

Metal Interactions with Microbial Biofilms in Acidic and Neutral pH Environments

F. G. FERRIS,[1]† S. SCHULTZE,[2] T. C. WITTEN,[2] W. S. FYFE,[1] AND T. J. BEVERIDGE[2]*

Department of Geology, University of Western Ontario, London, Ontario N6A 5B7,[1] and Department of Microbiology, University of Guelph, Guelph, Ontario N1G 2W1,[2] Canada

Received 17 October 1988/Accepted 21 February 1989

Microbial biofilms were grown on strips of epoxy-impregnated filter paper submerged at four sites in water contaminated with metals from mine wastes. At two sample stations, the water was acidic (pH 3.1); the other sites were in a lake restored to a near neutral pH level by application of a crushed limestone slurry. During a 17-week study period, planktonic bacterial counts increased from 10^1 to 10^3 CFU/ml at all sites. Biofilm counts increased rapidly over the first 5 weeks and then leveled to 10^6 CFU/cm² in the neutral pH system and 10^5 CFU/cm² at the acidic sites. In each case, the biofilms bound Mn, Fe, Ni, and Cu in excess of the amounts adsorbed by control strips covered with nylon filters (pore size, 0.22 μm) to exclude microbial growth; Co bound under neutral conditions but not under acidic conditions. Conditional adsorption capacity constants, obtained graphically from the data, showed that biofilm metal uptake at a neutral pH level was enhanced by up to 12 orders of magnitude over acidic conditions. Similarly, adsorption strength values were usually higher at elevated pH levels. In thin sections of the biofilms, encapsulated bacterial cells were commonly found enmeshed together in microcolonies. The extracellular polymers often contained iron oxide precipitates which generated weak electron diffraction patterns with characteristic reflections for ferrihydrite ($Fe_2O_3 \cdot H_2O$) at d equaling 0.15 and 0.25 nm. At neutral pH levels, these deposits incorporated trace amounts of Si and exhibited a granular morphology, whereas acicular crystalloids containing S developed under acidic conditions.

The behavior of dissolved metals in natural bodies of water is strongly influenced by particulate inorganic and organic material (23, 39). Hydrous metal oxides (31, 38), clays (35), humic substances (22, 26, 36), and biota (25, 28) are all capable of binding metallic ions from solution. This effectively enhances the partitioning of metals into sediments and contributes to authigenic mineral formation during the course of diagenesis (16, 33). Of the various metal-complexing agents in aquatic systems, microorganisms and their constituent polymers are among the most efficient scavengers of metallic ions. For example, planktonic microbial forms have been implicated in metal (i.e., Fe and Mn) uptake within horizontally advected hydrothermal plumes along the East Pacific Rise and southern Juan de Fuca Ridge (10, 11). Similarly, soluble metals are bound by the capsular material which often surrounds bacteria associated with sedimenting colloidal particles in freshwater lakes (32). Certainly, a few specific natural microbial metal interactions (i.e., those of the iron- and manganese-depositing bacteria) have been well studied (19, 20), but unfortunately most of our information concerning general microbial immobilization of metals comes from short-duration laboratory experiments on isolated bacterial cell walls and extracellular polymers (3, 37). For this reason, it is important to develop a better understanding of the reactivity between metallic ions and natural microbial populations.

The formation of nontransient adherent communities (i.e., biofilms) of microorganisms on submerged surfaces is common in both freshwater and marine environments (17, 18, 30, 41). These attached microbial populations benefit from the enriched nutrient status of solid-liquid interfaces and may be more active in terms of metabolic activity than their planktonic counterparts (15). Previous studies have used microbial surface colonization for in situ growth (6), nutrient uptake (29), and biomass determinations (34). A similar approach is taken in this investigation on interactions between metals and microorganisms in their native environment. Biofilms were grown on strips of epoxy-impregnated filter paper strips submerged in water contaminated with metals from mine wastes. At regular intervals over a 17-week study period, samples were analyzed for adsorbed metal and examined by electron microscopy. The results showed that microbial biofilms are not only capable of binding significant quantities of metallic ions under natural conditions but they also serve as templates for the precipitation of insoluble mineral phases.

MATERIALS AND METHODS

Site description. Metal adsorption studies by adherent microbial populations were conducted within acidic and neutral pH environments of the Moose Lake watershed at Onaping, northwest of Sudbury, Ontario, Canada. Above Moose Lake, mine drainage and casual water seep through waste rock and then pass over and through two mill tailing ponds, one of which is still active (Fig. 1). Acid conditions are generated in these areas by the oxidation of pyrrhotite (FeS_{1+x}) and other metal sulfides present in the mine wastes. The acidic metal-laden waters, some of which pass through Cranberry Lake, eventually collect in Upper Moose Lake. Upon entering Lower Moose Lake, the water is treated with a crushed limestone slurry to restore circumneutral pH

* Corresponding author.
† Present address: NOVA HUSKY Research Corporation, Bioscience Group, Calgary, Alberta T2E 7K7, Canada.

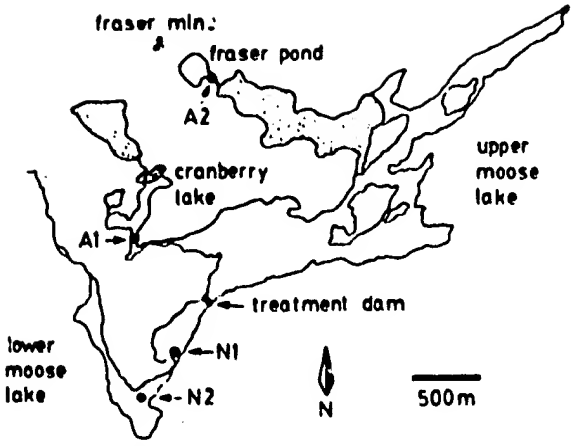

FIG. 1. Map of Moose Lake area showing location of sample sites, Fraser mine, treatment dam, and tailing impoundments (shaded areas).

conditions and reduce downstream dissolved metal concentrations.

Sample stations were established at four sites in the last week of April 1987 (Fig. 1). Anchored buoys were placed in the south end of Cranberry Lake (site A1) in 6.0 m of water and near the discharge of Fraser Mine Pond (site A2) at a depth of 3.0 m. The pH level at both sites was 3.1 and remained constant over the sampling season. Similarly, buoys were anchored in areas of Lower Moose Lake 5.0 to 6.0 m deep, above (site N1) and below (site N2) a narrow channel separating two arms of the lake. At these sites, the pH level was more variable but stayed within a range of 6.5 to 6.9. Also, during the first 8 weeks, surface water temperatures at the four sample stations increased from near 8°C to a stable level of approximately 15°C. Temperature and pH levels were determined whenever samples were collected (see below).

Sampling procedures. Strips of Whatman no. 1 filter paper (Fisher Scientific Co.) were impregnated with an epoxy resin (Epon 812; CanEM), cured, and mounted in plastic Gepe 35-mm photographic slide binders (5.0 × 5.0 cm). Control slides were prepared by sandwiching the support strips between 0.22-μm Nylon 66 micron filters (Schleicher and Schuell, Inc.) to inhibit microbial penetration to the support strips. A UV laminar flow cabinet was used at all times to reduce exogenous contamination of the slides. Test and control slides were threaded onto separate lines attached firmly to weighted plastic hangers. These were subsequently suspended 1.5 m below the anchored buoys at each sample station.

After an initial in situ incubation of 1 week and at approximately 5-week intervals thereafter, paired sets of slides were carefully recovered from each of the sample stations. In each case, the slides were aseptically placed into sterile petri plates for immediate transport to a field laboratory. At the same time, water samples were collected with 4.0-liter acid-leached and autoclaved polypropylene bottles. All samples were prepared for analysis within an hour of being collected.

Enumeration of bacteria. Sterile scalpels were used to cut three 1.0-cm^2 samples from the test and control strips. Of these specimens, two were retained for metal analyses and electron microscopy; the remaining squares were transferred directly into sterile tubes containing 4.0 ml of M-9 salts (GIBCO) adjusted to pH 5.0 or 7.0 for the acidic and neutral pH stations, respectively. A combination of mechanical disruption with a sterile stainless steel spatula, homogenization in a water bath sonicator, and vortexing was used to disperse attached bacteria. By phase microscopy, we could not see any bacteria remaining attached to the support strips. After serial dilution of each suspension in M-9 salts, plates were prepared in duplicate with minimal medium (M-9 salts supplemented with 1.0% [wt/vol] glucose and 0.5% [wt/vol] yeast extract) adjusted to the appropriate pH level. Dilutions of each water sample were also prepared to enumerate planktonic bacteria. After incubation at 20°C for 3 weeks, all plates with fewer than 300 colonies were counted to estimate viable heterotrophic bacterial population density values. In addition, Gram stains of cells from individual colonies were made to determine the distribution of attached or planktonic gram-positive and gram-negative bacteria.

Metal analyses. Specimens from both control and test strips were placed into 30-ml acid-leached polypropylene bottles containing 1.0 ml of 2.0% (vol/vol) HNO_3 (Fisher). Each square was leached for 2 weeks at 20°C before dilution to 10.0 ml with high-resistance (ca. 5 MΩ/cm) deionized distilled water. Water samples were also transferred to polypropylene bottles and acidified with nitric acid to a final concentration of 0.2% (vol/vol). A Perkin-Elmer model 2280 atomic absorption spectrometer operating in the graphite furnance mode was used to determine sample concentrations of Mn, Fe, Co, Ni, and Cu. The instrument was routinely calibrated with corresponding J. T. Baker metal standards.

Data analysis. Biofilm metal adsorption isotherms were graphically constructed by using an empirically derived version of the James-Healy model for metallic ion interactions at solid-liquid interfaces (24). The original equation takes the form of a Freundlich isotherm and relates metal adsorption to electrostatic surface potential. Under conditions of constant ionic strength, surface potential varies directly with charge density which, in a biofilm, should be proportional to the number of attached cells. If ionic strength is assumed to be constant, a logarithmic relationship between biofilm metal adsorption and population density can be established; $\log \Gamma_i = 1/\theta_i \log[\mathrm{CFU}] - pX_i$, where Γ_i is micromoles of metal i bound per cm^2, θ_i is an index of the adsorption strength, [CFU] is CFU per cm^2 (an estimate of the total number of attached cells), and X_i is a conditional adsorption capacity constant expressed as micromoles of metal i adsorbed per CFU. The biofilm metal adsorption data were fit to this equation by linear least-squares regression analysis.

Electron microscopy. Thin wedges cut from the specimen squares were transferred to polypropylene tubes containing 1.0% (vol/vol) glutaraldehyde (CanEM) in water from the corresponding sample stations. In this way, the attached microorganisms were fixed for electron microscopy under conditions similar to those experienced in situ. The samples were subsequently dehydrated through an ethanol-propylene oxide series (both chemicals were from Fisher) and embedded in Epon 812 (CanEM). A Reichert-Jung Ultracut E ultramicrotome was then used to cut sections of ca. 150-nm thickness perpendicular to the wedge surfaces. Duplicate sets of thin sections were prepared from each specimen and mounted on Formvar carbon-coated copper or aluminum grids; one of the grids was routinely stained with uranyl acetate and lead citrate. The unstained grids were imaged directly in the electron microscope relying on the metals complexed in the native environment for electron contrast.

The thin-sectioned specimens were examined with either a Philips EM 300 at 60 kV or a Philips EM 400T at 100 kV. The EM 400T was equipped with a scanning transmission electron microscope unit, goniometer stage, and an EDAX energy-dispersive X-ray spectrometer interfaced to a Tracor Northern series 5500 multichannel analyzer. Both electron microscopes were operated with liquid nitrogen-cooled anticontamination devices in place at all times. Energy dispersive X-ray spectroscopy was conducted by using electron beam spot sizes of 200 nm or less, and spectra were obtained by collecting counts for 100 s (live time). In some samples, selected area electron diffraction was used to examine mineral precipitates. The *d*-spacing of selected-area electron diffraction patterns was calculated with evaporated aluminum as a standard for camera-length calibrations.

RESULTS

Biofilm growth. The planktonic and adherent heterotrophic bacterial population density values for each sample station are plotted in Fig. 2. At each site, there was a significant but variable increase in cell counts over the study period. In contrast, bacteria were not detected on any of the control support strips (i.e., those covered with 0.22-μm-pore nylon filters) until week 11. The numbers of bacteria on the controls at that time and after the last sampling were 10- to 100-fold lower than corresponding values from the freely exposed test strips (data not shown).

Of the four sample stations, acidic site A1 in Cranberry Lake (Fig. 2C) had the highest initial counts of both planktonic and attached bacteria. This observation suggests that the concentration of free-living bacteria plays an important role in determining the initial rate of microbial surface colonization. After week 1, however, the growth rates of the attached bacterial populations appeared to be independent of their planktonic counterparts. The curves for the adherent bacteria were generally hyperbolic as expected for systems controlled primarily by cellular adsorption and growth, coupled with a concomitant emigration of daughter cells (6, 27). In contrast, the free-living bacteria exhibited sinusoidal population curves which are more characteristic of microbial population responses to seasonal warming.

The general pattern of biofilm growth was the same for the two neutral pH sites (Fig. 2, A and B). After a rapid increase in cell numbers over the first 5 weeks, the biofilm growth rate decreased progressively until the last sampling when a population density of 2.0×10^6 CFU/cm^2 was recorded. Similarly, the numbers of attached bacteria at the acidic stations increased in parallel with one another (Fig. 2, C and D). However, a marked decrease in growth rate was observed after week 5, with final population density values reaching levels of only 4.0×10^3 CFU/cm^2. The lower numbers of attached bacteria found at the acidic sites suggest that attachment and growth are stressed by low pH levels and possibly by high dissolved metal concentrations.

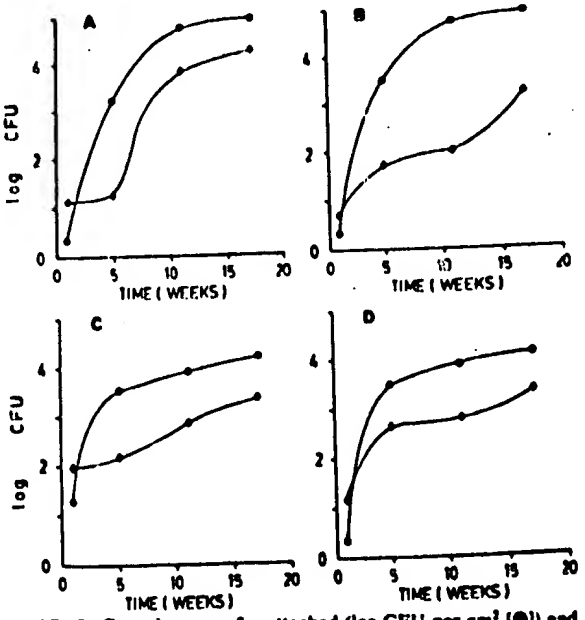

FIG. 2. Growth curves for attached (log CFU per cm^2 [●]) and planktonic heterotrophic bacteria (log CFU per milliliter [◆]) at neutral pH sites N1 (A) and N2 (B) and at acidic sites A1 (C) and A2 (D).

Direct examination of all biofilms by phase-contrast light microscopy revealed small ocherous precipitates (>1.0 μm in diameter) and some remnants of diatom frustules. Distinct bacteria were difficult to directly image against the background of the epoxy-impregnated strips. At the neutral pH stations, filamentous cyanobacteria were occasionally observed with rarely more than a single filament present in one field of view. Eucaryotic algae were not observed in these samples; however, small motile unicellular algae (possibly *Chlamydomonas* species) were found on some samples from the acidic sites. Periphytic grazing protozoans were not encountered on any of the biofilm strips. Gram stains of cells from individual bacterial colonies randomly selected from the dilution plates from each site throughout the season (both in the water and on the biofilm strips) revealed that gram-negative bacteria accounted for 75 to 80% of the bacteria.

Metal retention. The mean aqueous metal concentration values for each sample station over the 17-week study period

TABLE 1. Mean aqueous metal concentrations for the sample stations over the 17-week study period

Station	Mean concentration ± SD (μg/ml [ppm])[a] of:				
	Mn	Fe	Co	Ni	Cu
N1	0.65 ± 0.14	2.71 ± 0.67	0.08 ± 0.02	2.10 ± 0.30	0.02 ± 0.01
N2	0.52 ± 0.16	12.56 ± 5.41	0.05 ± 0.04	2.08 ± 0.46	0.02 ± 0.01
A1	1.64 ± 0.02	37.23 ± 15.81	0.29 ± 0.11	5.57 ± 0.72	0.21 ± 0.11
A2	3.57 ± 0.60	62.50 ± 22.62	5.76 ± 2.76	62.92 ± 30.87	1.74 ± 0.65

[a] Figures represent an average of at least five determinations for each sample plus or minus the standard deviation of the mean (ppm, parts per million).

TABLE 2. Amount of metal adsorbed by control surfaces and biofilms after 17 weeks of in situ incubation

Sample[a]	Mean amt ± SD of indicated metal adsorbed (μg/cm²)[b]				
	Mn	Fe	Co	Ni	Cu
N1-C	0.15 ± 0.01	269.50 ± 29.90	0.05 ± 0.01	0.26 ± 0.04	0.09 ± 0.03
N1-B	0.17 ± 0.04	3,145.00 ± 198.06	0.05 ± 0.02	1.98 ± 0.01	0.81 ± 0.10
N2-C	0.06 ± 0.02	238.50 ± 29.05	0.07 ± 0.02	0.24 ± 0.09	0.23 ± 0.01
N2-B	20.09 ± 0.10	11,596.00 ± 238.45	0.25 ± 0.17	11.52 ± 0.36	2.18 ± 0.13
A1-C	0.06 ± 0.03	48.60 ± 9.30	0.01 ± 0.01	0.14 ± 0.03	0.01 ± 0.01
A1-B	0.18 ± 0.01	994.40 ± 137.09	NB[c]	0.07 ± 0.02	0.16 ± 0.04
A2-C	0.09 ± 0.02	9.55 ± 1.65	0.03 ± 0.01	0.18 ± 0.05	0.06 ± 0.01
A2-B	0.10 ± 0.02	50.00 ± 21.25	NB	0.69 ± 0.31	0.09 ± 0.02

[a] C, Control surface; B, biofilm.
[b] Figures represent an average of at least five determinations for each sample plus or minus the standard deviation of the mean. The biofilm values are expressed in terms of metal adsorbed in excess of the corresponding control surface.
[c] NB, Not bound.

are summarized in Table 1. Iron was the most abundant metal species at all sites, accounting for up to 83 mol% of the five assayed transition metals. Consecutively lower levels of nickel, manganese, cobalt, and copper were recorded, with a 3- to 100-fold concentration decrease for all metals in the circumneutral pH system. Of the two acidic sites, station A2 had the highest aqueous metal concentrations. This reflects the small size, upstream location, and limited dilution of Fraser Pond by casual runoff. In contrast, similar concentrations of manganese, cobalt, nickel, and copper were found at both neutral pH stations. However, approximately four times more iron was found at site N2. Since Lower Moose Lake tends to become partially meromictic during the summer months, site N2 was probably situated in or near an upwelling current of iron-rich anoxic water from the chemocline.

The biofilms bound each metal species, with the exception of cobalt under acidic conditions, in excess of the amounts adsorbed by the corresponding control surfaces (Table 2). Metal adsorption was enhanced at neutral pH values, particularly at site N2 where a thick (ca. 1.0-mm) coating of iron-oxide precipitates developed throughout the biofilms. Such ocherous deposits were not evident on the control strips and formed only thin biofilm-associated accretions at the other sample stations.

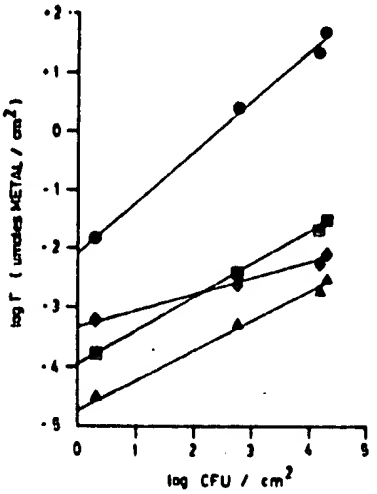

FIG. 3. Biofilm metal adsorption isotherms for Mn (▲), Fe (●), Ni (◆), and Cu (■) under neutral pH conditions at site N1.

A set of metal adsorption isotherms for the biofilms at site N1 are shown in Fig. 3. Similar plots were obtained with data from the other sample stations. In each case, regression analysis yielded straight lines with correlation coefficients of 0.98 to 0.99. These Freundlich-type isotherms provided estimates of the conditional metal-binding capacity constants (X_i) for the biofilms and an index of adsorption strength (θ_i) for each metal species (Table 3). The lower pX_i values at stations N1 and N2 show that biofilm metal adsorption was enhanced by up to 12 orders of magnitude over the two acidic sites. Also, the adsorption strength values associated with the metals were usually higher at elevated pH levels; iron was the only exception and exhibited similar θ_i values at all sites. These trends indicate that microbial biofilms are more efficient scavengers of metals under neutral pH conditions.

Biofilm mineralization. Microcolonies of encapsulated bacteria were commonly found in stained thin sections of the biofilms (Fig. 4). The extracellular polymeric material surrounding the cells typically exhibited a fibrous structure and often contained an abundance of iron-rich precipitates. In specimens from the two neutral pH stations, these deposits were distinguished by a granular appearance, whereas clumps of acicular crystalloids developed under acidic conditions (compare Fig. 4A and 4B). Both types of mineralization generated diffuse prismatic diffraction bands, with characteristic reflections for ferrihydrite ($Fe_2O_3 \cdot nH_2O$) centered on d equaling 0.25 and 0.15 nm. However, energy-dispersive X-ray spectroscopic analyses revealed distinct differences in trace element composition between the two

TABLE 3. Biofilm metal adsorption capacity constants and adsorption strength values

Metal	Values found in station:							
	N1		N2		A1		A2	
	θ_i	pX_i	θ_i	pX_i	θ_i	pX_i	θ_i	pX_i
Mn	2.04	4.71	1.47	3.21	0.25	17.08	0.32	13.85
Fe	1.16	2.09	1.08	1.63	1.06	2.39	1.28	3.23
Co	0.96	7.66	0.80	7.87	NB[a]	NB	NB	NB
Ni	1.82	3.98	1.41	4.08	0.63	8.34	0.75	6.67
Cu	2.24	3.31	2.08	3.58	0.42	11.38	0.58	9.09

[a] NB, Not bound.

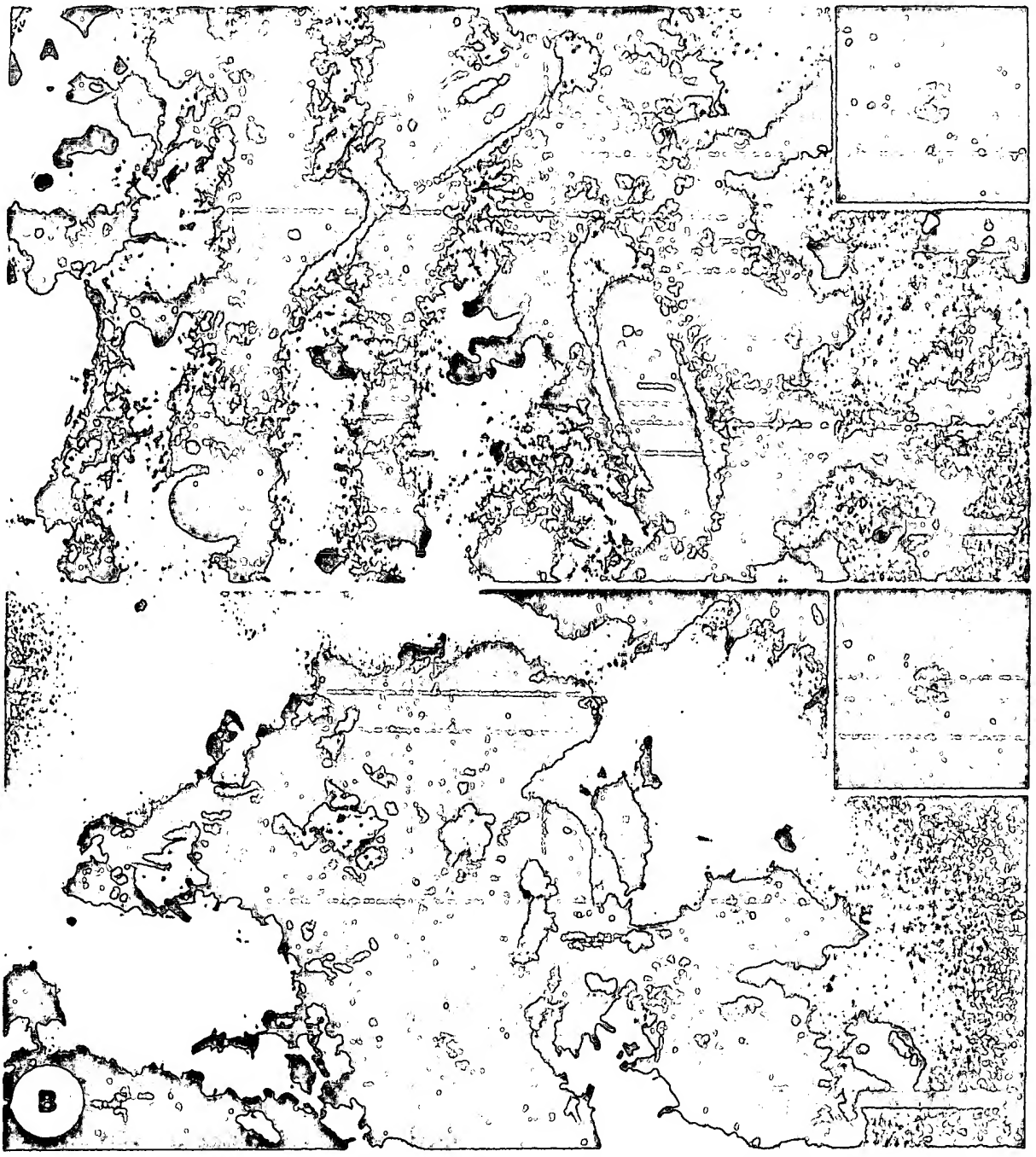

FIG. 4. Transmission electron micrographs of stained thin sections showing mineralized bacterial microcolonies in biofilms from sample stations N2 (A) and A1 (B). Insets show corresponding selected area electron diffraction patterns for the ferrihydrite precipitates (bars, 500 nm).

types of ferrihydrite precipitates (Fig. 5). Th se which formed at neutral pH values contained Al, Si, and Cl as minor indigenous element impurities, whereas S was incorporated under acidic conditions.

The direct examination f unstained specimens provided electron-scattering profiles f microcolonies in early stages of mineralization. In these micrographs, individual cells typically appeared as ghosts enmeshed in an electron opaque matrix containing small crystallites (Fig. 6A). Energy-dispersive X-ray spectroscopy showed that iron was the principle source of contrast inherent to these specimens. Furthermore, a close association between the fibrous capsular

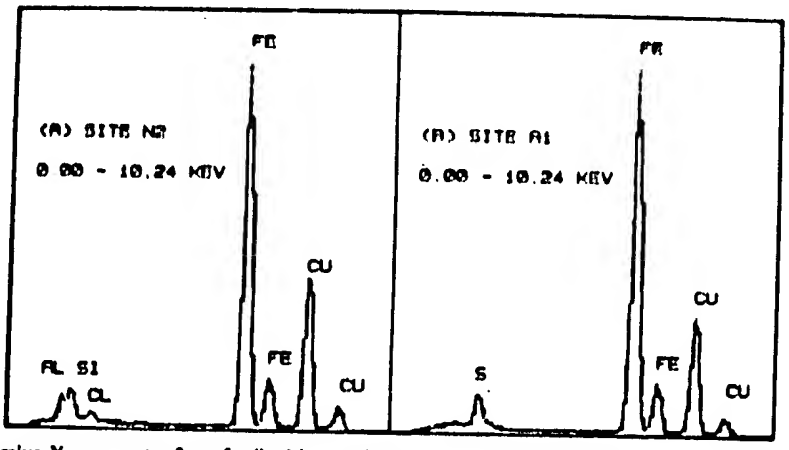

FIG. 5. Energy-dispersive X-ray spectra from ferrihydrite precipitates associated with biofilms at sites N2 (A) and A1 (B). Fe (Kα and Kβ), Al, Si, Cl and S peaks are from the specimens; Cu (Kα and Kβ) peaks are from the supporting grids.

polymers surrounding the bacteria and the nascent ferrihydrite precipitates could be discerned after staining (Fig. 6B). This confirmed that the attached bacteria served directly as nucleation sites for the precipitation of iron.

DISCUSSION

The plate counts for attached and planktonic heterotrophic bacteria were generally similar to those obtained in other aquatic environments stressed by metal-laden acid mine drainage (29, 40). Extremely low pH conditions, in particular, are known to adversely affect microbial metabolic activities and growth rates (34). This accounts for the relatively poor response to seasonal warming of suspended bacteria at the two immediately impacted sites in Fraser Pond and Cranberry Lake. Evidence of acid-induced stress is also seen in comparisons of the biofilm communities. The attached bacterial populations in the circumneutral pH systems demonstrated significantly higher rates of growth over the last 12 weeks of the investigation as expected for a more vigorous guild of microorganisms.

A number of recent studies suggest that the initial colonization of submerged surfaces of microorganisms is dominated by the simultaneous attachment and growth of individual planktonic cells (6, 27). This effectively supports a rapid onset of population growth, particularly when the concentration of free-living cells is high (cf. Fig. 2A through 2D). However, as the density of attached cells increases and surface area becomes limiting (i.e., fewer attachment sites), the attachment rate is greatly reduced (6). At the same time, emigration of cells from larger unstable microcolonies occurs with increasing frequency (27). The later stages of microbial surface colonization are therefore characterized by progressively slower rates of population growth. These observations explain the overall pattern of biofilm formation at each of our four sample stations.

The differences in biofilm metal adsorption between the neutral and acidic pH sites can be attributed partly to variations in population density. However, reactions between metallic ions and polymeric organic substrates are strongly influenced by pH level (39). This solution property determines the extent to which protons dissociate from reactive acidic groups and effectively controls surface charge density (24). At a low pH level, the availability of negatively charged sites such as carboxylates and phosphates is greatly reduced so fewer metal cations are adsorbed. Conversely, metallic ion adsorption is usually enhanced under neutral pH conditions by a proportional increase in the number of ionized acidic groups. These effects are reflected in the total amounts of metal bound by the biofilms (Table 2) and the corresponding pX_i values (Table 3).

The reduction of surface charge density with decreasing pH levels also serves to weaken electrostatic free energy contributions to metallic ion adsorption (24). This accounts for the observed trend towards lower (or unmeasurable in the case of cobalt) θ_i values for manganese, nickel, and copper at the two acidic sites. However, electrostatic interactions may additionally be weakened through the partial hydrolysis of a metal cation. The adsorption behavior of iron is explained by this later process. At elevated pH levels, cationic colloidal elements [i.e., $Fe(OH)^{2+} \cdot 5H_2O$ or $Fe(OH)^{+} \cdot 4H_2O$] tend to form via the hydrolysis of ferric iron (9). This probably caused a decrease in the overall strength of adsorption by counteracting the increase in electrostatic interactions which usually accompany the higher surface charge density expected at neutral pH levels.

Previous studies have demonstrated that bacterial cells are capable of serving as nucleation sites for a wide range of authigenic minerals (4, 13, 14). The ability of bacteria to serve as templates for mineralization depends primarily on the inherent capacity of their anionic surface polymers to bind metallic ions (3, 12). Once immobilized, complexed metals can be precipited at the cell surface by complete hydrolysis, a change in oxidation state, or through reactions with other counter ions in solution (14). The secondary growth of these mineral precipitates may then proceed via homogeneous crystal nucleation reactions (2). A similar series of events starting with the oxidation and hydrolysis of cell-bound ferrous or ferric iron probably accounts for the mineralization which developed in association with the biofilms.

The morphological characteristics of the ferrihydrite mineralization associated with the biofilms correlates well with the trace element composition of the precipitates. Synthesis experiments have shown that the incorporation of silicate or sulfate anions not only suppresses the ordering of ferrihydrite but also hinders the formation of more stable anhydrous iron oxides such as goethite or hematite (1, 5, 8). The

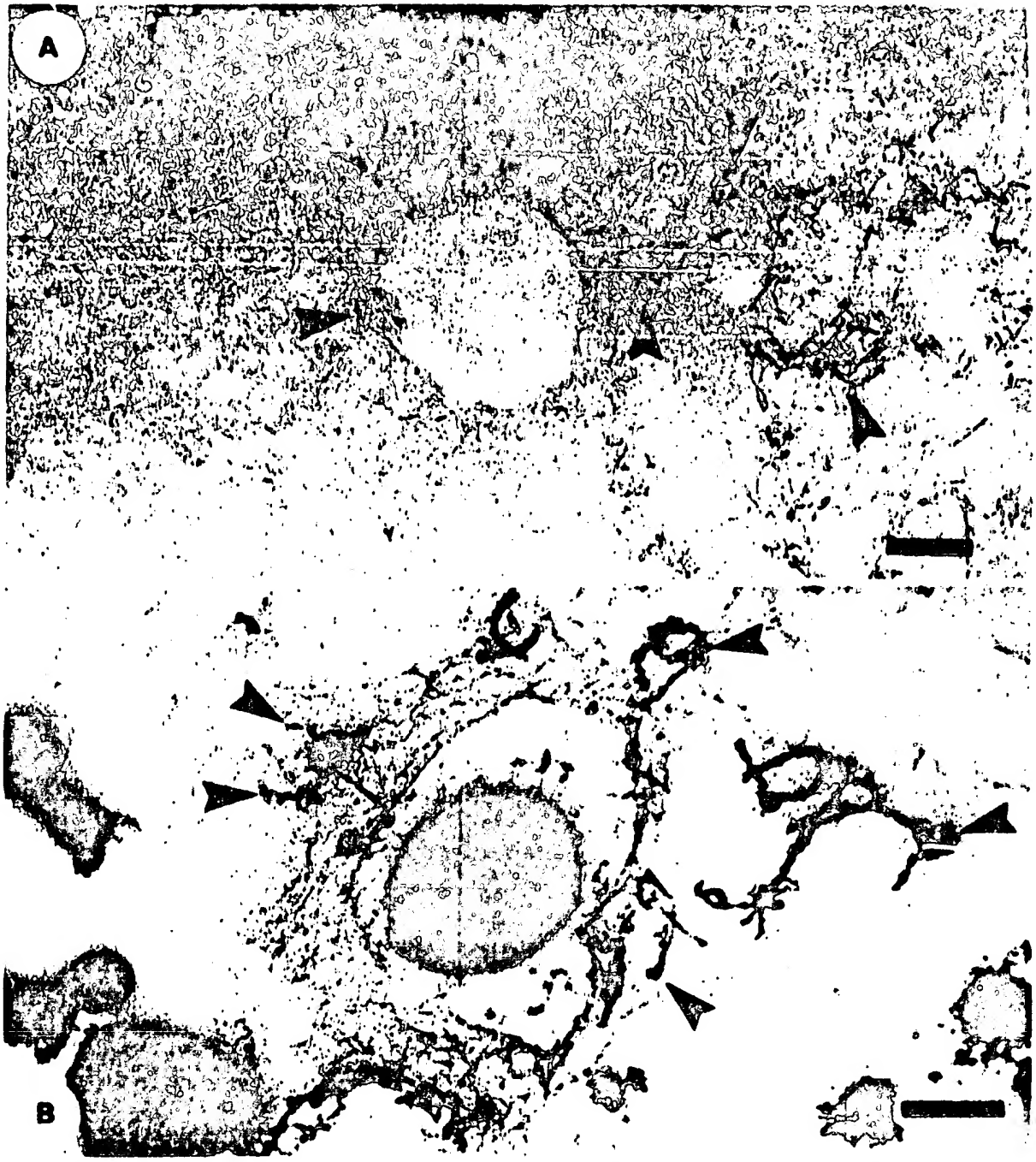

FIG. 6. Thin-section profiles of encapsulated bacteria in unstained (A) and stained (B) biofilm specimens from site N2. Arrows indicate some nascent ferrihydrite precipitates associated with the extracellular polymers of the bacteria (bars, 200 nm).

exact reasons for this are not yet clear. However, the available evidence suggests that negatively charged ions effectively cross-link colloidal particles of ferrihydrite and promote the formation of an unreactive immobile mineral phase (8). In the case of sulfate, this seems to result in the production of fibrous networks of acicular ferrihydrite crystalloids similar to those observed in association with biofilms from the acidic sites (5). However, siliceous ferrihydrites commonly exhibit a more granular morphology reminiscent of the iron precipitates which developed in conjunction with the neutral pH biofilms (7, 8).

This work heightens our awareness of the importance of microbial biofilms as natural metal-immobilizing matrices. Clearly, there are differences between metal affinities and

mineral species produced by the acidic and neutral natural systems reported here; this is presumably a reflection of their different aqueous chemistries and microbial communities. In both cases, metal sorption went well beyond that of the control surfaces. Preliminary data on the the microbiota of the deep subsurface (21) suggest that mineral development on bacterial surfaces may be more widespread than first imagined (Fig. 1 and 2 in reference 21). Given the antiquity of bacteria and the terrestrial depths at which they can reside, microbial metal immobilization and mineralization cannot be a trivial affair (3).

ACKNOWLEDGMENTS

This work was supported by funds from the Ontario Geological Survey, the Natural Sciences and Engineering Research Council (NSERC) of Canada, and Falconbridge Ltd. to T.J.B. and W.S.F. F. G. Ferris was the recipient of an NSERC postdoctoral fellowship, and T. C. Witten received an NSERC summer research assistantship. The EM 400T was purchased with funds from NSERC and is maintained by funds from the University of Guelph and NSERC and by user fees.

We are grateful to Tracor Northern Canada Ltd. for the use of the TN series 5500 on the EM 400T.

LITERATURE CITED

1. **Anderson, P. R., and M. M. Benjamin.** 1985. Effect of silicon on the crystalization and adsorption properties of ferric oxides. Environ. Sci. Technol. 19:1048–1053.
2. **Berner, R. A.** 1980. Early diagenesis: a theoretical approach. Princeton University Press, Lawrenceville, N.J.
3. **Beveridge, T. J., and W. S. Fyfe.** 1985. Metal fixation by bacterial cell walls. Can. J. Earth Sci. 22:1892–1898.
4. **Beveridge, T. J., J. D. Meloche, W. S. Fyfe, and R. G. E. Murray.** 1983. Diagenesis of metals chemically complexed to bacteria: laboratory formation of metal phosphates, sulfides, and organic condensates in artificial sediments. Appl. Environ. Microbiol. 45:1094–1108.
5. **Brady, K. S., J. M. Bigham, W. F. Jaynes, and T. J. Logan.** 1986. Influence of sulfate on Fe-oxide formation: comparisons with a stream receiving acid mine drainage. Clays and Clay Miner. 34:266–274.
6. **Caldwell, D. E., D. K. Brannan, M. E. Morris, and M. R. Betlach.** 1981. Quantitation of microbial growth on surfaces. Microb. Ecol. 7:1–11.
7. **Carlson, L., and U. Schwertmann.** 1981. Natural ferrihydrites in surface deposits from Finland and their association with silica. Geochim. Cosmochim. Acta 45:421–429.
8. **Cornell, R. M., R. Giovanoli, and P. W. Schindler.** 1987. Effect of silicate species on the transformation of ferrihydrite into goethite and hematite in alkaline media. Clays and Clay Miner. 35:21–28.
9. **Cotton, F. A., and G. Wilkinson.** 1972. Advanced inorganic chemistry. John Wiley & Sons, Inc., New York.
10. **Cowen, J. P., and K. W. Bruland.** 1985. Metal deposits associated with bacteria: implications for Fe and Mn marine biogeochemistry. Deep-Sea Res. 32:253–272.
11. **Cowen, J. P., G. J. Massoth, and E. T. Baker.** 1986. Bacterial scavenging of Mn and Fe in a mid- to far-field hydrothermal particle plume. Nature (London) 322:169–171.
12. **Degens, E. T., and V. I. Ittekkot.** 1981. *In situ* metal staining of biological membranes in sediments. Nature (London) 298:262–264.
13. **Ferris, F. G., T. J. Beveridge, and W. S. Fyfe.** 1986. Iron-silica crystallite nucleation by bacteria in a geothermal sediment. Nature (London) 320:609–611.
14. **Ferris, F. G., W. S. Fyfe, and T. J. Beveridge.** 1987. Bacteria as nucleation sites for authigenic minerals in a metal contaminated lake sediment. Chem. Geol. 63:225–232.
15. **Fletcher, M.** 1985. Effect of solid surfaces on the activity of attached bacteria, p. 339–362. *In* D. C. Savage and M. Fletcher (ed.), Bacterial adhesion: mechanisms & physiological significance. Plenum Publishing Corp., New York.
16. **Forstner, U.** 1982. Accumulative phases for heavy metals in limnic sediments. Hydrobiologia 91:269–284.
17. **Geesey, G. G., R. Mutch, J. W. Costerton, and R. B. Green.** 1978. Sessile bacteria: an important component of the microbial population in small mountain streams. Limnol. Oceanogr. 23: 1214–1223.
18. **Geesey, G. G., W. T. Richardson, H. G. Yeomans, R. T. Irvin, and J. W. Costerton.** 1977. Microscopic examination of natural sessile bacterial populations from an alpine stream. Can. J. Microbiol. 23:1733–1736.
19. **Ghiorse, W. C.** 1984. Biology of iron and manganese depositing bacteria. Annu. Rev. Microbiol. 38:515–550.
20. **Ghiorse, W. C.** 1986. Applicability of ferromanganese—depositing microorganisms to industrial metal recovery processes, p. 141–148. *In* H. L. Erlich and D. S. Holmes (ed.), Workshop on biotechnology for the mining, metal-refining and fossil fuel processing industries. John Wiley & Sons, Inc., New York.
21. **Ghiorse, W. C., and J. T. Wilson.** 1988. Microbial ecology of the terrestrial subsurface. Adv. Appl. Microbiol. 33:107–172.
22. **Huljev, D. J.** 1986. Interaction of some metals between marine-origin humic acids and aqueous solutions. Environ. Res. 40: 470–478.
23. **Hunter, K. A., and P. S. Liss.** 1979. The surface charge of suspended particles in estuarine and coastal waters. Nature (London) 282:823–825.
24. **James, R. O., and T. W. Healy.** 1972. Adsorption of hydrolyzable metal ions at the oxide-water interface. III. A thermodynamic model of adsorption. J. Colloid Interface Sci. 40:65–81.
25. **Jardim, W. F., and H. W. Pearson.** 1984. A study of the copper-complexing compounds released by some species of cyanobacteria. Water Res. 18:985–989.
26. **Kerndorf, H., and M. Schnitzer.** 1980. Sorption of metals on humic acid. Geochim. Cosmochim. Acta 44:1701–1708.
27. **Lawrence, J. R., P. J. Delaquis, D. R. Korber, and D. E. Caldwell.** 1987. Behavior of *Pseudomonas fluorescens* within the hydrodynamic boundry layers of surface microenvironments. Microb. Ecol. 14:1–14.
28. **Mann, H., and W. S. Fyfe.** 1985. Algal uptake of U and some other metals: implications for global geochemical cycling. Precambrian Res. 30:337–349.
29. **Mills, A. L., and L. M. Mallory.** 1987. The community structure of sessile heterotrophic bacteria stressed by acid mine drainage. Microb Ecol. 14:219–232.
30. **Mills, A. L., and R. Maubrey.** 1981. Effect of mineral substrate composition on bacterial attachment to submerged rock surfaces. Microb Ecol. 7:315–322.
31. **Millward, G. E., and R. M. Moore.** 1982. The adsorption of Cu, Mn and Zn by iron oxyhydrate in model estuarine solution. Water Res. 16:981–985.
32. **Mittelman, M. W., and G. G. Geesey.** 1985. Copper-binding characteristics of exopolymers from a freshwater-sediment bacterium. Appl. Environ. Microbiol. 49:846–851.
33. **Nissenbaum, A., and D. J. Swaine.** 1976. Organic matter-metal interactions in recent sediments: the role of humic substances. Geochim. Cosmochim. Acta 40:809–816.
34. **Palumbo, A. V., M. A. Boyle, R. R. Turner, J. W. Elwood, and P. J. Mulholland.** 1987. Bacterial communities in acidic and circumneutral streams. Appl. Environ. Microbiol. 53:337–344.
35. **Reid, J. D., and B. McDuffie.** 1981. Sorption of trace cadmium on clay minerals and river sediments: effects of pH and Cd (II) concentrations in a synthetic river water medium. Water Air Soil Pollut. 15:375–386.
36. **Reuter, J. H., and E. M. Perdue.** 1977. The importance of heavy metal-organic interactions in natural water. Geochim. Cosmochim. Acta 41:325–334.
37. **Rudd, T., R. M. Sterritt, and J. N. Lester.** 1984. Formation and

conditional stability constants of complexes formed between heavy metals and bacterial extracellular polymers. Water Res. 18:379–384.
38. Schoer, J. 1985. Iron-oxo-hydroxides and their significance to the behavior of heavy metals in estuaries. Environ. Technol. Lett. 6:189–202.
39. Stumm, W., and J. J. Morgan. 1981. Aquatic chemistry. John Wiley & Sons, Inc., New York.
40. Wassel, R. A., and A. L. Mills. 1983. Changes in water and sediment bacterial community structure in a lake receiving acid mine drainage. Microb. Ecol. 9:155–169.
41. Weise, W., and G. Rheinheimer. 1978. Scanning electron microscopy and epifluorescence investigation of bacterial colonization of marine sand sediments. Microb. Ecol. 4:175–188.

STIC-ILL

10/9/10

41670

From: Marx, Irene
Sent: Tuesday, September 10, 2002 9:19 AM
To: STIC-ILL
Subject: 09/777664

Importance: High

Please send to Irene Marx, Art Unit 1651; CM1, Room 10E05, phone 308-2922, Mail box in 11B01

Observations on the ionic composition of blue-green algae growing in saline lagoons
AU Pillai, V. K.
SO Proc. Natl. Inst. Sci. India, (19550000) vol. 21, no. 2, pp. 90-102.
DT Journal

Dalrymple, D.W., 1965, "Calcium carbonate deposition associated with blue green algal mats, Baffin Bay.:, Texas: Institute of Marine Science Publication 10, p. 187-200

Black, M., 1933, "The algal sedimentation... ", Royal Society of London Philosphical transactions, Ser. B, V. 222, p. 165-192

Lowenstam HA (1981), Science, 211:1126-1131

Ferris et al., Earth Sci., 47:233-250 (1993)

Ferris et al., Appl. and Environm. Microbiol.,1989, 55:1249-1257

Kazmierczak et al., (1990), Science, 250:1244-1248

Kempe et al., Facies, 28:1-32, 1993.

Kempe et al., 1994, Bull, Inst. Oceanogr., Monaco no. spec., 13:61-117.

Merz, M.U.E, 1992, Facies, 26:81-102

Pentecost et al., 1986, Calcification in cyanobacteria, In "Biomineralization of Lower plants and animals (Leadbeater et a., ed. 73-90, Clarendon Press, Oxford.

Riding, R., 1982, Nature, 299:814-815

Thompson eta., 1990, Geology, 18:995-998

Irene Marx
Art Unit 1651
CMI 10-E-05,
Mail Box 11-B-01
703-308-2922

THE BRITISH LIBRARY D.S.C. FAX TRANSMISSION IN RESPONSE TO A COPYRIGHT FEE PAID REQUEST

COPYRIGHT: OUR LICENCE EFFECTIVELY RESTRICTS FAX TO PAPER TO PAPER DELIVERY. VIEWING THIS DOCUMENT ON A SCREEN OR CONTINUING TO STORE IT ELECTRONICALLY AFTER THE RECEIPT OF A SATISFACTORY PAPER COPY, IS NOT PERMITTED.

This document has been supplied by
The British Library Document Supply Centre,
on behalf of
Chemical Abstracts Service.
Warning: further copying of this document
(including storage in any medium by electronic means),
other than that allowed under the copyright law, is not
permitted without the permission of the copyright
owner or an authorised licensing body.

CAS Document Detective Service
2540 Olentangy River Road
P.O. Box 3012
Columbus, OH 43210-0012

Cyanobacterial precipitation of gypsum, calcite, and magnesite from natural alkaline lake water

J. B. Thompson*
Department of Geology, Syracuse University, Syracuse, New York 13244

F. G. Ferris*
Department of Geology, University of Western Ontario, London, Ontario N6A 5B7, Canada

ABSTRACT

Results from transmission electron microscopy provide direct evidence for cyanobacterial biomineralization of gypsum and calcite in aquatic environments. Laboratory simulations using filter-sterilized natural lake water inoculated with *Synechococcus* sp., isolated from Fayetteville Green Lake, New York, revealed epicellular biomineralization of gypsum, calcite, and magnesite. Experimental, electron microscopical, and sedimentological evidence indicates that *Synechococcus* is responsible for a major proportion of the marl sediment and carbonate bioherms in Green Lake. The elucidated role of *Synechococcus* in biomineralization and its ubiquitous distribution in nature have widespread implications for cyanobacterial mineralization in marine and freshwater environments since late Archean time.

INTRODUCTION

The role of bacteria and cyanobacteria in large-scale precipitation of calcium carbonate in natural aquatic environments has long been a subject of controversy (Lane, 1903; Hale, 1903; Drew, 1911, 1913; Pollock, 1918; Black, 1933; Greenfield, 1963; McCallum and Guhathakurta, 1970; Krumbein, 1974, 1979; Morita, 1980; Novitsky, 1981). Although microorganisms have been linked to calcification (Drew, 1911; Krumbein, 1974; Morita, 1980; Pentecost, 1985; Pentecost and Bauld, 1988), direct experimental evidence for microbial calcification in natural waters is lacking. The best direct evidence for microbial calcification has come from transmission electron microscopy (TEM) studies of bacteria from the human oral cavity (dental calculi) and urinary tract (kidney stones) (Ennever, 1963; Ennever and Takazoe, 1973; McLean et al., 1985; Nickel et al., 1987). We present experimental data for the direct natural biomineralization of gypsum, calcite, and magnesite by a small unicellular coccoid cyanobacterium of the genus *Synechococcus*.

METHODS

To experimentally investigate the role of these small cyanobacteria (picoplankton, 0.2–2.0 μm) in calcite precipitation in nature we isolated a pure culture of *Synechococcus* sp. from Fayetteville Green Lake, New York (Fig. 1A). *Synechococcus* sp. was isolated from Green Lake using serial dilutions of homogenized active carbonate bioherm (thrombolite; Thompson et al., 1990) material on BG-11 (a commonly used cyanobacterial growth medium) agar. This *Synechococcus* isolate is taken to represent the same numerous "rounded or oval, very small cells" (Davis, *in* Walcott, 1914, p. 88) entombed within the calcite grains from Green Lake (Fig. 1B; Bradley, 1929, 1963; Howe, 1932).

Figure 1. A: Phase contrast photomicrograph of *Synechococcus* sp. isolated from Fayetteville Green Lake and used in laboratory simulations. B: Petrographic thin-section photomicrograph of calcite crystal from Green Lake showing evidence for occlusions of numerous small bacterial cells within calcite grain (arrows). Note similar size of *Synechococcus* cells in A and occluded bacterial cells in B (scale bars = 5 μm).

To test the calcite-forming capabilities of our isolate in natural alkaline waters we inoculated test tubes with 9.0 ml of cold filter-sterilized (0.22 μm nylon filters) Green Lake water with 1.0 ml of standard suspension of *Synechococcus* containing 10^3 colony-forming units per milliliter. The cultures were incubated under fluorescent light (24 h/day) at 20 °C for periods of up to 72 h. At sampling times of 4, 24, 48, and 72 h, a test tube was removed for experimental analysis. The cells and/or precipitates were harvested by centrifugation and initially analyzed using whole-mount preparations in the TEM. The remaining material was fixed in 1% glutaraldehyde and embedded in an epoxy resin for thin sectioning and detailed electron microscopy. All whole mounts and thin sections were examined using a Philips EM300 or a Philips EM400T equipped with an energy dispersive X-ray spectrometer (EDS). The supernatant was analyzed for changes in water chemistry, including pH, Ca^{2+}, Mg^{2+}, and SO_4^{2-}. Calcium and magnesium concentrations were determined via inductive coupled plasma emission spectroscopy, and sulfate concentrations were determined by liquid chromatography. Alkalinity was determined from acid titration to a pH 4.30 end point. Ion-activity coefficients were calculated using the extended Debye-Hückel equation. Apparent dissociation constants for carbonic acid were calculated using the Güntelberg approximation and saturation indices according to $SI = \log IAP/K_{sp}$, where SI = saturation index, IAP = ion activity product, and K_{sp} = solubility product. Ionic strength was calculated according to Stumm and Morgan (1981), and pH was measured using standard combination electrodes and National Bureau of Standards buffers. Controls consisted of test tubes with no inoculum, inoculated tubes kept in constant darkness, and tubes containing only bacterial (*Bacillus subtilis*) cell walls.

RESULTS

Surface waters in this marl-rich lake are alkaline and rich in calcium, magnesium, and sulfate derived from the surrounding Silurian bedrock (Table 1). TEM results of the experimental time course indicate a progressive biomineralization

*Present addresses: Thompson, Department of Microbiology, University of Guelph, Guelph, Ontario N1G 2W1, Canada; Ferris, Bioscience Group, NOVA HUSKY Research Corporation, Calgary, Alberta T2E 7K7, Canada.

of gypsum, calcite, and magnesite from the lake water. Epicellular biomineralization of gypsum on the cell wall of *Synechococcus* occurred within 4 h (Fig. 2). Epicellular calcite precipitation was first recognized after 24 h had elapsed.

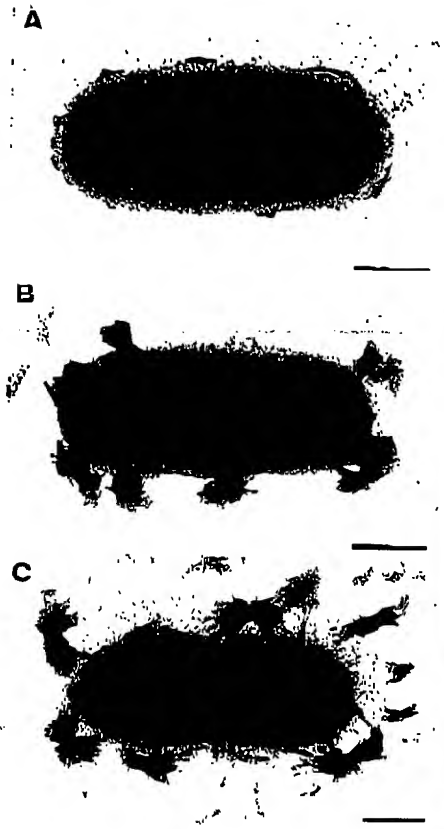

Figure 2. Series of transmission electron micrographs showing progression of gypsum precipitation on cell wall of *Synechococcus* (whole mounts). A: Initiation of numerous nucleation sites on cell surface. B: Gypsum precipitation spreading away from cell. Gypsum still appears to be covered by thin layer of bacterial slime. C: Dividing *Synechococcus* cell shedding some of precipitated gypsum (scale bars = 500 nm).

Epicellular calcite precipitation was more massive and disruptive to the *Synechococcus* cells than the fibrous gypsum precipitation (Figs. 2 and 3). Calcification directly coincided with a small increase in pH that occurred between the 4 and 24 h sampling periods (Table 2). The photosynthetic metabolism of *Synechococcus* was directly responsible for the alkalinization of the experimental microenvironment, because the pH did not increase in any of the control samples.

Measured changes in water chemistry from the simulations were consistent with the biomineralization inferred from TEM (Table 2). Calcium concentration decreased throughout the entire experiment, coinciding with the precipitation of $CaSO_4$ and $CaCO_3$. Magnesium concentration was unaltered during the 72 h, although electron microscopic results obtained at 72 h suggest the possible precipitation of magnesite as the pH continued to increase. Sulfate concentrations decreased during the first 48 h, but showed a slight increase thereafter. Carbonate-ion concentration increased after 4 h due to the corresponding increase in pH (Table 2). Precipitation of gypsum and calcite was verified by EDS and electron diffraction, whereas the magnesite precipitation was suggested by a single strong magnesium peak using EDS. We may have recognized some hydrated form of magnesium carbonate. No precipitation or alkalinization was evident in the sterile controls or in the controls containing only bacterial cell walls. No calcite precipitation or alkalinization took place in inoculated controls kept in the dark, which indicates that calcite precipitation was directly related to photosynthesis by *Synechococcus*. Gypsum was observed in the dark controls and therefore its formation appears to be unrelated to the *Synechococcus* photosynthetic alkalinization process. Sterile controls elevated to an equivalent pH (8.5; Table 2) by adding base (NaOH) also did not precipitate calcite.

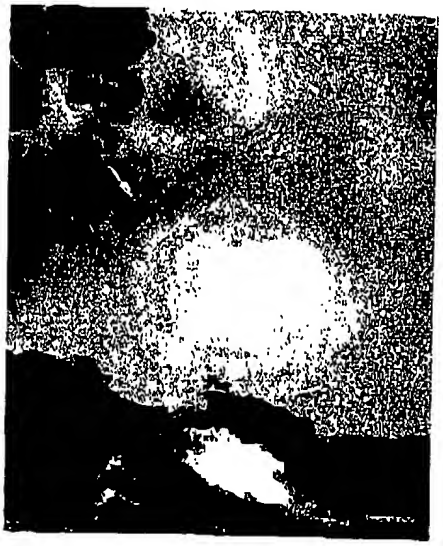

Figure 3. Thin-section transmission electron micrograph of two *Synechococcus* cells and calcite from 72 h culture (cell is represented by white oval area between arrows). Arrows point to calcite (electron dense material) on cell surface. Cells are unstained due to dissolution of calcite by acidic heavy-metal stains used to provide contrast to biological specimens (scale bar = 200 nm).

Mineral saturation indices, calculated from the experimental results in Table 2, also agree with the observed mineralization trends (Fig. 4). Initially the lake water was slightly oversaturated with gypsum (SI = 1.16) and calcite (SI = 2.73). Photosynthetic alkalinization by *Synechococcus* perturbed water chemistry by increasing conditions of oversaturation with respect to calcite solubility (Fig. 4A). Within 24 to 48 h the calcification process had reduced Ca^{2+} activity to the condition that solutions were no longer oversaturated with respect to gypsum solubility. Experimental evidence indicates that some gypsum may have redissolved as the system became undersaturated with respect to gypsum solubility after 48 h; this is shown by the increasing sulfate concentration recorded at 72 h (Table 2). The experimental system was oversaturated with respect to magnesite solubility after approximately 72 h (Fig. 4B). Magnesite was found to be associated with large *Synechococcus* aggregates. The pH associated with large

TABLE 1. CHEMISTRY OF FAYETTEVILLE GREEN LAKE WATER

Date/depth	Ca^{2+}	Mg^{2+}	SO_4^{2-}	Alkalinity	Ionic strength	pH
	(millimoles/liter)					
9-15-1988 (5 m)	11.39	2.67	9.30	3.20	55.20	7.97
12-16-1966* (10 m)	10.48	2.96	11.66	3.28	53.00†	7.94†

*Data from Brunskill and Ludlam (1969).
†Data from Brunskill (1969).

TABLE 2. CHEMICAL ANALYSIS OF EXPERIMENTAL TIME COURSE

Hours	Ca^{2+} (mmol/L)	Mg^{2+} (mmol/L)	SO_4^{2-} (mmol/L)	CO_3^{2-} (mmol/L)	pH
0	11.39	2.67	9.30	$10^{-3.36}$	7.97
4	11.28	2.67	8.81	$10^{-3.35}$	7.97
24	11.20	2.67	8.34	$10^{-4.73}$	8.28
48	10.19	2.61	8.27	$10^{-4.01}$	8.34
72	9.37	2.65	8.38	$10^{-4.15}$	8.57

cell aggregates was possibly higher than the experimentally recorded pH (Table 2), resulting in magnesite precipitation (Fig. 4B).

Subsequent analysis of the actively growing portion of the natural bioherm in Green Lake and filters used in filtering Green Lake water revealed the presence of gypsum in the lake. The outermost surface of the active bioherms (Thompson et al., 1990) was examined by EDS and X-ray diffraction after the sample material was treated with weak hydrochloric acid. These methods revealed the presence of gypsum in trace amounts (<2%) only in the outer part of the bioherms. Therefore, experimental and sedimentological evidence suggest that gypsum in Green Lake is redissolved and/or replaced by calcite over time.

DISCUSSION

Our results clearly indicate that the small cyanobacterium *Synechococcus* is capable of epicellular biomineralization (Mann, 1986) of gypsum and calcite in natural alkaline aquatic environments. The role of bacteria or cyanobacteria in gypsum precipitation has never been reported, except for a possible indirect physical control on the evaporation of seawater (Braithwaite and Whitton, 1987). It is well known that many microorganisms can bind cations, including calcium, to their cell surface and extracellular glycocalyx (a polyanionic polysaccharide matrix) (Morita, 1980; Costerton et al., 1981; Beveridge and Fyfe, 1985). Calcium cations concentrated on the cell surface may act as nucleation sites for both gypsum and calcite precipitation (Fig. 5).

The photosynthetic metabolism of *Synechococcus* was directly responsible for the alkalinization of the microenvironment due to its ability to use HCO_3^- as its primary source of inorganic carbon (Miller and Colman, 1980; Badger et al., 1985). Miller and Colman (1980) reported a similar alkalinization during photosynthesis by *Synechococcus*. They suggested that *Synechococcus* conducts a HCO_3^-/OH^- exchange process across the cell membrane and that the hydroxyl ions were produced as a result of HCO_3^- fixation in photosynthesis. Our experimental results support such an exchange process; the pH of the experimental microenvironment continued to increase throughout the experiment (Table 2). Therefore, *Synechococcus* induces calcification in alkaline environments due to its photosynthetic alkalinization process (HCO_3^-/OH^- exchange system) (Fig. 5). Gypsum initially precipitated on the surface of *Synechococcus* because of the binding of calcium cations (which results in a calcium-enriched microenvironment at the cell surface) and because of the presence of high sulfate concentrations in the lake water. Calcium ions are also actively excluded from all bacterial cells in order to maintain a low concentration of intracellular calcium (Rosen, 1987). Therefore, photosynthetic bacteria in general may have a calcium-enriched microenvironment around their cell due to a light-driven calcium efflux (Rosen, 1987). Subsequently, *Synechococcus* induced calcification in the presence of light by increasing the pH of the microenvironment around the cells.

The microenvironment around *Synechococcus* consists of an envelope of water in which diffusion of materials to and from the bacterial cell occurs (Purcell, 1977). Simple solution chemistry cannot apply in this microenvironment because there is a fluid-solid interface in which thermodynamic activation energies can be reduced and chemical reactions are made possible. These small unicellular cyanobacteria are ubiquitous within the mixolimnion of Green Lake (10^5 cells/ml; Thompson et al., 1990) and many other aquatic environments (Bailey-Watts et al., 1968; Whitton, 1973; Waterbury et al., 1979; Li et al., 1983; Murphy and Haugen, 1985; Wyman et al., 1985; Guillard et al., 1985; Stockner, 1988).

Our data resolve the long-standing controversy over calcification in Green Lake (Davis, *in* Walcott, 1914; Bradley, 1929, 1963; Howe, 1932; Brunskill, 1969) and have broad implications for other natural environments. Early investigators of the carbonate sediment and bioherms in Green Lake referred to the possible precipitation of these deposits by numerous "rounded or oval, very small cells" (Davis, *in* Walcott, 1914, p. 88; Bradley, 1929, 1963; Howe, 1932). Bradley (1963, p. 921) recognized occluded bacterial cells within the calcite crystals from Green Lake and concluded that "the process by which Green Lake bacteria are entombed still goes on, though we do not yet know exactly how they operate." Unfortunately, Bradley (1968) retracted this important paper because he was convinced that what he had observed was an artifact. Brunskill (1969) stated that the calcification in Green Lake was the result of inorganic precipitation largely due to the effects of seasonally increasing temperatures. The data presented here are contrary to Brunskill's (1969) interpretation. If temperature were the major control, calcite should have precipitated in sterile control samples. The natural lake water used in these experiments was kept at 4 °C until the experiment was started. Our data show that *Synechococcus* is responsible for the predominant calcification in Green Lake and that *Synechococcus* cells are continually entombed within the growing calcite crystals (Fig. 1B; Bradley, 1963).

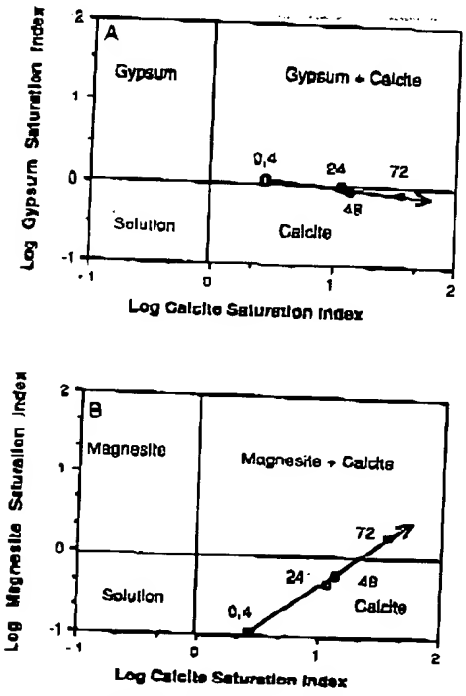

Figure 4. Mineral saturation indices (SI) determined from results of water chemistry. Numbers represent sampling time intervals (0, 4, 24, 48, and 72 h). A: Gypsum vs. calcite saturation; note that alkalinization of microenvironment by *Synechococcus* has raised level of oversaturation with respect to calcite solubility to 35 times by 72 h. SI of gypsum has dropped, becoming undersaturated between ~24 and 48 h. B: Magnesite vs. calcite saturation; note that experimental microenvironment actually became oversaturated with magnesite by 72 h. SI for magnesite at 72 h was 1.71.

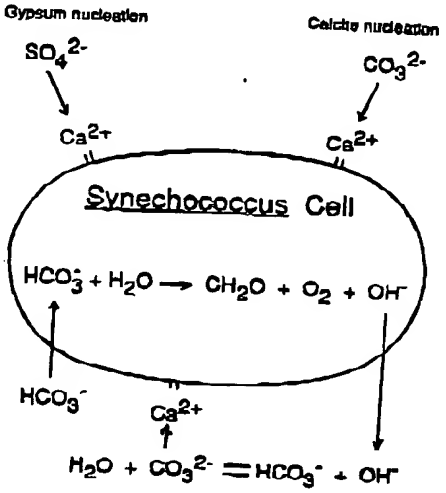

Figure 5. Schematic model for *Synechococcus* calcification. *Synechococcus* is responsible for direct alkalinization of its surrounding microenvironment due to HCO_3^-/OH^- exchange process across its cell membrane. Exchange process is result of HCO_3^- fixation in photosynthesis (Miller and Colman, 1980). *Synechococcus* also provides ideal nucleation site for calcification within this microenvironment due to its high surface-to-volume ratio and its ability to bind calcium cations to cell surface.

The direct role of *Synechococcus* in biomineralization along with its universal abundance in natural aquatic environments has widespread implications for the examination of whiting events (freshwater and marine), carbonate mud deposition, and bioherm development since late Archean time in environments other than Fayetteville Green Lake. Unicellular cyanobacteria, similar to *Synechococcus*, have existed since late Archean to Early Proterozoic time (Knoll and Barghoorn, 1975, 1977; Cloud, 1976; Awramik, 1976, 1984).

Our preliminary results on the biomineralization of gypsum and magnesite indicate that more field and laboratory investigations are warranted. A detailed examination of naturally occurring gypsum and sedimentary magnesite deposits is needed. Magnesite biomineralization may be occurring in natural high pH (8.5–10.0) aquatic environments rich in magnesium.

REFERENCES CITED

Awramik, S.M., 1976, Gunflint stromatolites: Microfossil distribution in relation to stromatolite morphology, *in* Walter, M.R., ed., Stromatolites (Developments in sedimentology 20): New York, Elsevier, p. 311–320.

——1984, Ancient stromatolites and microbial mats, *in* Cohen, Y., Castenholz, R.W., and Halvorson, H.O., eds., Microbial mats: Stromatolites: New York, Alan R. Liss, Inc., p. 1–22.

Badger, M.R., Bassett, M., and Comins, H.N., 1985, A model for HCO_3^- accumulation and photosynthesis in the cyanobacterium *Synechococcus* sp.: Plant Physiology, v. 77, p. 465–471.

Bailey-Watts, A.E., Bindloss, M.E., and Belcher, J.H., 1968, Freshwater primary production by a blue-green alga of bacterial size: Nature, v. 220, p. 1344–1345.

Beveridge, T.J., and Fyfe, W.S., 1985, Metal fixation by bacterial cell walls: Canadian Journal of Earth Sciences, v. 22, p. 1893–1898.

Black, M., 1933, The precipitation of calcium carbonate on the Great Bahama Bank: Geological Magazine, v. 70, p. 455–466.

Bradley, W.H., 1929, Algae reefs and oolites of the Green River Formation: U.S. Geological Survey Professional Paper 154-G, p. 203–223.

——1963, Unmineralized fossil bacteria: Science, v. 141, p. 919–921.

——1968, Unmineralized fossil bacteria: A retraction: Science, v. 160, p. 437.

Braithwaite, C.J.R., and Whitton, B.A., 1987, Gypsum and halite associated with the cyanobacterium *Entophysalis*: Geomicrobiology Journal, v. 5, p. 43–55.

Brunskill, G.J., 1969, Fayetteville Green Lake, New York, II. Precipitation and sedimentation of calcite in a meromictic lake with laminated sediments: Limnology and Oceanography, v. 14, p. 830–847.

Brunskill, G.J., and Ludlam, S.D., 1969, Fayetteville Green Lake, New York. I. Physical and chemical limnology: Limnology and Oceanography, v. 14, p. 817–829.

Cloud, P., 1976, Beginnings of biosphere evolution and their biogeochemical consequences: Paleobiology, v. 2, p. 351–387.

Costerton, J.W., Irvin, R.T., and Cheng, K.J., 1981, The bacterial glycocalyx in nature and disease: Annual Review of Microbiology, v. 35, p. 299–324.

Drew, G.H., 1911, The action of some denitrifying bacteria in tropical and temperate seas and the bacterial precipitation of calcium carbonate in the sea: United Kingdom Marine Biological Association Journal, v. 9, no. 2, p. 142–155.

——1913, On the precipitation of calcium carbonate in the sea by marine bacteria, and on the action of denitrifying bacteria in tropical and temperate seas: United Kingdom Marine Biological Association Journal, v. 9, no. 4, p. 479–524.

Ennever, J., 1963, Microbiologic calcification: New York Academy of Sciences Annals, v. 109, p. 4–13.

Ennever, J., and Takazoe, I., 1973, Bacterial calcification, *in* Zipkin, I., ed., Biological mineralization: New York, Wiley Interscience, p. 629–648.

Greenfield, L.J., 1963, Metabolism and concentration of calcium and magnesium and precipitation of calcium carbonate by a marine bacterium: New York Academy of Sciences Annals, v. 109, p. 23–45.

Guillard, R.R.L., Murphy, L.S., Foss, P., and Liaaen-Jensen, S., 1985, *Synechococcus* spp. as likely zeaxanthin-dominant ultraphytoplankton in the North Atlantic: Limnology and Oceanography, v. 30, p. 412–414.

Hale, D.J., 1903, Theories of origin of bog lime or marl: Geological Survey of Michigan Annual Report, v. 8, p. 41–64.

Howe, M.A., 1932, The geologic importance of the lime secreting algae: U.S. Geological Survey Professional Paper 170-E, p. 57–69.

Knoll, A.H., and Barghoorn, E.S., 1975, Precambrian eukaryotic organisms: A reassessment of the evidence: Science, v. 190, p. 52–54.

——1977, Archean microfossils showing cell division from the Swaziland System of South Africa: Science, v. 198, p. 396–398.

Krumbein, W.E., 1974, On the precipitation of aragonite on the surface of marine bacteria: Naturwissenschaften, v. 61, p. 167.

——1979, Calcification by bacteria and algae, *in* Trudinger, P.A., and Swaine, D.J., eds., Biogeochemical cycling of mineral-forming elements: Amsterdam, Elsevier, p. 47–68.

Lane, A.C., 1903, Notes on the origin of Michigan bog limes: Geological Survey of Michigan Annual Report, v. 8, p. 199–223.

Li, W.K.W., SubbaRao, D.V., Harrison, W.G., Smith, J.C., Cullen, J.J., Irwin, B., and Platt, T., 1983, Autotrophic picoplankton in the tropical ocean: Science, v. 219, p. 292–295.

Mann, S., 1986, Biomineralization in lower plants and animals—Chemical perspectives, *in* Leadbeater, B.S.C., and Riding, R., eds., Biomineralization in lower plants and animals: Oxford, England, Clarendon Press, p. 39–54.

McCallum, M.F., and Guhatbakurta, K., 1970, The precipitation of calcium carbonate from seawater by bacteria isolated from Bahama Bank sediments: Journal of Applied Bacteriology, v. 33, p. 649–655.

McLean, R.J.C., Nickel, J.C., Nookes, V.C., and Costerton, J.W., 1985, An in vitro ultrastructural study of infectious kidney stone genesis: Infection and Immunity, v. 49, p. 805–811.

Miller, A.G., and Colman, B., 1980, Evidence for HCO_3^- transport by the blue-green alga (cyanobacterium) *Coccochloris peniocystis*: Plant Physiology, v. 65, p. 397–402.

Morita, R.Y., 1980, Calcite precipitation by marine bacteria: Geomicrobiology Journal, v. 2, p. 63–82.

Murphy, L.S., and Haugen, E.M., 1985, The distribution and abundance of phototrophic ultraplankton in the North Atlantic: Limnology and Oceanography, v. 30, p. 47–58.

Nickel, J.C., Olson, M., McLean, R.J.C., Grant, S.K., and Costerton, J.W., 1987, An ecological study of infected urinary stone genesis in an animal model: British Journal of Urology, v. 59, p. 21–30.

Novitsky, J.A., 1981, Calcium carbonate precipitation by marine bacteria: Geomicrobiology Journal, v. 2, p. 375–388.

Pentecost, A., 1985, Association of cyanobacteria with tufa deposits: Identity, enumeration, and nature of the sheath material revealed by histochemistry: Geomicrobiology Journal, v. 4, p. 285–299.

Pentecost, A., and Bauld, J., 1988, Nucleation of calcite on the sheaths of cyanobacteria using a simple diffusion cell: Geomicrobiology Journal, v. 6, p. 129–135.

Pollock, J.B., 1918, Blue-green algae as agents in the deposition of marl in Michigan lakes: Michigan Academy of Science Annual Report, v. 20, p. 247–261.

Purcell, E.M., 1977, Life at low Reynolds number: American Journal of Physics, v. 45, p. 3–11.

Rosen, B.P., 1987, Bacterial calcium transport: Biochimica et Biophysica Acta, v. 906, p. 101–110.

Stockner, J.G., 1988, Phototrophic picoplankton: An overview from marine and freshwater ecosystems: Limnology and Oceanography, v. 33, p. 765–775.

Stumm, W., and Morgan, J.J., 1981, Aquatic chemistry. An introduction emphasizing chemical equilibria in natural waters (second edition): New York, Wiley Interscience, 780 p.

Thompson, J.B., Ferris, F.G., and Smith, D., 1990, Geomicrobiology and sedimentology of the mixolimnion and chemocline in Fayetteville Green Lake, New York: Palaios, v. 5, p. 52–75.

Walcott, C.D., 1914, Pre-cambrian Algonkian algal flora: Smithsonian Miscellaneous Collections, v. 64, p. 77–157.

Waterbury, J.B., Watson, S.W., Guillard, R.R.L., and Brand, L.E., 1979, Widespread occurrence of a unicellular, marine planktonic, cyanobacterium: Nature, v. 277, p. 293–294.

Whitton, B.A., 1973, Freshwater plankton, *in* Carr, G., and Whitton, B.A., eds., The biology of blue-green algae: Berkeley, University of California Press, p. 353–367.

Wyman, M., Gregory, R.P.F., and Carr, N.G., 1985, Novel role for phycoerythrin in a marine cyanobacterium, *Synechococcus* strain DC2: Science, v. 230, p. 818–820.

ACKNOWLEDGMENTS

Supported by funds from the Upstate Freshwater Institute to Thompson and an Ontario Geological Survey grant to W. S. Fyfe and T. J. Beveridge. All electron microscopy was performed in the Natural Sciences and Engineering Research Council of Canada Guelph regional Scanning Transmission Electron Microscopy Facility at the University of Guelph. We thank G. Spiers for his assistance with chemical analyses; T. Marian and W. Murray, New York State Office of Parks, Recreation and Historic Preservation, Central Region, for their cooperation; and T. J. Beveridge for laboratory support at the University of Guelph.

Manuscript received March 1, 1990
Revised manuscript received May 14, 1990
Manuscript accepted May 30, 1990

Printed in U.S.A.

STIC-ILL

MLC
Pl. 1.12

From: Marx, Irene
Sent: Tuesday, September 10, 2002 9:19 AM
To: STIC-ILL
Subject: 09/777664

Importance: High

Please send to Irene Marx, Art Unit 1651; CM1, Room 10E05, phone 308-2922, Mail box in 11B01

Observations on the ionic composition of blue-green algae growing in saline lagoons
AU Pillai, V. K.
SO Proc. Natl. Inst. Sci. India, (19550000) vol. 21, no. 2, pp. 90-102.
DT Journal

Dalrymple, D.W., 1965, "Calcium carbonate deposition associated with blue green algal mats, Baffin Bay.:, Texas: Institute of Marine Science Publication 10, p. 187-200

Black, M., 1933, "The algal sedimentation... ", Royal Society of London Philosphical transactions, Ser. B, V. 222, p. 165-192

Lowenstam HA (1981), Science, 211:1126-1131

Ferris et al., Earth Sci., 47:233-250 (1993)

Ferris et al., Appl. and Environm. Microbiol.,1989, 55:1249-1257

Kazmierczak et al., (1990), Science, 250:1244-1248

Kempe et al., Facies, 28:1-32, 1993.

Kempe et al., 1994, Bull, Inst. Oceanogr., Monaco no. spec., 13:61-117.

Merz, M.U.E, 1992, Facies, 26:81-102

Pentecost et al., 1986, Calcification in cyanobacteria, In "Biomineralization of Lower plants and animals (Leadbeater et a., ed. 73-90, Clarendon Press, Oxford.

Riding, R., 1982, Nature, 299:814-815

Thompson eta., 1990, Geology, 18:995-998

Irene Marx
Art Unit 1651
CMI 10-E-05,
Mail Box 11-B-01
703-308-2922

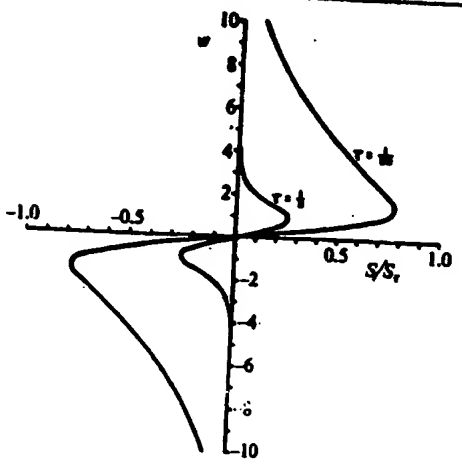

Fig. 4 Vertical profiles of the S concentration at a diffusing interface with $D_{12}=0$ and with the initial contrast in S concentration between the two layers equal to zero. The vertical coordinate w is equal to $z/2\sqrt{D_{22}t}$ and the reference S value S_r is $(\Delta T/2)\,(D_{21}/D_{22})\,\tau/(1-\tau)$.

fingers is not affected by coupled diffusion and the flux of T between the fingers is mainly due to the cross-diffusive flux of T caused by the positive value of D_{12} (satisfying inequality (7)) and the S gradient between the fingers. Note that in both *a* and *b* of Fig. 3 the horizontally averaged density gradient is statically stable ($\bar{\rho}_z<0$) and that the downgoing fingers are more dense than the surrounding upgoing fingers.

The theoretical arguments outlined above have all related to regions in which there are constant vertical gradients of the two diffusing properties. A more common experimental situation, however, is one in which a layer of fluid is placed above another layer of different composition, with initially a sharp interface between them. When two solutions are placed one above the other, the diffusion of the two species T and S across the bounding interface may set up gradients which are favourable for the formation of fingers. Figure 4 shows the profiles of S as a function of $w=z/2\sqrt{D_{22}t}$ when the difference in S concentration between the layers is zero and one of the cross-diffusion coefficients, D_{12}, is also equal to zero. The S gradient is proportional to the cross diffusion coefficient D_{21} and to the difference in the T concentrations between the layers, ΔT. The S gradient is conductive to fingering in this interfacial region where the T gradient maintains the hydrostatic stability. This subject of diffusion at an initially sharp interface is discussed in more detail in ref. 9, including cases where both properties are initially set up in the hydrostatically 'stable' sense.

To test our belief that fingers can form due to cross-diffusion without needing to invoke any other special properties of polymers, we initiated experiments using two layers of sodium chloride solution at different temperatures, the cross diffusion term being now the Soret coefficient. According to published values of the coefficients, the criterion for instability to fingering motions (inequality (4)) could just be satisfied at low temperatures (where D_{21} is positive), with the upper layer a few degrees warmer than the lower. This system was, however, too sensitive to extraneous effects such as heating at the side walls and evaporation at the surface, and we concluded that a definitive experimental test of the theoretical ideas presented here will have to be carried out in a solute–solute system.

Cussler[11] lists references to measurements of all four ternary diffusion coefficients in various systems, showing that one of the few substances to exhibit large cross-diffusion fluxes is another polymer, polystyrene, of molecular weight of 190,000. Cussler and Lightfoot[12] used the polystyrene–toluene–cyclohexane combination and found values of $D_{12}/D_{11}<-1$. They also give a simple explanation of the large cross-diffusion effect in terms of the chemical potential as a function of temperature for the two binary mixtures, polystyrene–toluene and polystyrene–cyclohexane.

In order to understand the mechanism of finger formation in situations such as those discussed by Preston *et al.*[2,4] we suggest that the next logical step is to endeavour to measure the cross-diffusion fluxes for some of these long chain polymers in the presence of each other.

Received 7 May; accepted 4 August 1982.

1. Huppert, H. E. & Turner, J. S. *J. Fluid Mech.* **106**, 299–329 (1981).
2. Preston, B. N., Laurent, T. C., Comper, W. D. & Checkley, G. J. *Nature* **287**, 499–503 (1980).
3. Williams, A. *J. J. geophys. Res.* **86**, 1917–1928 (1981).
4. Comper, W. D. (in preparation).
5. Wendt, R. P. *J. phys. Chem.* **66**, 1740–1742 (1962).
6. Schechter, R. S., Prigogine, I. & Hamm, J. R. *Phys. Fluids* **15**, 379–385 (1972).
7. Velarde, M. G. & Schechter, R. S. *Phys. Fluids* **15**, 1707–1714 (1972).
8. Huppert, H. E. & Turner, J. S. *J. Fluid Mech.* **106**, 299–329 (1981).
9. McDougall, T. *J. J. Fluid Mech.* (in the press).
10. Huppert, H. E. & Manins, P. C. *Deep-Sea Res.* **20**, 315–323 (1973).
11. Cussler, E. L. *Multicomponent Diffusion* (Elsevier, New York, 1976).
12. Cussler, E. L. & Lightfoot, E. N. *J. phys. Chem.* **69**, 1135–1144 (1965).

Cyanophyte calcification and changes in ocean chemistry

Robert Riding

Department of Geology, University College, Cardiff CF1 1XL, UK

Cyanophytes range from at least 2,200 Myr (ref. 1) to the Recent, but they only produced common marine shelly fossils during the Palaeozoic and Mesozoic (570–80 Myr) (Fig. 1). This contrasts with the pattern of metazoan evolution in which rapid diversification near the Precambrian–Cambrian boundary was closely accompanied by skeletonization[2] which has been retained in marine environments to the Recent. Attempts to explain this unusual geological distribution of marine calcareous cyanophytes cannot be made solely by reference to biological processes because these algae are mainly dependent on environmental conditions for their calcification[3]. Thus, the presence or absence of calcified cyanophytes may be a general indication of long-term changes in seawater chemistry. This likelihood has been recognized previously[4] but has not been explored in any detail. Here I outline some possible explanations and suggest that cyanophyte calcification was facilitated by enhancement of marine $CaCO_3$ precipitation rates in the late Precambrian because of decrease in the Mg^{2+}/Ca^{2+} ratio, linked to falling P_{CO_2} levels and extensive dolomite formation. Scarcity of calcareous cyanophytes in Cenozoic marine environments again implicates the Mg^{2+}/Ca^{2+} ratio, inferred from oöid mineralogy to have increased in the late Mesozoic[5], as a factor influencing cyanophyte calcification in the sea.

Calcareous cyanophytes, represented by microscopic fossils such as *Angulocellularia*, *Girvanella* and *Ortonella*, are consistently present in normal marine shelf environments from the Nemakit–Daldyn Horizon of latest Precambrian age in Siberia[6] until the Jurassic and possibly also Cretaceous[7]. But they have not been reported from Cenozoic marine deposits and the very few records of them in Recent seas indicate that they are extremely rare, are not calcified to the same degree as Palaeozoic and Mesozoic examples, and tend to be limited to marginal marine situations[8,9]. Similarly, calcareous cyanophytes appear to be absent from most Precambrian rocks despite intensive study of stromatolite microfabrics. The best evidence for Precambrian calcareous cyanophytes is weakly calcified traces of filaments from Upper Riphean and younger rocks in the Soviet Union[6].

In attempting to account for the paucity of calcareous cyanophytes in the sea during the Precambrian and Cenozoic,

0028-0836/82/430814-02$01.00

© 1982 Macmillan Journals Ltd

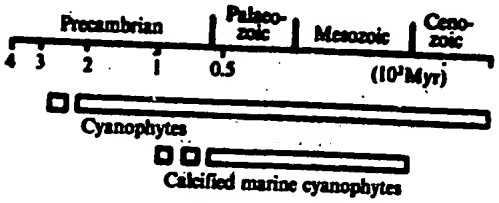

Fig. 1 Precambrian to Recent range of cyanophytes[1] compared with the Palaeozoic–Mesozoic occurrence of marine calcified cyanophytes.

both biological and environmental factors needed to be considered. The possibility that cyanophytes evolved calcification in the latest Precambrian cannot be ruled out, but silicified cyanophytes from the Proterozoic are similar to Recent forms[10] and do not show morphological differences that could account for an absence of calcification. Furthermore, there is no good evidence that cyanophytes capable of calcification either became extinct or were excluded from marine environments in the late Mesozoic. The suggestion that cyanophytes in the sea were outcompeted by red and green algae[4] is not supported by direct evidence[11,12], and it is known that Recent genera which calcify in freshwater can live uncalcified in the sea[4]. Consequently, an environmental control to account for marine cyanophyte calcification is not unreasonable, despite the fact that suggestions of changes in seawater composition near the Precambrian–Cambrian boundary to account for metazoan skeletonization have received little support recently[2]. Mg^{2+}/Ca^{2+} ratio changes near the Precambrian–Cambrian boundary have been suggested in this context[13], but metazoan skeletonization probably does not share the environmental dependence of cyanophyte calcification. However, it is remarkable that calcification in cyanophytes and metazoans began almost synchronously near 570 Myr.

Thermodynamically, an increase in temperature, partial pressure of CO_2 in buffered seawater, pH, or $a_{Ca^{2+}}$ will enhance the magnitude of $CaCO_3$ precipitation. A decrease in salinity resulting in increases of $\gamma_{Ca^{2+}}$ and $\gamma_{CO_3^{2-}}$ will have the same effect[14]. However, these parameters do not necessarily reflect the rate of precipitation of calcareous sediments. In marginal marine embayments it is possible to modify substantially temperature, pH and salinity, but these local changes in restricted environments cannot be invoked as long-term effects on general seawater chemistry. The occurrence of calcareous cyanophytes in reef environments from Cambrian to Jurassic–Cretaceous time[7] requires modification of normal shelf seawater to be sustained for hundreds of millions of years. The rate of nucleation and growth of calcite, aragonite and dolomite, has been shown to depend on Mg^{2+} ion concentrations and a plausible explanation for changes in cyanophyte calcification can be invoked on the basis of kinetic considerations involving this ion.

The mutual interdependence of P_{CO_2} and the ratio of Mg^{2+}/Ca^{2+} in carbonated buffered seawater is well documented[15]. For example, an increase in P_{CO_2} will lead to $CaCO_3$ deposition and thus an increase of the Mg^{2+}/Ca^{2+} ratio. Conversely, any decrease in P_{CO_2} during the Precambrian[16] would thus decrease the Mg^{2+}/Ca^{2+} ratio of seawater. As it has been demonstrated[17,18] that relative decreases of Mg^{2+} concentrations greatly enhance the rate of nucleation of $CaCO_3$ it might be expected that cyanophyte calcification would be stimulated as a result. Extensive formation of late Precambrian dolomites[19], suggested to be primary[20], would also have depressed the Mg^{2+} content of seawater. Reversal of this condition—increase of the Mg^{2+}/Ca^{2+} ratio—in the late Mesozoic has been attributed to widespread deposition of $CaCO_3$ by pelagic microorganisms as calcareous oozes, now preserved as chalks[5]. Hence, changes in the Mg^{2+}/Ca^{2+} ratio can be inferred which correlate with both the appearance of calcareous marine cyanophytes near the Precambrian–Cambrian boundary and their disappearance in the late Mesozoic.

Calcification may have conferred biological advantages on cyanophytes and certainly resulted in important changes in their sedimentological roles, whatever its cause may have been. An environmental control is plausible and implies that cyanophyte calcification could be an index of marine $CaCO_3$ precipitation rates which reflects times when inorganic carbonate production was increased. If this is so then it should also correlate with enhanced oölid formation and subsea cementation in the geological record. The presence of weakly calcified ?cyanophytes in the upper Proterozoic[5] suggests a period of transition before the abrupt appearance of heavily calcified forms in the Nemakit–Daldyn. More information is required from the late Mesozoic to see whether a similar phase preceded the disappearance of calcareous marine cyanophytes at that time.

This research was supported by the NERC and also by the Humboldt Foundation through a Fellowship at the Technical University, Munich. I thank Peter Williams for advice on carbonate chemistry, and Robin Bathurst, Martin Brasier, Dianne Edwards, and Maurice Tucker for critically reading the manuscript.

Received 28 June; accepted 16 August 1982.

1. Cloud, P. *Paleobiology* **2**, 351–387 (1976).
2. Stanley, S. M. *Am. J. Sci.* **276**, 56–76 (1976).
3. Golubic, S. in *The Biology of Blue-Green Algae* (eds Carr, N. G. & Whitton, B. A.) 434–473 (Blackwell, Oxford, 1973).
4. Monty, C. L. V. *Ann. Soc. geol. Belg.* **95**, 585–624 (1973).
5. Sandberg, P. A. *Sedimentology* **22**, 497–538 (1975).
6. Riding, R. & Voronova, L. G. *Naturwissenschaften* (in the press).
7. Wray, J. L. *Developments in Palaeontology and Stratigraphy* Vol. 4 (Elsevier, Amsterdam, 1977).
8. Winland, H. D. & Matthews, R. K. *J. sedim. Petrol.* **44**, 921–927 (1974).
9. Golubic, S. & Campbell, S. E. in *Phanerozoic Stromatolites* (ed. Monty, C.) 209–229 (Springer, Berlin, 1981).
10. Schopf, J. W. *Scient. Am.* **239**, 85–102 (1978).
11. Gebelein, C. D. in *Developments in Sedimentology* Vol. 20 (ed. Walter, M. R.) 499–515 (Elsevier, Amsterdam, 1976).
12. Stanley, S. M. *Paleobiology* **2**, 209–219 (1976).
13. Durov, S. A. *Trudy novocherk. politekh. Inst.* **98**, (1960).
14. Garrels, R. M. & Christ, C. L. *Solutions, Minerals and Equilibria* (Harper & Row, New York, 1965).
15. Holland, H. D. *Proc. natn. Acad. Sci. U.S.A.* **53**, 1173–1182 (1965).
16. Berkner, L. V. & Marshall, L. C. *Discuss. Faraday Soc.* **37**, 122–141 (1964).
17. Pytkowicz, R. M. *J. Geol.* **73**, 196–199 (1965).
18. Berner, R. A. *Soc. Econ. Paleont. Miner. Spec. Publ.* **20**, 37–43 (1974).
19. Ronov, A. B. *Geokhimiya* **8**, 715–743 (1964).
20. Tucker, M. E. *Geology* **10**, 1, 7–12 (1982).

Evidence for a central Eurasian source area of Arctic haze in Alaska

G. E. Shaw

Geophysical Institute, University of Alaska, Fairbanks, Alaska 99701, USA

During winter when the polar oceans are frozen, air masses entering Alaska from the Arctic are charged with suspended submicrometre particles whose chemical signatures show evidence of being derived from man-made sources of pollution[1–3]. Occasionally, the aerosol loading is large enough to reduce visibility and thus the phenomenon has come to be referred to as 'Arctic haze'. We report here three strong episodes of Arctic haze in Alaska which were examined during February–April 1982 and which were found to be possibly associated with air emissions in central Eurasia.

Figure 1 illustrates th episodic nature of Arctic haze in interior Alaska during late winter 1982. The cross-hatched regions are synonymous with incidences of visible haze, which occurred in association with low air temperatures, increased particle concentration for particles near 0.13-μm diameter (determined with a laser spectrometer) and, as the maps at the

0028–0836/82/430815—04$01.00

1982 Macmillan Journals Ltd

STIC-ILL

X09/10

411626

From: Marx, Irene
Sent: Tuesday, September 10, 2002 9:19 AM
To: STIC-ILL
Subject: 09/777664

Importance: High

Please send to Irene Marx, Art Unit 1651; CM1, Room 10E05, phone 308-2922, Mail box in 11B01

Observations on the ionic composition of blue-green algae growing in saline lagoons
AU Pillai, V. K.
SO Proc. Natl. Inst. Sci. India, (19550000) vol. 21, no. 2, pp. 90-102.
DT Journal

Dalrymple, D.W., 1965, "Calcium carbonate deposition associated with blue green algal mats, Baffin Bay.:, Texas: Institute of Marine Science Publication 10, p. 187-200

Black, M., 1933, "The algal sedimentation... ", Royal Society of London Philosphical transactions, Ser. B, V. 222, p. 165-192

Lowenstam HA (1981), Science, 211:1126-1131

Ferris et al., Earth Sci., 47:233-250 (1993)

Ferris et al., Appl. and Environm. Microbiol.,1989, 55:1249-1257

Kazmierczak et al., (1990), Science, 250:1244-1248

Kempe et al., Facies, 28:1-32, 1993.

Kempe et al., 1994, Bull, Inst. Oceanogr., Monaco no. spec., 13:61-117.

Merz, M.U.E, 1992, Facies, 26:81-102

Pentecost et al., 1986, Calcification in cyanobacteria; In "Biomineralization of Lower plants and animals (Leadbeater et a., ed. 73-90, Clarendon Press, Oxford.

Riding, R., 1982, Nature, 299:814-815

Thompson eta., 1990, Geology, 18:995-998

Irene Marx
Art Unit 1651
CMI 10-E-05,
Mail Box 11-B-01
703-308-2922

9/11

LC 9/11 SMP WDS

FACIES	28	1-32	Pl. 1-8	9 Figs.	11 Tab.	ERLANGEN 1993

Satonda Crater Lake, Indonesia: Hydrogeochemistry and Biocarbonates

Stephan **Kempe**, Hamburg and Józef **Kaźmierczak**, Warsaw

KEYWORDS: BIOCARBONATES – STROMATOLITES – CYANOBACTERIA (PLEUROCAPSALES) – HYDROGEOCHEMISTRY (QUASI-MARINE) – SATONDA ISLAND (INDONESIA) – RECENT

CONTENTS

SUMMARY

The results of detailed hydrochemical and biosedimentological studies of the sea-linked Satonda Crater Lake, Sumbawa Island/Indonesia are presented. They revealed that the mildly alkaline, mid-water stratified and species-poor lake supports growth of cyanobacterial-red algal calcareous reefs comparable with some ancient marine biocarbonates. The chemical and biotic changes during the last 4,000 years of the lake history have been reconstructed. They indicate that the chemistry of the lake evolved from initially fresh water, through highly alkaline to the modern slightly alkaline quasi-marine conditions with corresponding biotic changes. The influence of the 1815 eruption of the nearby located Tambora Volcano on the lake chemistry and resulting lithological and biotic changes is also discussed. The lake proves to be a good model for the recently proposed hypothesis of an early alkaline (soda) ocean.

1 INTRODUCTION

On November 22nd, 1983, the 'Soda Ocean Hypothesis' (SOH) was born during a public lecture on the global carbon cycle. Its theoretical background has since been published in KEMPE & DEGENS (1985, 1986) and in KEMPE et al. (1989). The SOH maintains that the Precambrian ocean was highly alkaline, of high pH and of low Ca concentrations. It is based on the observation that the weathering of silicate rocks with carbonic acid (the Urey-reaction, UREY, 1951) produces, in general, solutions with equivalent ratios $[Ca^{2+} + Mg^{2+}] < [HCO_3^-]$ and $[Na^+ + K^+] > [Cl^- + SO_4^{2-}]$. Upon evaporation, these solutions will reach the solubility product of the alkaline earth carbonate minerals first. Precipitation of calcite, aragonite or even dolomite will leave Na^+, K^+ and HCO_3^- (plus Cl^- and SO_4^{2-}) behind, i.e., highly alkaline conditions (GARRELS & MACKENZIE, 1967; HARDIE & EUGSTER, 1970; EUGSTER & HARDIE, 1978). Today, we find alkaline lakes (so-called soda lakes) in volcanic areas associated with active plate boundaries worldwide (KEMPE et al., 1989).

However, comparing the chemistry of 'isolated' lakes with that of the early ocean, does not seem to be very convincing. The chance to find a contemporary alkaline but marine environment came during the Dutch-Indonesian Snellius II expedition to the Flores Sea in November 1984 (participants from Hamburg: E. T. Degens, V. Ittekkot and S. Kempe). One of us (S. K.) noticed on the map that the small volcanic island Satonda contained a lake, seemingly at sea level and therefore possibly filled with seawater. Professor D. Eisma, chief-scientist of the Snellius II-leg, kindly agreed to send a landing party to Satonda. In the morning of November 22nd, 1984, one year after the SOH had been formulated, Stephan Kempe, Doeke Eisma, Theo Buisma, Haruna Mappa and Surino set out from the R/V Tyro by rubber boat to inspect the island and its lake.

The first glance already proved that we had found what was expected: the water tasted salty like seawater but had a pH of 8.55! And, even more important, there were groups of large,

Addresses: Dr. S. Kempe Institute for Biogeochemistry and Marine Chemistry, Center of Marine and Climate Research, University of Hamburg, Bundesstr. 55, D-2000 Hamburg 13, Fed. Rep. of Germany; Prof. Dr. J. Kaźmierczak, Institute of Paleobiology, Polish Academy of Sciences, Zwirki i Wigury 93, PL-02089 Warsaw, Poland.

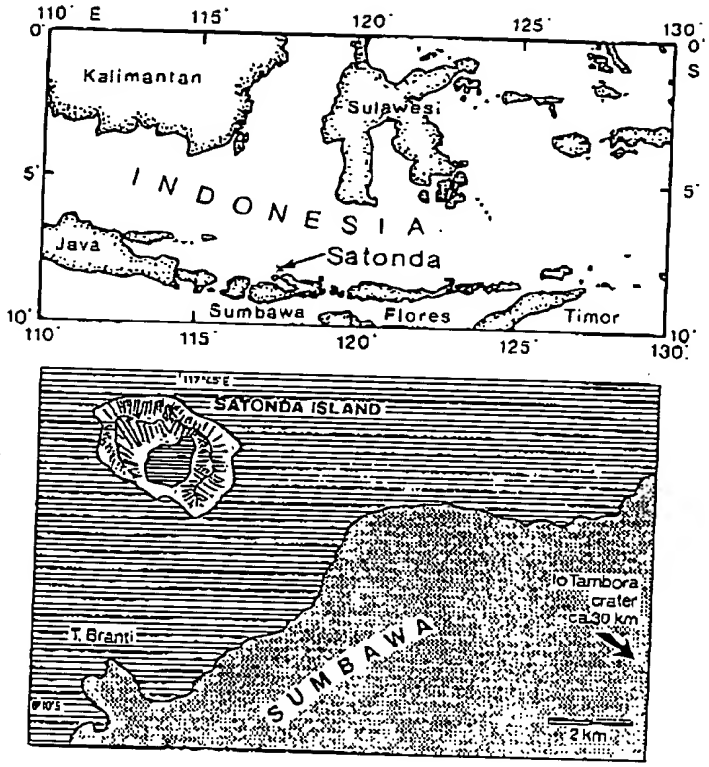

Fig. 1. Sketch map of the Island of Satonda and its location north of the Sanggar Peninsula on Sumbawa/ Indonesia.

semicircular pillars made of carbonate dotting the shore (Pl. 1/1). Because November is the end of the dry season, the heads of these pillars lay dry. During the wet season the lake level obviously stands more than a meter higher as marked by bands of dry algae on rocks. The beach of the lake otherwise consists of black volcanic sand. T. Buisma scuba dived down to 10 m where the water was as warm as at the surface, i.e., 32 °C. S. Kempe snorkeled in the murky water along the shore observing that the pillars rise vertically from depth, some of them seemed to be taller than 10 m. The pillars are overgrown with long filaments of non-calcified green algae. The fauna in the lake evidently consists of only a few species: one sponge, one fish and one thin-shelled, small, black gastropod even though 100 m across the crater rim the tropical reef houses hundreds of species. Two water samples (for chemical data of surface sample see Table 1) were taken proving that the lake was mixed down to a depth of 10 m. These samples showed that not only the pH but also the total alkalinity is elevated in the lake as compared with modern seawater, while the Ca concentration is much lower than in seawater of comparable salinity.

The carbonate pillars were sampled for microscopic inspection. These pieces were later examined by J. Kazmierczak, who discovered that the carbonate is not an inorganic precipitate, but has been mainly precipitated by cyanobacteria (blue-green algae). The microscopic structure, either laminated, cystous or clotty, reminds one of Precambrian stromatolites, the only macroscopic fossil preserved from the ancient pre-metazoan sea (KEMPE et al., 1992).

These first results showed that Satonda crater lake could serve in fact as a contemporary model of the Precambrian ocean: it contains seawater of a higher alkalinity and pH and lower Ca concentration than any recent seawater and it promotes the growth of in situ calcifying cyanobacterial stromatolites, not reported from any other modern marine site previously.

These were the known facts when the German-Indonesian R/V Sonne 45B expedition was planned by the late Professor E. T. Degens in 1985. From the beginning it was clear that Satonda Island should be paid an extended visit during that expedition. At first, a few days were thought to be sufficient, but then, as planning became more detailed, it was decided to launch a more extensive program and to have a land party on the island throughout most of the cruise. This land party would in part cooperate with the 'Tambora' land party (D. Jung, K. Heyckendorf, K. Paluskova and company) and would receive logistic help from aboard the R/V Sonne. The land party consisted of the two authors, the research divers G. Landmann and A. Lipp, and two Indonesian colleagues from Bandung University: Y. Surachman and D. Susanto. The party arrived at Satonda October 2nd with two rubber boats from Den Passar and was taken aboard the R/V Sonne October 13th, 1986. The Tambora land party visited Satonda October 3rd when also one of the rubber boats was carried over the crater rim into the lake. On October 4th, the R/V Sonne stopped at Satonda delivering Professor How Kin Wong and Uwe Salge with their seismic gear. They mapped the bathymetry of the lake and left one day later. On the 5th water samples were taken to be analyzed for nutrients by Dr. G. Liebezeit aboard the R/V Sonne. A more detailed trip report is found in the Interims Report to the BMFT 'Tambora Volcano, Cruise SO 45-B', December 1986, Kazmierczak et al., unpublished (1986). All rock and sediment samples were taken in duplicates, one set for the University of Bandung and one set for the University of Hamburg. All notes and data tables were

Parameter	Satonda surface		Salch Bay surface	
pH	8.55		8.27	
Temp.	31.3	°C	29.3	°C
Sal.	- *	o/oo	34.23	°/oo
Cl^-	17.96	g/l	19.44	g/l
Ca^{2+}	9.58	meq/l	19.8	meq/l
Mg^{2+}	92.92	meq/l	104.60	meq/l
Mg/Ca	9.75		5.8	
Alk	3.65	meq/l	2.28	meq/l
$o\text{-}PO_4^{3-}$	0.28	µM/l	0	µM/l
H_2SiO_4	29.9	µM/l	0	µM/l
Urea	0.8	µM/l	-	µM/l
NH_4^+	1.0	µM/l	< 0.1	µM/l
NO_3^-	0.2	µM/l	0	µM/l
NO_2^-	0.01	µM/l	0	µM/l

Table 1: Comparison of chemical data of two surface water samples collected in Satonda Crater Lake and in nearby Salch Bay (Sample TAM2). Nutrient data by R. De Vries.

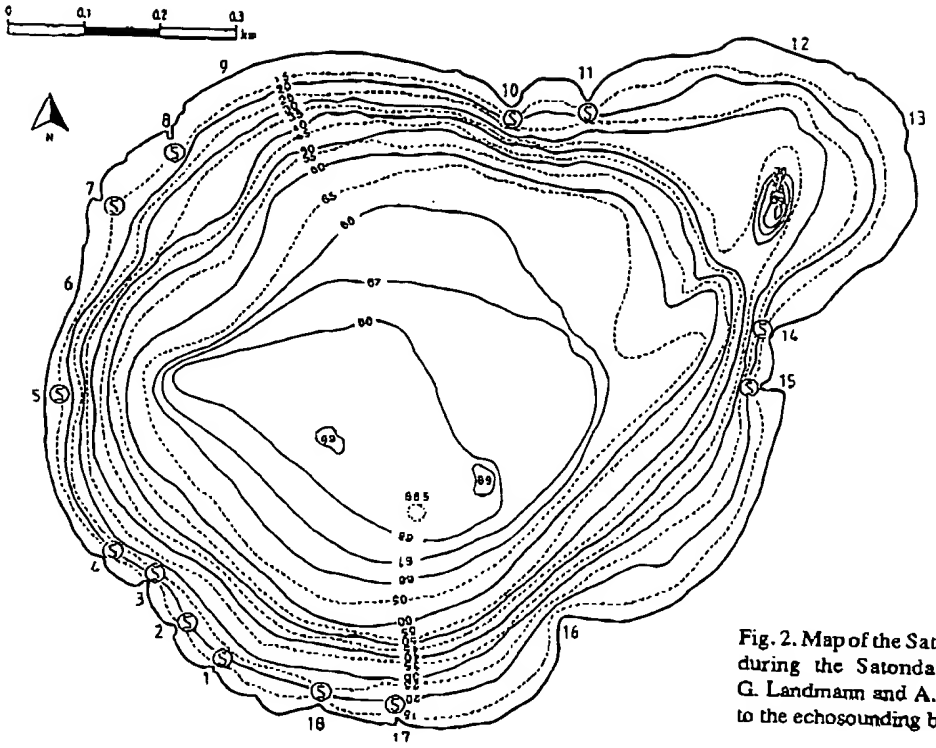

Fig. 2. Map of the Satonda Crater Lake as surveyed during the Satonda expedition by S. Kempe, G. Landmann and A. Lipp. Bathymetry according to the echosounding by H.K. Wong and U. Salge.

copied aboard the R/V Sonne for the University of Bandung. The video tapes were later copied at Hamburg and given to the Indonesian colleagues on occasion of their visit at Hamburg.

This paper documents the results of the Satonda land party and discusses some of the implications from these findings as to our understanding of the nature of the Precambrian ocean (KEMPE et al., 1992). A short account of the principal findings of the expedition has been published by KEMPE & KAZMIERCZAK (1990a). Specific aspects of the stromatolite structure have been published by KAZMIERCZAK & KEMPE (1990 and 1992).

2 GEOGRAPHIC AND GEOLOGICAL SETTING

Satonda is a small volcanic island 3 km off the northern shore of the Sanggar peninsula on Sumbawa/Indonesia (Fig. 1). Its geographical coordinates are 8°7' S and 117°45'E. The island is about 30 km away from the Tambora volcano, the last eruption of which in 1815 was the largest paroxysm of historic times worldwide (SELF et al., 1984).

The Satonda Volcano belongs to the string of Quaternary and Recent volcanoes following the inner part of the 6,000 km long Sunda Island Arc between Sumatra and the eastern Banda Sea. West of Flores, the Indian ocean plate (of Jurassic age) is subducted, while to the east of Flores the arc collides with the Australian continent. In the vicinity of Sumbawa the crust is relatively thin and its seismic characteristics are oceanic (HAMILTON, 1979). The structural elements of the arc at Sumbawa include -from south to north- the Java trench (which marks the beginning of the underthrusting of the Indian plate), the non-volcanic outer arc (mostly submarine), the inner arc basins (up to 4,000 m deep south of Lombok-Sumbawa) and the volcanic island arc. Between Java and eastern Flores most of the volcanoes occur 125 to 200 km above the active Benioff zone. At first, the Benioff zone dips at a shallow angle to the north and the volcanoes are 300 km away from the trench axis. Then the zone steepens and reaches 600 km depth within 200 km farther north under the Flores Sea (HAMILTON, 1974, 1979). The Tambora, its associated eruption centers, the Sangeang Api and Satonda occur 175 to 200 km above the Benioff zone. Satonda marks the most outward subaerial eruption center with regard to the depth of the Benioff zone in all of the Lesser Sunda Islands.

The oldest rocks on Sumbawa are Lower Miocene in age and their volcanic rocks belong to the calc-alkaline series (basalt - andesite - dacite association) normal for island arcs. The material of the Tambora and the Sangeang Api, however, is marked by an unusual potassium affinity (potassic ne-trachybasalt-trachyandesite association). Such rocks normally occur over much deeper parts of the Benioff zone and the SiO_2 - K_2O ratio is much smaller than expected for the young age of the volcanos (FODEN & VARNE, 1980; BARBERI et al., 1983 a,b). The Tambora is a large (40-50 km diameter) shield volcano made up of basaltic lava. Explosive eruptions producing pyroclastics occurred only recently. The last one, literally annihilating the 1,500 m high summit cone of the then 4,300 m high volcano, was possibly triggered by the intrusion of water into a shallow magma chamber (BARBERI et al., 1983a; SELF et al., 1984; SIGURDSSON & CAREY, 1988). The eruption ejected 50 km³ of rock (150 km³ of pumice and pyroclastics) on April 10th, 1815. On the island 92,000 people died because of the eruption or because of the following famine. Due to the stratospheric dust produced by the eruption, the summer of 1816 was extremely cold

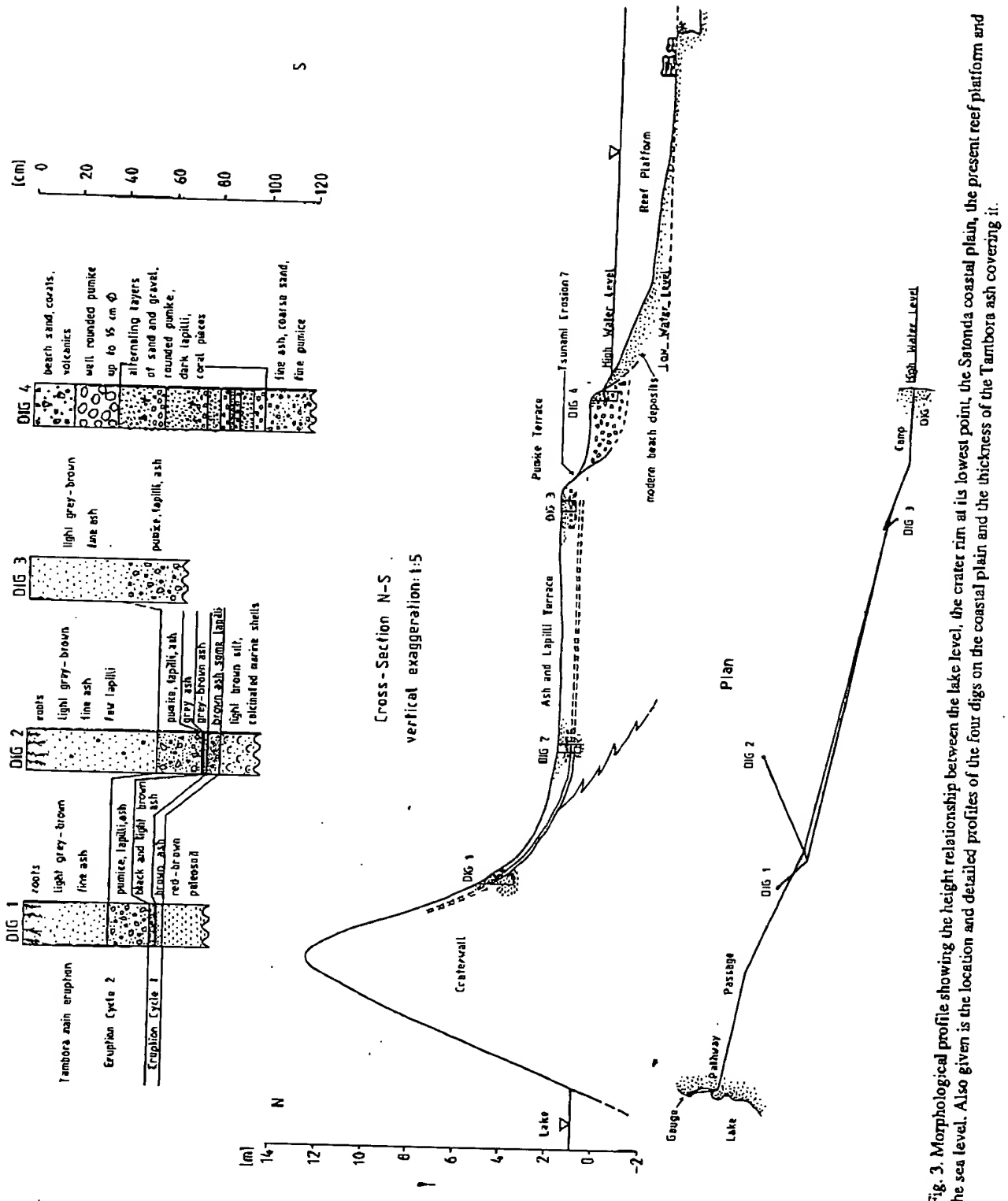

Fig. 3. Morphological profile showing the height relationship between the lake level, the crater rim at its lowest point, the Satonda coastal plain, the present reef platform and the sea level. Also given is the location and detailed profiles of the four digs on the coastal plain and the thickness of the Tambora ash covering it.

throughout the northern hemisphere (STOMMEL & STOMMEL, 1979), causing severe crop failures. In Scotland and England alone 65,000 people died because of hunger that year (SIGURDSSON & CAREY, 1988).

The island of Satonda is shown on a satellite image of the Tambora published on the front cover of th 1984 November edition of Geology. The island is about 3 x 2 km in size, with an elongated axis striking NW-SE. It forms a caldera about 2 x 2 km large and the caldera walls rise up to 300 m above sea level (a.s.l.). The eastern wall is very steep and not covered by vegetation. Here various strata of pyroclastic deposits can be seen interrupted by a few harder banks. Lava

Depth (m)	A, cumulative (km^2)	V of Layer (10^{-3} km^3)	V, cumulative (10^{-3} km^3)
0	0.772	10.98	34.10
15	0.692	3.33	23.12
20	0.642	3.09	19.79
25	0.596	2.87	16.70
30	0.554	2.63	13.82
35	0.498	2.39	11.19
40	0.457	2.22	8.80
45	0.430	2.07	6.58
50	0.402	1.93	4.51
55	0.369	1.74	2.58
60	0.328	0.30	0.84
65	0.272	0.23	0.54
68	0.067	0.03	0.03

Total area:	0.772	km^2
Total volume:	0.0341	km^3
Mean depth:	44.2	m
Maximal depth, main crater:	69.5	m
Maximal depth, small crater:	39	m
Perimeter:	3700	m
Length:	1220	m
Width:	945	m

Tab. 2. Area and volume data of Satonda Crater Lake.

No	Depth	Location	Date	Hour	Remarks
0	0.2	Satonda Bay	5/10/86	10.15	seawater, reef platform
1	0.1	Lake	5/10/86	11.15	Java sand beach, foamy
2	0.1	Lake, Sta.1	5/10/86	11.45	shallow lagoon, mats
3	0.2	Lake, Sta.1	5/10/86	12.00	in front of reef, 10 cm above algal mats
4	0.1	Lake, Sta.1	5/10/86	12.05	50 cm in front of reef
5	0.1	Lake, Sta.1	5/10/86	12.10	before reef on small bench with algal rafts
6	0.1	Lake, Sta.1	5/10/86	12.15	shallow lagoon, partly decaying algal mats
7	0.05	Lake, Sta.1	5/10/86	12.20	inner end of 10 cm deep lagoon, decaying algae, some fish
8	0.05	Lake, Sta.1	5/10/86	12.25	channel between $CaCO_3$ pillars
9	0.02	Lake, Sta.1	5/10/86	13.00	inner end of 3-4 cm deep lagoon, grey, muddy sediment, dead algae
10	0.05	Lake, Sta.1	5/10/86	12.50	30 cm wide channel between tops of $CaCO_3$ pillars
11	0.5	Lake Center	5/10/86	14.30	Secchi Depth 4.5 m
12	5	Lake Center	5/10/86	14.40	Sampler slightly open
13	10	Lake Center	5/10/86	14.50	Sampler slightly open
14	20	Lake Center	5/10/86	15.00	Sampler slightly open
15	30	Lake Center	5/10/86	15.10	Sampler slightly open
16	40	Lake Center	5/10/86	15.20	Sampler slightly open
17	50	Lake Center	5/10/86	15.30	Sampler slightly open
18	65	Lake Center	5/10/86	15.40	Sampler slightly open
20	2	Lake Center	7/10/86	08.20	air temperature 29.3°C
21	10	Lake Center	7/10/86	08.35	
22	20	Lake Center	7/10/86	09.00	
23	22	Lake Center	7/10/86	09.15	
24	24	Lake Center	7/10/86	09.25	black-brown due to manganese oxide particles
25	26	Lake Center	7/10/86	14.10	
26	30	Lake Center	7/10/86	14.20	
27	40	Lake Center	7/10/86	14.28	
28	50	Lake Center	7/10/86	14.40	
29	60	Lake Center	7/10/86	15.15	water with strong greenish tint, degasses slowly
30	55	Lake Center	9/10/86	9.00	as above
31	62	Lake Center	9/10/86	9.20	as above
32	0	Spring, Sta.16	9/10/86	10.00	spring 10 cm above lake level

Tab. 3. List of water samples, Satonda Crater Lake.

outcrops were not observed but a few intrusions, typified by dense rocks with large phenocrysts, were observed. These form hard ridges in the caldera wall and protrusions along the outer circumference of the cone. The volcano rises from about 1,000 m water depth and has the steep slope typical of tuff cones. As yet, no date is available for the last eruption of Satonda. According to the deep erosional ravines in the tuff ring, one would imagine that this eruption occurred several thousand, if not tens of thousands of years ago. Possibly the volcano was built when the sea level stood lower during the last Glacial.

The center of the island is occupied by a lake (Fig. 2). It appears to fill two individual but intersecting basins, one 950 m in diameter in the south and one 400 m in diameter in the north, giving the lake the appearance of a figure eight. The larger crater is now 69 m deep, the smaller 39 m; between them are remnants of a ridge which stand 10 m above the bottom.

The only access to the lake is from the south of the island where, at one point, the height of the crater rim is reduced to 13 m a.s.l. and the width of the wall has decreased to about 30 m (Fig. 3). Possibly the crater wall has collapsed on this side of the island, forming a semicircular bay now occupied half by a coastal plain and half by a coral platform. Another elongated plain exists at the eastern side of the island. Here a few huts have been built and the only two permanent residents of the island cultivate a few banana and cocos trees. They have a small well of brackish ground water but must import their drinking water from the main island.

The island is surrounded by coral reefs, which form extended shallows at the eastern side of the island. To the north and west, the slopes of the volcano fall steeply into the depth of the Flores Sea. There are a few beaches of mixed coarse-grained coral and volcanic sand. These beaches can be reached by rubber boat or by outrigger. The island cannot be rounded along the shore on foot because of occasional steep cliffs and because of dense vegetation. It is covered by an contiguous forest with an unpassable thorny and dense underbush.

There is rich terrestrial animal life on the island. We observed monkeys and the inhabitants reported huge pythons. Most noteworthy is, however, the large colony (possibly up to one thousand individuals) of flying foxes which rest during the day on trees in the southeastern corner of the caldera. Scorpions and large millipedes exist from which we received a few bites, luckily none with major consequences.

3 METHODS

3.1 Survey

The lake's circumference was surveyed first. In order to do so, 18 stations (S, Fig. 2) were set up at prominent points and marked by about 2 m tall poles. These poles later served as navigation aids both for echo-sounding, water sampling and coring and for points of reference in identifying the individual stromatolite stations. Next a base line was established with tape and compass between S1 and S18. This base line is 134.8 m long, striking 118°N. Then the angles between the 17 other stations and the base line were measured with a simple theodolite from each of the end points of the base line. In addition the distances were measured with a 3 m long

No.	Depth m	Temp. °C	Cond. mS/cm	pH	Eh mV	O_2 mg/l	Tot.Alk. meq/l	CO_3^{2-} meq/l	ΣCO_2 mmol/l
0	0.2	29.5	42.7	8.27	-	-	2.16	0.36	1.98
1		33.1	38.7	8.45	357	7.33	3.88	0.58	3.44
2		35.2	38.9	8.60	347	-	-	-	-
3		31.8	38.9	8.48	367	-	-	-	-
4		31.8	38.6	8.50	403	10.31	3.72	0.76	3.34
5		34.0	38.9	8.70	354	-	-	-	-
6		37.0	39.2	8.89	382	-	-	-	-
7		37.9	39.6	8.64	383	-	-	-	-
8		34.8	38.9	8.84	403	-	-	-	-
9		39.0	43.6	8.38	324	7.89	3.44	0.68	3.10
10		36.4	39.5	8.79	386	9.43	-	-	-
11	0	30.4	38.9	8.45	360	-	-	-	-
12	5	30.4	38.9	8.44	367	-	-	-	-
13	10	(30.0	38.2	8.44	356)	-	-	-	-
14	20	(28.4	39.0	8.31	350)	-	-	-	-
15	30	(29.1	44.7	7.40	-93	H_2S)	-	-	-
16	40	(29.1	42.3	7.76	-45	H_2S)	-	-	-
17	50	(29.2	42.3	7.60	-59	H_2S)	-	-	-
18	65	(29.5	41.0	7.70	-41	H_2S)	-	-	-
20	2	29.9	38.8	8.43	411	6.67	3.60	0.64	3.28
21	10	29.8	38.8	8.42	333	6.69	3.68	0.64	3.36
22	20	28.6	38.5	8.33	339	3.36	3.60	0.52	3.34
23	22	28.3	38.6	8.29	330	2.80	3.68	0.56	3.40
24	24	28.7	43.1	7.31	-66	0.00	5.76	0.0	5.76
25	26	29.7	45.4	7.13	-138	H_2S	6.60	0.0	6.60
26	30	29.8	45.4	7.27	-123	H_2S	6.44	0.0	6.44
27	40	29.0	45.4	7.33	-136	H_2S	6.56	0.0	6.56
28	50	29.0	45.5	7.12	-143	H_2S	7.72	0.0	7.72
29	60	29.2	49.5	6.92	-192	H_2S	38.8	0.0	38.8
30	55	29.1	47.8	6.90	-210	H_2S	33.88	0.0	33.88
31	62	28.9	50.0	6.87	-224	H_2S	49.6	0.0	49.6
32	0	29.2	21.3	7.08	16	-	4.56	0.0	4.56

Tab. 4. Field data from Satonda Crater Lake. ( ) = samples from leaky samplers.

measuring pole and a graded scale in the telescope of the theodolite. This worked only accurately for stations less than 150 m away while for farther away stations distances had to be estimated to ± 50 m. Triangulations and rough distances agreed fairly well and a set of survey points was thus established. The remaining coast line was added by visual inspection once the station network had been plotted at a scale of 1:2,500. Accuracy of this procedure is not very high but considered sufficient for the purpose.

The largest depth of the lake (69 m) was established first by plumb line. Later echo-sounding with a 3.5 KHz pinger system yielded a detailed bathymetric map (Fig. 2). The pinger electronics and a generator were mounted on the inflatable and the pinger was towed at its side. A total of 15 profiles were recorded between the shore stations, covering the lake like a spider web. Due to the high gas content of the surface sediments, the acoustic signal could not penetrate much of the sediments, so that the sedimentary structures remain largely unknown.

The bathymetric map was used to determine the area of the individual isobaths and the volume of the layers between isobaths (assumed to have the shape of truncated cones). The results are listed in Table 2. The total area of the lake is 0.77 km² and the total volume is 0.034 km³. The average depth of the lake is 44 m.

Poles with marks were set both in the crater and at Satonda Bay to record tides. The pole at the bay was washed away several times during the night so that a continuous water level record could not be obtained. Total water level differences amounted to over two meters during our stay. The average water level fell toward the end of our stay (neap tides) and high levels occurred during storms. Average tides amounted to about 1 m. Within the crater the water level stayed constant within the accuracy of the measurements (± 2 mm).

This observation shows that the lake level is hydraulically disconnected from the sea and that tidal waves do not penetrate the crater rim. It was therefore necessary to run a levelling between the lake and the bay (Fig. 3). The levelling was done with the spirit level of the theodolite and the 3 m long measuring bar. Accuracy is probably better than ± 2cm (mm could be estimated on the meter bar). All measurements were repeated. It was found that the lake stood 86.5 cm above the highest wash line at the bay, i.e., even at the end of the dry season, the lake did not fall below sea level. Marks on rocks show that the lake stands 105 cm higher during the rainy season. The lowest point of the passage over the crater rim was found to be 12.57 m above the wash zone or 11.7 m above the lake level.

No.	Depth m	Fe_{tot} mg/l	Mn_{tot} mg/l	Ca mg/l	Mg mg/l	Mg/Ca mol-ratio	K mg/l	Na mg/l
0	0.2	0.24	0.05	435	1283	4.86	379	10,087
1		0.35	0.07	213	1016	7.86	764	9,346
4		0.26	0.05	224	990	7.28	454	9,406
9		0.40	0.19	266	1141	7.07	491	10,361
20	2.0	0.37	0.07	216	1082	8.26	444	9,428
21	10.0	0.68	0.06	222	1056	7.84	445	9,410
22	20.0	0.37	0.05	216	1051	8.01	441	9,314
23	22.0	0.56	0.09	221	1050	7.80	440	9,355
24	24.0	0.59	2.37	259	1207	7.68	495	10,541
25	26.0	0.33	0.70	265	1247	7.75	528	11,018
26	30.0	0.31	0.39	266	1260	7.80	524	10,923
27	40.0	0.24	0.37	287	1244	7.14	526	10,935
28	50.0	0.16	0.39	279	1250	7.38	526	10,805
29	60.0	0.24	0.45	292	1395	7.87	601	11,909
30	55.0	0.26	0.52	278	1402	8.31	600	11,750
31	62.0	0.24	0.39	275	1446	8.66	603	12,036
32	0	0.11	0.04	178	605	5.60	185	4,816

Tab. 5. AAS laboratory data.

3.2 Water Samples

At the shore and close to the calcareous reefs water samples were taken with hand-held PE bottles. From the water column samples were taken with a 1.5 liter Nansen bottle mounted on a hand-held nylon line. A total of 32 samples were tak n (Table 3).

No.	Depth m	NO_3^- µmol/l	NO_2^- µmol/l	NH_4^+ µmol/l	ΣN_i µmol/l	P_{tot} µmol/l	$\Sigma N_i/P$	SiO_2 µmol/l
0	0.2	1.15	0.05	0.56	1.76	0.0	-	4.35
1		-	-	-	-	-	-	-
2		0.71	0.08	2.95	3.74	0.07	53	56.6
3		0.69	0.06	2.19	2.94	0.12	24	48.8
4		0.35	0.03	8.45	8.83	0.03	294	49.2
5		0.33	0.05	1.14	1.52	0.08	19	34.5
6		0.34	0.04	3.74	4.12	0.01	412	29.5
7		0.49	0.22	2.93	3.64	0.10	36	65.0
8		0.39	0.03	5.08	5.50	0.00	-	36.3
9		0.49	0.21	9.56	10.26	0.11	93	96.1
10		0.81	0.36	4.99	6.16	0.08	77	51.0
11	0	0.15	0.03	1.68	1.86	0.06	31	6.1
12	5	0.13	0.03	1.05	1.21	0.01	121	5.5
13	10	0.14	0.01	0.63	0.78	0.02	39	4.1
14	20	0.12	0.13	1.85	2.10	0.01	210	7.3
15	30	-	0.25	47.95	48.20	0.02	2410	37.9
16	40	-	0.22	43.61	43.83	0.12	365	10.7
17	50	-	0.24	36.53	36.77	0.33	111	19.3
18	65	-	0.27	42.20	42.47	0.68	62	00.1

Tab. 6. Ship-board data, nutrients.

When samples 12 to 18 were taken, the Nansen bottle did not close correctly, which resulted in the contamination of the sample with water from above the point where the sampler was originally closed. Except for nutrients, which therefore have to be regarded as minimum values, these samples were later retaken and re-analyzed.

The following parameters were determined immediately after recovery of the sample:

-- Temperature (with the thermoprobe of the conductometer);

-- Conductivity (with a digital hand-held WTW LF-91 conductometer, standardized versus standard 35 ‰ seawater at 20°C);

-- pH and Eh (with a hand-held digital WTW pH-91 meter and an INGOLD PT-408 combination pH-redox electrode standardized against INGOLD solutions 9896 pH = 7.385 at 25°C and 9807 pH = 9.180 at 25°C, DIN 19266 and NBS);

-- Oxygen was preserved with $MnSO_4$ and KI-KOH solution for later titration in a Winkler bottle.

-- A limited set of subsamples for $\delta^{18}O$ and $\delta^{13}C$ determination were taken.

At the field camp aliquots of the samples were acidified with HCl to pH 2 for later determination of cations concentrations (Na, K, Mg, Ca, Fe, Mn) by standard atomic absorption methods (courtesy A. Reimer). Subsamples were filtered through 0.45 µm membrane filters (MF) and through glass fibre filters (GF). The MF were also used in scanning electron microscopy. The GF were used in the analysis of suspended matter for particulate organic carbon (POC). GF filtered water was poisoned with a few drops of saturated $HgCl_2$ solution for later determination of the dissolved organic carbon (DOC).

With a HACH hand-held titrator the following parameters were determined in the field camp:

-- Alkalinity (using phenolphthalein and methyl orange as indicators and 1.6n H_2SO_4 as acid)

-- Oxygen (after WINKLER).

G. Liebezeit analyzed nutrient concentrations (NO_3^-, NO_2^-, NH_4^+, PO_4^{3-}, SiO_2) of samples 1-18 aboard the R/V Sonne a few hours after the samples had been taken according to standard methods.

Results of all chemical determinations are given in Tables 4 (field data), 5 (AAS data), 6 (nutrient data), and 7 (carbon data).

3.3 Sediment Samples

Rock samples were taken with a hammer from the stromatolitic reefs both from above the water surface and from depth by diving. The hard rock samples were dried in the sun before packaging. The divers also collected shells and other biological samples from the lake floor and the living surface of the stromatolites and took a series of underwater photographs.

One sediment core was successfully taken from the center of the deep crater at a depth of 64 m with a small gravity corer and a hand line. The location was between S17 and S10 about 1/3 of the total distance away from S10.

At the shore two digs were made in the mud between the

No.	Depth m	DOC mg/l	TOC mg/l	DIC mg/l	$DIC_{cal.}$ mg/l	POC% * (wt)	PN% * (wt)	C/N (wt)	$\delta^{18}O$ water	$\delta^{13}C$ DIC
0	0	1.2	-	23.4	23.4	-	-	-	-	-
1	0	5.4	-	39.3	41.3	-	-	-	-	-
9	0	7.5	-	36.5	37.2	-	-	-	-	-
20	2	7.1	8.3	39.8	39.4	-	-	-	+ 2.79	-
21	10	6.0	8.0	39.1	40.3	1.20	0.17	7.1	+ 3.05	- 8.44
22	20	5.6	8.4	39.0	40.1	1.09	0.16	6.8	+ 2.58	-
23	22	5.5	8.4	38.8	40.8	0.72	0.12	6.0	-	-
24	24	5.6	5.1	55.0	69.1	1.55	0.22	7.0	+ 2.93	-
25	26	4.5	3.8	59.0	79.2	1.00	0.11	9.1	-	-
26	30	6.5	5.3	60.0	77.3	1.17	0.08	14.6	-	-
27	40	9.6	6.3	58.0	78.7	0.06	0.08	7.5	+ 2.99	- 11.76
28	50	7.5	6.2	62.0	92.6	0.78	0.17	4.6	-	-
29	60	10.3	7.1	290.0	465.6	0.70	0.15	4.7	+ 2.53	- 21.36
30	55	7.2	7.2	338.0	406.6	0.67	0.10	6.7	-	-
31	62	8.4	7.8	380.0	595.2	2.54	0.29	8.8	-	-
32	0	1.0		54.3	54.7	1.06	0.11	9.6	-	-

Tab. 7. Carbon data.

DOC values determinded on samples filtered in the field, fixed with Hg Cl_2.

TOC values determinded on samples fixed with $HgCl_2$ and tightly sealed without air space.

DIC values down to sample 23 (22) were taken from DOC-bottles (filtered water), below DIC was measured in unfiltered (TOC) samples to avoid CO_2 degassing on filtration and transport as much as possible. DIC cal. values from Σ CO_2 of Table 4 times 12 (mg C/mmol CO_2/l).

* Filters made carbonate-free by H_2PO_4.

No.	Depth m	in situ T °C	Conductivity mS/cm	Salinity °/oo	Chlorinity °/oo	Sigma θ	Sigma T	Sigma 20°C
0	0.2	29.5	42.7	34.37	19.02	27.62	21.44	24.04
1		33.1	38.7	30.78	17.04	24.73	17.51	21.39
4		31.8	38.6	30.69	16.99	24.66	17.91	21.32
9		39.0	43.6	35.18	19.47	28.27	18.50	24.65
20	2	29.9	38.8	30.87	17.09	24.81	18.70	21.45
21	10	29.9	38.8	30.87	17.09	24.81	18.73	21.45
22	20	28.6	38.5	30.61	16.94	24.59	18.93	21.26
23	22	28.3	38.6	30.69	16.99	24.66	19.09	21.32
24	24	28.7	43.1	34.73	19.22	27.91	21.98	24.31
25	26	29.7	45.4	36.82	20.38	29.60	23.22	25.86
26	30	29.8	45.4	36.82	20.38	29.60	23.18	25.86
27	40	29.0	45.5	36.82	20.38	29.60	23.45	25.86
28	50	29.0	45.0	36.91	20.43	29.67	23.52	25.93
29	60	29.2	49.5	40.60	22.47	32.65	26.23	28.64
30	55	29.1	47.8	39.02	21.60	31.38	25.08	27.48
31	62	28.9	50.0	41.06	22.73	33.03	26.69	28.99
32	0	29.2	21.3	15.90	8.80	12.77	7.78	10.27

Tab. 8. Calculated data, salinity, density.

Sample No.	Depth m	Na	K	Mg	Ca	Sr	Cl	SO_4	Br	F	Alk.tot
						meq/kg					
0	0.2	460.8	9.46	102.23	21.20	0.18	535.4	55.45	0.83	0.07	2.109
1		421.1	19.31	81.16	10.41	0.16	477.7	49.67	0.74	0.06	3.799
4		428.8	11.37	79.09	10.94	0.16	476.4	49.52	0.74	0.06	3.642
9		491.7	12.26	90.86	12.95	0.18	546.9	56.76	0.85	0.07	3.357
20	2	425.2	11.12	86.43	10.55	0.16	479.3	49.81	0.74	0.06	3.524
21	10	427.0	11.14	84.35	10.84	0.16	479.2	49.81	0.74	0.06	3.603
22	20	423.1	11.04	83.97	10.55	0.16	475.2	49.38	0.74	0.06	3.525
23	22	424.5	11.02	83.88	10.80	0.16	476.5	49.52	0.74	0.06	3.603
24	24	478.8	12.36	96.14	12.62	0.18	537.5	56.03	0.84	0.07	5.623
25	26	510.8	13.16	99.18	12.89	0.19	569.4	59.41	0.89	0.07	6.434
26	30	509.8	13.06	100.22	12.94	0.19	569.6	59.41	0.89	0.07	6.278
27	40	510.0	13.11	98.94	13.96	0.19	569.5	59.41	0.89	0.07	6.395
28	50	511.5	13.11	99.41	13.57	0.19	569.8	59.55	0.89	0.07	7.525
30	55	534.3	14.93	111.33	13.50	0.20	577.4	62.96	0.94	0.08	32.974
29	60	561.5	14.94	110.65	14.17	0.21	597.2	65.50	0.98	0.08	37.720
31	62	566.3	14.99	114.66	13.34	0.21	594.0	66.25	0.99	0.08	48.203
32	0	212.3	4.68	48.86	8.79	0.08	244.2	25.65	0.38	0.03	4.514

Tab. 9. Measured and calculated total ionic composition.

stromatolites. Samples were collected in plastic bags. Four further digs were made at the outer slope of the crater rim, in the coastal plain, on the beach wall and directly on the beach in order to sample the Tambora ash and the underlying strata (Fig. 3).

4 DISCUSSION OF HYDROCHEMICAL DATA

The water samples can be grouped into several categories:
— seawater from Satonda Bay (sample 0),
— lake water from lagoons between stromatolitic reefs (samples 1-10),
— lake water from a depth profile at the center of the lake (samples 11-31), and
— water from a small spring 10 cm above lake level near S16 (sample 32).

The discussion will center on the samples from the depth profile and will use sample 0 as a reference sample.

4.1 Recalculation procedures

Before the measured values could be interpreted geochemically, it was necessary to calculate standard parameters such as salinity, density, formality (mol/kg) and a charge-balanced main ion distribution. Salinity, chlorinity and density were calculated from the standardized conductivity and temperature measurements. Results are given in Table 8. Then a model main ion composition was calculated by using the salinity/ion ratios given for seawater by MILLERO (1974). Next, the measured K, Mg, Ca and alkalinity concentrations were recalculated for formalities (by using the calculated density) and inserted into the ion composition model. This step offsets the salinity/ion ratio of the minor ions slightly and makes small adjustments of the Na and/or Cl concentrations necessary. In order to do these calculations conveniently, BASIC programs were written. The final result, a charge balanced model of the major ion composition in accord with the measured salinity, is given in Table 9.

In turn, the major ion composition served as input for a computerized carbonate model. The program WATMIX (WIGLEY & PLUMMER, 1976) calculates all parameters of the carbonate system in seawater taking respect of all ion pairs. The main outputs are the CO_2 pressure of the water plus the saturation indices (SI) of the minerals calcite and dolomite (SI_{Cc} and SI_{Dol}). The results of this calculation are given in Table 10. The chemistry of seawater carbonate systems is explained, e.g., in KEMPE (1982), BROECKER & PENG (1984), PEGLER & KEMPE (1988) and KEMPE & PEGLER (1991).

4.2 Stratification of the lake

In Fig. 4 the salinity profile of the lake is plotted. It reveals three distinct layers:

1) A mixed surface layer 22.8 m deep (exact depth established by diving) with a salinity of 30.6-30.9 ‰, i.e. 90 % of the salinity at Satonda Bay (sample 0). This layer has a total volume of 0.0215 km^3, i.e. it contains 63 % of the total lake volume (V_{tot}). Temperature in this layer was 29.9°C down to 10 m and below 29°C in its deeper part, suggesting that a seasonal thermocline had developed during the dry and sunny season of the year. As a consequence of this heating, evaporation was able to slightly increase the salinity in the upper ten meters compared to the layer below (cf. Table 8).

2) A well mixed middle layer down to a depth of about 50 m with a salinity of 36.8-36.9 ‰, i.e., 108 % of the salinity

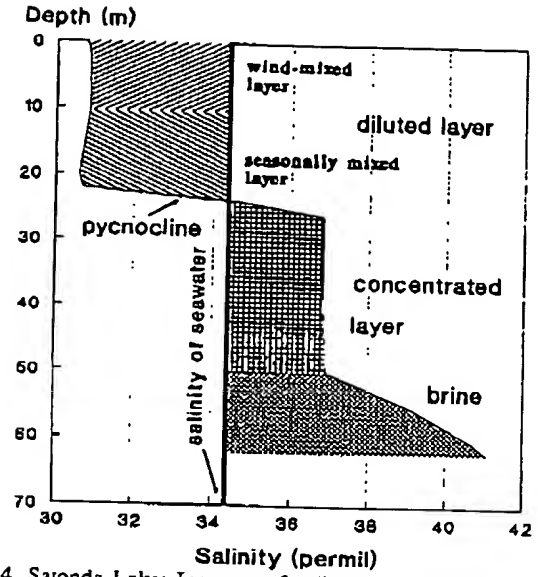

Fig. 4. Satonda Lake: Increase of salinity with depth. Vertical structure of water column.

of the surrounding seawater. The layer has a volume of 0.0081 km³, i.e. 24 % of V_{tot}.

3) A deep layer between 50 m depth and the bottom with an increasing salinity reaching 41.06 ‰ in the deepest sample recovered (118 % of surrounding seawater). The volume of this layer is 0.0044 km³ or 13% of V_{tot}. Temperatures stay at around 29°C throughout the deeper water column, excluding the possibility of a larger source of hydrothermal water.

The upper and the middle layers are separated by a very steep pycnocline. Between 22 and 26 m depth the density increases by 4 $\sigma\vartheta$ units (Table 8). For comparison: in the Black Sea, the most stably stratified larger body of seawater known, the density difference amounts to 3 $\sigma\vartheta$ in 200 m only. Thus, Satonda Crater Lake shows an extremely stable stratification. This pycnocline was discovered rather unexpectedly. Because Satonda is situated in the tropics we expected that the evaporation during the dry season would increase the salinity in the surface layer enough to cause convection of the total lake volume as is typical for most tropical lakes (polymixis). Thus the stratification must be a feature attesting to some unusual vent in the history of the lake.

The consequences of this stratification is seen when a variety of other parameters measured is plotted versus depth (Fig. 5): At the interface, the redox potential drops from values typical for fully oxygenated water (330-410 mV) to negative values within 2 m and H_2S smell is present in all samples below 24 m. As is typical for such interfaces, a manganese oxide particle layer exists slightly above the 0-redox potential interface at exactly 22.8 m (by diving). Looking along the layer, it appeared to be a midwater lake floor and a hand put into it disappeared like in a magician's trick: no light can penetrate into the Mn-oxide layer. In fact, the reducing conditions below the pycnocline are more intense than in the Black Sea (Kempe, unpublished cruise reports) but similar to the Black Sea the concentration of total Mn increases significantly below the pycnocline when the Mn^{4+} is reduced to the more soluble Mn^{2+} ion. At the interface (Table 5) a total of 2.37 mg Mn/l were measured, much more than in the Mn-particle layer of the Black Sea. The concentration of iron is, however, larger in the surface layer then in the reducing layer (0.3-0.6 mg/l versus 0.16-0.31 mg/l) even though iron is also completely reduced in waters of <-100 mV. The explanation for this decrease in spite of the increased solubility is the formation of insoluble iron sulfides which remove the iron from the water column as fast settling particles.

As is expected in reducing waters, ammonia is the main nitrogen-bearing species and it increases considerably below the pycnocline. It is, however, also the main species in the oxygenated part of the water column, possibly indicating a slow upward loss of this nutrient by diffusion from the middle layer or its production in the water. In contrast to open ocean conditions, concentrations of nitrate are always lower than those of ammonia. Nitrite increases below 20 m. Total reactive phosphorus content of the water increases significantly only below 40 m and not at the pycnocline. This finding is different from that from the Black Sea where a P maximum occurs at the onset of the H_2S increase (e.g., KEMPE et al., 1991). The mol ratio of total inorganic nitrogen to total phosphorus is even more interesting: it is always higher than the Redfield ratio of 15, which is characteristic of seawater in general (BROECKER & PENG, 1984). This indicates that the lake receives, in contrast to phosphorus, a surplus of nitrogen or generates it internally. The N/P ratio even increases in the middle layer, reaching over 2,000 at 30 m. At this depth nitrogen bearing material settling from above seems to be remineralized preferentially.

The waters of the lake appear to be murky and the Secchi depth

No.	Depth m	Ionic Strength	$pPCO_2$	PCO_2 ppmv	CO_2 mmol/kg	SI Cc	SI Dol	SI Gyp
0	0.2	0.655	3.51	309	0.008	0.73	2.39	-0.63
1	-	0.578	3.44	363	0.009	0.88	2.91	-0.93
4	-	0.576	3.53	297	0.008	0.90	2.93	-0.91
9	-	0.662	3.43	369	0.008	0.88	2.88	-0.82
20	2	0.581	3.45	351	0.009	0.81	2.78	-0.93
21	10	0.581	3.43	372	0.010	0.82	2.79	-0.92
22	20	0.576	3.32	476	0.013	0.73	2.60	-0.93
23	22	0.577	3.26	546	0.015	0.72	2.57	-0.92
24	24	0.654	1.99	10120	0.270	0.09	1.31	-0.85
25	26	0.692	1.75	17740	0.459	-0.01	1.12	-0.84
26	30	0.692	1.90	12450	0.321	0.12	1.38	-0.83
27	40	0.692	1.96	10890	0.286	0.21	1.52	-0.80
28	50	0.693	1.68	21090	0.554	0.07	1.24	-0.81
29	60	0.753	0.78	167100	4.313	0.58	2.28	-0.79
30	55	0.727	0.81	153500	3.990	0.48	2.11	-0.81
31	62	0.759	0.62	238800	6.195	0.61	2.36	-0.81
32	0	0.303	1.78	16480	0.471	-0.25	0.46	-1.04

SI = Saturation Index

Tab. 10. Carbonate system data.

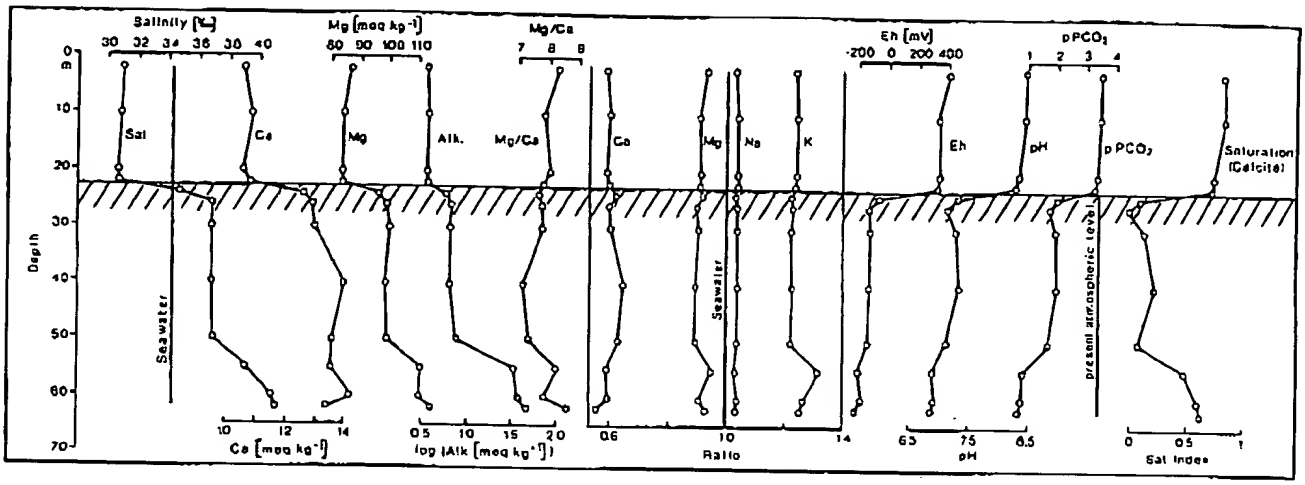

Fig. 5. Hydrophysical and hydrochemical structure of water column of Satonda Crater Lake, October, 1986 (for data see samples 20 to 31 in Tables, for explanations of variables see Tables and text). „Ratio" curves refer to elemental ratios between seawater and Satonda Lake water with seawater having the ionic composition at the respective Satonda salinities. Note that CO_2 pressure is given as negative decadic logarithm ($pPCO_2$). Concentration of alkalinity is also given in logarithmic form.

was only 4.5 m. However, tows with a ± 50 µm plankton net did not yield any larger phyto- or zooplankton specimens. Near the reefs abundant fecal pellets of gastropods were caught.

Filters clogged easily, demonstrating the presence of very fine and 'slimy' organic matter probably of bacterioplankton origin. DOC concentrations are very high throughout the water column, values range between 5.4 and 10.3 mg/l (for comparison: Satonda Bay water had 1.2 mg DOC/l, a common value for surface seawater) (Table 7). The particulate matter collected on the filters had C/N values at about the Redfield ratio (C/N = 7), i.e., they were typical of average organic matter. Possibly the contribution of cyanobacteria to the plankton in the water and their nitrification heterocysts influence the C/N ratio. Inspection of some of the filters by SEM showed in fact cyanobacteria chains (*Anabaena*-like). Also small pennate diatoms, coccolithophorids and curled rods (bacteria?) were found in addition to undefined organic debris and some mineral grains.

All the major ions (Fig. 5) increase significantly in concentration at the interface and in the bottom layer. This increase is, however, largely in proportion to the salinity increase; the ratios of Ca, Mg, K and Na to the concentrations these elements would have in seawater of identical salinity change little with depth (Fig. 5, center). In other words, the relative major ion composition of the lake water is nearly constant. The main difference to seawater is the enrichment of the alkalinity and the depletion of alkaline earth ions. In particular, Ca is depleted to 60% of its amount in normal seawater.

4.3 Carbonate system

The only major parameter which increases with depth in excess of the salinity increase is alkalinity. Measured values in the surface, middle and bottom layers amounted to 3.5-3.8, 6.2-7.5 and 33-48 meq/kg respectively. Compared to seawater (2.1 meq/kg in Satonda Bay, Table 9, sample 0) it is greatly enriched in the lake.

This increased alkalinity is responsible for the high pH of 8.4-8.9 in the surface layer as compared to 8.1-8.3 for surface seawater (Fig. 5., Table 4). Calculation of the CO_2 pressure (PCO_2) (Table 10) shows that the surface layer (PCO_2 = 300 - 370 ppmv) is in equilibrium with the atmosphere (PCO_2 = 350 ppmv). However, this PCO_2 increases very rapidly with depth. In the middle layer values between 10,000 and 20,000 ppmv were measured while in the bottom layer the PCO_2 increased to over 200,000 ppmv (or 0.2 atm.). In fact, the high PCO_2 causes a water sample raised to the surface to degass spontaneously. If this pressure were to

Plate 1 Stromatolites and sponge, Satonda Crater Lake, Indonesia, October 1986

Fig. 1. Circular and semicircular stromatolitic reefs protruding above the water level of Satonda crater lake at the end of the dry season, station 1, 5. 10. 1986

Fig. 2. Underwater photograph of living stromatolite surface at a depth of ca. 17 m, station 1. Scale of picture ca. 40 cm

Fig. 3. Sponge (*Suberites* sp.) growing on the stromatolite surfac . In the background uncalcified green algae. A few specimen of the gastropod *Rhinoclavis sinensis* (Cerithiidae) (GMELIN, 1791) graze on the sponge (center). Height of sponge 8 cm.

Fig. 4. Calcareous stromatolitic reefs exposed at the end of the dry season, 12. 11. 1984. Reefs in the foreground form fringes around volcanic rocks. Reef in the center extends to more than 22 m of water depth. The caldera walls in the background of the lake (1 km in diameter) rise up to 300 m above sea level.

Plate 1

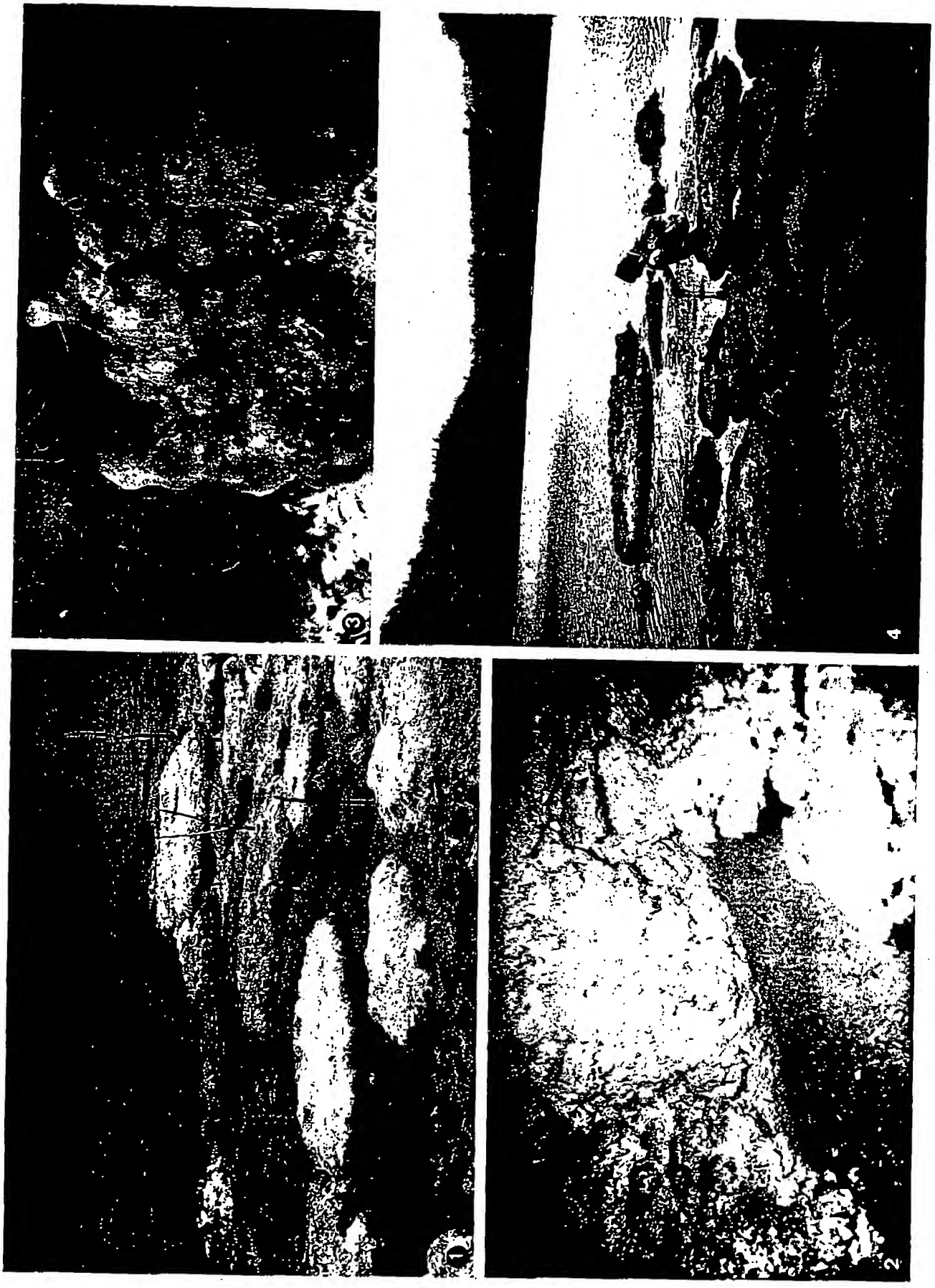

increase by a factor of 30, then th PCO_2 would match the hydrostatic pressure of the water column and the lake could degass spontaneously similarly to the 1986 disaster of Lake Nyos in Cameroon (KLING et al., 1987).

The increase of the PCO_2 causes the pH to decrease drastically with depth (Fig. 5, Table 4). Across the pycnocline the pH decreases by 1 unit in a few meters. In the bottom layer pH values of below 7 were recorded.

These low pH values mask in a sense the true alkaline nature of the water. If one would degas water from the middle and bottom layers and bring them into equilibrium with atmospheric PCO_2 the water would acquire considerably larger pH values. Such a degassing can be done numerically with the WATMIX program. Sample 31 from a depth of 62 m would assume a pH of 9.17 and sample 25 taken at a depth of 26 m would assume a pH value of 8.61 if degassed to a 350 ppmv PCO_2 without changing their composition.

The large alkalinity of the lake can clearly be attributed to the bicarbonate and carbonate ions present, i.e., to dissolved inorganic carbon (DIC). By comparing the DIC calculated from alkalinity titration with the independently determined DIC in poisoned samples (Table 7), one sees that they are very similar in the surface water (samples 0, 1, 9, 20, 21, 22). In bottom waters, the measured DIC is always smaller than the calculated DIC. This is expected because samples degassed their excess CO_2 during transport and precipitated $CaCO_3$.

The high alkalinity leads to a concentration of CO_3^{2-} in the surface layer of 0.5 to 0.9 meq/l, values much higher than in normal surface seawater (Satonda Bay: 0.36 meq/l). This fact is very important, because one could assume that the lower Ca concentration would cause a lower calcite saturation in the lake than in seawater. If one calculates the calcite saturation index (SI_{Cc} = the logarithm of the ratio between the ion activity product of $[Ca^{2+}]$ and $[CO_3^{2-}]$ and the dissolution constant at the in situ temperature), then one finds that Lake Satonda is in fact much more supersaturated with respect to calcite than normal surface seawater (Table 10, Fig. 5). SI_{Cc} of 0.8 to 0.9 were found in the surface samples of Satonda whereas normal surface seawater has a SI_{Cc} of 0.4-0.6 (e.g., PEGLER & KEMPE, 1988). At the pycnocline the SI_{Cc} is drastically reduced but it never becomes undersaturated at depth in spite of the large increases in PCO_2. This is because of the concomitant large increase in the alkalinity. Calcite particles settling to the lake bottom will not therefore be dissolved under present chemical conditions and the sediment in fact contains carbonate minerals (see section 6.3). Dolomite is, as under open ocean conditions, much more supersaturated than calcite (Table 10).

The origin of the large amounts of DIC in the lake (as ΣO_2 and alkalinity) was revealed by $\delta^{13}C$ measurements (Table 7). Samples from 10, 40 and 60 m depth yielded -8.4, -11.8 and -21.4 ‰ PDB, respectively. This suggests that the DIC is a mixture of marine DIC ($\delta^{13}C$ close to 0 ‰) and biogenic carbon ($\delta^{13}C$ close to -25 ‰) with ratios of 66:34, 53:47 and 14:86 % in the three layers. Contrary to what we first expected, volcanic CO_2 does not seem to play a significant role ($\delta^{13}C$ close to -7 ‰). Washed in and decaying plant debris from the crater rim is most probably the main cause of the high PCO_2 in the lake.

During the decay of the organic matter under anaerobic conditions, sulfate is reduced and the charge originally balanced by it is transferred to a bicarbonate formed from free CO_2 and H_2O, causing the alkalinity to rise. This

Plate 2 Recent and fossil gastropods and bivalves, Satonda Crater Lake, Indonesia, October 1986. EDAX structure of stromatolite

Fig. 1. Shells of the only gastropod species *Rhinoclavis sinensis* (Cerithiidae) (GMELIN, 1791) living in Satonda Crater Lake. Dense population of this gastropod is associated with the living cyanobacterial-red algal cover of the calcareous reefs. Station 1, depth 50 cm; scale bar = 1 cm

Fig. 2. Fossil (ca. 4,000 years old) specimens of the above illustrated gastropod species. Compared with the living forms the fossil specimens which thrived during the early period of Satonda Crater Lake history are slightly larger, better ornamented and have thicker shells. Station 1, dig 1 (level 30-50 cm); scale bar = 1 cm

Figs. 3., 4., 5. Examples of shelled molluscs living in Satonda Crater Lake during its early history (ca. 4,000 years ago): Fig. 3: specimens of another species of cerithiid gastropod, Fig. 4: muricid gastropod *Ocenebra* sp., Fig. 5: venerid bivalve ? *Lioconcha* sp. Station 1, dig 1 (level 30-50 cm); scale bar = 1 cm

Fig. 6. Subfossil shells of the bivalve *Pinctada* sp. overgrown by serpulids and calcareous cyanobacterial crust. Specimens collected from the lake bottom near the steep cyanobacterial-red algal calcareous reef wall. Sample 28, station 17, depth 19-21 m; scale bar = 3 cm

Fig. 7. EDAX-spectra of the section Fig. 8 showing the relative abundance of Mg, Si, S, cl and Ca in the aragonitic layer (dotted line) and in the high Mg-calcitic layer (hatched curve). Note the high Mg concentration in the calcitic compared to the aragonitic layer.

Fig. 8. SEM view of cross-fractured and EDTA-etched fragment of the Satonda Crater Lake fossil calcareous stromatolite (for transmitted light picture see Plate 8, Fig. 6), showing the contact between the in vivo with high Mg calcite permineralized coccoid cyanobacterial layer and the post mortem with aragonite permineralized layer of decomposed coccoid cyanobacteria.

Fig. 9. EDAX-mapping of the same section showing magnesium distribution within both layers; scale bar for Fig. 8 and Fig. 9 = 3 µm.

Plate 2

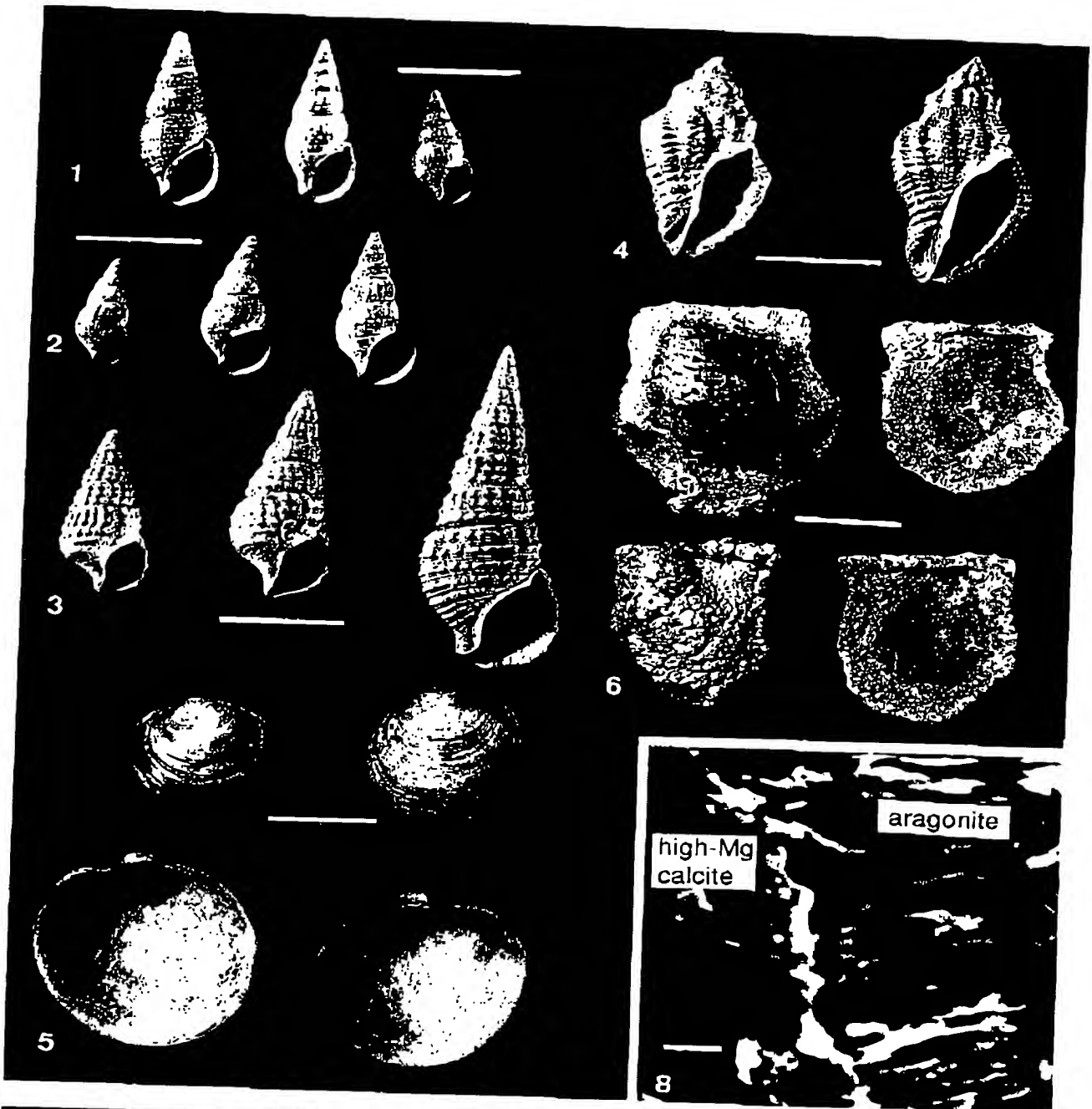

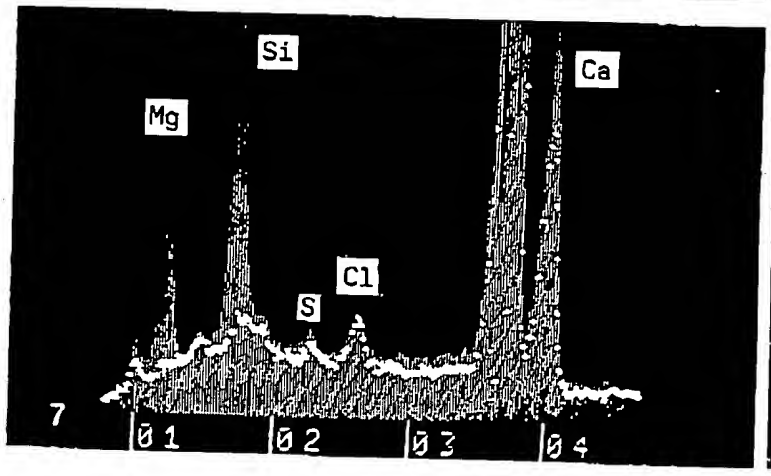

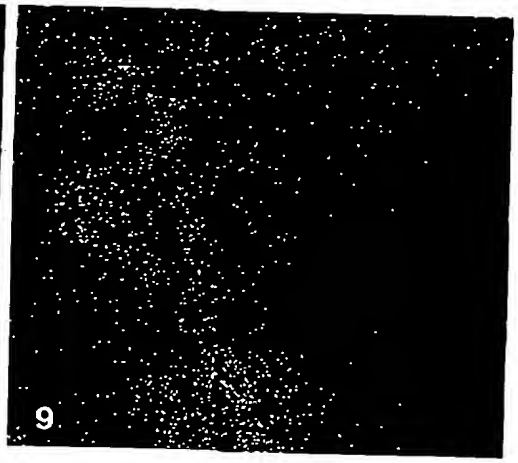

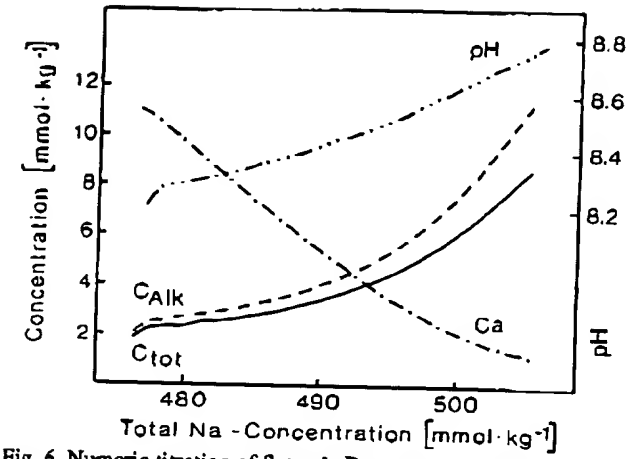

Fig. 6. Numeric titration of Satonda Bay seawater by incremental addition of $NaHCO_3$ (X-axis) and subtraction of $CaCO_3$ to stabilize supersaturation at +0.81 SI_{Ca}, calculated with WATMIX (WIGLEY & PLUMMER, 1976), calculations assume an open system with a PCO_2 of 350 ppmv. Titration starts at left with seawater less than +0.81 SI_{Ca} but quickly reaches the threshold SI_{Ca} from where on $CaCO_3$ is subtracted to keep supersaturation constant (note inflection in curves). The increase in pH, total alkalinity (C_{Alk}), and ΣCO_2 (C_{tot}) is shown as well as the decrease in Ca concentration.

alkalinity producing process was termed 'alkalinity pump' (KEMPE, 1990). Additional alkalinity could be generated by the dissolution of volcanic glass in the lake, i.e., by silicate weathering under a high PCO_2. Silicate weathering would cause the release of additional cations, mostly Na^+ and K^+. How much each of these two processes have contributed to the large increase in alkalinity in Satonda Lake cannot be calculated from the current data set because sulfate and H_2S concentrations were not measured and Na^+ concentrations cannot be determined precisely enough by AAS due to its high concentration.

One can, however, model the process of alkalinity addition numerically. Such a calculation with a modified WATMIX program is shown in Figure 6 where $NaHCO_3$ was added to the composition of normal seawater in increments, so that the alkalinity is increased gradually. This causes an increase in the SI_{Ca} and as soon as the threshold value was reached (+0.81) $CaCO_3$ was subtracted by the program in an amount to keep the solution at the threshold SI_{Ca}. This threshold value was chosen since in Satonda and in other stromatolite forming environments massive calcite precipitation proceeds at this value (KEMPE & KAZMIERCZAK, 1990b). It was further assumed that the system was open, i.e., in equilibrium with atmospheric PCO_2 (340 ppmv). Starting from normal seawater composition, the solution increases in alkalinity (C_{Alk}), in total dissolved carbonate (C_{tot}) and in pH but decreases in calcium concentration. At a pH of 8.4 the Ca concentration and the alkalinity roughly match the actual concentrations in Satonda Lake surface waters. Satonda water has, however, a somewhat lower Na concentration since it is diluted by 10 % relative to seawater.

4.4 Samples from lagoons among calcareous reefs

The first 10 water samples (Table 3, for locations see Fig. 7) were from lagoons among the algal reef of S1. They illustrate how water composition can differ over short distances in the shallow pools on top of the calcareous reefs which are filled with dense carpets of *Cladophoropsis*.

A few regularities can be noted in the data: All of the reef associated samples are much warmer than in the open water (at least during the daytime). Samples 6, 7, 9, and 10 taken in inner lagoons have significantly higher conductivities than at the open lake surface. This is due to intense evaporation in these shallow pools. Near photosynthesizing mats oxygen and pH values are higher than at the lake surface (i.e., PCO_2 is lower). Nutrient concentrations are highly variable (Table 6). Nitrite concentrations are highest landward (samples 7, 9, 10). Ammonia concentrations are higher

Plate 3 Recent green algae, and macroscopic views of stromatolites, Satonda Crater Lake, Indonesia, October 1986

Figs. 1.-3. Green algae associated with the cyanobacterial-red algal living cover of the calcareous reefs in Satonda Crater Lake: 1: *Cladophora* sp., 2: *Cladophoropsis* sp., 3: *Chaetomorpha* sp., scale bars = 500 µm

Fig. 4. Vertical section through the highly porous calcareous crust near the living surface. Arrow indicates the sharp boundary between the younger, upper part of the specimen composed predominantly of calcified thalli of crustose red algae (*Peyssonnelia* and *Lithoporella*) alternating with layers of calcified coccoid cyanobacteria (the cyanobacterial-red algal zone) and the older lower part of the specimen built almost exclusively by weakly laminated, clotty cyanobacterial carbonate encompassing numerous shells of cerithiid gastropods and tubes of serpulids (the peloidal zone). Sample 29, station 17, depth 23 m; scale bar = 2 cm

Fig. 5. Top view of the strongly mammilated living surface of the cyanobacterial-red algal calcareous reef. Sample 5, station 7, depth 3 m; scale bar = 1 cm

Fig. 6. Vertical section through the cyanobacterial-red algal zone of the calcareous reef overgrowing a large lava block extending slightly above the water table. The specimen is composed of foliaceous thalli of calcified squamariacean red algae (*Peyssonnelia* sp.) alternating with layers of variously calcified coccoid cyanobacteria; these two components are arranged in indistinct vertical columns. Sample 46, station 10; scale bar = 3 cm

Fig. 7. Cross-section of a calcareous pipe formed by cyanobacterial-red algal encrustation around a tree branch sunken in the lake (now decayed). The whitish outer zone of the specimen is built predominantly of calcareous red algae, whereas the rest is composed almost exclusively of calcified aggregates of coccoid cyanobacteria. Sample 86, station 7, depth 6 m; scale bar = 2 cm

Plate 3

among the mats than in the open water. Highest phosphorus values correspond to highest temperatures (samples 7 and 9) indicative of the release of nutrients in water too warm for algal activity. Sample 9 has also high SiO_2, Fe, Mn, and DOC concentrations but a low alkalinity, a low measured DIC concentration and the lowest Mg/Ca ratio of all samples. The PCO_2 was near atmospheric pressure and the SI_{ca} not higher than in the other samples. The lagoon of sample 9 was filled with decaying algae and dead gastropods, a place which has experienced first intensive photosynthesis and then aerobic remineralization.

These samples illustrate that the water chemistry near the algal mats is highly variable according to season, weather, time of day, water level and biological activity admitted by these factors. This fact is important to the discussion of carbonate precipitation on the cyanobacterial mats.

5 DISCUSSION OF SEDIMENT ANALYSES

5.1 Calcareous reefs

5.1.1 Setting and macroscopic appearance

Massive calcareous reefs occur along the lake shore at thirteen rocky points (Fig. 2). The largest reef bodies are located on the southwestern shore of the lake (S 1-4 and S 16-18). The reefs appear typically as low mounds or irregularly shaped crusts 0.5-1.2 m in thickness (Figs. 7-8). They grow outward from the steep substratum as lobated overhanging ledges. The living cover of the reefs has been observed by direct diving down to the O_2/H_2S interface. Dead reef surface has been observed below the chemocline, testifying deeper extension of the oxic layer in the past. The top of the reefs is almost flat with slightly raised outer edges covered with strongly corroded subcircular heads emerged about 30 cm above the water level at the end of the dry season (October 1986) (Pl. 1/1, 1/4).

The submerged reef surface has, down to the depth of ca. 8 m, a cauliflower-like appearance due to the presence of numerous granules, mammilae and knobs, a few mm to 2 cm high (Pl. 3/5). Deeper, it is distinctly smoother, bearing in places low cyst-like elevations (Pls. 1/2; 3/4).

The outer 10-15 cm of the reef are highly porous and briule. Older parts of the reef structure are built of massive, hard limestone (Pl. 3/6).

Calcareous crusts of various thickness have also been observed on pieces of wood and tree branches washed into the lake from the crater wall. The woody material is often decayed, leaving calcareous tubes and chimneys behind (Pl. 3/7).

5.2.2 Living reef surface

Reef-forming biota

The biota taking part at present in the reef formation consists chiefly of in situ calcifying mats of coccoid cyanobacteria (*Pleurocapsa* group, sensu Rippka et al., 1981; see e.g., Pls. 5/5 and 6/4, 6) intergrowing with two kinds of crustose red algae: the monostromatous corallinacean Lithoporella sp. (e.g., Pls. 5/2; 6/7; 7/1) and the less abundant squamariacean *Peyssonnelia* sp. (e.g., Pls. 4/6, 5/1-3). At depths below 12 m down to the O_2/H_2S interface nubecullinid foraminifers participate also significantly in the reef framework formation (Pls. 5/4 and 6/1). Aggregations of nubecullinid calcareous tests encrust particularly densely shadowed reef surfaces such as overhangs, crypts and cavities. Individual nubecullinid tubes also occur, though rarely, on the reef surface at lesser depths and on better illuminated areas. The main groups of the reef-forming organisms are distributed on the reef surface in patches leaving some places uncolonized. Periodic (probably seasonal) domination of one group over the other is visible in the recent history of the reef communities. During the time of our stay, the reef surface was largely covered by a thin film of soft or only weakly encrusted pleurocapsalean cyanobacteria over-growing mostly non-living thalli of *Lithoporella* and

Plate 4 Diatoms, coccolithophorid and red algae associated with the cyanobacterial stromatolites, Satonda Crater Lake, Indonesia, October 1986.

Fig. 1. SEM picture of a colony of pennate diatom (*Fragilaria* sp.) from the surface of a calcified coccoid cyanobacterial layer. Sample 11, station 11, depth 9 m; scale bar = 30 µm

Fig. 2. Enlarged fragment of the above showing a broken specimen of a smaller benthic pennate diatom *Mastogloia* sp.; scale bar = 3 µm

Fig. 3. SEM picture of an almost intact coccolithophorid coccosphere (*Syracosphaera mediterranea*) from the surface of a calcified cyanobacterial layer. Sample 10, station 7, depth 8 m; scale bar = 10 µm

Fig. 4. Magnification of the above to show the details of the coccoliths and the granular character of the $CaCO_3$ covering the cyanobacterial aggregates; scale bar = 3 µm

Fig. 5. Vertical section through the uppermost part of the calcareous cyanobacterial-red algal zone demonstrating the rapid changes in the crust-forming biota and associated sediments; a: layer dominated by the crustose coralline algae *Lithoporella* sp. intergrowing with variously calcified pleurocapsalean cyanobacteria; b: layer built of closely adhering crustose thalli of the squamariacean red algae *Peyssonnelia* sp.; c: layer of silicified coccoid cyanobacterial aggregates; d: layer of clotty (thrombolitic) micrite; e: layer composed of loosely distributed foliaceous thalli of the squamariacean red algae *Peyssonnelia* sp. alternating with irregular accumulations of pelletoid and clotty (peloidal) calcareous material. Sample 29, station 17, depth 23 m; scale bar = 500 µm

Fig. 6. Continuation of layer e from above to show the squamariacean framework of the crust and the pelletoid-peloidal character of the internal sediment filling partially the spaces between the foliaceous thalli of the red algae; scale bar = 500 µm

Plate 4

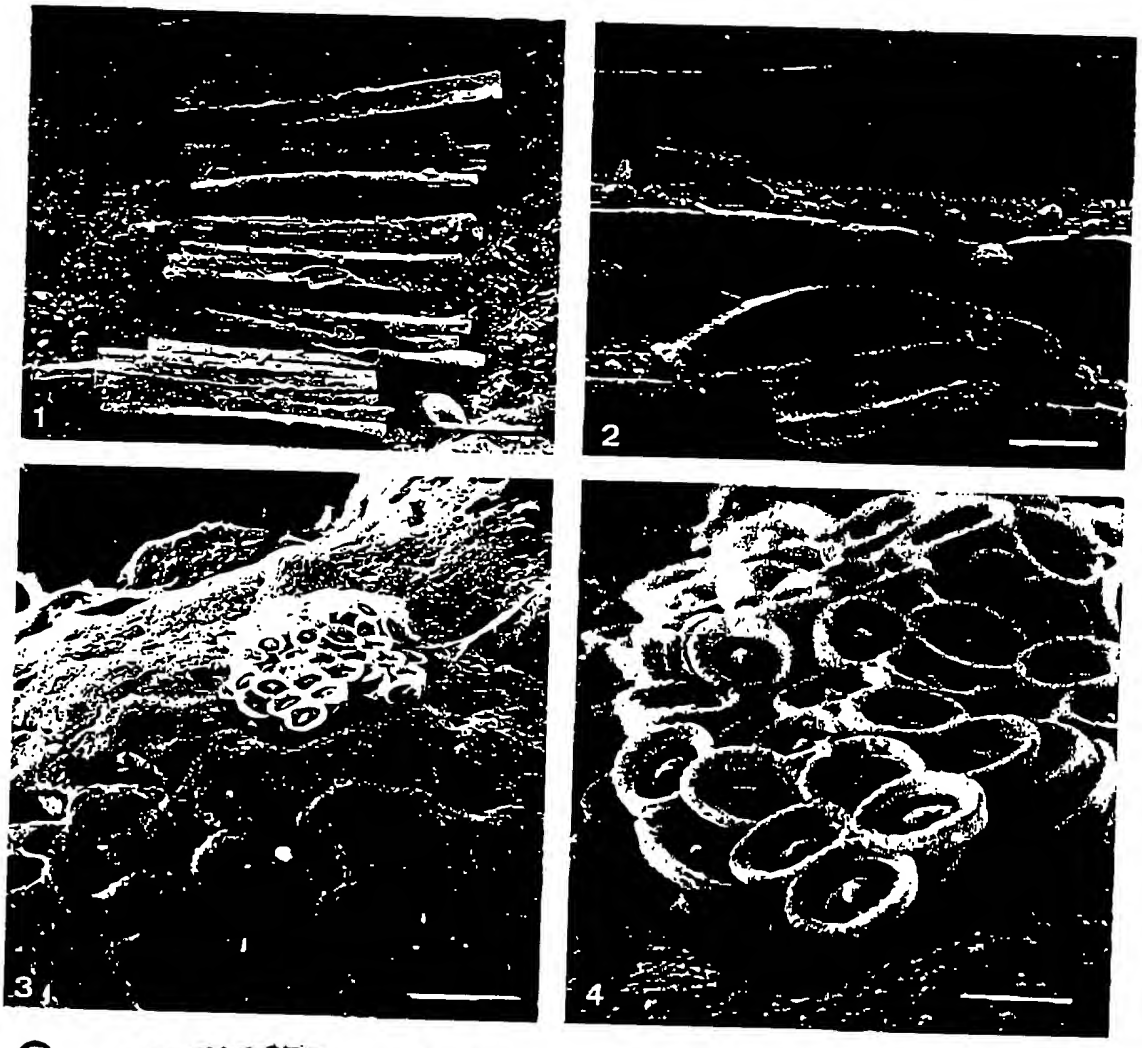

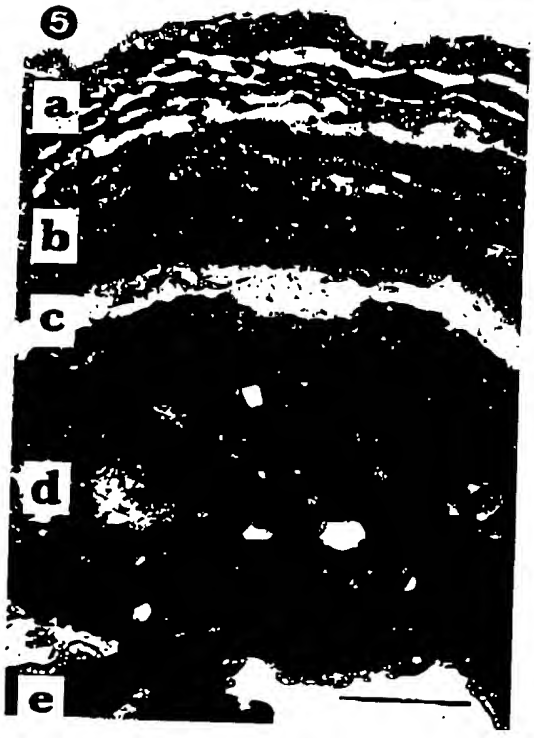

Peyssonnelia (Pl. 6/7). Encrustations consisted of fine, granular Mg calcite. The number of living red algae during that time was significantly higher in depths between 2 and 15 m. Close to the O_2/H_2S interface the reef surface was almost entirely overgrown by pleurocapsalean cyanobacteria.

Noteworthy is the great variety of skeletal mineralogies of the reef-forming organisms. Hence, *Lithoporella*, like other corallinaceans, secretes high Mg calcite (ADEY & MACINTYRE, 1973), whereas *Peyssonnelia* has an aragonitic skeleton (WRAY, 1977; JAMES et al., 1988). The cyanobacteria and the nubecullinid foraminifers produce in turn high Mg calcite.

Reef-associated biota

Macrobiota: Green algae, sponges and gastropods are the main groups of macroorganisms associated with the cyanobacterial-red algal reef surface. Three species of siphonocladalean algae belonging to the genera *Cladophora*, *Cladophoropsis* and *Chaetomorpha* thrive in dense clusters close to the reef wall. They are very abundant to water depths of about 4 m, less common deeper and disappear below 8 m. The specimens of *Cladophoropsis* are always attached to the reef surface, whereas *Cladophora* and *Chaetomorpha* grow both attached to the reef surface or float free as bunches of filaments. The green algae as a rule do not calcify except for the brushy carpets of *Cladophoropsis* growing in evaporative pools on the top of the reef where the tips of their filaments are encrusted with thin layers of calcium carbonate.

Sponges are represented by one species of brown to bright orange colored monaxonid demosponge identified as *Suberites* sp. (Pl. 1/3) bearing only one kind of tylote spicules (Pl. 6/1-2). Post mortem accumulations of *Suberites* spicules are strewed over the reef surface (Pl. 6/1). The spicules dissolved, however, quickly close to the reef surface and have not been encountered incorporated into the cyanobacterial-red algal carbonate framework.

A large population of the cerithiid gastropod *Rhinoclavis sinensis* (GMELIN) is grazing both on the cyanobacteria and red algae as well as on the siphonocladalean algae. Empty gastropod shells are often encrusted and embedded in the reef framework. Post mortem accumulations of gastropod shells washed downward form a few cm thick coquina blankets on the lake bottom close to the reef wall. Gastropod fecal pellets are common components of internal sediment, filling the interskeletal reef cavities. (pl. 7/3

It is interesting to note that the large population of grazing gastropods has apparently no adverse effect on the cyanobacterial-algal community living on the Satonda Lake reef surface. This is in contrast to views attributing the decline in stromatolite formation in the past marine environments to the activity of grazing animals, particularly in the time close to the Precambrian/Cambrian boundary (GARRETT, 1970; WALTER & HEYS, 1985).

Skeletal microbiota: No special studies have been carried out on the reef-associated microbiota. It is, however, interesting to note the occurrence of pennate benthic diatoms *Fragilaria* sp. and *Mastogloia* sp. (Pl. 4/1-2) and the coccolithophorid *Syracosphaera mediterranea* (Pl. 4/3-4) on the reef surface. The association of *Fragilaria* and *Mastogloia* is known to prefer alkaline conditions (e.g., HAVORTH, 1972) and lower salinities. *Syracosphaera* as well as the rare miliolid foraminifers living on the reef surface (*Quinqueloculina*, *Miliolinella*) are cosmopolitan forms tolerating varying salinities.

5.2.3 Biota and lithology of the fossil reef framework

The calcareous reef framework below the living cover can be divided vertically into three zones which differ significantly in their biotic and lithologic composition. The-

Plate 5 Red algae, foraminifers and cyanobacteria of the stromatolites, Satonda Crater Lake, Indonesia, October 1986.

Fig. 1. Magnification of the layer e from other specimen to show the structure of the aragonitic thalli of the squamariacean red algae *Peyssonnelia* sp. and the peloidal material filling the space between successive thalli. Noteworthy are the botryoid aragonitic fans (a) attached to the basal surface of the upper thallus shown in the picture. Sample 57, station 10, depth 21 m; scale bar = 200 µm

Figs. 2-3. Vertical sections of the living calcareous crust surface close to the chemocline. Dominating organisms are monostromatous corallinaceans *Lithoporella* sp. (cl) intergrowing with crustose squamariaceans *Peyssonnelia* sp. (sq). The surface of most red algae is covered by a thin film of pleurocapsalean cyanobacteria (comp. Plate 6), which often penetrate the upper parts of the red algal thalli. Cross-sections of rare tubes of nubecullinid foraminifers (arrowed) are visible between the thalli of red algae. A thicker layer of clotty cyanobacterial micrite (t) silicified at the top (white zone) is shown in Fig. 3. Sample 29, station 17, depth 23 m; scale bar = 100 µm

Fig. 4. Vertical section of a dense aggregation of tubes of nubecullinid foraminifers from the living crust surface. They usually encrust shadowed areas of the crust surface and intergrow with squamariacean red algae (sq). Empty nubecullinid tubes are often filled with calcified pleurocapsalean cyanobacteria or tubes of younger generation of nubecullinids. Sample 9, station 7, depth 7 m; scale bar = 200 µm

Fig. 5. Phase contrast photomicrograph of living aggregate of pleurocapsalean cyanobacteria from the reef surface (arrowed). Sample 9, station 7, depth 7 m; scale bar = 10 µm

Fig. 6. Organically preserved remnants of the pleurocapsalean sheaths (glycocalyx) from the silicified part of the clotty layer shown in (Pl. 5/4); scale bar = 10 µm

Plate 5

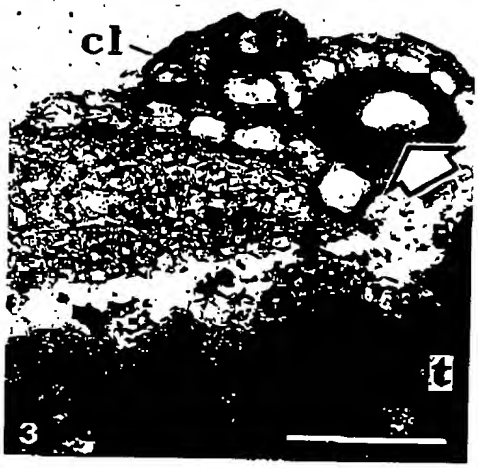

se are (from the top): 1. the cyanobacterial-red algal zone, 2. the peloidal zone, and 3. th stromatolitic-siphonocladalean zone.

The cyanobacterial-red algal zone

At the first few millimeters below the surface the skeletal framework is composed of biota identical to those living on the reef surface, i.e., mainly thalli of Lithoporella alternating with thin layers of calcified sheaths of pleurocapsalean cyanobacteria (Pl. 4/5, layer a). The next 2-3 mm of the reef section are built of a dense layer composed of *Peyssonnelia* thalli alternating with thin films of calcified pleurocapsalean cyanobacteria (Pl. 4/5, layer b). Below, a 2-4 mm thick layer of weakly translucent thrombolitic (clotty) limestone occurs which is silicified at the top (Pl. 4/5, layers c and d) and encloses in many places well-preserved remnants of pleurocapsalean sheaths (Pl. 5/6). The thrombolitic layer passes into a broader zone composed of irregularly wrinkled or slightly arched foliaceous thalli of *Peyssonnelia* giving the reef structure a cystous appearance (see Pl. 3/4, above the arrow). The zone is thicker at shallow water depths (0-5 m) where it attains 15-25 cm, and much thinner (3-4 cm) close to the O_2/H_2S interface. The arcuate sheets of the peyssonnelid algae, on the average 250-300 µm thick, are loosely attached to the substratum, overlapping and often curling back on themselves (Pl. 4/5, layer e, 4/6 and 5/1). The cavities between the sheets are either empty or partially or entirely filled with internal sediment composed predominantly of clotty (peloid) micrite and sparry cement (Pl. 4/6 and 5/1). Some peyssonnelid thalli display hypobasal calcification in the form of botryoidal aragonite fringes, 100-250 µm thick, very similar to those described recently by JAMES et al. (1988) in Holocene peyssonnelid algae from the Bahamas. The hypobasal aragonite in peyssonnelids and other corallines has been interpreted as syngenetic and probably the product of metabolic activity of the algae (WALKER & MOSS, 1984; JAMES et al., 1988; BOSENCE, 1991). In the Satonda specimens, however, the botryoids usually replace micritic sediment evidently predating the hypobasal calcification. It seems therefore that the botryoids represent rather early diagenetic calcification (cf. ALEXANDERSSON, 1974) evoked probably shortly after the death of the algae by microbial decomposition of the non-calcified hypobasal algal rhyzoids. The latter, in fact, have never been found preserved in the Satonda peyssonnelids.

The lowermost part of the multitiered peyssonnelid canopies comprises a dense set of thalli forming a 2-5 mm thick band, distinctly separating the cyanobacterial-red algal zone from the underlying peloidal zone (Pls. 3/4 and 7/3).

The peloidal zone

The lithology and biotic composition of this unit differs significantly from the overlying cyanobacterial-red algal limestone described above. The sharp contact between the two zones has a discontinuous character (Pls. 3/4 and 7/3, marked by arrows). This discontinuity can probably be attributed to a rapid change in Satonda Lake chemistry caused by the eruption of the nearby Tambora Volcano in 1815 (ashfall). The zone attains an average thickness of 15-20 cm and passes downward continuously into the stromatolitic-siphonocladalean zone. The lower boundary of the peloidal zone has been arbitrarily placed at the level where the first stromatolitic (microlaminated) structures appear abundantly and the reef changes from a highly porous and brittle to a massive and hard structure.

The porous sediment is composed mainly of micritic peloids 30-250 µm in size with a significant contribution of thrombolitic micrite in places. The peloids are not well-sorted but are sometimes graded and form micritic laminae. Many of the peloids are surrounded by rims of structureless

Plate 6 Red algae, sponge spicules and coccoidal cyanobacteria of the stromatolites, Satonda Crater Lake, Indonesia, October 1986.

Fig. 1. Vertical section of the living surface of the calcareous crust built of corallinacean (*Lithoporella* sp.) and squamariacean (*Peyssonnelia* sp.) red algae intercalating with calcareous tubes of nubecullinid foraminifers visible in cross-sections as variously sized cysts (thin arrow). The cyanobacterial-red algal-nubecullinid community is associated with large population of monaxonid demosponges (*Suberites* sp.) which spicules cover in many places the living surface (bold arrow). Sample 8, station 7, depth 6 m; scale bar = 50 µm

Fig. 2. A bunch of monaxonic spicules (tylostyles) of *Suberites* sp. (Demospongiae) associated with the reef-forming cyanobacterial-red algal community. Sample same as above; scale bar = 50 µm

Fig. 3. Magnified section of (Fig. 1) showing remnants of pleurocapsalean sheaths preserved due to early post mortem silicification; scale bar = 30 µm

Fig. 4. SEM picture of soft and calcified pleurocapsalean capsules from the desiccated surface of the living cyanobacterial-red algal crust in a top view. Sample 11, station 7, depth 9 m; scale bar = 30 µm

Fig. 5. SEM picture of a multiple fissioned pleurocapsalean cell aggregate from the living surface of the cyanobacterial-red algal calcareous crust in a top view (desiccated specimen). Note the microgranular character of the high Mg calcite permineralizing the cyanobacterial sheaths. Sample 11, station 7, depth 9 m; scale bar = 10 µm

Fig. 6. SEM picture showing various degrees of calcification of desiccated pl urocapsalean capsules from the living surface of th cyanobacterial-red algal calcareous crust in a top view; scale bar = 10 µm

Fig. 7. SEM picture of cross-fractured surficial portion of the cyanobacterial-red algal zone (for a top view of the same see Fig. 4). The top layer is built of calcified pleurocapsalean sheaths encrusting a monostromatous thallus of strongly calcified corallinacean alga *Lithoporella* sp. Sample 10, station 7, depth 9 m; scale bar = 10 µm

Plate 6

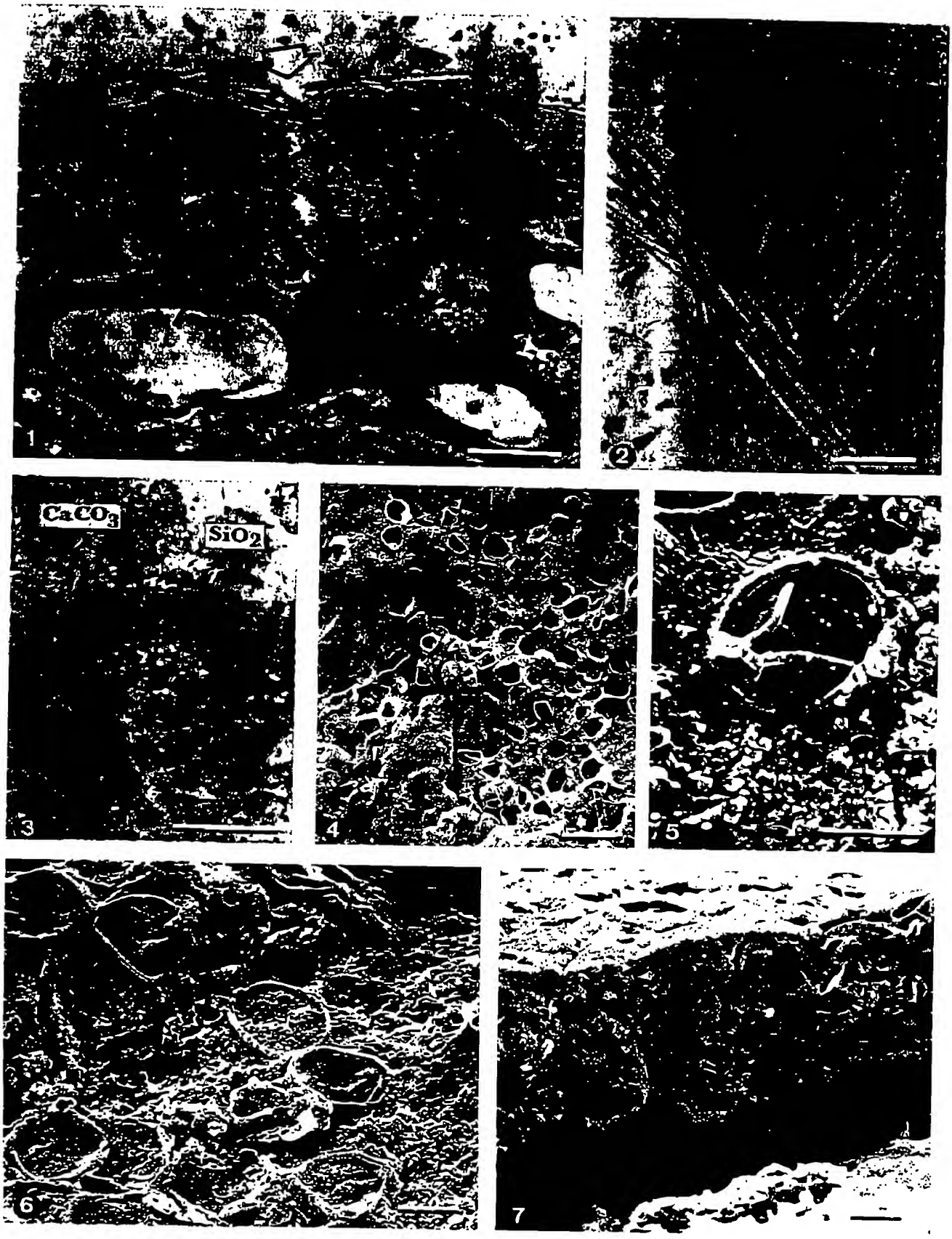

sparry calcite 15-25 µm thick. Calcified ellipsoidal to fusiform fecal pellets of cerithiid gastropods, up to 800 µm in length, are also present and may in places occur in dense accumulations (Pl. 7/3). Shells of the gastropods are often found immurated in the peloid sediment. Some of them are encrusted by thin layers of stromatolitic sediment. Some larger peloids and part of the gastropod fecal pellets are silicified. The silicification may be complete or is limited only to the outer part of the grains (Pl. 7/4). Skeletal grains associated with the peloids include foraminifers (miliolids and undetermined uniserial textularids), ostracods and tiny serpulids.

Peloidal sediments similar to those from Satonda Lake are present in carbonate build-ups of a variety of ages. They may occur as internal sediments and in open spaces between reef frame builders (e.g., PALMER & FÜRSICH, 1981; KREBS, 1974; STEIGER & WURM, 1980; DABRIO et al., 1981; REID, 1987; REID et al., 1990). It is uncertain whether the genesis of peloids was inorganic or organically induced. Heterotrophic bacteria have been recently suggested as possible precipitating agents (CHAFETZ, 1986). Association of some silicified Satonda Lake peloids with remnants of coccoid pleurocapsalean cyanobacteria suggests that they may represent decomposed and diagenetically altered aggregates of calcified coccoid cyanobacteria, i.e., microbial structures closely related to in situ calcified cyanobacterial stromatolites. This suggestion needs to be supported by further detailed studies.

The stromatolitic-siphonocladalean zone

This zone comprises the bulk of the Satonda Lake reef framework and directly overlies the lava substratum. Its thickness varies considerably with lake depth, attaining 50-80 cm near the lake surface and only 2-5 cm close to the reef base.

The rock is composed of variously sized, elongated and irregularly twisted microlaminated bodies densely intergrown to form a massive calcareous structure. Small spaces between the laminated bodies are filled with clotty micrite or they remain empty (Pl. 7/6).

The central part of each microlaminated body is occupied mostly by one, rarely by two or three empty cylindrical tubes not adhering to each other, attaining 90-220 µm in diameter (Pl. 7/6-7). The tubes are, as a rule, equidimensional with occasional constrictions and scarce lateral branches. The size and shape of the tubular structures leaves little doubt that they represent remnants (moulds) of siphonocladalean green algae and are essentially similar to filaments of *Cladophoropsis* associated with the living reef surface. Similar to the living *Cladophoropsis* the tubular structures are most densely distributed in the microlaminated rock which has been formed in shallow water. The distribution density of the tubes decreases apparently with depth. Below 10 m they are lacking and the rock is composed exclusively of microlaminated columns and nodules of various sizes. The mostly central position of the algal tubes in the microlaminated structures indicates that the siphonocladalean filaments formed originally the growth base for the calcareous encrustations. After decay they left the empty tubes behind.

The laminated deposits surrounding the siphonocladalean tubes are clearly of microbial, i.e., stromatolitic origin. Since the individual stromatolites are not visible to the unaided eye they can be classified as microstromatolites (HOFMANN, 1969). Their texture is in optical micrographs defined by alternating dark-light couplets of micritic and sparitic laminae (Pl. 7/6-7). The dark laminae are thinner (15-50 µm) than

Plate 7 Cyanobacterial-red algal zone, peloidal zone and stromatolitic-siphonocladalean zone of stromatolites, Satonda Crater Lake, Indonesia, October 1986.

Fig. 1. SEM picture of the single-layered thalli of *Lithoporella* sp. from the living surface of the cyanobacterial-red algal zone in a top view (desiccated specimen). Attached to *Lithoporella* are shrunken capsules of uncalcified pleurocapsalean cyanobacterial (arrowed). Sample 29, station 17, depth 23 m; scale bar = 30 µm

Fig. 2. SEM picture (EDTA etched cross-fracture) of the cyanobacterial-red algal zone close to the living surface. Clearly visible is the difference between the cells of the crustose squamariacean alga *Peyssonnelia* sp. permineralized with aragonite and the pleurocapsalean cell aggregates permineralized with dense, microgranular high Mg calcite. Sample 8a, station 7, depth 6 m; scale bar = 30 µm

Fig. 3. Vertical section through the subsurficial portion of the calcareous reef showing the sharp boundary (arrowed) between the cyanobacterial-red algal zone and the underlying peloidal zone enclosing numerous fecal pellets of cerithiid gastropods. For macroscopic photograph of the boundary between the two units see Pl. 3/4. Sample 29, station 17, depth 23 m; scale bar = 500 µm

Fig. 4. Examples of silicified peloids (arrowed) from the peloidal zone shown in Fig. 3; scale bar = 200 µm

Fig. 5. Fragment of the peloidal zone with section of an immurated shell of cerithiid gastropod covered by a few stromatolitic layers. Sample 8, station 7, depth 7 m; scale bar = 500 µm

Fig. 6. Thin section of the stromatolitic-siphonocladalean zone of the reef framework. The massive rock is built almost exclusively of stromatolitic layers; their complex configuration is due to various calcifications of subsequent coccoid cyanobacterial layers overgrowing filaments of now decayed siphonocladalean green algae (some of them are arrowed). Sample 47, station 10, above water mark; scale bar = 500 µm

Fig. 7. Magnified fragment of the same as above to show the subcystose pattern of the stromatolitic structure in vertical section. Arrow indicates cross-section of a filament of green algae forming the basis for the cyanobacterial growth; scale bar = 200 µm

Plate 7

the light ones (20-300 µm). They display subparallel to subcystose or cystose arrangement (Pl. 7/7) and are often gathered in sets separated by thicker light bands. Pillar- and column-shaped micritic structures occur sometimes at junctions between neighboring cysts. The texture of the Satonda microstromatolites is remarkably similar to internal patterns observed in vertical thin sections of, e.g., Lower Proterozoic stromatolites (subcystose patterns; see WALTER, 1983, photo 8-11), certain Ordovician and Lower Carboniferous stromatoporoid stromatolites (cystose to subclathrate patterns; see GALLOWAY, 1961; DONG, 1964), and Quaternary lacustrine stromatolites (subparallel to subcystose patterns; see CASANOVA, 1987; HILLAIRE-MARCEL & CASANOVA, 1987), or even Paleozoic biostructures known as *Wetheredella* WOOD, 1948, and related problematic fossils. We have addressed this questions in two separate papers (KAZMIERCZAK & KEMPE, 1990, 1992).

SEM analyses revealed that the dark and light laminae differ sharply both in their microstructural and mineralogical characters. SEM pictures and EDAX mapping of etched sections show that the dark laminae have an irregular porous microstructure and are composed of microgranular high Mg calcite, whereas the light ones are compact and built of fibrous aragonite (Pl. 2/8-9; Pl. 8/1-2, 4).

The remnants of the original microbial community generating the stromatolitic structures are recognizable in the dark as well as in the light laminae. They are much better preserved in the dark laminae, where they occur as patchy to semicontinuous clusters of coccoid microfossils which can be easily identified as $CaCO_3$ permineralized capsules (sheaths) or moulds of capsules of pleurocapsalean cyanobacteria. Very similar, if not identical, capsules have been described from other modern and fossil stromatolites (e.g., HORODYSKI & VONDER HAAR, 1975; KRUMBEIN & GIELE, 1979; KAZMIERCZAK & KRUMBEIN, 1983; BRATHWAITE et al., 1989). In the light laminae the remains of the original pleurocapsalean cyanobacteria are occasionally preserved in the aragonitic matrix as indistinct patches of former cell aggregates (Pl. 8/2) or residues f the outer common sheaths (glycocalyx) which surround the cell aggregates during life (Pl. 8/6). Careful etchings with EDTA demonstrate that traces of a continuous mass of coccoid aggregates can be detected throughout the aragonitic layers. They are visible as shallow, roundish depressions etched within the horizontally striated aragonitic background (Pl. 8/4-5). The size and mode of distribution of these depressions correspond exactly with the well preserved pleurocapsalean aggregates from the dark laminae. This permits the conclusion that the entire microstromatolitic structure was produced by the same kind of cyanobacteria and that the final textural, microstructural, and mineralogical differences expressed in the microstromatolites were to a large extent controlled by abiotic environmental factors.

It seems that two basically different calcification processes of the coccoid cyanobacterial mat were involved in the formation of the microstromatolites. The dark calcitic laminae originated most probably as the result of rapid in vivo calcification of the coccoid mat surface. The fast calcification was presumably the crucial factor enhancing the relatively good preservation of the microbiota noticed in the dark laminae. The microgranular calcite permineralizing of the coccoids in the dark laminae is identical to that covering the living cyanobacteria today. The light aragonitic laminae, in turn, appear to be the product of early diagenetic (early post mortem) calcification of the subsurface masses of coccoid cells which, due to periodic formation of the in vivo calcified surficial cell layers, have been closed in cryptic microenvironments where they underwent microbial decomposition and concomitant permineralization by aragonite. Thread-like bodies occurring in some aragonitic laminae of the Satonda microstromatolites which are reminiscent of sheaths of sulfur bacteria or flexibacteria seem to support such an interpretation. Calcification processes in decaying cyanobacterial mats evoked by bacterial degradation (mostly sulfate reducers) below the zone of photosynthesis have been recently advanced as major factor in $CaCO_3$ formation

Plate 8 Details of the structure of the stromatolitic-siphonocladalean zone of the Satonda Crater Lake stromatolites, Indonesia, October 1986.

Fig. 1. Vertical section through the stromatolitic-siphonocladalean zone of the Satonda Crater Lake calcareous reef in transmitted light. The light layers are composed of aragonite and the much thinner dark layers of high Mg calcite. Sample 47, station 10, above water table; scale bar = 100 µm

Fig. 2. SEM picture of (Fig. 1) (formic acid etched vertical section) showing the sharp textural difference between the fibrous aragonitic layer and the spongy high Mg calcitic layer the basal part of which is slightly silicified. Arrow indicates a remnant of strongly obliterated pleurocapsalean aggregate preserved within the aragonitic layer; scale bar = 10 µm

Fig. 3. SEM picture of formic acid etched, vertical section showing remnant of a pleurocapsalean cell aggregate as shown in Fig 1 from the dark high Mg calcitic layer surrounded by the remains of the common mucus sheath; scale bar = 10 µm

Fig. 4. SEM picture (EDTA etched, vertical section) of the finely striated aragonitic layer figured in(Fig. 1; the numerous etching depressions represent traces of early post mortem decomposed pleurocapsalean aggregates; scale bar = 30 µm

Fig. 5. A magnified, formic acid etched fragment of Fig. 4; scale bar = 10 µm

Fig. 6. SEM picture (EDTA etched, vertical section) of the aragonitic stromatolitic layer with organically preserved remnants of the outer common sheaths of pleurocapsalean cell aggregates (glycocalyx) preserved within the early diagenetic fibrous aragonite; scale bar = 30 µm

Plate 8

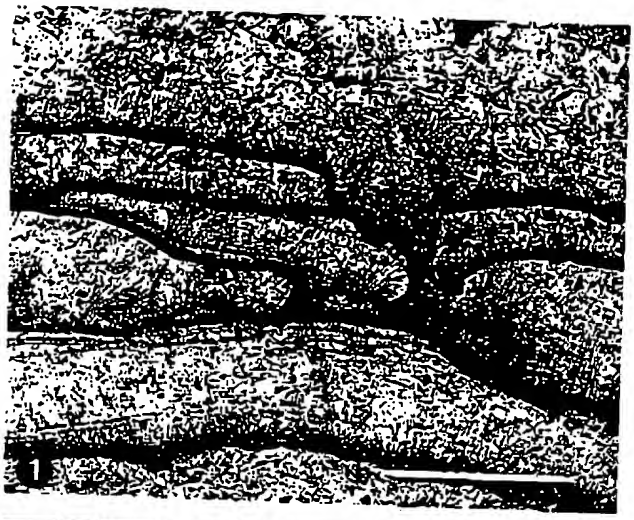

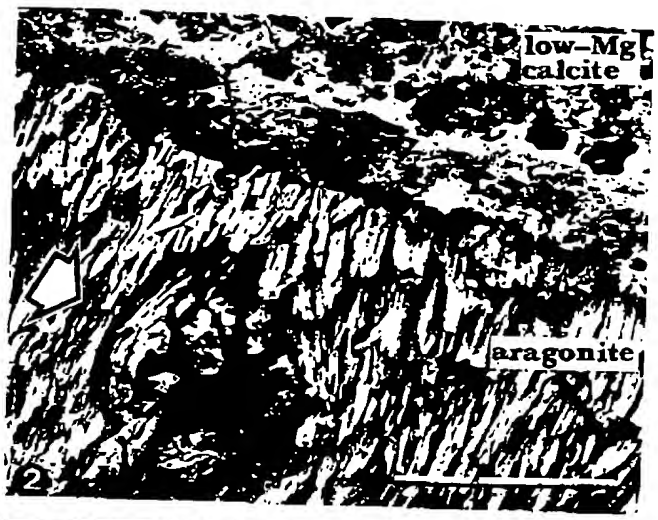

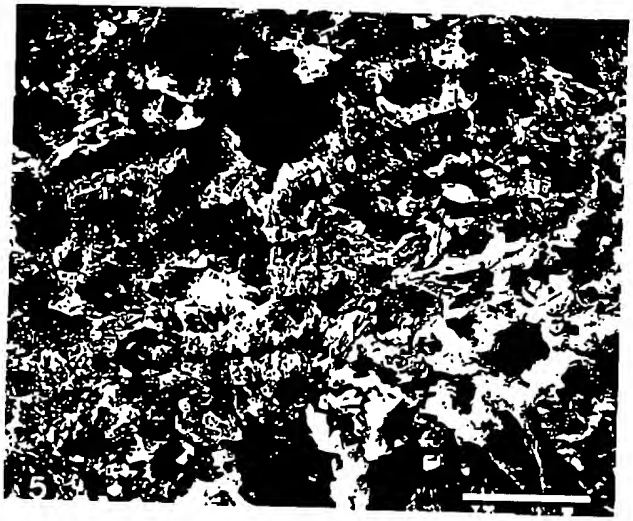

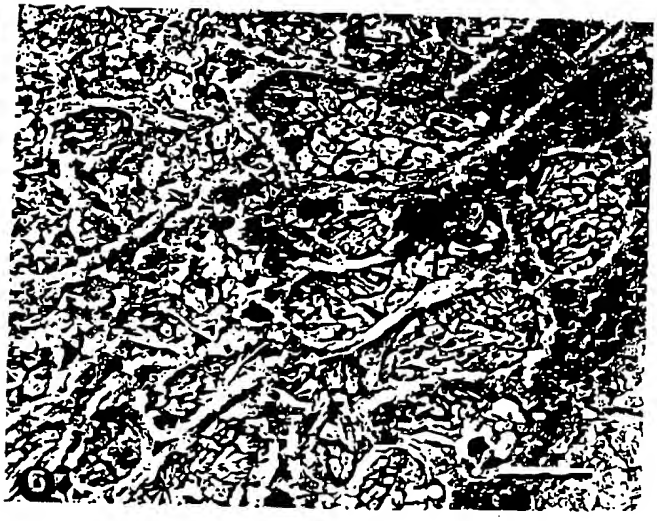

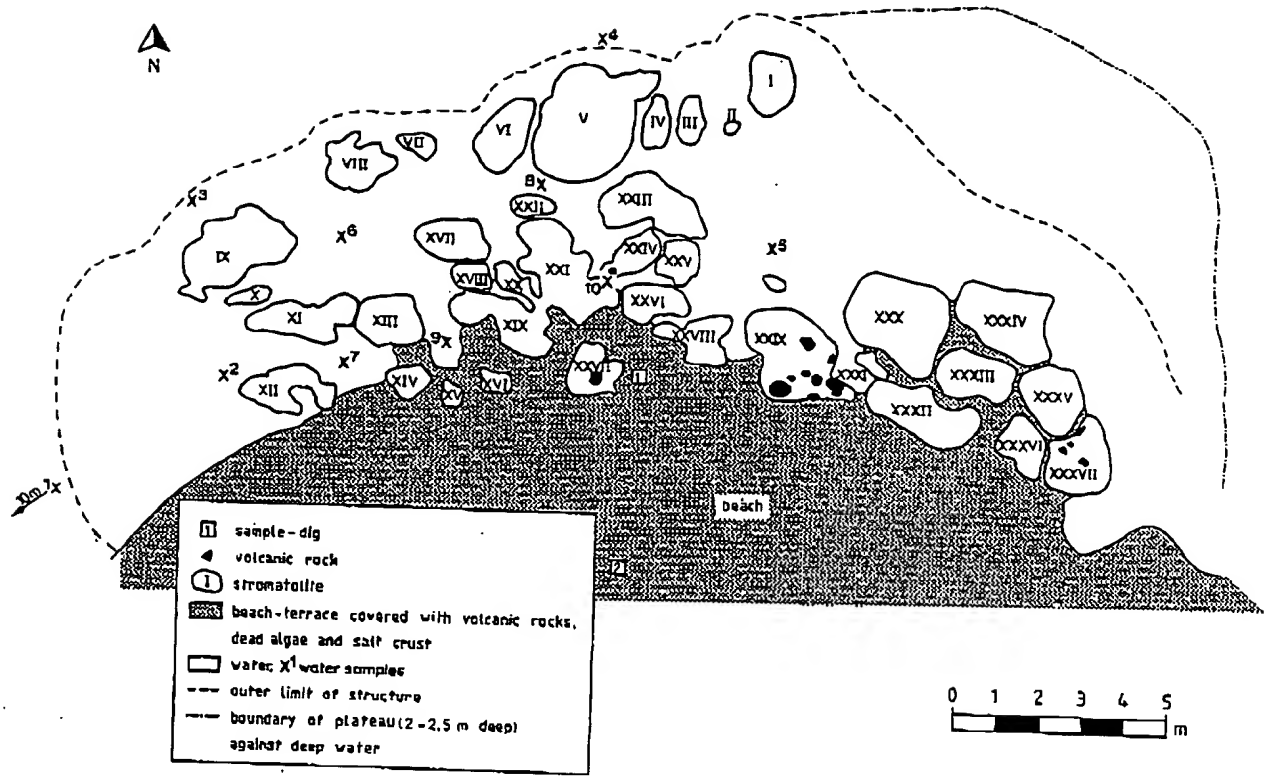

Fig. 7. Sketch map showing the heads of the calcareous stromatolitic structures exposed above the water level; Satonda Crater Lake; station 1; October 9th, 1986.

(KRUMBEIN & COHEN, 1977; LYONS et al., 1984). Similar carbonate precipitation mechanisms involving anaerobic respiration has been also suggested as morphogenetic agent for some Precambrian microstromatolites (LANIER, 1988).

5.2 Onshore digs

At station 1 two digs were made (for locations see Fig. 7, squares 1, 2). The lithologic profiles of these digs are given in Fig. 8. Both sites were covered with about 9 cm of volcanic ash and sand washed down to the beach from the crater wall. In dig 1 several layers of calcareous mud and sand mixed with volcanic sand and lapilli occur.

Numerous molluscs shells have been found embedded in this sediment. These are: two cerithiid gastropod species, a muricid gastropod *Ocenebra* sp., *Neritina* sp., and a venerid bivalve ?*Lioconcha* sp. - see Pl. 2/2-6.

The sediment enclosing the mollusc shells is very rich in both calcareous and agglutinated benthic foraminifers, diatoms, ostracods, and small skeletal fragments of echinoderms and bryozoans. Following foraminifers have been identified: *Ammonia beccarii* (LINNÉ) forma *tepida* (CUSHMAN), *A. beccari* (LINNÉ) forma *parkinsoniana* (D'ORBIGNY), *Rosalina bradyi* (CUSHMAN), *Discorbis* cf. *vesicularis* (LAMARCK), *Cymbaloporetta* cf. *plana* (CUSHMAN), *Peneroplis* sp., *Elphidium* sp., *Bolivina* sp., *Glabratella* sp., miliolids (among others representatives of *Triloculina*, *Quinqueloculina* and *Miliolinella*), *Textularia* sp., ?*Buliminoides* sp., ?*Laterostomella* sp., and numerous unidentifiable incrusting forms. Compared with normal marine specimens the calcareous foraminifers from Satonda have strikingly small and thin tests what may indicate a lower salinity of the Satonda Crater Lake water during their lifetime. The ostracods associated with the foraminifers ('*Hermanites*' sp., *Bairdia* sp., *Cytheropsis* sp., *Semicytherula* (?) sp.) are also known as forms tolerating low salinity.

At the depth of 55 cm a dark brown organic mud with many plant remains and pieces of wood was found which was devoid of any shells or carbonate sediments. The same layer was found in dig 2 immediately below the upper ash layer. A piece of wood from this layer was dated by ^{14}C. It yielded an age of 3920 ± 30 years BP.

A series of digs was also conducted on the coastal plain of Satonda Bay (Fig. 3). Digs 1, 2 and 3 uncovered the Tambora 1815 sequence of ashes, lapilli and pumice. Slightly up the crater rim this layer was 60 cm thick and covered a red-brown paleosoil. On the plain the Tambora ash was 85 cm thick and covered a light brown silt with apparently calcinated and/or weathered marine shell and coral debris. One of these shells was dated also by ^{14}C yielding an age of 310 ± 50 years BP (international agreed conventional age minus 400 years for apparent age of seawater).

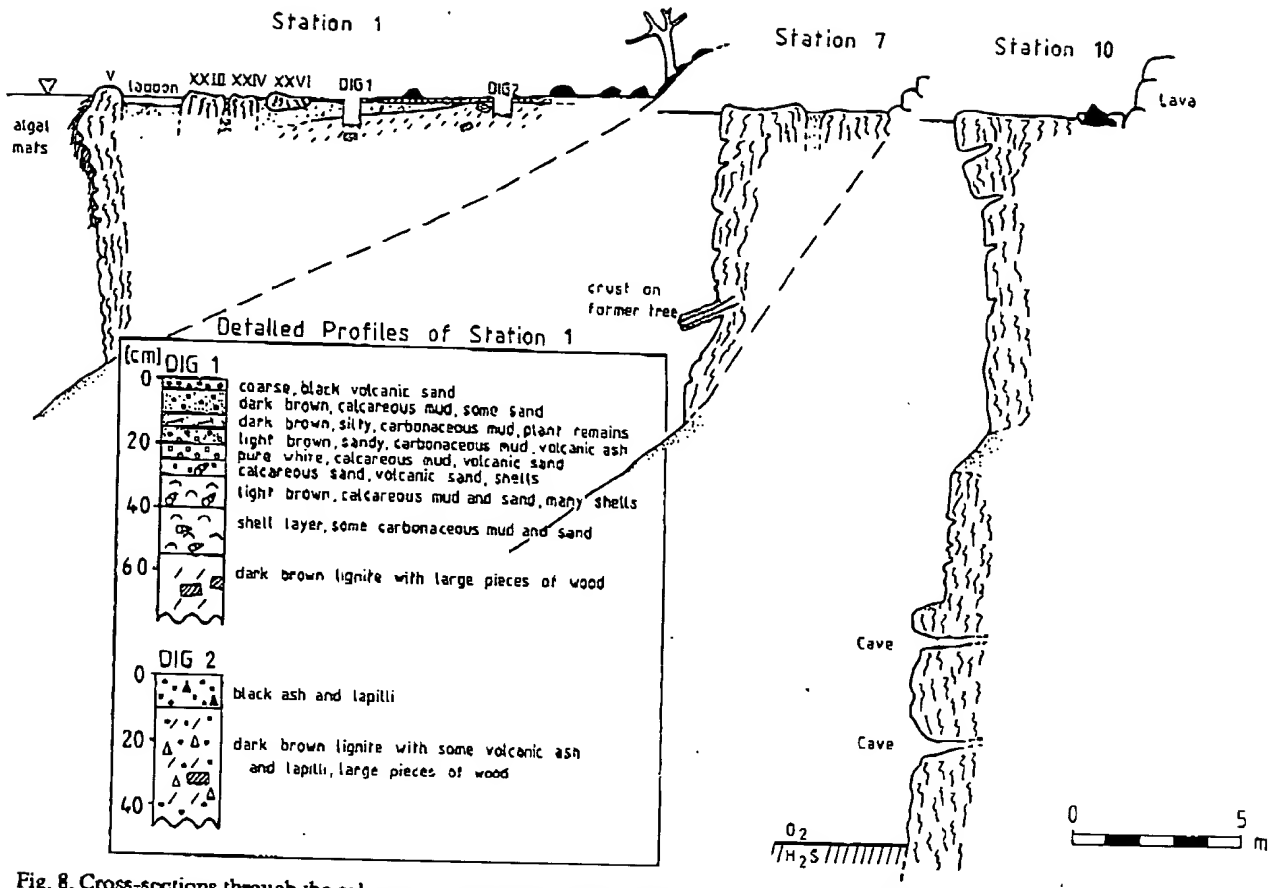

Fig. 8. Cross-sections through the calcareous stromatolitic reefs, of Satonda Crater Lake, at stations 1, 7, and 10, and lithologic profiles of digs 1 and 2 at station 1.

5.3 Sediment core

We recovered one sediment core from the center of the lake. Because it had a very high water content, we could only open and cut it after it had ample time to dry. One can easily discern 13 lithologic units within the core (Fig. 9). Some of the core sections are varved (units I, VI, VII, VIII) others are mottled or structureless. The varves consist of couplets of light, calcareous lamina and darker, carbonaceous lamina. The existence of varves attests to anaerobic bottom waters devoid of burrowing benthic life.

In the light bands, $CaCO_3$ concentrations rise to over 50% (Table 11). Microscopic investigations show that they are composed of wheat-grain aragonite. The preservation of aragonite at the bottom of the lake shows that bottom waters must have been supersaturated with regard to all Ca and Mg carbonate minerals for quite a long time (aragonite is the most soluble alkaline earth carbonate mineral). In the upper 15 cm of the core, nine distinct carbonate layers can be identified. They may represent years of intensive plankton blooms, causing unusual depletion of free CO_2, a high pH and a high CO_3^{2-} concentration and a high carbonate mineral supersaturation. Unit VIII is composed of a series of such white bands, the lower section of which appears to be slightly disturbed by slumping.

It is difficult to discern if the unvarved sections are turbidites, slump masses or regular sediments not influenced by seasonal variations. Conspicuous are two ash layers (units III and X). They were inspected microscopically by K. Heyckendorf who observed biotite and spherical pumice in both layers. These are components typical of the 1815 Tambora ejecta. He therefore suggested that at least the upper layer is redeposited ash. In order to test this assumption unit VIII which contains enough organic carbon (Table 11) was dated by ^{14}C. The result yielded 140 ± 140 years, suggesting that unit X is the Tambora ash proper and that unit III is redeposited. However, the thickness of both layers together amounts to only a few centimeters, not at all comparable to the 60-80 cm of ash deposited on Satonda. Either an appreciable amount of the ash has dissolved in the lake water (compare siliceous layer in the cyanobacteria-red algal stromatolite layer) and the larger pieces of pumices floated to shore or the core did not reach the in situ Tambora ash at all and unit X contains also only redeposited Tambora material.

The chemistry of the sediment is quite variable as far as its $CaCO_3$ and organic carbon content is concerned (Table 11). In contrast to this, the phosphorus content is quite constant and does not show any correlation with the C_{org} content. C/P ratios fluctuate between 220 and 20, i.e., they are relatively high. Contributions by inorganic phosphorus especially in

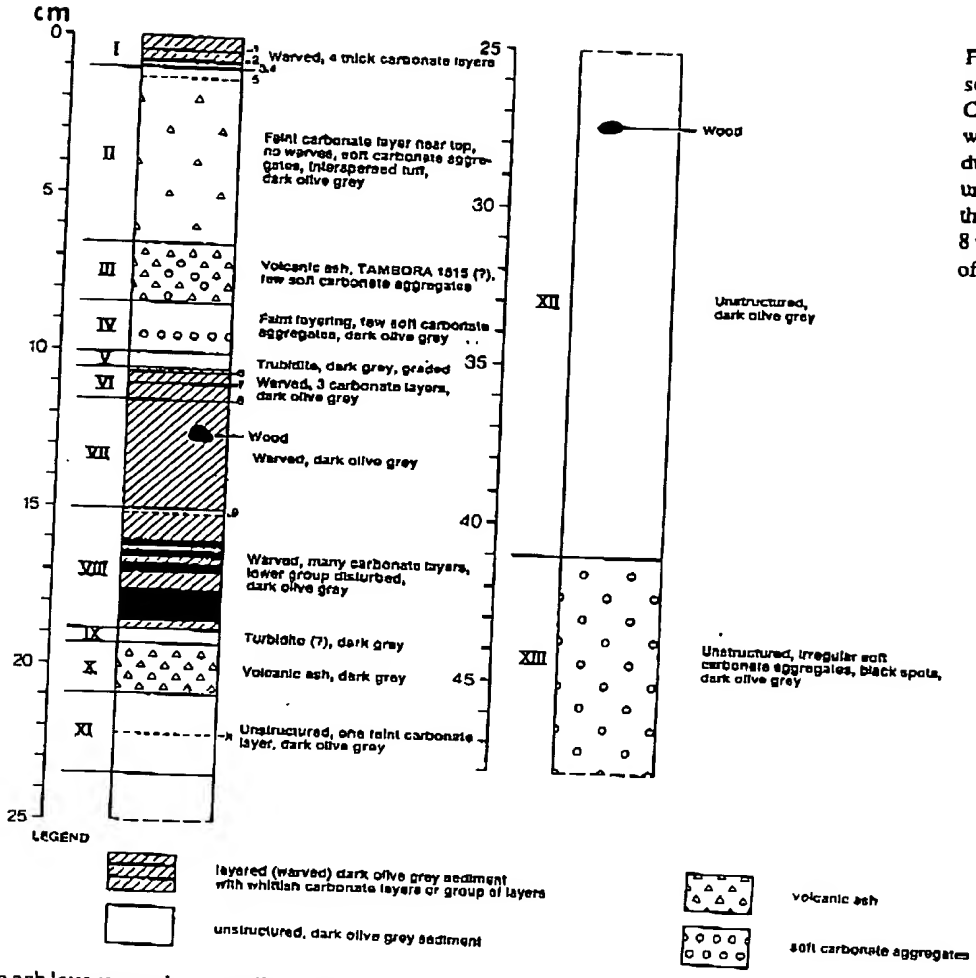

Fig. 9. Lithologic profile of a sediment core from Satonda Crater Lake, recovered from a water depth of 64 m. Note that due to slumping the ash layers of units III and X contain ash from the Tambora 1815 eruption. Unit 8 was dated by ^{14}C giving an age of 140 ± 140 years.

the ash layers may be a possible explanation. The $\delta^{13}C$ values of the organic carbon are quite constant, as is expected if most of the organic carbon is of terrestrial origin. $\delta^{13}C$ values of the carbonate are on the other hand quite variable, the lowest values occur in the lower units of the core, suggesting a shift in the carbonate isotope composition of the surface water of the crater since the Tambora eruption.

In units I, II, VI and VIII a rich microfossil fauna was found, consisting of up to six diatom species, a species of a calcareous foraminifera, up to two species of silicoflagellates and broken monaxonid sponge spicules. Also, subspherical carbonate bodies were found formed around spiral trichomes of *Anabaena*. The other units did not contain identifiable organic remains, except of broken sponge spicules.

6 CHEMICAL AND BIOTIC EVOLUTION OF SATONDA CRATER LAKE

The hydrochemical, sedimentological and radiometric age data collected permit a tentative reconstruction of the depositional history of Satonda Crater Lake.

After the last eruption of Satonda Volcano several thousand years ago, its two crater were filled with fresh water as witnessed by the organic mud we found below the calcareous sediments at the lake beach. About 4,000 years ago the fresh water was replaced by seawater. This may have been caused by a partial collapse of the southern crater rim which left a large semicircular theater-like scar: the present Satonda Bay. The width of the crater rim at its most narrow place was only 30 m allowing the penetration of heavier seawater into the crater. In the beginning, the lake was not as alkaline as today, allowing the settlement of the marine organisms listed above (see Chapter 5.2) along the lake shore whereas others, like the serpulids and the bivalves Pinctada (see Pl. 1/6) colonized slightly deeper water. Evaporation in small lagoons at the beach formed gradually seawater of high salinity which collected at the bottom of the crater, creating permanently anaerobic bottom waters. Organic matter accumulating in this layer produced subsequently via sulfate reduction and/or silicate dissolution an increase in alkalinity. The lake itself was mixed down to 50 m depth due to evaporation induced salinity convection in the dry season. During that time additional seawater would infiltrate the lake increasing its salinity to 108 % that of seawater. During the rainy season a fresh water lens might have been formed on top of the lake, rising its level and causing outflow of relatively fresh water to the sea. With increasing salinity and alkalinity in the lake water, calcification of cyanobacterial mats growing on rocky grounds started forming quickly the bulk of the reefs (the stromatolitic-siphonocladalean zone). The molluscs gradually died out with th exception of one species of

No.	Unit	Description	P_{tot} µmol P/g	TOC %	$CaCO_3$ (%)	$\delta^{13}C_{carb}$ ‰	$\delta^{18}O_{carb}$ ‰	$\delta^{13}C_{org}$ ‰
continuous samples								
1	1	dark layers above carbonate layer 1	29.8	8.02	2.7	- 3.58	+ 3.44	- 24.74
2	1	carbonate layer 1, dark layers in middle of unit 1 & carbonate layer 2	27.1	5.78	30.3			
3	1	carbonate layers 3 and 4	20.4	5.47	57.3	- 1.65	- 0.18	- 26.56
4	2	upper third of unit 2	25.3	2.90	2.2	- 3.21	- 0.17	- 25.71
5	2	middle third of unit 2	24.5	2.30	4.0			
6	2	lower third of unit 2	23.6	1.79	3.2	- 3.52	- 0.44	- 25.86
7	3	ash layer	21.9	0.95	3.2	- 3.52	- 0.44	- 25.87
8	4	top half of unit 4	25.4	3.65	0.7	- 0.49	- 0.91	- 25.78
9	4	bottom half of unit 4	23.3	3.80	1.5			
10	5	unit 5 (grey)	23.8	0.07	0.6	---	---	- 23.85
11	6	upper part of unit 6, including carbonate layers 6 and 7	18.3	6.70	7.4	- 1.43	- 0.77	- 25.73
12	6/7	bottom of unit 6 & 7 including carbonate layer 8 & 3 mm of top of unit 7 (above wood)	22.8	6.70	8.7			
13	7	middle of unit 7 including wood	17.9	6.68	1.4	---	---	- 25.36
14	7	bottom of unit 7	19.0	6.85	2.3			
15	8	top of unit 8, light carbonate layers	21.6	8.67	18.3	- 4.33	- 2.02	- 24.18
16	8	thick white series of carb. layers	23.9	4.65	53.4			
17	8	thin dark double layer & white intermediate layer	---	9.42	12.4			
18	8	2nd thick band of white carbonate layer	21.0	6.39	44.3			
19	8	thick dark band in center of unit 8	23.5	5.07	6.1	---	---	- 24.89
20	8	lower thick white band	23.4	3.66	29.8	- 4.24	- 0.93	- 25.19
21	8/9	lower dark layer of unit 8 unit 9	24.9	1.35	0.4			
22	10	top of sandy ash layer	24.2	0.87	0.2	---	---	- 26.31
23	10	bottom of sandy ash layer	23.7	0.56	0.7			
24	11	top of unit 11 including carbonate layer X	22.2	0.94	3.7	- 4.66	- 0.20	- 25.59
25	11	bottom of unit 11	24.8	1.29	1.9			
discontinuous samples								
26	12	sample 2 cm below top of unit 12	20.0	2.01	8.7	- 5.60	- 0.02	- 24.74
27	12	sample 3 cm above border of unit 12/13	20.0	2.21	10.2	- 6.30	+ 0.24	- 24.94
28	13	top of unit 13 including a large chunck of white carbonate	19.6	2.88	9.5			
29	13	bottom of core 45 - 46.5	20.8	2.61	9.8			

Tab. 11. Description of samples and geochemical parameters from sediment core, Satonda Crater Lake, 64 m water depth. Length of core originally 64 cm. Length of core on June 9, 1988: 47 cm. Of this, 28 cm are more or less original in length, while the upper 36 cm shrank to 19 cm.

cerithiid gastropod. The stromatolitic reef growth graded into the peloidal sediment.

Then, prior to the Tambora eruption 1815, but later than 400 years BP Satonda Bay fell dry. This is evidenced by shells and coral fragments located 1.2 m above the present high water level underneath the Tambora ash in the inner part of Satonda Bay (Fig. 3). Possibly the island and part of the Tambora peninsula was uplifted at this time. Terraces in the Peti Crater/Saleh Bay attest also to this uplift. Whether this uplift was related to a doming of the Tambora prior to its eruption remains to be seen. For the lake the uplift meant the interruption of its connection to the sea. Rain water accumulated in the lake which could not flow out to the sea and created an upper layer with a salinity lower than before, thus insulating the middle layer from contact with air making it anaerobic as well. The lake became stratified in mid water.

The slight uplift of the Satonda Island caused the decrease of the lake water salinity to a quasi marine level and enabled the colonization of red algae and nubecullinid foraminifers on the cyanobacterial reef framework. Large influx to the lake of ash and pumice (60-80 cm layer) after the 1815 Tambora eruption have interrupted for a short time the growth of the stromatolitic structures and resulted in a rapid increase in SiO_2 in the water column, leading to silification of some originally calcareous cyanobacterial layers (Pl. 4/5). An apparent trend to increasing alkalinity is visible at present in the chemical evolution of lake which is documented by the dominance of cyanobacterial mats in the living reef cover.

7 CONCLUSIONS

The calcareous reefs in Satonda Crater Lake grow essentially by in situ calcification of cyanobacteria. The most important environmental factor responsible for cyanobacterial calcification is, in our opinion, the high supersaturation with regard to calcium carbonate minerals. At Satonda, calcification proceeds at a SI_{Ca} of +0.8. Values for normal surface seawater range from 0.4 to 0.6 (e.g., PEGLER & KEMPE, 1989; KEMPE & PEGLER, 1991). At such levels of supersaturation only enzymatic calcification can proceed, whereas non-enzymatic precipitation, like that induced by cyanobacteria, cannot occur under normal marine conditions. Cyanobacterial calcification is reported from a wide spectrum of different water types: from hypersaline alkaline lakes, from low mineralized alkaline lakes and from hard-water environments. In a recent paper we compared four settings of cyanobacterial reef growth (Walker Lake, hypersaline; Lake Tanganyika, low salinity; Andros Island Ponds-Bahamas, hard water) and found that all of them are characterized by very high supersaturation indices similar to the supersaturation index measured for the Satonda Crater Lake water (KEMPE & KAZMIERCZAK, 1990a, b). Other factors such as high alkalinity, the calcium concentrations, and a high Mg/Ca ratio are only of importance as part of the thermodynamic system producing high supersaturation. Increasing the concentration of the carbonate ion is most easily done in systems of high alkalinities and high productivity. The withdrawal of CO_2 and the conservation of the charge balance is the key reaction:

$$2\,HCO_3^- \text{----> } CO_2 + CO_3^{2-} + H_2O$$

The example of Satonda shows that, given the right geological surrounding, even modern seawater can be transformed into an environment generating calcareous stromatolites.

The microstructure f the Satonda stromatolites has many similarities to that of Precambrian and Paleozoic calcareous microbialites (both stromatolitic and thrombolitic). There is no principal difference among them and many

of our thin sections have identical matches in the fossil record. It is therefore plausible to conclude that the Precambrian Ocean had a high carbonate mineral supersaturation and that it was most probably more alkaline than the sea of today. In a sense, Satonda is a big experimental vessel where Precambrian environmental conditions can be studied and where seemingly extinguished life styles have been recreated. The growth of stromatolites is therefore a predictable feature and not a trick nature knew how to play a billion years ago and has forgotten in the meantime.

The results presented are definitely not the final word about Satonda. At best our conclusions can be tentative at this moment. Much needs to be learnt about the early phases of the reefs and their microstructure. Longer sediment cores could resolve the history of the last 4,000 years in greater detail and more isotopic measurements are needed to decipher the complex story of mass balances and isotopic fractionations not even touched upon in this study.

The role of cyanobacteria in the lake is also felt in the nutrient budget: the dominance of ammonia over nitrite and nitrate, the high N/P ratios in the dissolved nutrients and the low C/N ratios in the suspended matter. Nitrification seems to run high in the lake. Unusual for seawater is also the ability of the lake to maintain high DOC concentrations. Both the high ammonia and the high DOC concentrations could prove to be interesting details in a discussion of the chemistry of the cyanobacteria-dominated early ocean.

ACKNOWLEDGEMENTS

The investigations on Satonda would not have been possible without the full-hearted scientific support by the late Professor Egon T. Degens. From the beginning he was convinced that the carbonate deposits on the island were worthwhile to study, even though he has never seen the deposits himself. He shaped the Sonne 45 B cruise to give us a maximum in time and an optimum in logistic support for our investigations on Satonda.

The authors gratefully acknowledge the assistance by Günter Landmann, Andreas Lipp, Yusuf Surachman and Dwi Susanto during the field work. Without their physical efforts and their good humor the expedition would not have been successful. Professor How Kin Wong and Uwe Salge kindly interrupted their seismic studies aboard the R/V Sonne to assist us in mapping the crater lake. Analytical assistance was given to us by Prof. W. Mook, Groningen ($\delta^{13}C$, $\delta^{18}O$ and ^{14}C), by Dr. G. Liebezeit, Hamburg (nutrient chemistry) and by A. Reimer, Hamburg (AAS). Laboratory assistance was provided by M. Sternhagen and R. Koop. Their contributions are gratefully acknowledged. Special thanks are extended to Drs. Janina Szczechura, Danuta Peryt, and Waclaw Baluk, Warszawa, for helping in identification of molluscs and skeletal microbiota, and to Zbigniew Strak, Warszawa, for technical assistance. We are also indebted to the captain and crew of the R/V Sonne for help in transportation and for provisions. Thanks are also due to the manager of the Hotel Tambora and to the police at Calabai for their friendly reception and logistic help.

Financial support from the German Federal Ministry of Research and Technology (Grant No 524 03R372/7) as well as from the Alexander von Humboldt Foundation to one of us (J.K.) is greatly appreciated. The paper is a contribution to the IGCP Project No. 261 'Stromatolites'.

REFERENCES

ADEY, W.H. & MACINTYRE, I.G. (1973): Crustose coralline algae: A re-evaluation in the geological sciences. - Geol. Soc. Amer. Bull. 84, 883-904, Boulder

ALEXANDERSSON, E.T. (1974): Carbonate cementation in coralline algal nodules in the Skagerrak, North Sea: Biochemical precipitation in undersaturated waters. - J. Sed. Petrol., 44, 7-26, Tulsa

BARBERI, F., BIGIOGGERO, B., BORIANI, A., CAVALLIN, A., CIONI, R., EVA, C., GELMINI, R., GIORGETTI, F., IACARINO, S., INNOCENTI, F., MARINELLI, G., SCOTTI, A., SUETKO, D., SUDRADJAT, A., & VILLA, I. (1983a): Magmatic evolution and structural meaning of the Island of Sumbawa, Indonesia. - IUGG Interdis. Symp. Hamburg August 15-27, 1983, Progr. Abstr. 1, 49, Hamburg

BARBERI, F., BIGIOGGERO, B., BIZOUARD, H. BORIANI, A., CIONI, R., CLOCCHIATTI, R., INNOCENTI, F., & MARINELLI, G. (1983b): Tambora Volcano, Island of Sumbawa, Indonesia. - IUGG Interdis. Symp. Hamburg August 15-27, 1983, Progr. Absr. 1, 48, Hamburg

BOSENCE, D.W.J. (1991): Coralline algae: mineralization, taxonomy, and paleoecology. - In: RIDING, R. (ed.): Calcareous Algae and Stromatolites. – 98-113, Berlin (Springer)

BRAITHWAITE, C.J.R., CASANOVA, J., FREVERT, T. & WHITTON, B.A. (1989): Recent stromatolites in the landlocked pools on Aldabra, western Indian Ocean. - Paleogeogr. Paleoclimat. Paleoecol. 69, 145-166, Amsterdam

BROECKER, W.C. & PENG, T.-H. (1984): Tracers in the Sea. - Lamont-Doherty Geological Observatory, 690 pp, Palisades, N.Y.

CASANOVA, J. (1987): Stromatolites et hauts niveaux lacustres Pléistocénes du bassin Natron-Magadi (Tanzanie-Kenya). - Sci. Géol. Bull. 40, 135-153, Strasbourg

CHAFETZ, H.S. (1986): Marine peloids: a product of bacterially induced precipitation of calcite. - J. Sed. Petrol. 56, 812-817, Tulsa

DABRIO, C.J., ESTEBAN, M. J.M. & MARTIN, J.M. (1981): The coral reef of Níjar, Messinian (Uppermost Miocene), Almería Province, southeast Spain. - J. Sed. Petrol. 51, 521-539, Tulsa

DONG, D.Y. (1964): Stromatoporoids from the early Carboniferous of Kwangsi and Kuiechow. - Acta Palaeont. Sinica 12, 280-299, Nanking

EUGSTER, H. P. & HARDIE, L. A. (1978): Saline lakes. - In: LERMAN, A. (ed.): Lakes- Chemistry, Geology, Physics. – 237-293, New York (Springer)

FODEN, J. D. & VARNE, R. (1980): The petrology and tectonic setting of Quaternary-Recent volcanic centres of Lombok and Sumbawa, Sunda Arc. - Chem. Geol. 30, 201 - 226, Amsterdam.

GALLOWAY, J.J. (1961): Ordovician Stromatoporoidea of North America. - Bull. Amer. Paleont. 43, 5-102, Ithaka

GARRELS, R. M. & MACKENZIE, F. T. (1967): Origin of the chemical composition of some springs and lakes. - In: Equilibrium Concepts in Natural Water Systems. – Amer. Chem. Soc., Advances in Chemistry, 67, 222 - 242, Washington D.C.

GARRETT, P. (1970): Phanerozoic stromatolites: Non-competitive ecologicrestriction by grazing and burrowing animals. - Science 169, 171-173, Washington D.C.

HAMILTON, W. (1974): Earthquake map of the Indonesian region. - U. S. Geol. Surv., Miscell. Invest. Ser. Map 1-875-C, scale 1:5,000,000, Washington D.C.

— (1979): Tectonics of the Indonesian region. - U. S. Geol. Surv. Prof. Pap. 1078, Washington D.C.

HARDIE, L. A. & EUGSTER, H. P. (1970): The evolution of closed-basin brines. - Mineral. Soc. Amer., Spec. Publ. 3, 273 - 290, Washington D.C.

HAVORTH, E.Y. (1972): Diatom succession in a core from Pickerel Lake, northeastern south Dakota. - Geol. Soc. Amer. Bull. 83, 157-172, Boulder

HILLAIRE-MARCEL, C. & CASANOVA, J. (1987): Isotopic hydrology and paleohydrology of the Magadi (Kenya) -Natron (Tanzania) basin during the late Quaternary. - Paleogeogr. Paleoclimat. Paleoecol. 58, 155-181, Amsterdam

HOFMANN, H.J. (1969): Attributes of stromatolites. - Geol. Surv. Can. Pap. 69-35, 1-77, Ottawa

HORODYSKI, R.J. & VONDER HAAR, S.P. (1975): Recent calcareous stromatolites from Laguna Mormona (Baja California), Mexico. - J. Sed. Petrol. 45, 894-906, Tulsa

JAMES, N.P., WRAY, J.L. & GINSBURG, R.N. (1988): Calcification of encrusting aragonitic algae (Peyssonneliaceae): implications for the origin of late Paleozoic reefs and cements. - J. Sed. Petrol. 58, 291-303, Tulsa

KAZMIERCZAK, J., KEMPE, S., LANDMANN, G., LIPP, A., SURACHMAN, Y. & SUSANTO, D. (1986): Satonda excursion, trip report, 2 - 13 October, 1986. - In: Tambora Volcano, Cruise SO 45-B. – Interims Report to the BMFT, 34 pp. (unpublished), Hamburg

KAZMIERCZAK, J. & KEMPE, S. (1990): Modern cyanobacterial analogues of Paleozoic stromatoporoids. - Science 250, 1244-1248, Washington, D.C.

— & — (1992): Recent cyanobacterial counterparts of Paleozoic *Wetheredella* and related problematic fossils. - Palaios 7, 294-304, Tulsa

KAZMIERCZAK, J. & KRUMBEIN, W.E. (1983): Identification of calcified coccoid cyanobacteria forming stromatoporoid stromatolites. - Lethaia 16, 207-215, Oslo

KEMPE, S. (1982): Valdivia Cruise, October 1981: Carbonate equilibria in the estuaries of Elbe, Weser, Ems and in the southern German Bight. - In: DEGENS, E.T. (ed.): Transport of Carbon and Minerals in Major World Rivers, Part 1. – Mitt. Geol.-Paläont. Inst. Univ. Hamburg, SCOPE/UNEP, Spec. Vol., 52, 719-742, Hamburg

— (1990): Alkalinity: The link between anaerobic basins and shallow water carbonates? - Naturwissenschaften 77, 426-427.

KEMPE, S. & DEGENS, E. T. (1985): An early soda ocean? - Chem. Geol. 53, 95-108, Amsterdam

— & — (1986): Enthielt der urzeitliche Ozean Soda statt Kochsalz? - Spektrum der Wissenschaft 11, Weinheim.

KEMPE, S., KAZMIERCZAK, J. & DEGENS, E. T. (1989): The soda ocean concept and its bearing on biotic evolution. - In: CRICK, E. (ed.): Origin, Evolution and Modern Aspects of Biomineralization in Plants and Animals. – Proc. 5th Int. Symp. Biomineralization, Arlington, Texas, May, 1986). – 29-43, New York (Plenum Press)

KEMPE, S. & KAZMIERCZAK, J. (1990a): Chemistry and stromatolites of the sea-linked Satonda Crater Lake, Indonesia: A recent model for the Precambrian sea? - Chem. Geol. 81, 299-310, Amsterdam

— & — (1990b): Calcium carbonate supersaturation and the formation of in situ calcified stromatolites. - In: ITTEKKOT, V.A., KEMPE, S., MICHAELIS, W. & SPITZY, A. (Eds.): Facets of / Modern Biogeochemistry. – Festschrift for E.T. Degens on occasion of his 60th birthday, 255-278, Berlin (Springer)

KEMPE, S. & PEGLER, K. (1991): Sinks and sources of CO_2 in coastal seas: the North Sea. - Tellus 43B, 224-235, Copenhagen

KEMPE, S., DIERCKS, A.-R., LIEBEZEIT, G. & PRANGE, A. (1991): Geochemical and structural aspects of the pycnocline in the Black Sea (R/V KNORR 134-8 leg 1, 1988). - In: IZDAR, E. & MURRAY, J.W. (eds.): Black Sea Oceanography. – NATO Advanced Studies Institute Series C, Vol. 351, 89-110, Dordrecht (Kluwer)

KEMPE, S., KAZMIERCZAK, J., KONUK, T., LANDMANN, G., LIPP, A. & REIMER, A. (1992): Mikrobialithe in alkalischen Seen - lebende Zeugen des Urozeans? - Spektrum der Wissenschaft 1, 14-15, Weinheim

KLING, G. CLARK, M.A., COMPTON, H.R. et al., (1987): The 1986 Lake Nyos gas disaster in Cameroon, West Africa. - Science 236, 169-175, Washington, D.C.

KREBS, W. (1974): Devonian carbonate complexes of Central Europe. - In: LAPORTE, L.F. (ed.): Reefs in Time and Space. – Soc. Econ. Paleont. Miner. Spec. Pub. 18, 155-208, Tulsa

KRUMBEIN, W.E. & COHEN, Y. (1977): Primary production, mat formation and lithification: Contribution of oxygenic and facultative anoxygenic cyanobacteria. - In: FLÜGEL, E. (ed.): Fossil Algae: Recent Results and Developments. – 37-56, Berlin (Springer)

KRUMBEIN, W.E. & GIELE, C. (1979): Calcification in a coccoid cyanobacterium associated with the formation of desert stromatolites. - Sedimentology 26, 593-604, Oxford

LANIER, W.P. (1988): Structure and morphogenesis of microstromatolites from the Transvaal Supergroup, South Africa. - J. Sed. Petrol. 58, 89-99, Tulsa

LYONS, W.B., LONG, D.T., HINES, M.E., GAUDETTE, H.E. & ARMSTRONG, P.B. (1984): Calcification of cyanobacterial mats in Solar Lake, Sinai. - Geology 12, 623-626, Boulder

MILLERO, F.J. (1974): The physical chemistry of seawater. - Ann. Res. Earth Planet. Sci. 2, 101-150, Amsterdam

PALMER, T.J. & FÜRSICH, F.T. (1981): Ecology of sponge reefs from the Upper Bathonian of Normandy. - Palaeontology 24, 1-25, Oxford

PEGLER, K. & KEMPE, S. (1988): The carbonate system of the North Sea: determination of alkalinity and TCO_2 and calculation of PCO_2 and SI_{cal} (spring 1986). - In: KEMPE, S., LIEBEZEIT, G., DETHLEFSEN, V. & HARMS, U. (eds.): Biogeochemistry and Distribution of Suspended Matter in the North Sea and Implications to Fisheries Biology. – Mitt. Geol.-Paläont. Inst. Univ. Hamburg, SCOPE/UNEP Sonderbd., 65, 35-87, Hamburg

REID, R.P. (1987): Nonskeletal peloidal precipitates in Upper Triassic reefs, Yukon Territory (Canada). - J. Sed. Petrol. 57, 983-990, Tulsa

REID, R.P., MACINTYRE, I.G. & JAMES, N.P. (1990): Internal precipitation of microcrystalline carbonates: a fundamental problem for sedimentologists. - Sediment. Geol. 68, 163-170, Amsterdam

RIPPKA, R., WATERBURY, J.B. & STANIER, R.Y. (1981): Provisional generic assignments for cyanobacteria in pure culture. - In: STARR, M.P. et al. (eds.): The Prokaryotes. – 247-256, Berlin (Springer)

SELF, S., RAMPINO, M. R., NEWTON, M. S. & WOLF, J. A. (1984): Volcanological study of the great Tambora eruption in 1815. - Geology 12, 659 - 663, Boulder

SIGURDSSON, H. & CAREY, S. (1988): The far reach of Tambora. - Nat. Hist. 6/88, 67-73, New York

STEIGER, T. & WURM, D. (1980): Facies patterns of Upper Jurassic platform carbonates (Plassen Limestone, Northern Alps, Styria/ Austria). - Facies 2, 241-283, Erlangen

STOMMEL, H. & STOMMEL, E. (1979): The year without a summer. - Scient. Amer. 240, 134-140, New York

UREY, H. C. (1951): The origin and development of the Earth and other terrestrial planets. - Geochim. Cosmochim. Acta 1, 209 - 277, Oxford

WALKER, R. & MOSS, B. (1984): Mode of attachment of six epilithic crustose Corallinaceae (Rhodophyta). - Phycologia, 23, 321-329, Oxford

WALTER, M.R. (1983): Archean stromatolites: evidence of the Earth's earliest benthos. - In: SCHOPF, J.W. (ed.): Earth's Earliest Biosphere. – 187-213, Princeton (Univ. Press)

WALTER, M.R. & HEYS, G.R. (1985): Links between the rise of the Metazoa and the decline of stromatolites. - Precambrian Res. 29, 149-174, Amsterdam

WIGLEY, T.M.L. & PLUMMER, L.N. (1976): Mixing of carbonate waters. - Geochim. Cosmochim. Acta 40, 989-995, Oxford

WRAY, J.L. (1977): Calcareous Algae. - 185 pp., Amsterdam (Elsevier)

Manuscript accepted January 16, 1993

STIC-ILL

9/10

From: Marx, Irene
Sent: Tuesday, September 10, 2002 9:19 AM
T : STIC-ILL
Subject: 09/777664

411618

Importance: High

Please send to Irene Marx, Art Unit 1651; CM1, Room 10E05, phone 308-2922, Mail box in 11B01

Observations on the ionic composition of blue-green algae growing in saline lagoons
AU Pillai, V. K.
SO Proc. Natl. Inst. Sci. India, (19550000) vol. 21, no. 2, pp. 90-102.
DT Journal

Dalrymple, D.W., 1965, "Calcium carbonate deposition associated with blue green algal mats, Baffin Bay.:, Texas: Institute of Marine Science Publication 10, p. 187-200

Black, M., 1933, "The algal sedimentation... ", Royal Society of London Philosphical transactions, Ser. B, V. 222, p. 165-192

Lowenstam HA (1981), Science, 211:1126-1131

Ferris et al., Earth Sci., 47:233-250 (1993)

Ferris et al., Appl. and Environm. Microbiol.,1989, 55:1249-1257

Kazmierczak et al., (1990), Science, 250:1244-1248

Kempe et al., Facies, 28:1-32, 1993.

Kempe et al., 1994, Bull, Inst. Oceanogr., Monaco no. spec., 13:61-117.

Merz, M.U.E, 1992, Facies, 26:81-102

Pentecost et al., 1986, Calcification in cyanobacteria, In "Biomineralization of Lower plants and animals (Leadbeater et a., ed. 73-90, Clarendon Press, Oxford.

Riding, R., 1982, Nature, 299:814-815

Thompson eta., 1990, Geology, 18:995-998

Irene Marx
Art Unit 1651
CMI 10-E-05,
Mail Box 11-B-01
703-308-2922

9/11

LC
9/11
SMP
NOS

FACIES	26	81-102	Taf. 19-20	7 Abb.	2 Tab.	ERLANGEN 1992

The Biology of Carbonate Precipitation by Cyanobacteria

Martina U. E. **Merz**, Marburg

KEYWORDS: CYANOBACTERIA – *SCHIZOTHRIX, SCYTONEMA* – CALCIFICATION – STABLE ISOTOPES – FRESHWATER CARBONATE – EVERGLADES (FLORIDA) – RECENT

CONTENT

SUMMARY

In the freshwater areas of the Everglades, Florida, U.S.A., carbonate is precipitated in dense cyanobacterial mats. Precipitation is linked with photosynthesis in the mats in a quantitative relationship.

On ground of field observations and experiments a model for precipitation in the filamentous cyanobacteria *Scytonema* is proposed, which links precipitation to bicarbonate use in photosynthesis and subsequent release of OH^- ions.

Besides supersaturation of the water with respect to carbonate and photosynthetic bicarbonate use, precipitation requires a suitable sheath structure and composition. The characteristics of the sheath seem to be responsible for a distinct crystal morphology in the two genera *Scytonema* and *Schizothrix*, as well as for the restriction of calcification to the outer sheath in *Scytonema*. In the immediate vicinity of the trichom precipitation seems to be inhibited.

Comparison of this form of calcifying cyanobacteria with calcification in calcareous algae shows many similarities and rises the question of the biological significance of calcification or precipitation.

The precipitated carbonate shows equilibrium precipitation in its δ oxygen values, while it is enriched in ^{13}C relative to the ambient water. This agrees with a model of precipitation in which the carbonate derives from the water immediately surrounding the filament. There the water is depleted in ^{12}C which is preferably taken up for photosynthesis. No respiratory carbon is involved in precipitation.

From measurements of the amount of precipitation in the field and in experiments the annual sedimentation rate is estimated to be 0.024 to 0.24 mm. These values fall within the range of laminae thicknesses in fossil algal laminites.

1 INTRODUCTION

From the Precambrian-Cambrian boundary until the end of the Cretaceous, calcifying cyanobacteria frequently occur in normal marine environments. After the end of the Cretaceous, however, they seem to be restricted to non-marine settings. In the Modern, calcification of cyanobacteria occurs almost exclusively in freshwater, and hypersaline or brackish waters. Because the precipitation is extracellular, this change in environmental distribution is believed to reflect changes in sea water chemistry. It has been proposed that the calcium/magnesium ratio (RIDING, 1982) or the degree of supersaturation with respect to carbonate (KEMPE & KAZMIERCZAK, 1990) of the oceans changed, leading to less favourable conditions for precipitation. To determine, what other environmental factors may have affected this change in geological distribution, it is neccessary to know which mechanisms of calcification exist in cyanobacteria and how the mutual influence of organic and inorganic factors in precipitation might vary in different environments.

Photosynthesis and photosynthetic uptake of bicarbonate

Address: Dr. M. Merz, Institut für Geologie und Paläontologie, Hans Meerwein Str., Lahnberge, D-3550 Marburg

have been shown to be the driving mechanism for the calcification in many calcareous algae (Borowitzka, 1990). The same was suggested for cyanobacteria (for example: Golubic, 1972; Braithwaite et al., 1989). Conclusive evidence from field observations or experimental data, however, are scarce. It has been shown by Gleason that in the Florida Everglades the timing of carbonate precipitation in cyanobacterial mats coincides with photosynthetic activity and that inorganic factors seem to play a neglegible role in precipitation (Gleason, 1972; Gleason & Spackman, 1974). The Florida Everglades, therefore, have been chosen as an excellent location for field experimentation on the mechanism of carbonate precipiation.

2 INTRODUCTION TO CYANOBACTERIA

2.1 Photosynthesis

Photosynthetic activity is an important factor in the calcification of calcareous algae. By its effect on water composition and especially pH, it creates an environment where carbonate precipitation can easily be induced.

Photosynthesis transforms light energy into chemical energy, which can be used for the formation of organic molecules from CO_2 and other inorganic substances. The photosynthetic apparatus of plants and cyanobacteria, which absorbs the energy, consists of two photosystems (PS I and PS II) in which photosynthetically active pigments, generally chlorophylls, absorb light of an appropriate wavelength. The absorbed light energy is then transformed into chemical energy (NADPH and ATP) via two electron transport chains. Thereby water is reduced in PS II. While the hydrogen is used in the electron transport chains, the oxygen is released by the cells into the medium. The energy stored in NADPH and ATP is used for the synthesis first of a hexose, and subsequently of various other substances.

The synthesis of these substances begins with the attachment of CO_2 to RuBP ('carboxylation'). The reaction is catalyzed by the enzyme RUBISCO-carboxylase. In this reaction the CO_2 can be substituted by O_2, which leads to the unintentional oxidation of RUBISCO instead of its carboxylation. Photosynthesis is more effective, the higher the ratio is of CO_2 to O_2, because less energy is lost by the oxidation of RUBISCO. Plants and cyanobacteria developed various techniques to increase the concentration of CO_2 relative to O_2. The RUBISCO of cyanobacteria has an especially low affinity for CO_2 (Raven & Lucas, 1985). Nevertheless cyanobacteria photosynthesize rapidly even at low CO_2-concentrations. They posses a mechanism which allows them to increase the intracellular concentration of inorganic carbon (DIC) up to 1000-fold above that of the ambient water (Lucas, 1983; Volokita et al., 1984; Kaplan et al., 1987). The DIC concentrating mechanism consists of an energy consuming pump-system, which actively tak sup DIC and transports it into the cells (Kaplan et al., 1987; Badger & Price, 1989). CO_2 is taken up preferentially, but bicarbonate is taken up as well, especially at high pH-values (Miller & Colman, 1980; Price & Badger, 1989 a; Miller et al., 1990). The species arriving at the inside of the cell seems to be always HCO_3^- (Badger et al., 1985; Ogawa & Kaplan, 1987; Reinhold et al., 1987). In the cell interior, the conversion of HCO_3^- to CO_2 is catalyzed by the enzyme carboanhydrase (CA). Whichever carbon species was taken up, only CO_2 is finally used for the carboxylation of RuBP. Nevertheless, in the following 'HCO_3^- use in photosynthesis' will be used if the original species taken up was bicarbonate.

The energy required to run the DIC-pump is balanced by the increase in the rate of photosynthesis under low-CO_2 conditions. In environments where CO_2 supply rather than the available light energy limits the rate of photosynthesis, the active uptake of HCO_3^- gives an advantage over organisms which have to rely on CO_2 uptake alone. Under high O_2 concentrations, as frequently found in microbial mats, the intracellular accumulation of DIC might help to suppress oxydation of RuBP (Prins & Elzenga, 1989; Raven & Lucas, 1985).

Another positive effect of the DIC concentration could be as a protection from photoinhibition (Badger & Andrews, 1982; Kaplan, 1985; Krause, 1988). Photoinhibition occurs when more light energy is absorbed by the photosystems than can be used for the formation of NADPH and ATP. Some of the excessive energy is released in the form of fluorescence or heat, but the rest might irreversibly damage the photosynthetic apparatus. An active DIC pump allows higher rates of carbon fixation, so that higher light levels could be utilized. In addition some of the potentially damaging energy could directly be used to run the pump (Kaplan, 1981).

2.2 Carbonate Precipitation Associated with Cyanobacteria

Cyanobacteria can live as single cells (coccoid cyanobacteria) or several cells may be linked to form cell rows, called trichom. If the trichom is surrounded by a mucilagenous sheath, the structure is called a filament. The main constituents of the sheath are polysaccharides. The function of the sheath is still unclear, but it seems to be involved in the ability of many benthic cyanobacteria to glide towards optimum light conditions.

The occurence of cyanobacteria is frequently linked to the deposition of carbonate. By trapping sediment between the filaments, they are involved in the formation of stromatolites in both sea water and freshwater. Cyanobacteria can also calcify when carbonate is precipitated in association with the organism. The result of precipitation is often a micritic tube surrounding the filament or the trichom. Similar tubes can be found in the fossil record in marine environments from the Precambrian-Cambrian boundary until the end of the Cretaceous. Various names are given to these fossils depending on the tube diameter, possible branching, and overall growth form. While some of the names might unite several biological species under the same fossil name (Riding, 1977 b), and others might be due to organisms other than cyanobacteria, there is little doubt that most of them do represent calcified cyanobacteria. From the Cretaceous onward, calcification seems basically restricted to non-marine

environments (PENTECOST & RIDING, 1986).

In the Modern, calcification occurs in a variety of environments, often in shallow water poor in nutrients (GLEASON, 1972; SABATER, 1989), and nearly always non marine. In freshwater, calcifying cyanobacteria can frequently be found in spring tufas or oncolites. It has been estimated that in tufas the photosynthetic activity of the cyanobacteria can only account for 1 to 2 % of the precipitated carbonate while the rest of the carbonate is precipitated because of equilibration of the water with the atmospheric conditions (PENTECOST, 1978). Calcification of filaments also occurs in shallow hypersaline environments, which might be exposed to periods of emersion or freshwater influx (GOLUBIC, 1983; HORODYSKI & VONDER HAAR, 1975) and in desert crusts or caves where the cyanobacteria are living in a subaerial environment (COX et al., 1989; JONES & KAHLE, 1986; KRUMBEIN & GIELE, 1979). Calcification of living cyanobacteria in a normal marine setting is only described by GOLUBIC & CAMPBELL (1981), as a species specific calcification of various *Rivularia* species. The degradation of dead cyanobacterial material also seems to promote calcification in cyanobacterial mats (DEFARGE et al., 1985; LYONS et al., 1984), although it is not always clear whether cyanobacteria have been calcified alive or post mortem (BRAITHWAITE et al., 1989). It seems unlikely that the mechanism of calcification and the degree of biologic influence is the same in all these environments.

In calcification of modern cyanobacteria, a distinction has to be made between two different forms of calcification because they may reflect two different ways of precipitation concerning the degree of influence by the cyanobacteria. One is the encrustation of the sheath with carbonate, where the crystals nucleate outside on the sheath surface. This form has been called 'encrusted sheath' by RIDING (1977 a). The result is a carbonate tube with an inner diameter reflecting the diameter of the filament. This form of calcification often occurs in environments such as tufas, where mostly inorganic factors such as CO_2 degassing or temperature increase lead to precipitation. An influence of photosynthesis on tufa deposition could not be shown (GOLUBIC, 1972; PENTECOST, 1980; PENTECOST & RIDING, 1986).

The other form of calcification is the impregnation of the sheath with carbonate crystals. In this form, which is termed 'impregnated sheath', are the crystals precipitated completely within the sheath (RIDING, 1977 a). The outer diameter of the resulting micrite tube corresponds to the outer diameter of the filament, while the inner diameter might have the same or a larger diameter than the trichom. It is this second form of calcification which seems to be controlled by the organism, with precipitation being closely tied to the physiological activity of the cyanobacteria.

The calcification of the sheath also seems to depend on taxa-specific characteristics (PENTECOST & RIDING, 1986). *Plectonema* shows similar forms of calcification in different environments such as stromatolitic crusts in the Borrego Desert, California, (KRUMBEIN & POTTS, 1979) and temporary freshwater ponds on the Aldabra Atoll (RIDING, 1977 a). On the other hand, do different species calcify differently in the same environment (KRUMBEIN & GIELE, 1979; GOLUBIC & CAMPBELL, 1981; LEINFELDER, 1985; OBENLUNESCHLOSS & SCHNEIDER, 1990). The different morphology of the crystals is probably due to differences in the chemical composition and the arrangement of the polysaccharides in the sheaths. The polysaccharides probably provide a suitable surface for nucleation. They absorb calcium ions, which consequently serve as binding sites for carbonate ions.

In both cases, encrustation and impregnation of the sheath, the mineralogy of the precipitated carbonate corresponds to the chemistry of the ambient water. Aragonite is precipitated in sea water, high-magnesian calcite in brackish water, and low-magnesian calcite in freshwater (PENTECOST & RIDING, 1986).

3 METHODS

Temperature and pH were measured in the field with a portable Orion pH/T/volt meter (model SA 230) and an Orion combination electrode. For measurements of the pH in the cyanobacterial mats an Ingold combination electrode with a tip diameter of 3.5 mm was used. Temperature was measured with a resolution to 0.1 C, accuracy +/-1.0 C, pH with a resolution to 0.01, accuracy ±0.02.

Oxygen was measured in the field with a portable oxygen-meter from YSI, model 52, with a resolution to 0.1 ppm. The electrode was calibrated against air, following the procedure described in the YSI manual.

Water depth was measured against an arbitrary scale with a zero mark at the sediment surface. The light intensity was measured in the air with a portable lux meter from Lutron, model LX 101.

For measurements of calcium and chloride concentration and of alkalinity, water samples were taken to the laboratory. For the calcium and alkalinity measurements, 30 ml samples were filtered in the field (Whatman G/F glasfiber filters) and poisened with one drop of concentrated $HgCl_2$ to prevent alteration by biological activity. For chloride determination filtered 15 ml samples were taken but no $HgCl_2$ was added.

Alkalinity was titrated in 10 ml samples with 0.1 or 0.05n HCl, following the method by GRAN (1952), using a Corning combination electrode to measure the pH changes after the addition of acid. Reproducibility of the results was better than 0.02 meq. 1, 2, and 3 meq laboratory standards of $NaCO_3$ were used for standardization.

Calcium was titrated with 10 or 1 mmol EGTA according to the method of GIESKES (1986). Reproducibility was 1 ppm (0.025 mmol). A 50 ppm $CaCO_3$ solution was used as a standard.

Chloride was also titrated following the method by GIESKES (1986). The titrant was diluted to 0.01 mol. Reproducibility was better than 5 %. Better results could not be determined because of the very low chloride concentrations in the samples.

The amount of dissolved inorganic carbon (DIC) was calculated from the measurements of pH, temperature, alkalinity, and calcium and chloride concentration, using the equilibrium constants by MILLERO (1979), corrected for the ionic strength as described by HELDER (1988). The amount of precipitation was calculated by the changes in calcium

concentration and alkalinity, with the decrease in calcium being equal to, and the change in alkalinity being twice the amount of precipitation. For the cyanobacteria the change in calcium reflects th amount of precitated carbonate while the change in alkalinity reflects precipitation as well as the amount of DIC being concentrated inside the cells. Normally, however, the amount of intracellular DIC can be assumed to be very small as compared with the amount of precipitated carbonate. Total DICs were calculated from pH, temperature, and water analyses before and after the experiments. The photosynthetic CO_2 uptake was calculated assuming that the total decrease of DIC in the water, minus that removed by precipitation, reflects the DIC used in photosynthesis.

Cyanobacterial mats, water, sediment, and gastropod shells were measured for their carbon and oxygen isotopic composition. All samples were measured with a Finnigan-MAT mass spectrometer, model MAT 251.

Oxygen isotopes in the water were measured following the method by EPSTEIN & MAYEDA (1953).

Carbon isotopic composition of the DIC in the water was measured in CO_2 liberated from the water, following the addition of 0.5 ml concentrated phosphoric acid to a 5 ml water sample. The samples taken at the beginning of the wet season (7/16/89 to 9/26/89) were allowed to equilibrate with 10 ml of air. This leaves oxygen isotopic composition basically unaffected, carbon isotopic composition, however, might have changed towards equilibrium values with the atmosphere. As the measured values are well below equilibrium values, the original composition must have been even lighter.

Samples of the sediment and gastropods were always collected from the same horizon of a core to obtain samples of the same age that probably precipitated from a water of comparable isotopic composition. The shells were carefully cleaned from the attached sediment before being measured. The isotopic composition was measured in the CO_2 produced after treatment with phosphoric acid.

All laboratory work was done under supervision of Dr. P.K.Swart in the Stable Isotope Laboratory of the Rosenstiel School of Marine and Atmospheric Sciences, University of Miami.

Sediment cores of the Holocene carbonate muds were taken manually with 8 cm diameter aluminum tubes. They were frozen, slabbed, and oven dried. For thin sections and polished slabs, the cores were vacuum-impregnated with resin.

Cyanobacteria samples for microscopic observations were fixed for several hours by the addition of 3.5 % glutaraldehyde in filtered water from the sampling site to preserve organic structures. The samples were then gradually transferred into a 70 % alcohol solution. Samples for the electron microscope were critical point dried. This method minimizes the disruption of organic structures by dehydration. First the samples have to be transferred into ethyleneglycol then into 100 % acetone. The acetone is then replaced by liquid CO_2. Finally the samples are dried at the critical temperature and pressure conditions of CO_2, when the liquid and the gaseous phase coexist. Drying under these conditions causes minimal shrinkage in the organic material. Th storage in alcohol, h wever, leads to a certain volume change.

For observations of the carbonate crystals in the sheaths, the specimen were treated with sodiumhypochlorite (Clorox) to disintegrate the organic material.

The amount of organic versus inorganic material was determined by ashing the samples at 55° C for 3 hours. The change in weight reflects the amount of organic material, whereby an amount of 7 % ash was assumed (WOLK, 1973).

For the experiments, 0.4 to 1.0 g (dry weight) of cyanobacterial mats covering floating parts of submerged plants were used, after being cleaned from plant material. They were incubated in beakers holding up to 600 ml of sampling-site water. The experiments were generally started in the early morning, before the onset of photosynthesis, and run until the late afternoon when decreasing oxygen concentrations indicated the cease of photosynthesis. Some experiments were run over 24 hours or even over several days, to measure dissolution as well as precipitation. The experiments were run in sets of 2 to 5 replicates and the same experimental setup was repeated on several days.

Experiments were made with dichlorphenyldimethylurea (DCMU), an inhibitor for the activity of PS II, and ethoxyzolamide, an inhibitor for bicarbonate use in photosynthesis. DCMU was dissolved in methanol and added to the incubated samples to give final concentrations of 10^{-5}, $5x10^{-5}$, and 10^{-6} mol DCMU. Ethoxyzolamide was dissolved in Dimethylsulfoxide (DMSO) and appropriate amounts were added to give final concentrations of $2x10^{-4}$, $4x10^{-4}$, and $6x10^{-4}$ mol ethoxyzolamide (PRICE & BADGER, 1989 b).

As the effect of the inhibitors was variable on different days, each set of experiments included 2 to 5 untreated controls consisting of cyanobacteria incubated in pure sampling-site water. The controls always showed significantly higher amounts of precipitation than the cyanobacteria treated with an inhibitor.

In most experiments, no attempt was made to inhibit gas exchange with the atmosphere in order to prevent a buildup of high oxygen concentrations and therefore favouring photooxidation. Only when it was intended to measure the amount of photosynthesis were the experiments carried out in tightly covered beakers or in sealed Erlenmeyer flasks. While pH, temperature, and oxygen were generally measured every hour, measurements in the closed containers were only taken at the beginning and end of every experiment.

A slight underestimation of the amount of precipitation due to an increase of ion concentration by evaporation in the uncovered beakers does not affect the interpretation of the experimental data, because the results are always interpreted in relation to untreated controls of the same day.

To allow a comparison of the amount of precipitation in the various containers, precipitation was calculated, knowing the amount of incubated cyanobacterial material, as the theoretical amount of carbonate precipitated by 1 g cyanobacteria out of 1 l of water in 10 hours (mmol/g/l/10h).

4 CYANOBACTERIAL MATS IN THE FLORIDA EVERGLADES

4.1 The Environment

The Everglades are situated at the southernmost tip of the Florida mainland. The most important environmental feature is the seasonal runoff of freshwater to the south and southwest over six to eight months per year, temporarily covering extensive areas in the Everglades with shallow water. Where the freshwater mixes with the marine waters of Florida Bay, a mangrove belt is developed protecting the areas to the north from marine influence. The typical sediment is a mangrove peat of varying thickness. Northward, in the freshwater prairies, there is a vegetation which can withstand several months of complete dessication, consisting mostly of sawgrass (*Cladium jamaicensis*), a few scattered mangroves, and extensive cyanobacterial mats. Carbonate muds accumulate in these areas. GLEASON has shown that the carbonate is precipitated during the day, within the cyanobacterial mats, rather than being caught between the filaments (GLEASON, 1972; GLEASON & SPACKMAN, 1974). Inorganic factors are unlikely to play a significant role in precipitation in the Everglades. As the water flows over large distances and is very shallow (up to 50 cm), it is well equilibrated with the atmosphere except for a temporal disequilibrium caused by the biologic activity of the microbial mats. During times of complete water cover, flow velocities up to 25 cm per second (8/27/91) were estimated.

The sampling site is located in the freshwater prairies, east of Paurotis Pond, along the road from Florida City to Flamingo (fig. 1). It is covered by water from about July to January or February. During this time cyanobacterial mats develop, covering the sediment surface and submerged parts of plants. Well-developed mats are one to two centimeters thick. The surface of the mats is greyish brown or yellow because of a high content of protective carotenoids. Most of the chlorophyll is concentrated in the deeper layers of the mats, causing a deeply green colour.

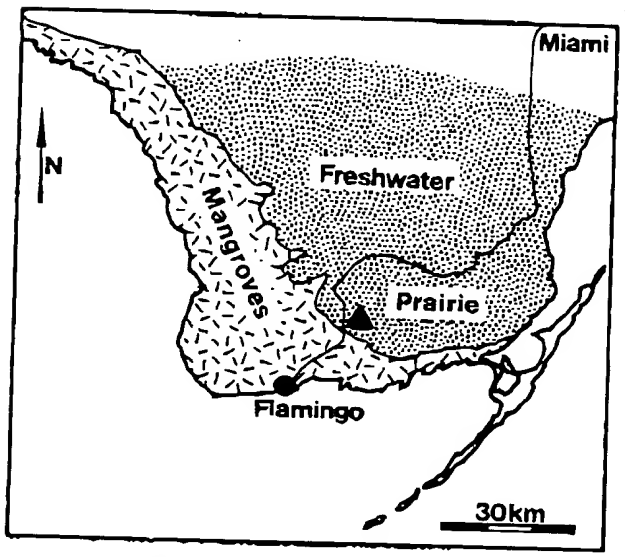

Fig. 1. The sampling site, marked with a black triangle, is located in the freshwater areas of the Everglades National Park, east of Paurotis Pond, at the road from Florida City to Flamingo.

The mats are dominated by calcifying species of filamentous cyanobacteria, *Schizothrix* and *Scytonema* (determination by courtesy of S.GOLUBIC).

4.1.1 The Water

The 1989/90 wet season (e.g. period of complete water cover at the sampling site) was relatively short due to little rainfall in this and the previous season. It lasted from the first week of July to the end of December. By this time the site was completely dry again. During the wet season the alkalinity of the water rose from 1.5 meq in July to 2.5 meq at the end of December. The calcium concentration rose in the same time from 1.1 to 1.25 mmol. Only in the first week of July were both concentrations higher, with an alkalinity of 1.7 meq and a calcium content of 4.5 mmol. Both alkalinity and calcium showed their lowest concentrations in September and October, when the water level was highest. As can be seen in fig. 2, the concentrations show a distinct peak in the middle of August, possibly related to a change in the flow direction of the water (in the figure indicated by arrows). At low water level (less than 5 cm), the water at the sampling site flows to the east, while at higher water levels it flows westward over the sampling site. With the changing flow directions, water from slightly different source areas might reach the site.

The concentration of chloride varied during the wet season between 1.0 and 7.5 mmol after it dropped from 18 mmol to 1.3 mmol in the first three weeks of water cover. The extremely high chloride concentration at the beginning of the season might be caused by the dissolution of easily soluble minerals that were precipitated during the period of dessication.

The measured water temperature at the sampling site showed extremes of more than 41°C in August to around 10°C at the end of December. The average temperature lies around 25° C (SWART et al., 1990; MERZ, 1990).

While most of the seasonal variations in water composition are due to the effects of evaporation and run-off, alkalinity, calcium concentration, oxygen and pH also show strong daily variations caused by the activity of the microbial mats. The concentration of chloride is neither influenced by physiological activities nor by carbonate precipitation and was therefore measured as a reference to determine the importance of biological factors.

Daily variations:

In the first week of complete water cover, before the cyanobacterial mats were developed at the sampling site, alkalinity, pH, and calcium concentration were measured over 24 hours. The concentration of calcium rose slightly during the day (from 4.69 mmol at 9 am to 4.79 mmol at 7 pm), alkalinity showed a week maximum in the midmorning (1.89 meq at 7 am, 1,90 meq at 11 am, and 1,68 meq at 7 pm). The pH varied unsystematically between 6.93 and 7.75. Later in the season, over well-developed cyan bacterial mats, temperature, pH, oxygen, calcium concentration, and alkalinity fluctuate systematically within 24 hours (Fig. 3).

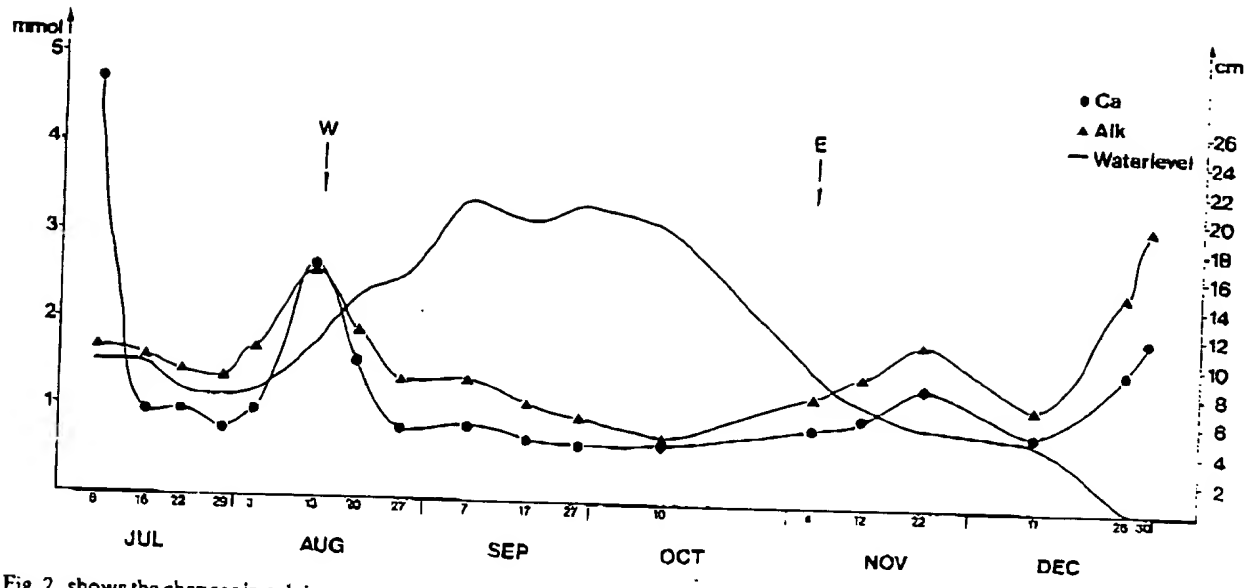

Fig. 2. shows the changes in calcium concentration, alkalinity, and water level from the first week of complete water cover at the sampling site (7/8/89) until the site was dried out at the end of December. All samples were taken around 6 pm. The arrows indicate changes in flow direction, to the East in the beginning of the wet season, to the West from August to November, and then, with decreasing water level, again to the East.

The pH can rise during day time more than one unit, up to values above pH 9. The lowest measured value was 7.04 in the early morning (8/20/89). The oxygen concentration, together with the pH, rises during daytime above equilibrium values with the atmosphere. In the evening it begins to fall. The minimum values of oxgen are measured in the early morning.

The concentration of chloride is constant throughout a day, indicating that the changes in calcium and oxygen concentration, alkalinity, and pH are caused by the biological activity in the microbial mats.

Both pH and oxygen concentration depend on the photosynthetic and respiratory activity of the microbial mats. Photosynthetic CO_2 uptake causes the pH to rise. Simultaneously, oxygen is released by the cells. Respiration is reflected by a decrease of oxygen concentration and pH, because of the release of CO_2.

Calcium concentration and alkalinity show, 1-2 hours out of phase, the reverse rhythm from oxygen concentration and pH. They decrease during the day, indicating carbonate precipitation during photosynthesis. The lowest values are reached about one hour before sunset. During the night they increase, when carbonate is dissolved by the respiratory activity in the microbial mats.

Several times measurements have been made of the water in the mat. During the daytime the pH was always significantly higher than in the water above the mats, while in the night it was lower. Although it was not possible to take samples of the mat water without any contamination of the overlying water, the calcium concentration and the alkalinity were always significantly higher in the mats.

4.1.2 The Sediment

The Holocene freshwater carbonate muds in the Everglades reach a thickness of up to 50 cm, depending on the relief of the underlying Pleistocene carbonates. In push cores it can be seen that the first few centimeters have a dark brown colour, rapidly fading with depth, because of a decrease in the content of organic material. Most of the sediment is a light brown to grey, unstructured carbonate mud, frequently containing plant roots and freshwater snails. The carbonate tubes of *Scytonema* appear to disintegrate rapidly as they could not be found in either thin section or by scanning electron microscopy.

While other carbonate muds associated with cyanobacterial mats often exhibit a distinct lamination (Andros Island, Bahamas, Monty, 1972; Hardie & Ginsburg, 1977), lamination in the sediment cores from the Everglades are restricted to the top few centimeters. The laminations are rapidly obscured with depth. This could be due to a different structure of the mats themselves, to a less pronounced periodicity in sediment accumulation, or to a higher rate of bioturbation in the Everglades.

Despite the proximity of the marine environment to the freshwater carbonate muds, no marine fossils are found. This fact is probably due to the protection by the mangrove belt which inhibits landward transport of marine sediments. In the fossil record, the carbonates of the Everglades would appear as unstructured micrites with a low fossil diversity, containing only a few species of freshwater snails.

4.2 Microscopic Observations

In the Everglades, the trichoms of *Scytonema* are surrounded by a sheath that is differentiated into two distinct layers. The inner sheath is dense, structured, and birefringent under crossed nicols and is always uncalcified (Pl. 19/1-3). The inner sheath is surrounded by a less dense outer sheath. The outer sheath is impregnated by micritic calcite crystals and encloses the inner sheath like bark a tree. In samples that have been critical point dried the outer sheath might break

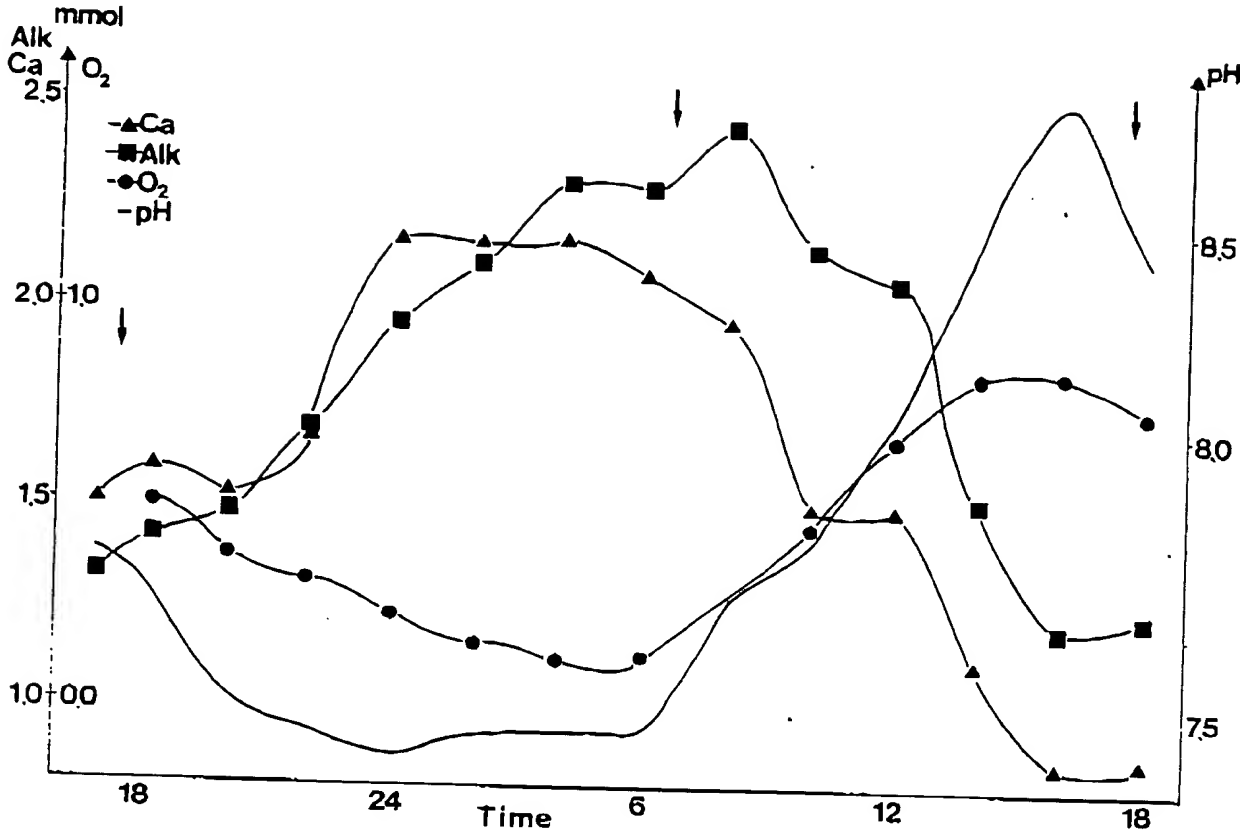

Fig. 3. Oxygen concentration and pH decrease after sunset (indicated by the arrow), while calcium concentration and alkalinity rise. After sunrise (arrow), the increase in oxygen concentration and pH indicates the onset of photosynthesis with an simultaneous decrease of calcium concentration and alkalinity. The time is given in 24 hours.

off and exhibit the smooth surface of the uncalcified inner sheath (Pl. 19/7). The crystals in the outer sheath may be as small as 2-3 µm, but are generally 5-7 µm long (Pl. 19/5).

The two sheaths seem to differ in structure as well as in chemical composition. Treatment with sodiumhypochlorite (Clorox) leads to the rapid disintegration of the outer sheath and the trichom, while the inner sheath remains preserved for an extended period of time. In most of the *Scytonema* filaments, the impregnation of the outer sheath leads to the formation of a dense carbonate tube (Pl. 19/6). The outer diameter of the tube is constant along the filament. As there is no precipitation in the inner sheath, the inner diameter of the tube reflects the diameter of the trichom plus the inner sheath. Close to the filament tip the diameter of the tube decreases. The filament tip itself is always uncalcified (Pl. 19/1). Calcification never exceeds the outer sheath. This is shown by the constant tube diameter, as well as by the fact that in critical point dried samples, the organic material of the sheath covers the outer surfaces of the crystals (Pl. 19/8). Treatment with Alizarin Red S leads to a staining of the organic material in the outer sheath. The crystals remain unstained which indicates that they are covered by organic material and therefore are not accessible to the stain.

Some of the *Scytonema* filaments show a completely different mode of calcification. Calcification is restricted to single rings within the outer sheath (Pl. 20/2-4). Some of them have the shape of straight cylinders (Pl. 20/3), while others are funnel shaped (Pl. 20/2, 4). The occurrence of the rings is independent of any morphological features of the filament. Rarely are the rings produced by the alternation of denser and less densely calcified zones of a continous tube.

Observations indicate that calcification of *Scytonema* and *Schizothrix* in the Everglades is different. These differences are similar to those reported by GLEASON & SPACKMAN (1974). Due to the small size of the filaments of *Schizothrix*, the structure of the sheath and the location of crystals within it is not as easily observed as in *Scytonema*. It can be seen, however, that the filaments are not as densely calcified. The calcification is generally restricted to single crystals or crystal conglomerates, that are probably embedded in sheath material (Pl. 20/1).

The morphology of the single crystals of the two taxa, as well as of the two different forms of calcification in *Scytonema* is distinctly different. Typical crystals of the *Scytonema* tubes are well developed rhombohedra that do not show any preferred orientation with respect to the trichom. The crystal faces in contact with the inner sheath are sometimes flattened, probably due to dissolution (Pl. 19/2). The crystals may form a tight tube, in which case the crystal morphology is not as distinct (Pl. 19/6).

The crystals in the carbonate rings of *Scytonema* have another morphology. They consist of single needles, or possibly dendritic crystals (Pl. 20/8). The morphologic difference is obvious even under the light microscope where

the crystals have a star-like appearance (Pl. 20/3). They appear to be embedded in organic material with a denser structure than the outer sheath of the other filaments. Due to this organic coating, the boundaries between single crystals are invisible (Pl. 20/8).

The calcite crystals in *Schizothrix* also have a distinct morphology. Their most remarkable feature is the dendritic growth which leads to the development of aggregates of calcite needles, following the crystallographic directions of calcite (Pl. 20/5-7). Some of them have a triangular form and seem to be oriented with their base parallel to the trichom (Pl. 20/7). The crystals may coalesce to form larger aggregates of dendrites enclosing short segments of the filament.

4.3 Carbonate Precipitation, Sedimentation Rates

Sedimentation rates of a freshwater carbonate mud, precipitated by cyanobacteria, can be estimated from the field and experimental data obtained in the Everglades. The alkalinity of water is not changed by photosynthetic CO_2 uptake and in freshwater (total) alkalinity is about equal to carbonate alkalinity (DREVER, 1988). Therefore it can be assumed that changes in alkalinity and in calcium concentration of a water both reflect carbonate precipitation or dissolution.

In this way the amount of precipitated and dissolved carbonate was calculated for 12 and 24 hour sampling periods of the 1989/90 wet season. Precipitation was calculated by subtracting the minimal values of alkalinity and calcium measured in the evening from the maximum values in the morning. Dissolution was calculated accordingly, by subtracting the maximum values in the morning from the minimum values of the previous evening. Because the maximum and minimum values were taken, the calculated timespans are slightly different at the different days. Tab. 1 shows the amount of precipitation, calculated for various days. On the 8/20 and 8/27 only precipitation has been measured, while on the 9/25, 10/10, 11/4, and 12/12/89 dissolution has been measured as well.

As can be seen in Tab. 1, the amounts of precipitation and dissolution per day vary considerably, but do not show any seasonal pattern. Precipitation varies from 0.09 to 0.46 mmol (assuming that the value of 1.10 mmol (11/4/89), estimated by the change in calcium concentration, is due to an analytical error). During the night, some of the carbonate, 0.05 to 0.5 mmol, is redissolved.

By subtracting the amount of dissolved carbonate from the amount of carbonate precipitated during the day, the net amount of precipitation from 1 l water in 24 hours can be estimated. As there seems to be hardly any sediment influx other than the carbonate precipitated by the cyanobacteria the estimated net precipitation reflects the amount of sedimentation. When the net sedimentation is calculated with field data it can be seen that there is net precipitation in two out of four days, while at the other two days the values indicate net dissolution.

From these data, 0.015 mmol $CaCO_3$ per liter water in 24 hours is taken as an average amount of precipitation throughout the wet season. In 1989 the duration of water cover at the sampling site lasted about 180 days, from the first week of July to the last week of December. As this wet season was comparatively short, because of a succession of especially dry summers, a normal duration of water cover of 200 days will be assumed for calculations of the annual sedimentation. The average water depth at the sampling site is taken to be 10 cm, estimated from the recorded water depth in 1989 (Fig. 2).

For a daily net precipitation of 0.015 mmol and a density of calcite of 2.7, a pore space free volume of 111 mm^3 $CaCO_3$ per wet season can be calculated. This gives an annual sediment layer with a thickness of 0.011 mm per

Plate 19 Light microscopical and SEM photographs of calcified *Scytonema* filaments, Everglades, Florida. All samples were taken in the freshwater algal marshes east of Paurotis Pond.

Fig. 1. Uncalcified filament tip of *Scytonema*. The structured inner sheath is clearly visible. The trichom is shorter than the sheath, which might be an artefact because of shrinkage during preparation. The outer sheath is vaguely visible. Sample fixed in 3.5 % glutaraldehyde. x 460

Fig. 2. Calcified filament of *Scytonema*. The inner sheath, surrounding the central trichom, appears dark. Single crystals are located in the outer sheath. The sides of the crystals facing the inner sheath are flattened, which might be a dissolution feature.Sample fixed in 3.5 glutaraldehyde. x 230

Fig. 3. Calcified filament of *Scytonema*. The layered structure of the uncalcified inner sheath is clearly visible, while in the outer sheath there are well developed calcite rhombohedra. Sample fixed in 3.5.% glutaraldehyde. x 460

Fig. 4. Filament of *Scytonema*, being enclosed in carbonate crystals. The single crystal rhombohedra are still clearly visible. Sample fixed in 3.5 % glutaraldehyde. x 460

Fig. 5. SEM photograph of a *Scytonema* filament, treated with sodiumhypochlorite. Well developed calcite rhombohedra are laying on the surface of the undisintegrated inner sheath.

Fig. 6. SEM photograph of a calcified *Scytonema* filament. The carbonate crystals coalesce to form a dense calcite tube around the trichom and the inner sheath. Sample treated with sodiumhypochlorite.

Fig. 7. SEM photograph of a calcified *Scytonema* filament. The outer sheath, heavily impregnated with carbonate crystals, broke off and exposed the smooth surface of the uncalcified inner sheath. Sample fixed in 3.5 % glutaraldehyd, critical point dried.

Fig. 8. SEM photograph of a calcified *Scytonema* filament. The organic material of the dried and collapsed outer sheath completely covers the calcite crystals. Sample fixed in 3.5 % glutaraldehyd, critical point dried.

Plate 19

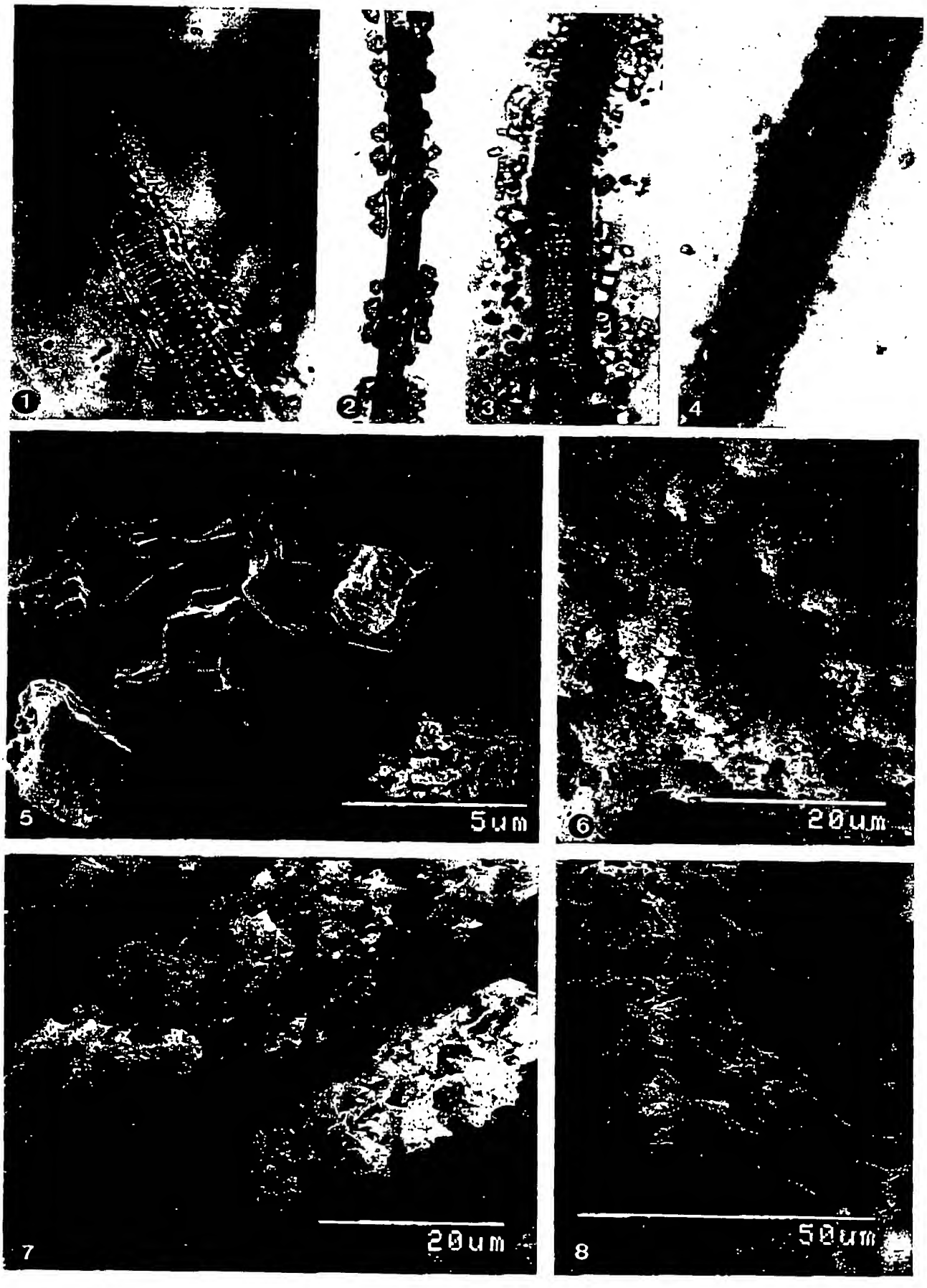

Date	20.8.89	27.8.89	25.9.89	10.10.9	4.11.89	12.12.89
Precipitati n						
Time	7-19:00	8-18:00	8-18:00	9-18:00	8-16:00	8-15:30
Ca^{2+}	0,340	0,350	0,194	0,111	1,105	0,456
Alk	0,090	0,325	0,185	0,150	0,615	0,460
Dissolution						
Time			18-8:00	18-9:00	8-16:00	15:30-7:30
Ca^{2+}			-0,212	-0,048	-0,467	-0,474
Alk			-0,230	-0,085	-0,565	-0,485
Net						
Ca^{2+}			-0,018	0,063	0,638	-0,018
Alk			-0,045	0,065	0,050	-0,025

Tab. 1. Amount of carbonate precipitation in mmol measured at various days during the 1989/90 wet season.

square dm (= precipitation out of 1 l of water with an average water depth of 10 cm).

The same calculations were made with the data obtained from cyanobacteria precipitating over 24 or 36 hours in experiments in 500 ml beakers. Again, the amount of net precipitation varied on different days. Experiments performed on 12/30/89 gave a net amount of 0.080 mmol/24 hrs from 1 liter, while experiments performed the 11th through 13th of January gave values of 0.200 mmol/24 hrs/liter. Taking the calculated values again as average values for precipitation throughout the wet season, annual sediment thicknesses of 0.60 to 0.148 mm are estimated. Because they were measured in closed containers rather than in running water, these values should be more exact than the data obtained from the field measurements.

Assuming 60% pore space the thickness of the annually accumulated sediment layer would be 0.018 mm (1.8 cm/1000 yrs) for the field data, and 0.1 and 0.24 mm (10 and 24 cm/1000 yrs) for the experimental results. These calculations are made ignoring a possible contribution by organic material (30 % dry weight of the cyanobacteria).

Scholl et al. (1969) estimated the sedimentation rates in the Everglades from ^{14}C-data to be 1.6 cm/1000 yrs, with higher rates immediately after flooding of the platform about 4000 yrs b.p. and slowly decreasing later (1.2 mm/yr in the first 1000 yrs). Their estimates give sedimentation rates that are 10 times higher than the ones calculated in this study from the field data, but they fall within the range calculated from the experimental data (for the representativity of the experimental data see Chapter 4. 6.1).

When comparing the data from the Everglades with the laminae thicknesses of fossil laminites, it must be kept in mind that the volume changes during diagenesis might be considerable and highly variable. It is difficult to estimate how much of the original porosity will be destroyed by compaction and how much might be preserved by early cementation. The data from the Everglades, however, lie well within the range of laminae thicknesses given by Müller-Jungbluth for the Hauptdolomite, Triassic, Northern Calcareous Alps. He measured laminae of 0.08 to 1.0 mm thickness in the Middle Hauptdolomite, and 0.1 to 5 mm in the Lower Hauptdolomite (Müller-Jungbluth, 1968; 1970).

4.4 Organic Material

The field observations show a close temporal relationship between photosynthesis and the precipitation of car-

Plate 20 Lightmicroscopical photographs of *Scytonema* and *Schizothrix*, SEM photographs of calcification in *Schizothrix*. All samples were taken in the freshwater algal marshes east of Paurotis Pond, Everglades, Florida.

Fig. 1. *Schizothrix* filament in the light microscope. The crystals appear star like in the light microscope. The tiny filament is vaguely visible between the carbonate crystals. It apparently is surrounded by a voluminous unstructured sheath. Sample fixed in 3.5 glutaraldehyde. x 460

Fig. 2.-4. Ring calcification in *Scytonema*. The rings can be funnel shaped (2), cylindrical (3), or look like shallow bowls (4). The morphology of the crystals in the rings is similar to the crystal morphology in *Schizothrix*. As in the continously calcified *Scytonema* filaments (Plate 19) remains the inner sheath always uncalcified. Under the light microscope it is clearly visible because of its darker colour and layered structure. Samples fixed in 3.5 % glutaraldehyde.

Fig. 5. SEM photograph of a single dendritic *Schizothrix* crystal. Sample treated with sodiumhypochlorite.

Fig. 6. SEM photograph of a calcified *Schizothrix* filament, densely encrusted by dendritic calcite crystals. Sample treated with sodiumhypochlorit .

Fig. 7. SEM photograph of a calcified *Schizothrix* filament. The dendritic crystals are triangular and their base seems to be oriented parallel to the filament.

Fig. 8. SEM photograph of ring calcification in *Scytonema*. The crystals, possibly dendritic, seem to be embedded in organic material denser than the outer sheath of the continously calcified *Scytonema* filaments.

Plate 20

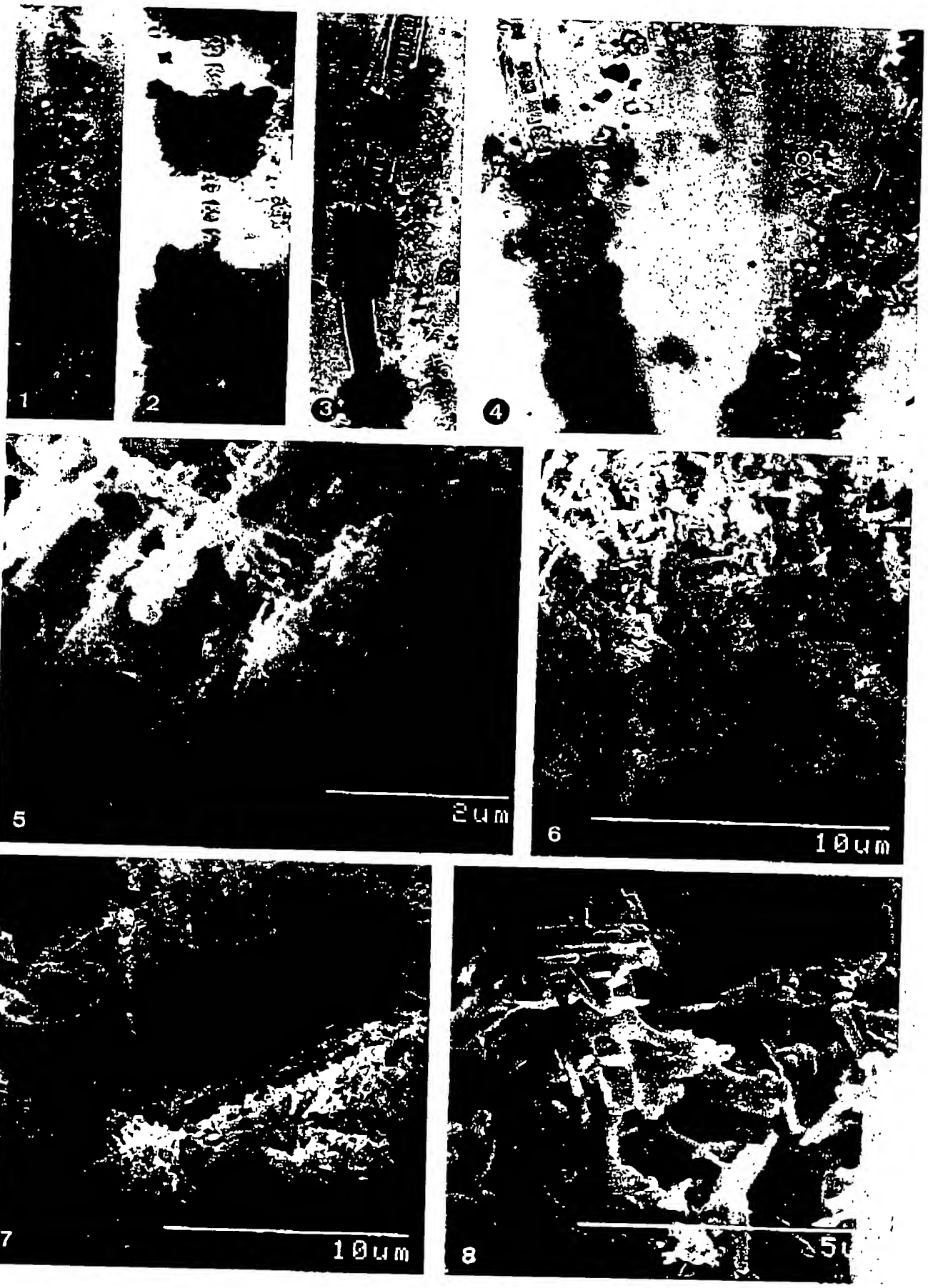

bonate. They do not allow, however, deductions to be drawn about how actively the carbonate is precipitated by the cyanobacteria. Precipitation could simply be a byproduct of photosynth sis, which the organism is unable to inhibit. If this is the case, the amount of precipitation would be expected to depend on environmental conditions, such as the ion concentrations, temperature, and- biologically influenced- the pH. But if precipitation is a more active process, it should have a stronger relation to the rate of photosynthesis than to environmental factors.

To distinguish between these two possibilities, the amount of photosynthesis versus the amount of precipitated carbonate has been measured. Different methods were used, each showing constant ratios between photosynthesis and precipitation of 1 mol precipitated carbonate for 1 to 2 mol organically fixed carbon.

Measuring the percentage of organic material in 29 samples of cyanobacterial mats gives values close to 32 %. This percentage is constant throughout the season, independent of the time when the sample was taken, showing that there is no stronger calcification in older cyanobacteria. In order to compare the amount of precipitation with the amount of organically fixed carbon, the amount of carbon in the organic material was calculated, assuming that the organic material of cyanobacteria contains 46 % carbon (Wolk, 1973). The amount of carbon fixed organically and the amount precipitated in carbonate shows a constant relationship with an average ratio of 1.86 mmol organic carbon to carbonate.

While this methods gives an average ratio of photosynthesis to precipitation over several weeks or months, the ratio can also be directly measured over a few hours. This has been done in closed containers, in which the amount of photosynthesis was calculated either by measuring CO_2 uptake or by measuring O_2 release. The CO_2 uptake was measured in beakers which were tightly covered to inhibit gas exchange with the atmosphere. As oxygen equilibrates with the atmosphere much quicker, oxygen was measured with an electrode in tightly sealed Erlenmeyer beakers. Precipitation was again measured by the decrease of alkalinity and calcium concentration. In all th containers cyanobacteria were incubated for several hours.

The equation

(DIC - precipitation)/precipitation = V

gives the ratio V of photosynthesis versus precipitation. It can be seen from the equation that the method of calculation increases any possible analytical error in the determination of precipitation. On the other hand, alkalinity is used for the calculation of the amount of photosynthesis as well as for the calculation of precipitation, which leads to a weak artificial correlation. The ratios calculated in this way should therefore be taken as estimates rather than exact values. They do, however, indicate a constant relationship between photosynthesis and precipitation. Around 1.15 mol carbon is fixed organically for every mol precipitated carbonate (1.10 to 1, according to the estimates by Ca^{2+}, 1.20 to 1, according to the estimates by alkalinity), (Tab. 2).

Despite these inaccuracies, the calculated results show fairly good accordance with the ratios found by direct measurements of photosynthesis by measuring oxygen evolution. For every mol of CO_2 fixed in photosynthesis, one mol of O_2 is released. The amount of oxygen therefore corresponds exactly to the amount of carbon fixed. The ratios of oxygen to precipitated carbonate are given in Table 2. The values are slightly lower than the previously calculated ones, indicating that for every mol CO_2 used in photosynthesis, one mol of carbonate is precipitated. The low value of sample 890 is probably caused by a loss of O_2, due to a defect seal on the beaker. The low value for sample 891 also occurs in the Ca^{2+}-calculation for the CO_2-uptake calculations, indicating an analytical error in the titration of calcium.

Irregardless of which method was used, it can be said that for one to two mol carbon fixed organically there is one mol

Sample	Cl	Ca2+	Alk	CO2/Ca2+	CO2/Alk	O2/Ca2+	O2/Alk
Control							
888	0,484	0,227	0,225	1,13	1,15	0,93	0,94
889	0,508	0,254	0,235	1,00	1,16	0,86	0,93
890	0,597	0,332	0,280	0,80	1,13	0,47	0,56
891	0,433	0,296	0,200	0,46	1,17	0,67	0,99
892	0,587	0,256	0,275	1,29	1,13	0,93	0,87
893	0,439	0,178	0,200	1,46	1,19		
894	0,215	0,111	0,095	0,94	1,27		
895	0,352	0,182	0,160	0,95	1,20		
896	0,324	0,121	0,145	1,68	1,23		
897	0,379	0,143	0,170	1,65	1,23		
898	0,457	0,210	0,210	1,18	1,18		
899	0,428	0,210	0,195	1,04	1,19		
900	0,386	0,165	0,175	1,34	1,20		
901	0,412	0,189	0,190	1,18	1,17		
902	0,720	0,328	0,340	1,19	1,12		
995	0,395	0,219	0,175	0,08	1,26		
996	0,322	0,134	0,145	1,40	1,22		
997	0,238	0,153	0,105	0,55	1,27		
Ethoxyzolamide							
998	0,051	0,012	0,010	3,24	4,08		
999	0,214	0,061	0,085	2,51	1,52		
1000	0,094	0,076	0,025	0,024	2,77		

Tab. 2. Ratio of photosynthesis to precipitation in untreated samples and samples treated with the inhibitor ethoxyzolamide. Photosynthesis was calculated from the amount of CO_2 uptake and measured from the amount of O_2 released by the cells.

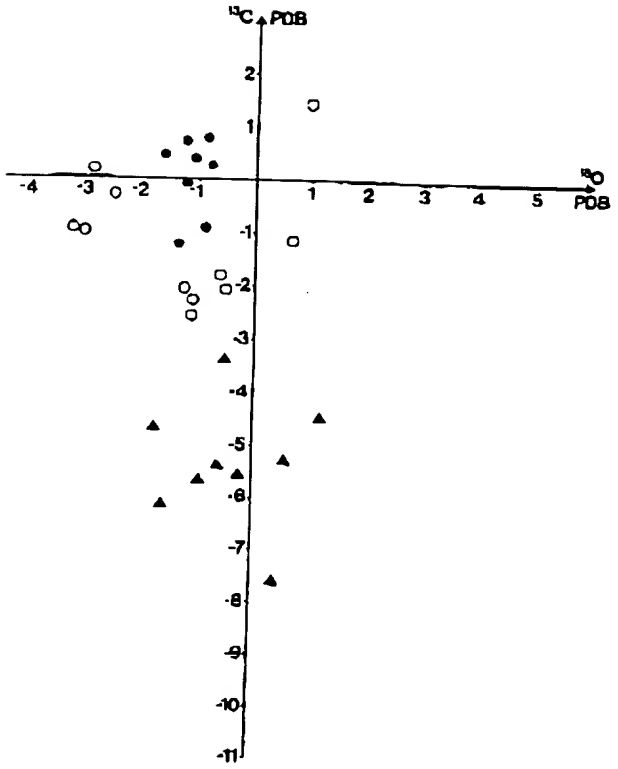

Fig. 4a. Isotopic composition of carbonate precipitated during the 1989/90 wet season (circles), carbonate sediment from push cores (solid dots), and gastropod shells (triangles). Data are all given versus PDB.

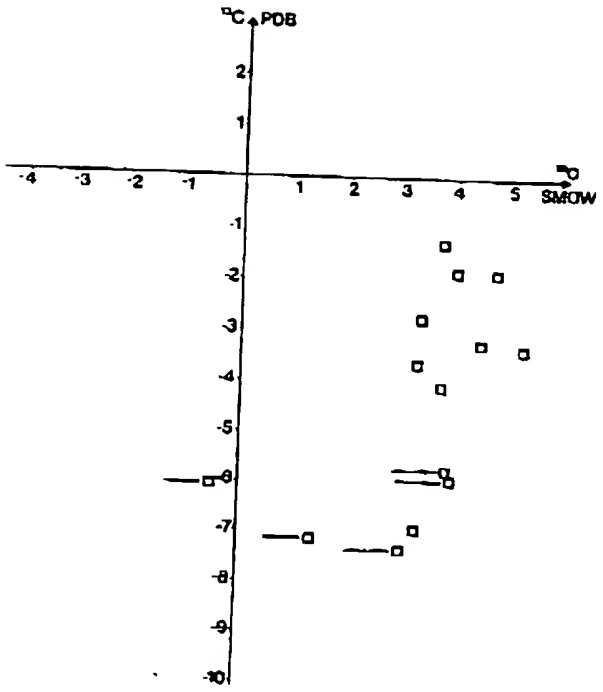

Fig. 4b. Isotopic composition of water, measured throughout the wet season 1989/90. The arrows mark samples which are possibly slightly to heavy in 13C due to storage before measuring. Carbon data are given versus PDB, oxygen data versus SMOW.

of carbonate precipitated. This is a constant relationship, apparently relatively independent of inorganic factors. The amount of carbonate never exceeded the amount of organically fixed carbon in either the experiments or in the cyanobacterial mats.

4.5 Stable Isotopes

Stable carbon (versus PDB) and oxygen (versus SMOW) isotopic compositions of the water in the Everglades have been measured throughout the duration of the wet season. In addition stable isotopic compositions have been determined for calcite precipitated in the water during the same time span, for carbonate mud sampled from the sediment cores, and for gastropod shells sampled from the same horizons in the cores as the carbonate mud (carbon and oxygen versus PDB). The carbon data of the water samples from the beginning of the wet season are possibly depleted, in ^{13}C due to equilibration with 10 ml of air (see chap. 3). In fig. 4 b these data are marked with an arrow.

Carbon and oxygen isotopic compositions of gastropod shells have been measured as a reference for equilibrium precipitation. The gastropods were used because it has been shown that molluscs precipitate in equilibrium with both the carbon and the oxygen compositions of the surrounding waters (Epstein et al., 1951; Fritz & Poplawski, 1974; Mook & Vogel, 1968).

The oxygen isotopic composition of carbonate precipitated by cyanobacteria during the 1989/90 wet season indicates precipitation in equilibrium with the ambient water. The same is true when comparing the values of the carbonate mud from the cores and the gastropods. According to the equation given by O'Neil (1969, in McConnaughey, 1989) carbonate, precipitated from water of $\delta^{18}O$=5.269 (12/26/89) to $\delta^{18}O$= -1.882 (7/8/89) should have a composition of $\delta^{18}O$=3.499 to -3.652. This is assuming an average temperature of 25° C, which is the average temperature given by Swart et al. (1989) for Florida Bay following temperature data from a weather station in Key West. It is confirmed by calculating the average temperature for three days in September, November, and December of 1989, when the temperature at the sampling site was measured over 24 hours. These data give an average temperature at the sampling site of 26.6° C.

The measured oxygen data of the carbonates fall within the range of the lighter calculated values. Equilibrium precipitation is also supported by a comparison of the isotopic data obtained from gastropod shells and the carbonate sediment from the cores. Taking into account that calcite is about 0.6 permil lighter than coprecipitated aragonite, the $\delta^{18}O$ values of the shells and the sediment fall within the same range.

The carbon isotopes, however, show an enrichment of ^{13}C in the cyanobacterial carbonate relative to the water. An average value of -5.5 permil $\delta^{13}C$ was assumed for the water. The fractionation of carbon is independent of the temperature of precipitation. In equilibrium precipitation carbonate is always about 2 permil heavier in ^{13}C than the DIC of the water it precipitated from. Carbonate in equilibrium with the

water during the 1989/90 wet season should therefore have a composition of about -3.5 permil. The sediment values, however, range between 0.25 to -2.6 permil. The sediment is therefore heavy (i.e. enriched in ^{13}C), relative to the values calculated from the water isotopic composition.

Comparing again the $\delta\,^{13}C$ values of the gastropod shells with the sediment composition, it can be seen that the sediment is considerably heavier than equilibrium precipitation. The aragonite shells show $\delta^{13}C$ values between -1.25 and 0.7 permil. In addition, a fractionation between aragonite and calcite has to be taken into account, with calcite being 1.8 permil depleted in ^{13}C relative to aragonite (RUBINSON & CLAYTON, 1969). The sediment is therefore 6-7 permil heavier than the water it was precipitated from, the water composition being reflected by the gastropod shells.

The ^{13}C enrichment in the carbonate precipitated by the cyanobacteria is understandable when considering the carbon fractionation in photosynthesis. The enzyme RUBISCO (Chapter 2.2.1) is generally discriminating against ^{13}C up to -27 permil (SWART, 1983; SHARKEY & BERRY, 1985). In cyanobacteria, the degree of discrimination depends on the environmental DIC concentration. It varies between -18 permil and 0 permil, being reduced by active DIC uptake (CALDER & PARKER, 1973; ESTEP, 1984).

The enrichment of ^{13}C in the carbonate is an effect of preferential ^{12}C uptake during photosynthesis, which increases the ^{13}C concentration in the immediate vicinity of the filaments. This enrichment indicates that the precipitated carbon is derived completely extracellular, and that no respiratory carbon is incorporated.

The same effect, i.e a ^{13}C enrichment in carbonate due to photosynthetical ^{12}C uptake, can be seen in some calcareous algae and in corals with a high density of zooxanthellae and consequent high rates of photosynthesis (KEITH & WEBER, 1965; BOROWITZKA, 1986; SWART, 1983; MCCONAUGHEY, 1989; CUMMINGS & MCCARTY, 1982). In contrast, some coralline red algae show relatively light $\delta^{13}C$ values because of incorporation of respiratory carbon in the skeleton (BOROWITZKA, 1986 and compilation by SWART, 1983, Fig. 1).

STUIVER (1970) measured the isotopic composition of various lacustrine carbonates and found an enrichment of ca. 5 permil relative to mollusc shells in ^{13}C, which he explained by photosynthetic ^{12}C depletion by phytoplankton. A ^{18}O enrichment, which he found in his sediments, can not be confirmed from the Everglades data.

In comparison with fossil cyanobacteria carbonates it has to be considered that in addition to the water composition, active DIC uptake might change the degree of carbon fractionation in photosynthesis and hence the isotopic composition of the residual carbon pool for precipitation.

4.6 Experiments on Precipitation

Experimental data on carbonate precipitation by cyanobacteria are scarce, probably due to difficulties in inducing precipitation under laboratory conditions (PENTECOST, 1978). The same phenomenon, i.e. a weaker or lacking calcification in laboratory cultures as compared with field grown specimens, is described from calcareous algae (GIRAUD & CABIOCH, 1979). The experiments have therefore been conducted in the field. An advantage of field experiments are

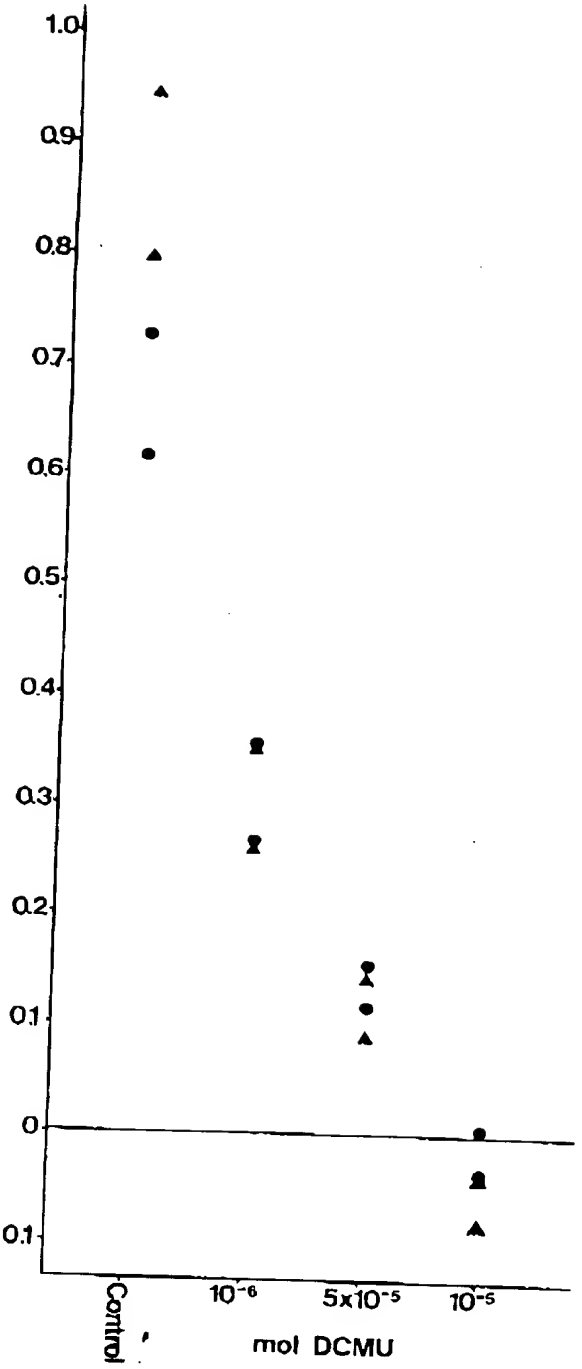

Fig. 5. gives the amount of carbonate (in mmol) precipitated in experiments with various amounts of the photosynthesis inhibitor DCMU and an untreated control experiment (10/11/89). The amount of precipitated carbonate decreases with an increasing inhibitor concentration. At a concentration of 10^{-5} mol DCMU the net result is carbonate dissolution, because the amount of (uninhibited) respiration in the cyanobacteria exceeds the amount of photosynthesis. Precipitation was estimated from changes in calcium (solid circles) and alkalinity (triangles).

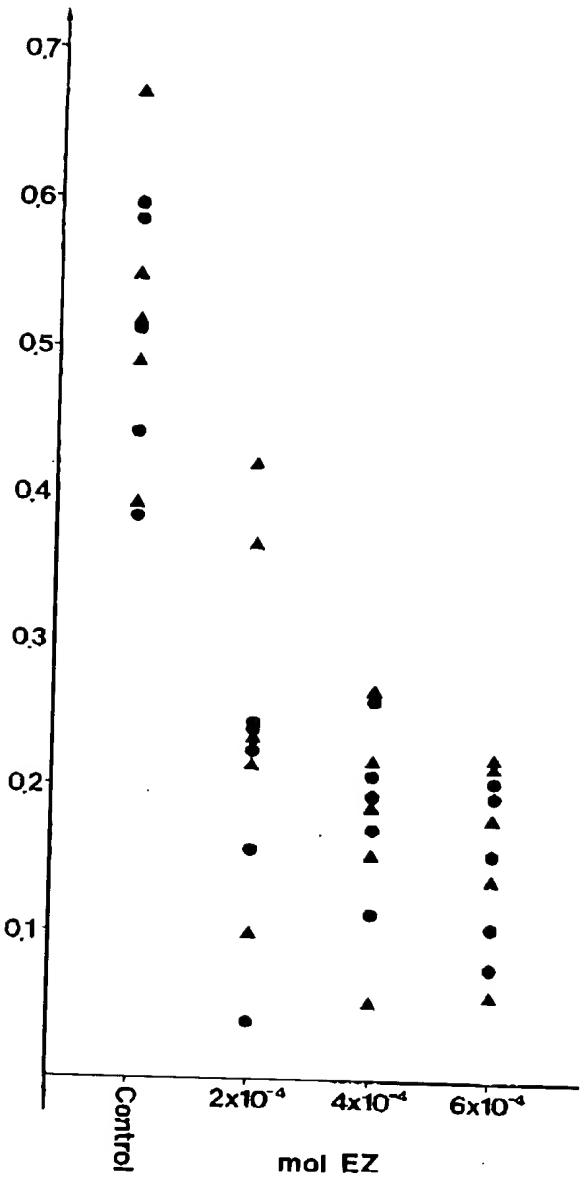

Fig. 6. gives the amount of precipitation in experiments with various amounts of the inhibitor ethoxyzolamide and an untreated control experiment. Precipitation decreases with an increasing concentration of the inhibitor. Precipitation was estimated from changes in calcium (solid circles) and alkalinity (triangles).

the natural conditions in temperature, illumination, and water composition. A disadvantage is that these factors cannot be controlled and are subject to both daily and seasonal variations.

4.6.1 Untreated Cyanobacteria

The amount of precipitation in containers with untreated controls was not only used as a reference for the inhibitor experiments, but also allows the evaluation of how closely the amount of precipitation measured in the experiments resembles the amount of precipitation under natural conditions. As the cyanobacteria start to grow soon after the site is completely covered by freshwater, the age of the cyanobacteria is about the same as the duration of the wet season. The cyanobacteria used in the experiments on January 11th to 13th had a carbonate content of 1.3 to 1.9 g. They precipitated this amount in 180 days, from July to December 1989. This gives a daily amount of precipitation of 7.2 to 10.5 mg carbonate. In the experiments they precipitated an net amount of 15 mg (0.150 mmol, January 11./12.) and 5 mg (0.050 mmol, January 12./13.). This calculation shows that at least in experiments of several hours or a few days the amount of precipitated carbonate corresponds to precipitation under natural conditions.

4.6.2 Experiments with Inhibitors

Precipitation starts in the morning with the onset of photosynthesis and ends in the evening when photosynthesis ceases. To actually prove, however, that precipitation depends on photosynthesis, cyanobacteria were treated with the inhibitor DCMU (Dichlorphenyldimethylurea). This inhibitor blocks the electron transport from photosystem II to photosystem I in photosynthesis. For *Synechococcus* a 10^{-5} molar DCMU solution was shown to completely inhibit photosynthesis (BADGER & ANDREWS, 1982).

Because of the poor solubility of DCMU in water, appropriate amounts of a concentrated stock solution of DCMU in methanol (0.012 g in 50 ml methanol) were added to sampling site water to get the desired final DCMU concentrations of 10^{-5}, $5x10^{-6}$, and 10^{-6} mol DCMU. The maximum methanol concentration of 1 % showed no negative effect on the viability of the cyanobacteria.

Fig. 5 shows the results of an experiment with various concentrations of DCMU (10^{-6}, $5x10^{-6}$, 10^{-5}; 10/11/89). It is obvious that the amount of precipitated carbonate decreases with the increasing concentration of the inhibitor, corresponding to the decreasing photosynthetic activity. When transferred from the DCMU solution to pure water, the cyanobacteria immediately began to photosynthesize and carbonate was precipitated.

Ethoxyzolamide

Ethoxyzolamide (EZ) is an inhibitor for the activity of the enzyme carboanhydrase (CA), which catalyses the conversion of HCO_3^- to CO_2 (Chapter 2.2). In which way EZ affects photosynthesis of cyanobacteria is yet not clear (5.1). Appropriate amounts of a stock solution of EZ in DMSO (Dimethylsulfoxide) were added to incubated cyanobacteria to give final inhibitor concentrations of $2x10^{-4}$, $4x10^{-4}$, and $6x10^{-4}$ mol. As a consequence of the addition of EZ, the pH dropped in the containers 0.04 to 0.1 pH units. All the inhibitor experiments therefore inevitably have a slightly lower initial pH.

Fig. 6 shows the amount of carbonate precipitated by controls and by cyanobacteria treated with various EZ concentrations. It can be seen that the amount of precipitation decreases with the increasing concentration of the inhibitor.

Comparing the amounts of dissolution occurring over night in all the samples, it can be seen that there is as much dissolution in the inhibitor experiments as in the control

samples, because th inhibitor does not affect the pentose-phosphate pathway and thus CO_2 release and dissolution. The net result in 24 hours is therefore precipitation in the controls, but dissolution for the EZ treated cyanobacteria.

Calculating the ratio of photosynthesis to precipitation for the EZ experiments, gives values significantly different from the ones in the control samples Tab. 2). While in the controls the ratio lies around 1.15 to 1 are the values for the EZ experiments considerably higher, up to 4 to 1. The inhibitory effect on precipitation is stronger than on photosynthesis. The ratio of respiration to dissolution occuring over night, shows, as expected, no differences between the untreated cyanobacteria and the EZ samples. This ratio is, however, always slightly more variable than the ratio of photosynthesis to precipitation, varying beween 1 to 2 mol respired carbon for every mol dissolved carbonate.

DMSO

PRICE & BADGER (1989 b) found a slightly negative effect on photosynthesis by DMSO concentrations above 0.2%. Therefore some experiments were run to test the effect of the DMSO concentrations used in the EZ experiments. In these tests, no influence of pure DMSO were found, neither on photosynthesis nor on carbonate precipitation.

5 DISCUSSION

PENTECOST (1988) concluded that the high amount of carbonate as compared to organic material in the green alga *Gongrosira* sp. was an indicator of a high incidence of inorganic precipitation. In tufas the amount of organic material derived from cyanobacteria is estimated to be as low as 1 to 0.3-0.4 % (PENTECOST, 1978; 1985). RAVEN et al. (1986) measured the ratio of organic material versus carbonate in characeans and found more organic carbon than carbon in carbonate. They interpreted this as a reflection of little inorganic influence on precipitation.

The ratio of organic versus inorganic carbon seems to be an indicator of the relative percentage of organic and inorganic influences on precipitation. A ratio of more than 1:1 is the result of organic dominated precipitation, while a higher amount of carbonate than organic carbon (e. g. a ratio below 1) reflects the influence of inorganic factors. The crystal morphology can in both cases be specifically influenced by the organic material, which might provide the nucleation sites for precipitation.

In the Everglades, the amount of carbon precipitated in carbonate is always lower than the amount of organic carbon. The restriction of calcification to the sheath also indicates biological precipitation. If inorganic factors were the cause of precipitation, calcification would be expected to exceed the outer sheath, because of continous growth following crystal nucleation. All these observations suggest active carbonate precipitation by cyanobacteria.

5.1 The Mechanism f Precipitation

Cyanobacteria grown under high CO_2 conditions (above equilibrium with the atmosphere) have the ability to actively take up CO_2 and transport it into the cells. When grown under low CO_2 conditions (equilibrium with the atmosphere and less) they activate a mechanism which allows them to take up bicarbonate as well. Bicarbonate use causes the release of equivalent amounts of OH^- ions, which are produced by the conversion of HCO_3^- to CO_2 (KAPLAN, 1985; SCHERER et al., 1988 a; PRINS & ELZENGA, 1989). It was shown by MILLER & COLMAN (1980) for *Coccochloris* sp. that the amount of OH^- ions released into the medium exactly equals the amount of $NaHCO_3$ provided for photosynthesis. The mechanism of DIC uptake is presently discussed, and there are still considerable uncertainties. It is not yet clear, if one or two transport systems are involved in the uptake of the two carbon species, and how the pumps work. The pump, however, appears to have a carboanhydrase-like moiety in the cell wall (BADGER et al., 1985; BADGER & PRICE, 1989; ESPIE et al., 1989; MILLER & COLMAN, 1980; PRICE & BADGER, 1989 a;). EZ might inhibit the uptake mechanism by impeding the CA-moiety of the pump and/or by inhibiting the intracellular conversion of bicarbonate to CO_2 and OH^- (PRICE & BADGER, 1989 a,b). The experimental results show, however, different effects of EZ in different species, possibly indicating differences in the structure of the pump systems. There also may be variations caused by environmental conditions, with cells grown in the presence of low CO_2 concentrations using a more complex mechanism than those functioning in an environment more rich in CO_2 (PRICE & BADGER, 1989 b). VOLOKITA et al. (1984) found a stronger inhibition of CO_2 uptake than of HCO_3^- uptake in *Anabaena variabilis*. According to PRICE & BADGER, *Synechococcus* posses one pump, transporting CO_2 as well as HCO_3^- into the cells. In their experiments EZ affects the uptake of both species equally, which they interpret as an indication of inhibition of the pump system. An additional effect of EZ on the intracellular CA activity is possible (PRICE & BADGER, 1989 b). ESPIE et al. (1989; *Synechococcus*), however, propose an uptake mechanism consisting of two pump systems because, according to the authors, the uptake of each of the two carbon species can be specifically inhibited.

The experimental results from the Everglades suggest preferential inhibition of bicarbonate uptake. An equal inhibition of both bicarbonate and CO_2 uptake should lead to an equal decrease in photosynthesis and precipitation. The preferential decrease in precipitation shows that the two processes can, to a certain degree, be separated. Taking into account the considerable differences between the experimental conditions and the natural conditions existing in the Everglades, and, in addition, the different species involved, differences are not surprising.

The quantitative relationship of photosynthesis and precipitation and the preferential inhibition of precipitation by EZ, suggest a model in which precipitation is linked to photosynthetic bicarbonate use rather than general DIC uptake. Fig. 7 shows the proposed model in *Scytonema*. HCO_3^- is taken up, CO_2 is used for photosynthesis, and OH^- ions are released from the cells. In the sheath they either react with another HCO_3^- ion to form water and a carbonate ion, or they are neutralized by the uptake of H^+ ions (among others: ESPIE et al., 1989). Either way, there are carbonate ions formed in the immediate vicinity of the cell. As the percent-

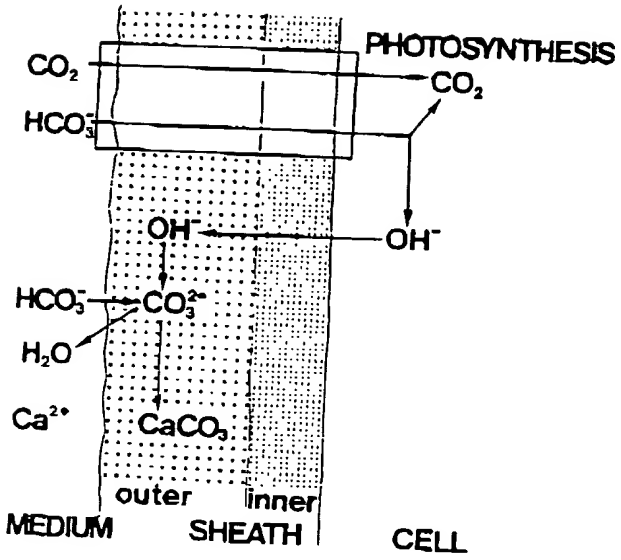

Fig. 7. Schematic model for precipitation in *Scytonema*. DIC is taken up, either in form of CO_2 or HCO_3^-, by an active pump system. The pump system is indicated by the frame. It's structure is presently discussed. When HCO_3^- is the carbon species used for photosynthesis, hydroxyl ions are liberated. Either they are released by the cells, or H^+ ions are taken up for neutralization. Either way there are carbonate ions quantitatively formed in the outer sheath, subsequently leading to precipitation by attracting calcium ions.

age of HCO_3^- use in photosynthesis increases, more carbonate ions are formed. In cyanobacteria the sheath acts as a diffusion barrier resulting in a local increase in the concentration of carbonate ions. The carbonate ions react with calcium being absorbed by the polysaccharides of the sheath, and calcium carbonate is precipitated. When CO_2 is the carbon species taken up, no OH^- ions are formed and no precipitation occurs. Therefore the ratio of organically to inorganically fixed carbon depends on the relative percentage of HCO_3^- in photosynthesis. If the percentage is low, due to low pH values or the inhibition of HCO_3^- use, the amount of photosynthesis is relatively high as compared to the amount of precipitation. This is demonstrated by the results of the EZ experiments, in which up to four times as much carbon was taken up for photosynthesis than was precipitated in carbonate. If the percentage of HCO_3^- used in photosynthesis is high, then a ratio of photosynthesis to precipitation of 1 can result.

The result of this purely biological calcification might be an impregnation of the sheath, while an encrustation indicates inorganic precipitation. In this case, sheath impregnation should preferentially occur in environments where photosynthetic bicarbonate use occurs.

5.2 Biological Influence

The restriction of calcification to the outer sheath in *Scytonema* and the different crystal morphologies in the two taxa, despite all the natural variations in ion concentration, temperature, and probably crystallization rate throughout the wet season, suggest a taxa specific influence of the cyanobacteria over calcification.

The crystal morphology can be strongly influenced by the rate of crystallization (ADDADI & WEINER, 1985), which depends on the rate of ion supply as well as on the rate of ion incorporation into the crystal lattice. Variations in sheath structures and compositions, by allowing different diffusion rates for Ca^{2+}-ions, might lead to different crystallization rates, subsequently resulting in differences in crystal morphology. For example, higher crystallization rates in *Schizothrix* might have lead to the growth of dendritic crystals, while the rhombohedral crystals in *Scytonema* might be due to a relatively slower growth rate. It has been demonstrated that the polysaccharides of the sheaths can serve as an interface for mediating and controlling crystal nucleation because of their high affinity for Ca^{2+} ions (SOMERS & BROWN, 1978), onto which CO_3^{2-} ions are subsequently absorbed (Ionotrophy; GREENFIELD et al., 1984). In addition, WECKESSER et al. (1988) showed a different capacity for calcium absorption in different cyanobacterial genera. Those differences could also be reflected in the distinct crystal morphologies observed in *Scytonema* and *Schizothrix* (MERZ & ZANKL, submitted).

5.3 Environmental Influence

Calcifying cyanobacteria only occur in waters supersaturated with respect to carbonate, but even there calcification is restricted to certain genera (*Homoethrix, Phormidium, Plectonema, Rivularia, Schizothrix, Scytonema;* PENTECOST & RIDING, 1986). None of these genera, however, are obligate calcifiers.

The occurrence of calcified and uncalcified cyanobacteria living under the same environmental conditions indicates that supersaturation is not always sufficient for calcification.

The results from this study show that two other factors can be of major importance. One is bicarbonate uptake by cyanobacteria, and the other is the suitability of the sheath for carbonate nucleation. Any environmental factor that influences either one of these factors will influence the cyanobacteria's ability to calcify.

The bicarbonate pump is induced when the CO_2 supply from the ambient water is low relative to the potential rate of photosynthesis. It should be active in an environment where CO_2 concentrations are low, either due to low total DIC concentrations or to high pH values. But also in environments where high light intensities sustain or even require especially high rates of photosynthesis, bicarbonate uptake might be advantageous for the reduction of photoinhibition (Chapter 2.2). In these environments photosynthetic bicarbonate use could then lead to carbonate precipitation.

Structure and composition of the sheath also seem to be essential for calcification. Differences among species in their affinity for calcium were described by WECKESSER et al. (1988). But the affinity for calcium might also depend on environmental conditions (WHEELER & SIKES, 1984; GREENFIELD et al., 1984), thus possibly changing the suitability of the sheath for nucleation. The thickness of the

sheath as a diffusion limited site for precipitation is also influenced by environmental conditions (TUFFERY, 1969).

5.4 Possible Biological Significance of Calcification

The question about the environmental factors influencing calcification is closely linked to the question about possible benefits for the cyanobacteria. In principle there seem to be no differences in the calcification of cyanobacteria and of calcareous algae. In algae, calcification depends on the activity of the enzyme carboanhydrase, the uptake of bicarbonate for photosynthesis (LUCAS, 1979; SIKES & WILBUR, 1982; BOROWITZKA, 1990), or on the presence of a polysaccharide matrix. Green algae calcify extracellulary, either in diffusion limited intracellular spaces (*Halimeda*; BOROWITZKA & LARKUM, 1977), or within sheath material containing polysaccharides (*Penicillus*, *Udotea*; BOROWITZKA, 1986). DCMU inhibits precipitation in *Halimeda*, as it does in cyanobacteria, while diamox, an inhibitor for carboanhydrase activity, greatly reduces calcification (BOROWITZKA & LARKUM, 1976). As in cyanobacteria seem the polysaccharides in *Halimeda* to control the orientation of the crystals to a certain degree. It was shown that in characeans (chlorophyceae, chlorophyta) precipitation occurs in localized bands of OH^- release, which are formed by the use of bicarbonate in photosynthesis (LUCAS, 1979; BOROWITZKA, 1982). There seems to be no organic material involved in precipitation by characeans.

In the calcification of corallinaceans (rhodophyta) and coccolithophoridae, obviously under biologic control, polysaccharides play an important role. Corallinaceans precipitate within the cell wall. The orientation of the crystals is regulated by organic molecules.

These comparisons show that some forms of calcification in cyanobacteria and calcareous algae may basically be the same. Therefore there is, for cyanobacteria as for calcareous algae, the question, if there is any beneficial effect from calcification or precipitation for the organism as is suggested by the restriction of calcification to certain taxa and the control calcifying cyanobacteria can exert on precipitation.

5.4.1 Light Protection

When there is more light energy absorbed than can be used in photosynthesis for the formation of organic molecules, a severe damage of the reaction centers in the photosynthetic apparatus might occur. The rate of photosynthesis can be reduced or the reaction centers might be irreversibly damaged. Some of the carotenoids in cyanobacteria absorb the potentially hazardous radiation and thus protect the photosynthetically active pigments. It has been proposed that the calcification of some cyanobacteria and algae might have a light shading function (Cyanobacteria, VAN LIERE & WALSBY, 1982; Corallinaceae, LITTLER, 1976; Characeae, RAVEN et al., 1986). The same has been proposed for the fossil calcifying cyanobacteria *Renalcis* and *Epiphyton* (ROWLAND & GANGLOFF, 1988).

Calcifying cyanobacteria occur, besides being common in tufa deposits and similar environments, often in areas of extremely shallow water where they are exposed to very high light intensities. C mparing the measured light intensities in the Everglades with literature data on the intensity optimum for photosynth sis by cyanobacteria it can be seen that the optimum values are exceeded more than ten fold. For some strains WALSBY (1968) and HÄDER (1987) give values of 500 to 1000 lx. For mat forming Oscillatoriaceans in a natural environment the light optimum is about 3000 lx, while they show photophobic reactions when the irradiance exceeds 10000 lx (PENTECOST, 1984). CASTENHOLTZ (1982) describes phototactic movements up to 10000 lx. Generally, cyanobacteria prefer low light intensities.

There are two ways, how a strong light irradiance might induce conditions favourable for carbonate precipitation.

The stress of living in high light environments could induce secretion of sheath material neccessary for precipitation (KAZMIERCZAK et al., 1990; SCHERER et al., 1988 b), and a calcified sheath might physically shade the filament. But high light intensities might also affect precipitation via an induction of the bicarbonate pump. Some of the absorbed light energy has to be used for the maintenance of the pump, and would thus not be able to damage the photosynthetic apparatus. Calcification would then occur as a secondary consequence of the high radiation.

5.4.2 Ion Sink

Precipitation might help to buffer the pH rise caused by CO_2 uptake during photosynthesis. This was proposed by RAVEN et al., (1986) for characeans and by PAASCHE (1964) and SIKES et al. (1980) for coccoliths. The hydroxyl ions would lead to rapid increase of pH, if they would be released into a weakly buffered medium. By their reaction with an extracellular bicarbonate ion and the subsequent precipitation of carbonate, the pH rise is reduced. Therefore carbonate precipitation might allow higher rates of photosynthesis in weakly buffered waters. The occurrence of calcifying cyanobacteria, however, does not seem to be restricted to environments with a low natural buffer capacity.

Carbonate precipitation could also be used as a sink for carbonate ions being inevitably formed as a consequence of hydroxyl ion release. Carbonate ions cannot be used in photosynthesis. Therefore they may have a negative effect on bicarbonate uptake when they get attached to the pump and block it (LUCAS, 1983). The carbonate precipitation might be a way to protect the pump from the carbonate ions, thus ensuring a constant high rate of photosynthesis by unimpaired DIC uptake. The effect would be similar to the spatial separation of bicarbonate uptake and hydroxyl release in characeans (LUCAS, 1983).

Although there are too few experimental data on the calcification of cyanobacteria to decide, what factors finally cause precipitation, it can be seen that there are various ways how the organisms may benefit from it.

ACKNOWLEDGEMENTS

This paper is a summary of a PhD thesis supervised by Prof. H. Zankl, Marburg. I thank Prof. R.N. Ginsburg, Miami, for hospitality at Fisher Island, Prof. P.K. Swart,

Miami, for generously allowing me to use his lab facilities and for measuring the stable isotopes, Prof. S. Golubic, Boston, for valuable discussions and determination of the cyanobacteria, Prof. L. Brand, Miami, for his support, A. Titze, Marburg, for the SEM photographs, Dr. G.M. Grammer, Miami, for proof reading the English text, and the Everglades National Park Service for the sampling permit.

The research was founded with a stipend for graduate students by the German Academic Exchange Service to M. Merz and a research grant to H. Zankl by the German Science Foundation (Za 22/33-1). An anonymous reviewer gave hints to impove the manuscript.

REFERENCES

ADDADI, L. & WEINER, S. (1985): Interactions between acidic proteins and crystals: Stereochemical requirements in biomineralization. - Proc. Natl. Acad. Sci. U.S.A., 82/6, 4110-4114, 5 Figs., Washington

BADGER, M.R. & ANDREWS, T.J. (1982): Photosynthesis and inorganic carbon usage by the marine cyanobacterium, *Synechococcus* sp.. - Plant Physiol., 70/2, 517-523, 9 Figs., 1 Tab., Lancaster, Pa.

BADGER, M.R., BASSETT, M. & COMMINS, H.N. (1985): A model of HCO_3^- accumulation and photosynthesis in the cyanobacterium *Synechococcus* sp.. - Plant Physiol., 77/2, 465-471, 7 Figs., Lancaster, Pa.

BADGER, M.R. & PRICE, G.D. (1989): Carbonic anhydrase activity associated with the cyanobacterium *Synechococcus* PCC 7942. - Plant Physiol., 88/1, 51-60, 2 Tabs., 5 Figs., Lancaster, Pa.

BOROWITZKA, M.A. (1982): Mechanisms in algal calcification. - In: ROUND, F.E., CHAPMAN, D.J. (eds.): Progress in Phycological Research, vol. 1, 137-178, 11 Figs., 2 Tab., Amsterdam (Elsevier Biomedical Press)

-- (1986): Physiology and biochemistry of calcification in the Chlorophyceae. - In: LEADBEATER, B.S.C., RIDING, R. (eds.): Biomineralization in Lower Plants and Animals. – The Systematic Association, Spec. Vol. 30, 400 pp., 107-124, 2 Figs., 1 Tab., Oxford (Clarendon Press)

BOROWITZKA, M.A. (1989): Carbonate calcification in algae-Initiation and control. - In: MANN, S., WEBB, J., WILLIAMS, R.J.P. (eds.): Biomineralization: chemical and biochemical perspectives. – 541 pp., 63-94, 10 Figs., 4 Tabs., Weinheim (VCH Verlagsgesellschaft mbH)

BOROWITZKA, M.A. & LARKUM, A.W.D. (1976): Calcification of the green algae *Halimeda*; IV. The action of metabolic inhibitors on the photosynthesis and calcification. - J. Exp. Bot., 27, 894-907, 5 Figs., 4 Tabs., Oxford

– & -- (1977): Calcification in the green algae *Halimeda*; I; An ultrastucture study of thallus development. - J. Phycol., 13/1, 6-16, 24 Figs., New York

BRAITHWAITE, C.J.R., CASANOVA, J., FREVERT, F., WHITTON, B.A. (1989): Recent stromatolites in landlocked pools on Aldabra, western Indian Ocean. - Paleogeogr., Paleoclimat., Paleoecol., 69/3-4, 145-165, 4 Pls., 23 Figs., Amsterdam

CALDER, J.A., PARKER, P.L. (1973): Geochemical implications of induced changes in 13C fractionation by blue-green algae. - Geochim. Cosmochim. Acta, 37/1, 133-140, 2 Figs., 3 Tabs., New York

CASTENHOLZ, R.W. (1982): Motility and taxes. - In: CARR, N.G. & WHITTON, B.A. (eds.): The Biology of Cyanobacteria. – 688 pp., 414-439, Oxford (Blackwell)

COX, G., JAMES, J.M., LEGGETT, K.E.A., OSBORNE, R., ARMSTRONG, L. (1989): Cyanobacterially deposited speleothems: subaerial stromatolites. - Geomicrobiol. J., 7, 245-252, 7 Figs., New York

CUMMINGS, C.E., MCCARTHY, H.M. (1982): Stable carbon istope ratios in *Astrangia danae*: evidence for algal modification of carbon pools used in calcification. - Geochim. Cosmochim. Acta. 46/6, 1125-1129, 2 Figs., 2 Tabs., New York

DEPARGE, C., TRICHET, J., SIN, P. (1985): First data on the biogeochemistry of Kopara deposits from Rangiroa Atoll. - Proceed. 5th Int. Coral Reef Congress, Tahiti, 3, 365-370, 6 Figs., 2 Tabs., Moorea

DREVER, J. (1988): The Geochemistry of Natural Waters. - 2nd Ed., 437 pp., Englewood Cliffs (Prentice Hall)

EPSTEIN, S. & MAYEDA, T. (1953): Variation of ^{18}O content of waters from natural sources. - Geochim. Cosmochim. Acta, 4/5, 213-224, 3 Figs., 1 Tab., New York

ESPIE, G.S., MILLER, A.G. & CANVIN, D.T. (1989): Selective and reversible inhibition of active CO_2 transport by hydrogen sulfide in a cyanobacterium. - Plant. Physiol., 91/1, 387-394, 7 Figs., Lancaster, Pa.

ESTEP, M.F. (1984): Carbon and hydrogen isotopic compositions of algae and bacteria from hydrothermal environments, Yellowstone National Park. - Geochim. Cosmochim. Acta, 48/3, 591-599, 6 Figs., 10 Tabs., New York

FRITZ, P., POPLAWSKI, S. (1974): 18O and 13C in the sheaths of freshwater molluscs and their environments. - Earth Planet. Sci. Lett., 24, 91-98, 6 Figs., 1 Tab., Amsterdam

GIESKES, J. (1986): Water chemistry procedures aboard Joides Resolution - some coments. - Ocean Drilling Program, Technical Note No. 5, 46 pp., College Station

GIRAUD, G. & CABIOCH, J. (1979): Ultrastructure and the elaboration of calcified cell-walls in the coralline algae (Rhodophyta, Cryptonemiales). - Biol. Cellulaire, 36, 81-86, Paris

GLEASON, P.J. (1972): The origin, sedimentation and stratigraphy of a calcitic mud located in the southern fresh-water Everglades. - PhD-Thesis, Pennsylvania State Univ., 355 pp., University Park

GLEASON, P.J. & SPACKMAN, W.JR. (1974): Calcareous periphyton and water chemistry in the Everglades. - In: GLEASON, P.J. (ed.): Environments in South Florida, Present and Past – 146-181, 34 Figs., 9 Tab., Miami

GOLUBIC, S. (1972): The relationship between blue-green algae and carbonate deposits. - In: CARR, N.G. & WHITTON, B.A. (eds.): The Biology of Blue-Green Algae. – 676 pp., 434-472, 19 Figs., Oxford (Blackwell)

– (1983): Stromatolites, fossil and recent: a case history. - In: WESTBROEK, P., DE JONG, E.W. (eds.): Biomineralization and biological metal accumulation. – 313-326, 6 Figs., Dordrecht (Reidel)

GOLUBIC, S. & CAMPBELL, S.E. (1981): Biogenically formed aragonite concretions in marine *Rivularia*. - In: MONTY, C. (ed.): Phanerozoic Stromatolites: Case histories. – 249 pp., 209-229, 3 Pls., 2 Figs., 1 Tab., Berlin (Springer)

GRAN, G. (1952): Determination of the equivalence point in potentiometric titrations, Part I. - Analyst, 77, 661-671, London

GREENFIELD, E.M., WILSON, D.C. & CRENSHAW, M.A. (1984): Ionotropic nucleation of calcium carbonate by molluscan matrix. - Am. Zool., 24/4, 925-932, 7 figs., Bloomington, Indiana

HÄDER, D.-P. (1987): Photomovement. - In: FAY, P., VAN BAALEN, C. (eds.): The Cyanobacteria. – 325-345, 10 Figs., 1 Tab., Amsterdam (Elsevier)

HARDIE, L.A. & GINSBURG, R.N. (1977): Layering: The origin and environmental significance of lamination and thin bedding. - In: HARDIE, A. (ed.): Sedimentation on the Modern Carbonate Tidal Flats of NW Andros-Island, Bahamas. – Johns Hopkins Univ. Studies in Geol., 22, 203 pp., 50-123, 94 Figs., 16 Tabs., Baltimore

HELDER, R.J. (1988): A quantitative approach to the inorganic carbon in aqueous media used in the biological research; dilute solutions isolated from the atmosphere. - Plant Cell Environment, 11, 211-230, 4 Figs., 5 Tabs., Oxford

HORODYSKI, R.J. & VONDER HAAR, S.P. (1975): Recent calcareous stromatolites from Laguna Mormona (Baja California) Mexico. - J. Sed. Petrol., 45/4, 894-906, 7 Figs., Tulsa

JONES, B. & KAHLE, C.F. (1986): Dendritic calcite crystals formed

by calcification of algal filaments in a vadose environment. - J. Sed. Petrol., 56/2, 217-222, 7 Figs., Tulsa

KAPLAN, A. (1981): Photoinhibition in *Spirulina platensis*: Response of photosynthesis and HCO_3^- uptake capability to CO_2-depleted conditions. - J. Exp. Bot., 32/2, 669-677, 4 Figs., 1 Tab., Oxford

-- (1981): Photoinhibition in *Spirulina platensis*: Response of photosynthesis and HCO3- uptake capability to CO_2-depleted conditions. - J. Exp. Bot., 32/2, 669-677, 4 Figs., 1 Tab., Oxford

-- (1985): Adaptation to CO_2 levels: Induction and the mechanism for inorganic carbon uptake. - In: LUCAS, W.J. & BERRY, J.A. (eds.) Inorganic Carbon Uptake by Aquatic Photosynthetic Organisms,. – Am. Soc. Plant Physiol., 325-338, 9 Figs., Rockville, MD.

KAPLAN, A., MARCUS, Y., ZENVIRTH, D., OMATA, T., REINHOLD, L. & OGAWA, T. (1987): The mechanism of inorganic carbon uptake by cyanobacteria: energetization and activation by light. - In: BIGGINS, J. (ed.): Progress in Photosynthesis Research, vol. IV, 6.301-6.307, 8 Figs., Dordrecht (M.Nijhoff Publ.)

KAZMIERCZAK, J., ITTEKOT, V. & DEGENS, E.T. (1985): Biocalcification through time: environmental challenge and cellular response. - Paläontolog. Zeitschr., 59/1-2, 15-33, 6 Figs., Stuttgart

KEITH, M.L. & WEBER, J.N. (1965): Systematic relationships between carbon and oxygen isotopes in carbonates deposited by modern corals and algae. - Science, 150, 498-501, 2 Figs., 1 Tab., Washington

KEMPE, S. & KAZMIERCZAK, J. (1990): Calcium carbonate supersaturation and the formation of in situ calcified stromatolites. - In: ITTEKKOT, V, KEMPE, S., MICHAELIS, W., SPITZY, A. (eds.): Facets of modern biogeochemistry, 433 pp., 161 Figs., 255-278, 4 Figs., 4 Tabs., Berlin (Springer)

KRAUSE, G.H. (1988): Photoinhibition of photosynthesis. An evaluation of damaging and protective mechanisms. - Physiol. Plant., 74/3, 566-574, 2 Figs., Copenhagen

KRUMBEIN, W.E. & GIELE, C. (1979): Calcification in a coccoid cyanobacterium associated with the formation of desert stromatolites. - Sedimentology, 26/4, 593-604, 9 Figs., Amsterdam

Krumbein, W.E. & Potts, M. (1979): Girvanella-like structures formed by Plectonema gloeophilum (Cyanophyta) from the Borrego desert in Southern California. - Geomicrobiol. J., 1/3, 211-217, 4 Figs., 1 Tab., New York

LEINFELDER, R.R. (1985): Cyanophyta calcification, morphotypes and depositional environments (Alenquer bncolite, Upper Kimmeridgian?, Portugal). - Facies, 12, 253-274, 2 Pls., 3 Figs., 2 Tab., Erlangen

LITTLER, M.M. (1976): Calcification and its role among macroalgae. - Micronesia, 12/1, 27-41, 7 Figs., 3 Tabs., Agana

LUCAS, W.J. (1979): Alkaline band formation in Chara corallina. - Plant Physiol., 63/2, 248-254, 9 Figs., 1 Tab., Lancaster, Pa.

LUCAS, W.J. (1983): Photosynthetic assimilation of exogenous HCO3- by aquatic plants.- Ann. Rev. Plant Physiol., 34, 71-104, 5 Figs., Palo Alto, Pa.

LYONS, B.W., LONG, D.T., HINES, M. E., GAUDETTE, H.E., ARMSTRONG, P.B. (1984): Calcification of cyanobacterial mats in Solar Lake, Sinai. - Geology, 12/10, 623-626, 1 Fig., 2 Tabs., Boulder

MCCONAUGHEY, T. (1989): ^{13}C and ^{18}O isotopic disequilibrium in biological carbonates: I. patterns. - Geochim. Cosmochim. Acta, 53/1, 151-162, 15 Figs., 2 Tabs., New York

MERZ, M.U.E. (1990): Karbonatfällung durch Cyanobakterien im Süßwasserbereich der Everglades, Florida. - unpubl. PhD-Thesis, Univ. of Marburg, 71 pp., 19 Figs., 7 Tabs., Marburg

MERZ, M.U.E. & ZANKL, H. (submitted): The influence of the sheath on carbonate precipitation by cyanobacteria. - submitted to Boll. Soc. Pal. Italiana, Modena

MILLER, A.G. & COLMAN, B. (1980): Evidence for HCO_3^- transport by the blue.green alga (cyanobacterium) *Coccochloris peniocystis*. - Plant Physiol., 65/2, 397-402, 7 Figs., Lancaster, Pa.

MILLER, A.G., ESPIE, G.S. & CANVIN, D.T. (1990): Physiological aspects of CO_2 and HCO_3^- transport by cyanobacteria: a review. - Can. J. Bot., 68/6, 1291-1302, 10 Figs., Ottawa

MILLERO, F.J. (1979): The thermodynamics of the carbonate systems in seawater. - Geochim. Cosmochim. Acta, 43/10, 1651-1661, 9 Figs., 9 Tabs., New York

MONTY, C.L.V. (1972): Recent algal stromatolitic deposits, Andros Island, Bahamas, Preliminary report. - Geol. Rdsch., 61, 742-783, 32 Figs., 1 Tab., Stuttgart

MOOK, W.G. & VOGEL, J.C. (1968): Isotopic equilibrium between shells and their environment. - Science, 159, No. 3817, 1 Fig., Washington

MÜLLER-JUNGBLUTH, W.-U. (1968): Sedimentary petrologic investigation of the Upper Triassic 'Hauptdolomit' of the Lechtaler Alps, Tirol, Austria. - In: MÜLLER, G. & FRIEDMAN, G. (eds.) Recent Developments in Carbonate Sedimentology in Central Europe. – 255 pp., 228-239, 14 Figs., Berlin (Springer)

-- (1970): Sedimentologische Untersuchung des Hauptdolomit der Östlichen Lechtaler Alpen, Tirol. - Festbd. Geol. Inst. 300-J.-Feier Univ. Innsbruck, 255-308, Innsbruck

OBENLÜNESCHLOSS, J. & SCHNEIDER, J. (1990): Ecology and calcification patterns of Rivularia (Cyanobacteria). - In: ANAGNOSTIDIS, K., HICKEL, B. & KOMAREK, J. (eds.)Proc. 11th Symp. IAC, – Arch. Hydrobiol., Suppl. Vol, 'Algological Studies', Berlin

OGAWA, T. & KAPLAN, A. (1987): A model for inorganic carbon accumulation in cyanobacteria. - In: BIGGINS, J. (ed.): Progress in Photosynthesis Research, vol. IV. – 6.297-6.300, 3 Figs., 1 . Tab., Dordrecht (M.Nijhoff Publ.)

PAASCHE, E. (1964): A tracer study of the inorganic carbon uptake during coccolith formation and photosynthesis in the coccolithophorid Coccolithus huxleyi. - Physiol. Plant. (suppl.) III, 1-82, Copenhagen

PENTECOST, A. (1978): Blue-green algae and freshwater carbonate deposits. - Proc. R. Soc. London, Ser. B, 200, 43-61, 1 Pl., 11 Figs., 10 Tab., London

-- (1980): Calcification in plants. - Int. Rev. Cytol., 62, 1-26, 2 Tabs., New York

-- (1984): Effects of sedimentation and light intensity on a mat-forming Oscillatoriaceae with particular reference to *Microcoleus lyngbyaceus* GOMONT. - J. Gen. Microbiol., 130, 983-990, 4 Figs., London

-- (1985): Association of cyanobacteria with tufa deposits: Identity, enumeration, and nature of the sheath material revealed by histochemistry. - Geomicrobiol. J., 4/3, 286-297, 7 Tab., New York

-- (1988): Observations on the growth and calcium carbonate deposition in the green alga Gongrosira. - New Phytol., 110/2, 2 Figs., 7 Tab., 249-253, London

PENTECOST, A. & RIDING, R. (1986): Calcification in cyanobacteria. - In: LEADBEATER, B.S.C., RIDING, R. (ed.) The Systematic Association Spec. Vol. 30, Biomineralization in Lower Plants and Animals. – 400 pp., 73-90, 6 Figs., Oxford (Clarendon Press)

PRINS, H.B.A. & ELZENGA, J.T.M. (1989): Bicarbonate utilization: Function and mechanism. - Aquatic Bot., 34/1, 59-83, 3 Figs., 1 Tab., Amsterdam

PRICE, G.D. & BADGER, M.R. (1989 a): Ethoxyzolamide inhibition of CO2 uptake in the cyanobacterium Synechococcus PCC 7942 without apparent inhibition of internal carbonic anhydrase activity. - Plant Physiol., 89/1, 37-43, 8 Figs., Lancaster, Pa.

PRICE, G.D. & BADGER, M.R. (1989 b): Ethoxyzolamide inhibition of CO_2-dependent photosynthesis in the cyanobacterium Synechococcus PCC 7942. - Plant Physiol., 89/1, 44-50, 3 Figs., 8 Tabs., Lancaster, Pa.

RAVEN, J.A. & LUCAS, W.J. (1985): Energy costs of carbon acquisition.- In: LUCAS, W.J., & BERRY, J.A. (eds.): Inorganic Carbon Uptake by Aquatic Photosynthetic Organisms. - Am. Soc. Plant Physiol., 305-325, Rockville

RAVEN, J.A., SMITH, F.A. & WALTER, N.A. (1986): Biomineralization in the Charophyceae sensu lato. - In: LEADBEATER, S.C., RIDING, R. (eds.) The Systematic Association, Spec. Vol. 30, Biomineralization in Lower Plants and Animals. – 400 pp., 125-139, 1 Tab., Oxford (Clarendon Press)

REINHOLD, L., ZVIMAN, M. & KAPLAN, A. (1987): Inorganic carbon

fluxes in cyanobacteria: A quantitative model. - In: BIGGINS, J. (ed.): Progress in Photosynthesis Research, vol. IV, 6.289-6.296, 6 Figs., Dordrecht (M.Nijhoff Publ.)

RIDING, R. (1977 a): Calcified *Plectonema* (blue-green algae), a recent example of *Girvanella* from Aldabra Atoll. - Palaeontology, 20/1, 33-46, 1 Pl., 5 Figs., London

-- (1977 b): Problems of affinity in Paleozoic calcareous algae. - In: FLÜGEL, E. (ed.): Fossil algae, recent results and developements. – 375 pp., 202-211, 2 Tabs., Berlin (Springer)

-- (1982): Cyanophyte calcification and changes in ocean chemistry. - Nature, 299, No. 5886, 814-815, 1 Fig., London

ROWLAND, S.M. & GANGLOFF, R.A. (1988): Structure and paleoecology of Lower Cambrian reefs. - Palaios, 3, Reefs Issue, 111-135, 18 Figs., Tulsa

RUBINSON, M. & CLAYTON, R.N. (1969): Carbon-13 fractionation between aragonite and calcite. - Geochim. Cosmochim. Acta, 33/8, 997-1002, 3 Tabs., New York

SABATER, S. (1989): Encrusting algal assemblages in a mediterranean river basin. - Arch. Hydrobiol., 114/4, 555-573, 5 Figs., 6 Tabs., Berlin

SCHERER, S., RIEGE, H. & BÖGER, P. (1988 a): Light-induced proton efflux of the cyanobacterium *Anabaena variabilis*. - In: ROGERS, L.J., GALLON, J.P. (eds.) Biochemistry of the algae and cyanbacteria. – 121-129, Oxford (Clarendon Press)

SCHERER, S., CHEN, T.W. & BÖGER, P. (1988 b): A new UV-A/B absorbing pigment in the terrestrial cyanobacterium Nostoc commune. - Plant Physiol., 88/2, 1055-1057, 4 Figs., 1 Tab., Lancaster, Pa.

SCHOLL, D.W., CRAIGHEAD, F.C. & STUIVER, M. (1969): Florida submergence curve revised: its relation to coastal sedimentation. - Science, 163, No. 3867, 562-564, 3 Figs., Washington

SHARKEY, T.D. & BERRY, J.A. (1985): Carbon isotope fractionation of algae as influenced by an inducible CO_2 concentrating mechanism. - In: LUCAS, W.J. & BERRY, J.A. (eds.) Inorganic carbon uptake by aquatic photosynthetic organisms. – Am. Soc. Plant Physiol., 389-403, 4 Figs., 1 Tab., Rockville

SIKES, C.S., ROER, R.D. & WILBUR, K.M. (1980): Photosynthesis and coccolith formation: Inorganic carbon sources and net inorganic reaction of deposition. - Limnol. Oceanogr., 25/2, 248-261, 7 Figs., 2 Tabs., Baltimore

SIKES, C.S. & WILBUR, K.M. (1982): Functions of coccolith formation. - Limnol. Oceanogr., 27/1, 18-26, 3 Figs., 3 Tabs., Baltimore

SOMERS, G.F. & BROWN, M. (1978): The affinity of trichomes of blue-green algae for calcium ions. - Estuaries, 1, 17-28, 2 Figs., 7 Tabs., Solomons

SWART, P.K. (1983): Carbon and oxygen isotope fractionation in scleractinian corals: a review. - Earth Sci. Rev., 19, 51-80, 10 Figs., Amsterdam

SWART, P.K., STERNBERG, L.D.S.L., STEINEN, R. & HARRISON, S.A. (1989): Controls on the oxygen and hydrogen isotopic composition of the waters of Florida Bay, U.S.A.. - Chem. Geol., Isotope Geosci., 10, 113-125, 8 Figs., 2 Tabs., Amsterdam

TUFFERY, A.A. (1969): Light and electron microscopy of the sheath of a blue-green alga. - J. Gen. Microbiol., 57/1, 41-50, 5 Pls., London

VAN LIERE, L. & WALSBY, A.E. (1982): Interactions of cyanobacteria with light. - In: CARR, N.G., WHITTON, B.A. (eds.):The Biology of Cyanobacteria. – Bot. Monographs, Vol. 19, 688 pp., 9-45, 13 Figs., 2 Tabs., Oxford (Blackwell)

VOLOKITA, M., ZENVIRTH, D., KAPLAN, A. & REINHOLD, L. (1984): Nature of the inorganic carbon species actively taken up by the cyanobacterium Anabaena variabilis. - Plant Physiol., 76/3, 599-602, 5 Figs., Lancaster

WALSBY, A.E. (1968): Mucilage secretion and the movement of blue-green algae. - Protoplasma, 65/1-2, 223-238, 17 Figs., Wien

WECKESSER, J., HOFMANN, K., JÜRGENS, U.J., WHITTON, B.A. & RAFFELSBERGER, B. (1988): Isolation and chemical analysis of the sheaths of the filamentous cyanobacteria *Calothrix parietina* and *C. scopulorum*. - J. Gen. Microbiol., 134/3, 629-634, 1 Fig., 2 Tabs., London

WHEELER, A.P. & SIKES, S. (1984): Regulation of carbonate calcification by organic matrix. - Amer. Zool., 24/4, 933-944, 3 Figs., 1 Tab., Bloomington, Indiana

WOLK, P.C. (1973): Physiology and cytobiological chemistry of blue-green algae. - Bacteriological Rev., 37/1, 32-101, 16 Figs., 11 Tabs., Baltimore

Manuscript received October 7, 1991
Revised manuscript accepted November 28, 1991

STIC-ILL

From: Marx, Irene
Sent: Tuesday, September 10, 2002 9:19 AM
To: STIC-ILL
Subject: 09/777664

Importance: High

Please send to Irene Marx, Art Unit 1651; CM1, Room 10E05, phone 308-2922, Mail box in 11B01

Observations on the ionic composition of blue-green algae growing in saline lagoons
AU Pillai, V. K.
SO Proc. Natl. Inst. Sci. India, (19550000) vol. 21, no. 2, pp. 90-102.
DT Journal

Dalrymple, D.W., 1965, "Calcium carbonate deposition associated with blue green algal mats, Baffin Bay.:, Texas: Institute of Marine Science Publication 10, p. 187-200

Black, M., 1933, "The algal sedimentation... ", Royal Society of London Philosphical transactions, Ser. B, V. 222, p. 165-192

Lowenstam HA (1981), Science, 211:1126-1131

Ferris et al., Earth Sci., 47:233-250 (1993)

Ferris et al., Appl. and Environm. Microbiol.,1989, 55:1249-1257

Kazmierczak et al., (1990), Science, 250:1244-1248

Kempe et al., Facies, 28:1-32, 1993.

Kempe et al., 1994, Bull, Inst. Oceanogr., Monaco no. spec., 13:61-117.

Merz, M.U.E, 1992, Facies, 26:81-102

Pentecost et al., 1986, Calcification in cyanobacteria, In "Biomineralization of Lower plants and animals (Leadbeater et a., ed. 73-90, Clarendon Press, Oxford.

Riding, R., 1982, Nature, 299:814-815

Thompson eta., 1990, Geology, 18:995-998

Irene Marx
Art Unit 1651
CMI 10-E-05,
Mail Box 11-B-01
703-308-2922

VI. *The Algal Sediments of Andros Island, Bahamas.*

By MAURICE BLACK, *Trinity College, Cambridge.*

(*Communicated by* O. T. JONES, *F.R.S.*)

(Received November 4, 1932—Read February 9, 1933.)

[PLATES 21, 22.]

CONTENTS.

I.—INTRODUCTION.

In the course of a geological reconnaissance of Andros Island, in the Bahamas, it was found that the lower forms of plant life, especially the Blue-green Algæ, play an important part in the process of sedimentation. In addition to those forms which

[Published May 2, 1933.

SEP 12 2002 09:54 FR CISTI ICIST 613 998 5283 TO 17033084516 P. 04

actively contribute calcium carbonate to the sediment, there are other species which function primarily as sediment binders, without necessarily precipitating any lime themselves. Such sediment-binding algæ usually impart characteristic structures to the medium in which they grow; and in the interior of Andros, where such deposits are

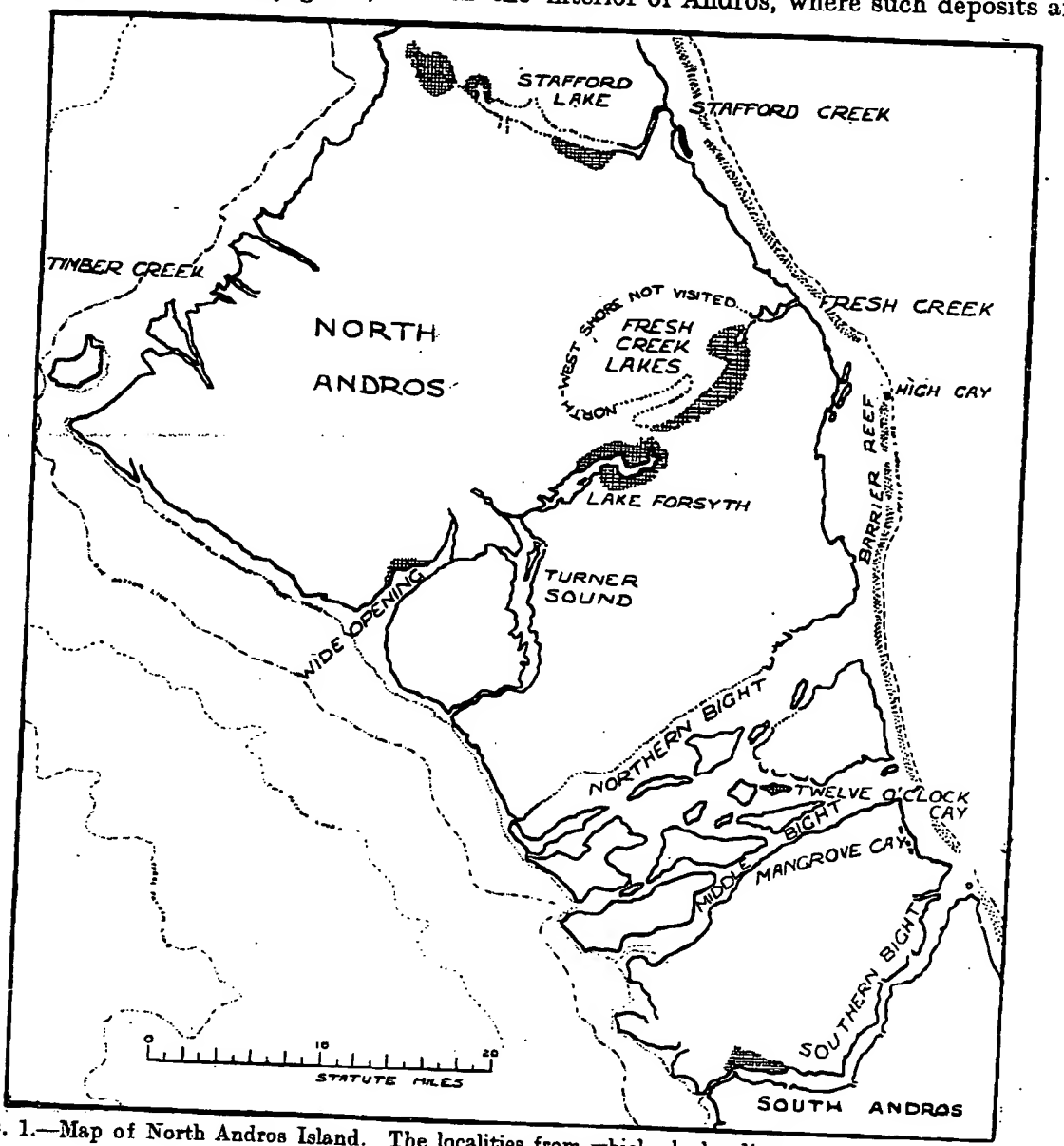

FIG. 1.—Map of North Andros Island. The localities from which algal sediments are described in this paper are shaded.

now accumulating over large areas, structures are being produced which are reminiscent of those found in some of the great limestone formations of the Lower Palæozoic and Upper Precambrian. In view of this, and of the supposed algal origin of certain of these limestone structures, it is felt that a detailed description of the Bahaman sedi-

SEP 12 2002 09:54 FR CISTI ICIST 613 998 5283 TO 17033084516 P. 05

ments will provide an example of a modern Cyanophyceous deposit, which may prove useful for comparison with older limestones of similar structure.

The field work on which this paper is based was undertaken during the spring of 1930, in the course of an expedition to Andros Island, made possible through the assistance of the Rouse Ball Fund of Trinity College, Cambridge, and of the Percy Sladen Fund of London. It is the author's pleasant duty to acknowledge his gratitude to the trustees of these two funds for their generous support. This expedition to the interior of Andros Island formed part of the programme of the International Expedition to the Bahamas, under the general direction of Dr. RICHARD M. FIELD, of Princeton, U.S.A.

The Bahama Bank is a region of shallow water limestone sedimentation. It consists of a great submarine plateau, standing almost at sea level, and thus forming a great stretch of shallow sea, surrounded on all sides by deep water. The rocks which form the islands are very pure limestones of Pleistocene Age, and the modern sediments on the bank are also entirely of calcite and aragonite, without any admixture of siliceous or argillaceous material. Thus the region is one of exclusively limestone sedimentation, and in this respect is closely comparable with some of the seas of Palæozoic and later Precambrian times, in which carbonate sediment prevailed over considerable areas.

Andros Island, in which the algal beds are found, has an area of some two thousand square miles, and is the largest island in the Bahamas. Along the east coast there is a well developed barrier reef, backed by a narrow ridge of limestone hills, but the interior and the western part of the island are of entirely different character. Low-lying, marshy plains, interspersed with shallow lakes and outcrops of limestone, are found in the interior, whilst in the westernmost part of the island, locally known as "The Marl," the limestone outcrops disappear, and the country consists of white, unconsolidated limestone-mud, known as *Drewite*. This is a desolate region, with bare white drewite flats, very sparsely covered with halophytic vegetation. The whole island, but especially the western part, is dissected by an intricate system of tidal creeks and mangrove swamps, which render it liable to heavy flooding under favourable circumstances. As this flooding has an important effect upon the growth of the algal deposits, by providing an intermittent supply of sediment, and possibly by causing an alteration in the salinity of the surface water, we shall return to this question in more detail later.

II.—Ecology of the Algal Flora.

(*a*) *Distribution of the Genera.*

The western edge of the Great Bahama Bank lies some eighty miles off the coast of Andros, and the intervening shallow water never reaches a depth greater than about four fathoms. The sea floor is mantled with bottom deposits of white, mostly fine-grained, calcium carbonate sediments, with occasional outcrops of Pleistocene lime-stone. Owing to the shallowness and clarity of the water, and to the whiteness of the

SEP. 12 2002 09:55 FR CISTI ICIST 613 998 5283 TO 17033084516 P. 06

bottom deposits, the light intensity on the sea floor is very great, and the bottom flora consists very largely of Chlorophyceæ and marine angiosperms. Dredgings between the edge of the bank and the west coast of Andros brought up mainly specimens of *Penicillus, Rhipocephalus, Udotea, Halimeda, Batophora* and *Caulerpa*. It was evident, in examining the dredgings, that the basal filaments of the algæ, in permeating the surface layers of the unconsolidated muds and sands upon which they grow, have a considerable binding effect upon the sediment. This is even more conspicuous in the zone between tides, where the purely filamentous forms, such as *Derbesia*, assist in producing the same effect. Although the sediment is by no means hard, it becomes tenaciously cohesive, and resists the erosive action of ordinary tidal currents.

Above the intertidal belt, the Chlorophyceæ are no longer dominant, and are almost completely replaced by the Cyanophyceæ. Wherever the surface sediments were examined, they were found to be permeated by algal filaments and cells, or to be covered by a skin consisting of algal colonies growing on the surface. In regions of intermittent sedimentation, such as the coastal belt, and some of the flat, low-lying areas in the interior of the island, these algæ were found to play an active part in the process of sediment accumulation. The colonization of newly deposited sediment by filamentous algæ first of all binds together the sediment, preventing its being easily washed away again, and then produces a felt of algal filaments, which is sometimes quite thick and dense. In nearly all the species involved, the filament is enclosed in a mucilaginous sheath, to which mineral particles very readily adhere. Thus any fresh sediment brought into the region is at once trapped amongst the filaments.*

The most important species in the Bahaman sediments are :—

Gloeocapsa atrata (Turpin) Kützing.
G. granosa (Berkeley) Kützing var. *chlora* nov.†
G. fusco-lutea (Naegli) Kütz.
G. gelatinosa Kütz.
G. magma (Brebisson) Kütz.
G. rupestris Kütz.
G. viridis sp. nov.
Aphanocapsa grevillei (Hassal) Rabenhorst.
A. marina Hansging.
Symploca læte-viridis Gomont.
Phormidium tenue (Meneghini) Gomont.
Schizothrix braunii Gomont.
Plectonema atroviride sp. nov.
Scytonema androsense sp. nov.
S. crustaceum Agardh. var. *catenula* nov.

It will be noticed that the Rivulariaceæ, so frequently associated with the formation of lake balls and water biscuits, are of no importance here.

These algæ were found to be growing, not in pure colonies, but in rather complex communities, which are still under investigation, and will not be described in detail

* This sediment-binding action of filamentous algæ is also of common occurrence in regions where the sediment consists of non-calcareous mud, and colonization of fresh sediment by such species as *Microcoleus chthonoplastes* and *Vaucheria thuretii* has been shown to be important in tidal salt marshes. For example, see Carey and Oliver, 1918, p. 173, and Plate XV, upper figure.

† The new species and varieties of algæ are described in section VII, p. 186.

SEP 12 2002 09:56 FR CISTI ICIST 613 998 5283 TO 17033084516 P. 07

until more of the species involved have been grown in artificial culture. Roughly speaking, it may be said that the communities in areas affected by the tides are dominated by *Symploca lætе-viridis* and several non-filamentous forms; that as one goes from the tidal belt inland towards the less saline water, species of *Scytonema* appear, and grow intimately with a large number of other species, important amongst which are *Schizothrix* and *Aphanocapsa*; and finally, that in places where the ground water is not saline, or which are affected by rain-water alone, almost pure colonies of *Scytonema* are found, without admixture of any species belonging to the Oscillatoriaceæ. Thus we have the distribution shown in Table I.

TABLE I.

Maximum Salinity: parts per 1000.	Nature of Habitat.	Flora.
30–40	Shoal water below tides	Chlorophyceæ: *Udotea*, *Penicillus*, *Halimeda*.
15–36	Between tides, near H.W.M.	Cyanophyceæ: *Phormidium*, *Symploca*, and unicellular forms.
? ca. 2	Above H.W.M. Inland Marl flats	Cyanophyceæ: *Scytonema*, *Plectonema*, *Schizothrix*, and unicellular forms.
0	Above H.W.M. Limestone outcrops	*Scytonema* alone.

III.—Description of the Algal Sediments.

Where definite algal structures are developed in the sediments, their growth form depends to a large extent upon local conditions, and a different type of algal head is found in each of the geographical belts mentioned above.

Under the shoal waters of the Great Bahama Bank, no complex algal heads were observed, and the Cyanophyceæ, which are elsewhere responsible for these structures, were not found to be present in large numbers. The Chlorophyceæ, which make up the bulk of the flora here, were found to permeate the sediment and bind the particles together, without producing any banded or radial structure. It was only above low-water mark, where the Cyanophyceæ are the prevalent algæ, that alga-controlled lamination and algal heads with characteristic internal structures were found.

The simplest type, fig. 2, and figs. 21 and 22, Plate 22, was found in localities which were frequently flooded by sea water. Round the western entrance to Southern Bight, filaments of *Symploca lætе-viridis* permeate the sediment as it is deposited, and play an important part in binding it, thus preventing re-erosion. During intervals of non-deposition the alga continues to grow in company with several other species, and a thin organic layer is produced. Beyond this, however, the alga does little to modify

SEP 12 2002 09:56 FR CISTI ICIST 613 998 5283 TO 17033084516 P. 08

the structure of the sediment, except by accentuating the mechanically formed laminations.

Somewhat more distinctively alga-controlled sediments were found about high-water mark at Twelve O'clock Cay and in the Wide Opening, figs. 17 and 18, Plate 21, where, in addition to this kind of lamination, simple algal heads are developed, fig. 3, and fig. 24, Plate 22. These take the form of irregularly scattered domes usually an inch or two high, and four or five inches in diameter, each possessing a crude concentric lamination.

It was in the interior of Andros Island that the most highly developed type of algal head was found, and where the most extensive algal deposits were discovered. Bordering the fresh-water lakes, and forming the flat ground between the limestone ridges, are large stretches of drewite marshes, which are covered with circular algal heads possessing a peculiar structure of approximately concentric laminæ, fig. 5, and figs. 19 and 20, Plate 21.

In all these forms, parallel or concentric lamination is the dominant element in the structure of the algal heads, and the mineral matter is soft and uncemented sediment, mechanically entrapped by the algæ, without any perceptible addition of secondary crystals. On slightly more elevated ground, however, the algal heads assume an entirely different structure, fig. 28, Plate 22. The colonies consist of radiating filaments, without much interstitial sediment, and the whole algal head is often strongly cemented with carbonate crystals precipitated round the filaments. Two main factors are probably responsible for this difference in structure: firstly, the absence of sediment, which leaves the algal head porous, and secondly, the different properties of the water, which is rain-water with a certain amount of freshly dissolved calcium carbonate in solution, but practically no other dissolved salts.

The types of algal structures described below are restricted to the sedimentary forms; those algal heads in which the clastic sediment does not play an essential part are still under investigation, and will be dealt with in a later publication. In the paragraphs immediately following, only the positions of the localities are indicated, and the local conditions are described in more detail in Section V, p. 179, after the significance of the environment has been discussed.

(*a*) *Deposits of Type A.*

Locality.—Southern Bight, Andros Island, Bahamas, on the north shore near the western entrance to the bight. Lat. 24° 3′ N., and Long. 77° 49′ W.

Growth Form, fig. 2.—This is the simplest form of alga-controlled sediment which was recognized, and consists of drewite, with a strongly marked organic lamination parallel with the surface. In fresh specimens, the thin darker laminæ, fig. 21, Plate 22, have a greenish tinge, and the thicker ones are white; in older material the green colour is replaced by brown. The algal filaments do not seem to modify the form of

SEP 12 2002 09:57 FR CISTI ICIST 613 998 5283 TO 17033084516 P. 09

the upper surface of the sediment, but they accentuate the mechanical lamination by producing a dark organic film between the layers of sediment. By permeating each layer as it is deposited, the filaments bind together the sediment and tend to preserve it from re-erosion.

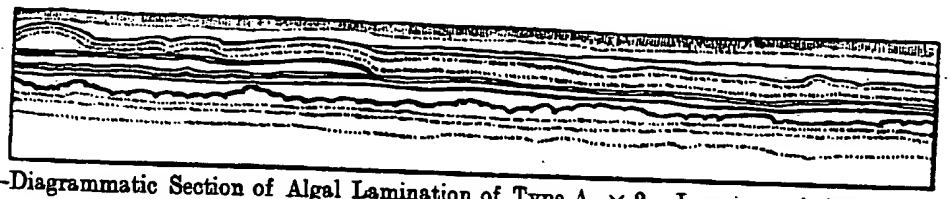

FIG. 2.—Diagrammatic Section of Algal Lamination of Type A, × 2. Layers consisting largely of algal material are shaded.

The Algæ.—The algal filaments are almost invisible in ordinary rock-sections, but are readily seen when the carbonate has been removed by acid; in such preparations, two filamentous forms are found—*Symploca læte-viridis* in conspicuous, bright grass-green tufts, and *Phormidium tenue*, in slender, solitary filaments of pale blue green cells. In the deeper layers of the sediment, the cell-contents are no longer present, and these two algæ are represented by colourless, empty sheaths. There are, in some of the laminæ, traces of *Scytonema*, but these remains are too badly preserved to be specifically identifiable; compared with the other two species, this form is rare. Of the Chroococcaceæ, *Gloeocapsa magma* and *G. fusco-lutea* are found, but not in any appreciable quantities.

Material which had been dried out at the time of collection gave, in the laboratory, a strong culture of *Symploca læte-viridis* and *Phormidium tenue*; under suitable conditions, the *Symploca* produced erect tufts of grassy-green filaments, closely similar to those found embedded in the sediment. It appears to be this species which gives the pale enamel-green colour to the more recently deposited layers of the sediment.

The Sediment.—The sediment occurs in two kinds of laminæ. The thicker laminæ are usually between 0·5 mm. and 1·75 mm. thick, and contain detrital grains of all sizes up to 0·1 mm., or a little more. The arrangement of the grains suggests that each lamina was deposited by a single process, for the grains grade from coarse at the bottom to finer on top within each lamina. Frequently there is a slight suggestion of a palisade structure resulting from a parallel arrangement of vertically growing filaments; this is restricted to the upper surface of the lamina. Interbedded with these obviously sedimentary laminæ, there are somewhat thinner layers of very fine-textured sediment, usually little more than one-tenth of a millimetre in thickness. These layers seem to represent the sediment entrapped in the mucilaginous sheaths of the algal filaments.

(*b*) *Deposits of Type B.*

Locality.—Twelve O'clock Cay, between Middle and Northern Bights, Andros Island. Lat. 24° 18′ N., Long. 77° 48′ W.; and in the mangrove flats bordering the northern shore of the Wide Opening, Lat. 24° 29′ N., Long. 78° 8′ W.

SEP 12 2002 09:57 FR CISTI. ICIST 613 998 5283 TO 17033084516 P. 10

Growth Form, fig. 3.—The surface layers of the sediment, which is here rather sandy, are impregnated and bound together by a gelatinous substance formed from the mucilaginous investments of blue-green algæ. The characteristic algal heads in these localities consist of low, rounded, domes, rising above the normal surface of deposition of sediment. The domes are irregularly scattered, and are usually four or five inches across.

The algal heads contain a very small proportion of organic matter, and this can only be seen near the outer surface, where addition of new sediment and active algal growth are still going on. Although concentric laminæ appear to be present in the central parts of the dome, this structure is lost as soon as the sediment is disturbed, and it was only found possible to collect material from the other shell, to a thickness of about half an inch. These specimens, when sectioned, show the lamination to be due to sharp differences in grain size in successive layers in the sediment, fig. 24, Plate 22, in addition to the alternation of light and dark layers, in which the sand grains can be seen to be embedded in the remains of algæ.

The conspicuous dark layers in the sediment owe their colour to the presence of two deeply tinted species of *Gloeocapsa*—the copper red *G. magma*, and the brilliant green

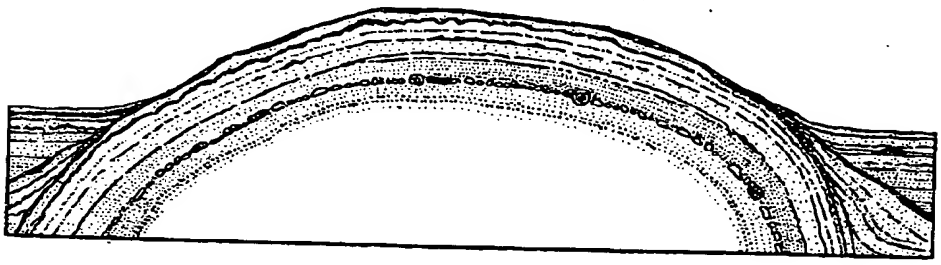

FIG. 3.—Diagrammatic Section of an Algal Head of Type B, natural size. Dark organic layers, made up of cells of *Gloeocapsa*, are represented by black lines. The intervening layers, consisting of sediment bound together by *Symploca* and *Aphanocapsa*, are dotted or unshaded.

G. viridis. Mixed with the cells of these two species are scattered colonies of *G. fusco-lutea* and *G. gelatinosa*. The lighter layers, which are not noticeably coloured in a hand specimen, are permeated by a remarkable, colourless gelatinous mass of *Aphano-capsa marina*, through which are threaded innumerable unconnected filaments of *Symploca læte-viridis*; at certain levels, the *Symploca* filaments are closely entwined, giving rise to bright green tufts, similar to those found in Type A. Remains of *Scytonema* are distinctly rare.

The Sediment.—The sediment in this kind of algal head is rather similar to that found in Type A, except that in the specimens examined it was found to be distinctly coarser, and grains up to one millimetre in diameter are quite frequent. The grains include well-rounded, almost spherical or ellipsoidal grains of limestone, fragments of molluscan shells, and tests of Foraminifera, especially of *Peneroplis proteus* D'ORBIGNY. Again the more organic layers are very much finer in grain size, and much thinner than the coarsely detrital laminæ.

(c) *Deposits of Type C.*

Locality.—The flat country bordering Lake Forsyth, Lat. 24° 35′ N., Long. 77° 56′ W., and also round Stafford Lake, Lat. 24° 50′ N., Long. 78° 0′ W., in North Andros.

Growth Form.—In their position of growth, algal heads of this type appear as regularly spaced, raised discs, usually four or five inches in diameter, figs. 19 and 20, Plate 21. They are entirely unlithified, and in their natural condition they have a somewhat rubber-like consistency. Cross sections show a colour banding, with laminæ parallel with the upper surface, the laminæ being alternately white and brown, fig. 25, Plate 22. This colour banding is found to go much deeper below ground than the surface discs.

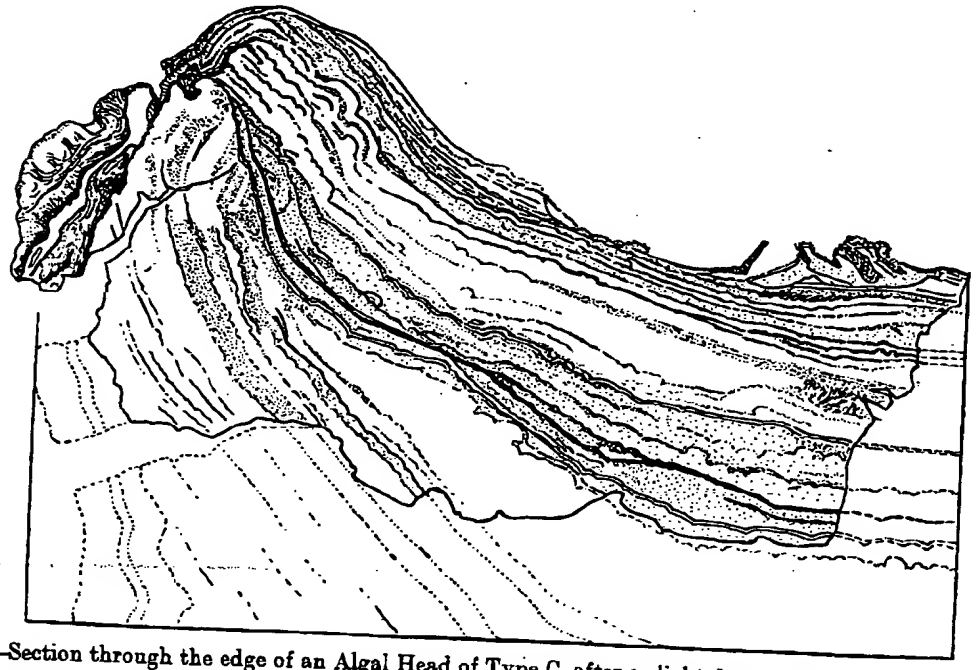

FIG. 4.—Section through the edge of an Algal Head of Type C, after a slight drying, showing the upturning of the edge. × 2.

This growth form is the resultant of two opposing tendencies. The growth process, by itself, gives rise to flat or smoothly rounded, convex forms, similar to those of Type B; this simple shape, however, is rarely retained for long, and is constantly liable to modification during periods of partial drying. Owing to the large proportion of organic matter, and the fine texture of the sediment in the algal heads, drying causes the upper layers to contract, fig. 4, and a concave shape results, fig. 8. Renewed growth of the algæ produces further layers, at first concentric with the concave surfaces of the older part of the algal head, but gradually re-establishing the convex form again. This process may continue for a considerable time, and unless the structure is inter-

SEP 12 2002 09:58 FR CISTI ICIST 613 998 5283 TO 17033084516 P. 12

fered with, the algal heads develop into cylindrical columns, with transverse laminations, more or less concave upwards.

The Algæ.—The association of species found in these algal heads is a complicated one, remarkable for the intense jade-green colours of many of the species, and the absence or great rarity of species whose sheaths are not green, olive brown, or hyaline. The most important species are :—

Gloeocapsa atrata.	*Schizothrix braunii.*
G. fusco-lutea.	*Plectonema atroviride.*
G. viridis.	*Scytonema androsense.*
Aphanocapsa marina.	*S. crustaceum* var. *catenula.*

In thin sections the dark laminæ appear as translucent brown streaks, made up of algal filaments closely pressed together, and enclosing very little sediment amongst them. No orderly arrangement of the filaments is noticeable, except a rough parallelism induced by compression. In sections prepared as rock slices, it is impossible to recognize the individual filaments ; they were investigated by cutting shavings from the hand specimen, swelling them in water, and then clearing with dilute acid. The residue is in the form of a felt of interlocking filaments, and with care can be removed to a slide and mounted. By this means, the algæ can be observed in a relatively uncompressed condition, and unobscured by sediment.

The brown laminæ consist of closely matted filaments of the two species of *Scytonema*, mingled with a few tangled sheaths of *Schizothrix*. The sediment between the dark layers consists of extremely small and irregularly shaped carbonate grains, which do not appear to be in contact with one another. The spaces between the carbonate crystals are occupied by algal material which is colourless and not visible in a petrological section. Sections cleared with acid at once reveal the organic matrix as a colourless, jelly-like material, which appears to be made up of an extended mass of *Aphanocapsa marina*, mixed with a profusion of filaments of *Schizothrix braunii*. Both of these have pale coloured cells, set in an abundance of clear, colourless mucilage.

Running through these laminæ of loosely packed sediment, there are occasionally narrow tubes, usually about sixteen microns in diameter, with walls of closely packed carbonate crystals, fig. 26, Plate 22. They are best seen in petrological sections examined between crossed nicols. There can be little doubt that these tubes also have an algal origin, for it is possible to tease out from untreated sediment, filaments of *Scytonema* with a similar calcareous investment made up of crystals embedded in the mucilaginous sheaths of the filaments.

The Sediment.—The sediment consists of rather angular grains of calcite, with no obvious crystal outlines, but rather with the shape of detrital grains. The average size is about four microns, and grains above eight microns in diameter are very rare in most samples. The sediment on the floor of Lake Forsyth includes somewhat coarser grades than this, and grains of ten microns form quite an appreciable pro-

SEP 12 2002 09:59 FR CISTI ICIST 613 998 5283 TO 17033084516 P. 13

portion of the sediment. This seems to indicate that only the finer material is carried in suspension over the algal flats.

(*d*) *Deposits of Type D.*

Locality.—On the rocky flats bordering the lakes at the headwaters of Fresh Creek, Lat. 24° 38′ N., Long. 77° 54′ W.

Growth Form, fig. 5.—These algal bodies differ from the forms already described in their frequent occurrence in an unattached condition. In their early development, they are in the shape of circular, plano-convex lenses, some two or three inches in diameter. They resemble, in their internal structure, the earliest formed parts of algal heads of Type C, except in their having a larger proportion of organic material to sediment, and in the less orderly form of the laminations. They differ mainly in their behaviour during desiccation, when they roll up and become completely detached from the sediment below.

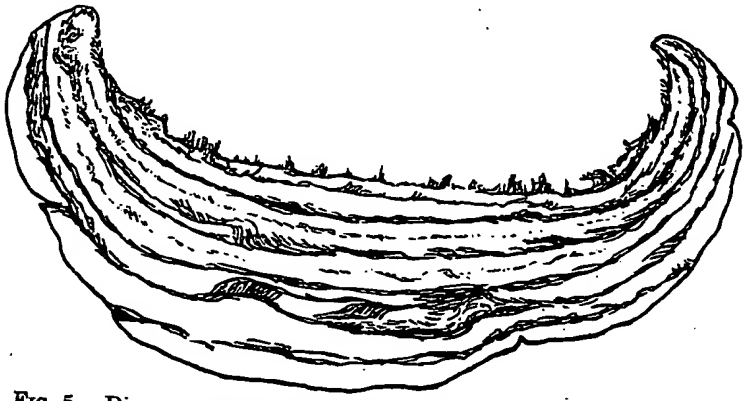

FIG. 5.—Diagrammatic Section of an Algal Head of Type D. × 2.

The Algæ.—The algæ in this type are of the same species as those found in Type C, but in the material under consideration, the proportion of *Scytonema* is very much greater than in the Type C specimens from either Lake Forsyth or from Stafford Lake, and the gelatinous matrix of *Aphanocapsa* is proportionately reduced.

The Sediment.—The sediment is of extremely fine grain size; most of the particles are two microns or less in diameter, and very few are as much as ten microns. The larger grains have angular or ragged outlines, whilst the shape of the smaller grains is difficult to determine.

IV.—THE SIGNIFICANCE OF THE LAMINATION.

Each of the four types of algal head described above is characterized by the possession of a laminated structure, which may arise in one or more of three ways:—

(1) Rhythmic variation in the quantity of filaments of one species or group of species, with relation to the quantity of sediment.
(2) Alternation of two species or of two groups of species.
(3) Sedimentary lamination in mineral particles enclosed between the filaments.

SEP 12 2002 10:00 FR CISTI ICIST 613 998 5283 TO 17033084516 P. 14

In each development of concentrically laminated sediment investigated on Andros Island, it was found that the presence of two of these laminating processes could be traced. Thus :—

The lamination in Type A arises from a combination of 1 and 3.
" " Type B " " 2 and 3.
" " Types C and D " " 1 and 2.

There can be little doubt that each of these laminating processes represents a response to some definite recurrent or rhythmic change in the environment, and it is a matter of considerable stratigraphical interest to know what these changes are, and to what extent we can rely upon the evidence of these laminated bodies to reconstruct the external conditions under which such sediments were formed. It is impossible to enter into the question exhaustively until more results of experimental work on the algæ in culture are available, but one or two of the more important environmental conditions as observed in the field may be discussed here.

(*a*) *Deposition of the Sediment.*

The simplest rhythm is that expressed in the sediment itself, but even here there are several factors involved. In the lower part of the tidal belt, shifting and redeposition of sediment takes place as a result of tidal scour, and as a result of storms. Our observations went to show that on the marl flats where the algal deposits are found, tidal action by itself was not responsible for any appreciable sedimentation, but may become quite important during violent storms, when large quantities of sediment are stirred up into the water. If the sediment in suspension is very fine grained, the mucilaginous sheaths of the algæ entrap quite an appreciable quantity, and appear to do this selectively for the smallest grains in suspension. Thus, if a mixture of mud, silt, and sand is drifted over the algal heads at a velocity sufficient to keep the sand grains moving, the mud particles cling to the mucilage of the filaments, but very little sand is retained. Laminæ which have the characteristics of ordinary gravity sedimentation are also formed in most algal deposits in the tidal belt of the island ; in these, each lamina begins with comparatively coarse grains, often between 0·1 mm. and 1·0 mm. in diameter, and passes upwards into fine mud. Such laminæ are frequently about one millimetre thick, but may vary considerably from this. They appear to effect a complete smothering of the algal head, probably by sediment settling out after a heavy storm ; we were not fortunate enough to observe the actual deposition of this kind of lamina in progress, but abundant examples were found where algal heads had quite recently been smothered by fresh deposits of mechanical sediment.

In the widespread algal deposits of the interior of Northern Andros Island, no trace

SEP 12 2002 10:00 FR CISTI ICIST 613 998 5283 TO 17033084516 P. 15

of mechanical lamination was discernible, and the sediment is all extremely fine in texture. The interior lakes are not tidal, but here again the sediment is supplied to the algal marshes by a process of flooding. This takes place in two entirely different ways: by heavy rainfall, and by invasion by sea water from the banks to the west. In the first case the salinity of the ground water is reduced, and the transportation of sediment is very small, being a slight washing of material from the land into the lakes and creeks. There is possibly also a little transference of sediment from the lake floors on to submerged parts of the algal flats, when the bottom deposits are stirred up by waves, and drifted by wind-blown surface currents on to flooded areas bordering the lakes. The solution effects are probably more important.

In the second case conditions are quite reversed; vast quantities of sea water are piled up on the shoals, and are swept over the low-lying parts of Andros as a result of violent westerly winds. During such storms, the water over the banks is laden with churned-up sediment and the whole of the flooded area is liable to be smothered under a film of fine white mud, which is left behind when the flood water retreats. The prevailing winds are easterly in direction, and do not cause this kind of flooding. It is probably produced on a grand scale only by hurricanes, which are liable to visit this region during the autumn months. These are circular storms, revolving in an anti-clockwise direction, and travelling along a north-westerly course across the archipelago. Consequently, during the earlier part of a storm, the shoal water on the banks is violently agitated, and becomes strongly charged with suspended sediment. When the wind reverses, and blows from the west, a great wave of drewite-laden water is forced over the island. If the storm is particularly violent, this flood water crosses the island completely, and finds its way through the eastern creeks into the lagoon behind the barrier reef—a cross-country journey of some forty miles.

The sediment brought into the centre of the island by such flood water is extremely fine grained, since all the coarser constituents are deposited before the water has travelled far in from the west coast. This uniformity of grain size prevents any mechanical lamination, or any noticeable difference in size between the particles agglutinated round the mucilage of the algæ, and those particles which settled out under gravity.

(*b*) *Growth of the Algæ.*

The growth rate of any particular colony of algæ is probably controlled by a complex set of conditions, important variables amongst which are:—humidity, supply of carbon dioxide, temperature, salinity of the ground water, and deposition of sediment. These conditions are now being investigated experimentally with the algæ in culture but owing to the extremely slow growth rate of most of the species involved, and the difficulty of obtaining cultures free from bacteria and fungi, it will be some time before a satisfactory series of measurements can be made. Field observations were made on the variations of salinity, sedimentation, and water level, and the effects of

SEP 12 2002 10:01 FR CISTI ICIST 613 998 5283 TO 17033084516 P. 16

rhythmic fluctuations of these upon the growth of the algal heads was qualitatively examined.

(i) *The Effect of Salinity.*—In this region, *Symploca læte-viridis* and *Phormidium tenue* seem to be characteristic of salt water, in the case of *Symploca* ranging up to 36 parts per thousand. Experimental work, however, indicates that these two species can tolerate considerable ranges of salt concentration, and can flourish both in nearly fresh water and in highly saline water. With *Scytonema* and *Plectonema*, on the other hand, the salinity has a strong controlling influence. Very little *Scytonema* was found in places liable to be washed by undiluted sea water. With salinities between 1·0 and 10·0 per thousand, there tends to be an alternation between *Scytonema* and the *Schizothrix-Aphanocapsa* association. Where the salt content of the water is appreciably less than one part per thousand, flourishing colonies of pure *Scytonema* were found. The growth habit assumed in these circumstances is quite unlike the forms already described in this paper; the filaments assume a radial arrangement, and deposit a finely crystalline cement of calcium carbonate between the filaments. In North Andros, this kind of structure is best developed in places where the main supply of water is fresh rain-water, and where there is only a negligible influx of water-borne sediment.

It is thus possible that an intermittent growth of *Scytonema* might be controlled by fluctuations in salinity; for instance, the layers with *Scytonema* in the high level mud flats at Southern Bight may represent periods during which the mud flats were free from flooding by sea water, and the salt leached out of the surface layer by rain.

(ii) *The Effect of Sedimentation.*—Experimental work on the two most important groups of species—those belonging to the Scytonemataceæ, and those belonging to the Oscillatoriaceæ—has already shown that whereas the former are extremely slow-growing, the Oscillatoriaceæ are capable of surprisingly rapid growth in a fresh culture. Indeed, an ordinary lamina of sediment, a few millimetres in thickness, could be permeated and bound fast by filaments of *Schizothrix*, *Symploca* or *Phormidium* in a few days, whereas it would be a matter of months before a skin of *Scytonema* could form over the new surface. Thus intermittent access of fresh sediment to a region equally advantageous to each of the two genera, would undoubtedly cause laminæ with a prepondernace of *Scytonema* to alternate with laminæ containing a preponderance of *Schizothrix*, which is, indeed, what occurs in the Lake Forsyth region.

The same kind of process is probably responsible for the dark organic layers in the specimens from Twelve O'clock Cay. Here the sedimentary layers contain chiefly a filamentous form (probably *Symploca* again), and the more organic layers consist of a complex colony of deeply coloured unicellular forms, which make a dense film over the whole surface of the structure. The filamentous forms probably grow comparatively quickly through the newly deposited sediment; the unicellular forms, however, do not do this, but only colonize the exposed outer surface, where they form

SEP 12 2002 10:01 FR CISTI ICIST 613 998 5283 TO 17033084516 P. 17

a dark coloured, mucilaginous layer which protects the sediment underneath from re-erosion.

(iii) *Effect of Fluctuations in Water Level.*—The seasonal rise and fall of water level in the interior of Andros has the effect of alternately gently flooding and draining the algal flats, but desiccation is probably quite rare. The effect of partial drying is to suspend the growth of the algæ, and possibly induce the formation of resting spores. On re-wetting, *Scytonema* takes a very long time to begin a fresh growth, whilst *Schizothrix* produces an abundance of filaments comparatively quickly.

V.—Relationship to the Environment.

(a) *Lake Forsyth.*

The Lake Forsyth country forms part of the interior belt of low salinity which runs through the centre of Andros Island. Wide expanses of drewite flats surround the north-easterly part of the lake, and stretch for considerable distances north and south. They are colonized by algal heads of Type C, which form a closely set pavement of raised discs, and give a very characteristic appearance to the ground, figs. 19 and 20, Plate 21. To the north-east the algal flats are interrupted by a low outcrop of limestone, fig. 6, which separates this region from a series of brackish lakes draining into Fresh Creek. Towards this limestone ridge, upon which drewite deposits rest unconformably, the spermophyte vegetation becomes more important, and conditions become unsuitable for the formation of well-shaped algal heads. There are also regions within the marl flats where algal heads are not formed, and the algal beds give place to undifferentiated sediments, as, for instance, in local developments of mangrove swamp, where the ground is permanently under water. In these localities a greyish coloured ooze, consisting of drewite with a large proportion of organic matter, is being deposited.

The lake is not tidal, and appears to derive enough water from the drainage of the surrounding country to keep its outlet, the White River, in constant flow. For the same reason, although the surface of the lake is only a few feet above sea level, the salinity of its water is normally quite low, and our observations showed it to vary but little from 1·25 parts per thousand. The territory surrounding the lake is subject to a gentle seasonal flooding, caused directly by fluctuations in the rainfall. During the time when we were in camp on the shore of the lake, the water level was high enough to swamp parts of the algal flats, but a large proportion of the marshes still stood above water. The floor of the lake is covered with a very fine-grained deposit of calcium carbonate, and it is possible that storms such as ordinary Northers, which stir up sediment into the water, may also be responsible for depositing it over the marshes during these seasonal floods. However, this may be, the hurricane floods appear to be the most important agents in spreading subaqueous sediments over the land.

SEP 12 2002 10:02 FR CISTI ICIST 613 998 5283 TO 17033084516 P. 18

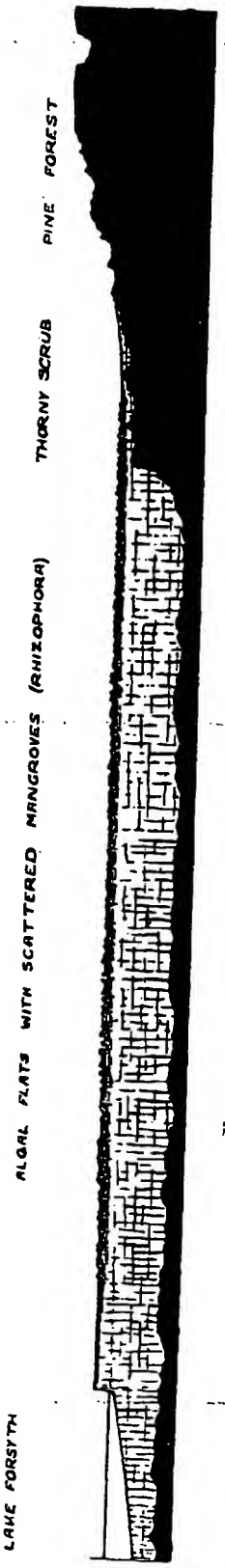

Fig. 6.—Section of the Algal Flats near the head of Lake Forsyth.

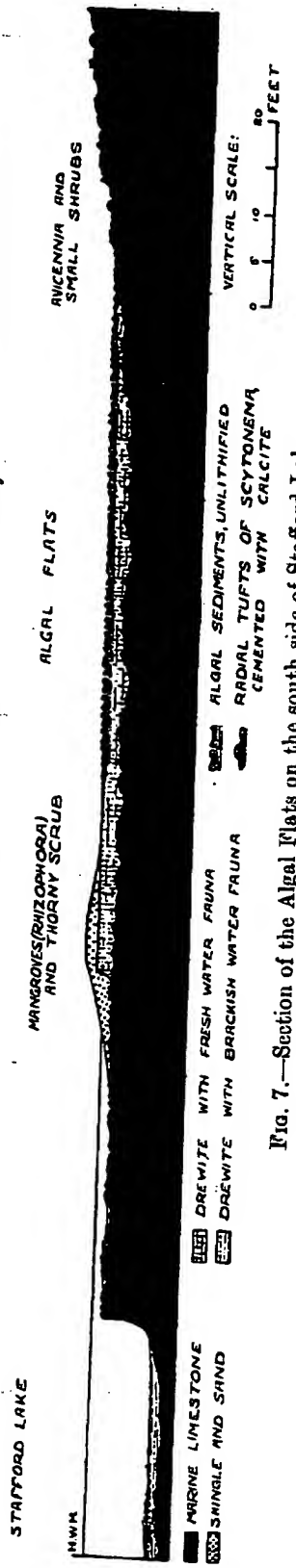

Fig. 7.—Section of the Algal Flats on the south side of Stafford Lake.

(*b*) *Stafford Lake.*

The eastern end of Stafford Lake is bordered at water level by a limestone platform which is locally covered by a thin deposit of peaty drewite, see fig. 7. At the junction between the drewite and the limestone, several distinct growth forms of algal colonies are to be found, but where the drewite is thick enough to mask the limestone completely, algal heads exactly like those of Lake Forsyth appear, with the same species of *Schizothrix* and *Scytonema*. At the eastern end of the lake, such deposits are restricted in area by the limestone outcrops, but further west, the thickness of unlithified sediment becomes greater, and the drewite flats increase in extent until they stretch completely across the lake. The ground water conditions appear to be more closely related to the fresh water areas in the south and west, rather than to Stafford Lake itself, which is in part tidal, and distinctly saline (14–20 parts per thousand at our camp, lat. 24° 50′ N., long. 78° 0′ W.). This difference is also borne out by the fossil fauna of the surface layers of drewite, which show a freshwater (Amnicolid) assemblage, quite distinct from the brackish water assemblage in the sediments now accumulating on the floor of Stafford Lake. Consequently, although the drewite flats on which the algal beds are now being formed border a saline lake, it appears that the local conditions of growth are similar to those at the headwaters of Lake Forsyth. The algal flats are separated from the shores of Stafford

Lake by a ridge of partly cemented gravel, and where this is absent, it is found that there is an area with no algal deposits at all comparable with those of Lake Forsyth.

On the rugged outcrops of limestone which rise through the drewite marshes at the eastern end of the lake, the conditions for algal growth are quite different from those which prevail on the marshes themselves. The supply of sediment is negligible, the available moisture is restricted to rain-water, and the rock surface drains fairly rapidly. The algal heads found here are of the radial type mentioned on p. 170.

(*c*) *The Southern Bight.*

The north shore of Southern Bight is bordered by drewite mud flats which rise with an almost imperceptible slope from the bight to higher ground beyond the reach of flooding by ordinary spring tides. The lowest belt, which remains covered by a few inches of water at low tide, supports a vegetation dominated by green algæ; *Caulerpa paspaloides* on the soft mud, and *Batophora oestedi* where there is a solid substratum. Separated from this lower mud flat by a slight step in the surface of the ground, is a higher mud flat which is not reached by ordinary neap tides, but is slightly flooded by spring and other heavy tides. This forms an area of slow deposition, for if such flooding happens to coincide with rough weather, during which sediment is stirred up into the sea, this belt of land is covered by a thin film of mud which settles out before the water retreats again. This mud flat is colonized by *Symploca*, and the sediment takes on the conspicuously laminated structure (Type A) described on p. 171. Going further beyond the reach of ordinary tides, the surface of the drewite is found to be slightly lithified, presumably through the action of rain-water, and outcrops of Pleistocene limestones also appear; conditions here become favourable for the uninterrupted growth of *Scytonema*, and the sedimentary structures give place to partly calcified algal heads, similar to those found at Stafford Lake and near the headwaters of Fresh Creek.

(*d*) *Twelve O'clock Cay.*

Twelve O'clock Cay is a small island lying in the land-locked sea between Middle and Northern Bights. The algal heads, which are here all of Type B, are of particular interest because they occur on a mud flat which is washed at every tide by water of essentially the same salinity as the sea, 36–38 parts per thousand on the Great Bahama Bank. Although this region is normally sheltered from heavy wave action, the sediment is subjected to constantly shifting currents, and a considerable amount of the finer material is consequently winnowed away, leaving a sediment of a distinctly sandy texture. The tide rises over the algal flats quite gently, and with normal weather conditions there is no transport of sediment. It is probably only during quite severe storms that sediment is swept over the algal flats and deposited there. Towards low-water mark, the algal deposits pass laterally, with no abrupt transition, into loose submarine sediments with no organic matrix or structure.

SEP 12 2002 10:03 FR CISTI ICIST 613 998 5283 TO 17033084516 P. 20

(e) *The Wide Opening.*

The algal beds which occur on the north side of the Wide Opening are similar to those of Twelve O'clock Cay, except in their being colonized to a greater extent by mangroves. They are probably washed at every tide unless the wind sets strongly off shore, when the water is blown out of the Wide Opening. The salinity varies considerably, since there is a substantial amount of brackish water drainage entering this gulf. Our only determination gave a salinity of 17·87 parts per 1000, but as this sample was taken at lowest ebb tide, the figure is undoubtedly lower than the normal; with the rising tide, the Wide Opening fills up with sea water—37·8 per 1000—and by the time that the water level is high enough to flood the algal beds, the salinity must have risen to between 36 and 37 parts per 1000.

(f) *The Fresh Creek Lakes.*

The lakes at the head of Fresh Creek present an interesting series of algal deposits, which are still under investigation. In the localities examined, which are all along the southern shore of this lake system, there are extensive outcrops of limestone. The ground stands several feet above the surface of the lakes, and appears to receive sediment at very rare intervals. Although the lake water is slightly saline, the ground water is fresh, and the recent sediments have a hard, cemented crust. Most of the algal deposits are non-sedimentary, and resemble the cemented forms from Stafford Lake and Southern Bight. There is, however, one sedimentary form (Type D), which is remarkable because the algal heads become completely detached, and are transported by the wind until they are deposited finally in one of the lakes.

(g) *Review of Relationship to the Environment.*

Reviewing the geographical relationships of these algal deposits, we see that they mark a borderline facies between land and water—and, indeed, they often occupy territory which the cartographer hesitates to assign to either. Their structure depends upon several rhythmic processes, foremost amongst which is the alternate flooding and draining of the areas in which the algæ grow. Since they are essentially mechanical sediments, as opposed to the organic accumulations of coenoplase and calcareous algæ, they can only develop in regions where calcium carbonate is the dominant sediment. Thus, unlike the lime extracting algæ, they could not produce their characteristic forms in streams or lakes, unless there were also a sediment of solid carbonate in suspension.

(h) *Early Development of the Algal Heads, and Relation with the Sediment below.*

In all the localities examined, the surface of the sediment between the algal heads, no matter what its former irregularities, is completely covered by a mucilaginous algal skin, and there can be little doubt that the algal sediments described in this paper

SEP 12 2002 10:04 FR CISTI ICIST 613 998 5283 TO 17033084516 P. 21

originated as algal films on mechanically deposited sediments. In the early stages of development, the form which an algal head may take seems to depend to some extent upon the nature of the sediment. In regions of sandy sediment, such as Twelve O'clock Cay, the characteristic, dome-shaped structure probably originates round some irregularity on the surface of the sediment; this becomes colonized by algæ, which begin to accumulate sediment around them. Once the domed structure has been initiated, the algal head will tend to increase its size by the addition of fresh layers deposited concentrically round the earlier ones, producing algal heads of Type B.

In the interior of Andros, round Lake Forsyth and Stafford Lake, the algal heads are initiated, most probably, in a different way. The sediment is of a fine enough

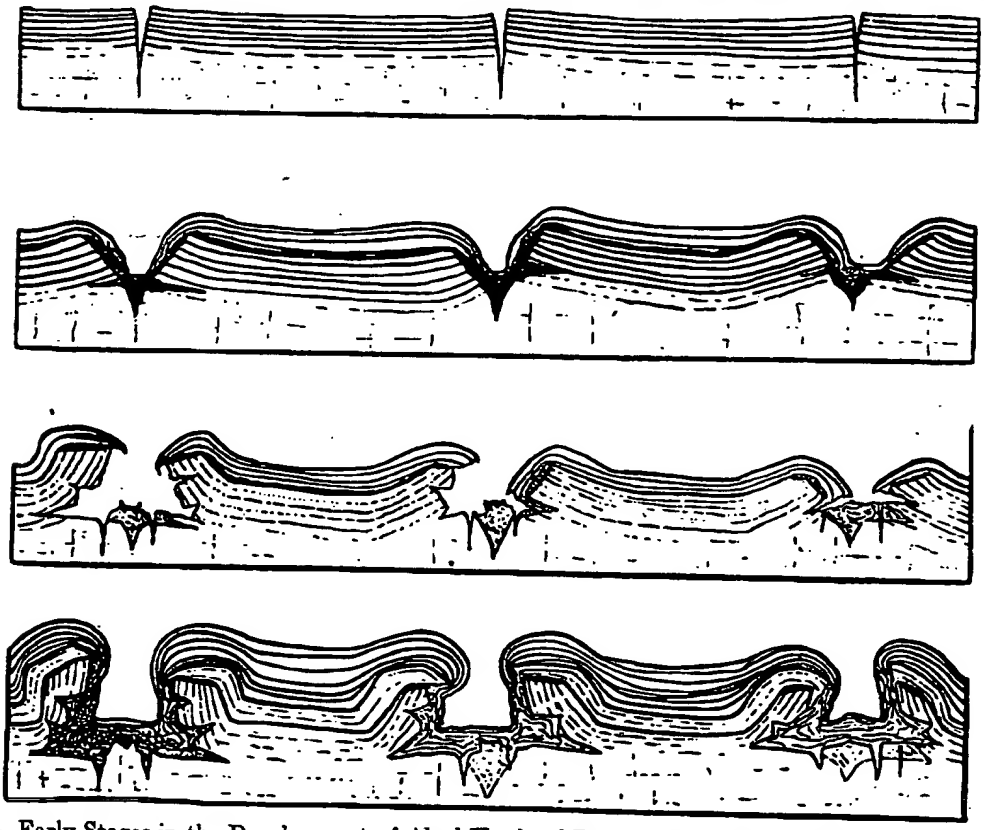

FIG. 8.—Early Stages in the Development of Algal Heads of Type C. × ½. For explanation, see the text.

texture to produce desiccation cracks on a slight drying out of the surface layers, fig. 8. Once this has happened, each desiccation polygon becomes sheathed in a felt of algal filaments, and with further growth, the polygonal outline is lost, and a circular disc is produced. Further growth tends to fill up the gaps between the disks, and to cause a doming of the upper surface. A repetition of desiccation at this stage causes the upper layers of the algal head to shrink; the peripheral part then tears away from the material filling the interspaces between neighbouring algal heads, and a slight upward curling of the outer edge gives a concave or saucer-shaped form to the upper surface (see fig. 4). A renewal of growth then gives rise to the characteristic structure

SEP 12 2002 10.04 FR CISTI ICIST 613 998 5283 TO 17033084516 P. 22

of Type C. The development of Type D probably follows the same plan, but does not appear to go so far as in that of Type C.

When algal heads of Type C attain a considerable thickness, it is often found that only the top inch or inch-and-a-half retains an appreciable quantity of organic matter, and although the earlier formed layers still retain their laminated appearance, the laminæ are now marked out as alternating grey and white bands, with relatively little plant material left. That the disappearance of this organic matter is brought about by bacterial decomposition, is made probable by the recent discovery of very active cellulose and hemi-cellulose destroying bacteria, and also of agar-liquefying bacteria, in the mangrove swamps of western Andros. (BAVENDAMM, 1931 and 1932.)

VI.—COMPARISON WITH OTHER RECENT CYANOPHYCEOUS DEPOSITS.

Amongst recent calcareous algal deposits, the Bahaman sediments stand apart from all other recorded examples in being completely unlithified, and in consisting of clastic material collected by, but not precipitated by, the algæ concerned. This tendency of the Cyanophyceæ to collect clastic material and retain it amongst the mucilaginous sheaths of the thallus, is no recent discovery, and the importance of these plants as pioneer colonizers of newly deposited mudflats has long been recognized. These phenomena have, however, mainly been observed in regions where argillaceous (and to a less extent, arenaceous) sediments are predominant, as for example on the shores of estuaries and deltas (CAREY and OLIVER, 1918, pp. 170–173), and the possibility of the development of this kind of algal colonization on a vaster and more elaborate scale in regions of limestone sedimentation has not fully been realized.

Numerous occurrences of calcareous concretions have been described in which the lime is believed to have been precipitated through the activity of blue-green algæ. In all these, the calcium carbonate is thrown out of solution because the physiological activities of the plant cells disturb the chemical equilibrium of the surrounding water; the solid carbonate, as a consequence, is completely external to the plant cells, and may either come down as a loose precipitate, or as a hard stony encrustation round the algal colonies. All the limestones which are known to originate in this way are being precipitated in fresh-water lakes and streams, in contrast with the Bahaman sedimentary deposits, which range from fresh lake water to water of ocean salinity. A further point of importance is that all the previously described cyanophyceous limestones either require a nucleus or hard substratum upon which to grow, or else they take the form of nodules with a structure of hard, concentric envelopes. The stratigraphical relationships of the Bahaman deposits are somewhat different, for here the algal beds themselves form an incident in the deposition of a series of stratified sediments, and they develop on the surface of completely unconsolidated material.

An example of a cyanophyceous deposit which shows some interesting points in common with the Bahaman material is described by W. WETZEL (1926) from the valley of the Rio Loa, where it flows through the Atacama Desert in Chile. The unlithified

SEP 12 2002 10:05 FR CISTI ICIST 613 998 5283 TO 17033084516 P. 23

algal structures form a tough leathery coating (*Lederhäute*), on the granite blocks of the river bed. They are found to contain *Oscillatoria*, *Nostoc*, and a filamentous bacterium, *Crenothrix*. The river water is slightly saline (3·49 parts per 1000), which is a suggestive point when it is remembered that these *Lederhäute*, and the Bahaman deposits, which are also mostly in somewhat saline water, have in common the peculiarity of remaining unlithified. Another point of interest is that the Atacama *Lederhäute* also enclose clastic sediment, which, however, is non-calcareous, but consists of fine sand and mud, insoluble in hydrochloric acid. Consequently, if detrital calcite is assumed to be absent, it is possible to estimate the relative proportions of precipitated carbonate and clastic sediment. An analysis gave the following results, showing the clastic material and carbonate to be present in approximately equal amounts :—

Organic Matter	9·5
Clastic Sediment	45·0
Calcium Carbonate	37·8
Magnesium Carbonate	4·2

In the Bahaman deposits there is no such ready method of distinguishing between clastic and precipitated material, since both consist entirely of soluble carbonates. Nevertheless, in Type A and Type B the texture of the sediment is sufficiently coarse for many of the individual grains to be easily recognized as fragments of molluscan or foraminiferal shells, or as clastic grains derived from older limestones. Type B can thus be seen at a glance to consist almost entirely of clastic material, and Type A very largely so.

The hard, stony cyanophyceous limestones have much less in common with the Bahaman deposits. They generally occur as discoidal or spherical bodies, up to a foot or more in diameter; internally they are often cavernous, and the general structure may be roughly radial, or, occasionally, concentric. "Water Biscuits" and "Lake Balls" have been recorded and described from many localities, amongst which are the Finger Lakes of New York State (Clarke 1900), various lakes in Michigan and Minnesota (Powell 1903), and streams in Pennsylvania (Roddy 1915). The concentric arrangement becomes more noticeable where a seasonal or other change in water-level causes alternate drying and moistening; a roughly concentric structure is found in specimens from the flat gravel banks on the shore of the Rhine near Konstanz, where the algæ are covered only when the river is high (Pia 1926, pp. 45–47).

In an extremely interesting occurrence described by Sir Douglas Mawson from the Robe district, South Australia, the water biscuits have a well-developed concentric structure, owing to alternate desiccation and flooding (Mawson 1929). The region in which the deposits are found is flat and almost at sea level, and is subjected to seasonal flooding; the conditions thus appear to have much in common with those prevailing in parts of Andros Island. The algal deposits, nevertheless, show interesting differences, for whereas the Bahaman algal heads are unlithified, and merely

SEP 12 2002 10:05 FR CISTI ICIST 613 998 5283 TO 17033084516 P. 24

form a surface modification of the sediment upon which they grow, the water biscuits are formed each as a separate, lithified individual, completely detached from its substratum, and deriving its carbonate largely or entirely by precipitation. Thus each water biscuit consists of a series of concentric shells, each one entirely enclosing the previously-formed part of the structure—an arrangement in strong contrast with the construction of the Bahaman deposits.

The author knows of no records of modern cyanophyceous limestones in process of formation in the open sea. HØEG has recently described a series of post-glacial stromatolitic plates, discovered on the cliffs of Malmø and Svenør, in the Oslo Fjord, and has shown that they are probably of marine origin. Unfortunately, their growth appears to have ceased some considerable time ago, and it is difficult to reconstruct the conditions which favoured the deposition of calcite in this particular from. HØEG (1929) suggests that the carbonate was precipitated from sea water through the agency of blue-green algæ or of bacteria, and points out that the structure and arrangement of the stromatolitic plates is strongly in agreement with an origin by precipitation. In this they differ entirely from the Bahaman deposits, for they are thoroughly lithified and have a compact crystalline structure.

A comparison with the Precambrian and early Palæozoic stromatolites, to which the Bahaman sediments show a certain resemblance, is beyond the scope of this paper, and will be considered separately in a later communication.

VII.—Description of Species.

Gloeocapsa granosa (Berkeley) Kützing, fig. 9.—A plant resembling *G. granosa* in its habit was found in the marshes near Lake Forsyth. It differs from typical

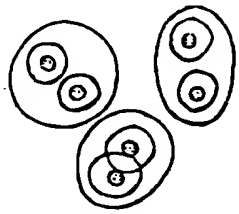

Fig. 9.

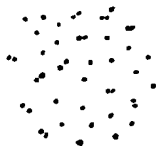

Fig. 12.

Fig. 10.

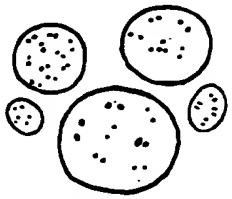

Fig. 11.

Fig. 9.—*Gloeocapsa granosa* var. *chlora*, Lake Forsyth. × 400. Fig. 10.—*Gloeocapsa viridis*, sp. nov., Twelve O'clock Cay. × 400. Figs. 11 and 12.—*Aphanocapsa marina*, in oval colonies from Lake Forsyth (fig. 11), and in the diffuse form, from Twelve O'clock Cay (fig. 12). × 1000.

SEP 12 2002 10:06 FR CISTI ICIST 613 998 5283 TO 17033084516 P. 25

material in its larger size, and also in the conspicuous jade-green pigmentation of the sheaths, especially in the case of families of four or more cells, in which the innermost sheaths are often deeply coloured. This form is therefore best regarded as a variety of *G. granosa*, for which the name *chlora* is proposed.

G. granosa (BERKELEY) var. *chlora* nov. Cells apple-green, 4–6 microns in diameter; individual sheaths olive-green to jade-green in colour, more strongly pigmented in the older colonies, non-lamellose, 12–14 microns in diameter. Colonies up to 75 microns in size, the inner common sheaths pale green, the outer ones colourless.

Habitat.—Amongst other Cyanophyceæ on the moist surface of chalk marshes; at the type locality, the water is almost fresh.

Locality.—Lake Forsyth, Andros Island, Bahamas.

Gloeocapsa viridis sp. nov., fig. 10.—Cells 0·75–1·0 microns in diameter; sheaths 2·5–5·0 microns, bright grass-green, usually strongly lamellose; plants in clusters from a few cells to groups of about twenty microns.

Habitat.—On sandy ground, liable to be flooded by sea water; at the type locality, intimately associated with *G. magma*.

Locality.—Twelve O'clock Cay, Middle Bight, Andros Island, Bahamas.

Aphanocapsa marina HANSGING, figs. 11 and 12.—The small *Aphanocapsa* which is found in great abundance at Lake Forsyth, and at Twelve O'clock Cay, only differs from the typical *A. marina* in the rather greater size of its cells, which range from 0·5 to 0·75 microns, as compared with 0·4 to 0·5 microns in the material described by HANSGING and by FOSLIE (1890, p. 169). The cells of the Bahaman material are pale green; near Lake Forsyth, where the water is almost fresh, the plant is sometimes found in well-defined, oval colonies, up to 12 microns in diameter, but it is usually in the form of a gelatinous, shapeless, mass, filling the spaces between other blue-green algæ. At Twelve O'clock Cay, the plant was found abundantly near high-water mark, as a colourless extended mass, pervading the spaces between sand grains, or amongst other algæ.

Plectonema atroviride sp. nov., fig. 13.—Filaments 4–5 microns in diameter, straight, rarely with a slight spiral tendency, branched freely at first, but later sparingly; false branches usually solitary. Sheaths firm, the outermost one hyaline, the inner deeply coloured, dark jade-green, almost opaque. Trichome one micron broad, with cells 6–8 microns in length.

Habitat.—Growing amongst other Cyanophyceæ, especially in tufts of *Scytonema*, in chalk marshes which are liable to be flooded by fresh water.

Locality.—At the head of Lake Forsyth, and near the southern shore of Stafford Lake, Andros Island, Bahamas.

Remarks.—This species resembles *P. nostocorum* in its form and habit, but differs in its thick and deeply coloured sheaths, and also in the greater length of its cells. In its unusually long cells, it may be compared with *P. terebrans*, but differs again in its stout sheaths. It also shows some similarity to *P. radiosum*, but is a distinctly smaller

SEP 12 2002 10:06 FR CISTI ICIST 613 998 5283 TO 17033084516 P. 26

plant. From all other species of *Plectonema* with a similar size or habit, it differs in the elongate shape of its cells.

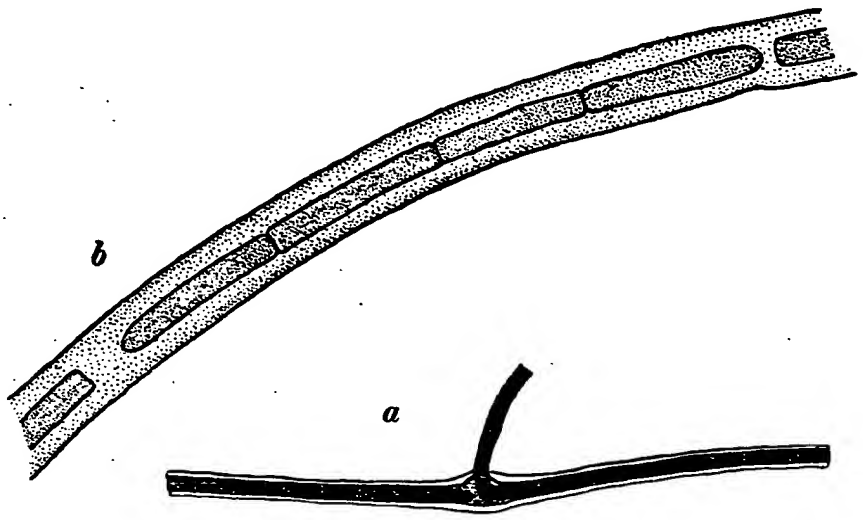

FIG. 13.—*Plectonema atroviride* sp. nov., Lake Forsyth, Andros. (*a*) Part of a filament, to show the two sheaths, the inner one deeply pigmented, and also the method of branching. × 700. (*b*) Part of a filament with the inner sheath bleached to show the trichome. × 3000.

Scytonema androsense sp. nov., fig. 14.—Plants forming matted strata and small woolly tufts, dark lead-grey to deep green in colour. Filaments with a very sharp outer edge, 15–30 microns in diameter, and up to a centimetre in length. Sheaths strongly lamellose; the innermost lamella is deep sage-green in colour, and is sometimes dark enough to obscure the trichome inside; outer sheaths, very pale green to colourless; at certain levels, the lamellæ are strongly divergent, and spread out to form broad, pale green or colourless funnel-shaped ocreae. Trichome 6–10 microns in diameter, with cells quadrate or slightly longer than broad; cell contents pale blue-green. Heterocysts the same width as the trichome, or a little wider, one-and-a-half times or twice as long as broad; outer wall of the heterocyst hyaline, enclosing an inner, golden yellow, granular centre. False branches free, and usually divergent at the base.

Habitat.—In chalk marshes, moistened by water with a salinity of 1·25 parts per thousand, or less.

Locality.—Lake Forsyth, Stafford Lake, and near the Fresh Creek Lakes, in Northern Andros Island, Bahamas.

Remarks.—This species falls into the division *Petalonema* of BORNET and FLAHAUT, but differs from other ocreate species of similar dimensions and structure in its intense green colour. It differs further from most of the species in this group, such as *S. densum*, *S. velutinum*, and *S. alatum*, by its characteristic heterocysts; from *S. crustaceum*, which it resembles in size and shape of heterocysts, it differs strongly in the lack of any trace of cohesion between the false branches.

SEP 12 2002 10:07 FR CISTI ICIST 613 998 5283 TO 17033084516 P. 27

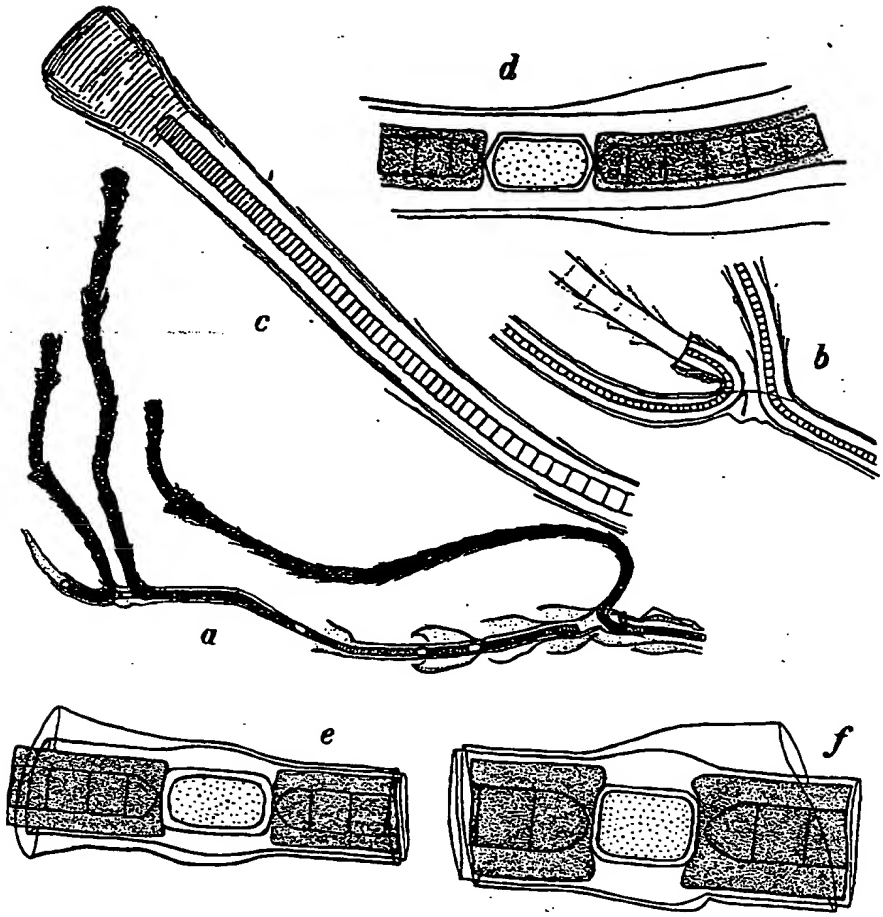

FIG. 14.—*Scytonema androsense* sp. nov., Lake Forsyth. (*a*) Part of the plant to show the spreading habit of the ocreae. × 120. (*b*) Method of branching. × 240. (*c*) Characteristic growing apex of a filament. × 480. (*d*) Part of a filament to show the deeply pigmented inner sheath broken at a heterocyst. × 800. (*e*) and (*f*) Typical heterocysts. × 800.

Scytonema crustaceum AGARDH, figs. 15 and 16.—Associated with *S. androsense* in the interior of Andros Island, is another species of *Scytonema*, which approaches *S. crustaceum* var. *incrustans* in many of its characteristics, but differs in the behaviour of its false branches. Unlike the typical *S. crustaceum*, and its variety *incrustans*, which give rise to branches in pairs, this form most commonly produces its false branches singly, and a paired arrangement is less frequently seen. Where the false branches do arise in pairs, they are usually immediately ascending, and are free for their entire length, fig. 16a. False branches arising singly, however, frequently pierce only the innermost sheath of the parent filament, and run within the outer sheaths for some distance before they break free, fig. 16b. Where the false branches entirely fail to break through the sheaths of the parent filament, fig. 16c, a peculiar disorganization of the trichome is sometimes observed to take place, fig. 16d; the filament produces a bulbous swelling, within which the trichome develops into a tangled mass of *Nostoc*-like chains, or may even break down into separate spherical cells.

SEP 12 2002 10:07 FR CISTI ICIST 613 998 5283 TO 17033084516 P. 28

In view of these peculiarities, this plant is best regarded as a variety of *S. crustaceum*, for which the name *catenula* is proposed.

S. crustaceum AGARDH. var. *catenula* nov.—Plants forming matted strata and woolly tufts, dark grey to deep green in colour. Filaments 20–45 microns in diameter, often with an irregular outer edge. Sheaths of strongly divergent lamellæ, olive-brown in colour. Spreading ocreæ absent. Trichome 5·0–12·5 microns in breadth, with spherical

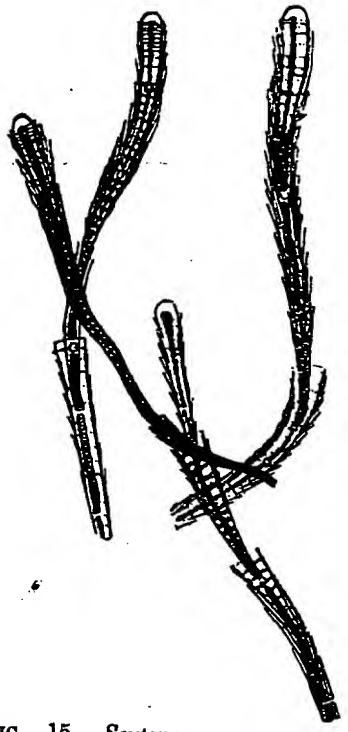

FIG. 15.—*Scytonema crustaceum* var. *catenula*, Lake Forsyth. Part of plant to show the divergent sheaths. × 150.

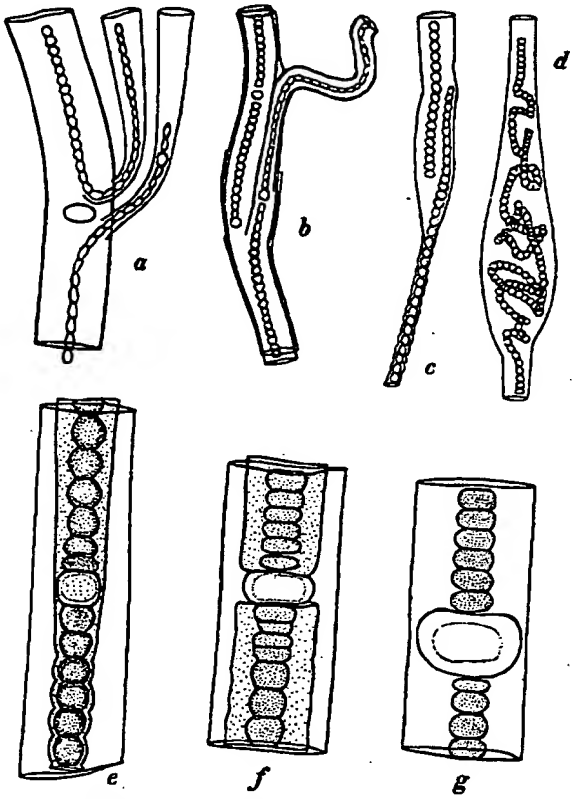

FIG. 16.—*Scytonema crustaceum* var. *catenula*. (*a*) Normal method of branching. × 200. (*b*)–(*d*) Branches with only partial rupture or non-rupture of the sheaths. × 150. (*e*)–(*g*) Typical heterocysts. × 500.

or compressed barrel-shaped cells; cell contents pale blue-green. Heterocysts compressed, wider than the trichome, and broader than their own length, colourless or olive-green, homogeneous. False branches usually arising singly, less commonly in pairs; solitary false branches frequently failing to pierce one or more of the outer sheaths, so that the branch runs within the parent filament, between two of the sheaths, or produces a bulbous swelling, within which the trichome becomes loosely aggregated or even disorganized into separate spherical cells.

Habitat.—In chalk marshes, associated with *S. androsense*.

Locality.—Marshes round the head of Lake Forsyth, Stafford Lake, and the Fresh Creek Lakes, Andros Island, Bahamas.

SEP 12 2002 10:08 FR CISTI ICIST 613 998 5283 TO 17033084516 P. 29

VIII.—Summary.

(1) Algal deposits, with characteristic structures, in some respects resembling certain Palæozoic stromatolites, are developing over a considerable area in Northern Andros Island.

(2) Several geographical belts can be recognized in the island, and the algal deposits in each belt possess a growth form distinct from that shown by algal deposits growing in other belts.

(3) The calcium carbonate which goes to make up these deposits is not necessarily precipitated by the algæ responsible for the structures, but consists of essentially mechanically entrapped sediment.

(4) The algal deposits are entirely unlithified, and do not require a solid substratum upon which to grow. They originate normally as a surface modification of unconsolidated sediments, and well-developed algal sediments are found to pass laterally and also downwards, into ordinarily bedded sediments.

(5) Generally the characteristic structure is produced, not by a single species, but by a community of organisms ; this is especially true of the structures with a dominantly concentric arrangement, as opposed to a radial one.

(6) Any particular species of alga may enter into, and help to build up, more than one type of rock structure.

(7) Although this kind of structure is best developed in regions of low salinity, it is also found in localities where the salinity is essentially that of the open ocean.

IX.—References.

Bavendamm, W. (1931). 'Ber. deuts. bot. Ges.,' vol. 49, p. 288.
(1932). 'Arch. Mikrobiol.,' p. 205.
Carey and Oliver (1918). "Tidal Lands, a Study in Foreshore Problems," Blackie & Sons.
Clarke, J. M. (1900). 'Bull. N.Y. State Museum,' No. 39, vol. 8, p. 195.
Foslie, M. (1890). "Marine Algæ of Norway."
Høeg, O. A. (1929). 'K. norske Vidensk. Selsk. Skr.,' No. 1.
Mawson, Sir Douglas (1929). 'Quart. J. Geol. Soc.,' vol. 85, p. 613.
Pia, J. (1926). "Pflanzen als Gesteinsbildner." Berlin, Gebr. Borntraeger.
Powell, H. (1903). 'Minn. Bot. Stud.,' p. 75.
Roddy, H. J. (1915). 'Proc. Amer. Phil. Soc.,' vol. 54, p. 246.
Wetzel, W. (1926). 'Centralbl. Min.,' B, 354–361.

EXPLANATION OF PLATES.

PLATE 21.

FIG. 17.—Mangrove flats on the North shore of the Wide Opening, seen at ebb tide. These flats are colonized by algal heads of Type B.

FIG. 18.—Algal heads of Type B at Twelve O'clock Cay. The photograph was taken looking down through a few inches of water, gently flooding the algal beds with the rising tide.

FIG. 19.—Algal heads of Type C, near the North Eastern shore of Lake Forsyth.

FIG. 20.—Surface view of the algal flats near the headwaters of Lake Forsyth. The individual discs are 4 or 5 inches in diameter.

PLATE 22.

FIG. 21.—Type A. Section in Reflected Light, showing the surface and uppermost laminæ. × 10.

FIG. 22.—Type A. Slab etched with acid to show the relative thicknesses of organic layers (dark) and sedimentary layers (light). The individual filaments of *Symploca* and *Phormidium* cannot be distinguished at this magnification, and the algal material appears as rather ill-defined layers of jelly. Filaments of *Scytonema* may be distinguished in the lower part of the figure. Reflected light. × 10.

FIG. 23.—Type A. Thin section showing the relation between the algal filaments and the grains of sediment at the surface. Transmitted light. × 100.

FIG. 24.—Type B. An algal layer, consisting mainly of deeply pigmented *Gloeocapsa magma* and *G. viridis*, runs across the centre of the figure. The normal texture of the sediment in this locality is seen in the lower half of the figure. Near the top of the section is a band of much finer grained sediment, enmeshed between filaments of *Symploca*. Reflected light. × 10.

FIG. 25.—Type C. Part of a mature algal head, sectioned in artificial resin. The dark layers consist of compressed algal filaments, mainly belonging to species of *Scytonema*. Reflected light. × 10.

FIG. 26.—Type C. Thin section, showing sections of algal tubes (*Scytonema*, spp.). Transmitted light. × 100.

FIG. 27.—Type D. Thin section, showing the large proportion of organic matter (dark), and the extremely fine grain of the sediment. Transmitted light. × 100.

FIG. 28.—Radial algal head, from Stafford Lake. The open, porous structure is in strong contrast with the compact forms shown in the other figures of this plate. Reflected light. × 2.3.